



CATALYTIC SYSTEMS ADAPTED TO GLYCEROL MEDIUM. APPLICATIONS IN SELECTIVE PROCESSES.

Marta Rodríguez Rodríguez

ADVERTIMENT. L'accés als continguts d'aquesta tesi doctoral i la seva utilització ha de respectar els drets de la persona autora. Pot ser utilitzada per a consulta o estudi personal, així com en activitats o materials d'investigació i docència en els termes establerts a l'art. 32 del Text Refós de la Llei de Propietat Intel·lectual (RDL 1/1996). Per altres utilitzacions es requereix l'autorització prèvia i expressa de la persona autora. En qualsevol cas, en la utilització dels seus continguts caldrà indicar de forma clara el nom i cognoms de la persona autora i el títol de la tesi doctoral. No s'autoritza la seva reproducció o altres formes d'explotació efectuades amb finalitats de lucre ni la seva comunicació pública des d'un lloc aliè al servei TDX. Tampoc s'autoritza la presentació del seu contingut en una finestra o marc aliè a TDX (framing). Aquesta reserva de drets afecta tant als continguts de la tesi com als seus resums i índexs.

ADVERTENCIA. El acceso a los contenidos de esta tesis doctoral y su utilización debe respetar los derechos de la persona autora. Puede ser utilizada para consulta o estudio personal, así como en actividades o materiales de investigación y docencia en los términos establecidos en el art. 32 del Texto Refundido de la Ley de Propiedad Intelectual (RDL 1/1996). Para otros usos se requiere la autorización previa y expresa de la persona autora. En cualquier caso, en la utilización de sus contenidos se deberá indicar de forma clara el nombre y apellidos de la persona autora y el título de la tesis doctoral. No se autoriza su reproducción u otras formas de explotación efectuadas con fines lucrativos ni su comunicación pública desde un sitio ajeno al servicio TDR. Tampoco se autoriza la presentación de su contenido en una ventana o marco ajeno a TDR (framing). Esta reserva de derechos afecta tanto al contenido de la tesis como a sus resúmenes e índices.

WARNING. Access to the contents of this doctoral thesis and its use must respect the rights of the author. It can be used for reference or private study, as well as research and learning activities or materials in the terms established by the 32nd article of the Spanish Consolidated Copyright Act (RDL 1/1996). Express and previous authorization of the author is required for any other uses. In any case, when using its content, full name of the author and title of the thesis must be clearly indicated. Reproduction or other forms of for profit use or public communication from outside TDX service is not allowed. Presentation of its content in a window or frame external to TDX (framing) is not authorized either. These rights affect both the content of the thesis and its abstracts and indexes.

Catalytic Systems Adapted to Glycerol Medium. Applications in Selective Processes

PhD Thesis presented by:

Marta Rodríguez Rodríguez

Developed under the supervision of:

Prof. Montserrat Gómez and Prof. Miquel A. Pericàs

Departament de Química Analítica i Química Orgànica (URV)
Institut Català d'Investigació Química (ICIQ)
Laboratoire Hétérochimie Fondamentale et Appliquée (UPS)

January 2017





UNIVERSITAT ROVIRA I VIRGILI



Prof. MONTSERRAT GÓMEZ and Prof. MIQUEL A. PERICÀS BRONDO,

STATE, that the present Doctoral Thesis entitled: "**Catalytic Systems Adapted to Glycerol Medium. Applications in Selective Processes**", presented by Marta Rodríguez Rodríguez to receive the degree of Doctor, has been carried out under their supervision between the Université de Toulouse 3 - Paul Sabatier (UPS) and the Institute of Chemical Research of Catalonia (ICIQ).

Toulouse, 18th November 2016

Tarragona, 28th November 2016

Prof. Montserrat Gómez

Prof. Miquel Àngel Pericàs
Brondo

The work developed in the present doctoral thesis has been possible thanks to the funding received from Centre National de la Recherche Scientifique (CNRS), the Université de Toulouse 3 - Paul Sabatier and Fundació Institut Català d'Investigació Química (ICIQ). The work has been developed in the framework of the CTQ2012-38594-C02-01 and CTQ2015-69136-R (MINECO/FEDER) projects and the Severo Ochoa Excellence Accreditation SEV-2013-0319 from the Spanish Ministry of Economy and Competitiveness and the 2014SGR827 from the Generalitat de Catalunya.



Acknowledgements

En primer lugar, quiero agradecer a mis dos directores de tesis Montserrat Gómez y Miquel A. Pericàs por darme esta gran oportunidad. Los dos me habéis enseñado muchísimas cosas y me habéis apoyado en todo momento. Estoy enormemente agradecida por todo.

I would like to thank Silvia Díez González, Joaquín García Álvarez, Sergio Castellón and Karine Philippot for agreeing to be part of my Ph.D jury and reading this dissertation.

Ayant commencé à Toulouse, je voudrais commencer par remercier l'LHFA. Tout d'abord, je voudrais remercier le directeur du laboratoire, Didier Bourissou, de m'avoir accueilli durant une année et demi à l'LHFA, ce fût une expérience incroyable. C'était pour moi la première fois que je partais de Valladolid, ma ville natale. Les débuts de cette aventure furent difficiles mais vous l'avez rendue très facile à vivre et vous l'avez surtout rendue inoubliable. Je voudrais commencer par mon équipe, l'équipe SYMAC. Faouzi, tu m'as beaucoup aidé au commencement, je n'oublierai jamais le temps passé avec toi au travail, merci beaucoup. Isabelle, la femme « Macgyver », que aurais fait-je sans toi !!, tu es une très belle personne, un grand merci à toi Isabelle. Antonio, para mi Antoñito, hemos vivido grandes momentos juntos en el laboratorio, no olvidaré nunca tu gran apoyo incluso en la distancia, ha sido muy importante. Ying-Ying, merci beaucoup pour ton sourire permanent, je suis très contente de t'avoir connu. Trung and Garima, it was a pleasure to meet you. Je voudrais également remercier Christian Pradel pour toutes les analyses de TEM et aussi pour ses encouragements. Daniel, merci beaucoup pour t'aide. Et je voudrais par la même occasion remercier tous le personnel de l'LHFA, ça a été un grand plaisir d'avoir partagé du temps avec vous. Florian, un grand ami, merci beaucoup pour ton soutien ainsi que pour ton aide, qui, a été très importante pour moi. Natalia, hemos pasado juntas muy buenos momentos en Toulouse, muchísimas gracias por tu apoyo en esta experiencia. Amos, el grandullón, nunca olvidaré tu frase estrella : « La vida es chula », muchísimas gracias « muchachito ». Gracias también a Noel Nebra, me han ayudado mucho tus consejos el tiempo que coincidimos allí. La liste des personnes est très très longue. Mille mercis à tous mes collègues de labo : Anne Fred, Mathieu, Alexia, Sebastien, Anthony, Koyel, Noemi,

Momo, Dimitri, Cristóbal, Ferial, Gwen, Marc, Max, Richard, Frank, DianDian, Abdallah, Sam, Noel, Laura, Raphaël et Morelia. Merci aussi à Olivier Volpato, Olivier Thillaye du Boullay et Romaric pour votre grand travail. Je voudrais remercier à Abder, Nicolas, Rinoi, Julien, Blanca pour vos nombreux couragements.

Maryse et Serah, merci beaucoup pour tout votre aide avec toutes les procédures administratives. Vous faites un travail magnifique au LHFA.

Merci aux personnels des différentes plates-formes techniques et d'analyses d'avoir toujours été présents dès que j'en avais besoin.

...y después de pasar un año y medio genial en el LHFA, me trasladé al ICIQ en Tarragona...

La experiencia en el ICIQ ha sido también inolvidable, no voy a olvidar nunca el tiempo que he pasado aquí en el grupo Pericàs. Empiezo con Carles Rodríguez, muchísimas gracias por todo, he tenido mucha suerte de haberte conocido. Cada vez que he hablado contigo he aprendido una cosa nueva, he aprendido hasta cómo jugar al volley (al menos, defenderme). Sonia, muchísimas gracias por ayudarme, apoyarme y confiar en mí en todo momento, ha sido muy importante para mí. Pablo!! Qué habría hecho yo sin tí... no tengo suficientes palabras para agradecerte todo lo que me has enseñado (y aguantado también!). Patri, qué haríamos todos sin ti, muchísimas gracias por tu gran trabajo y tu apoyo (y por haberme introducido en el mundo del zumba). Ada, una pena no haberte conocido antes, voy a echar de menos tu buen humor permanente y tu positividad, muchas gracias por tu ayuda. Laura Osorio, muchas gracias por tus ánimos y los buenos momentos que he pasado contigo, un placer haberte conocido. Paola, me ha encantado conocerte, qué manera de reír contigo, mil gracias por tu ayuda también. Carles Ayats, vaya bajón cuando te fuiste!, no voy a olvidar nunca las risas contigo. Lidia, compañera de viaje, ha sido un placer conocerte, ánimo que ya casi lo tienes. Laura Buglioni, mi italiana preferida, también una pena no haberte conocido antes, gracias por esos grandes momentos. Alba, la de "Lleide", una grandísima compañera, vaya unas risas contigo también, muchas gracias. Sara Ranjbar, we had fantastic moments together inside the thesis room (and outside), thank you for your encouraging words. Tharun, the best photographer ever, it was a pleasure to meet you. Santi y Lluís, los más jovencillos del grupo, muchos ánimos chicos, estoy muy contenta de haberos conocido. Dina, la mujer viajera, pasé muy buenos momentos contigo

compartiendo mesa, muchas gracias. Javi, sólo compartí unos meses contigo y es una pena que no hayan sido más, muchas gracias por tu ayuda y las risas que nos hemos echado juntos. Esther, muchas gracias también por los ánimos. Y la lista no acaba nunca, Montserrat, Anna, Irina, Carmen, Shoulei, Junshan, Francesca, MarcoN, MarcoM...mil gracias por todo vuestro apoyo.

Sara García, qué habría hecho yo sin tu ayuda con todos los trámites administrativos. Haces un trabajo espléndido. Muchísimas gracias por todo.

Muchas gracias también a todo el personal de las áreas de soporte a la investigación y personal administrativo del ICIQ por su ayuda siempre que lo he necesitado.

Hay también dos piezas muy importantes en esta etapa en Tarragona, Caye y Sope. Caye, compañera de carrera, de piso, de tesis, de penas y de alegrías, una grandísima amiga. Hemos pasado mucho tiempo juntas y la verdad, ha sido genial. Muchísimas gracias por todo Caye, me ha ayudado muchísimo tenerte al lado. We did it!!! Sope, el mejor palentino del mundo, muchas gracias por estar ahí siempre, eres un gran amigo. Os voy a echar mucho de menos a los dos, al “tierra de sabor” team.

Quería también dar las gracias a toda la gente que he conocido en el ICIQ, de los que también he recibido muchos ánimos: Leti, Giacomo, Luca, Giulia, Katia, Jeroen, Luis, Sofía, Lucas, Bala, Neus, Marta, Eloisa, Kike, Andrea, Dani, Ilario y Nicola.

Quiero agradecer también a Alicia Maestro todo lo que me enseñó en mi último año de carrera y en mi Máster. El tiempo que pasé allí trabajando y aprendiendo con ella me motivo aún más a hacer una tesis. Muchísimas gracias por todo Alicia.

No me olvido de mis amigos en Valladolid que siempre han estado ahí cuando he vuelto de visita. Muchas gracias Judith, Lucía, Olga y Gorka por vuestros ánimos.

Agradezco también el apoyo de Mayte y de César, y también de César (hijo) por la imagen que me ha hecho para la portada de la tesis, eres todo un artista.

El apoyo de mi familia ha sido algo indispensable en esta tesis. Cada día mis padres y mi hermana han estado escuchándome, apoyándome y dándome consejos. No tengo palabras suficientes para agradecer todo lo que hacéis por mi y lo que me apoyáis. También quiero agradecer el apoyo recibido de mi tía Angelines, siempre ahí para todo, mi tío Antonio y mis primos Toño, Inma y Onti. Quiero agradecer a mi tía

Isabelita por su gran apoyo, a Alex y en especial a Helena que ha estado esperando siempre impaciente estos tres años a su “tata” y haciendo unos superdibujos increíbles que han decorado mi habitación todo este tiempo, ya acabé Helena!!. Quiero recordar también a mi abuela, que en mi cabeza ha estado siempre ahí, ayudándome. Esta tesis es para vosotros.

Le quiero agradecer a Iván todo su apoyo y paciencia. A pesar de la distancia, todos los días has estado a mi lado, escuchándome y entendiéndome. Tus visitas fueron esenciales siempre para mí. Mil gracias por todo.

A mi familia

“La patience est amère, mais son fruit est doux”

Jean-Jacques Rousseau

List of publications

“Metal-Free Intermolecular Azide-Alkyne Cycloaddition Promoted by Glycerol”

M. Rodríguez-Rodríguez, E. Gras, M. A. Pericàs and M. Gómez

Chem. Eur. J. **2015**, *21*, 18706

“Key non-metal ingredients for Cu-catalyzed “Click” reactions in glycerol: nanoparticles as efficient forwarders”

M. Rodríguez-Rodríguez, P. Llanes, C. Pradel, M. A. Pericàs and M. Gómez

Chem. Eur. J. **2016**, *22*, 18247

Summary

Solvents are used in huge amounts in the chemical industry and this is one of the biggest problems to be solved not only from an environmental point of view, but also for economic reasons. The solvents commonly used in the industry are volatile, toxic, inflammable and/or corrosives; then, their replacement by others less harmful represents a crucial objective. Glycerol appears as a promising candidate to substitute the conventional organic solvents. It is produced in huge amounts as a waste in biodiesel industry. Consequently, the valorisation of glycerol becomes an important concern. This compound possesses very interesting properties to be used as solvent such as its non-toxicity, large range in liquid state, negligible vapor pressure, capacity for solubilizing organic and inorganic compounds, low miscibility with other organic solvents and also its low price.

This Thesis deals with the development of new catalytic systems in glycerol medium. In particular, in this work we show how glycerol can facilitate the stabilization of copper(I) nanoparticles that are able to catalyze the 1,3-dipolar Huisgen cycloaddition between terminal alkynes and organic azides (known as click reaction). The reaction proceeds at room temperature and it is very efficient. Moreover, this reaction can be carried out in the absence of copper using internal alkynes, working under microwave irradiation. Glycerol favours the process in comparison with other solvents (including protic ones), probably due to its ability to form hydrogen bonds, which favors the interaction with microwave irradiation (accelerating the process). With the aim of studying stereoselective transformations, we have conceived new enantiopure ligands derived from PTA (1,3,5-triaza-7-phosphaadamantane). These innovative phosphines have been applied in enantioselective processes, such as pinacolboron addition to *N*-Boc-imines (Cu) or α -amination (Cu), among others, where the phosphine is involved as chiral ligand in metal-catalyzed processes, or as organocatalyst (Morita-Baylis-Hillman reaction).

Table of contents

Short Introduction and Objectives	3
Chapter 1. General Introduction	9
1.1 Glycerol: an eco-friendly and versatile solvent in catalysis	9
1.2 The azide–alkyne cycloaddition reaction	16
1.3 Glycerol-soluble derivatives for the development of new catalytic systems	18
1.4 References	21
Chapter 2. Metal-Free Intermolecular Azide–Alkyne Cycloaddition Promoted by Glycerol	27
2.1 Introduction	27
2.2 Results and discussion	32
2.3 Conclusions	49
2.4 Experimental section	50
2.5 References	60
2.6 Annex: NMR spectra of the isolated compounds	62
2.7 Published paper	80
Chapter 3. Key Non-Metal Ingredients for Cu-Catalysed Azide–Alkyne Cycloaddition in Glycerol	87
3.1 Introduction	87
3.2 Results and discussion	92
3.3 Conclusions	111
3.4 Experimental section	112
3.5 References	117
3.6 Annexes	120
3.6.1 Mass spectra of the impurities of the contaminated benzyl azide	120

3.6.2 GC-MS-EI chromatograms of “inactive” benzyl azides	123
3.6.3 NMR spectra of “inactive” benzyl azides	125
3.6.4 TEM images	128
3.6.5 NMR spectra of the isolated compounds	132
3.6.6 Published paper	146
Chapter 4. Preparation of new enantiopure PTA-based derivatives. Some applications in enantioselective catalysis	155
4.1 Introduction	155
4.2 Results and discussion	159
4.2.1 Preparation of the enantiopure PTA phosphines	159
4.2.2 Applications of the enantiopure PTA derivatives	171
4.3 Summary and outlook	181
4.4 Experimental section	182
4.5 References	201
4.6 Annex: NMR spectra of the isolated compounds	204
Conclusions and Perspectives	227

Short introduction and objectives

Short introduction and objectives

The *Green Chemistry* concept was defined for the first time at the beginning of the 1990s^[1] as the “*design of chemical products and processes to reduce or eliminate the use and generation of hazardous substances*”. The use of solvents is perhaps one of the most important areas of *Green Chemistry*, because they are widely recognised to represent a great environmental concern. In the chemical industry, solvents are used in huge amounts as media for chemical reactions, for chemical separations/purifications and for analysis. Moreover, many conventional solvents are toxic, flammable, and/or corrosive. According to one of the twelve principles of *Green Chemistry*,^[2] the reduction of the use of harmful solvents is one of the priorities. The European Solvents Industry Group (ESIG) has been created to promote the use of solvents in a more environmentally friendly and safe way.^[3] One of the targets is to produce new bio-based solvents. The bio-based solvent consumption in the European Union was 0.63 million tons in 2008, a 12.6% of the total (5 million tons) and it is estimated to growth up to 1.1 million tons by 2020.^[4]

The development of solvent-free processes would be ideal,^[5] however, solvents have in most of the cases a crucial role in the chemical transformations.^[6] Thus, the strategy to solve this problem is to replace petroleum-based solvents by others obtained from renewable resources or by ones that show better environmental, health and safety properties. Regarding these considerations, water is the first-choice solvent,^[7] and it has already been used on an industrial scale; however, its negligible capacity to solubilise organic and organometallic compounds and the high energy cost for water removal after completion of processes, limits its applications.

1,2,3-Propanetriol (glycerol) appears as a concomitant product in the production of biodiesel (approx. 10 wt% of the total output). The biodiesel industry has grown exponentially in the last few years and the utilisation of huge amounts of the glycerol generated in this process presents a problem for this technology. For this reason, the search for new uses of glycerol becomes an important challenge for researchers. In this sense, glycerol represents an attractive candidate to be used as solvent in chemical transformations. Together with its low price, its non-toxicity, the high boiling point (290 °C), the negligible vapour pressure and the ability to dissolve a variety of organic as well as inorganic compounds make it especially interesting for applications in catalysis.

In recent years, our group has been interested in the application of glycerol as solvent in catalytic transformations. Particularly, the stabilisation of Pd nanoparticles in this medium led to a highly efficient catalytic system for several chemical transformations.^[8] Glycerol also allowed us to stabilise Cu nanoparticles that were active in C–N and C–S bond formation reactions, azide–alkyne cycloadditions and tandem processes merging both afore mentioned transformations.^[9] Moreover, our research group could prove the important role of glycerol in the Rh-catalysed Pauson-Kand carbocyclisations.^[10]

Following these promising results, the main objective of this Thesis has been the development of new catalytic systems adapted to glycerol medium. We focused our attention on the azide–alkyne cycloaddition reaction. Despite the tremendous importance of this transformation, not only for applications in chemistry but also in biochemistry and material science, it has not been deeply studied in glycerol medium. For this reason we wanted to go further in this topic and take advantage of the properties of glycerol as solvent to discover new procedures to afford 1,2,3-triazoles. On the other hand, glycerol-soluble derivatives are required to build up catalytic systems in this medium considering that they can serve as ligands for organometallic complexes, as stabilisers for metallic nanoparticles or as catalysts by them self. In this context, the 1,3,5-triaza-7-phosphaadamantane (PTA) and its derivatives are found to be excellent water-soluble molecules very useful in reactions in water and also, as proved by our group, excellent glycerol-soluble ligands. Being focused on this, we envisioned the preparation of new enantiopure PTA derivatives to carry out catalytic asymmetric processes in this medium.

The **first chapter** gives an overview of the main topics of this Doctoral Thesis. First of all, the advantages of using glycerol as solvent for chemical transformations are explained. After this, a short introduction about the interest of 1,3-dipolar azide–alkyne cycloaddition reaction as well as about the need of glycerol-soluble derivatives to carry out catalytic reactions in this medium are also provided.

The aim of the **second chapter** is to develop a new metal-free synthetic procedure for the synthesis of 1,4,5-trisubstituted 1,2,3-triazoles from internal alkynes and organic azides using glycerol as solvent. Fully substituted triazoles are useful molecules in biochemistry. To avoid the use of transition metal catalysts in the synthesis of these molecules, a matter of importance to prevent contamination of the final products with traces of metals. The interesting physicochemical properties of glycerol, in particular its high boiling point, its negligible vapour

pressure and its high viscosity, offer the opportunity to use it under microwave dielectric heating and accelerate the reaction.

The **third chapter** deals with the Cu-catalysed azide–alkyne cycloaddition (CuAAC) using terminal alkynes in glycerol. The objective in this section is to look for milder reaction conditions with the aim of immobilising the catalyst. The effect of long-alkyl-chain amines as additives in the reaction medium has been studied in this section. They have a key role on the CuI-assisted azide–alkyne cycloaddition at room temperature, helping to the stabilisation of highly reactive copper nanoparticles in glycerol that can be recycled.

The objective of the **fourth chapter** is the preparation of novel glycerol-soluble enantiopure ligands derived from 1,3,5-triaza-7-phosphaadamantane (PTA), functionalised on the carbon atom nearest to phosphorus (“upper rim” functionalisation). The synthetic procedures as well as the preliminary tests of its activity in several asymmetric reactions (MBH, α -amination, addition of terminal alkynes to isatins and the hydroboration of imines) are shown in this chapter.

To summarise the work carried out in this Doctoral Thesis, this manuscript is completed by the main conclusions of the results obtained and some perspectives for the future.

- [1] P. T. Anastas, J. C. Warner, *Green Chemistry: Theory and Practice*, Oxford University Press, New York, **1998**.
- [2] P. Anastas, N. Eghbali, *Chem. Soc. Rev.* **2010**, *39*, 301–312.
- [3] <http://www.esig.org/>
- [4] BIOCHEM Project D2.3 Report on the "Assessment of the Bio-Based Products Market Potential for Innovation". [http://www.biochem-project.eu/download/toolbox/innovation/06/Bio-based product market potential.pdf](http://www.biochem-project.eu/download/toolbox/innovation/06/Bio-based_product_market_potential.pdf)
- [5] F. Kerton, R. Marriott, in *Alternative Solvents for Green Chemistry 2nd Ed., Chapter 3*, The Royal Society of Chemistry, **2013**, pp. 51–81.
- [6] C. Reichardt, T. Welton, in *Solvents and Solvent Effects in Organic Chemistry, 4th Ed.*, Wiley-VCH, Weinheim, **2010**, pp. 1–5.
- [7] F. Kerton, R. Marriott, in *Alternative Solvents for Green Chemistry 2nd Ed., Chapter 4*, The Royal Society of Chemistry, **2013**, pp. 82–114.
- [8] (a) F. Chahdoura, C. Pradel, M. Gómez, *Adv. Synth. Catal.* **2013**, *355*, 3648–3660; (b) F. Chahdoura, S. Mallet-Ladeira, M. Gómez, *Org. Chem. Front.* **2015**, *2*, 312–318; (c) F. Chahdoura, I. Favier, C. Pradel, S. Mallet-Ladeira, M. Gómez, *Catal. Commun.* **2015**, *63*, 47–51.
- [9] F. Chahdoura, C. Pradel, M. Gómez, *ChemCatChem* **2014**, *6*, 2929–2936.
- [10] F. Chahdoura, L. Dubrulle, K. Fourmy, J. Durand, D. Madec, M. Gómez, *Eur. J. Inorg. Chem.* **2013**, 5138–5144.

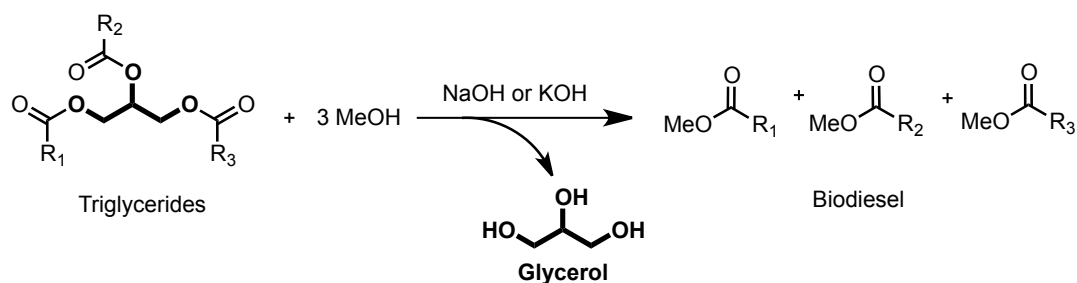
Chapter 1

General Introduction

Chapter 1. General introduction

1.1 Glycerol: an eco-friendly and versatile solvent in catalysis.

The huge industrial development and population growth are the principal causes of the current global energy crisis. To satisfy the demand of energy in all over the world, the non-renewal energy sources are being consumed in an unsustainable rate. Moreover, the combustion fossil fuels such as oil, gas and coal cause the emission of an alarming amount of hazardous substances into the atmosphere. Without the slightest doubt, these aspects are affecting drastically to the environment. This has led to a search of new alternatives to substitute fossil fuels, in particular the use of biofuels. Biodiesel has been identified as one of the options to replace or, at least, complement the traditional fuels.^[1] The preferred method to produce biodiesel is the transesterification of vegetable oils or animal fats with an alcohol (typically methanol) using a strong alkaline catalyst to produce esters (Scheme 1.1).^[2] In this process, glycerol is produced as a concomitant product. Generally, for each kilogram of biodiesel produced, approximately 100 g of glycerol are generated, which is nearly 10 wt.% of the total product.^[3]

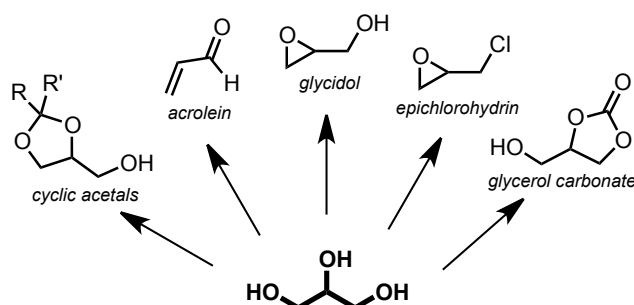


Scheme 1.1 General reaction for based-catalysed transesterification for biodiesel production.

One of the major obstacles for the commercialisation of biodiesel is the inevitable co-production of glycerol.^[4] The surplus of crude glycerol has supposed a dramatic impact in the prices of crude glycerol and consequently, in the biodiesel industry. Over the past few years, the crude glycerol prices dropped from 0.31€ to 0.04€ per kg.^[4-5] Moreover, depending on the biodiesel production process and the rapeseed used, the crude glycerol generated includes around 20% of impurities such as methanol, potassium and sodium salts, non-glycerol organic matter, soaps and water.^[6] The purification of crude glycerol is an expensive process and is riddled with handling and separation problems.^[7] Large-scale biodiesel producers can refine the crude glycerol to obtain a high pure form up to 99% of purity, which can be used in

pharmaceutical, food or cosmetic industries. Nevertheless, small-scale producers are looking for alternatives which permit the use of unrefined glycerol in profitable applications.^[8]

Clearly, the development of new strategies to convert glycerol into more valuable products or the search of new uses of this compound represents an urgent need. Actually, in 2013, the European Union initialised a project named GRAIL (“Glycerol Biorefinery Approach for the Production of High Quality Products of Industrial Value”) with the objective of coming up with solutions and technologies to utilise glycerol and transform it into beneficial products.^[9] In the last few years, much research has focused on this aim and several options and strategies have been developed. One of the most active areas of research is the transformation of glycerol into other small molecules like glycidol, epichlorohydrin, acrolein, glycerol carbonate or cyclic acetals, among others (Scheme 1.2).^[10] There are also interesting approaches such as the utilisation of glycerol for the synthesis of hydrogen, to use it as a fuel additive, as a substrate for fermentation, for methanol production, in waste water treatments and many others.^[4] In this context, the possible use of glycerol as solvent in chemical transformations has become a subject of particular interest.



Scheme 1.2 Some possible transformations of glycerol into intermediates of industrial interest.

Solvents are used in large quantities in fine-chemical and pharmaceutical industries for chemical transformations, separation and purification processes. Moreover, many conventional solvents are hazardous volatile compounds, toxic and harmful. One of the most important challenge of *Green Chemistry*^[11] is to minimise the environmental impact resulting from the use of solvents in chemical production. For this reason, the substitution of the conventional hazardous solvents by ones that shown better environmental, health and safety properties is an active and an important area of research. Bio-based solvents coming from renewable sources have emerged as one of these green alternatives.^[12] Boosted by the problematic of its overproduction, glycerol^[13] and its derivatives^[14] have appeared as one of these bio-based solvents together with others such as D-limonene, ethyl lactate^[15] or 2-

methyltetrahydrofuran.^[16] Glycerol is also widely used as one of the components of deep eutectic mixtures, known as Deep Eutectic Solvents (DESs).^[17] DESs are also promising alternatives for the replacement of common organic solvents. These eutectic mixtures are generally formed by two components: a hydrogen-bond acceptor (choline chloride, betaine, alanine, among others) and a hydrogen-bond donor (glycerol, ethylene glycol, urea, among others).^[18] DESs are mainly characterised by a freezing point lower than those of their neat components. They have similar physico-chemical properties to the well-known ionic-liquids but they are much cheaper and more environmentally friendly.

Glycerol is a clear, colourless, odourless and viscous liquid that possesses a unique combination of chemical and physical properties that make it an interesting solvent for catalysis. In order to compare with other alternative solvents, some properties of glycerol are collected in Table 1.1 together with those of water and [bmim][PF₆] (1-butyl-3-methylimidazolium hexafluorophosphate), one of the most used ionic liquids. In comparison with water and [bmim][PF₆], glycerol is very viscous at room temperature, but at higher temperatures (> 60 °C) becomes more fluid. Its melting point is higher than the one of water and [bmim][PF₆]. Like [bmim][PF₆], glycerol presents a high boiling point and a low vapour pressure in comparison with water. It is important to highlight the broad range of temperature (almost 300 °C) in which glycerol can maintain its liquid state. Finally, an important point is that glycerol is biodegradable, in contrast to [bmim][PF₆].

Table 1.1 Chemical and physical properties of glycerol, water and [bmim][PF₆].^[13a, 14a, 14c, 19]

Properties	Glycerol	Water	[bmim][PF ₆]
Chemical formula	C ₃ H ₈ O ₃	H ₂ O	C ₈ H ₁₅ F ₆ N ₂ P
Molecular mass (g/mol)	92.09	18.01	284.19
Density at 20 °C (g/mL)	1.26	1	1.36
Viscosity at 20 °C (cP)	1200	1	312
Melting point (°C)	18.2	0	-8
Boiling point (°C)	290	100	>350 ^[a]
Vapour pressure at 50 °C (mm Hg)	<1	92.5	<1
Biodegradable	Yes	-	Non

^[a] Decomposition temperature.

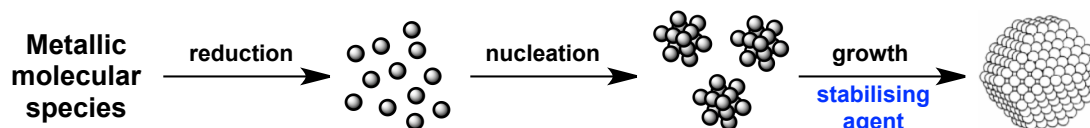
These data show that glycerol possesses some advantages in comparison with other alternative solvents in particular regarding catalytic applications and, along with other considerations, several points should be highlighted to show the main benefits of glycerol:

- Safety: due to its high boiling point and negligible vapour pressure, the reactions can be carried out at high temperatures, favouring the acceleration of processes. Moreover, the solvent is not evaporated, which increases the safety of the process on a large scale. Thanks to the high boiling point, distillation of products is also feasible.
- Toxicity: glycerol is a non-toxic compound with a median lethal dose (LD_{50}) of 12,600 mg/Kg (rats), which is the dose required to kill a half of the members of the tested population in a specific time. Moreover, it is found in numerous consumer products such as pharmaceuticals, cosmetics, tobacco, food and drinks.
- Environmental compatibility: glycerol is a biodegradable and reusable solvent. It has no harmful impact on the environment, which is very important in case of accidental spills. Aquatic toxicity measured by TLm96 parameter (defined as the concentration that would kill 50% of exposed organisms in 96 hours) is *ca.* 1,000 mg/L, an insignificant level.^[20]
- Economic consideration: glycerol is very cheap, crucial for applications at large scale.
- Solubility and miscibility: glycerol allows the dissolution of transition metal complexes, inorganic salts, acids, bases and enzymes. It also dissolves organic compounds usually insoluble in water. Glycerol is not miscible with hydrocarbons and ethers, which allows liquid-liquid extraction for product isolation.

Apart from all these benefits, the use of glycerol as solvent in chemical transformations shows also some drawbacks. The reactivity of the three hydroxyl groups with the reaction components can lead to undesired side products. In addition, the coordination ability of glycerol could be a problem for transition metal complex catalysts, because of the competition between the desired ligands and the hydroxyl groups for the coordination to the metal centre. Moreover, its high viscosity could make difficult the diffusion of the organic substrates in the medium. However, this limitation can be overcome by increasing the reaction temperature above 60 °C or adding co-solvents to improve the fluidity. In addition, the strong hydrogen-bonding network structure of glycerol^[21] makes it especially useful as solvent in microwave-promoted organic transformations.^[22] This supramolecular network is the responsible of its high viscosity, which is

correlated to the long relaxation time (that is, the time taken for the molecule to take up a random orientation when the electric field is switched off) observed for glycerol, in comparison with other protic solvents.^[23] This fact, together with its favourable dielectric properties, makes glycerol a cheap and environmental friendly solvent.

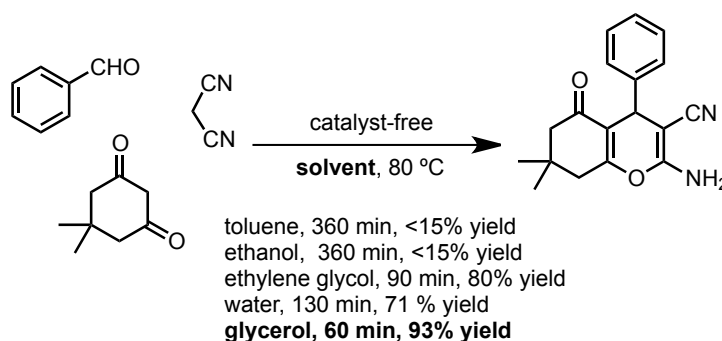
It is also remarkable the particular ability of glycerol to stabilise and immobilise metallic nanoparticles.^[13c] The bottom-up synthetic approach is one of the most convenient ways to control the size and morphology of metallic nanoparticles (MNPs) during its preparation (Scheme 1.3).^[24] Generally, the first step in this strategy consists in the reduction of transition metal salts or organometallic complexes (by adding a reducing agent). Then, naked atoms start to collide each other in the nucleation step leading to the formation of seeds (nuclei, *i.e.* small clusters). To control the particles growth, it is necessary the presence of a stabiliser, in order to avoid the thermodynamically tendency to give agglomerates and bulk material.^[25] Polyols, like glycerol, have been widely applied as solvents for the formation of MNPs because they can function as both reducing agent and stabiliser.^[26] This methodology is known as the polyol synthetic method and it was first developed by Fièvet *et al.* in 1989.^[27] Moreover, glycerol has the ability to immobilise MNPs, favouring the recycling of the catalytic phase by simple liquid-liquid extraction of the organic products and preserving the reactivity for the next runs. The supramolecular network of glycerol might be the responsible of such good immobilisation of the nanocatalysts, making easier the dispersion of nanoparticles and consequently avoiding their agglomeration, in contrast to the most part of common organic solvents. However neat glycerol cannot avoid the MNPs agglomeration.^[28]



Scheme 1.3 Bottom-up synthetic approach for the preparation of MNPs.

In relation to the applications in synthesis, glycerol has been used as solvent in many organic transformations since the middle of the last century.^[29] Nevertheless, it has not been considered as a green solvent until 2006, when Wolfson *et al.*^[30] reported the first examples using glycerol as solvent in Pd-catalysed Heck and Suzuki cross-couplings reactions. Since then, the number of publications reporting the benefits of the use of glycerol as solvent in chemical transformations including catalytic processes, has increased considerably.

Concerning the reports on non-catalysed reactions in glycerol medium, it is remarkable the pioneering contribution of Jérôme *et al.*^[31], in which they clearly demonstrated the advantages of glycerol over other conventional solvents, including water. Glycerol was found to be highly efficient in some organic transformations such as the aza-Michael reaction of amines and anilines, the Michael reaction of indoles or the ring-opening of styrene oxide with *p*-anisidine. After this contribution, the number of works using glycerol as solvent in non-catalysed reactions increased. For instance, Gu *et al.*^[32] showed that glycerol is an excellent solvent to carry out condensations of aldehydes with indoles and 1,3-cyclohexadiones, in the absence of any acid catalyst. Bhosale *et al.*^[33] reported the preparation of 5-substituted 1*H*-tetrazoles in glycerol medium under catalyst-free conditions using aryl nitriles, benzyl nitriles and also sterically hindered nitriles in combination with sodium azide. It should be also highlighted the work of Safaei and Shekouhy *et al.*^[34] in which they developed a one-pot chemoselective procedure for the synthesis of 4*H*-pyrans (Scheme 1.4).

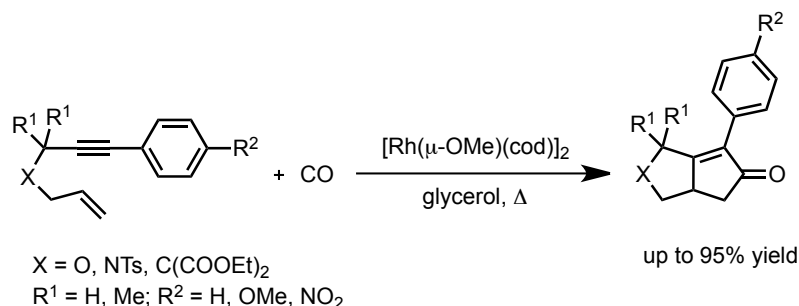


Scheme 1.4 Non-catalysed one-pot three-component synthesis of 4*H*-pyran derivatives in glycerol.^[34]

It has been speculated that glycerol facilitates these non-catalysed organic transformations due to its interaction by hydrogen bonding with the reactants, thus stabilising the corresponding transition states and intermediates.^[34] Concerning this last example, the authors proposed that in the first step of this reaction the OH groups of glycerol promote the formation of an *E*-olefin between the aldehyde and malononitrile.

The development of metallic catalytic systems in glycerol is one of the topics of research in our group.^[13c] We have contributed to the development of metallic homogeneous catalytic systems as well as the immobilisation of metal nanoparticles for catalysis in neat glycerol. Concerning the homogeneous systems, we have demonstrated the important role of glycerol in the Rh-catalysed Pauson–Khand carbocyclisation (Scheme 1.5).^[35] Although, as mentioned before, the potential reactivity and coordination ability of the hydroxyl groups in glycerol could be a limitation in catalysis, because of the formation of side products or the competition to

coordinate to metal centres, in that case it became the key of the success of the reaction. $[\text{Rh}(\mu\text{-OMe})(\text{cod})]_2$ catalysed the formation of bicyclo[3.3.0]octenones thanks to the coordinative behaviour of glycerol which stabilises the intermediates during the catalytic process.



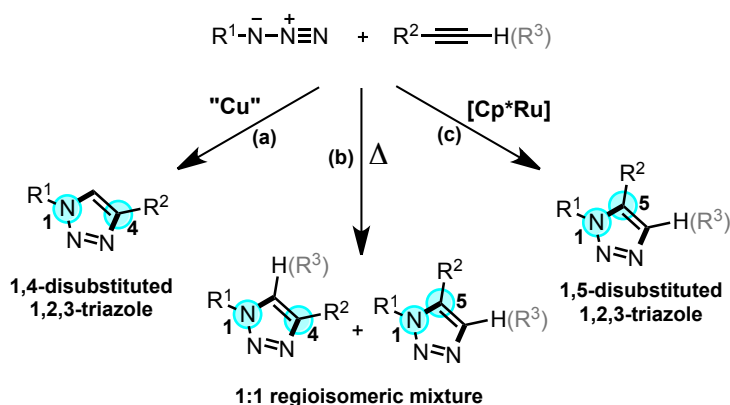
Scheme 1.5 Rh-catalysed Pauson-Khand carbocyclisations in neat glycerol.

Regarding the immobilisation of metal nanoparticles, we have reported the synthesis of well-defined copper(I) oxide nanoparticles (Cu_2ONPs)^[36] coated by poly(vinylpyrrolidone) (PVP) in glycerol for applications in different catalytic transformations such as C–heteroatom bond formation processes, 1,3-dipolar azide–alkyne cycloadditions and also tandem processes involving these two transformations. Concerning the 1,3-dipolar azide–alkyne cycloaddition, it should be pointed out that, despite the tremendous importance of this transformation, which transcends the chemistry community,^[37] it has not been deeply investigated in glycerol medium. This topic, which will be the subject of chapters 2 and 3 of the present Thesis, is analysed in section 1.2.

Moreover, our research group has described the synthesis and catalytic applications of palladium nanoparticles (PdNPs) using 3,3',3''-phosphanetriyltris(benzenesulfonic acid) trisodium salt (TPPTS),^[28, 38] 1,3,5-triaza-7-phosphaadamantane (PTA) derivatives^[39] and cinchona-based ligands as stabilisers.^[40] Glycerol-soluble derivatives are fundamental for developing catalytic systems in glycerol medium because they can serve as NPs stabilisers, ligands for organometallic complexes or as organocatalysts. Focusing our attention on the hydrosoluble phosphine PTA, this topic will be introduced and deeply explained in the section 1.3 of this chapter and in the chapter 4 of this Thesis.

1.2 The azide–alkyne cycloaddition reaction

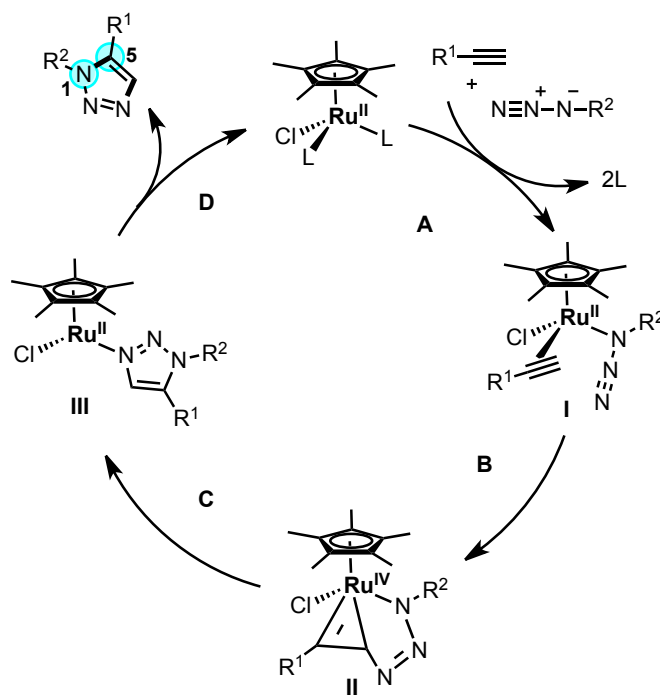
In 1893, Michael *et al.*^[41] reported the first example of a 1,3-dipolar cycloaddition reaction between phenyl azide and diethyl acetylenedicarboxylate. However, this publication did not attract the interest of the scientific community until approximately 70 years later, when Huisgen *et al.*^[42] deeply examined this class of reactions. The also called Huisgen 1,3-dipolar cycloaddition of organic azides and alkynes is a slow process, which requires high temperatures (Scheme 1.6b). Furthermore, it is not regioselective, leading to a mixture of both 1,4- and 1,5-disubstituted 1,2,3-triazoles. Although L'abbé first observed a copper-catalysed version of the 1,3-dipolar cycloaddition (CuAAC) in 1984,^[43] the importance of this discovery was not highlighted until 2002 when Medal *et al.*^[44] and Fokin and Sharpless *et al.*,^[45] independently, reported that Cu(I) species as catalysts are able to accelerate the process and make it fully regioselective, leading exclusively to 1,4-disubstituted 1,2,3-triazoles (Scheme 1.6a). Since then, the CuAAC has been widely applied due to the experimental simplicity, its robustness and the high yields obtained, being classified as the “click” reaction^[46] *par excellence*.^[47] On the other hand, years later, Fokin and Jia *et al.*^[48] developed the selective access to the complementary regioisomer (Scheme 1.6c). They reported that the use of [Cp*Ru] complexes as catalysts in the 1,3-dipolar cycloaddition (RuAAC) of organic azides and alkynes provided 1,5-disubstituted 1,2,3-triazoles in a regioselective manner.



Scheme 1.6 1,3-Dipolar cycloaddition reaction of organic azides and alkynes; a) Thermal AAC; b) CuAAC; c) RuAAC.

The RuAAC using [Cp*Ru] complexes as catalysts can also be applied to internal alkynes, in contrast to CuAAC which is generally applied with terminal alkynes, and this fact supports the different mechanistic pathway in comparison with CuAAC (detailed in Chapter 3). Based on DFT calculations,^[48c, 49] the proposed mechanism for RuAAC using [Cp*Ru] complexes (Scheme 1.7)

starts by the displacement of the spectator ligands on the initial Ru(II) complex (step A), leading to the intermediate I. At this point, a regioselective oxidative coupling between the terminal nitrogen on the azide and the alkyne (step B) to form a ruthenacycle intermediate II. Step C consists on a reductive elimination to afford the triazole ring (intermediate III), followed by the realising of the 1,5-regioisomer in step D. The π -coordination of the alkyne to the Ru centre (intermediate I) and the formation of the ruthenacycle (intermediate II) are the key points to explain why the RuAAC using $[\text{Cp}^*\text{Ru}]$ complexes leads to the 1,5-disubstituted 1,2,3-triazole and also to fully substituted triazoles, in contrast to CuAAC. In the case of the Cu-catalysed reaction, not only monometallic pathways have been proposed and it is generally limited to terminal alkynes (see Chapter 3). In spite of the potential of 1,5-isomers in several fields of medicinal chemistry and biochemistry, this RuAAC has not been as developed as the CuAAC due mainly to the higher cost of the catalysts and the harsher reaction conditions compared to Cu.^[50] It is important to note that using other Ru complexes as catalysts,^[51] the 1,4-regioisomer can also be obtained, as in the case of CuAAC.



Scheme 1.7 Proposed catalytic mechanism for RuAAC using $[\text{Cp}^*\text{Ru}]$ complexes providing the 1,5-disubstituted 1,2,3-triazoles.^[48c]

Apart from our contribution on this subject using Cu_2ONPs stabilised in glycerol, mentioned in the previous section, there is only one report published by García-Álvarez *et al.*^[52] concerning the CuAAC in this medium, in which they described an efficient simple CuI /glycerol catalytic

system for the preparation of 1,4-disubstituted 1,2,3-triazoles at room temperature (see Scheme 3.5 in Chapter 3).

1.3 Glycerol-soluble derivatives for the development of new catalytic systems.

Phosphines have been widely used in homogeneous catalysis as both ligands in organometallic catalysis^[53] and organocatalysts.^[54] In the context of the replacement of common organic solvents by others more environmental friendly solvents, the development of catalytic procedures in water medium has been one of the most studied areas. In this sense, varieties of water-soluble phosphines have appeared through the years,^[55] (see Figure 1.1 for some examples) and among them 1,3,5-triaza-7-phosphadamantane (PTA) and its derivatives (see Figure 1.2).^[56]

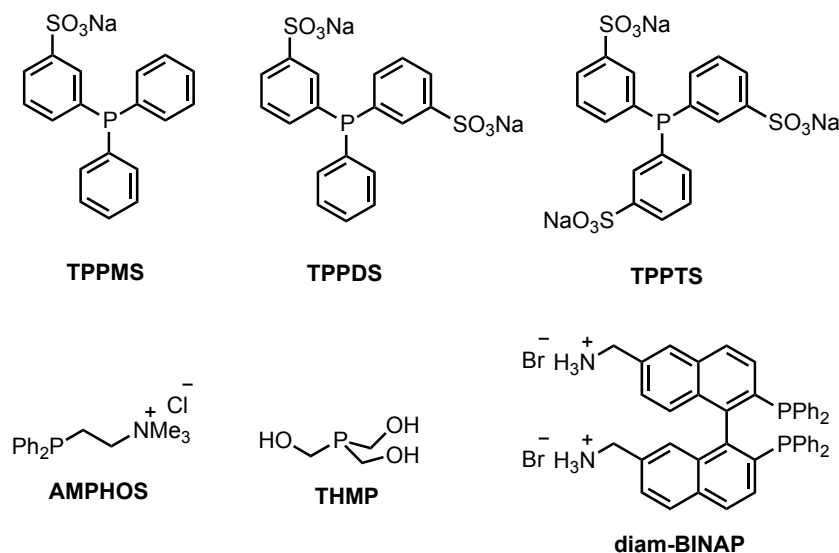


Figure 1.1 Water-soluble phosphines.

PTA has been functionalised in different ways to obtain several hydrosoluble PTA derivatives; some of them are collected in Figure 1.2. The PTA cage has been *N*-functionalised leading to *N*-monoalkylated quaternary ammonium salts (**PTAR**),^[39, 57] ring-opened dimethylated PTA (**dmoPTA**)^[58] or ring-opened diacetylated PTA (**DAPTA**).^[59] The functionalisation on the methylene position close to phosphorus atom has also led to other hydrosoluble PTA derivatives like phosphino alcohols such as **PTA-CRR'OH**^[60] or **PTA-CH(1-Melm)OH**,^[61] diphosphine derivatives such as **PTAPⁱPr**^[62] and aminophosphines such as **PTA-CRR'NHPh**.^[63]

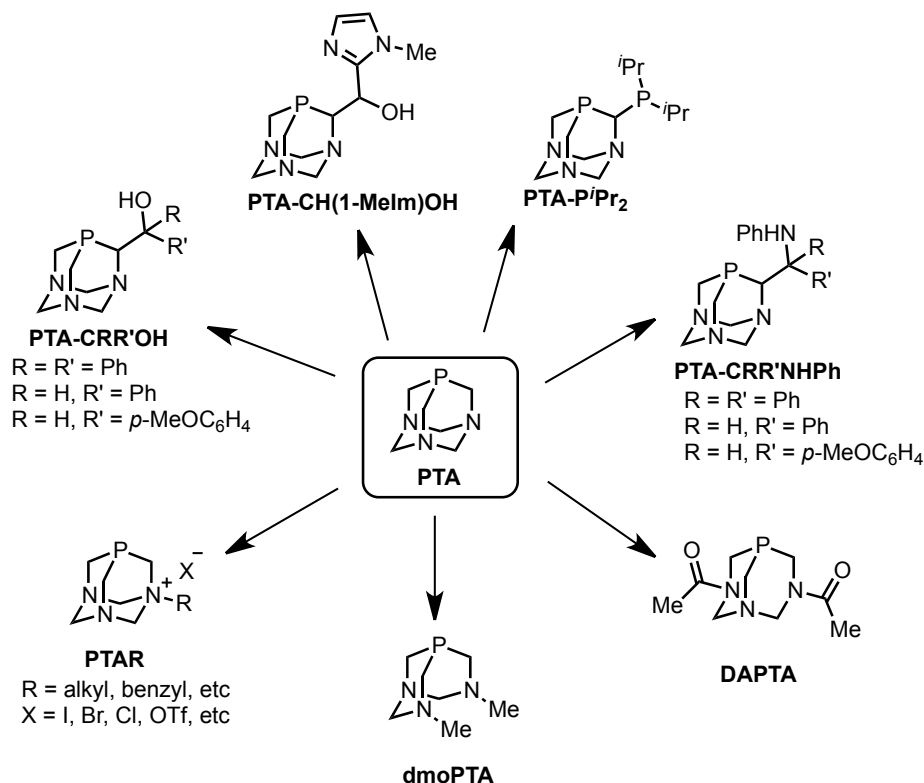
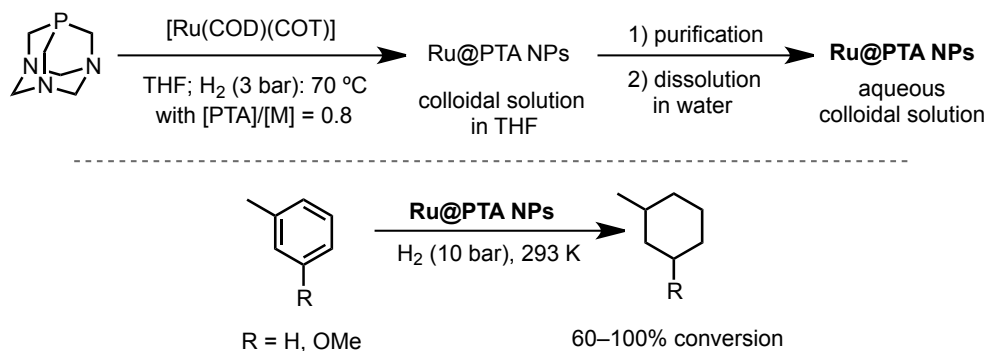


Figure 1.2 PTA and some selected hydrosoluble PTA derivatives.

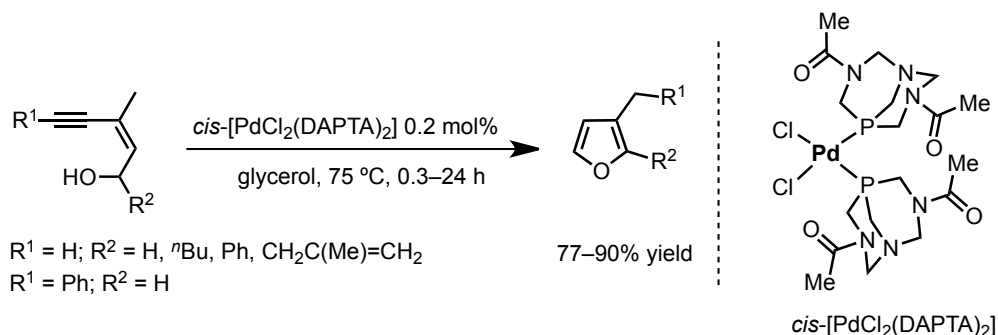
These PTA derivatives have been served mainly as ligands for organometallic complexes applied in homogeneous aqueous catalysis.^[56] Some of these organometallic complexes and their applications will be show in chapter 4. Few reports are dedicated to their use as stabiliser for MNPs (Ru, Pt, Pd or Ag) in water (Scheme 1.8).^[64]



Scheme 1.8 RuNPs stabilised by PTA reported by Philippot *et al.*^[64a, 64b]: synthesis of RuNPs (top) and their applications in hydrogenation of arenes (bottom)

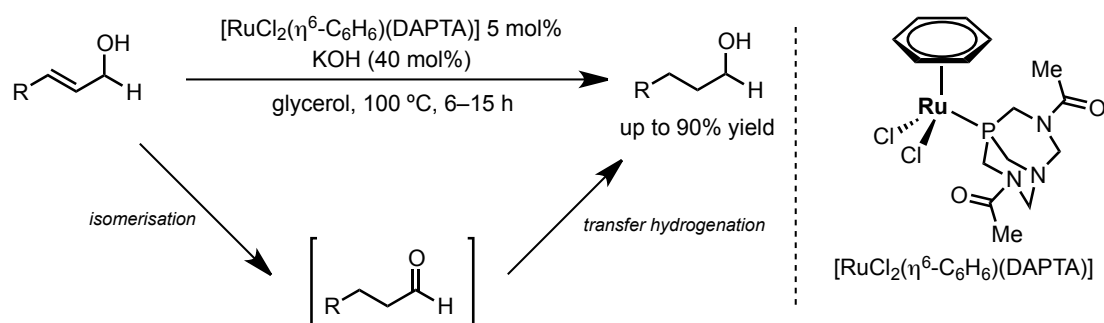
Following our aim of developing catalytic systems in glycerol and due to the similarity, in terms of polarity, between glycerol and water, all these hydrosoluble PTA derivatives could potentially serve as ligands for transition metal complexes, as stabilisers for MNPs or as catalysts by itself also in glycerol. Actually, although they have not been widely applied to develop

catalytic systems in this medium, few works have demonstrated that these PTA derivatives serve to this purpose. Cadierno *et al.* used glycerol as solvent in the Pd-catalysed intramolecular cycloisomerisation of (*Z*)-enynols using Pd complexes [PdCl₂L₂] containing PTA as ligand as catalytic precursors (Scheme 1.9).^[65]



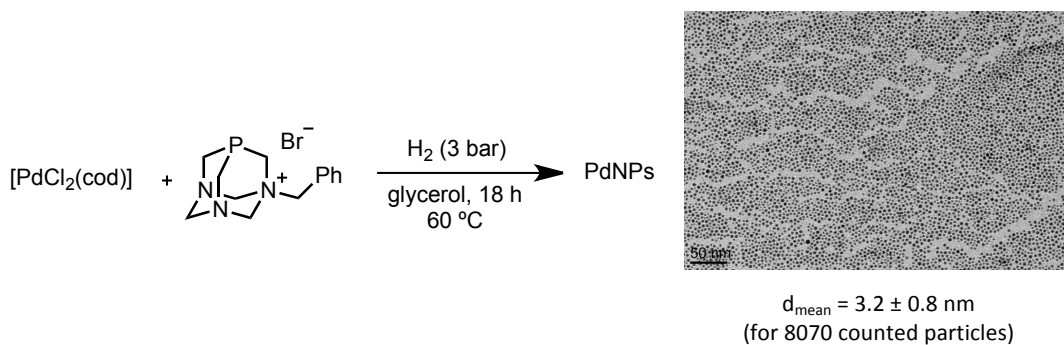
Scheme 1.9 Pd-catalysed intramolecular cycloisomerisation of (*Z*)-enynols using a Pd complex reported by Cadierno *et al.*^[65]

The same group also reported the use of glycerol as solvent and hydrogen donor in the reduction of allylic alcohols with Ru-based complexes containing PTA ligands (Scheme 1.10).^[66]



Scheme 1.10 Ru-catalysed reduction of allylic alcohols in glycerol reported by Crochet and Cadierno *et al.*^[66]

Our group has also contributed to this aim using the *N*-monoalkylated ammonium salts (**PTAR**) (see above Figure 1.2) as stabilisers for the preparation of PdNPs in glycerol (Scheme 1.11).^[39] The catalytic system was active in cross-couplings, hydrogenations and one-pot sequential processes, and the corresponding catalytic phase could be recycled thanks to the efficient catalyst immobilisation.



Scheme 1.11 Synthesis of PdNPs using PTA derivatives as stabilisers (left) and the TEM image of the PdNPs in glycerol (right), reported by our group.^[39]

On the bases of this literature overview we will next develop the different objectives of this thesis in the following three chapters.

1.4 References

- [1] E. F. Aransiola, T. V. Ojumu, O. O. Oyekola, T. F. Madzimbamuto, D. I. O. Ikhu-Omoregbe, *Biomass Bioenergy* **2014**, *61*, 276–297.
- [2] (a) S. Al-Zuhair, *Biofuels, Bioprod. Biorefin.* **2007**, *1*, 57–66; (b) S. Marx, *Fuel Process. Technol.* **2016**, *151*, 139–147.
- [3] J. M. Marchetti, V. U. Miguel, A. F. Errazu, *Renewable and Sustainable Energy Rev.* **2007**, *11*, 1300–1311.
- [4] M. Anitha, S. K. Kamarudin, N. T. Kofli, *Chem. Eng. J.* **2016**, *295*, 119–130.
- [5] C. A. G. Quispe, C. J. R. Coronado, J. A. Carvalho Jr, *Renewable and Sustainable Energy Rev.* **2013**, *27*, 475–493.
- [6] F. Yang, M. A. Hanna, R. Sun, *Biotechnol. for Biofuels* **2012**, *5*, 13.
- [7] W. N. R. Wan Isahak, Z. A. Che Ramli, M. Ismail, J. Mohd Jahim, M. A. Yarmo, *Sep. Purif. Rev.* **2015**, *44*, 250–267.
- [8] M. Pagliaro, M. Rossi, in *The Future of Glycerol (2)*, The Royal Society of Chemistry, **2010**, pp. 1–28.
- [9] http://cordis.europa.eu/project/rcn/110949_en.html
- [10] (a) M. Pagliaro, R. Ciriminna, H. Kimura, M. Rossi, C. Della Pina, *Angew. Chem. Int. Ed.* **2007**, *46*, 4434–4440; (b) A. Corma, S. Iborra, A. Velty, *Chem. Rev.* **2007**, *107*, 2411–2502; (c) C.-H. (Clayton) Zhou, J. N. Beltramini, Y.-X. Fan, G. Q. (Max) Lu, *Chem. Soc. Rev.* **2008**, *37*, 527–549; (d) Y. Zheng, X. Chen, Y. Shen, *Chem. Rev.* **2008**, *108*, 5253–5277; (e) B. Katryniok, H. Kimura, E. Skrzyńska, J.-S. Girardon, P. Fongarland, M. Capron, R. Ducoulombier, N. Mimura, S. Paul, F. Dumeignil, *Green Chem.* **2011**, *13*, 1960–1979.
- [11] (a) P. T. Anastas, J. C. Warner, *Green Chemistry: Theory and Practice*, Oxford University Press, New York, **1998**; (b) P. Anastas, N. Eghbali, *Chem. Soc. Rev.* **2010**, *39*, 301–312.
- [12] Y. Gu, F. Jérôme, *Chem. Soc. Rev.* **2013**, *42*, 9550–9570.
- [13] (a) Y. Gu, F. Jérôme, *Green Chem.* **2010**, *12*, 1127–1138; (b) A. Díaz-Álvarez, V. Cadierno, *Appl. Sci.* **2013**, *3*, 55–69; (c) F. Chahdoura, I. Favier, M. Gómez, *Chem. Eur. J.* **2014**, *20*, 10884–10893; (d) S. Tagliapietra, L. Orto, G. Palmisano, A. Penoni, G. Cravotto, *Chem. Pap.* **2015**, *69*, 1519–1531.
- [14] (a) A. E. Díaz-Álvarez, J. Francos, B. Lastra-Barreira, P. Crochet, V. Cadierno, *Chem. Commun.* **2011**, *47*, 6208–6227; (b) A. Wolfson, A. Snezhko, T. Meyouhas, D. Tavor, *Green Chem. Lett. Rev.* **2012**, *5*, 7–12; (c) J. I. García, H. García-Marín, E. Pires, *Green Chem.* **2014**, *16*, 1007–1033.
- [15] S. Aparicio, R. Alcalde, *Green Chem.* **2009**, *11*, 65–78.
- [16] V. Pace, P. Hoyos, L. Castoldi, P. Domínguez de María, A. R. Alcántara, *ChemSusChem* **2012**, *5*, 1369–1379.
- [17] (a) Q. Zhang, K. De Oliveira Vigier, S. Royer, F. Jérôme, *Chem. Soc. Rev.* **2012**, *41*, 7108–7146; (b) J. García-Álvarez, *Eur. J. Inorg. Chem.* **2015**, 5147–5157; (c) S. Khandelwal, Y. K. Tailor, M. Kumar, *J. Mol. Liq.* **2016**, *215*, 345–386; (d) D. A. Alonso, A. Baeza, R. Chinchilla, G. Guillena, I. M. Pastor, D. J. Ramón, *Eur. J. Org. Chem.* **2016**, 612–632.

- [18] (a) A. P. Abbott, R. C. Harris, K. S. Ryder, C. D'Agostino, L. F. Gladden, M. D. Mantle, *Green Chem.* **2011**, *13*, 82–90; (b) C. Vidal, J. García-Álvarez, A. Hernán-Gómez, A. R. Kennedy, E. Hevia, *Angew. Chem. Int. Ed.* **2016**, DOI: 10.1002/anie.201609929.
- [19] S. Carda-Broch, A. Berthod, D. W. Armstrong, *Anal. Bioanal. Chem.* **2003**, *375*, 191–199.
- [20] A. C. Venter, WO 2012176151 A1, **2012**.
- [21] T. Kusukawa, G. Niwa, T. Sasaki, R. Oosawa, W. Himeno, M. Kato, *Bull. Chem. Soc. Jpn.* **2013**, *86*, 351–353.
- [22] P. Cintas, S. Tagliapietra, E. Calcio Gaudino, G. Palmisano, G. Cravotto, *Green Chem.* **2014**, *16*, 1056–1065.
- [23] (a) D. M. P. Mingos, D. R. Baghurst, *Chem. Soc. Rev.* **1991**, *20*, 1–47; (b) C. Gabriel, S. Gabriel, E. H. Grant, B. S. J. Halstead, D. M. P. Mingos, *Chem. Soc. Rev.* **1998**, *27*, 213–224; (c) M. D. P. Mingos, *Microwave-Assisted Organic Synthesis* (Eds.: P. Lidström, J. P. Tierney), Blackwell, Oxford, **2005**.
- [24] (a) K. Philippot, B. Chaudret, *C. R. Chimie* **2003**, *6*, 1019–1034; (b) C. Amiens, D. Ciuculescu-Pradines, K. Philippot, *Coord. Chem. Rev.* **2016**, *308*, 409–432.
- [25] (a) A. Roucoux, J. Schulz, H. Patin, *Chem. Rev.* **2002**, *102*, 3757–3778; (b) B. Chaudret, *C. R. Physique* **2005**, *6*, 117–131; (c) N. Semagina, L. Kiwi-Minsker, *Catal. Rev. Sci. Eng.* **2009**, *51*, 147–217.
- [26] (a) T.-H. Tran, T.-D. Nguyen, *Colloids Surf. B* **2011**, *88*, 1–22; (b) A. J. Bicchì, R. E. Schaak, *ACS Nano* **2011**, *5*, 8089–8099; (c) H. Dong, Y.-C. Chen, C. Feldmann, *Green Chem.* **2015**, *17*, 4107–4132.
- [27] F. Fievet, J. P. Lagier, B. Blin, B. Beaudoin, M. Figlarz, *Solid State Ionics* **1989**, *32*, 198–205.
- [28] F. Chahdoura, C. Pradel, M. Gómez, *Adv. Synth. Catal.* **2013**, *355*, 3648–3660.
- [29] L. W. Clark, *J. Am. Chem. Soc.* **1955**, *77*, 6191–6192.
- [30] (a) A. Wolfson, C. Dlugy, D. Tavor, J. Blumenfeld, Y. Shotland, *Tetrahedron: Asymmetry* **2006**, *17*, 2043–2045; (b) A. Wolfson, C. Dlugy, *Chem. Pap.* **2007**, *61*, 228–232; (c) A. Wolfson, C. Dlugy, Y. Shotland, *Environ. Chem. Lett.* **2007**, *5*, 67–71.
- [31] Y. Gu, J. Barrault, F. Jérôme, *Adv. Synth. Catal.* **2008**, *350*, 2007–2012.
- [32] F. He, P. Li, Y. Gu, G. Li, *Green Chem.* **2009**, *11*, 1767–1773.
- [33] K. P. Nandre, J. K. Salunke, J. P. Nandre, V. S. Patil, A. U. Borse, S. V. Bhosale, *Chin. Chem. Lett.* **2012**, *23*, 161–164.
- [34] H. R. Safaei, M. Shekouhy, S. Rahmanpur, A. Shirinfeshan, *Green Chem.* **2012**, *14*, 1696–1704.
- [35] F. Chahdoura, L. Dubrulle, K. Fourmy, J. Durand, D. Madec, M. Gómez, *Eur. J. Inorg. Chem.* **2013**, 5138–5144.
- [36] F. Chahdoura, C. Pradel, M. Gómez, *ChemCatChem* **2014**, *6*, 2929–2936.
- [37] (a) L. Liang, D. Astruc, *Coord. Chem. Rev.* **2011**, *255*, 2933–2945; (b) S. Díez-González, *Catal. Sci. Technol.* **2011**, *1*, 166–178; (c) E. Haldón, M. C. Nicasio, P. J. Pérez, *Org. Biomol. Chem.* **2015**, *13*, 9528–9550; (d) M. S. Singh, S. Chowdhury, S. Koley, *Tetrahedron* **2016**, *72*, 5257–5283.
- [38] F. Chahdoura, S. Mallet-Ladeira, M. Gómez, *Org. Chem. Front.* **2015**, *2*, 312–318.
- [39] F. Chahdoura, I. Favier, C. Pradel, S. Mallet-Ladeira, M. Gómez, *Catal. Commun.* **2015**, *63*, 47–51.
- [40] A. Reina, C. Pradel, E. Martin, E. Teuma, M. Gómez, *RSC Adv.* **2016**, *6*, 93205–93216.
- [41] A. Michael, *J. Prakt. Chem.* **1893**, *48*, 94–95.
- [42] (a) R. Huisgen, *Angew. Chem. Int. Ed., Engl.* **1963**, *2*, 565–598; (b) R. Huisgen, *Angew. Chem. Int. Ed., Engl.* **1963**, *2*, 633–696.
- [43] G. L'Abbé, *Bull. Soc. Chim. Belg.* **1984**, *93*, 579–592.
- [44] C. W. Tornøe, C. Christensen, M. Meldal, *J. Org. Chem.* **2002**, *67*, 3057–3064.
- [45] V. V. Rostovtsev, L. G. Green, V. V. Fokin, K. B. Sharpless, *Angew. Chem. Int. Ed.* **2002**, *41*, 2596–2599.
- [46] A "click" reaction should be modular, wide in scope, it should give very high yields, it should produce no or inoffensive byproducts and it has to be stereospecific.
- [47] H. C. Kolb, M. G. Finn, K. B. Sharpless, *Angew. Chem. Int. Ed.* **2001**, *40*, 2004–2021.
- [48] (a) L. Zhang, X. Chen, P. Xue, H. H. Y. Sun, I. D. Williams, K. B. Sharpless, V. V. Fokin, G. Jia, *J. Am. Chem. Soc.* **2005**, *127*, 15998–15999; (b) L. K. Rasmussen, B. C. Boren, V. V. Fokin, *Org. Lett.* **2007**, *9*, 5337–5339; (c) B. C. Boren, S. Narayan, L. K. Rasmussen, L. Zhang, H. Zhao, Z. Lin, G. Jia, V. V. Fokin, *J. Am. Chem. Soc.* **2008**, *130*, 8923–8930.
- [49] E. Boz, N. Ş. Tüzün, *J. Organomet. Chem.* **2013**, *724*, 167–176.
- [50] J. R. Johansson, T. Beke-Somfai, A. Said Stålsmeden, N. Kann, *Chem. Rev.* **2016**, *116*, 14726–14768.
- [51] (a) P. N. Liu, J. Li, F. H. Su, K. D. Ju, L. Zhang, C. Shi, H. H. Y. Sung, I. D. Williams, V. V. Fokin, Z. Lin, G. Jia, *Organometallics* **2012**, *31*, 4904–4915; (b) P. N. Liu, H. X. Siyang, L. Zhang, S. K. S. Tse, G. Jia, *J. Org. Chem.* **2012**, *77*, 5844–5849.
- [52] C. Vidal, J. García-Álvarez, *Green Chem.* **2014**, *16*, 3515–3521.

- [53] S. Lühr, J. Holz, A. Börner, *ChemCatChem* **2011**, *3*, 1708–1730.
- [54] (a) C. Gomez, J.-F. Betzer, A. Voituriez, A. Marinetti, *ChemCatChem* **2013**, *5*, 1055–1065; (b) Y. Xiao, Z. Sun, H. Guo, O. Kwon, *Beilstein J. Org. Chem.* **2014**, *10*, 2089–2121.
- [55] (a) N. Pinault, D. W. Bruce, *Coord. Chem. Rev.* **2003**, *241*, 1–25; (b) K. H. Shaughnessy, *Chem. Rev.* **2009**, *109*, 643–710; (c) B. R. James, F. Lorenzini, *Coord. Chem. Rev.* **2010**, *254*, 420–430.
- [56] (a) A. D. Phillips, L. Gonsalvi, A. Romerosa, F. Vizza, M. Peruzzini, *Coord. Chem. Rev.* **2004**, *248*, 955–993; (b) J. Bravo, S. Bolaño, L. Gonsalvi, M. Peruzzini, *Coord. Chem. Rev.* **2010**, *254*, 555–607; (c) L. Gonsalvi, M. Peruzzini, in *Phosphorus Compounds: Advanced Tools in Catalysis and Material Sciences* (Eds.: M. Peruzzini, L. Gonsalvi), Springer Netherlands, Dordrecht, **2011**, pp. 183–212; (d) L. Gonsalvi, A. Guerriero, F. Hapiot, D. A. Krogstad, E. Monflier, G. Reginato, M. Peruzzini, *Pure Appl. Chem.* **2013**, *85*, 385–396.
- [57] (a) D. J. Daigle, A. B. Pepperman, S. L. Vail, *J. Heterocycl. Chem.* **1974**, *11*, 407–408; (b) S. Schäfer, W. Frey, A. S. K. Hashmi, V. Cmrecki, A. Luquin, M. Laguna, *Polyhedron* **2010**, *29*, 1925–1932.
- [58] (a) A. Mena-Cruz, P. Lorenzo-Luis, A. Romerosa, M. Saoud, M. Serrano-Ruiz, *Inorg. Chem.* **2007**, *46*, 6120–6128; (b) A. Mena-Cruz, P. Lorenzo-Luis, A. Romerosa, M. Serrano-Ruiz, *Inorg. Chem.* **2008**, *47*, 2246–2248.
- [59] D. J. Darensbourg, C. G. Ortiz, J. W. Kamplain, *Organometallics* **2004**, *23*, 1747–1754.
- [60] (a) G. W. Wong, W.-C. Lee, B. J. Frost, *Inorg. Chem.* **2008**, *47*, 612–620; (b) M. Erlandsson, L. Gonsalvi, A. Ienco, M. Peruzzini, *Inorg. Chem.* **2008**, *47*, 8–10.
- [61] D. A. Krogstad, A. Guerriero, A. Ienco, G. Manca, M. Peruzzini, G. Reginato, L. Gonsalvi, *Organometallics* **2011**, *30*, 6292–6302.
- [62] J. M. Sears, W.-C. Lee, B. J. Frost, *Inorg. Chim. Acta* **2015**, *431*, 248–257.
- [63] W.-C. Lee, J. M. Sears, R. A. Enow, K. Eads, D. A. Krogstad, B. J. Frost, *Inorg. Chem.* **2013**, *52*, 1737–1746.
- [64] (a) P.-J. Debouttière, V. Martinez, K. Philippot, B. Chaudret, *Dalton Trans.* **2009**, 10172–10174; (b) P.-J. Debouttière, Y. Coppel, A. Denicourt-Nowicki, A. Roucoux, B. Chaudret, K. Philippot, *Eur. J. Inorg. Chem.* **2012**, 1229–1236; (c) T. Gutmann, E. Bonnefille, H. Breitzke, P.-J. Debouttière, K. Philippot, R. Poteau, G. Buntkowsky, B. Chaudret, *Phys. Chem. Chem. Phys.* **2013**, *15*, 17383–17394; (d) M. Caporali, A. Guerriero, A. Ienco, S. Caporali, M. Peruzzini, L. Gonsalvi, *ChemCatChem* **2013**, *5*, 2517–2526; (e) T. J. Sherbow, E. L. Downs, R. I. Sayler, J. J. Razink, J. J. Juliette, D. R. Tyler, *ACS Catal.* **2014**, *4*, 3096–3104.
- [65] J. Francos, V. Cadierno, *Green Chem.* **2010**, *12*, 1552–1555.
- [66] A. E. Díaz-Álvarez, P. Crochet, V. Cadierno, *Catal. Commun.* **2011**, *13*, 91–96.

Chapter 2

Metal-Free Intermolecular Azide–Alkyne Cycloaddition Promoted by Glycerol

Chapter 2. Metal-Free Intermolecular Azide–Alkyne Cycloaddition Promoted by Glycerol

2.1 Introduction

Although the 1,2,3-triazole motif is not present in natural compounds, the “amide-triazole bioequivalence” of these heterocycles has been used for the synthesis of important bioactive molecules because of their physicochemical properties (peptide isosteres), in addition to their remarkable metabolic stability. In particular, the bioactivity depends, in a lot of cases, on the substituents on 1,4,5-site positions (Figure 2.1). These types of molecules act as anti-influenza agents (influenza is a respiratory disease), cannabinoid receptor antagonists (applied for treatments of obesity and drug addiction), Hsp90 inhibitors (anticancer agents), metabotropic glutamate receptor type 1 (mGluR1) antagonists (applied for treatment of psychotic disorders) and PET-based ligands (PET = Positron Emission Tomography) for imaging mGluR1 (in order to study the role of mGluR1 in the brain).^[1]

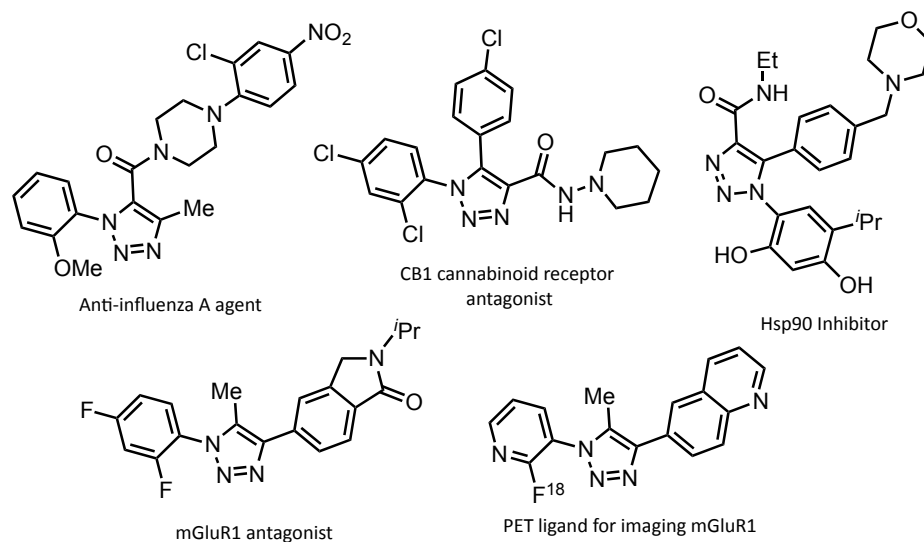
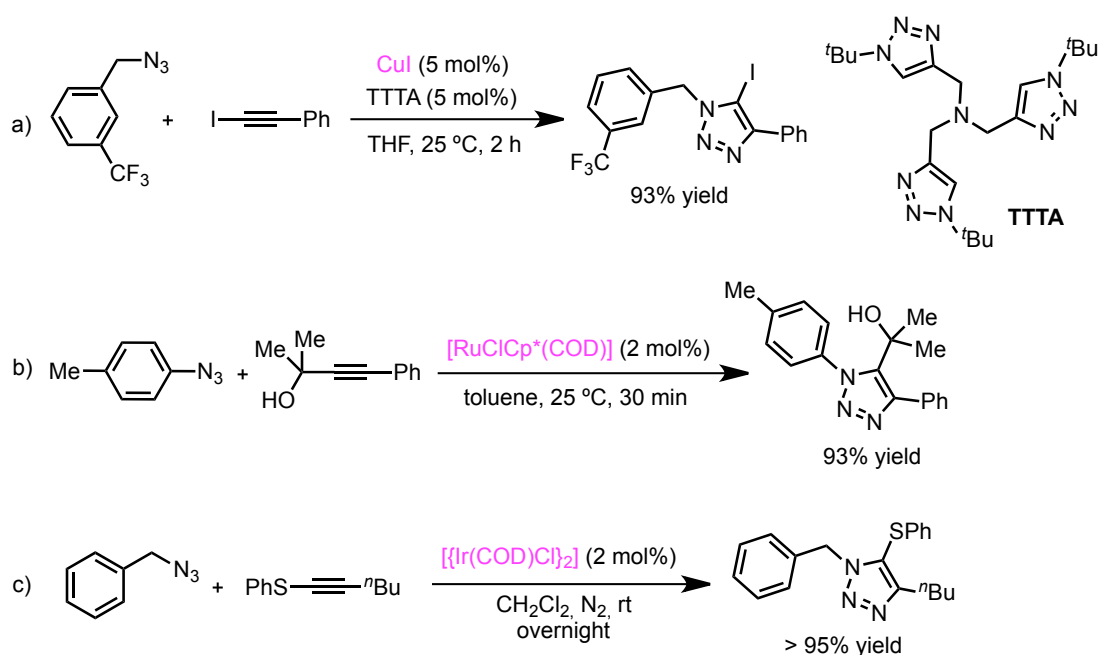


Figure 2.1 Biologically relevant fully substituted 1,2,3-triazoles.

The preparation of 1,4-disubstituted 1,2,3-triazoles have been widely investigated since 2002, when Meldal *et al.* and Fokin and Sharpless *et al.* independently established that the use of Cu(I) species as catalysts leads to fast, highly efficient and regioselective cycloadditions from the corresponding terminal alkynes and organic azides.^[2] On the contrary, the synthesis of fully substituted triazoles using internal alkynes remains as a challenge that it has been taken up by the scientific community. Several metal-catalysed processes have been studied pursuing this objective. A remarkably solution was reported by Hein and Fokin *et al.* who prepared 5-iodo-

1,2,3-triazoles from readily accessible 1-iodoalkynes using Cu(I) salts as catalytic precursors (Scheme 2.1a).^[3] The triazoles obtained were amenable to further functionalisation through a Pd-catalysed Suzuki-Miyaura cross-coupling reaction with arylboronic acids.^[4] Lin, Jia and Fokin *et al.* showed an alternative way to afford fully substituted triazoles using Ru complexes as catalysts, such as $[\text{RuClCp}^*(\text{PPh}_3)_2]$ and $[\text{RuClCp}^*(\text{COD})]$ (Scheme 2.1b).^[5] Good regioselectivities were achieved only with alkynes containing a hydrogen bond donor group, such as propargylic alcohols and amines, or those alkynes electronically biased. Jia and Sun *et al.* reported for the first time an efficient Ir-catalysed intermolecular azide-alkyne cycloaddition (AAC) of internal acetylenic thioethers (Scheme 2.1c).^[6]

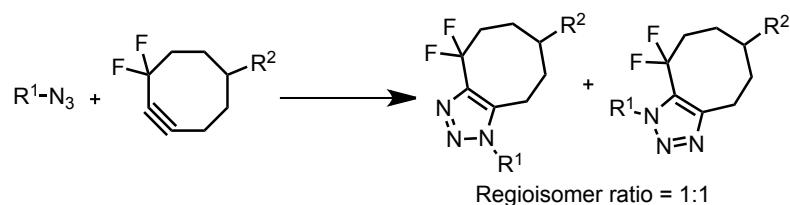


Scheme 2.1 Metal-catalysed intermolecular AAC with internal alkynes.

It should be also noted that the metal-catalysed direct arylation of 1,4-disubstituted 1,2,3-triazoles is also an important method for the synthesis of fully substituted triazoles.^[7] Several approaches have been reported in the literature using aryl halides and Pd^[8] or Cu^[9] catalysts.

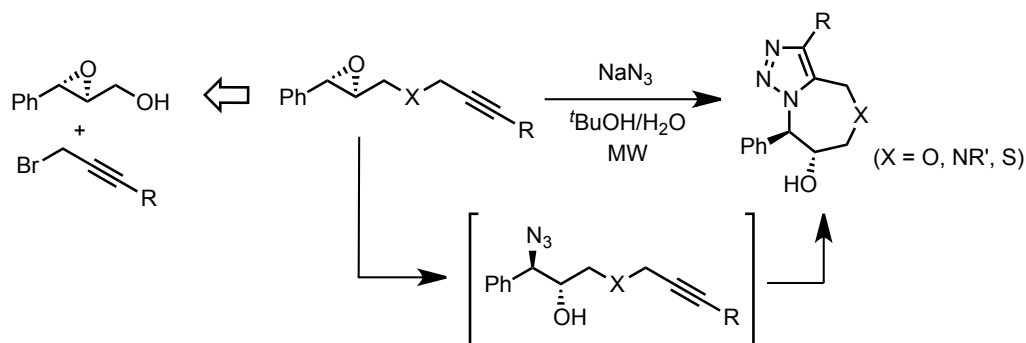
However, in some particular cases, the use of transition-metal catalysts can generate problems. Therefore, copper, despite of being an essential metal required by living cells, can become highly toxic and induce changes in cellular metabolism beyond certain concentrations.^[10] For this reason, the development of metal-free procedures to generate fully substituted triazoles from azides and internal alkynes is an interesting target for many research groups.^[10b]

The use of internal alkynes to obtain 1,4,5-trisubstituted 1,2,3-triazoles requires harsh conditions and activated alkynes that contain electron-withdrawing substituents in order to favour the intermolecular process.^[11] The strategy reported by Bertozzi has supposed an important progress in this field:^[12] the use of the ring strain as an alternative to the use of electron-poor alkynes, a concept that was firstly introduced by Witting and Krebs in 1961.^[13] The strain-promoted azide–alkyne cycloaddition (SPAAC) between cyclooctynes and azides leads to 1,4,5-trisubstituted triazoles under mild conditions, without regioselectivity control (Scheme 2.2). This metal-free strategy has been mainly used for selective modification of biomolecules and living cells. However, the synthetic pathway to afford cyclooctynes is tedious and it should be simplified in order to apply this methodology not only in biochemistry and medicinal chemistry, but also in other fields.



Scheme 2.2 The intermolecular strain-promoted azide–alkyne cycloaddition (SPAAC).

Another practical method to afford fully substituted 1,2,3-triazoles in the absence of metal is the intramolecular AAC.^[14] Under mild conditions, the cycloaddition can take place thanks to favourable entropy effects. This strategy involves the appropriate position of the azide and alkyne moieties in the structure of the substrate in order to favour the cyclisation; this approach has permitted to give a variety of chemical entities, exhibiting structural and biological significance. Pericàs *et al.* reported that 1,4,5-triazoles fused to seven-membered heterocycles can be easily obtained from accessible enantiopure phenylglycidyl propargyl ethers leading to benzodiazepine analogues (Scheme 2.3).^[14f]



Scheme 2.3 Metal-free intramolecular azide–alkyne cycloaddition leading to 1,4,5-triazoles fused to seven-membered heterocycles.

With the aim of providing a metal-free methodology for the preparation of fully substituted 1,2,3-triazoles following a challenge intermolecular strategy involving non-activated alkynes, we relied on the special physicochemical properties of glycerol as solvent. The copper-catalysed azide–alkyne cycloaddition in glycerol has been previously studied,^[15] to lead to 1,4-disubstituted 1,2,3-triazoles. With the suspicion of its non-innocent role in this transformation, we decided to compare the reactivity in glycerol with that carried out in other polar solvents, like alcohols or water. In order to make the procedure more efficient increasing the reaction rate, we planned the use of microwave dielectric heating taking advantage of the unique physicochemical properties of glycerol.

Microwave technology was not applied in organic synthesis until 1986.^[16] Since then, this technique has become an established methodology used by chemists from both academia and industry.^[17] Microwaves are a type of electromagnetic radiation in the frequency range of 0.3 to 300 GHz in which only molecular rotation is affected. In general, both domestic microwave ovens and those dedicated to synthesis operate at 2.45 GHz in order to avoid interferences with telecommunication and cellular phone frequencies. Microwave radiation is absorbed by a specific reagent or solvent and converted into heat at a given frequency and temperature.

The electric component of the electromagnetic field induces heating *via* two main mechanisms.^[17-18] The first one is the dipolar polarisation mechanism. In order to generate heat, a substance should possess a permanent dipole moment, which is sensitive to the electric component of the radiation, aligning itself with the electric field by rotation. As the applied field changes, the dipole tries always to be aligned with it and in this process energy is lost by molecular friction and collisions, generating dielectric heating. The frequency should be low enough to let the dipoles respond to the alternating electric field and rotate, and high enough to make dipoles to rotate and follow the alternating field. Therefore, the amount of heat generated depends on the frequency of the field and the ability of the substance to align itself. The second mechanism to induce heating is the conduction mechanism. In this case, the dissolved charged particles in the sample collide against each other under the influence of the electric field causing agitation or motion, that is, heat. This mechanism is able to generate much more heat than the dipolar polarisation mechanism.

Therefore, microwave heating is produced only in the presence of polar solvents and/or ions. To compare the heating characteristics of different solvents under microwave irradiation their dielectric properties should be taken into account. The ability of a specific substance to

convert electromagnetic energy into heat at a given frequency and temperature is determined by the loss tangent, $\tan \delta$, which is the quotient between the dielectric loss (ϵ'' , the efficiency in converting electromagnetic radiation into heat) and the dielectric constant (ϵ' , the polarizability of the molecules in the electric field). A high $\tan \delta$ means a high microwave absorption and rapid heating. As expected, polar molecules like alcohols show high loss tangent factors (>0.5 , Table 2.1). Polyalcohols exhibit the highest $\tan \delta$ values. However, as explained by Mingos *et al.*^[19], there is an added factor to take into account in these cases: the relaxation time (τ), that is, the time taken for a molecule to take up a random orientation when the electric field is switched off. Polyols form hydrogen bonds extensively making these solvents very viscous and this property is correlated with long relaxation times. Both factors, $\tan \delta$ values and relaxation times, make glycerol a perfect solvent for synthetic procedures based on microwave dielectric heating.^[20]

Table 2.1 Relaxation times, viscosities and $\tan \delta$ values of some polar solvents.^[19b, 19c]

Solvent	Relaxation time τ (ps)	Viscosity (mP)	Loss tangent (at 2.45 GHz)
Water	9.04	10.1	0.123
Methanol	51.5	5.5	0.659
Ethanol	170	10.8	0.941
Propan-1-ol	332	20	0.757
Ethyleneglycol	113	198 ^[21]	1.35
1,3-Propanediol	340	560 ^[22]	1.30
Glycerol	1216	9450	0.651

Surprisingly, despite of the unique characteristics of glycerol, there are few examples in the literature in which glycerol is used as solvent in chemical transformations under microwave dielectric heating.^[20] Perin *et al.*^[23] reported an efficient and clean protocol for the selective synthesis of vinyl sulphides using $\text{KF}/\text{Al}_2\text{O}_3$ in glycerol under microwave dielectric irradiation. Glycerol is also an efficient solvent for the microwave-assisted oxidation of thiols to sulphides, as demonstrated by Lenardão, Jacob *et al.*^[24] Another example is the ruthenium-catalysed ring-closing metathesis (RCM) of diethyl diallylmalonate in glycerol under microwave activation, reported by Colacino *et al.*^[25] In order to overcome the problem of side reactions between glycerol and ester substrates, the same group showed a micellar catalysis approach.^[26] Deligeorgiev *et al.*^[27] described an environmentally benign procedure for the synthesis of substituted 2-cyanomethyl-4-phenylthiazoles under microwave irradiation using glycerol as solvent. In addition, microwave dielectric heating has been also used for the synthesis of metal nanomaterials, using glycerol both as solvent and as a reducing agent (polyol methodology).^[28]

2.2 Results and discussion

Our work started studying the intermolecular azide–alkyne cycloaddition between benzyl azide and diphenylacetylene as model reaction. Under microwave dielectric heating, 1-benzyl-4,5-diphenyl-1,2,3-triazole (**1a**) was obtained in 85% isolated yield in only 30 min (Table 2.2, entry 1). Surprisingly, working under exactly the same conditions, the reaction did not work using other alcohol-based solvents, including ethanol or diols like ethylene glycol, propane-1,2-diol or propane-1,3-diol (Table 2.2, entries 2-5). The conversion was also very low using water as solvent (Table 2.2, entry 6). Aprotic polar solvents, such as fluorobenzene and 1,4-dioxane, did not neither promote the reaction (Table 2.2, entries 7 and 8). Even working under solvent-free conditions (Table 2.2, entry 9), the result was very poor comparing with that using glycerol as solvent. These promising results agree with the great heating characteristics of glycerol under microwave irradiation as explained above.

Table 2.2 Azide–alkyne cycloaddition between diphenylacetylene and benzyl azide under microwave dielectric heating in different solvents.^[a]

$\text{Ph}-\text{C}\equiv\text{C}-\text{Ph} + \text{BnN}_3 \xrightarrow[\text{100 }^\circ\text{C, 30 min}]{\text{solvent, MW}} \text{Bn}-\text{N}(\text{Ph})=\text{N}=\text{C}(\text{Ph})-\text{N}=\text{N}$

1
a
1a

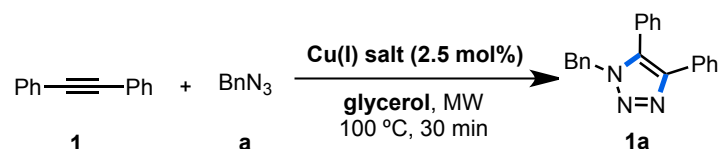
Entry	Solvent	Conversion (%) ^[b]	Yield (%) ^[c]
1	Glycerol	85	85 (85)
2	Ethanol	n.r.	-
3	Ethylene glycol	n.r.	-
4	Propane-1,2-diol	n.r.	-
5	Propane-1,3-diol	n.r.	-
6	Water	13	-
7	1,4-Dioxane	n.r.	-
8	Fluorobenzene	n.r.	-
9	Neat	20	18

^[a] Results from duplicate experiments. Reaction conditions: 0.4 mmol of benzyl azide and 0.6 mmol of diphenylacetylene in 1 mL of solvent, under microwave activation (250 W) at 100 °C for 30 min (temperature controlled by external infrared sensor). ^[b] Conversions based on benzyl azide and determined by ¹H NMR using 2-methoxynaphthalene as internal standard. ^[c] Determined by ¹H NMR using 2-methoxynaphthalene as internal standard; in brackets, isolated yield.

In order to investigate the effect of copper, the reaction was also carried out in the presence of 2.5 mol% of different copper(I) salts (Table 2.3). CuCl and CuI gave almost the same result as under metal-free conditions and the presence of Cu₂O even decreased the conversion.

It is important to mention that glycerol was analysed by ICP-AES in order to verify the absence of copper in the solvent used (<3 ppm).

Table 2.3 Azide–alkyne cycloaddition between diphenylacetylene and benzyl azide in the presence of Cu(I) salts.^[a]

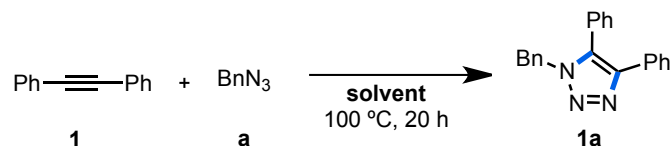


Entry	Cu(I) salt	Conversion (%) ^[b]	Yield (%) ^[b]
1	CuCl	85	85
2	CuI	86	67
3	Cu ₂ O	50	37

^[a] Results from duplicate experiments. Reaction conditions: 0.4 mmol of benzyl azide and 0.6 mmol of diphenylacetylene using 2.5 mol% of Cu(I) salt in 1 mL of glycerol, under microwave activation (250 W) at 100 °C for 30 min (temperature controlled by external infrared sensor). ^[b] Conversions (based on benzyl azide) and yields calculated by ¹H NMR using 2-methoxynaphthalene as internal standard.

Working under thermal activation (oil bath) at 100 °C for 20 h, the triazole **1a** was obtained in only 33% yield (Table 2.4, entry 1). The presence of a copper salt (2.5 mol% of CuCl) did not improve the result (Table 2.4, entry 2). Using other solvents, the reactivity observed followed the same trend (Table 2.4, entries 3, 5-6 and 8-9), except for ethylene glycol and water (Table 2.4, entries 4 and 7) where the yield was similar to the one obtained in neat glycerol

Table 2.4 Azide–alkyne cycloaddition between diphenylacetylene and benzyl azide under thermal activation in different solvents.^[a]



Entry	Solvent	Conversion (%) ^[b]	Yield (%) ^[b]
1	Glycerol	37	33
2 ^[c]	Glycerol	42	28
3	Ethanol	24	<5
4	Ethylene glycol	38	25
5	1,2-Propanediol	16	16
6	1,3-Propanediol	35	22
7	Water	46	31
8	1,4-Dioxane	7	7
9	Fluorobenzene	<5	-

^[a] Results from duplicate experiments. Reaction conditions: 0.4 mmol of benzyl azide and 0.6 mmol of diphenylacetylene in 1 mL of solvent, under thermal activation at 100 °C for 20 h, in a sealed tube. ^[b] Conversions (based on benzyl azide) and yields calculated by ¹H NMR using 2-methoxynaphthalene as internal standard. ^[c] In the presence of 2.5 mol% of CuCl.

The effect of microwave dielectric heating in the chemical transformations has been a matter of debate since the early days of microwave chemistry. Different explanations have been proposed to justify the fact that the reaction rate is generally higher under microwave irradiation, in comparison to conventional heating. The observed effects could be due to a purely thermal/kinetic phenomena (that is, due to the high internal temperatures achieved) as defended mainly by Kappe *et al.*^[29] or they could be due to non-thermal/specific effects by a direct influence of the microwave irradiation.^[30] For this reason, in many cases the results obtained under microwave dielectric heating have been compared with those obtained at the same conditions under thermal heating (that is, at the same temperature and at the same reaction time). However, this is not strictly correct; usually the microwave reactors are equipped with an external infrared (IR) sensor integrated into the cavity, which determines the temperature of the reaction vessel. In this way, it is assumed that the temperature fixed in the microwave reactor (the one given by the IR sensor) corresponds to the temperature inside of the reaction vessel and it is not always the case. Usually the internal temperature of the reaction is higher.

Since the microwave reactor used in this work was equipped only with an external IR sensor (CEM instrument), several tests were done in order to measure the internal temperature of the reaction. For that purpose, an Anton Paar Monowave 300 reactor equipped with both an internal fiber-optic (FO) sensor and external IR sensor was used (Figure 2.2).

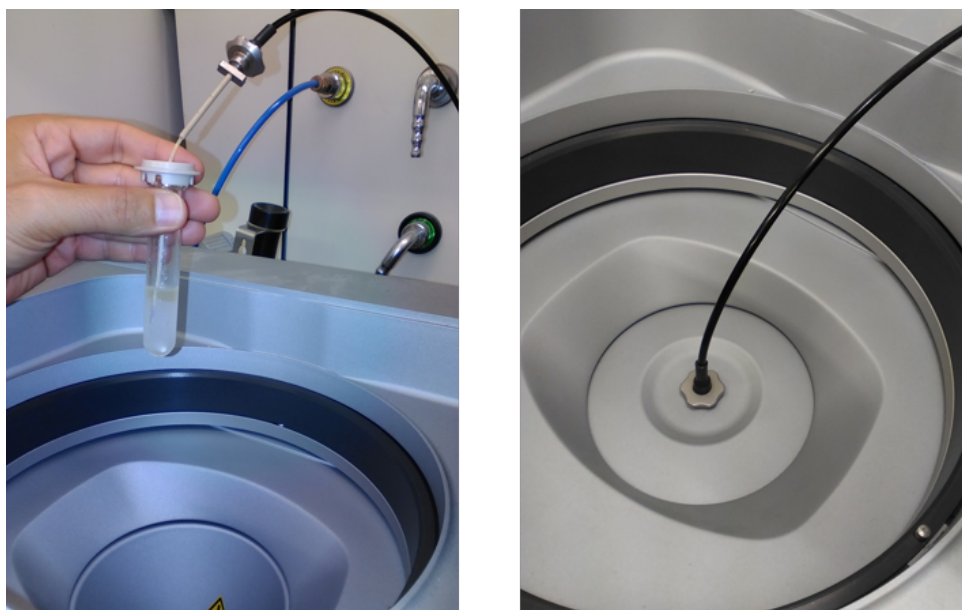
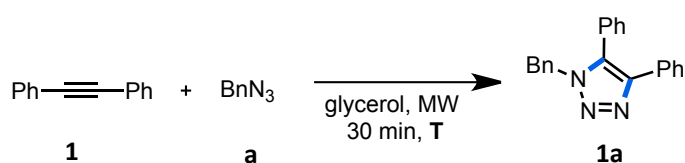


Figure 2.2 Pictures corresponding to the Anton Paar MW reactor equipped with an internal FO sensor: reaction vessel bearing the FO sensor (left) and reaction vessel inside of the reactor (right).

The benchmark reaction was carried out in this reactor at different temperatures (100 °C, 140 °C and 180 °C, according to the FO sensor) (Table 2.5). The yield obtained at 180 °C was the most similar to that obtained working with the CEM reactor equipped only with the external IR sensor (Table 2.5, entry 3). The reaction was also carried out under thermal heating (oil bath) at 180 °C for 30 minutes obtaining the product in a 65% yield (Table 2.5, entry 4) what can be explained by the efficient internal heating of the whole liquid volume simultaneously under microwave irradiation, in contrast to the conventional heating, which is less efficient.

Table 2.5 Azide–alkyne cycloaddition under MW irradiation using an Anton Paar MW reactor at different temperatures (according to the fiber-optic sensor).^[a]



Entry	T (°C)	Conversion (%) ^[b]	Yield (%) ^[b]
1	100	n.r.	-
2	140	22	15
3	180	92	84
4 ^[c]	180	72	65

^[a] Reaction conditions: 0.4 mmol of benzyl azide and 0.6 mmol of diphenylacetylene in 1 mL of glycerol, under microwave activation for 30 min (temperature controlled by the internal FO sensor). ^[b] Conversions (based on benzyl azide) and yields determined by ¹H NMR using 2-methoxynaphthalene as internal standard. ^[c] Under thermal heating (oil bath) for 30 min.

Once the reaction conditions were fixed, the reactivity using different internal alkynes was tested. From moderate to high yields (32–90%) were obtained using symmetrical disubstituted alkynes **2–5** (Table 2.6, entries 1–4). It is remarkable the good yield (71%) obtained when a non-activated alkyne (oct-4-yne, **5**) was used (after 1h under microwave irradiation, Table 2.6, entry 4).

Table 2.6 Scope of metal-free AAC using different internal alkynes.^[a]

$$\text{R}-\text{C}\equiv\text{C}-\text{R}' \xrightarrow[\text{glycerol, MW, 30 min, 100 }^\circ\text{C}]{\text{BnN}_3} \text{Bn}-\text{N}=\text{N}-\text{C}(\text{R})(\text{R}')-\text{C}\equiv\text{C}-\text{R}'$$

2-10 **a** **2a-10a**

Entry	Alkyne	Product	Conversion (%) ^[b]	Yield (%) ^[b]
1 ^[c]	<p>2</p>	<p>2a</p>	100	78
2	<p>3</p>	<p>3a</p>	96	90
3	<p>4</p>	<p>4a</p>	56	32
4 ^[d]	<p>5</p>	<p>5a</p>	73	71
5	<p>6</p>	<p>6a</p>	91	83 ^[e]
6	<p>7</p>	<p>7a</p>	49	49 ^[e]
7	<p>8</p>	<p>maj-8a + min-8a</p>	65	62 (9:1) ^[f]
8	<p>9</p>	<p>maj-9a + min-9a</p>	92	85 (9:1) ^[f]
9	<p>10</p>	<p>10a</p>	85	84 ^[g]

^[a] Results from duplicate experiments. Reaction conditions: 0.4 mmol of benzyl azide and 0.6 mmol of alkyne in 1 mL of glycerol, under microwave activation (250 W) at 100 °C for 30 min (temperature controlled by external infrared sensor). ^[b] Conversions (based on benzyl azide) and yields determined by ¹H NMR using 2-methoxynaphthalene as internal standard. ^[c] Reaction time: 15 min. ^[d] Reaction time: 60 min. ^[e] Regioisomer ratio: 1:1. ^[f] In brackets, regioisomer ratio. Only the major regioisomer is drawn. ^[g] Only one regioisomer was obtained (**10a**).

An equimolar mixture of regioisomers was obtained using unsymmetrical disubstituted alkynes **6** and **7** (Table 2.6, entries 5–6). However, high regioselectivity was achieved in the case of internal alkynes bearing a trimethylsilyl group (TMS), **8** and **9** (Table 2.6, entries 7–8) and only one regioisomer was obtained employing a *tert*-butyldimethylsilyl (TBDMS) alkyne **10** (Table 2.6, entry 9). Importantly, these 1,2,3-triazoles bearing silyl-based groups allow further functionalization, such as cross-coupling reactions, considering them valuable building blocks.^[31]

The TMS group was employed for the first time in 1972 as a directing group in the 1,3-dipolar cycloaddition.^[32] As explained in several works,^[33] there are two main reasons to explain this effect. The first one is the ability of the Si atom to stabilise a partial positive charge on the acetylene β -carbon (Figure 2.3a). This stabilisation can be possible thanks to the donation of electron density from the $\sigma_{\text{C-Si}}$ bond to the vacant p orbital of the carbon atom at β position, efficiently controlling the regiochemistry of the process (see the proposed transition state, Figure 2.3b). The second reason is the steric effect of the silyl-based groups. Therefore, the best regioselectivity was obtained using the alkyne bearing a much more sterically demanding TBDMS group in comparison with TMS.

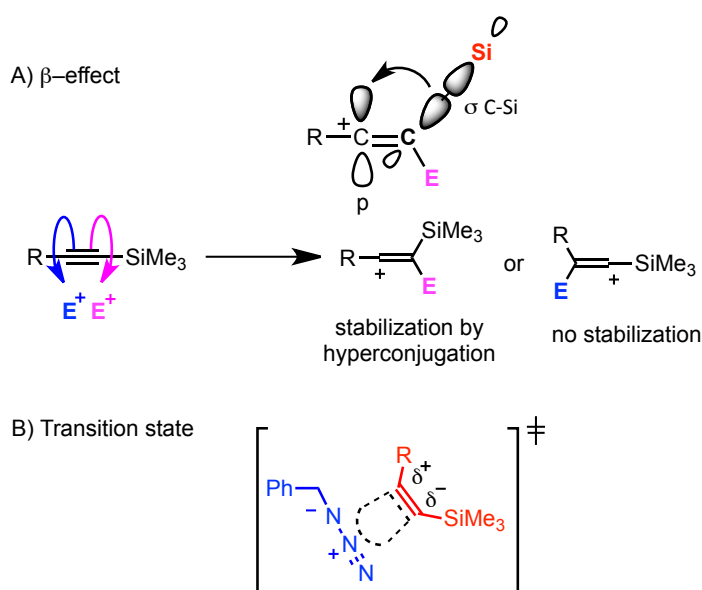


Figure 2.3 a) Stabilisation of a partial positive charge on the acetylene β -carbon because of the presence of the silyl-based group. b) Proposed transition state.

The structure elucidation of triazole **maj-8a** was carried out by NOESY NMR correlations (Figure 2.4). The Overhauser effect between the signal corresponding to the protons of the methylene group of the benzyl substituent and the one of the methyl at 5 position in the triazole cycle helped to directly determine that the major regioisomer was the 1-benzyl-4-trimethylsilyl-

5-methyl-1,2,3-triazole. Correlation between the signals corresponding to the aromatic protons and the signal of the $-\text{CH}_3$ could also be detected.

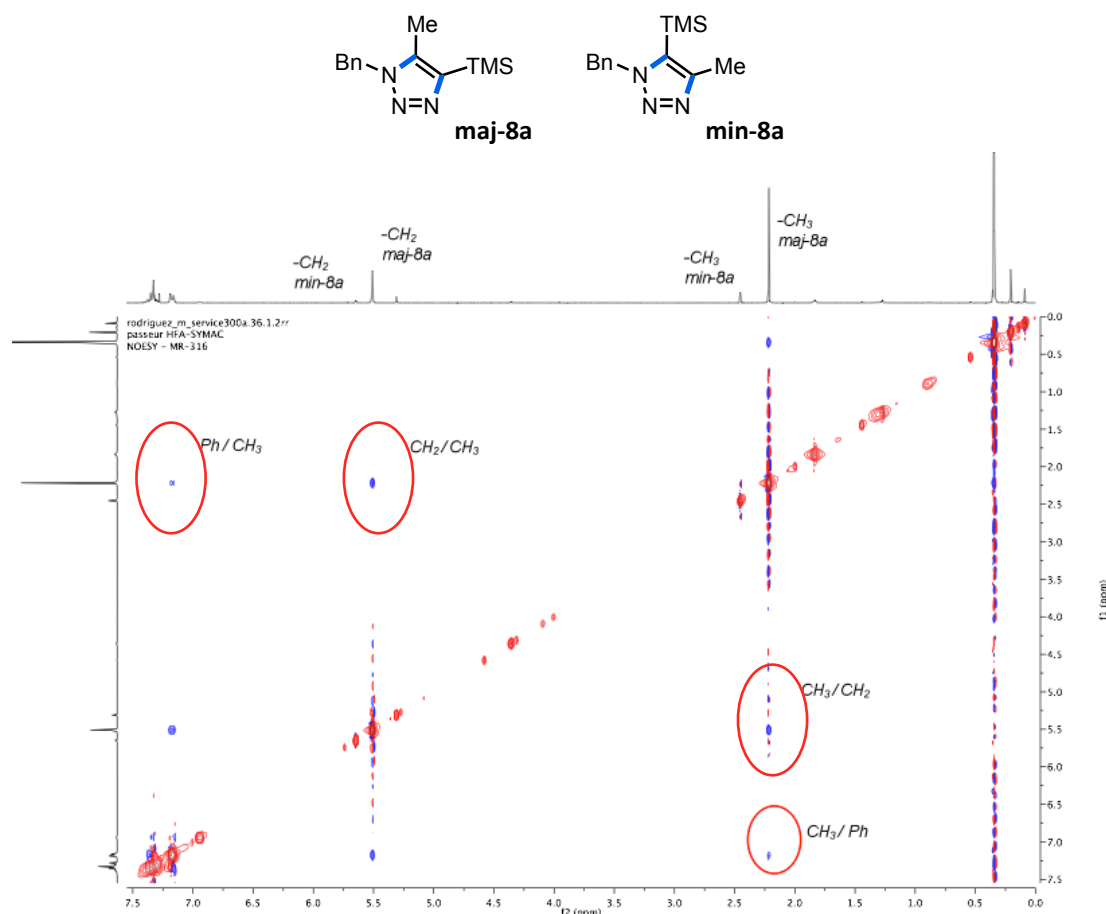
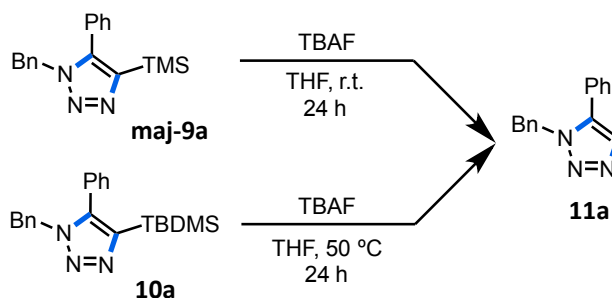


Figure 2.4 2D-NOESY NMR spectrum (300 MHz, CDCl_3) of the mixture of the two regioisomers of triazole **8a**. Red circles indicate NOE contacts for **maj-8a**.

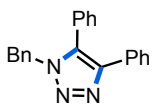
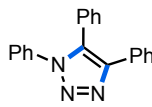
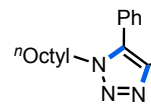
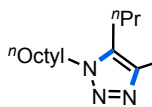
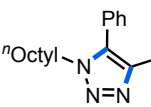
For **maj-9a** and **10a** the structure could not be established by NOESY NMR correlations. In these cases, the silyl group was eliminated by treatment with tetrabutylammonium fluoride (TBAF) obtaining the corresponding 1,5-disubstituted 1,2,3-triazole (the structure was established by NOESY NMR correlations) **11a** which directly allowed determining the major regioisomer (Scheme 2.4).



Scheme 2.4 The desilylation reaction of triazoles **maj-9a** and **10a** leading to the corresponding 1,5-regioisomer of triazole **11a**.

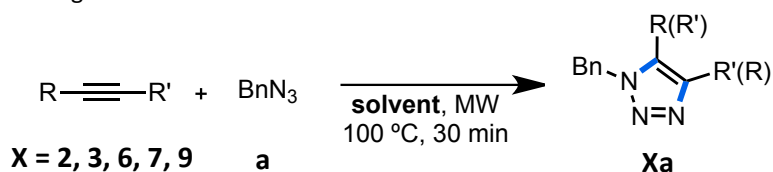
Other organic azides such as phenyl azide and octyl azide were also tested in the AAC reaction (Table 2.7). The reaction between phenyl azide (**b**) and alkyne **1** gave triazole **1b** in a lower conversion (78%) and yield (43%) comparing with the result obtained using benzyl azide and the same alkyne (triazole **1a**, 85% conversion, 85% yield; Table 2.2). Regarding the difference between conversion and yield, phenyl azide could be decomposing under MW conditions. Indeed, only 70% and 56% of phenyl azide was recovered under microwave activation in glycerol, when it was treated for 30 min at 150 and 250 W respectively, respectively. In contrast, under thermal heating (oil bath), 95% of PhN₃ was recovered after 20 h at 100 °C in glycerol. Octyl azide (**c**) gave good results using activated alkynes like **1** and **9** (giving triazoles **1c** and **9c**, respectively); however, using the alkyne oct-4-yne (**5**), the triazole **5c** was obtained in a poor conversion (28%) and yield (27%) even at a longer reaction time (120 min). In this last case, the poor reactivity can be explained because both reagents, the alkyne (**5**) and the azide (**c**) are non-activated with regard to the cycloaddition.

Table 2.7 Scope of AAC reaction using different organic azides.^[a]

					
	1a	1b	1c	5c	maj-9c
Time (min)	30 min	60 min ^[c]	60 min	120 min	30 min
Conversion (Yield) [%] ^[b]	85 (85)	78 (43)	83 (80)	28 (27)	84 (73) ^[d]

^[a]Results from duplicate experiments. Reaction conditions: 0.4 mmol of organic azide and 0.6 mmol of alkyne in 1 mL of glycerol, under microwaves activation (250 W) at 100 °C (temperature controlled by external infrared sensor). ^[b]Conversions (based on benzyl azide) and yields determined by ¹H NMR using 2-methoxynaphthalene as internal standard. ^[c]Power applied: 150 W. The reaction was protected from light. ^[d]Regioisomer ratio: 9:1.

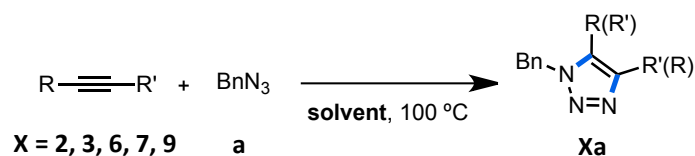
The effect of the solvent under microwave irradiation was also checked in the synthesis of some different 1,2,3-triazoles besides the benchmark reaction (Table 2.8). Essentially, in all the cases tested, the reactivity was higher using glycerol as solvent instead of other protic solvents like water, ethylene glycol or ethanol. There is an exception in the case of triazole **2a** (Table 2.8, entries 1–4) in which no difference in the reactivity was observed changing the solvent; the internal alkyne used (**2**) is so activated that the reactivity is high using any solvent. It should be noted that transesterification reactions between the alkyne **6** (or the triazole formed) and the solvent took place in the preparation of triazole **6a** in ethylene glycol medium (Table 2.8, entry 11) whereas using glycerol as solvent this was not observed. Once again, the usefulness of glycerol as solvent under microwave dielectric heating was verified.

Table 2.8 Effect of the solvent in the preparation of different fully substituted 1,2,3-triazoles under MW dielectric heating.^[a]

Entry	Product	Solvent	Conversion (%) ^[b]	Yield (%) ^[b]
1 ^[c]	2a (R = R' = CO ₂ Me)	Glycerol	100	78
2 ^[c]	2a (R = R' = CO ₂ Me)	Water	100	92
3 ^[c]	2a (R = R' = CO ₂ Me)	Ethylene glycol	100	81
4 ^[c]	2a (R = R' = CO ₂ Me)	Ethanol	100	87
5	3a (R = R' = OMe)	Glycerol	96	90
6	3a (R = R' = OMe)	Water	32	15
7	3a (R = R' = OMe)	Ethylene glycol	73	57
8	3a (R = R' = OMe)	Ethanol	25	10
9	6a (R = Ph, R' = CO ₂ Me)	Glycerol	91	83 ^[d]
10	6a (R = Ph, R' = CO ₂ Me)	Water	70	50 ^[d]
11	6a ^[e] (R = Ph, R' = CO ₂ Me)	Ethylene glycol	-	-
12	6a (R = Ph, R' = CO ₂ Me)	Ethanol	36	21 ^[d]
13	7a (R = Ph, R' = Me)	Glycerol	49	49 ^[d]
14	7a (R = Ph, R' = Me)	Water	19	<5 ^[d]
15	7a (R = Ph, R' = Me)	Ethylene glycol	25	7 ^[d]
16	7a (R = Ph, R' = Me)	Ethanol	14	<5 ^[d]
17	maj-9a (R = Ph, R' = TMS)	Glycerol	92	85 (9:1) ^[f]
18	maj-9a (R = Ph, R' = TMS)	Water	30	14 ^[g]
19	maj-9a (R = Ph, R' = TMS)	Ethylene glycol	63	52 (9:1) ^[f]
20	maj-9a (R = Ph, R' = TMS)	Ethanol	<5	<5 ^[g]

^[a] Reaction conditions: 0.4 mmol of benzyl azide and 0.6 mmol of the corresponding alkyne in 1 mL of solvent, under microwaves activation (250 W) at 100 °C for 30 min (temperature controlled by external infrared sensor). See Table 2.6 for the structures of alkynes and triazoles. ^[b] Conversions (based on benzyl azide) and yields determined by ¹H NMR using 2-methoxynaphthalene as internal standard. ^[c] Reaction time: 15 min. ^[d] Regioisomer ratio: 1:1 ^[e] Complex mixture due to transesterification reactions (HPLC-MS). ^[f] In brackets: regioisomer ratio. ^[g] The regioisomer ratio was not determined.

The effect of the solvent was also studied for the other triazoles (besides the model reaction) under thermal activation (Table 2.9). Once again, the same trend was observed; in almost all the examples, the reactivity in glycerol was higher than in other solvents. 1,2,3-Triazole **2a** was again an exception; no differences were observed using different solvents, probably due to the high reactivity of alkyne **2**. This behaviour seems to point out that glycerol is able to promote the azide-alkyne cycloaddition.

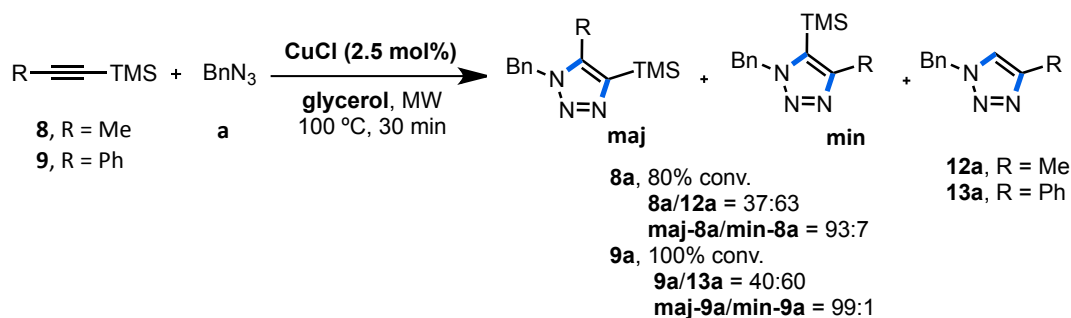
Table 2.9 Effect of the solvent in the preparation of different fully substituted 1,2,3-triazoles under thermal activation.^[a]

Entry	Product	Solvent	Time (h)	Conversion (%) ^[b]	Yield (%) ^[b]
1	2a (R = R' = CO ₂ Me)	Glycerol	2	100	87^[c]
2	2a (R = R' = CO ₂ Me)	Ethylene glycol	2	100	79
3 ^[d]	2a (R = R' = CO ₂ Me)	Ethanol	2	100	96
4	2a (R = R' = CO ₂ Me)	1,4-Dioxane	2	100	90
5	3a (R = R' = OMe)	Glycerol	20	86	73
6	3a (R = R' = OMe)	Ethylene glycol	20	66	55
7	3a (R = R' = OMe)	Ethanol	20	49	35
8	3a (R = R' = OMe)	1,4-Dioxane	20	45	32
9	6a (R = Ph, R' = CO ₂ Me)	Glycerol	2	80	73^{[c][f]}
10	6a (R = Ph, R' = CO ₂ Me)	Ethylene glycol	2	53	31 ^[f]
11	6a^[e] (R = Ph, R' = CO ₂ Me)	Ethanol	2	19	6 ^[g]
12	6a (R = Ph, R' = CO ₂ Me)	1,4-Dioxane	2	27	13 ^[g]
13	7a (R = Ph, R' = Me)	Glycerol	20	42	60^{[c][f]}
14	7a (R = Ph, R' = Me)	Ethylene glycol	20	27	16 ^[f]
15	7a (R = Ph, R' = Me)	Ethanol	20	18	<5 ^[g]
16	7a (R = Ph, R' = Me)	1,4-Dioxane	20	24	<5 ^[g]
17	maj-9a (R = Ph, R' = TMS)	Glycerol	20	77	70 (9:1)^[h]
18	maj-9a (R = Ph, R' = TMS)	Ethylene glycol	20	71	68 (9:1) ^[h]
19	maj-9a (R = Ph, R' = TMS)	Ethanol	20	30	31 (9:1) ^[h]
20	maj-9a (R = Ph, R' = TMS)	1,4-Dioxane	20	37	25 (9:1) ^[h]

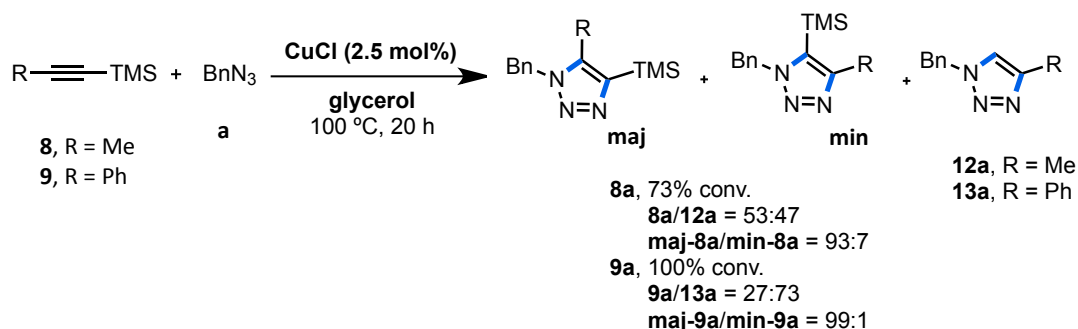
^[a] Reaction conditions: 0.4 mmol of benzyl azide and 0.6 mmol of the corresponding alkyne in 1 mL of solvent in a sealed tube. ^[b] Conversions (based on benzyl azide) and yields calculated by ¹H NMR using 2-methoxynaphthalene as internal standard. ^[c] Isolated yield. ^[d] Complex mixture due to transesterification reactions (NMR). ^[f] Regioisomer ratio: 1:1 ^[g] The regioisomer ratio was not determined. ^[h] In brackets: regioisomer ratio.

The presence of Cu(I) salts did not change the result, with the exception of TMS-based triazoles **8a** and **9a**. In the presence of 2.5 mol% of CuCl under microwave irradiation, not only the expected triazoles were obtained (**maj-8a** and **maj-9a**), but also the corresponding desilylated triazoles^[31b] as single regioisomers (**12a** and **13a**) (Scheme 2.5a). Under conventional thermal conditions, the same behaviour was observed (Scheme 2.5b). In the synthesis of the silyl-based triazole **10a** (bearing a TBDMS group instead of TMS), the presence of CuCl did not lead to the desilylated triazole.

a) Under microwave dielectric heating

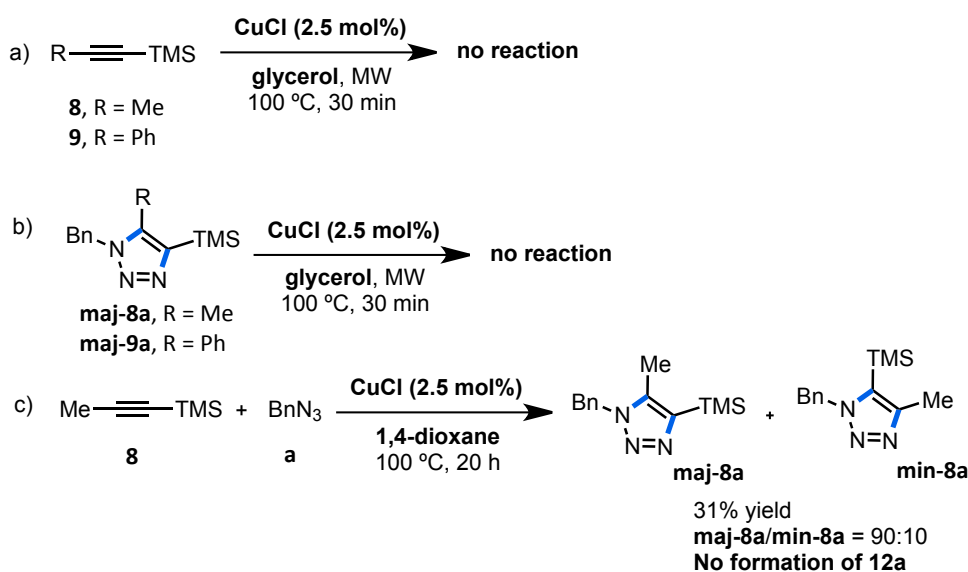


b) Under thermal conditions (oil bath)



Scheme 2.5 The effect of Cu(I) using TMS-based alkynes in the AAC reaction both under microwave irradiation (a) and conventional thermal conditions (b). Data from NMR analysis.

In order to explain the observed behaviour in the synthesis of TMS-based triazoles, several control experiments were carried out. No desilylation was observed on the alkyne **8** or **9** (Scheme 2.6a) and neither on the triazole **8a** and **9a** (Scheme 2.6b) in the presence of CuCl under the same reaction conditions. Moreover, the desilylation did not take place using 1,4-dioxane as solvent (Scheme 2.6c), instead of glycerol, what means that glycerol is involved in the process.



Scheme 2.6 Control experiments to explain the behavior observed when CuCl was present in the azide-alkyne cycloaddition between TMS-based alkynes **8** and **9** and benzyl azide **a**.

The reaction was also monitored by GC-MS observing that the formation of triazole **9a** was faster than the formation of the desilylated triazole **13a**. After 5 min, the ratio **9a/13a** was approximately 77:23 and after 15 min, when benzyl azide was totally consumed, the ratio was 58:42 approximately. After the full conversion of benzyl azide, phenylacetylene started appearing which indicates that the alkyne **9** started being desilylated.

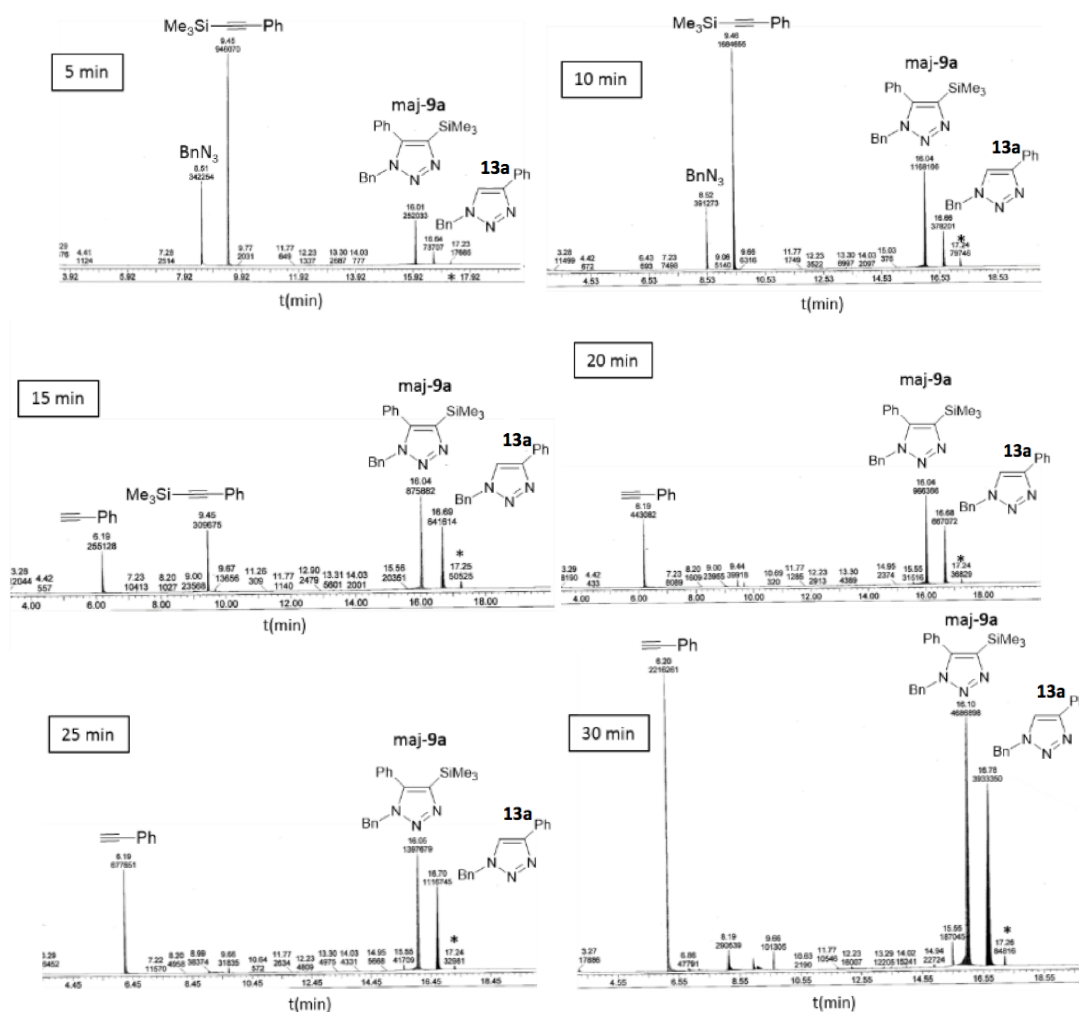
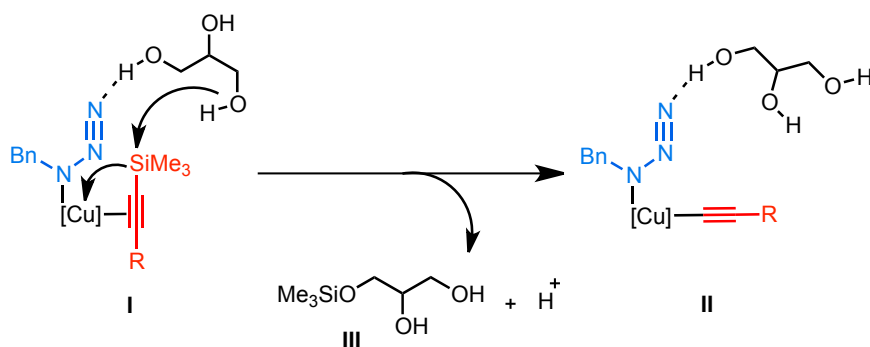


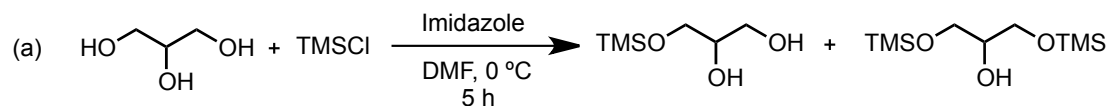
Figure 2.5 Chromatograms corresponding to the monitoring by GC-MS of the cycloaddition between alkyne **9** and benzyl azide **a** in the presence of CuCl. (*) The peak at 17.2 min corresponds to **min-9a**.

With these clues in hand a mechanism for the desilylation was proposed (Scheme 2.7). The silyl-based alkyne (**8** or **9**) should be coordinated to the metal centre triggering the desilylation promoted by glycerol, which thanks to the hydrogen bonds, is close to the coordination sphere Si interacting with the benzyl azide (intermediate **I**, Scheme 2.7). This situation should evolve to intermediate **II** in which the alkyne is coordinated to copper favouring the formation of the corresponding desilylated triazoles (**12a** or **13a**), obtaining only the 1,4-disubstituted regioisomer, according to the accepted Cu-catalysed mechanisms.^[2a, 34]

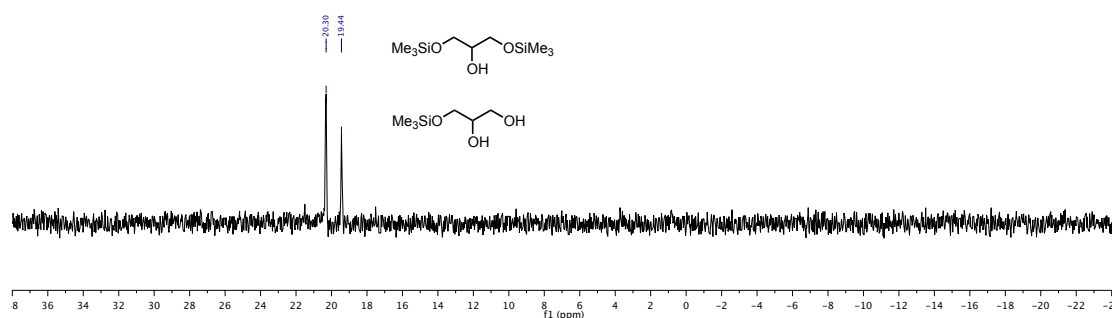


Scheme 2.7 Proposed mechanism for the Cu-mediated desilylation promoted by glycerol

The formation of the corresponding silyl derivative of glycerol (**III**) was detected by NMR. Silylated glycerol derivatives were directly prepared from glycerol and TMSCl (Figure 2.6a) and its ^{29}Si NMR spectrum compared with the crude reaction mixture of the formation of **8a** in the presence of CuCl in glycerol (Scheme 2.5a) (Figure 2.6b-c).



(b) ^{29}Si NMR



(c) ^{29}Si NMR

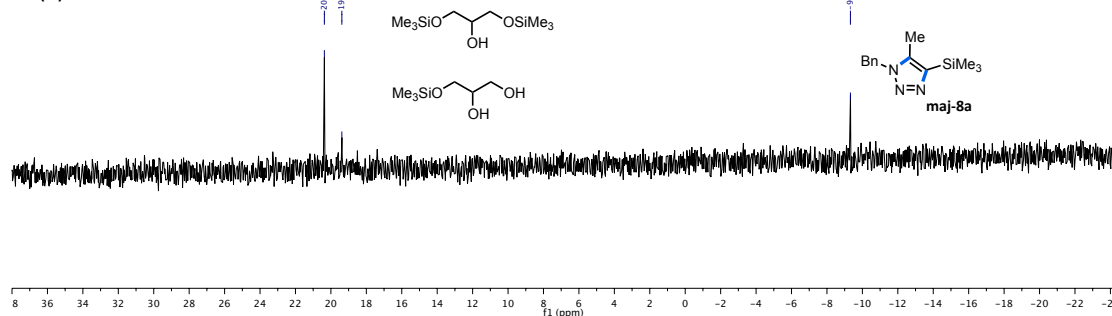


Figure 2.6 (a) Scheme corresponding to the silylation of glycerol; (b) ^{29}Si NMR (79.5 MHz, CDCl_3) spectrum corresponding to the mixture of mono- and bis-silylated glycerol derivatives obtained in (a); (c) ^{29}Si NMR (79.5 MHz, CDCl_3) spectrum corresponding to the crude of the reaction described in Scheme 2.5.

In order to rationalise this enhancement of the reactivity using glycerol as solvent under thermal conditions, the mechanism of the reaction should be taken into account. The azide-alkyne cycloaddition is a concerted pericyclic reaction which was first discovered by Michael in 1893.^[35] However, the reaction was mostly investigated by Huisgen in 1950s-70s^[36]. The reaction is an orbital symmetry-allowed cycloaddition [$\pi 4_s + \pi 2_s$] between a 1,3-dipole ($\pi 4_s$, azide) and a dipolarophile ($\pi 2_s$, alkyne). In this way, when the 1,3-dipole and the dipolarophile approach each other, their frontier orbitals interact forming new molecular orbitals (MO) in the transition state. Our model cycloaddition between benzyl azide and diphenylacetylene is classified according to the literature as type III.^[37] This means that the corresponding HOMO from the alkyne interacts with the LUMO of the benzyl azide (Figure 2.7). Therefore, a stabilising hydrogen bonding interaction between benzyl azide and glycerol might lower the energy of the LUMO, thus facilitating the reaction.

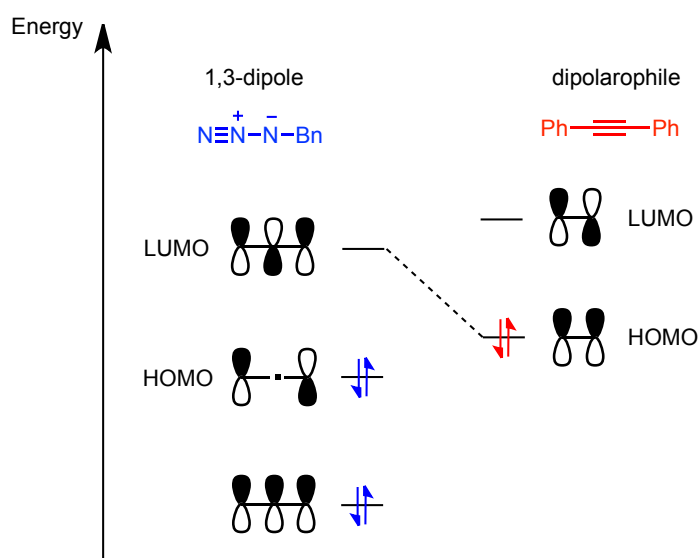


Figure 2.7 Frontier molecular orbital diagram representing the interaction between the frontier orbital HOMO of diphenylacetylene and LUMO of benzyl azide.

Theoretical calculations (DFT B3LYP, 6-31 G*) were carried out in order to study the interaction between glycerol and benzyl azide taking into account the ability of glycerol to form extensive hydrogen bonds.^[38] In order to compare, the interaction between benzyl azide and other alcohols like ethanol and diols (ethylene glycol, 1,2- and 1,3-propanediol) were also studied (Figure 2.8). The calculated charges showed that the dipolar character of benzyl azide increases in the resulting BnN_3 /alcohol adducts in comparison with neat benzyl azide.

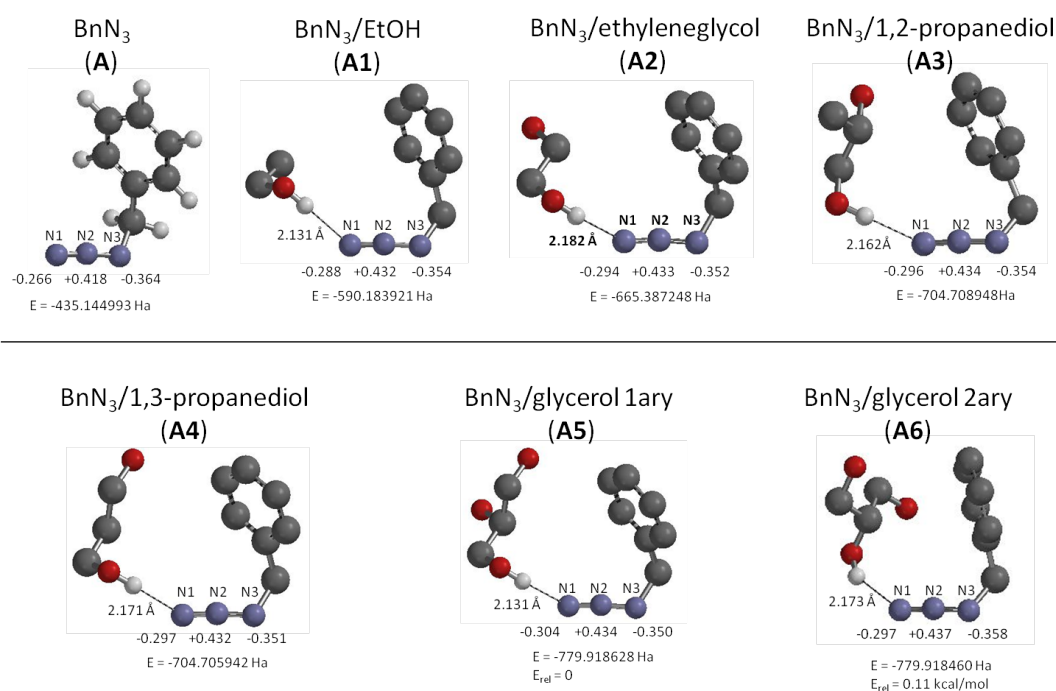


Figure 2.8 Calculated structures (DFT, B3LYP, 6-31G*) for neat BnN_3 (A) and the corresponding BnN_3 /alcohol adducts (A1-A6). Mulliken charges for nitrogen atoms are indicated below each corresponding atom. Hydrogen atoms are omitted for clarity, except for BnN_3 and hydrogen atoms involved in the hydrogen bonds. Lengths corresponding to hydrogen bonds between N1 and the corresponding oxygen are indicated for each adduct. Calculated energy is indicated for each structure. For glycerol, both adducts, for primary (A5) and secondary (A6) OH group, have been calculated, observing practically the same energy ($\Delta E = 0.11$ kcal/mol). Note: red spheres denote oxygen atoms; blue, nitrogen atoms; white, hydrogen atoms; grey, carbon atoms.

In addition, the stabilization of these BnN_3 /alcohol adducts is bigger when the intramolecular hydrogen bonds present in the case of polyols (glycerol, ethylene glycol and 1,2-propanediol) are considered (Figure 2.9).

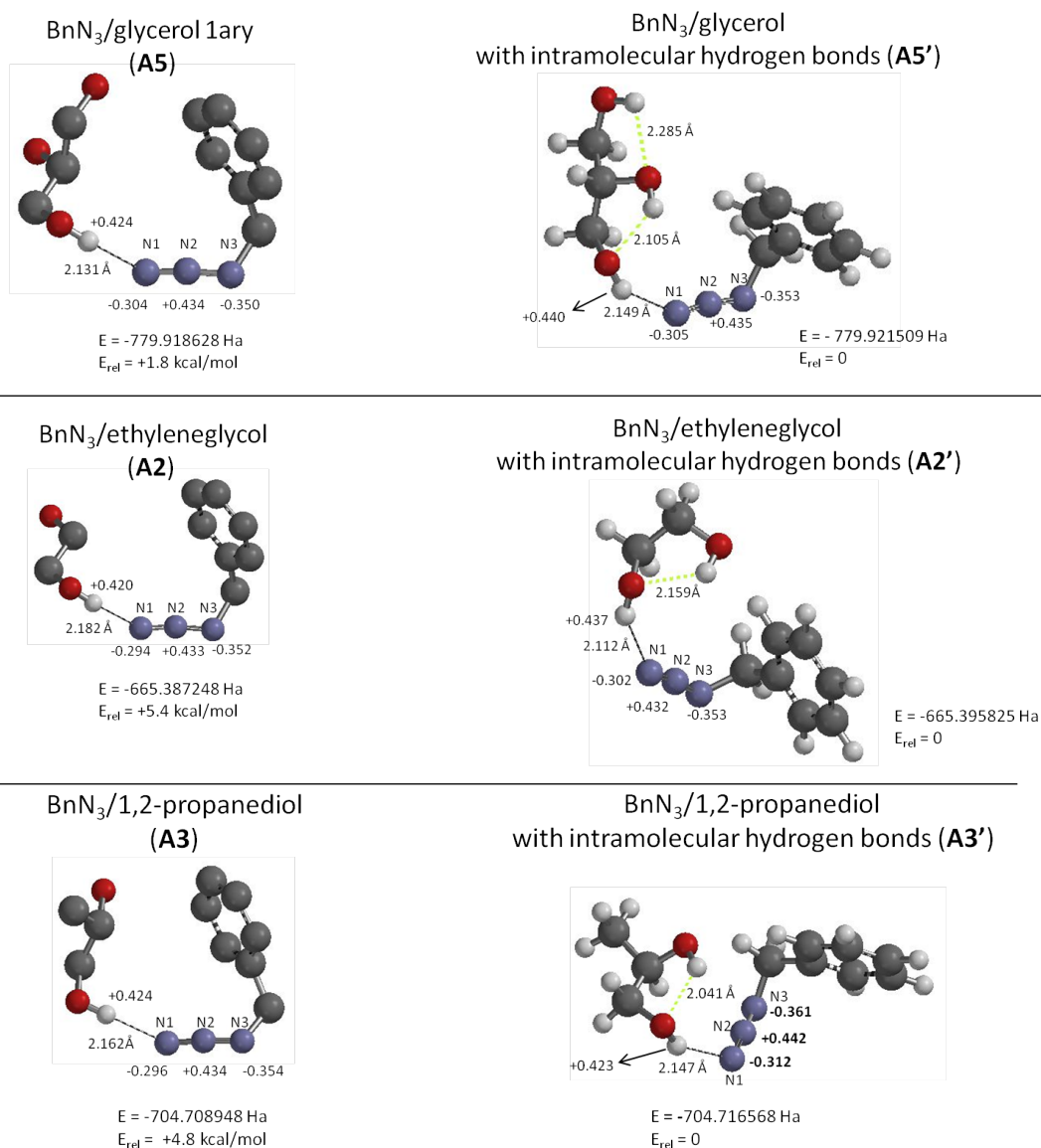


Figure 2.9 Calculated structures (DFT, B3LYP, 6-31G*) for BnN₃/alcohol adducts taking into account intramolecular hydrogen bonds (right: **A2'**, **A3'**, **A5'**); for comparative purposes, structures without intramolecular H bonds are represented (left: **A2**, **A3**, **A5**). Mulliken charges for nitrogen atoms and the hydrogen atom involved in the N---H bond are indicated. Hydrogen atoms are omitted for clarity for some structures. Lengths corresponding to the hydrogen bonds are indicated for each adduct. Calculated energy is indicated for each structure; for each pair of adducts (with and without intramolecular hydrogen bonds) the relative energy is indicated. Note: red spheres denote oxygen atoms; blue, nitrogen atoms; white, hydrogen atoms; grey, carbon atoms.

The relative energies of frontier orbitals for the different BnN₃/alcohol adducts were also analysed (Figure 2.10 and Table 2.10).

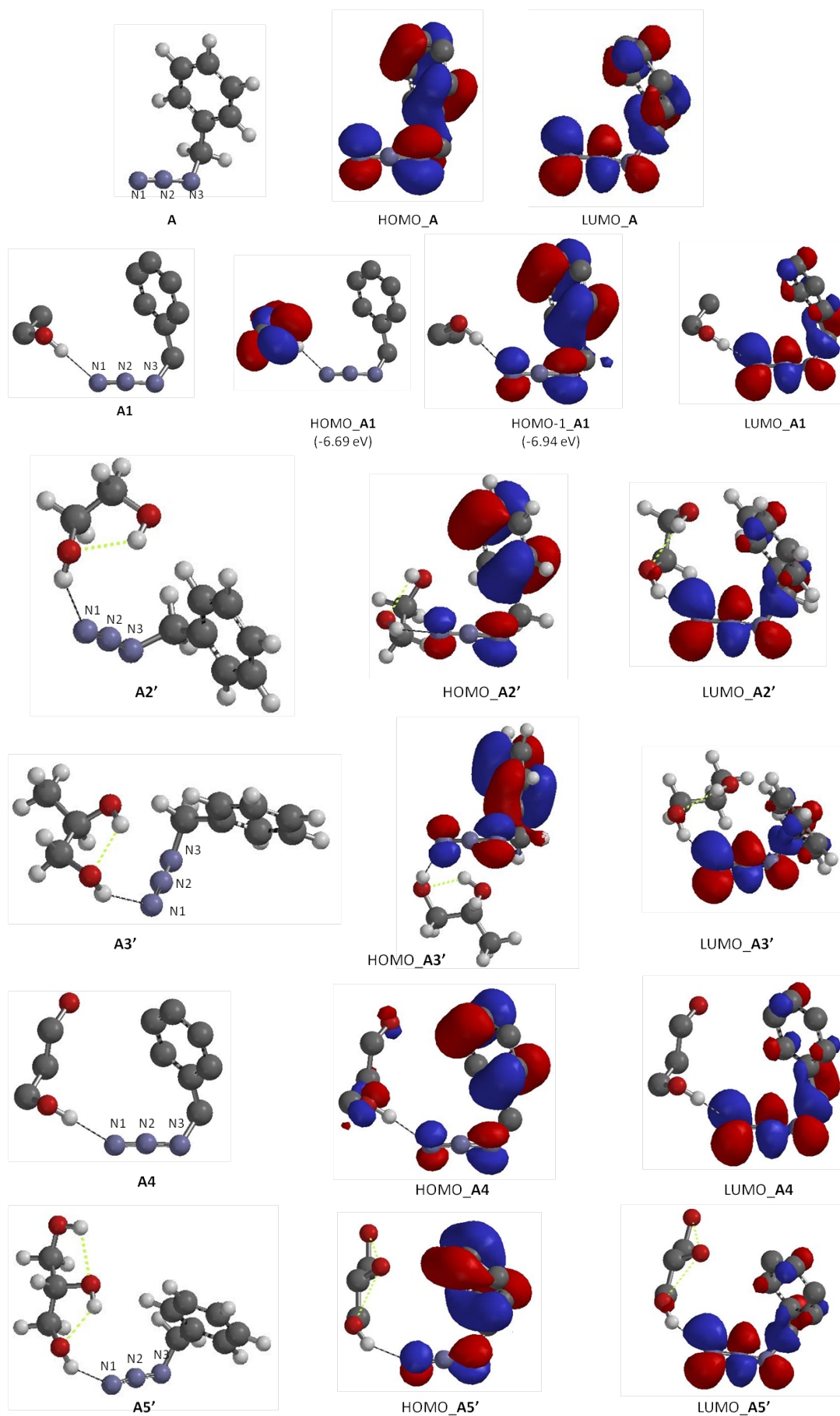


Figure 2.10 Frontier orbitals for A, A1, A2', A3', A4 and A5' involved in AAC processes.

Table 2.10 Calculated energy (DFT, B3LYP, 6-31G*) for frontier orbitals of neat BnN₃ and BnN₃/alcohol adducts (see Figure 2.10).

Energy (eV)	A	A1	A2'	A3'	A4	A5'
LUMO	-0.81	-1.17	-1.18	-1.05	-1.15	-1.31
HOMO	-6.72	-6.94 ^[a]	-6.86	-6.78	-6.80	-6.72

^[a] Corresponding to HOMO-1 (see Figure 2.10).

The BnN₃/glycerol LUMO (A5'), which overlaps with the diphenylacetylene HOMO, is more stable than the ones obtained for the other adducts (see Table 2.10). Therefore, the energy gap of the orbital interaction is lower when glycerol is present enhancing the reactivity (Figure 2.11), as observed in this work.

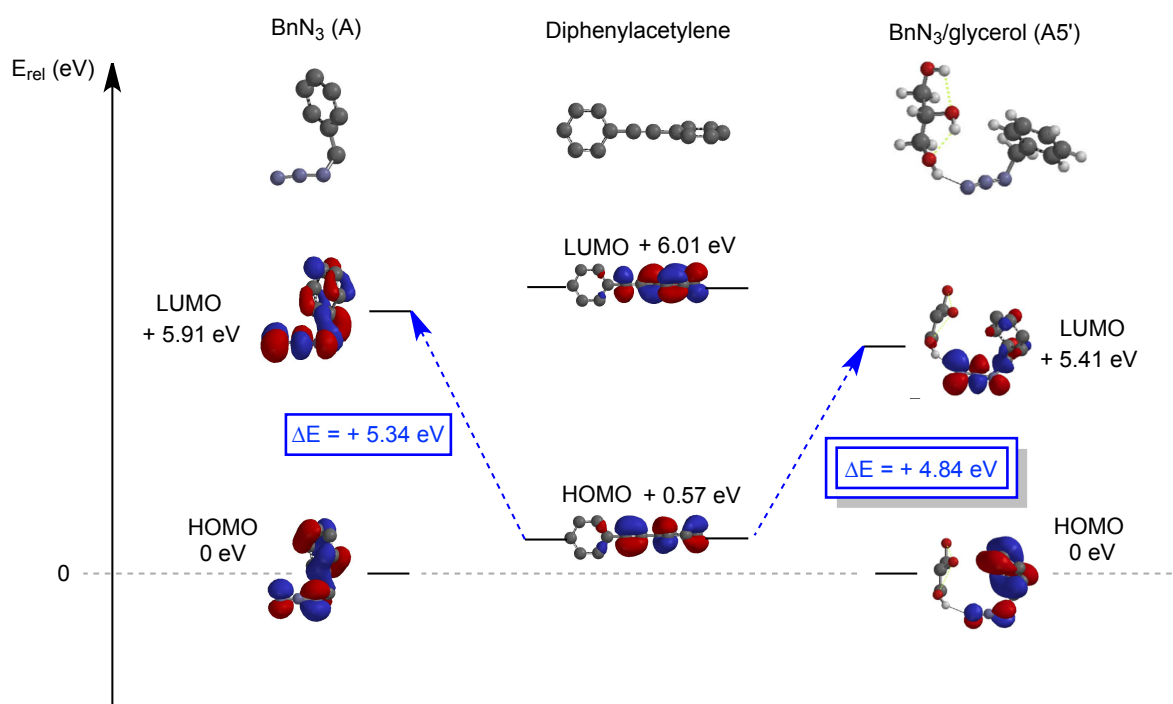


Figure 2.11 Frontier molecular orbitals diagram representing the overlapping between the HOMO of diphenylacetylene (center) and the LUMO of benzyl azide (A) (left) or the LUMO of BnN₃/glycerol adduct (A5') (right). The energy GAP is lower in second case.

2.3 Conclusions

In this chapter, we have demonstrated the important role of glycerol as solvent in the intermolecular azide-alkyne cycloaddition between internal alkynes and organic azides under metal-free conditions. Under conventional thermal heating (oil bath), the cycloaddition in glycerol is enhanced in comparison with other protic solvents. Theoretical calculations allowed us to demonstrate that the calculated energy for BnN₃/glycerol LUMO frontier orbital is lower than the ones obtained for neat benzyl azide or other adducts (such as BnN₃/propane-1,2-diol or

BnN₃/ethylene glycol), which favours the overlap with the corresponding dipolarophile HOMO (coming from the alkyne), enhancing then the reactivity (major rate) in glycerol.

Moreover, the reactivity of the cycloaddition was improved under microwave dielectric heating, proving that glycerol possesses unique properties that make it a useful solvent under microwave irradiation. Its ability to form multiple hydrogen bonds turns into a relaxation time much higher than other protic solvents and this is probably the key of the good behaviour of glycerol as solvent in microwave-assisted transformations.

In summary, metal-free AAC in glycerol, in particular under microwave activation, can be an interesting methodology for the synthesis of a wide range of fully substituted 1,2,3-triazoles, useful molecules in different fields, such as biochemistry and medicinal chemistry.

2.4 Experimental section

General

All manipulations were performed using standard Schlenk techniques under argon atmosphere unless otherwise noted.

Commercially available compounds (except glycerol) were used without previous purification. Glycerol (from Sigma- Aldrich, ≥99.5% purity) was heated overnight at 80 °C under vacuum before use. After that, it was kept under inert atmosphere. Benzyl azide (**a**),^[39] 1-phenyl-2-trimethylsilylacetylene (**9**)^[40] and *tert*-butyl dimethyl(phenylethynyl)silane **10**^[41] were prepared according to the literature procedure.

Three different **microwave reactors** were used during this work: (a) single-mode microwave CEM Explorer SP 48, 2.45 GHz, Max Power 300 W Synthesis System, (b) CEM Focused Microwave™ Synthesis System Model Discover and (c) Anton Paar Monowave 300.

Theoretical studies were carried out by Prof. Montserrat Gómez using the following software: SPARTAN'14 for Windows and Linux, Wavefunction, InC. 18401 Von Karmaan Avenue, suite 307, Irvine, CA 92612, USA. Calculations were carried out with Density Functional B3LYP by using the basis set 6-31 G*.

NMR spectra were recorded in CDCl₃ (unless otherwise cited) using a Fourier 300 MHz Bruker, a Bruker Avance 400 Ultrashield or a Bruker Avance 500 Ultrashield apparatus at 298 K. ¹H NMR spectroscopy chemical shifts are quoted in ppm relative to tetramethylsilane (TMS). Chemical

shifts are given in δ and coupling constants in Hz. ^{13}C NMR spectra are decoupled from ^1H and the chemical shifts are quoted in ppm relative to CDCl_3 ($\delta = 77.16$).

GC analyses were carried out on an Agilent GC6890 with a flame ionization detector using SGE BPX5 column composed of 5% of phenylmethylsiloxane.

Elemental analyses CHN were performed on a Thermo FlashEA 1112 elemental analyzer and F on a Metrohm761 Compact Ion Chromatograph (IC) at MedacLtd, United Kingdom.

FAB mass spectra were obtained on a Fisons V6-Quattro instrument, ESI mass spectra were obtained on a Waters LCT Premier Instrument and CI and EI spectra were obtained on a Waters GCT spectrometer.

IR spectra were recorded on a Bruker Tensor 27 FT-IR spectrometer and absorptions reported in wavenumbers (cm^{-1}).

Flash chromatography was carried out using 60 mesh silica gel and dry-packed columns or with a Teledyne Isco CombiFlash system with UV detector. Thin layer chromatography was carried out using Merck TLC Silicagel 60 F254 aluminum sheets. Components were visualized by UV light ($\lambda = 254 \text{ nm}$) and stained with KMnO_4 or phosphomolybdic acid dip.

Experimental procedures

General procedure for the azide-alkyne cycloaddition (GP1)

A sealed tube equipped with a stirring bar was successively charged with the corresponding alkyne (0.60 mmol) and the corresponding solvent (1 mL). The mixture was stirred at room temperature for 5 min. The azide (0.40 mmol) was then added and the tube was sealed. The mixture was magnetically stirred for the indicated time at the appropriate temperature or placed into the microwave reactor (100 °C, 250 W) for 30 min (or the appropriate time). It is important to note that, in the case of glycerol, ethylene glycol, water or 1,2- or 1,3-propanediol, the reaction mixture gave a kind of emulsion at room temperature, but at 100 °C a homogeneous solution was obtained (*i.e.* reagents and products were soluble). Using the mentioned solvents, the organic products were extracted with dichloromethane (6 x 2 mL). The combined chlorinated organic layers were filtered through a Celite pad and the resulting filtrate was concentrated under reduced pressure. When other solvents such as ethanol, 1,4-dioxane and fluorobenzene were used, the reaction mixture was homogeneous even at room

temperature. For these cases, the solvent was directly concentrated under reduced pressure at the end of the reaction. The products were purified by chromatography (silica short column, eluent: cyclohexane/EtOAc 1:1).

General procedure for the azide-alkyne cycloaddition using a copper catalyst (GP2)

A sealed tube equipped with a stirring bar was successively charged with copper catalyst (2.5 mol%) and the corresponding solvent (1 mL). The suspension was stirred at room temperature for 5 min. The alkyne (0.60 mmol) was added and the solution was stirred for a further 5 min. The organic azide (0.40 mmol) was also added to the mixture and the tube was sealed. The mixture was magnetically stirred for the indicated time at the appropriate temperature or placed into the microwave reactor (100 °C, 250 W) for 30 min (or the appropriate time). In the case of glycerol, ethylene glycol, water or 1,2- or 1,3-propanediol the organic products were extracted with dichloromethane (6 x 2 mL). The combined chlorinated organic layers were filtered through a Celite pad and the resulting filtrate was concentrated under reduced pressure. With other solvents such as ethanol, 1,4-dioxane and fluorobenzene, the solvent was directly concentrated under reduced pressure at the end of the reaction. The products were purified by chromatography (silica short column, eluent: cyclohexane/EtOAc 1:1).

Desilylation of **maj-9a**^[42]

To a solution of **9a** (120 mg, 0.4 mmol) in anhydrous THF (4 mL) was added a solution of TBAF (1 M in THF, 2 eq). The mixture was stirred overnight at rt. The reaction was then quenched with a saturated solution of NH₄Cl (20 mL) and extracted with EtOAc (3 x 10 mL). The organic phase was dried over MgSO₄ and concentrated under reduced pressure.

Desilylation of **10a**^[42]

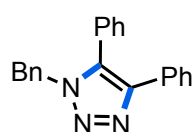
To a solution of **10a** (120 mg, 0.4 mmol) in anhydrous THF (4 mL) was added a solution of TBAF (1 M in THF, 3 eq). The mixture was stirred overnight at 50 °C. The reaction was then quenched with a saturated solution of NH₄Cl (20 mL) and extracted with EtOAc (3 x 10 mL). The organic phase was dried over MgSO₄ and concentrated under reduced pressure.

Silylation of glycerol

1*H*-Imidazole (1.63 g, 2.2 mmol) was dissolved in anhydrous DMF (60 mL) in a Schlenk flask under Ar atmosphere. After the addition of glycerol (9.92 g, 10 mmol), the solution was cooled

to 0 °C. Chlorotrimethylsilane (1.38 mL, 10.8 mmol) was then added dropwise during approximately 45 minutes. The reaction mixture was stirred during 5 h at 0 °C. After this period, Et₂O (60 mL) and brine (60 mL) were added to quench the reaction. The aqueous layer was further extracted with Et₂O (3 x 60 mL). The combined organic layers were washed with water (2 x 30 mL) and then dried over anhydrous MgSO₄, filtered and concentrated under vacuum. The product obtained was purified by chromatography (silica, short column) using cyclohexane/EtOAc 1:1 as eluent.

Characterization of organic compounds

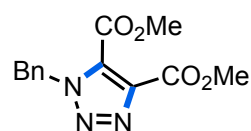


1-Benzyl-4,5-diphenyl-1H-1,2,3-triazole (1a)

The product was prepared following the general procedure **GP1** and purified by flash chromatography (pentane/Et₂O 3:1). Isolated as a white solid in 85% yield (105.5 mg, 0.34 mmol). The following spectroscopic data matched with those reported in the literature.^[43]

¹H NMR (300 MHz, CDCl₃): δ 5.45 (s, 2H, CH₂), 7.03–7.11 (m, 2H, H_{Ar}), 7.16–7.22 (m, 2H, H_{Ar}), 7.24–7.34 (m, 6H, H_{Ar}), 7.41–7.55 (m, 3H, H_{Ar}), 7.58–7.64 (m, 2H, H_{Ar}).

¹³C NMR (75 MHz, CDCl₃): δ 52.1 (CH₂), 126.7 (CH_{Ar}), 127.5 (CH_{Ar}), 127.7 (CH_{Ar}), 127.9 (C_{Ar}), 128.2 (CH_{Ar}), 128.5 (CH_{Ar}), 128.7 (CH_{Ar}), 129.2 (CH_{Ar}), 129.7 (CH_{Ar}), 130.1 (CH_{Ar}), 130.9 (C_{Ar}), 133.9 (C_{Ar}), 135.4 (C_{Ar}), 144.5 (C_{Ar}).

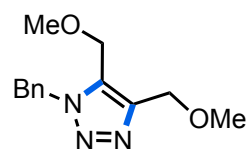


Dimethyl 1-benzyl-1H-1,2,3-triazole-4,5-dicarboxylate (2a)

The product was prepared following the general procedure **GP1** and purified by flash chromatography (cyclohexane/EtOAc 3:1). Isolated as a yellow oil in 68% yield (75 mg, 0.27 mmol). The following spectroscopic data matched with those reported in the literature.^[44]

¹H NMR (400 MHz, CDCl₃): δ 3.87 (s, 3H, CH₃), 3.95 (s, 3H, CH₃), 5.80 (s, 2H, CH₂), 7.23–7.29 (m, 2H, H_{Ar}), 7.30–7.37 (m, 3H, H_{Ar}).

¹³C NMR (100 MHz, CDCl₃): δ 52.7 (CH₂ or CH₃), 53.3 (CH₂ or CH₃), 53.9 (CH₂ or CH₃), 128.0 (CH_{Ar}), 128.8 (CH_{Ar}), 128.9 (CH_{Ar}), 129.8 (C_{Ar}), 133.9 (C_{Ar}), 140.2 (C_{Ar}), 158.8 (C=O), 160.4 (C=O).



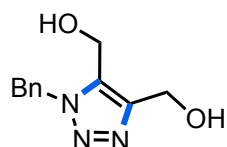
1-Benzyl-4,5-bis(methoxymethyl)-1H-1,2,3-triazole (3a)

The product was prepared following the general procedure **GP1** and purified by flash chromatography (cyclohexane/EtOAc 2:1). Isolated as a yellow oil in 88% yield (86.8 mg, 0.35 mmol). The following spectroscopic

data matched with those reported in the literature.^[45]

¹H NMR (300 MHz, CDCl₃): δ 3.28 (s, 3H, CH₃), 3.39 (s, 3H, CH₃), 4.40 (s, 2H, CH₂), 4.59 (s, 2H, CH₂), 5.62 (s, 2H, CH₂), 7.21–7.29 (m, 2H, H_{Ar}), 7.30–7.40 (m, 3H, H_{Ar}).

¹³C NMR (75 MHz, CDCl₃): δ 52.6 (CH₂), 58.1 (CH₃), 58.2 (CH₃), 61.5 (CH₂), 65.3 (CH₂), 127.6 (CH_{Ar}), 128.4 (CH_{Ar}), 128.9 (CH_{Ar}), 131.5 (C_{Ar}), 134.7 (C_{Ar}), 143.7 (C_{Ar}).

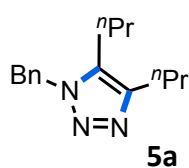


1-Benzyl-4,5-bis(hydroxymethyl)-1H-1,2,3-triazole (4a)

The product was prepared following the general procedure **GP1** and purified by flash chromatography (EtOAc). Isolated as a white solid in 46% yield (40 mg, 0.18 mmol). The following spectroscopic data matched with those reported in the literature.^[46]

¹H NMR (400 MHz, MeOH-*d*₄): δ 4.72 (s, 2H, CH₂), 4.77 (s, 2H, CH₂), 5.75 (s, 2H, CH₂), 7.31–7.49 (m, 5H, H_{Ar}).

¹³C NMR (100 MHz, MeOH-*d*₄): δ 51.2 (CH₂), 51.8 (CH₂), 54.3 (CH₂), 127.3 (CH_{Ar}), 127.9 (CH_{Ar}), 128.5 (CH_{Ar}), 134.5 (C_{Ar}), 135.2 (C_{Ar}), 144.9 (C_{Ar}).



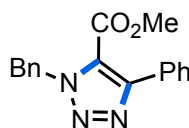
1-Benzyl-4,5-dipropyl-1H-1,2,3-triazole (5a)

The product was prepared following the general procedure **GP1** and purified by flash chromatography (cyclohexane/EtOAc 8:2). Isolated as a yellow oil in 69% yield (66.8 mg, 0.27 mmol). The following spectroscopic data matched with those reported in the literature.^[47]

¹H NMR (400 MHz, CDCl₃): δ 0.85 (t, ³J = 7.4 Hz, 3H, CH₃), 0.97 (t, ³J = 7.4 Hz, 3H, CH₃), 1.36 (tq, ³J = 7.7 Hz, ³J = 7.4 Hz, 2H, CH₂), 1.73 (tq, ³J = 7.7 Hz, ³J = 7.4 Hz, 2H, CH₂), 2.46 (t, ³J = 7.7 Hz, 2H, CH₂), 2.59 (t, ³J = 7.7 Hz, 2H, CH₂), 5.48 (s, 2H, CH₂), 7.10–7.18 (m, 2H, H_{Ar}), 7.26–7.37 (m, 3H, H_{Ar}).

¹³C NMR (100 MHz, CDCl₃): δ 13.8 (CH₃), 14.0 (CH₃), 22.1 (CH₂), 22.9 (CH₂), 24.5 (CH₂), 27.2 (CH₂), 51.9 (CH₂), 127.0 (CH_{Ar}), 128.1 (CH_{Ar}), 128.8 (CH_{Ar}), 133.0 (C_{Ar}), 135.6 (C_{Ar}), 145.5 (C_{Ar}).

Compound **6a** was obtained as a nearly equimolar mixture of both regioisomers (**maj-6a** and **min-6a**, 57:43). They were separated by flash chromatography (cyclohexane/EtOAc 10:1) for characterization. 2D-HMBC experiment was recorded to assign the regiochemistry.



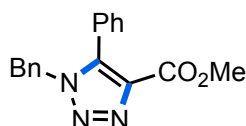
Methyl 1-benzyl-4-phenyl-1H-1,2,3-triazole-5-carboxylate (**min-6a**)

The product was prepared following the general procedure **GP1**. Isolated as a colorless oil in 51% yield (60.1 mg, 0.20 mmol). The following spectroscopic

data matched with those reported in the literature.^[48]

¹H NMR (400 MHz, CDCl₃): δ 3.80 (s, 3H, CH₃), 5.96 (s, 2H, CH₂), 7.30–7.50 (m, 7H, H_{Ar}), 7.70–7.76 (m, 3H, H_{Ar}).

¹³C NMR (100 MHz, CDCl₃): δ 52.3 (CH₂ or CH₃), 54.3 (CH₂ or CH₃), 123.8 (C_{Ar}), 127.9 (CH_{Ar}), 128.1 (CH_{Ar}), 128.4 (CH_{Ar}), 128.8 (CH_{Ar}), 129.0 (CH_{Ar}), 129.3 (CH_{Ar}), 130.2 (C_{Ar}), 135.1 (C_{Ar}), 150.6 (C_{Ar}), 159.6 (C=O).



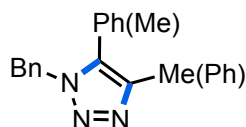
Methyl 1-benzyl-5-phenyl-1H-1,2,3-triazole-4-carboxylate (maj-6a)

The product was prepared following the general procedure **GP1**. Isolated as a colorless oil in 48% yield (56.3 mg, 0.19 mmol). The following spectroscopic data matched with those reported in the literature.^[49]

¹H NMR (400 MHz, CDCl₃): δ 3.85 (s, 3H, CH₃), 5.45 (s, 2H, CH₂), 6.98–7.05 (m, 2H, H_{Ar}), 7.19–7.32 (m, 5H, H_{Ar}), 7.42–7.56 (m, 3H, H_{Ar}).

¹³C NMR (100 MHz, CDCl₃): δ 51.9 (CH₂ or CH₃), 52.2 (CH₂ or CH₃), 125.8 (C_{Ar}), 127.5 (CH_{Ar}), 128.4 (CH_{Ar}), 128.6 (CH_{Ar}), 128.8 (CH_{Ar}), 129.7 (CH_{Ar}), 130.2 (CH_{Ar}), 134.5 (C_{Ar}), 136.8 (C_{Ar}), 141.4 (C_{Ar}), 161.3 (C=O).

Compound **7a** was obtained as a nearly equimolar mixture of both regioisomers (**maj-7a** and **min-7a**, 57:43). 2D-NOESY experiment was recorded to assign the regiochemistry.



1-Benzyl-5(4)-methyl-4(5)-phenyl-1H-1,2,3-triazole (**7a**)

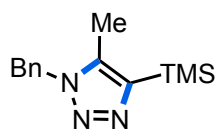
The product was prepared following the general procedure **GP1** and purified by flash chromatography (cyclohexane/EtOAc 3:1). Isolated as a yellow oil in 44% yield (44 mg, 0.18 mmol). The following spectroscopic data matched with those reported in the literature.^[50]

Signals of 1-benzyl-4-methyl-5-phenyl-1H-1,2,3-triazole (**maj-7a**) are marked with (*).

¹H NMR (400 MHz, CDCl₃): δ 2.32 (s, 3H*), 2.35 (s, 3H), 5.44 (s, 2H*), 5.57 (s, 2H), 7.01–7.08 (m, 2H*), 7.13–7.19 (m, 2H*), 7.20–7.25 (m, 2H), 7.26–7.29 (m, 3H*), 7.32–7.40 (m, 4H), 7.42–7.49 (m, 3H* + 2H), 7.68–7.75 (m, 2H).

¹³C NMR (100 MHz, CDCl₃): δ 9.2, 10.7*, 52.0, 52.1*, 127.1, 127.1, 127.3*, 127.5, 127.6*, 128.1*, 128.3, 128.7, 128.7*, 128.9, 129.0 (129.0*), 129.2*, 129.5*, 131.6, 134.6*, 134.8, 135.6*, 141.6*, 145.0.

Compound **8a** was obtained as an enriched mixture of both regioisomers (9:1). 2D-NOESY was recorded to assign the regiochemistry. Only **maj-8a** was described.


1-Benzyl-5-methyl-4-(trimethylsilyl)-1H-1,2,3-triazole (maj-8a)

The product was prepared following the general procedure **GP1** and purified by flash chromatography (cyclohexane/EtOAc 5:1). Isolated as a yellow oil in 54% yield (53.4 mg, 0.22 mmol).

$^1\text{H NMR}$ (500 MHz, CDCl_3): δ 0.35 (s, 9H, $\text{Si}(\text{CH}_3)_3$), 2.22 (s, 3H, CH_3), 5.51 (s, 2H, CH_2), 7.15–7.20 (m, 2H, H_{Ar}), 7.27–7.39 (m, 3H, H_{Ar}).

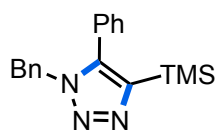
$^{13}\text{C NMR}$ (125 MHz, CDCl_3): δ -0.9 ($\text{Si}(\text{CH}_3)_3$), 9.3 (CH_3), 51.2 (CH_2), 127.2 (CH_{Ar}), 128.1 (CH_{Ar}), 128.9 (CH_{Ar}), 135.1 (C_{Ar}), 138.1 (C_{Ar}), 143.8 (C_{Ar}).

IR (neat): ν 1606 (C=C), 1497 (N=N), 1416 (Si-C), 1248 (C-N) cm^{-1} .

HRMS (ESI $^+$): m/z $[\text{M}+\text{H}]^+$ calculated for $\text{C}_{13}\text{H}_{20}\text{N}_3\text{Si}$: 246.1412; found: 246.1421.

Elemental analysis calculated (%) for $\text{C}_{13}\text{H}_{19}\text{N}_3\text{Si}$: C 63.63, H 7.80, N 17.11; found: C 63.22, H 7.88, N 16.94.

Compound **9a** was obtained as an enriched mixture of both regioisomers (9:1). The assignment was done after desilylation obtaining triazole **11a**. Only **maj-9a** was described.

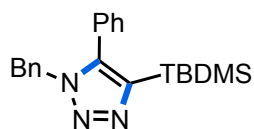

1-Benzyl-5-phenyl-4-(trimethylsilyl)-1H-1,2,3-triazole (maj-9a)

The product was prepared following the general procedure **GP1** and purified by flash chromatography (cyclohexane/EtOAc 6:1). Isolated as a yellow oil in 91% yield (111.8 mg, 0.36 mmol). The following spectroscopic data matched with those reported in the literature.^[31a]

$^1\text{H NMR}$ (400 MHz, CDCl_3): δ 0.15 (s, 9H, $\text{Si}(\text{CH}_3)_3$), 5.38 (s, 2H, CH_2), 6.98–7.04 (m, 2H, H_{Ar}), 7.07–7.13 (m, 2H, H_{Ar}), 7.22–7.28 (m, 3H, H_{Ar}), 7.36–7.47 (m, 3H, H_{Ar}).

$^{13}\text{C NMR}$ (100 MHz, CDCl_3): δ -0.9 ($\text{Si}(\text{CH}_3)_3$), 51.4 (CH_2), 127.6 (CH_{Ar}), 128.0 (CH_{Ar}), 128.4 (CH_{Ar}), 128.6 (CH_{Ar}), 128.6 (CH_{Ar}), 129.4 (CH_{Ar}), 130.0 (C_{Ar}), 135.6 (C_{Ar}), 143.5 (C_{Ar}), 145.0 (C_{Ar}).

Compound **10a** was the only regioisomer obtained. The assignment was done after desilylation obtaining triazole **11a**.


1-Benzyl-4-(tert-butyldimethylsilyl)-5-phenyl-1H-1,2,3-triazole (10a)

The product was prepared following the general procedure **GP1** and purified by flash chromatography (cyclohexane/EtOAc 3:1). Isolated as a yellow oil in 92% yield (128.5 mg, 0.37 mmol).

$^1\text{H NMR}$ (500 MHz, CDCl_3): δ 0.05 (s, 6H, $\text{Si}(\text{CH}_3)_2$), 0.90 (s, 9H, $\text{C}(\text{CH}_3)_3$), 5.35 (s, 2H, CH_2), 6.94–7.00 (m, 2H, H_{Ar}), 7.05–7.10 (m, 2H, H_{Ar}), 7.21–7.28 (m, 3H, H_{Ar}), 7.35–7.40 (m, 2H, H_{Ar}), 7.43–7.48 (m, 1H, H_{Ar}).

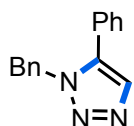
$^{13}\text{C NMR}$ (125 MHz, CDCl_3): δ -5.3 ($\text{Si}(\text{CH}_3)_2$), 26.6 ($\text{C}(\text{CH}_3)_3$), 51.4 (CH_2), 127.6 (CH_{Ar}), 127.9 (CH_{Ar}), 128.2 (CH_{Ar}), 128.5 (CH_{Ar}), 128.8 (C_{Ar} or $\text{C}(\text{CH}_3)_3$), 129.3 (CH_{Ar}), 130.4 (CH_{Ar}), 135.6 (C_{Ar} or $\text{C}(\text{CH}_3)_3$), 142.8 (C_{Ar} or $\text{C}(\text{CH}_3)_3$), 144.1 (C_{Ar} or $\text{C}(\text{CH}_3)_3$), 173.4 (C_{Ar} or $\text{C}(\text{CH}_3)_3$).

IR (neat): ν 1606 (C=C), 1497 (N=N), 1456 (Si–C), 1249 (C–N) cm^{-1} .

HRMS (ESI⁺): m/z $[\text{M}+\text{H}]^+$ calculated for $\text{C}_{21}\text{H}_{28}\text{N}_3\text{Si}$: 350.2050; found: 350.2047.

Elemental analysis calculated (%) for $\text{C}_{21}\text{H}_{27}\text{N}_3\text{Si}$: C 72.16, H 7.79, N 12.02; found: C 72.24, H 8.27, N 11.87.

1-Benzyl-5-phenyl-1H-1,2,3-triazole (11a)

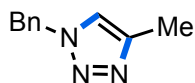


The product was prepared following the procedure of desilylation of **maj-9a** and purified by flash chromatography (CombiFlash[®] system, 4 g SiO_2 cartridge, 1st eluent: cyclohexane, 2nd eluent: 90:10 cyclohexane/EtOAc). Isolated as a white solid in 82% yield (77.5 mg, 0.33 mmol). Alternatively, the title compound was also obtained following the procedure of desilylation of **10a**. 2D-NOESY was recorded to assign the regiochemistry. The following spectroscopic data matched with those reported in the literature.^[43]

$^1\text{H NMR}$ (400 MHz, CDCl_3): δ 5.57 (s, 2H, CH_2), 7.05–7.15 (m, 2H, H_{Ar}), 7.25–7.36 (m, 5H, H_{Ar}), 7.39–7.50 (m, 3H, H_{Ar}), 7.77 (s, 1H, CH).

$^{13}\text{C NMR}$ (125 MHz, CDCl_3): δ 51.8 (CH_2), 126.9 (CH), 127.1 (CH_{Ar}), 128.1 (CH_{Ar}), 128.8 (CH_{Ar}), 128.9 (CH_{Ar}), 128.9 (CH_{Ar}), 129.5 (CH_{Ar}), 133.3 (C_{Ar}), 135.5 (C_{Ar}), 138.1 (C_{Ar}).

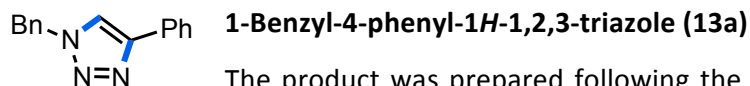
1-Benzyl-4-methyl-1H-1,2,3-triazole (12a)



The product was prepared following the general procedure GP2 and purified by flash chromatography (pentane/Et₂O 3:1). Isolated as a yellow oil in 30% yield (21.1 mg, 0.12 mmol). 2D-NOESY was recorded to assign the regiochemistry. The following spectroscopic data matched with those reported in the literature.^[51]

$^1\text{H NMR}$ (500 MHz, CDCl_3): δ 2.34 (s, 3H, CH_3), 5.50 (s, 2H, CH_2), 7.21 (s, 1H, CH), 7.26–7.30 (m, 2H, H_{Ar}), 7.34–7.42 (m, 3H, H_{Ar}).

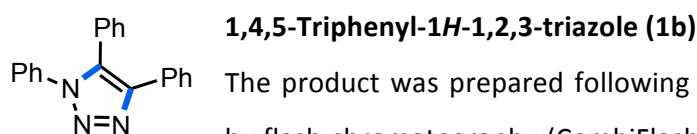
$^{13}\text{C NMR}$ (100 MHz, CDCl_3): δ 10.9 (CH_3), 53.9 (CH_2), 121.0 (CH), 128.0 (CH_{Ar}), 128.6 (CH_{Ar}), 129.0 (CH_{Ar}), 135.0 (C_{Ar}), 143.8 (C_{Ar}).



The product was prepared following the general procedure GP2 and purified by flash chromatography (pentane/Et₂O 2:1). Isolated as a white solid in 57% yield (53.5 mg, 0.23 mmol). 2D-NOESY was recorded to assign the regiochemistry. The following spectroscopic data matched with those reported in the literature.^[52]

¹H NMR (300 MHz, CDCl₃): δ 5.61 (s, 2H, CH₂), 7.27–7.51 (m, 8H, H_{Ar}), 7.70 (s, 1H, CH), 7.81–7.88 (m, 2H, H_{Ar}).

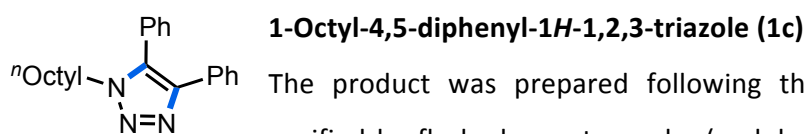
¹³C NMR (100 MHz, CDCl₃): δ 54.2 (CH₂), 119.5 (CH), 125.7 (CH_{Ar}), 128.1 (CH_{Ar}), 128.1 (CH_{Ar}), 128.8 (CH_{Ar}), 128.8 (CH_{Ar}), 129.2 (CH_{Ar}), 130.6 (C_{Ar}), 134.7 (C_{Ar}), 148.2 (C_{Ar}).



The product was prepared following the general procedure GP1 and purified by flash chromatography (CombiFlash® system, 12 g SiO₂ cartridge, 1st eluent: cyclohexane, 2nd eluent: 90:10 cyclohexane/EtOAc). Isolated as a white solid in 24% yield (28.1 mg, 0.09 mmol). The following spectroscopic data matched with those reported in the literature.^[50b]

¹H NMR (500 MHz, CDCl₃): δ 7.21–7.26 (m, 2H, H_{Ar}), 7.31–7.36 (m, 5H, H_{Ar}), 7.36–7.46 (m, 6H, H_{Ar}), 7.63 (dd, *J* = 8.1 Hz, *J* = 2.0 Hz, 2H, H_{Ar}).

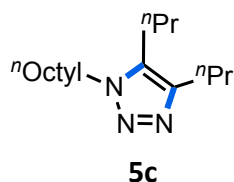
¹³C NMR (125 MHz, CDCl₃): δ 125.2 (CH_{Ar}), 127.4 (CH_{Ar}), 127.7 (C_{Ar}), 127.9 (CH_{Ar}), 128.5 (CH_{Ar}), 128.9 (CH_{Ar}), 129.0 (CH_{Ar}), 129.1 (CH_{Ar}), 129.4 (CH_{Ar}), 130.2 (CH_{Ar}), 130.8 (CH_{Ar}), 133.7 (C_{Ar}), 136.6 (C_{Ar}), 144.8 (C_{Ar}).



The product was prepared following the general procedure GP1 and purified by flash chromatography (cyclohexane/EtOAc 10:1). Isolated as a yellow oil in 73% yield (97.9 mg, 0.29 mmol). The following spectroscopic data matched with those reported in the literature.^[53]

¹H NMR (500 MHz, CDCl₃): δ 0.88 (t, ³*J* = 7.1, 3H, CH₃), 1.16–1.32 (m, 10H, CH₂), 1.80 (m, 2H, CH₂), 4.22 (t, ³*J* = 7.4 Hz, 2H, CH₂), 7.22–7.31 (m, 3H, H_{Ar}), 7.33–7.38 (m, 2H, H_{Ar}), 7.51–7.55 (m, 3H, H_{Ar}), 7.55–7.59 (m, 2H, H_{Ar}).

¹³C NMR (125 MHz, CDCl₃): δ 14.1 (CH₃), 22.6 (CH₂), 26.4 (CH₂), 28.8 (CH₂), 29.0 (CH₂), 30.1 (CH₂), 31.7 (CH₂), 48.3 (CH₂), 126.8 (CH_{Ar}), 127.6 (CH_{Ar}), 128.3 (C_{Ar}), 128.4 (CH_{Ar}), 129.3 (CH_{Ar}), 129.6 (CH_{Ar}), 130.0 (CH_{Ar}), 131.1 (C_{Ar}), 133.6 (C_{Ar}), 144.1 (C_{Ar}).

**1-Octyl-4,5-dipropyl-1H-1,2,3-triazole (5c)**

The product was prepared following the general procedure GP1 and purified by flash chromatography (cyclohexane/EtOAc 10:1). Isolated as a yellow oil in 28% yield (30.2 mg, 0.11 mmol).

$^1\text{H NMR}$ (500 MHz, CDCl_3): δ 0.89 (t, $^3J = 7.0$ Hz, 3H, CH_3), 0.98 (t, $^3J = 7.4$ Hz, 3H, CH_3), 0.98 (t, $^3J = 7.4$ Hz, 3H, CH_3), 1.20–1.40 (m, 10H, CH_2), 1.53–1.62 (m, 2H, CH_2), 1.68–1.77 (m, 2H, CH_2), 1.83–1.96 (m, 2H, CH_2), 2.55–2.61 (m, 4H, CH_2), 4.16–4.20 (m, 2H, CH_2).

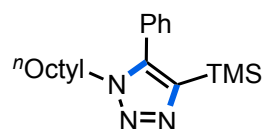
$^{13}\text{C NMR}$ (100 MHz, CDCl_3): δ 13.8 (CH_3), 14.0 (CH_3), 14.0 (CH_3), 22.6 (CH_2), 22.6 (CH_2), 22.9 (CH_2), 24.5 (CH_2), 26.7 (CH_2), 27.2 (CH_2), 29.1 (CH_2), 29.7 (CH_2), 30.3 (CH_2), 31.7 (CH_2), 47.9 (CH_2), 132.4 (C_{Ar}), 144.7 (C_{Ar}).

IR (neat): ν 1611 (C=C), 1570 (N=N), 1544 (Si–C), 1247 (C–N) cm^{-1} .

HRMS (ESI $^+$): m/z [M+H] $^+$ calculated for $\text{C}_{16}\text{H}_{32}\text{N}_3$: 266.2591; found: 266.2594.

Elemental analysis calculated (%) for $\text{C}_{16}\text{H}_{31}\text{N}_3$: C 72.40, H 11.77, N 15.83; found: C 72.13, H 12.28, N 15.53.

Compound **9c** was obtained as an enriched mixture of both regioisomers (9:1). Only **maj-9c** was described.

**1-Octyl-5-phenyl-4-(trimethylsilyl)-1H-1,2,3-triazole (maj-9c)**

The product was prepared following the general procedure GP1 and purified by flash chromatography (cyclohexane/EtOAc 10:1). Isolated as a white solid in 76% yield (100.8 mg, 0.30 mmol). The following spectroscopic data matched with those reported in the literature.^[54]

$^1\text{H NMR}$ (500 MHz, CDCl_3): δ 0.14 (s, 9H, $\text{Si}(\text{CH}_3)_3$), 0.87 (t, $^3J = 7.1$ Hz, 3H, CH_3), 1.15–1.33 (m, 10H, CH_2), 1.72–1.80 (m, 2H, CH_2), 4.15 (t, $^3J = 7.4$ Hz, 2H, CH_2), 7.24–7.30 (m, 2H, H_{Ar}), 7.47–7.52 (m, 3H, H_{Ar}).

$^{13}\text{C NMR}$ (125 MHz, CDCl_3): δ -0.9 ($\text{Si}(\text{CH}_3)_3$), 14.0 (CH_3), 22.6 (CH_2), 26.4 (CH_2), 28.8 (CH_2), 28.9 (CH_2), 30.3 (CH_2), 31.7 (CH_2), 47.7 (CH_2), 128.6 (CH_{Ar}), 129.1 (C_{Ar}), 129.3 (CH_{Ar}), 129.9 (CH_{Ar}), 143.2 (C_{Ar}), 144.3 (C_{Ar}).

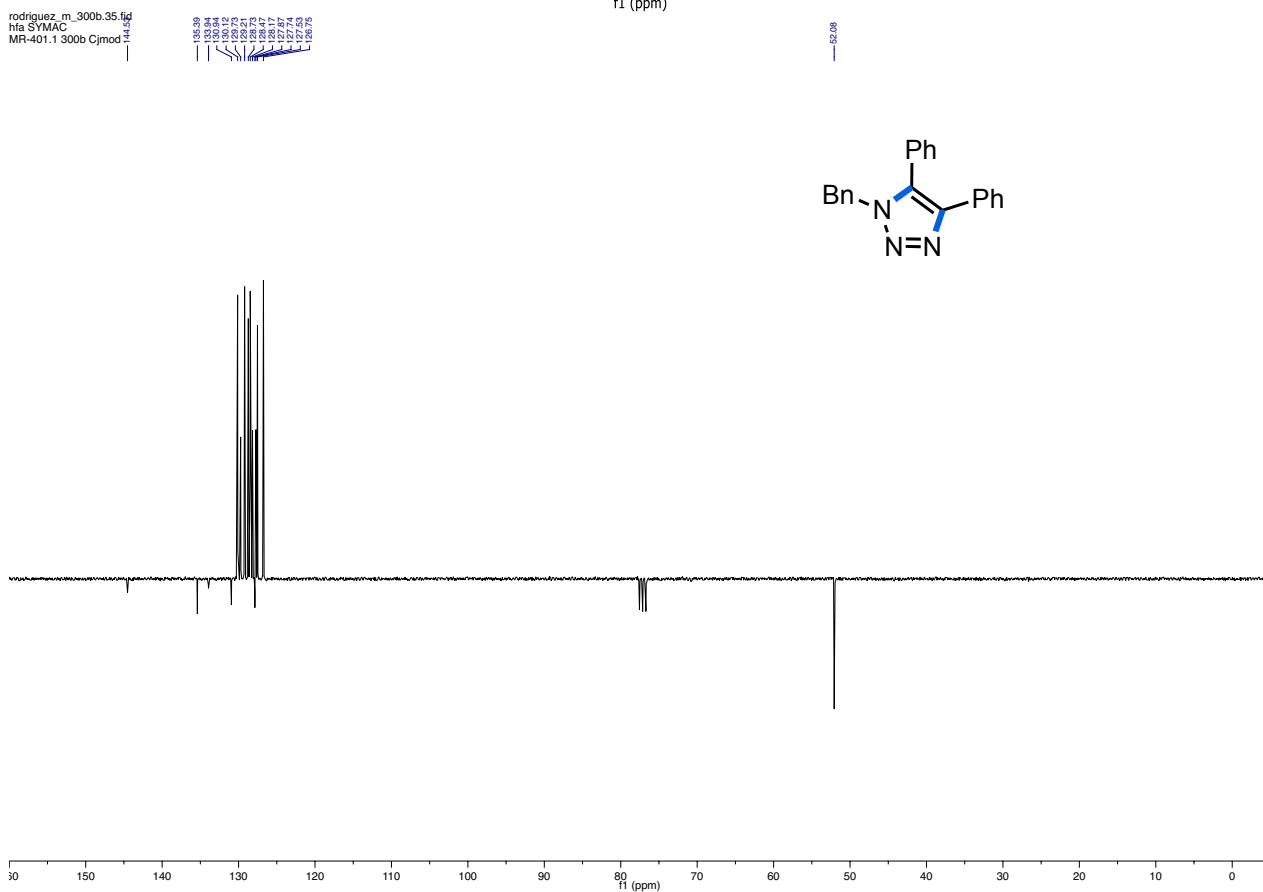
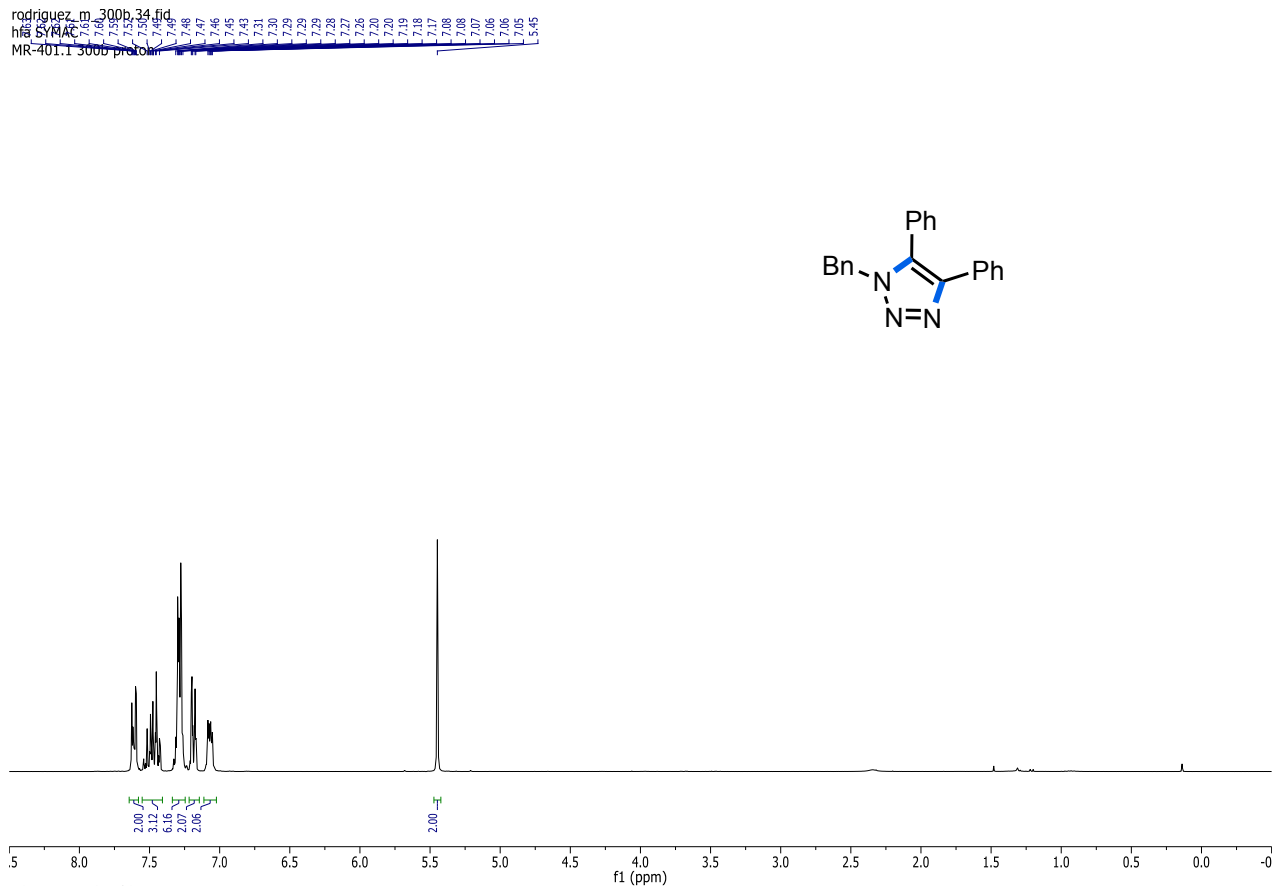
2.5 References

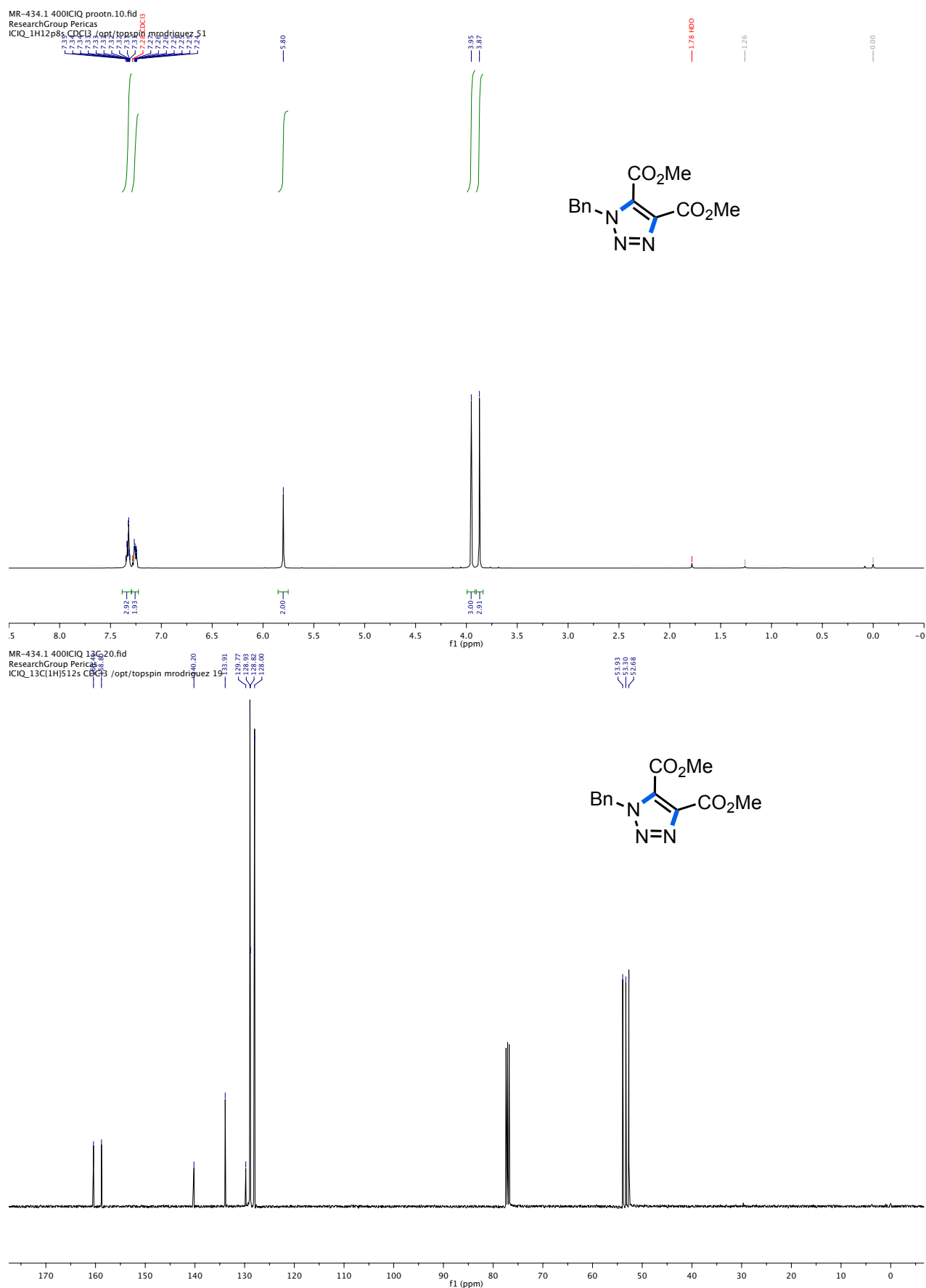
- [1] (a) H. Shu, S. Izenwasser, D. Wade, E. D. Stevens, M. L. Trudell, *Bioorg. Med. Chem. Lett.* **2009**, *19*, 891–893; (b) S. Ito, Y. Hirata, Y. Nagatomi, A. Satoh, G. Suzuki, T. Kimura, A. Satow, S. Maehara, H. Hikichi, M. Hata, H. Ohta, H. Kawamoto, *Bioorg. Med. Chem. Lett.* **2009**, *19*, 5310–5313; (c) M. Fujinaga, T. Yamasaki, K. Kawamura, K. Kumata, A. Hatori, J. Yui, K. Yanamoto, Y. Yoshida, M. Ogawa, N. Nengaki, J. Maeda, T. Fukumura, M.-R. Zhang, *Bioorg. Med. Chem.* **2011**, *19*, 102–110; (d) H. Cheng, J. Wan, M.-I. Lin, Y. Liu, X. Lu, J. Liu, Y. Xu, J. Chen, Z. Tu, Y.-S. E. Cheng, K. Ding, *J. Med. Chem.* **2012**, *55*, 2144–2153; (e) M. Taddei, S. Ferrini, L. Giannotti, M. Corsi, F. Manetti, G. Giannini, L. Vesci, F. M. Milazzo, D. Alloatti, M. B. Guglielmi, M. Castorina, M. L. Cervoni, M. Barbarino, R. Foderà, V. Carollo, C. Pisano, S. Armaroli, W. Cabri, *J. Med. Chem.* **2014**, *57*, 2258–2274.
- [2] (a) V. V. Rostovtsev, L. G. Green, V. V. Fokin, K. B. Sharpless, *Angew. Chem. Int. Ed.* **2002**, *41*, 2596–2599; (b) C. W. Tornøe, C. Christensen, M. Meldal, *J. Org. Chem.* **2002**, *67*, 3057–3064.
- [3] J. E. Hein, J. C. Tripp, L. B. Krasnova, K. B. Sharpless, V. V. Fokin, *Angew. Chem. Int. Ed.* **2009**, *48*, 8018–8021.
- [4] J. Deng, Y.-M. Wu, Q.-Y. Chen, *Synthesis* **2005**, 2730–2738.
- [5] B. C. Boren, S. Narayan, L. K. Rasmussen, L. Zhang, H. Zhao, Z. Lin, G. Jia, V. V. Fokin, *J. Am. Chem. Soc.* **2008**, *130*, 8923–8930.
- [6] S. Ding, G. Jia, J. Sun, *Angew. Chem. Int. Ed.* **2014**, *53*, 1877–1880.
- [7] F. Wei, W. Wang, Y. Ma, C.-H. Tung, Z. Xu, *Chem. Commun.* **2016**, *52*, 14188–14199.
- [8] (a) S. Chuprakov, N. Chernyak, A. S. Dudnik, V. Gevorgyan, *Org. Lett.* **2007**, *9*, 2333–2336; (b) L. Ackermann, R. Vicente, R. Born, *Adv. Synth. Catal.* **2008**, *350*, 741–748.
- [9] L. Ackermann, H. K. Potukuchi, D. Landsberg, R. Vicente, *Org. Lett.* **2008**, *10*, 3081–3084.
- [10] (a) L. M. Gaetke, C. K. Chow, *Toxicology* **2003**, *189*, 147–163; (b) J. M. Baskin, C. R. Bertozzi, *Aldrichimica Acta* **2010**, *43*, 15–23; (c) D. C. Kennedy, C. S. McKay, M. C. B. Legault, D. C. Danielson, J. A. Blake, A. F. Pegoraro, A. Stolor, Z. Mester, J. P. Pezacki, *J. Am. Chem. Soc.* **2011**, *133*, 17993–18001.
- [11] Z. Li, T. S. Seo, J. Ju, *Tetrahedron Lett.* **2004**, *45*, 3143–3146.
- [12] (a) N. J. Agard, J. A. Prescher, C. R. Bertozzi, *J. Am. Chem. Soc.* **2004**, *126*, 15046–15047; (b) N. J. Agard, J. M. Baskin, J. A. Prescher, A. Lo, C. R. Bertozzi, *ACS Chem. Biol.* **2006**, *1*, 644–648; (c) J. M. Baskin, J. A. Prescher, S. T. Laughlin, N. J. Agard, P. V. Chang, I. A. Miller, A. Lo, J. A. Codelli, C. R. Bertozzi, *Proc. Natl. Acad. Sci. U.S.A.* **2007**, *104*, 16793–16797; (d) S. T. Laughlin, J. M. Baskin, S. L. Amacher, C. R. Bertozzi, *Science* **2008**, *320*, 664–667.
- [13] G. Wittig, A. Krebs, *Chem. Ber.* **1961**, *94*, 3260–3275.
- [14] (a) A. I. Oliva, U. Christmann, D. Font, F. Cuevas, P. Ballester, H. Buschmann, A. Torrens, S. Yenes, M. A. Pericàs, *Org. Lett.* **2008**, *10*, 1617–1619; (b) R. Li, D. J. Jansen, A. Datta, *Org. Biomol. Chem.* **2009**, *7*, 1921–1930; (c) V. Declerck, L. Toupet, J. Martinez, F. Lamaty, *J. Org. Chem.* **2009**, *74*, 2004–2007; (d) E. Balducci, L. Bellucci, E. Petricci, M. Taddei, A. Tafi, *J. Org. Chem.* **2009**, *74*, 1314–1321; (e) R. A. Brawn, M. Welzel, J. T. Lowe, J. S. Panek, *Org. Lett.* **2010**, *12*, 336–339; (f) M. Sau, C. Rodríguez-Esrich, M. A. Pericàs, *Org. Lett.* **2011**, *13*, 5044–5047; (g) N. Das Adhikary, P. Chattopadhyay, *J. Org. Chem.* **2012**, *77*, 5399–5405.
- [15] (a) F. Chahdoura, C. Pradel, M. Gómez, *ChemCatChem* **2014**, *6*, 2929–2936; (b) C. Vidal, J. García-Álvarez, *Green Chem.* **2014**, *16*, 3515–3521.
- [16] (a) R. J. Giguere, T. L. Bray, S. M. Duncan, G. Majetich, *Tetrahedron Lett.* **1986**, *27*, 4945–4948; (b) R. Gedye, F. Smith, K. Westaway, H. Ali, L. Baldisera, L. Laberge, J. Rousell, *Tetrahedron Lett.* **1986**, *27*, 279–282.
- [17] C. O. Kappe, A. Stadler, *Microwaves in Organic and Medicinal Chemistry*, 1st ed., Wiley-VCH, Weinheim, **2005**.
- [18] (a) P. Lidström, J. Tierney, B. Wathey, J. Westman, *Tetrahedron* **2001**, *57*, 9225–9283; (b) C. O. Kappe, *Angew. Chem. Int. Ed.* **2004**, *43*, 6250–6284.
- [19] (a) D. M. P. Mingos, D. R. Baghurst, *Chem. Soc. Rev.* **1991**, *20*, 1–47; (b) C. Gabriel, S. Gabriel, E. H. Grant, B. S. J. Halstead, D. M. P. Mingos, *Chem. Soc. Rev.* **1998**, *27*, 213–224; (c) M. D. P. Mingos, *Microwave-Assisted Organic Synthesis* (Eds.: P. Lidström, J. P. Tierney), Blackwell, Oxford, **2005**.
- [20] P. Cintas, S. Tagliapietra, E. Calcio Gaudino, G. Palmisano, G. Cravotto, *Green Chem.* **2014**, *16*, 1056–1065.
- [21] H. Yue, Y. Zhao, X. Ma, J. Gong, *Chem. Soc. Rev.* **2012**, *41*, 4218–4244.
- [22] K. Kabiri, A. Azizi, M. J. Zohuriaan-Mehr, G. B. Marandi, H. Bouhendi, *J. Appl. Polym. Sci.* **2011**, *119*, 2759–2769.

- [23] E. J. Lenardão, M. S. Silva, R. G. Lara, J. M. Marczewski, M. Sachini, R. G. Jacob, D. Alves, G. Perin, *ARKIVOC* **2011**, *ii*, 272–282.
- [24] D. M. L. Cabrera, F. M. Líbero, D. Alves, G. Perin, E. J. Lenardão, R. G. Jacob, *Green Chem. Lett. Rev.* **2012**, *5*, 329–336.
- [25] N. Bakhrou, F. Lamaty, J. Martinez, E. Colacino, *Tetrahedron Lett.* **2010**, *51*, 3935–3937.
- [26] A. Hamel, M. Sacco, N. Mnasri, F. Lamaty, J. Martinez, F. De Angelis, E. Colacino, C. Charnay, *ACS Sustainable Chem. Eng.* **2014**, *2*, 1353–1358.
- [27] T. Deligeorgiev, S. Kaloyanova, N. Lesev, R. Alajarín, J. J. Vaquero, J. Álvarez-Builla, *GSC* **2011**, *1*, 170–175.
- [28] (a) A. Nirmala Grace, K. Pandian, *Mater. Chem. Phys.* **2007**, *104*, 191–198; (b) J. Kou, C. Bennett-Stamper, R. S. Varma, *ACS Sustainable Chem. Eng.* **2013**, *1*, 810–816; (c) J. Kou, R. S. Varma, *Chem. Commun.* **2013**, *49*, 692–694; (d) Y.-J. Zhu, F. Chen, *Chem. Rev.* **2014**, *114*, 6462–6555.
- [29] (a) M. A. Herrero, J. M. Kremsner, C. O. Kappe, *J. Org. Chem.* **2008**, *73*, 36–47; (b) D. Obermayer, C. O. Kappe, *Org. Biomol. Chem.* **2010**, *8*, 114–121; (c) C. O. Kappe, B. Pieber, D. Dallinger, *Angew. Chem. Int. Ed.* **2013**, *52*, 1088–1094; (d) C. O. Kappe, *Chem. Soc. Rev.* **2013**, *42*, 4977–4990; (e) C. O. Kappe, *Angew. Chem. Int. Ed.* **2013**, *52*, 7924–7928.
- [30] (a) A. Loupy, L. Perreux, M. Liagre, K. Burle, M. Moneuse, *Pure Appl. Chem.* **2001**, *73*, 161–166; (b) L. Perreux, A. Loupy, *Tetrahedron* **2001**, *57*, 9199–9223; (c) A. de la Hoz, A. Díaz-Ortiz, A. Moreno, *Chem. Soc. Rev.* **2005**, *34*, 164–178; (d) M. R. Rosana, Y. Tao, A. E. Stiegman, G. B. Dudley, *Chem. Sci.* **2012**, *3*, 1240–1244.
- [31] (a) J. Huang, S. J. F. Macdonald, J. P. A. Harrity, *Chem. Commun.* **2009**, 436–438; (b) L. Li, T. Shang, X. Ma, H. Guo, A. Zhu, G. Zhang, *Synlett* **2015**, 695–699.
- [32] L. Birkofer, M. Franz, *Chem. Ber.* **1972**, *105*, 1759–1767.
- [33] (a) A. Padwa, M. W. Wannamaker, *Tetrahedron* **1990**, *46*, 1145–1162; (b) D. J. Hlasta, J. H. Ackerman, *J. Org. Chem.* **1994**, *59*, 6184–6189; (c) S. J. Coats, J. S. Link, D. Gauthier, D. J. Hlasta, *Org. Lett.* **2005**, *7*, 1469–1472; (d) F. Kloss, U. Köhn, B. O. Jahn, M. D. Hager, H. Görls, U. S. Schubert, *Chem. Asian J.* **2011**, *6*, 2816–2824.
- [34] B. T. Worrell, J. A. Malik, V. V. Fokin, *Science* **2013**, *340*, 457–460.
- [35] A. Michael, *Journal für Praktische Chemie* **1893**, *48*, 94–95.
- [36] R. Huisgen, *Angew. Chem. Int. Ed.* **1963**, *2*, 565–632.
- [37] (a) R. Sustmann, *Tetrahedron Lett.* **1971**, *12*, 2717–2720; (b) K. N. Houk, J. Sims, C. R. Watts, L. J. Luskus, *J. Am. Chem. Soc.* **1973**, *95*, 7301–7315; (c) R. Huisgen, *J. Org. Chem.* **1976**, *41*, 403–419.
- [38] T. Kusukawa, G. Niwa, T. Sasaki, R. Oosawa, W. Himeno, M. Kato, *Bull. Chem. Soc. Jpn.* **2013**, *86*, 351–353.
- [39] S. G. Alvarez, M. T. Alvarez, *Synthesis* **1997**, 413–414.
- [40] H. Huang, G. Zhang, L. Gong, S. Zhang, Y. Chen, *J. Am. Chem. Soc.* **2014**, *136*, 2280–2283.
- [41] W. Uhl, D. Kovert, S. Zemke, A. Hepp, *Organometallics* **2011**, *30*, 4736–4741.
- [42] I. E. Valverde, A. F. Delmas, V. Aucagne, *Tetrahedron* **2009**, *65*, 7597–7602.
- [43] L. Zhang, X. Chen, P. Xue, H. H. Y. Sun, I. D. Williams, K. B. Sharpless, V. V. Fokin, G. Jia, *J. Am. Chem. Soc.* **2005**, *127*, 15998–15999.
- [44] S. C. Sau, S. R. Roy, T. K. Sen, D. Mullangi, S. K. Mandal, *Adv. Synth. Catal.* **2013**, *355*, 2982–2991.
- [45] T. Farooq, L. K. Sydnes, K. W. Törnroos, B. E. Haug, *Synthesis* **2012**, *44*, 2070–2078.
- [46] N. V. Dubrovina, L. Domke, I. A. Shuklov, A. Spannenberg, R. Franke, A. Villinger, A. Börner, *Tetrahedron* **2013**, *69*, 8809–8817.
- [47] B. Gold, P. Batsomboon, G. B. Dudley, I. V. Alabugin, *J. Org. Chem.* **2014**, *79*, 6221–6232.
- [48] Y. Zhou, T. Lecourt, L. Micouin, *Angew. Chem. Int. Ed.* **2010**, *49*, 2607–2610.
- [49] D. Gangaprasad, J. P. Raj, T. Kiranmye, S. S. Sadik, J. Elangovan, *RSC Adv.* **2015**, *5*, 63473–63477.
- [50] (a) J. Thomas, J. John, N. Parekh, W. Dehaen, *Angew. Chem. Int. Ed.* **2014**, *53*, 10155–10159; (b) A. B. Shashank, S. Karthik, R. Madhavachary, D. B. Ramachary, *Chem. Eur. J.* **2014**, *20*, 16877–16881.
- [51] M. S. Raghavendra, Y. Lam, *Tetrahedron Lett.* **2004**, *45*, 6129–6132.
- [52] P. Appukkuttan, W. Dehaen, V. V. Fokin, E. Van der Eycken, *Org. Lett.* **2004**, *6*, 4223–4225.
- [53] T. He, M. Wang, P. Li, L. Wang, *Chin. J. Chem.* **2012**, *30*, 979–984.
- [54] J. Huang, S. J. F. Macdonald, A. W. J. Cooper, G. Fisher, J. P. A. Harrity, *Tetrahedron Lett.* **2009**, *50*, 5539–5541.

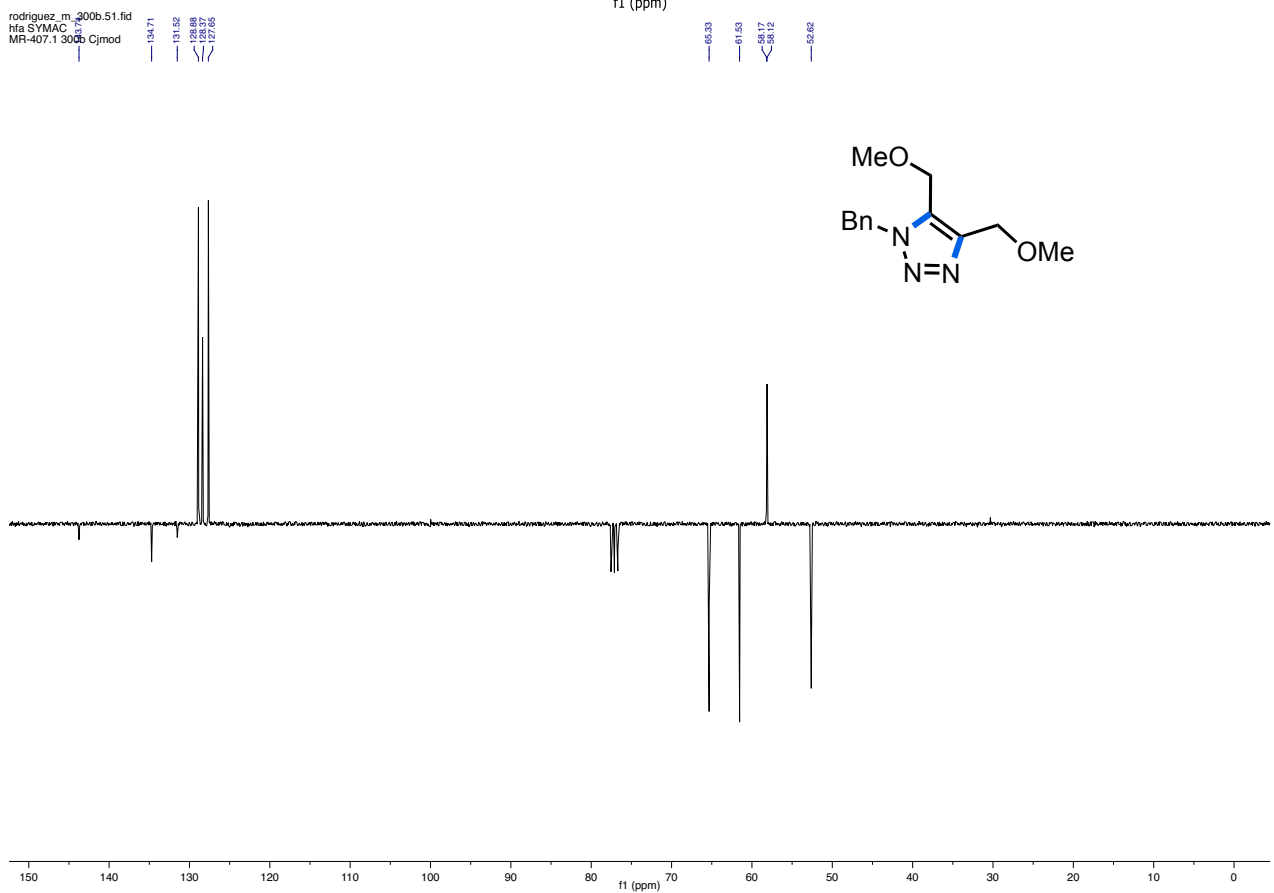
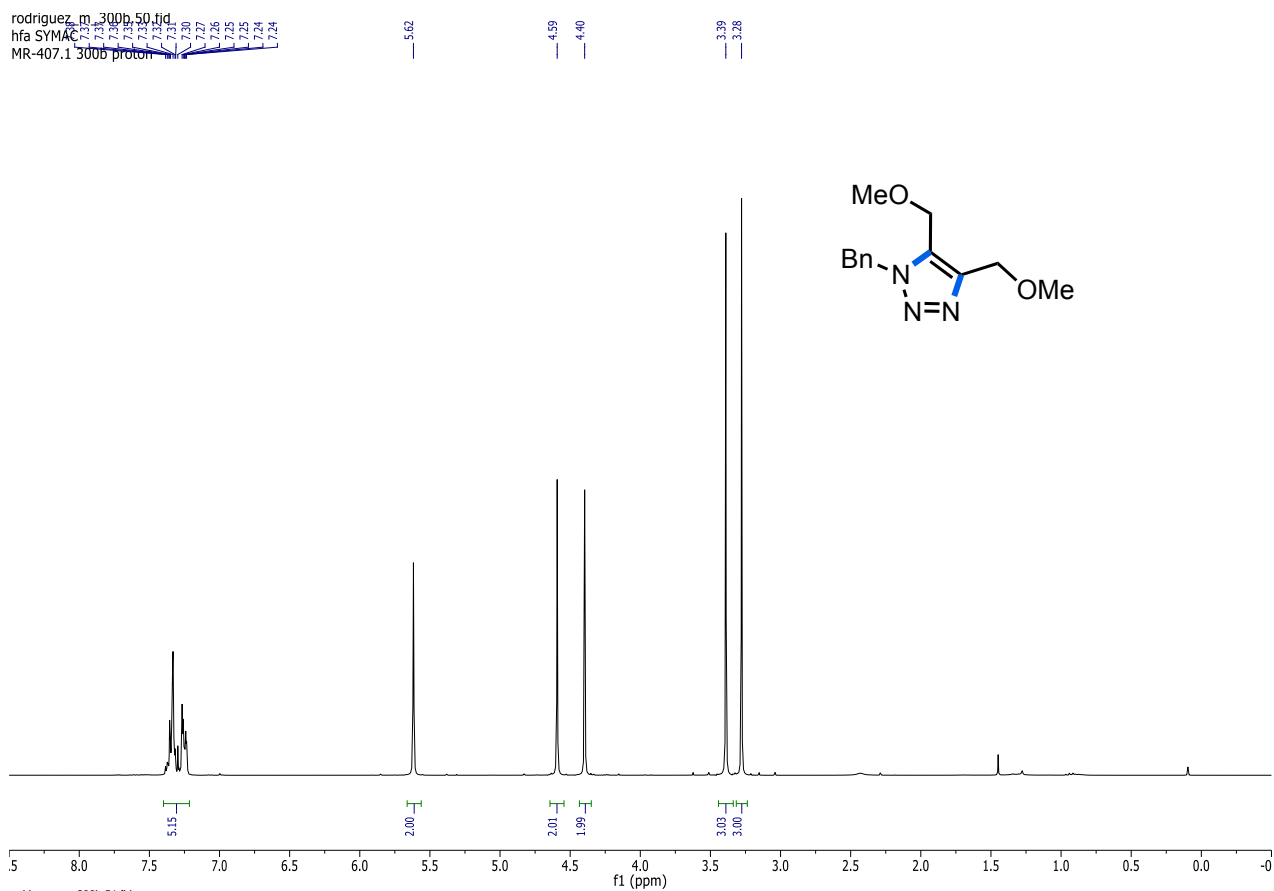
2.6 Annex: NMR spectra of the isolated compounds

¹H NMR (300 MHz) (top) and ¹³C NMR (75 MHz) (bottom) spectra in CDCl₃ for **1a**

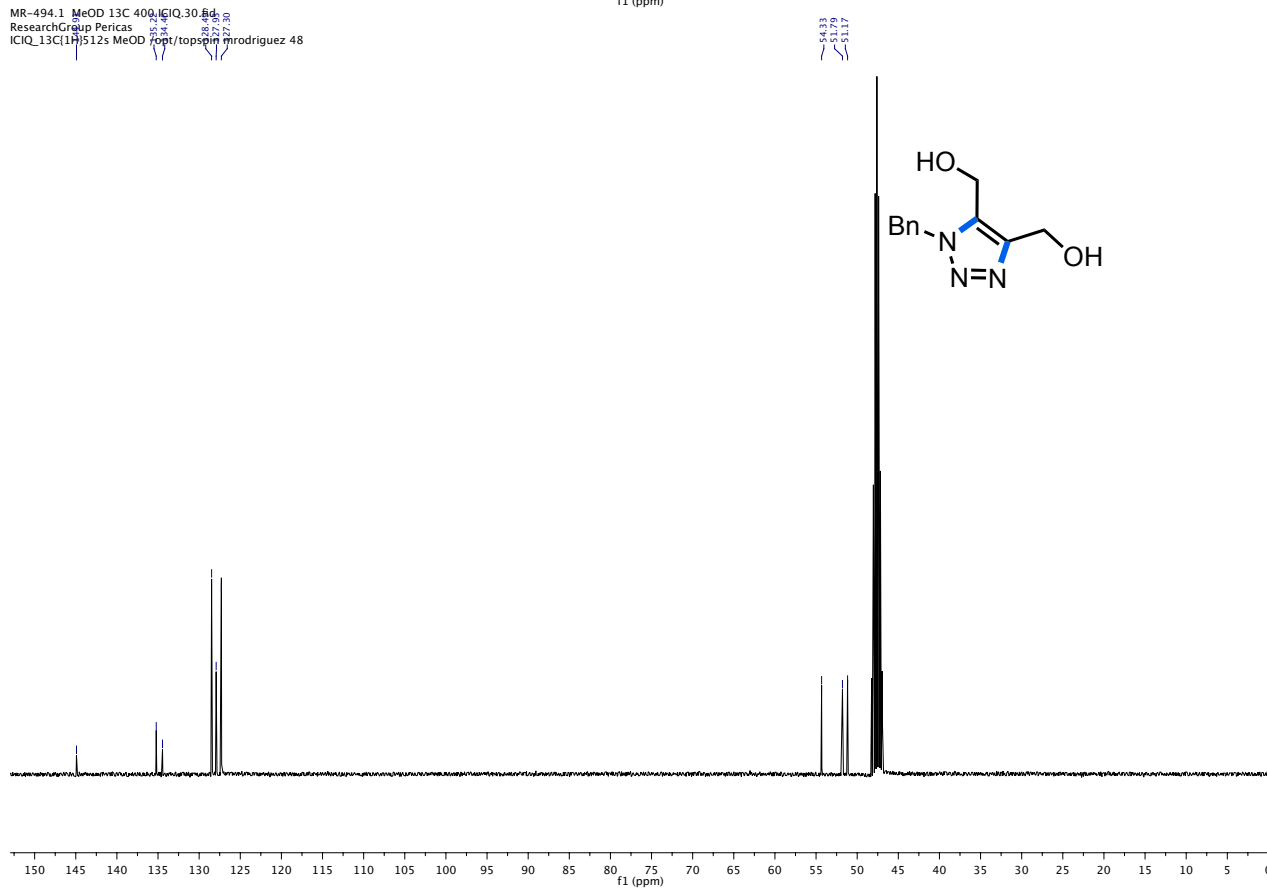
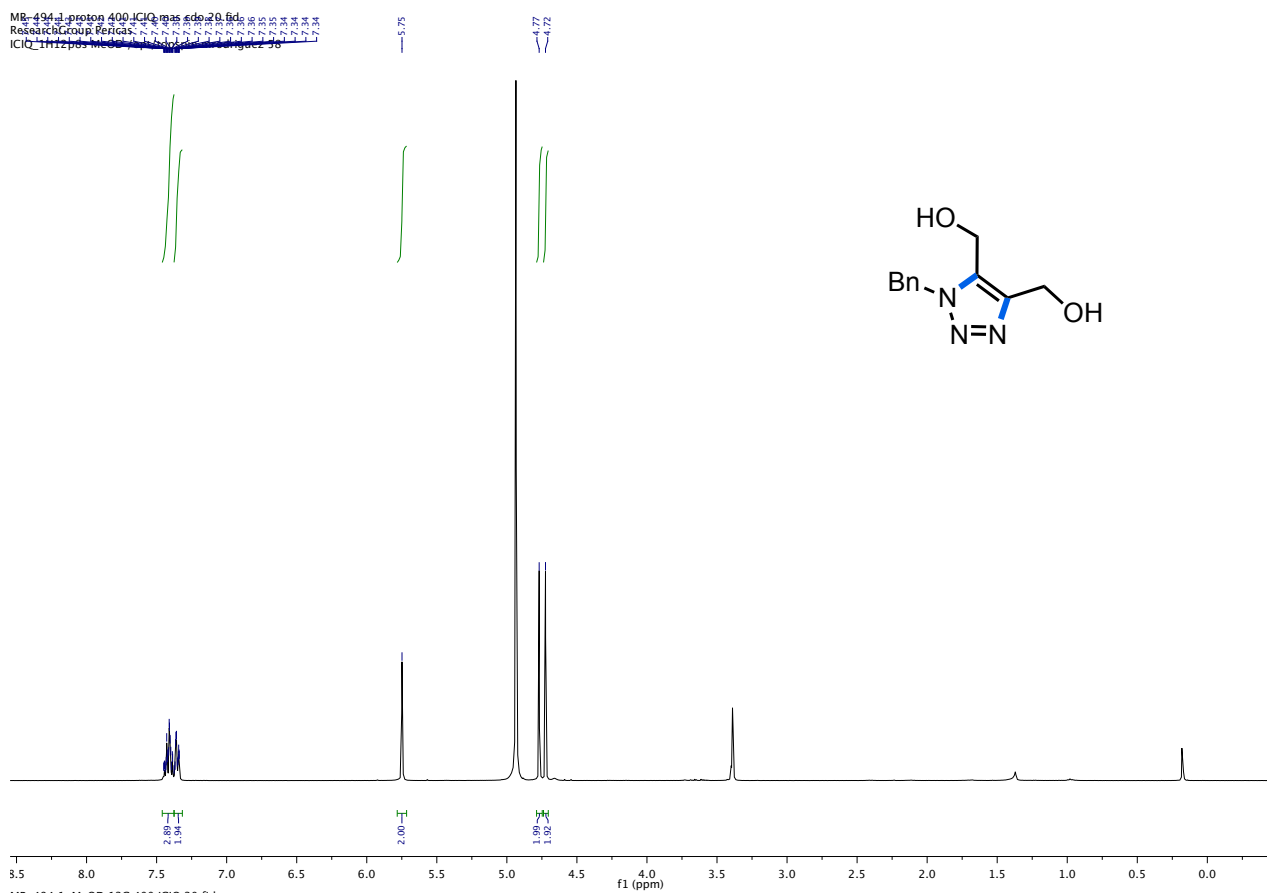


^1H NMR (400 MHz) (top) and ^{13}C NMR (100 MHz) (bottom) spectra in CDCl_3 for **2a**

^1H NMR (300 MHz) (top) and ^{13}C NMR (75 MHz) (bottom) spectra in CDCl_3 for **3a**

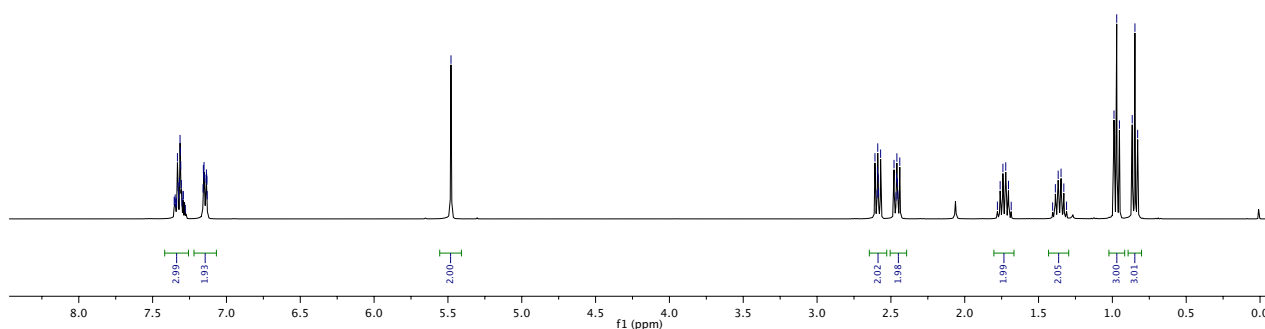
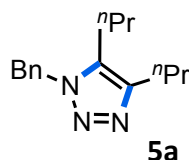


^1H NMR (400 MHz) (top) and ^{13}C NMR (100 MHz) (bottom) spectra in $\text{MeOH-}d_4$ for **4a**

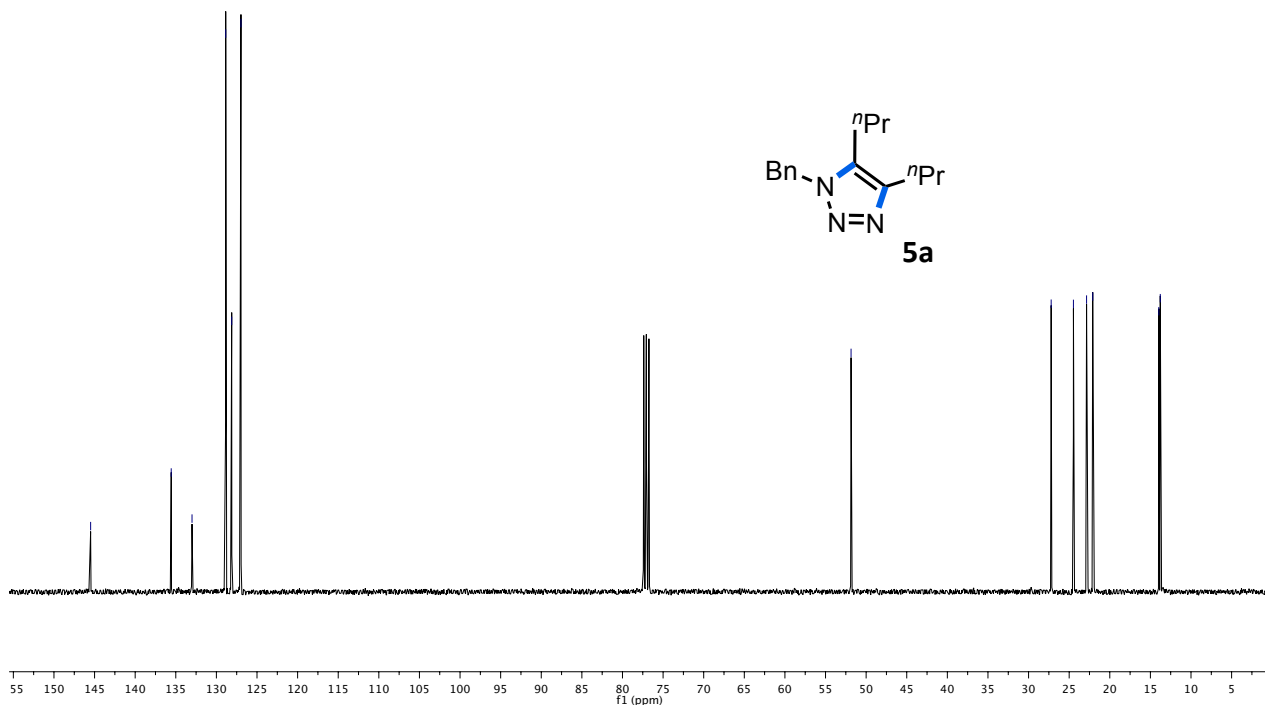
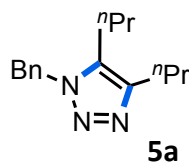


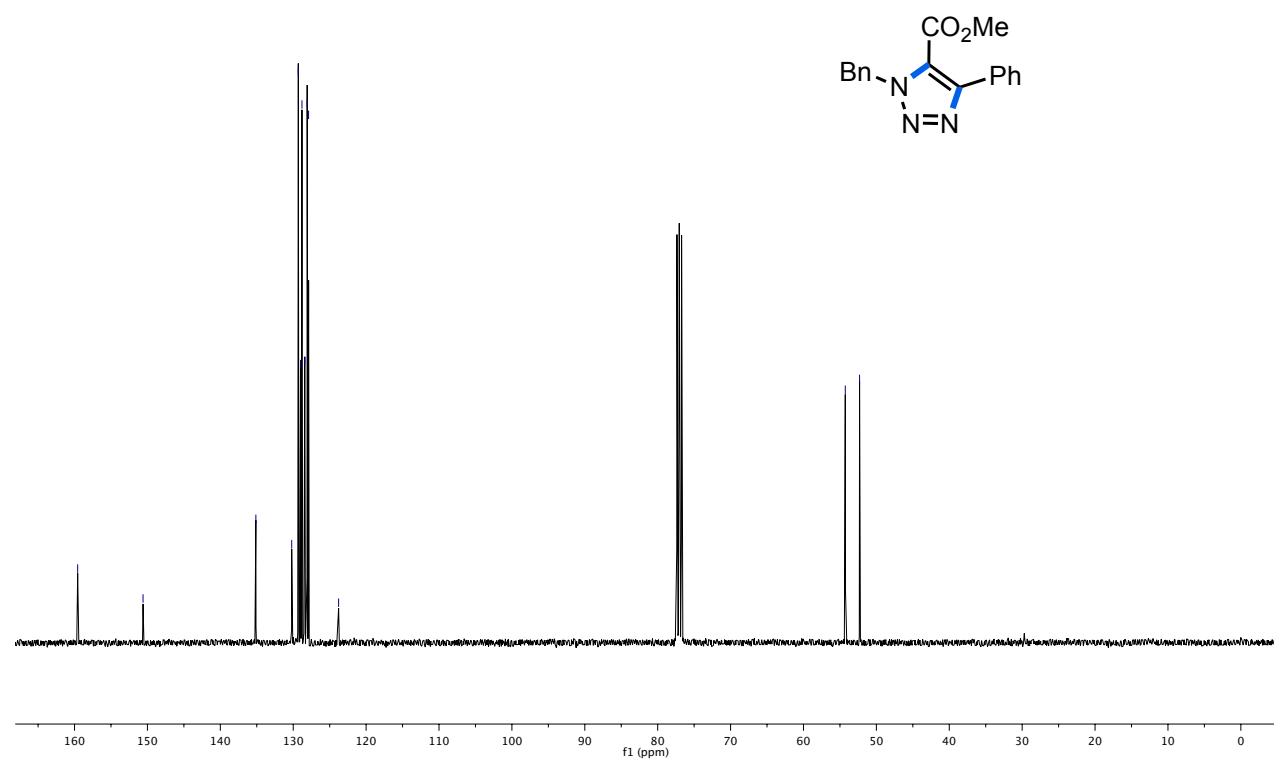
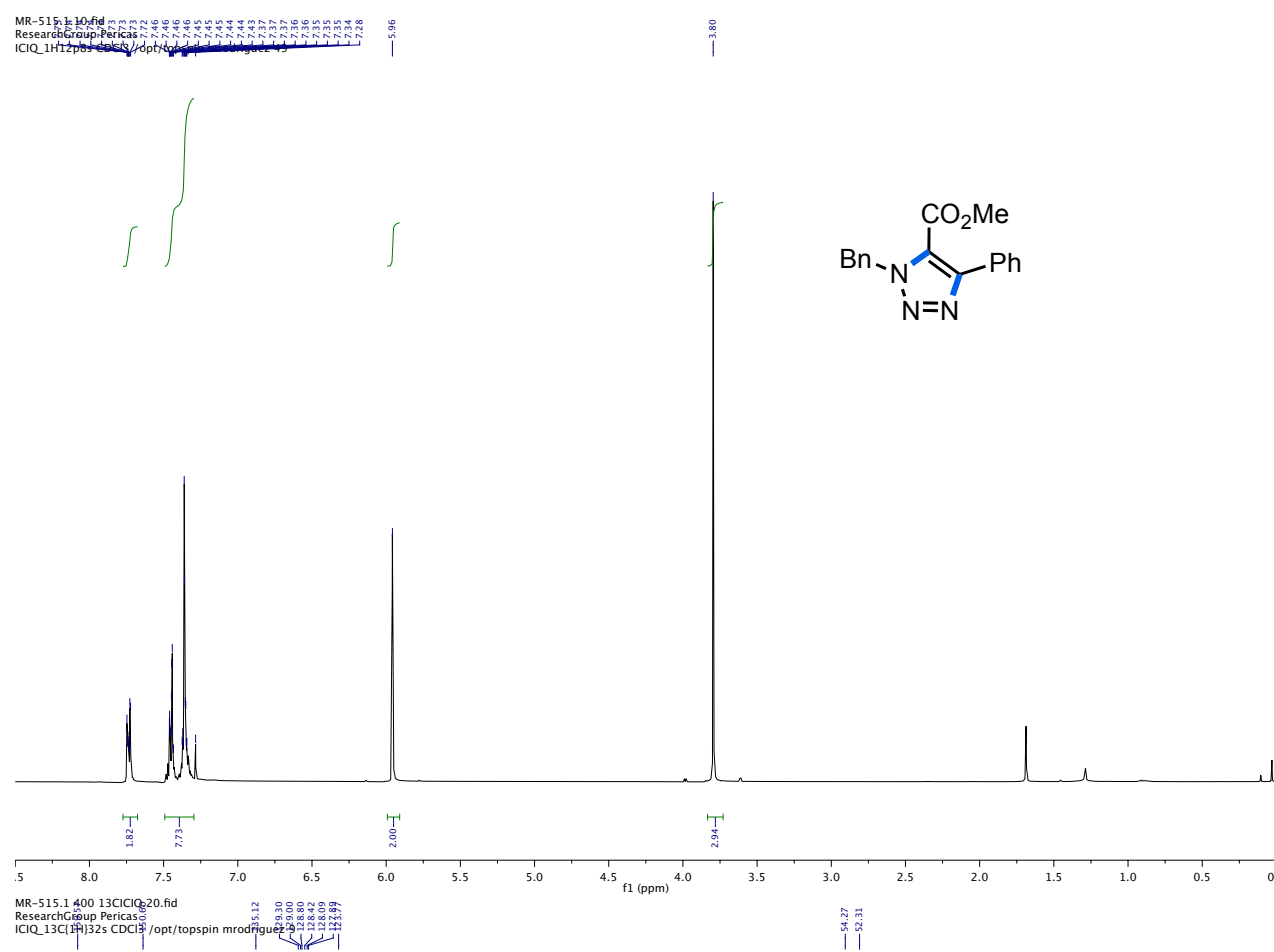
¹H NMR (400 MHz) (top) and ¹³C NMR (100 MHz) (bottom) spectra in CDCl₃ for **5a**

MR-457.1 PROTON-400 ICIQ.10.fid
 ResearchGroup:Pericas
 ICIQ_1H12pss CDCl3 /opt/topspin/mrodriguez/57

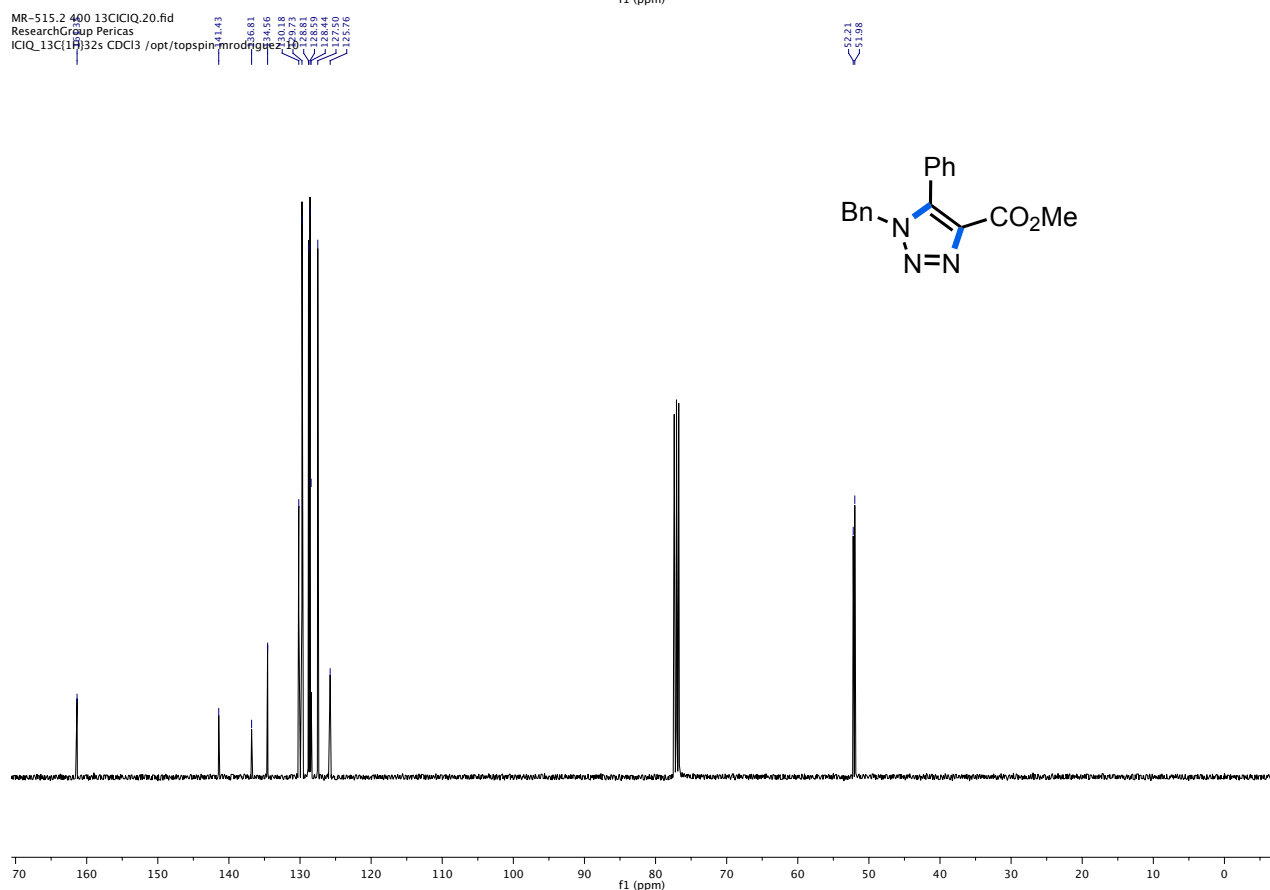
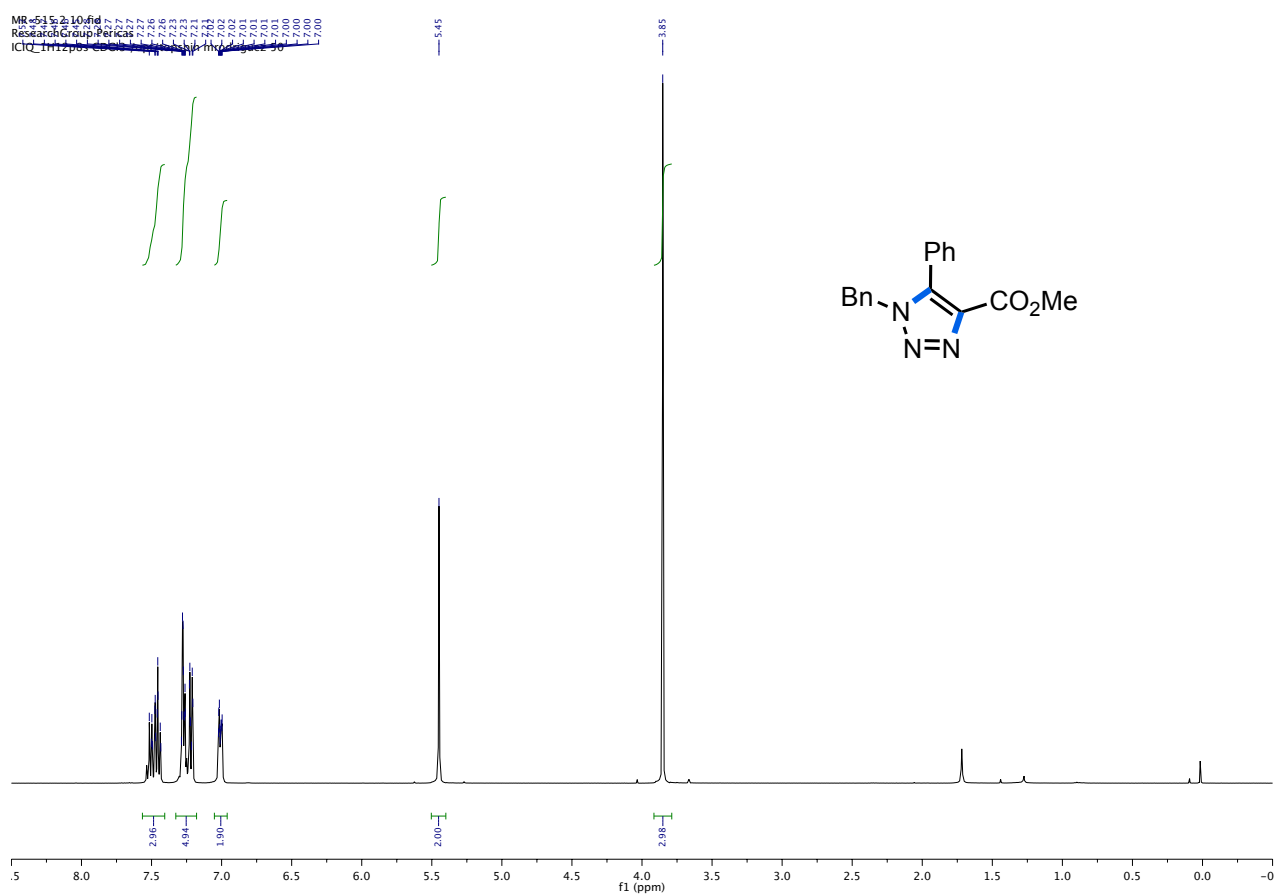


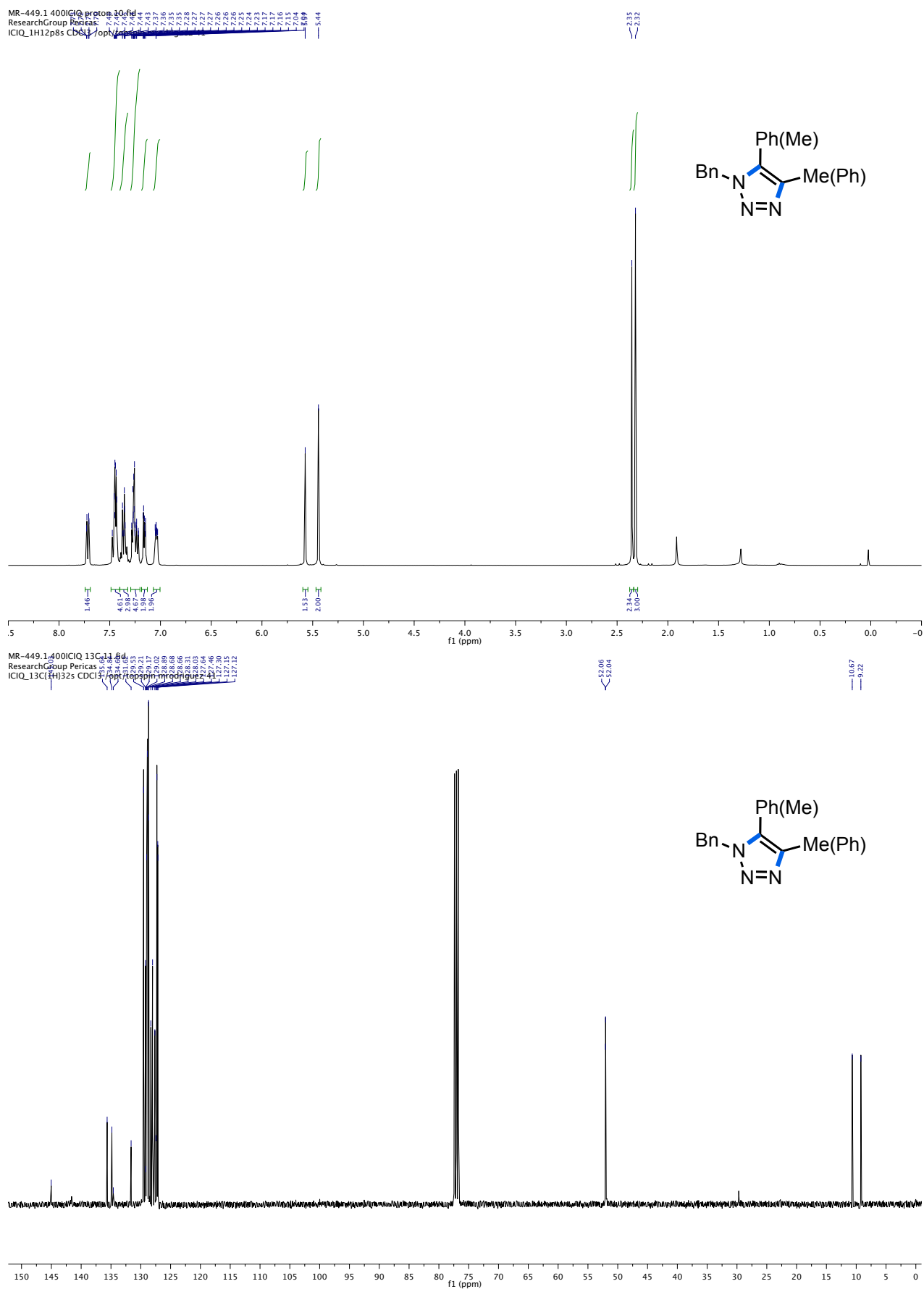
MR-457.1 13C-400 ICIQ.11.fid
 ResearchGroup:Pericas
 ICIQ_13C(1H)512s CDCl3 /opt/topspin/mrodriguez/57



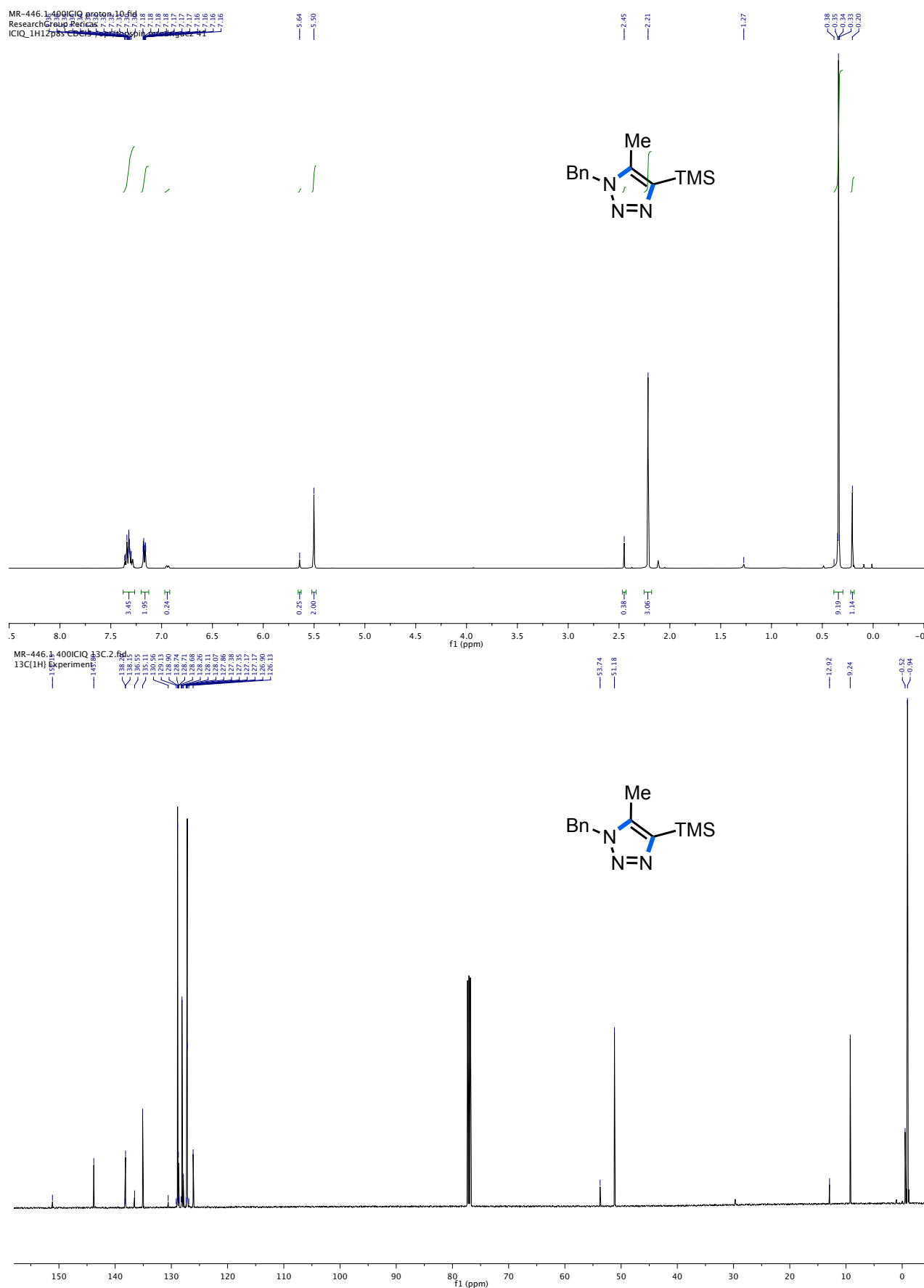
^1H NMR (400 MHz) (top) and ^{13}C NMR (100 MHz) (bottom) spectra in CDCl_3 for **min-6a**

^1H NMR (400 MHz) (top) and ^{13}C NMR (100 MHz) (bottom) spectra in CDCl_3 for **maj-6a**

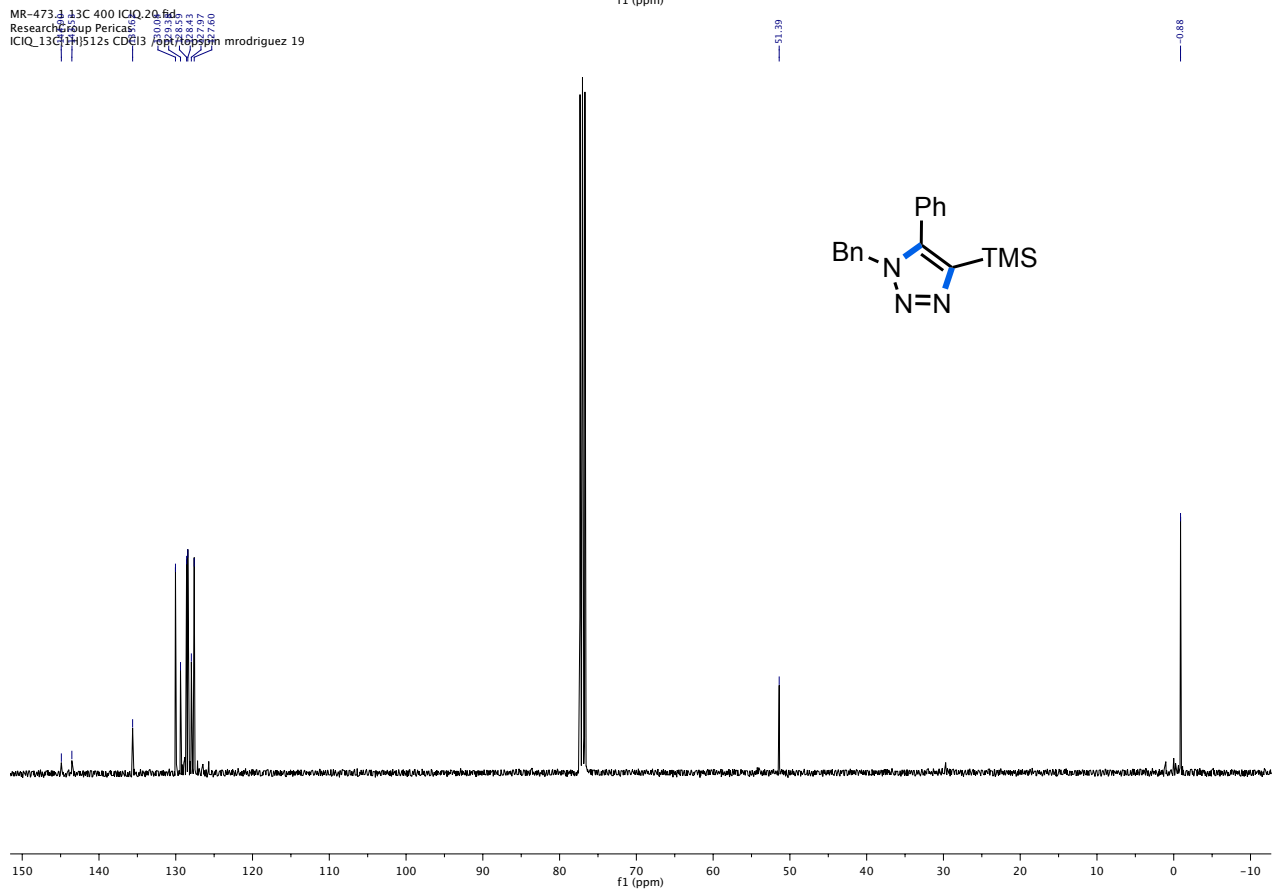
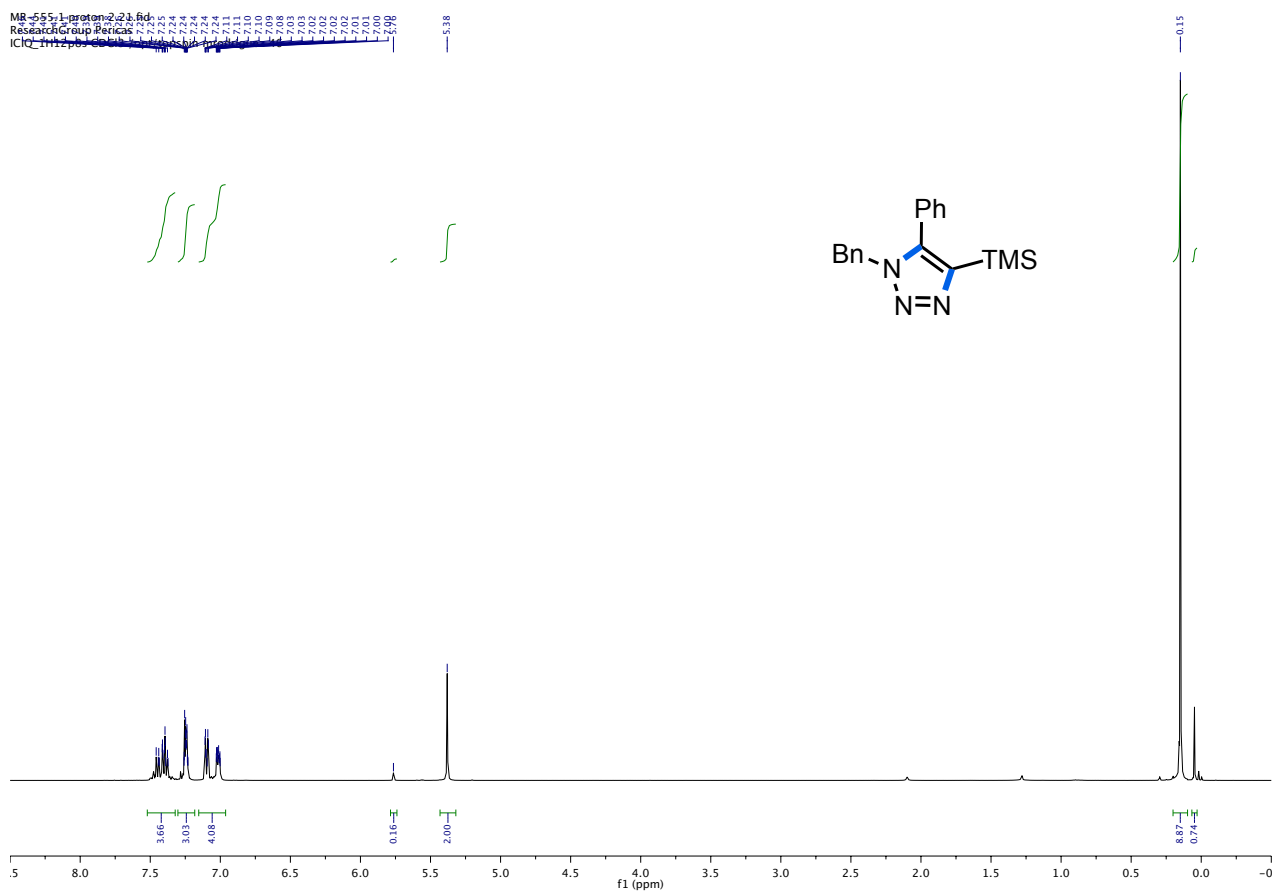


^1H NMR (400 MHz) (top) and ^{13}C NMR (100 MHz) (bottom) spectra in CDCl_3 for **7a**

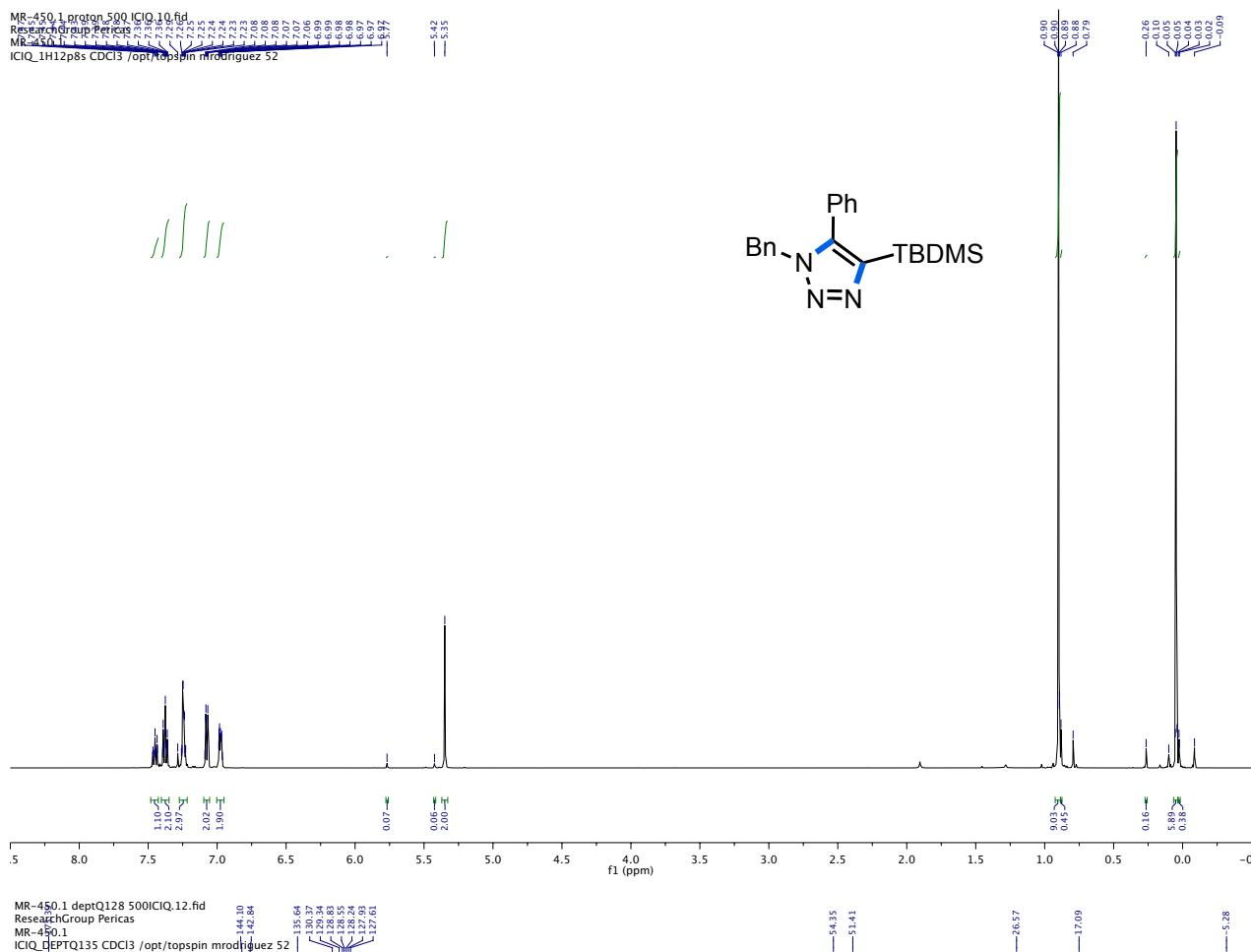
^1H NMR (500 MHz) (top) and ^{13}C NMR (125 MHz) (bottom) spectra in CDCl_3 for **maj-8a**



^1H NMR (400 MHz) (top) and ^{13}C NMR (100 MHz) (bottom) spectra in CDCl_3 for **maj-9a**

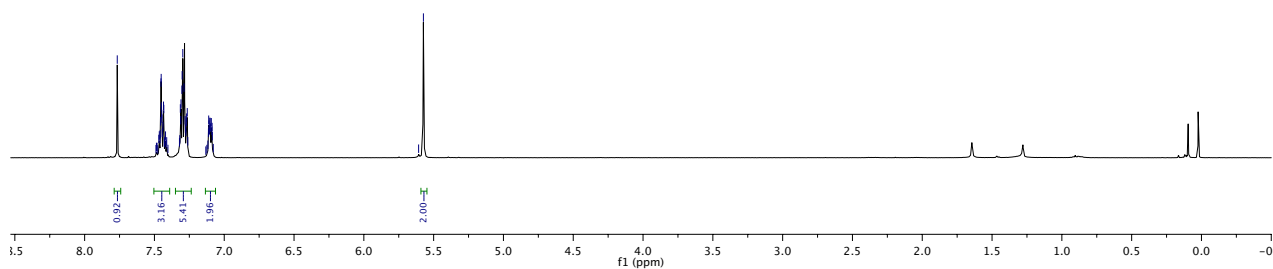
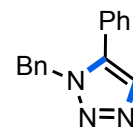
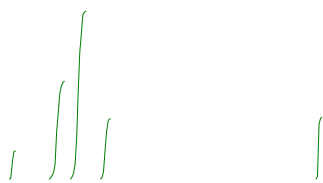


^1H NMR (500 MHz) (top) and ^{13}C NMR (125 MHz) (bottom) spectra in CDCl_3 for **10a**

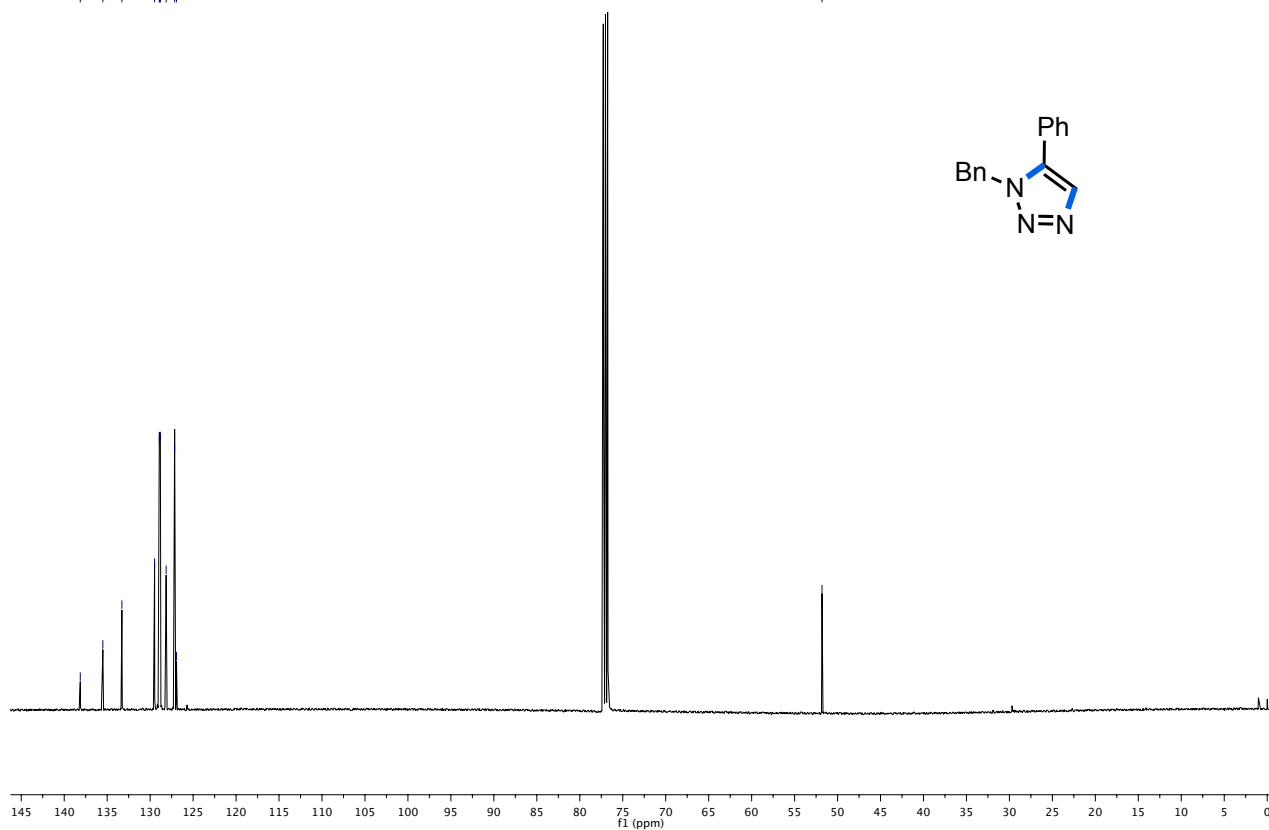
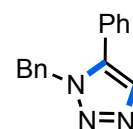


^1H NMR (400 MHz) (top) and ^{13}C NMR (125 MHz) (bottom) spectra in CDCl_3 for **11a**

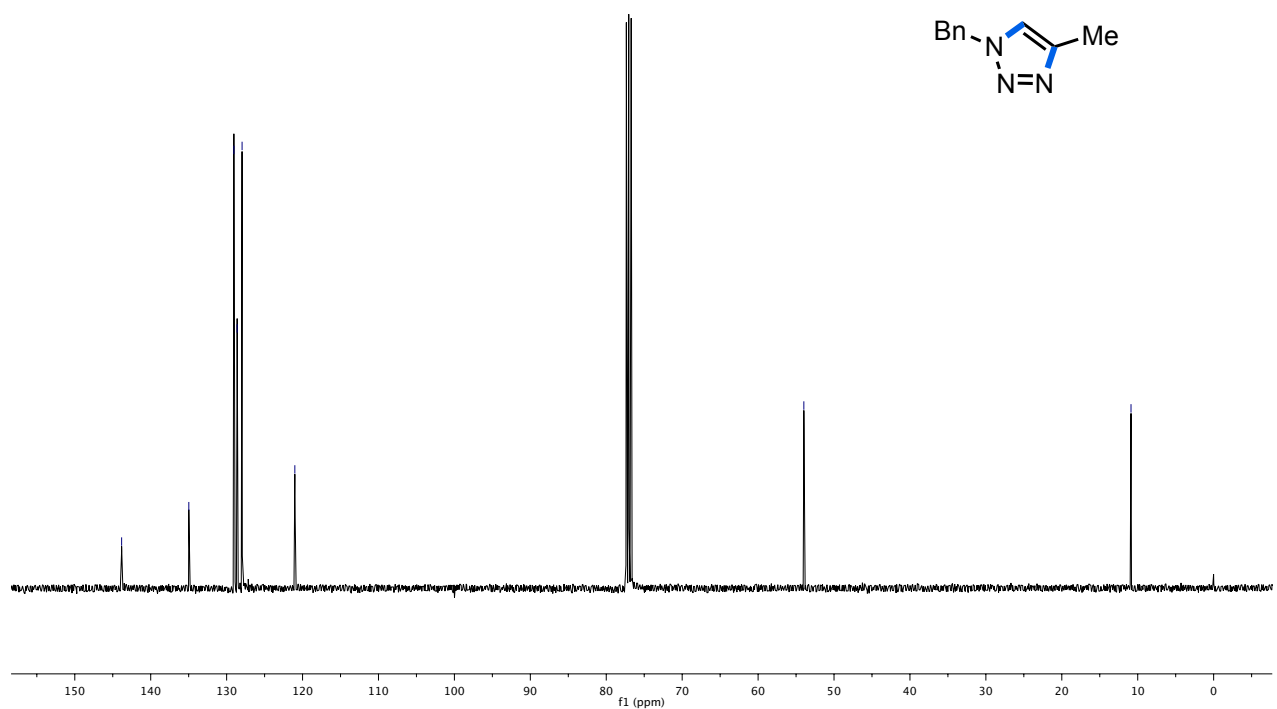
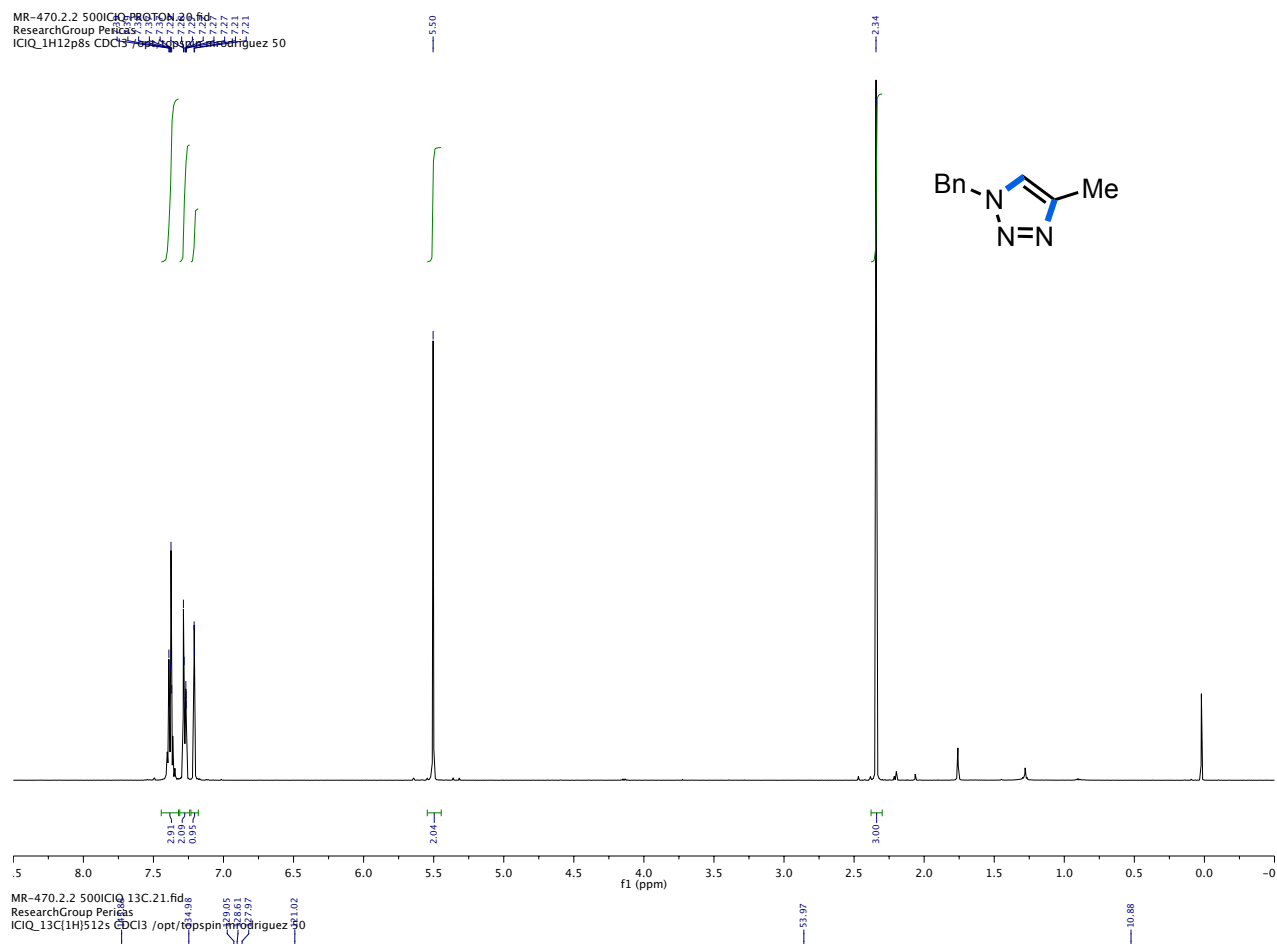
MR-497.1.10.fid
ResearchGroup Perkin
ICIQ_1H12p8s CDCl3

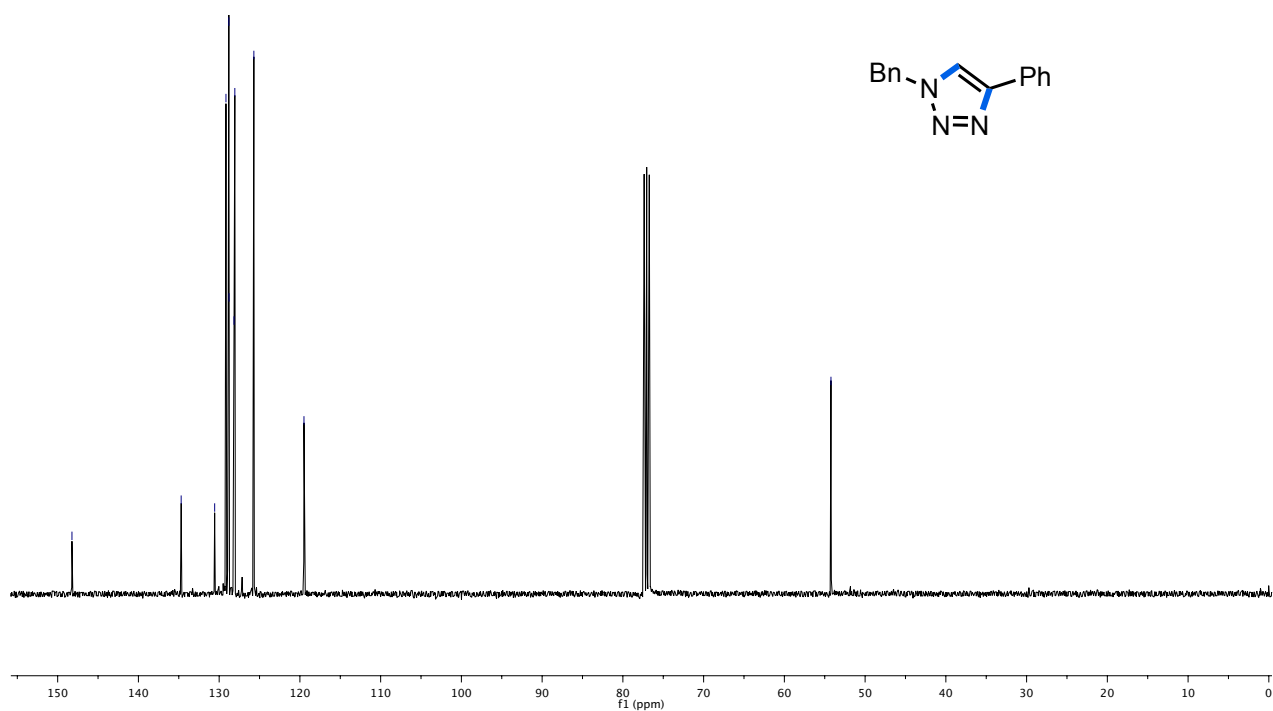
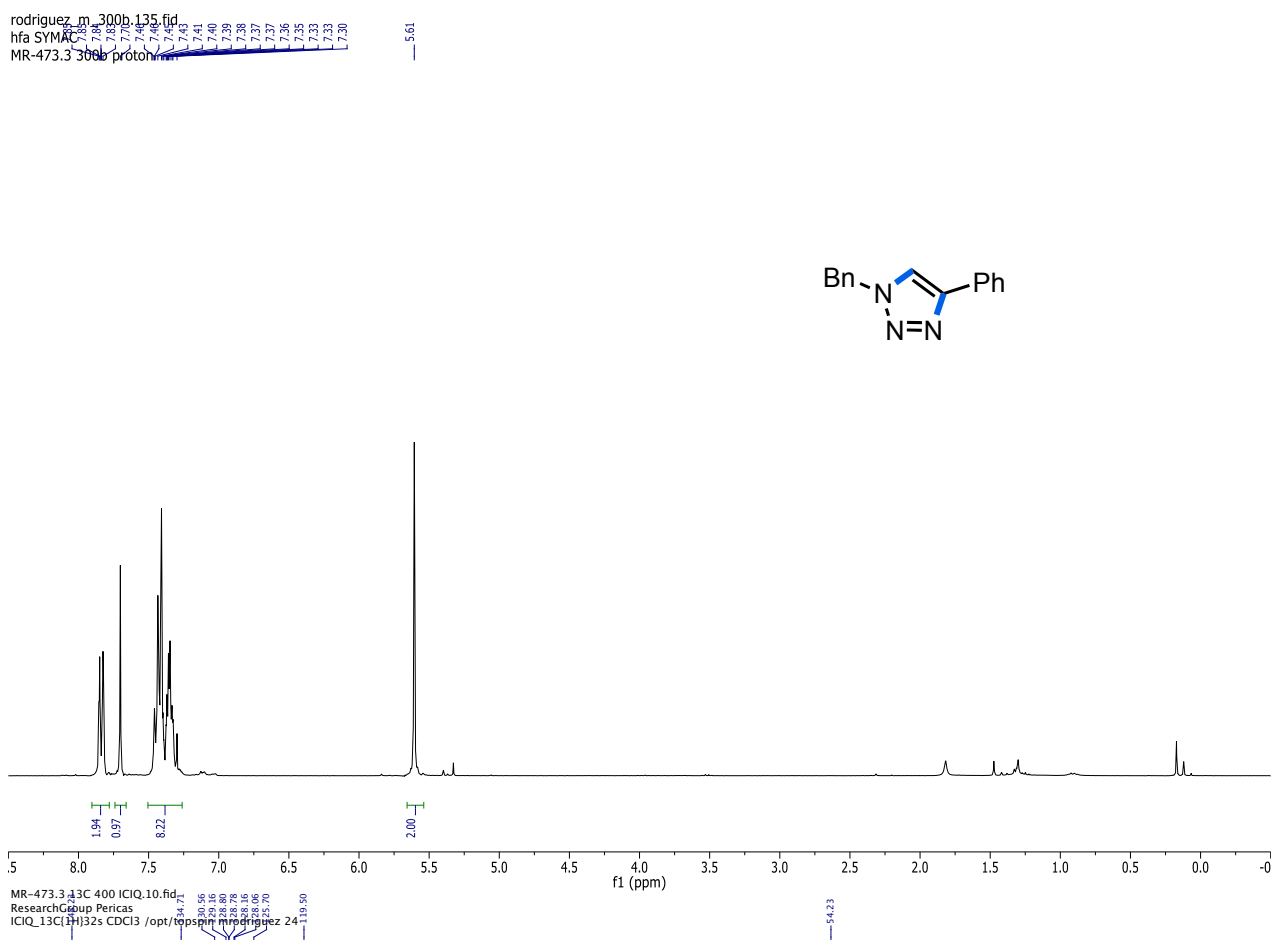


MR-497.1.13C 400 ICIQ_3.fid
13C(1H) Experiment

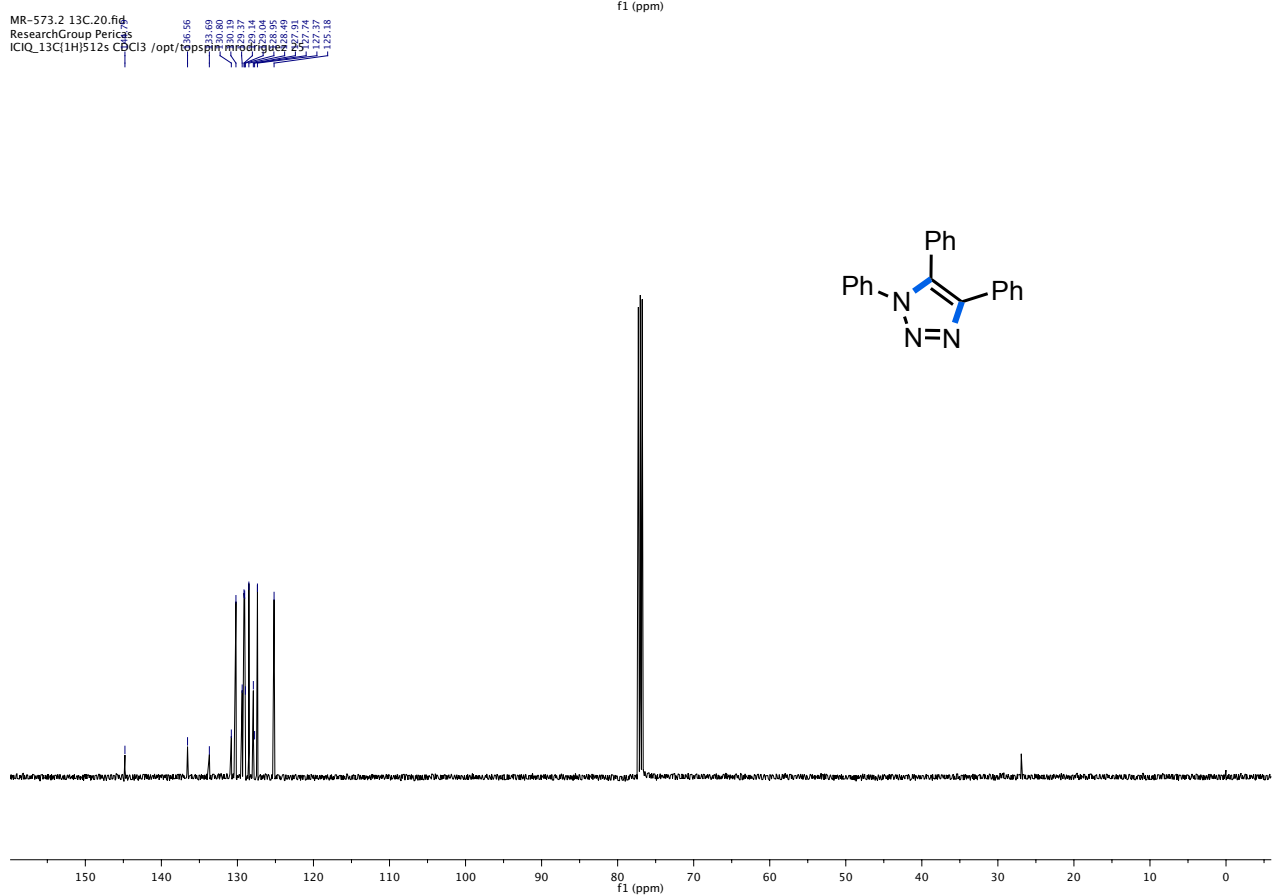
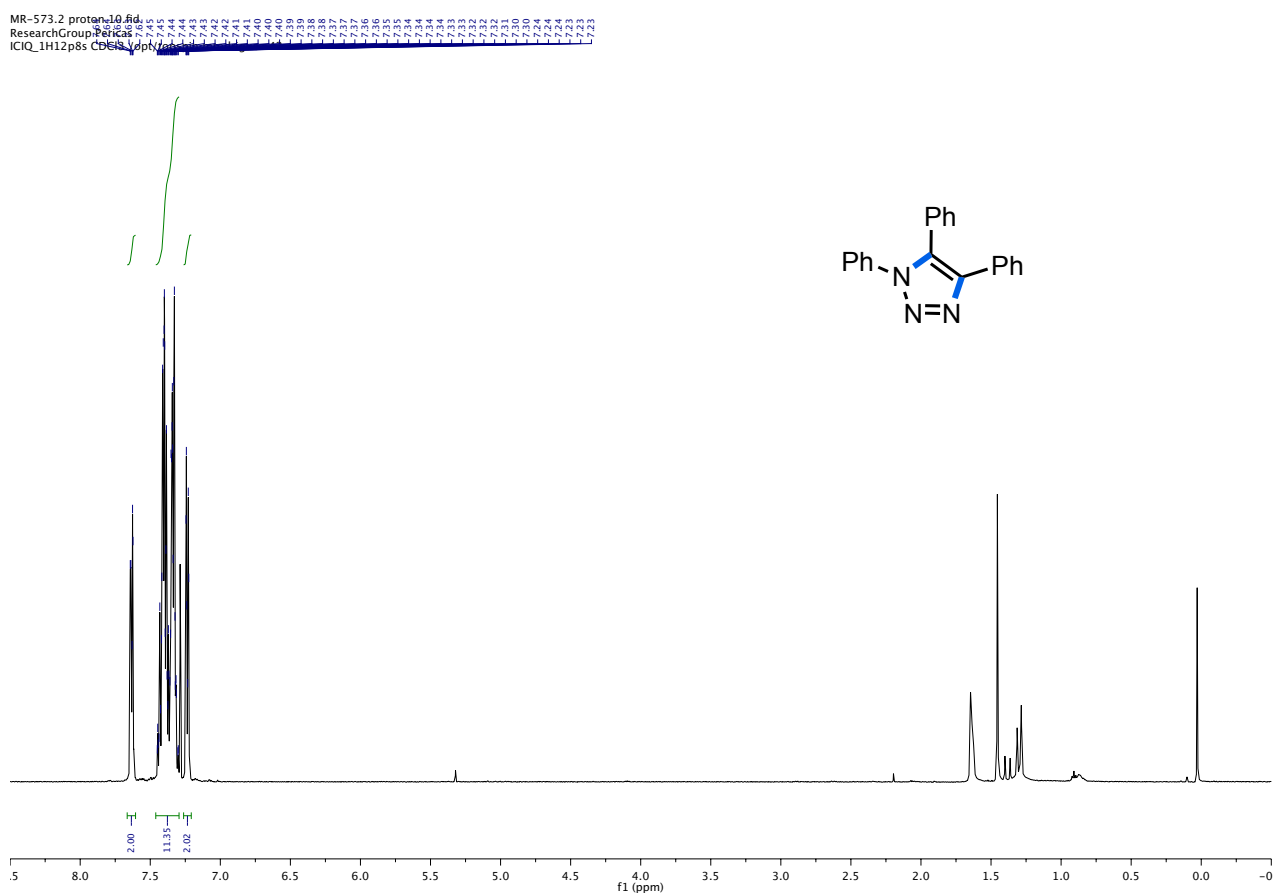


^1H NMR (500 MHz) (top) and ^{13}C NMR (100 MHz) (bottom) spectra in CDCl_3 for **12a**



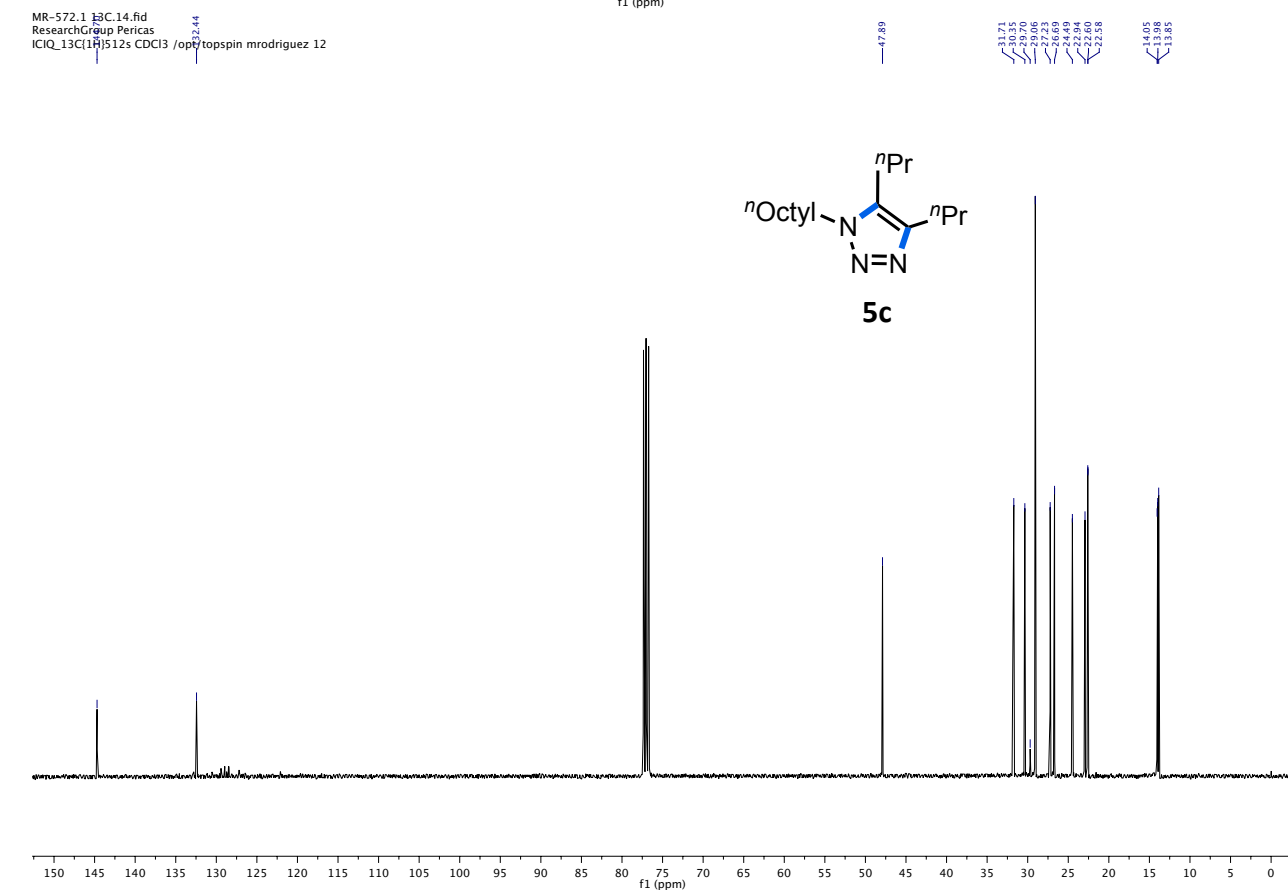
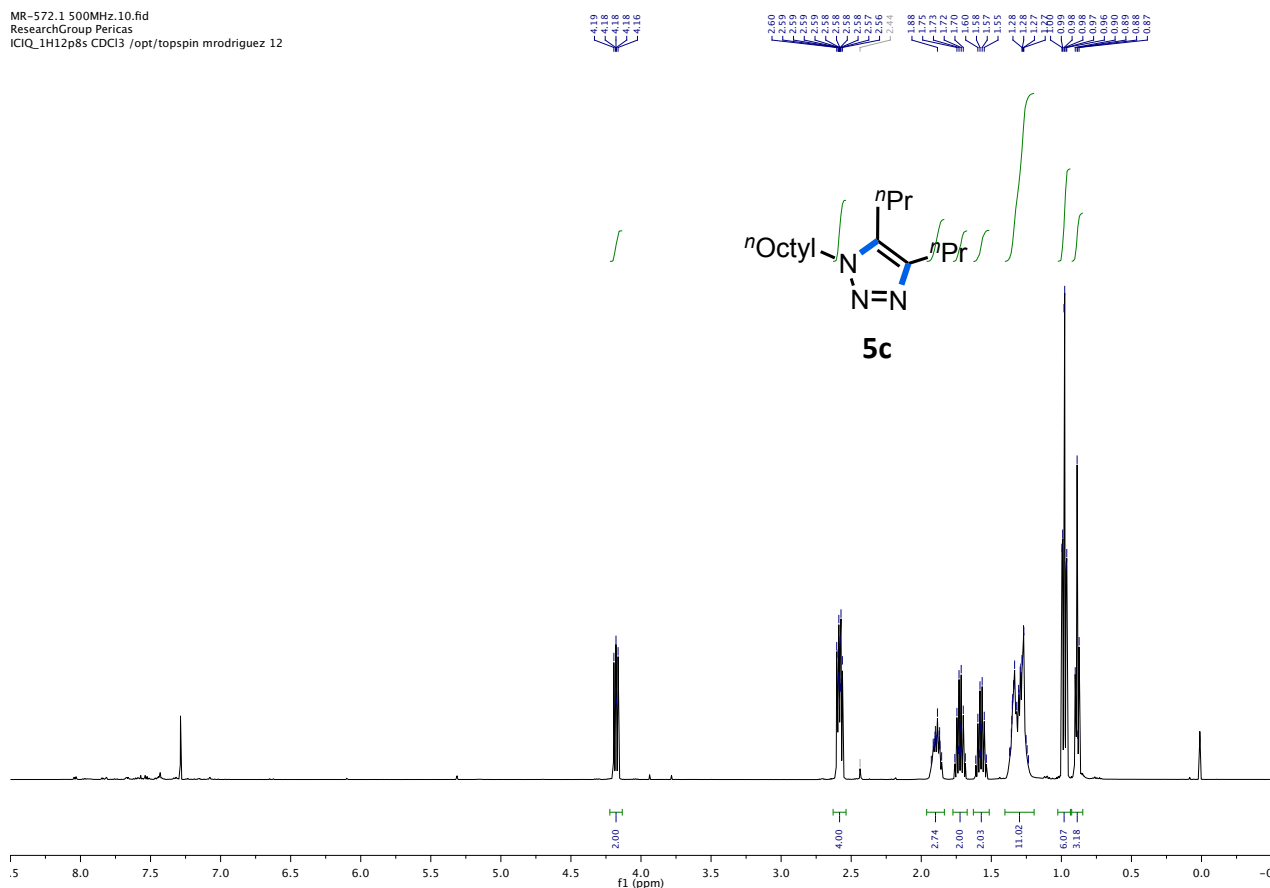
^1H NMR (300 MHz) (top) and ^{13}C NMR (100 MHz) (bottom) spectra in CDCl_3 for **13a**

¹H NMR (500 MHz) (top) and ¹³C NMR (125 MHz) (bottom) spectra in CDCl₃ for **1b**

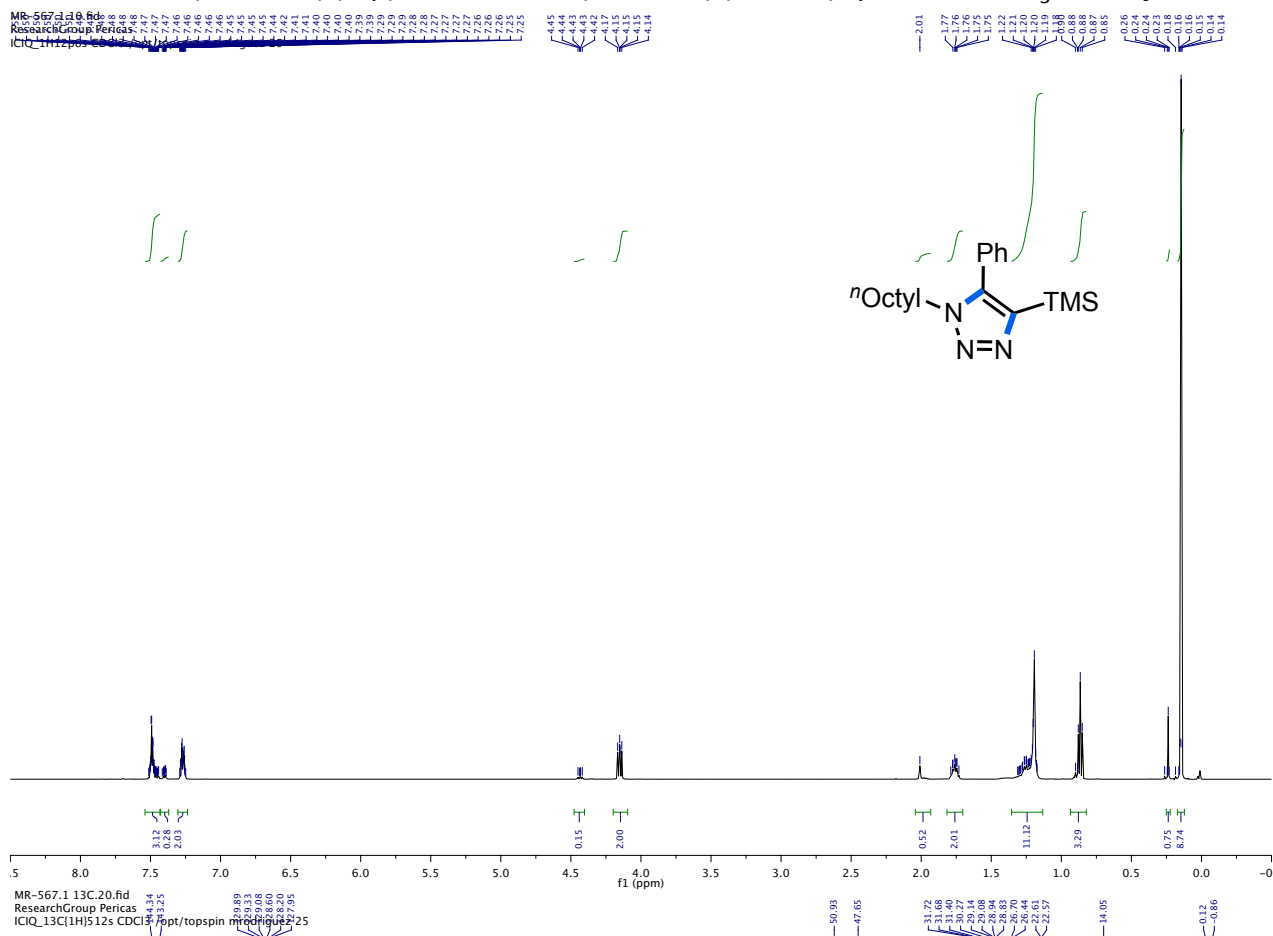


^1H NMR (500 MHz) (top) and ^{13}C NMR (100 MHz) (bottom) spectra in CDCl_3 for **5c**

MR-572.1 500MHz.10.fid
ResearchGroup Pericas
ICIQ_1H12p8s CDCl3 /opt/topspin mrodriguez 12



¹H NMR (500 MHz) (top) and ¹³C NMR (125 MHz) (bottom) spectra in CDCl₃ for **maj-9c**



2.7 Published paper



DOI: 10.1002/chem.201503858

CHEMISTRY
 A European Journal
 Full Paper

Synthetic Methods
Metal-Free Intermolecular Azide–Alkyne Cycloaddition Promoted by Glycerol

 Marta Rodríguez-Rodríguez,^[a, b] Emmanuel Gras,^[c] Miquel A. Pericàs,^{*, [b]} and Montserrat Gómez^{*, [a]}

Abstract: Metal-free intermolecular Huisgen cycloadditions using nonactivated internal alkynes have been successfully performed in neat glycerol, both under thermal and microwave dielectric heating. In sharp contrast, no reaction occurs in other protic solvents, such as water, ethanol, or diols. DFT calculations have shown that the BnN₃/glycerol adduct promotes a more important stabilization of the corresponding

LUMO than that produced in the analogous BnN₃/alcohol adducts, favoring the reactivity with the alkyne in the first case. The presence of copper salts in the medium did not change the reaction pathway (Cu(I) acts as spectator), except for disubstituted silylalkynes, for which desilylation takes place in contrast to the metal-free system.

Introduction

Azide–alkyne cycloadditions (AAC) represent a powerful tool for the synthesis of 1,2,3-triazoles, valuable heterocycles involved in diverse fields, such as biochemistry, organic synthesis, or materials science.^[1] Although this reaction was first reported in 1893 by Michael^[2] and in particular developed by Huisgen in the 1960s,^[3] it was not up to the beginning of the 21st century that the reaction found widespread practical interest after overcoming kinetic and regioselective concerns by transforming the thermally activated process into a catalytic reaction, mainly by using copper-based systems.^[1,4] Since then, many catalytic systems have been described, also including metals other than copper (such as Ag,^[5] Ru,^[6] Ir,^[7] or Ni^[8]), which allow access to substituted-1,2,3-triazoles from organic azides and alkynes. The use of internal alkynes leading to the formation of 1,4,5-trisubstituted 1,2,3-triazoles generally requires harsher conditions, and activated alkynes (either substituted by electron-withdrawing groups or strained).

For biological and pharmacological applications, metal-free AAC methodologies (back to the origins) still remain attractive approaches.^[9] Bertozzi and co-workers first used the strained-promoted strategy involving substituted cycloalkynes for bioconjugation purposes.^[10] Another elegant method is through intramolecular AAC reactions by taking advantage of the favorable entropy effects.^[11] However, to the best of our knowledge, intermolecular cycloadditions between organic azides and nonactivated internal alkynes under metal-free conditions remain an important challenge to be solved.

In the last years, with the purpose of using ecofriendly solvents, we have developed glycerol catalytic phases. They exhibit appealing properties mainly regarding the immobilization of the metal species, probably owing to the supramolecular arrangement shown by glycerol.^[12] In particular, Cu₂O nanoparticles prepared in neat glycerol led to the synthesis of 1,4-disubstituted-1,2,3-triazoles, permitting an easy recycling of the catalytic phase.^[13] With the assumption of glycerol having a noninocent role in this process, we decided to investigate the metal-free AAC in glycerol for the synthesis of 1,4,5-trisubstituted 1,2,3-triazoles.

[a] M. Rodríguez-Rodríguez, Prof. M. Gómez
 Laboratoire Hétérochimie Fondamentale et Appliquée (LHFA)
 Université de Toulouse, UPS and CNRS UMR 5069
 118, route de Narbonne, 31062 Toulouse cedex 9 (France)
 E-mail: gomez@chimie.ups-tlse.fr

[b] M. Rodríguez-Rodríguez, Prof. M. A. Pericàs
 Institute of Chemical Research of Catalonia (ICIQ)
 The Barcelona Institute of Science and Technology
 Avda. Països Catalans, 16, 43007 Tarragona (Spain)
 E-mail: mapericas@iciq.es

[c] Dr. E. Gras
 Laboratoire de Chimie de Coordination (LCC)
 Centre National de la Recherche Scientifique (CNRS)
 205, route de Narbonne, 31077 Toulouse cedex 4 (France)

Supporting information for this article is available on the WWW under <http://dx.doi.org/10.1002/chem.201503858>.

Results and Discussion

As a benchmark reaction, the intermolecular azide–alkyne cycloaddition (AAC) between diphenylacetylene (**1**) and benzyl azide (**a**) in neat glycerol under microwave dielectric heating for 30 minutes was chosen, affording 1-benzyl-4,5-diphenyl-1,2,3-triazole (**1a**; Table 1).^[14] The organic products were isolated by a biphasic liquid–liquid extraction after adding dichloromethane to the reaction mixture. The triazole **1a** was exclusively obtained in a high yield of 85% (Table 1, entry 1). With the aim of investigating the effect of copper in this reaction,^[15] we carried out the synthesis in the presence of a copper salt (2.5 mol% of CuCl), obtaining **1a** in almost the same isolated

yield (Table 1, entry 2). This evidences the spectator role of copper (see Table S1 in the Supporting Information).^[16] A similar trend was observed under classical thermal-promoted conditions (Table 1, entries 3 and 4), albeit in lower yields (< 35%) after 20 h. In the absence of glycerol (i.e., under solvent-free conditions), the product was obtained in only 18% yield (Table 1, entry 5). No copper was detected by ICP-AES analysis of neat glycerol (< 3 ppm).

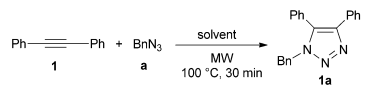
To better control the temperature (the reaction conditions were set at a targeted temperature, controlled by an external infrared temperature sensor),^[17] we employed a MW instrument combining both internal optical fiber and external infrared temperature sensors (Figure S1 in the Supporting Information). We carried out the cycloaddition at different temperatures (100, 140, and 180 °C, according to the internal optical fiber sensor) and observed that the yield obtained at 180 °C was comparable to that obtained working with the instrument equipped only with an infrared sensor (Table S2 in the Supporting Information). Under classical heating conditions (oil bath), only 65% yield was achieved at 180 °C in the same reaction time, which is consistent with a less efficient heat transfer.

Then, we decided to study the influence of the solvent under metal-free conditions. Surprisingly, no reaction took place when using other alcohol-based solvents, including ethanol and diols, such as ethylene glycol, propane-1,2-diol, and propane-1,3-diol (Table 1, entry 6). Water gave a very low conversion of benzyl azide of 13% (Table 1, entry 7). Aprotic polar solvents, such as 1,4-dioxane and fluorobenzene, also disfavored the cycloaddition (Table 1, entries 8 and 9). The varying reactivity observed by using different protic solvents can be explained by the solvent interaction with an external electric field. Alcohols, in particular polyols, form extensive hydrogen bonds, which in turn correlate with long relaxation times (the time taken to achieve the random state after being submitted to an external electric field).^[18] Therefore, water (9.2 ps), ethanol (170 ps), ethylene glycol (170 ps), or propane-1,3-diol (340 ps) exhibit shorter relaxation times than glycerol (1,215 ps), making it more relevant than other protic solvents for synthetic purposes under microwave conditions, as illustrated here for the AAC reaction.

Under thermal conditions (Table S3 in the Supporting Information), the reactivity in the different solvents follows the same trend, except for ethylene glycol and water for which **1a** was obtained in 25 and 31% yield, respectively (33% yield in glycerol; Table 1, entry 3), after 20 h at 100 °C. This clearly contrasts with the lack of reactivity observed under microwave heating (Table 1, entries 6 and 7), despite the high internal temperature achieved under MW activation (see above).

With these results in hand, we decided to study the scope of the process by using other internal alkynes (Table 2). For the symmetrical disubstituted alkynes **2–5** (Table 2, entries 1–4), moderate to high yields were obtained (32–90%). No transesterification reaction between the alkyne **2** or the triazole **2a** and glycerol was observed, in contrast to the reaction in ethanol (see Tables S4 and S5 in the Supporting Information). It is important to note that the nonactivated 4-octyne reacted with BnN_3 to give 1-benzyl-4,5-dipropyl-1,2,3-triazole **5a** in 71% iso-

Table 1. Azide–alkyne cycloaddition of diphenylacetylene and benzyl azide in neat glycerol.^[a]



Entry	Solvent	Conversion [%] ^{[b][c]}	Isolated yield [%] ^[d]
1	glycerol	85	85 (85)
2 ^[e]	glycerol	86	82 (80)
3 ^[f]	glycerol	37	33 (33)
4 ^{[e][f]}	glycerol	42	28 (27)
5	–	20	18 ^[g]
6 ^[h]	protic solvent	n.r.	–
7	H ₂ O	13	n.d.
8	1,4-dioxane	n.r.	–
9	fluorobenzene	n.r.	–

[a] Results from duplicate experiments. Reaction conditions: benzyl azide (0.4 mmol) and diphenylacetylene (0.6 mmol) in solvent (1 mL) under microwaves activation (250 W) at 100 °C for 30 minutes (temperature controlled by external infrared sensor). [b] Based on benzyl azide. [c] Determined by ¹H NMR spectroscopy using 2-methoxynaphthalene as an internal standard. [d] In brackets: yields determined by ¹H NMR spectroscopy using 2-methoxynaphthalene as an internal standard. [e] In the presence of 2.5 mol % of CuCl. [f] Reaction in a sealed tube under thermal activation at 100 °C for 20 h. [g] Determined by ¹H NMR spectroscopy using 2-methoxynaphthalene as an internal standard. [h] Results obtained with the following alcohols as solvents: ethanol, ethylene glycol, propane-1,2-diol, and propane-1,3-diol.

lated yield (after 1 h under microwave irradiation; Table 2, entry 4).

Unsymmetrically substituted alkynes **6** and **7** led to an almost equimolar mixture of both regioisomers (Table 2, entries 5 and 6). In view of synthetic applications and to explore the role of the silyl group as a directing group during the cycloaddition,^[19] we carried out the synthesis of triazoles **8–10** from the corresponding alkynes containing silyl-based groups, such as SiMe₃ (alkynes **8** and **9**; Table 2, entries 7 and 8) and Si(*t*Bu)Me₂ (**10**; Table 2, entry 9). As expected, the 4-silyl-substituted heterocycle was obtained as the major regioisomer^[20] and as the sole product for the bulky *tert*-butyldimethylsilyl (TBDMS) derivative (Table 2, entry 9).

Phenyl (**b**) and *n*-octyl (**c**) azides also gave the expected triazoles; conversions and yields were lower than those obtained when using benzyl azide (Figure 1).^[21] In contrast to benzyl and *n*-octyl azides, PhN₃ tends to decompose under the reaction conditions employed.^[22]

We studied the effect of Cu(I) in the synthesis of silyl-based triazoles **8a–10a**. For the synthesis of **10a**, bearing a TBDMS group, the reactivity was similar to the one observed in the absence of Cu(I). However, for the TMS-substituted ones (**8a**, **9a**), a mixture of two triazoles was obtained: the expected **8a** or **9a** and the desilylated 1-benzyl-4*R*-1,2,3-triazole (*R* = Me (**11a**), Ph (**12a**)), which was obtained as a single regioisomer (Scheme 1). Under the classical thermal conditions, the same behavior was observed (Scheme S1 in the Supporting Information).

Table 2. Azide-alkyne cycloaddition of internal alkynes and benzyl azide in neat glycerol.^[a]

Entry	Alkyne (R, R')	Product	Conv. [%] ^{[b][c]}	Yield [%] ^[d]
1 ^[d]	2 (CO ₂ Me)	2a	100	78
2	3 (CH ₂ OMe)	3a	96	90
3	4 (CH ₂ OH)	4a	56	32
4 ^[e]	5 (Pr)	5a	73	71
5	6 (Ph, CO ₂ Me)	6a	91	83 ^[f]
6	7 (Ph, Me)	7a	49	49 ^[f]
7	8 (Me, TMS)	maj- 8a	65	62 (9:1) ^[g]
8	9 (Ph, TMS)	maj- 9a	92	85 (9:1) ^[g]
9	10 (Ph, TBDMS)	10a	85	84 ^[h]

[a] Results from duplicate experiments. Reaction conditions: benzyl azide (0.4 mmol) and the corresponding alkyne (0.6 mmol) in solvent (1 mL) under microwaves activation (250 W) at 100 °C for 30 min (temperature controlled by external infrared sensor). [b] Based on benzyl azide. [c] Determined by ¹H NMR spectroscopy using 2-methoxynaphthalene as an internal standard. [d] Reaction time: 15 min. [e] Reaction time: 60 min. [f] Regioisomer ratio: 1:1. [g] In brackets: regioisomer ratio (major isomer: 1-benzyl-4-trimethylsilyl-5R-1,2,3-triazole (for R=Me: maj-**8a**; for R=Ph: maj-**9a**); minor isomer: 1-benzyl-5-trimethylsilyl-4R-1,2,3-triazole (for R=Me: min-**8a**; for R=Ph: min-**9a**)). [h] Only one isomer was obtained (1-benzyl-4-*tert*-butyldimethylsilyl-5-phenyl-1,2,3-triazole); see ref. [20].

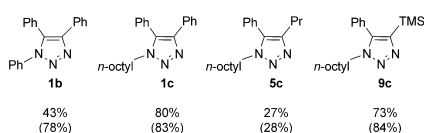
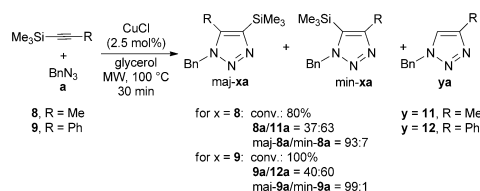
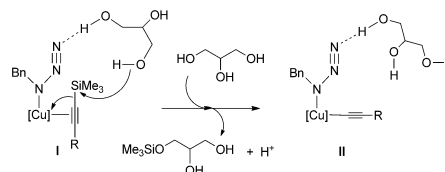


Figure 1. 1,4,5-Trisubstituted 1,2,3-triazoles from phenyl (**1b**) and *n*-octyl azides (**1c**, **5c**, **9c**). Isolated yields are given (conversions are given in brackets).



Scheme 1. Reactivity of silyl-based alkynes in the presence of CuCl under microwave activation. Data from NMR analysis.

Control experiments proved that the desilylation neither took place on the alkyne **8** or **9** nor on the triazole **8a** or **9a** (Scheme S2 in the Supporting Information). In addition, when the AAC reaction was carried out in dioxane, no corresponding desilylation occurred. Monitoring the reaction by GC-MS demonstrated that the formation of **9a** is faster than that corresponding to **12a** (after 5 min, the ratio **9a/12a** was approximately 3.4:1; after 15 min, the ratio was approximately 1.2:1, with full conversion of BnN₃). Once BnN₃ was consumed completely, desilylation of the alkyne **9** could be observed (Figure S4 in the Supporting Information). These facts led us to propose that the desilylation giving **12a** (and **11a**) occurs upon coordination of the alkyne to copper (intermediate **I** in Scheme 2), which is promoted by glycerol that is undoubtedly



Scheme 2. Plausible Cu-mediated desilylation of SiMe₃-based alkynes promoted by glycerol.

close to the coordination sphere owing to its interaction with BnN₃ through hydrogen bonds (see below). Intermediate **II** then evolves to give the favored regioisomer 1-benzyl-4R-1,2,3-triazole, according to the accepted Cu-catalyzed mechanisms.^[4b,23] The formation of the corresponding silyl derivative of glycerol was proven by NMR spectroscopy (see Figures S5 and S6 in the Supporting Information).^[24] Alkyne **10** did not give the corresponding desilylated triazole, probably as a consequence of the steric hindrance triggered by the TBDMS group around the metal center.

To rationalize the effect of glycerol in AAC reactions, we studied the interaction of glycerol with benzyl azide by theoretical calculations (DFT B3LYP, 6-31G*), taking into account the ability of glycerol to form hydrogen bonds.^[25,26] For comparative purposes, we also analyzed this effect with ethanol and several diols (ethylene glycol, 1,2-, and 1,3-propanediol). The resulting BnN₃/alcohol adducts increase the dipolar character of BnN₃ in relation to neat benzyl azide (see calculated charges

in Figure S7 in the Supporting Information). It is important to note that in the case of polyols (ethylene glycol, 1,2-propanediol, and glycerol) the intramolecular hydrogen bonds trigger an additional stabilization of the corresponding BnN_3 /alcohol adduct (see Figure S8 in the Supporting Information). The analysis of the relative energies of frontier orbitals for the different BnN_3 /alcohol adducts (see Figure S9 in the Supporting Information) showed that the BnN_3 /glycerol LUMO, which overlaps with the dipolarophile HOMO (diphenylacetylene was chosen for the calculations), is more stable than the ones obtained for the other adducts (see Table S6 in the Supporting Information). In consequence, the reactivity should be enhanced, as observed in this work for a range of alkynes.

Conclusion

We have shown that glycerol acts as a noninnocent solvent for metal-free azide–alkyne cycloadditions, promoting the reaction between internal alkynes and organic azides in contrast to other protic solvents, both under classical and dielectric heating. Moreover, the reactivity in glycerol was particularly enhanced by microwave heating, probably owing to the long relaxation time of glycerol in comparison with other protic solvents, which is related to its supramolecular arrangement through intermolecular hydrogen bonds. At a molecular level, analysis of the frontier orbitals for the BnN_3 /glycerol adduct pointed to a higher stabilization of the corresponding LUMO than that for comparable adducts involving ethanol and diols. This trend justifies the increase of the reaction rate according to a concerted pathway for the metal-free cycloaddition.

These results permit us to envisage the formation of fully substituted 1,2,3-triazoles by using a metal-free methodology, which is particularly interesting for the synthesis of drugs and natural products.

Experimental Section

General

All manipulations were performed by using standard Schlenk techniques under argon atmosphere. Unless stated otherwise, commercially available compounds were used without further purification. Glycerol was treated under vacuum at 80 °C overnight prior to use. NMR spectra were recorded on Bruker Avance 300, 400, and 500 spectrometers at 293 K. GC analyses were carried out on an Agilent GC6890 with a flame ionization detector using a SGE BPX5 column composed of 5% of phenylmethylsiloxane. Reactions under microwave activation were carried out on single-mode microwave CEM Explorer SP 48, 2.45 GHz, Max Power 300 W Synthesis System, CEM Focused Microwave™ Synthesis System Model Discover, and Anton Paar Monowave 300 instruments. Theoretical studies were carried out by using the following software: SPARTAN'14 for Windows and Linux, Wavefunction, Inc. 18401 Von Karman Avenue, suite 307, Irvine, CA 92612, USA. Calculations were carried out with Density Functional B3LYP by using the basis set 6-31G*.

General AAC procedure in glycerol under microwave activation

A sealed tube equipped with a stirring bar was successively charged with the corresponding alkyne (0.6 mmol) and glycerol (1 mL); the mixture was stirred at room temperature for 5 min. Benzyl azide (0.4 mmol, 53.2 mg) was then added and the sealed tube was placed into the microwave reactor (100 °C, 250 W) for 30 min (or the appropriate time). It is important to note that at room temperature the reaction mixture gave a kind of emulsion but that at 100 °C a homogeneous solution was obtained (i.e., reagents and products were soluble in glycerol).^[27] The organic products were extracted with dichloromethane (6 × 2 mL). The combined chlorinated organic layers were filtered through a Celite pad and the resulting filtrate was concentrated under reduced pressure. The products were purified by chromatography (silica short column, eluent: cyclohexane/ethyl acetate 1:1) to determine the isolated yields of the corresponding triazoles.

Compound maj-8a: Yellow oil; IR (neat): $\tilde{\nu}$ = 1606, 1497, 1416, 1248 cm^{-1} ; ^1H NMR (500 MHz, CDCl_3): δ = 0.35 (s, 9H), 2.22 (s, 3H), 5.51 (s, 2H), 7.15–7.20 (m, 2H), 7.27–7.39 ppm (m, 3H); ^{13}C (^1H) NMR (125 MHz, CDCl_3): δ = -0.9, 9.3, 51.2, 127.2, 128.1, 128.9, 135.1, 138.1, 143.8 ppm; HRMS (ESI^+): m/z [$M+H$] $^+$ calcd for $\text{C}_{13}\text{H}_{20}\text{N}_3\text{Si}$: 246.1412; found: 246.1421; elemental analysis calcd (%) for $\text{C}_{13}\text{H}_{19}\text{N}_3\text{Si}$: C 63.63, H 7.80, N 17.11; found: C 63.22, H 7.88, N 16.94.

Compound 10a: Yellow oil; IR (neat): $\tilde{\nu}$ = 1606, 1497, 1456, 1249 cm^{-1} ; ^1H NMR (500 MHz, CDCl_3): δ = 0.05 (s, 6H), 0.90 (s, 9H), 5.35 (s, 2H), 6.94–7.00 (m, 2H), 7.05–7.10 (m, 2H), 7.21–7.28 (m, 3H), 7.35–7.40 (m, 2H), 7.43–7.48 (m, 1H) ppm; ^{13}C (^1H) NMR (125 MHz, CDCl_3): δ = 5.3, 26.6, 51.4, 127.6, 127.9, 128.2, 128.5, 128.8, 129.3, 130.4, 135.6, 142.8, 144.1, 173.4 ppm; HRMS (ESI^+): m/z [$M+H$] $^+$ calcd for $\text{C}_{21}\text{H}_{28}\text{N}_3\text{Si}$: 350.2050; found: 350.2047; elemental analysis calcd (%) for $\text{C}_{21}\text{H}_{27}\text{N}_3\text{Si}$: C 72.16, H 7.79, N 12.02; found: C 72.24, H 8.27, N 11.87.

Compound 5c: Yellow oil; IR (neat): $\tilde{\nu}$ = 1611, 1570, 1544, 1247 cm^{-1} ; ^1H NMR (500 MHz, CDCl_3): δ = 0.89 (t, J = 7.0 Hz, 3H), 0.98 (t, J = 7.4 Hz, 3H), 0.98 (t, J = 7.4 Hz, 3H), 1.20–1.40 (m, 10H), 1.53–1.62 (m, 2H), 1.68–1.77 (m, 2H), 1.83–1.96 (m, 2H), 2.55–2.61 (m, 4H), 4.16–4.20 (m, 2H) ppm; ^{13}C (^1H) NMR (125 MHz, CDCl_3): δ = 13.85, 13.98, 14.05, 22.58, 22.60, 22.94, 24.49, 26.69, 27.23, 29.06, 29.70, 30.35, 31.71, 47.89, 132.44, 144.71 ppm; HRMS (ESI^+): m/z [$M+H$] $^+$ calcd for $\text{C}_{16}\text{H}_{32}\text{N}_3$: 266.2591; found: 266.2594; elemental analysis calcd (%) for $\text{C}_{16}\text{H}_{31}\text{N}_3$: C 72.40, H 11.77, N 15.83; found: C 72.13, H 12.28, N 15.53.

Acknowledgements

Financial support from the Centre National de la Recherche Scientifique (CNRS), the Université de Toulouse 3 – Paul Sabatier, and MINECO (grant CTQ2012-38594-C02-01) are gratefully acknowledged. The authors thank Pierre Lavedan and Stéphane Massou for NMR discussions and DOSY experiments. M.R. thanks the CNRS for a PhD grant.

Keywords: azide–alkyne cycloaddition · density functional calculations · glycerol · metal-free reactions · microwave activation

[1] For some selected recent reviews, see: a) R. Berg, B. F. Straub, *Beilstein J. Org. Chem.* **2013**, *9*, 2715–2750; b) N. V. Sokolova, V. G. Nenajdenko,

- RSC Adv. **2013**, *3*, 16212–16242; c) P. Thirumurugan, D. Matosiuk, K. Jozwiak, *Chem. Rev.* **2013**, *113*, 4905–4979; d) P. L. Golas, K. Matyjaszewski, *Chem. Soc. Rev.* **2010**, *39*, 1338–1354; e) P. Wu, V. V. Fokin, *Aldrichimica Acta* **2007**, *40*, 7–17; f) C. G. S. Lima, A. Ali, S. van Berkel, B. Westermann, M. W. Paixão, *Chem. Commun* **2015**, *51*, 10784–10796.
- [2] A. Michael, *J. Prakt. Chem.* **1893**, *48*, 94–95.
- [3] a) R. Huisgen, *Angew. Chem. Int. Ed. Engl.* **1963**, *2*, 565–598; *Angew. Chem.* **1963**, *75*, 604–637; b) R. Huisgen, *Angew. Chem. Int. Ed. Engl.* **1963**, *2*, 633–645; *Angew. Chem.* **1963**, *75*, 742–754.
- [4] For the first Cu-catalyzed works, see: a) C. W. Tornøe, C. Christensen, M. Meldal, *J. Org. Chem.* **2002**, *67*, 3057–3064; b) V. V. Rostovtsev, L. G. Green, V. V. Fokin, K. B. Sharpless, *Angew. Chem. Int. Ed.* **2002**, *41*, 2596–2599; *Angew. Chem.* **2002**, *114*, 2708–2711.
- [5] J. McNulty, K. Keskar, R. Vemula, *Environ. Chem. Chem. Eur. J.* **2011**, *17*, 14727–14730.
- [6] For the first report on Ru-catalyzed AAC reactions, see: a) L. Zhang, X. Chen, P. Xue, H. H. Y. Sun, I. D. Williams, K. B. Sharpless, V. V. Fokin, G. Jia, *J. Am. Chem. Soc.* **2005**, *127*, 15998–15999; for a selected recent review, see: b) Y. Yamamoto, *Heterocycles* **2013**, *87*, 2459–2493.
- [7] a) E. Rasolofonjatovo, S. Theeramunkong, A. Bouriaud, S. Kolodych, M. Chaumontet, F. Taran, *Org. Lett.* **2013**, *15*, 4698–4701; b) S. Ding, G. Jia, J. Sun, *Angew. Chem. Int. Ed.* **2014**, *53*, 1877–1880; *Angew. Chem.* **2014**, *126*, 1908–1911.
- [8] H. S. P. Rao, G. Chakibanda, *RSC Adv.* **2014**, *4*, 46040–46048.
- [9] J. M. Baskin, C. R. Bertozzi, *Aldrichimica Acta* **2010**, *43*, 15–23.
- [10] For a selected work, see: J. M. Baskin, J. A. Prescher, S. T. Laughlin, N. J. Agard, P. V. Chang, I. A. Miller, A. Lo, J. A. Codelli, C. R. Bertozzi, *Proc. Natl. Acad. Sci. USA* **2007**, *104*, 16793–16797.
- [11] For some representative examples, see: a) M. Sau, C. Rodríguez-Esrich, M. A. Pericàs, *Org. Lett.* **2011**, *13*, 5044–5047; b) R. A. Brawn, M. Welzel, J. T. Lowe, J. S. Panek, *Org. Lett.* **2010**, *12*, 336–339; c) V. Declerck, L. Toupet, J. Martínez, F. Lamaty, *J. Org. Chem.* **2009**, *74*, 2004–2007; d) A. I. Oliva, U. Christmann, D. Font, F. Cuevas, P. Ballester, H. Buschmann, A. Torrens, S. Yenes, M. A. Pericàs, *Org. Lett.* **2008**, *10*, 1617–1619.
- [12] a) F. Chahdoura, S. Mallet-Ladeira, M. Gómez, *Org. Chem. Front.* **2015**, *2*, 312–318; b) F. Chahdoura, I. Favier, C. Pradel, S. Mallet-Ladeira, M. Gómez, *Catal. Commun.* **2015**, *63*, 47–51; c) F. Chahdoura, I. Favier, M. Gómez, *Chem. Eur. J.* **2014**, *20*, 10884–10893; d) F. Chahdoura, C. Pradel, M. Gómez, *Adv. Synth. Catal.* **2013**, *355*, 3648–3660.
- [13] F. Chahdoura, C. Pradel, M. Gómez, *ChemCatChem* **2014**, *6*, 2929–2936.
- [14] For a selected contribution on the microwave-assisted synthesis in glycerol, see: W.-J. Zhou, X.-Z. Zhang, X.-B. Sun, B. Wang, J.-X. Wang, L. Bai, *Russ. Chem. Bull. Int. Ed.* **2013**, *62*, 1244–1247.
- [15] For the Cu-catalyzed synthesis of 1-benzyl-4,5-diphenyl-1,2,3-triazole by using preformed well-defined complexes (**15a**: 72% yield after 48 h at 80 °C; **15b**: 68% yield after 12 h at 120 °C in DMF) and heterogeneous catalyst (**15c**: 54% yield after 24 h at 80 °C), see: a) S. Hohloch, D. Scheffele, B. Sarkar, *Eur. J. Inorg. Chem.* **2013**, 3956–3965; b) B.-H. Lee, C.-C. Wu, X. Fang, C. W. Liu, J.-L. Zhu, *Catal. Lett.* **2013**, *143*, 572–577; c) P. Li, L. Wang, Y. Zhang, *Tetrahedron* **2008**, *64*, 10825–10830.
- [16] We tested different Cu(I) salts that gave similar results under the same catalytic conditions (see Table S1 in the Supplementary Information).
- [17] a) M. A. Herrero, J. M. Kremsner, C. O. Kappe, *J. Org. Chem.* **2008**, *73*, 36–47; b) D. Obermayer, C. O. Kappe, *Org. Biomol. Chem.* **2010**, *8*, 114–121.
- [18] C. Gabriel, S. Gabriel, E. H. Grant, B. S. J. Halstead, D. M. P. Mingos, *Chem. Soc. Rev.* **1998**, *27*, 213–223.
- [19] For selected contributions, see: a) L. Li, T. Shang, X. Ma, H. Guo, A. Zhu, G. Zhang, *Synlett* **2015**, 695–699; b) S. J. Coats, J. S. Link, D. Gauthier, D. J. Hlasta, *Org. Lett.* **2005**, *7*, 1469–1472; c) D. J. Hlasta, J. H. Ackerman, *J. Org. Chem.* **1994**, *59*, 6184–6189; d) A. Padwa, M. W. Wannamaker, *Tetrahedron* **1990**, *46*, 1145–1162.
- [20] For **8a**, the assignment of both regioisomers was carried out by NOESY NMR correlations (see Figure S2 in the Supporting Information). For **9a** and **10a**, desilylation reactions with tetrabutylammonium fluoride (TBAF) were carried out to unambiguously determine the major isomer (see Figure S3 in the Supporting Information).
- [21] Reaction conditions: azide (0.4 mmol) and the corresponding alkyne (0.6 mmol) in solvent (1 mL) under microwave activation (250 W) at 100 °C for 1 h (**1c**), 2 h (**5c**), or 30 min (**9c**). For **1b**, similar conditions were used but with applying a power of 150 W for 1 h. Reactions involving PhN₃ were protected from light.
- [22] 70 and 56% of PhN₃ were recovered from a glycerol solution of PhN₃ after 30 min under MW activation at 150 and 250 W, respectively. Under classical heating, 95% of PhN₃ was recovered after 20 h at 100 °C.
- [23] B. T. Worrell, J. A. Malik, V. V. Fokin, *Science* **2013**, *340*, 457–460.
- [24] A control experiment between glycerol and TMSCl was carried out to identify the major concomitant silylglycerol derivative observed (see Experimental part of the Supporting Information, Scheme S3 and Figures S5 and S6).
- [25] T. Kusukawa, G. Niwa, T. Sasaki, R. Oosawa, W. Himeno, M. Kato, *Bull. Chem. Soc. Jpn.* **2013**, *86*, 351–353.
- [26] DOSY NMR experiments were inconclusive on the effect of different solvents on the interaction with reagents involved in azide–alkyne cycloadditions (see Table S7 in the Supporting Information).
- [27] When using other solvents instead of glycerol (water, ethanol, ethylene glycol, propane-1,2-diol, propane-1,3-diol, dioxane, fluorobenzene), the reagents and products were soluble, even at room temperature for ethanol, dioxane and fluorobenzene.

Received: September 25, 2015
 Published online on November 6, 2015

Chapter 3

Key Non-Metal Ingredients for Cu-Catalysed Azide–Alkyne Cycloaddition in Glycerol

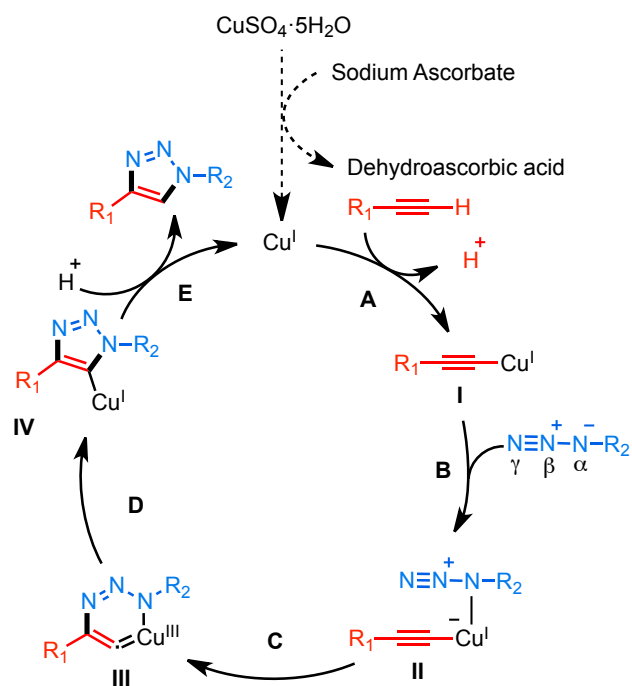
Chapter 3. Key Non-Metal Ingredients for Cu-Catalysed Azide–Alkyne Cycloaddition in glycerol.

3.1 Introduction

Since the work of Sharpless and Fokin *et al.*^[1] and Medal *et al.*^[2] in 2002, the copper catalysed azide-alkyne cycloaddition (CuAAC) has been considered the most useful procedure to prepare, in a regioselective manner, 1,4-disubstituted 1,2,3-triazoles. The more than 6,000 citing references of the work of Sharpless and Fokin and the ca. 4,500 citing references of the Medal's work are an overwhelming proof of this successful procedure,^[3] which has been widely investigated and applied.^[4]

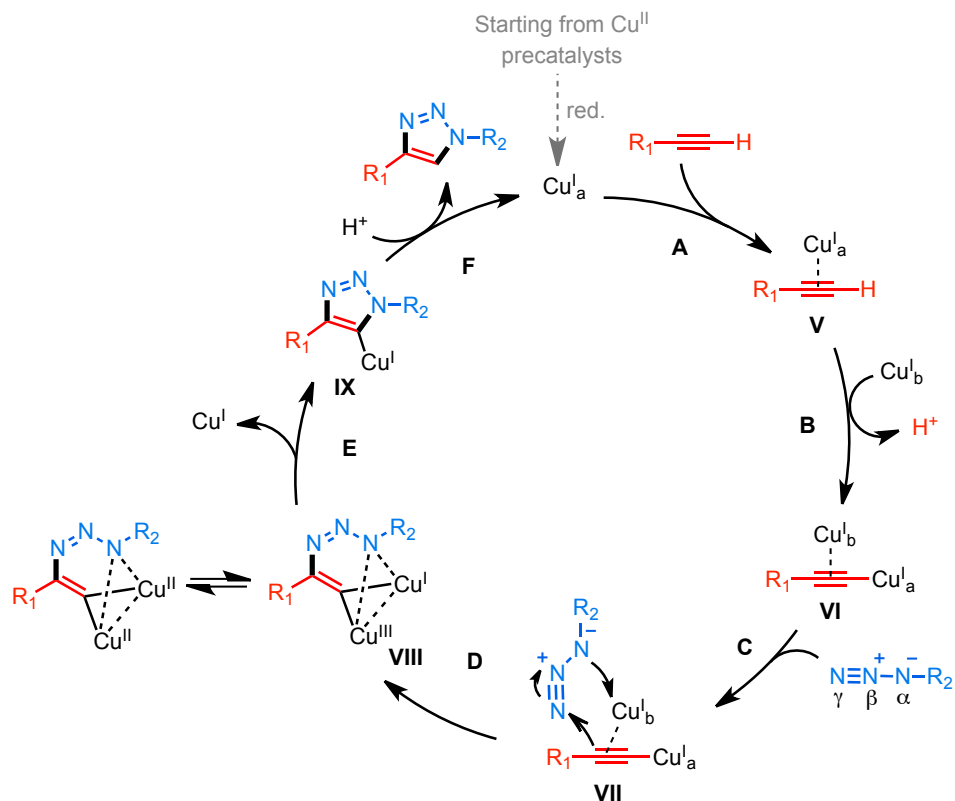
CuAAC is also well known as the “Click reaction” because this transformation is one of the most important examples that fulfils the requirements of the concept *Click Chemistry*,^[5] defined by Sharpless *et al.* in 2001. It tolerates a wide range of functional groups showing a large scope concerning both alkyne and azide reactants. Furthermore, this transformation can be carried out in a considerable variety of solvents. The reaction tolerates a wide range of pH values and it can be performed over a broad temperature range. In addition, azides and alkynes are quite stable substrates, which permit to work under different conditions: in the presence of oxygen and water, and also at high temperatures.

Despite the apparent simplicity of this reaction, the mechanism is still under debate in the scientific community.^[6] The vast array of conditions in which the CuAAC can proceed make the mechanism of this reaction difficult to be uniquely established. The first postulated stepwise mechanism^[1, 7] (Scheme 3.1) begins with the formation of the corresponding copper(I)-acetylide (intermediate **I**) by a simple acid-base reaction between the terminal alkyne and the copper(I) species (step A). After that, the formed copper-acetylide interacts with the organic azide (step B) by coordination of copper to the α nitrogen of the azide (intermediate **II**). At this point, an intramolecular oxidative insertion between the azide and the alkyne takes place (step C), leading to a six-membered Cu(III) metallacycle (intermediate **III**). A ring reductive contraction (step D) generates the corresponding copper(I)-triazolide (intermediate **IV**) which, after a final protonation (step E), leads to the reaction product, the 1,4-disubstituted 1,2,3-triazole and to the Cu(I) active species.



Scheme 3.1 First proposed mechanism for CuAAC.

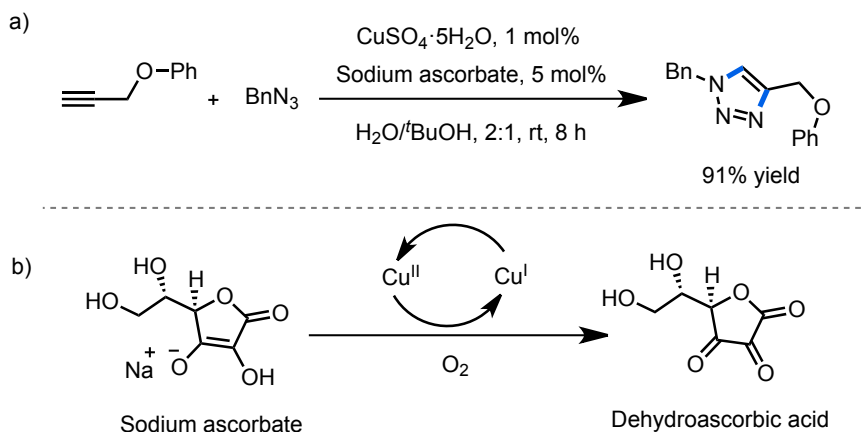
In a later work, Fokin, Finn *et al.*^[8] determined by kinetic studies the reaction rate to be second order in copper, which means the requirement of intermediates containing two copper atoms. Since then, mechanistic studies started focusing on explaining the formation of intermediate **III** (Scheme 3.1), which requires a high activation energy because of the ring strain. The introduction of another copper ion was suggested in order to prevent the formation of a strained metallacycle, decreasing in consequence the activation barrier.^[9] Up to date, there are many evidences of the participation of two copper(I) atoms in the rate-determining step.^[10] The accepted current pathway (Scheme 3.2) begins with the formation (steps A and B) of a σ,π -di(copper(I)) acetylide (intermediate **VI**). The π -bound enriched copper atom coordinated the azide (step C), leading to the complex **VII**. The nucleophilic attack at the γ nitrogen of the azide by the β carbon of the acetylide (step D) gives the strained (three fused cycles) metallacycle **VIII** in which one copper(I) has been oxidised to copper(III) (in equilibrium with the corresponding Cu(II) dinuclear core). After a ring closure, the copper(I) triazolide (**IX**) is obtained which after a subsequent protonation leads to the final product and the Cu(I) catalytic species. Among all the structures present in the mechanism, only the σ,π -di(copper) acetylide (**VI**)^[10c] and the copper(I) triazolide (**IX**)^[11] have been fully characterized. Intermediate **VII** has only been detected using a mass spectrometric method.^[10b] Using a copper isotope labelling experiment,^[10a] it was found that in the proposed metallacycle (**VIII**) occurs a rapid internal rearrangement equilibrium involving the two copper centres.



Scheme 3.2 The current dinuclear mechanism of CuAAC.

For both proposed Cu-catalysed mechanisms, the first step is the formation of the copper-acetylide intermediate, which means that the reactivity is restricted only to terminal alkynes, being the internal alkynes devoid of such reactivity. DFT calculations demonstrated that the initial formation of a π -complex between Cu(I) and the acetylene is highly disfavoured due to the high energetic barrier.^[7] Even though this lack of reactivity using internal alkynes seems to be explained, Nolan *et al.*^[12] and Vincent *et al.*^[13] reported that their preformed Cu(I) complexes can mediate the reaction between benzyl azide and 3-hexyne, proving the possibility of an alternative activation pathway.

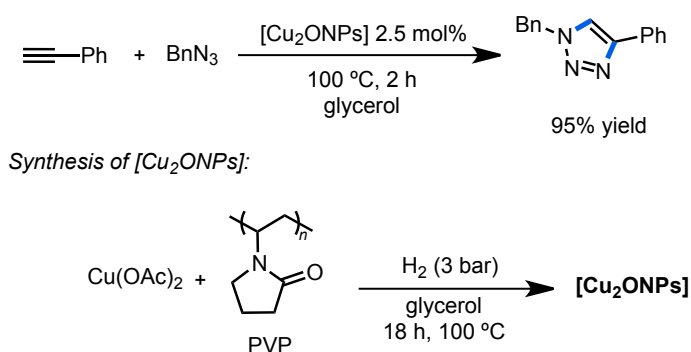
In spite of the debate about the mechanism of CuAAC, it is generally accepted the necessity of copper in the oxidation state +1 as catalytically active species to achieve an efficient reaction. To generate these catalytically active species, almost any copper source can be used as precatalyst. The most common method is the one initially reported by Sharpless and Fokin *et al.*^[1] in which $\text{CuSO}_4 \cdot 5\text{H}_2\text{O}$ is used in the presence of a reducing agent (sodium ascorbate) to generate the catalytically active Cu(I) (Scheme 3.3). The main advantage of this method is the compatibility with water and oxygen, which make it very attractive for bioconjugation. However, this methodology is limited to water-tolerant substrates.



Scheme 3.3 (a) CuAAC using the Cu(II)/sodium ascorbate system as catalyst; (b) redox process between sodium ascorbate and Cu(II) salts in an aerobic atmosphere.

Another way to achieve the desired Cu(I) species is the *in situ* oxidation of metal copper (Cu(0)), even though this method requires high catalyst loadings and takes longer times compared with the Cu(II)/sodium ascorbate system. It can be significantly accelerated applying microwave irradiation.^[14] Comproportionation of Cu(II) (available on the metal patina or added as CuSO₄) and Cu(0) generates the active Cu(I) species in solution. The main advantage of this protocol is the high purity of the products with lower levels of copper.

Copper nanoparticles (CuNPs) have been widely used as Cu(I) source for CuAAC.^[15] The advantages of using nanoparticles are mainly the high number of active species due to the large surface area and the easy separation and recyclability, which minimises the contamination of the products. In our group, we reported a highly efficient catalytic system consisting in copper(I) oxide nanoparticles (Cu₂ONPs) in neat glycerol.^[16] They were prepared starting from Cu(OAc)₂, under H₂ atmosphere (3 bar), at 100 °C and using PVP (poly(vinylpyrrolidone)) as stabiliser (Scheme 3.4). The mentioned Cu₂ONPs were successfully used as catalyst not only in CuAAC (Scheme 3.4), but also in C–heteroatom bond formation and AAC/coupling tandem processes. The catalytic phase could be recycled at least ten times, without any loss of activity.



Scheme 3.4 CuAAC catalysed by Cu₂ONPs in neat glycerol.

Copper(I) salts can be used directly as catalysts for CuAAC without the necessity of in situ generation of Cu(I) species from Cu(0) or Cu(II) starting materials. Copper(I) halides are commonly used despite being quite insoluble in most organic solvents.^[17] To improve the solubility of the copper species in the medium, the presence of additives is required. In general, Lewis bases (in particular amines, such as DIPEA^[21]) help to increase the solubility of copper species, inducing an acceleration of the process. Pre-formed copper(I) molecular complexes bearing nitrogen containing ligands are also commonly used in this transformation. In particular, polydentate nitrogen-based ligands are convenient not only to stabilise copper(I) species,^[18] but also to accelerate the process.^[19] In our group, we introduced tris(triazolyl)methanol (TTM, Figure 3.1a) as an excellent ligand for Cu(I).^[20] Its structure was proposed from NMR studies and by comparison with the crystal structure of a Cu(II) analogue (Figure 3.1b). This complex could efficiently catalyse AAC reactions in water or under solvent-free conditions, using low catalyst loadings (0.5 mol%) and at room temperature (Figure 3.1c).

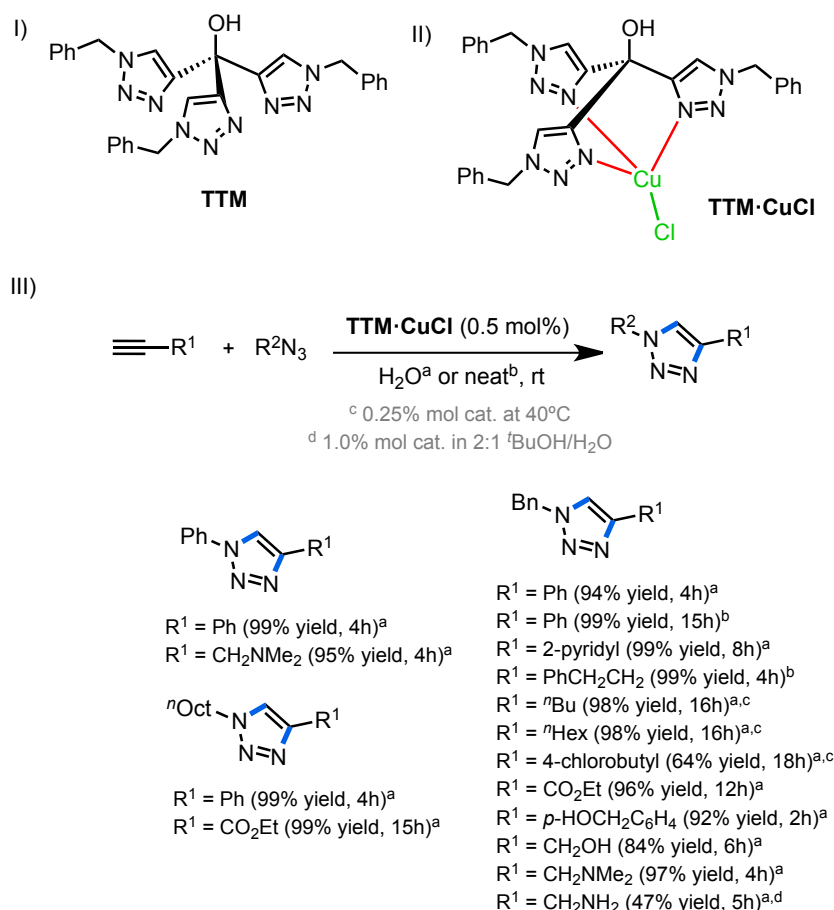
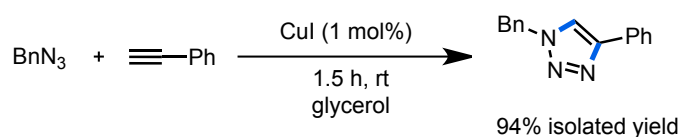


Figure 3.1 a) Tris(triazolyl)methanol ligand (TTM). b) Proposed structure of the copper(I) complex. (c) Scope of substrates using TTM·CuCl as catalyst on water or under neat conditions.

However, base-free CuAAC procedures using copper(I) halides as copper sources are rare. Therefore, we planned to study the CuAAC in the presence of copper(I) salts as catalyst working in glycerol medium, in the absence of any additive. In this way, we also wanted to understand the role of an added base in the transformation. To the best of our knowledge, there is only one work reported by García-Álvarez *et al.*,^[21] in which they carried out the Cu-AAC in the absence of any base (Scheme 3.5). The reaction proceeds under air, at room temperature, in a short period of time, tolerating a variety of substrates and permitting the catalyst recycling up to 6 times.



Scheme 3.5 Benchmark base-free CuAAC reaction in glycerol reported by García-Álvarez *et al.*^[21]

The mentioned work was published during the course of our researches. A serious discrepancy was found between the results reported and our work. Actually, the reaction described in Scheme 3.5 did not work in our hands, under “*exactly*” the same conditions. Taking into account the simplicity of the reaction, almost fulfilling the requirements in the Cornforth definition of an *ideal chemical process*,^[22] we suspected that an uncontrolled factor was participating in the process making impossible to reproduce this reaction.^[23] This impasse prompted us to try to rationalise this behaviour.

3.2 Results and discussion

The cycloaddition between benzyl azide (**a**) and phenyl acetylene (**13**) in glycerol was chosen as our model reaction. In the presence of 1 mol% of CuI as catalyst, the reaction did not work in 1.5 h (Table 3.1, entry 1). The yield was good only when the reaction time increased (24 h, Table 3.1, entry 1). In order to understand the absence of reproducibility of the results reported by García-Álvarez *et al.*,^[21] we checked all the components involved in the reaction. Different sources of glycerol, CuI and phenylacetylene were tested without observing any change in the reactivity. We arrived to the conclusion that the cause of irreproducibility was the benzyl azide. In fact, the efficiency of the reaction depends on the source of the azide (Table 3.1). Using our home-made benzyl azide,^[24] the reaction did not work (Table 3.1, entry 1), but using a commercial flask from Alfa-Aesar (Table 3.1, entry 2, two different lots) the reaction worked exactly as reported by García-Álvarez *et al.* Moreover, other commercial flasks from the

same company (but coming from a different Lot) (Table 3.1, entry 3) or from Sigma-Aldrich (Table 3.1, entry 4), did not give the reported result. Undoubtedly, some impurities were present in these sources of benzyl azide, triggering a dramatic effect in the catalytic transformation.

Table 3.1 CuAAC between phenylacetylene and benzyl azide using CuI as catalytic precursor.^[a]

$\text{Ph-C}\equiv\text{C-H} + \text{BnN}_3 \xrightarrow[\text{glycerol}]{\text{CuI (1 mol%), 1.5 h, rt}}$
 $\text{Bn-N}=\text{N}-\text{C}(\text{Ph})=\text{N}-\text{N}$

13 **a** **13a**

Entry	BnN ₃ Source/Batch code	Conversion (yield) (%) ^[b]
1	Home-made ^[c]	<5 <i>84 (69)^[d]</i>
2	Alfa-Aesar/C25Z013 ^[e]	100 (80)
3	Alfa-Aesar/AE040501	<5
4	Aldrich/BCBL4667V	<5

^[a] Reaction conditions: CuI (1 mol%), benzyl azide (0.5 mmol) and phenylacetylene (0.5 mmol) in glycerol (0.5 mL) at 25°C for 1.5 h. ^[b] Conversions (based on benzyl azide) and yields determined by ¹H NMR using 2-methoxynaphthalene as internal standard. ^[c] For synthesis, see experimental procedure in ^[24]. ^[d] In italics, result after 24 h. ^[e] Data coming from two different commercial flasks.

The active benzyl azide was analysed by GC-MS-EI (Figure 3.2), clearly evidencing the presence of impurities. The detailed analysis of the mass spectrum for each peak of the chromatogram (see Annex 3.6.1) allowed us to determine the nature of these impurities, corresponding very likely to long-alkyl chain amines. The same type of analysis was made for the rest of “inactive” benzyl azides (see Annex 3.6.2). The peaks observed in the analysis of the “active” (*i.e.* contaminated) benzyl azide were not found in the rest of chromatograms.

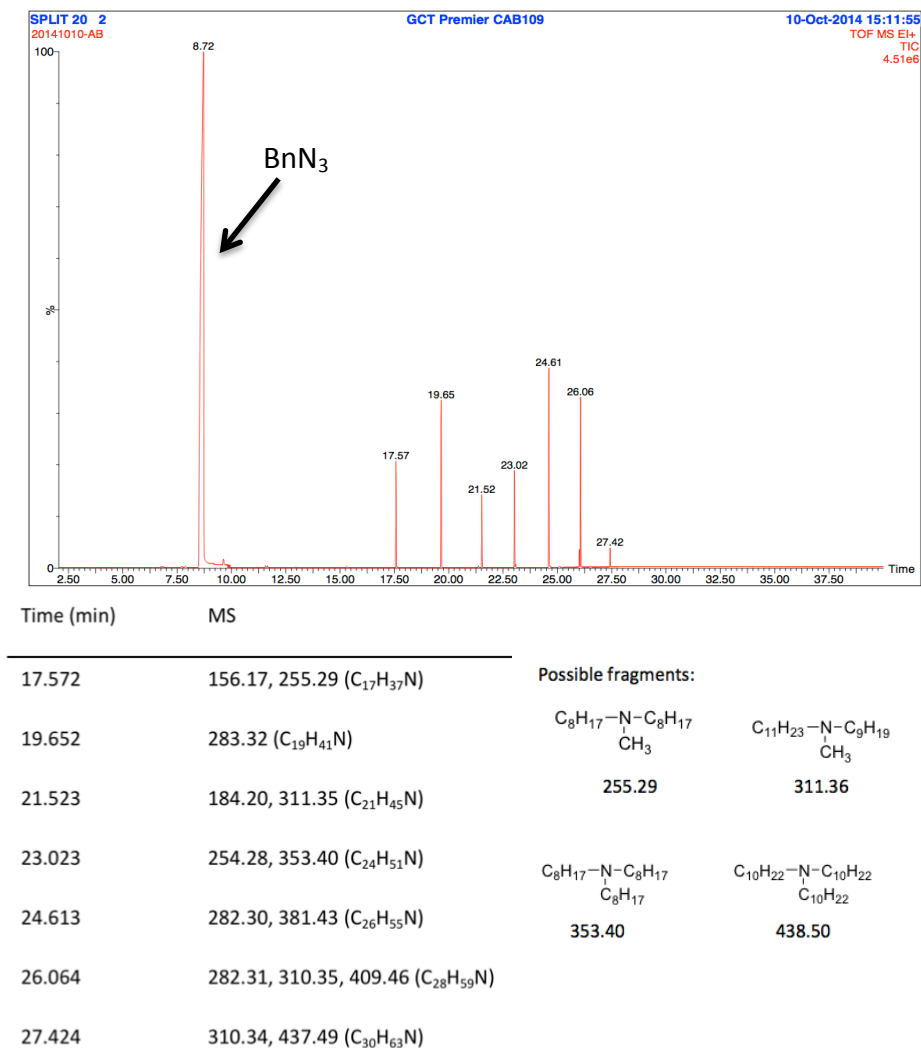


Figure 3.2 GC-MS-EI analysis for benzyl azide from Alfa-Aesar (Lot C25Z013). See Annex 3.6.1 for the mass spectrum for the peaks between 17.5 and 27.5 min retention times.

The “active” benzyl azide was also analysed by NMR (Figure 3.3). ¹H and ¹³C NMR spectra clearly exhibited the presence of impurities in this commercially available compound. These signals are in agreement with the presence of amines bearing long aliphatic chains, as suggested by the analysis by GC-MS-EI. The chemical shifts and the signals integrations are in agreement with these types of compounds. The rest of “inactive” benzyl azides were also analysed by ¹H and ¹³C NMR without finding any additional signal (see Annex 3.6.3).

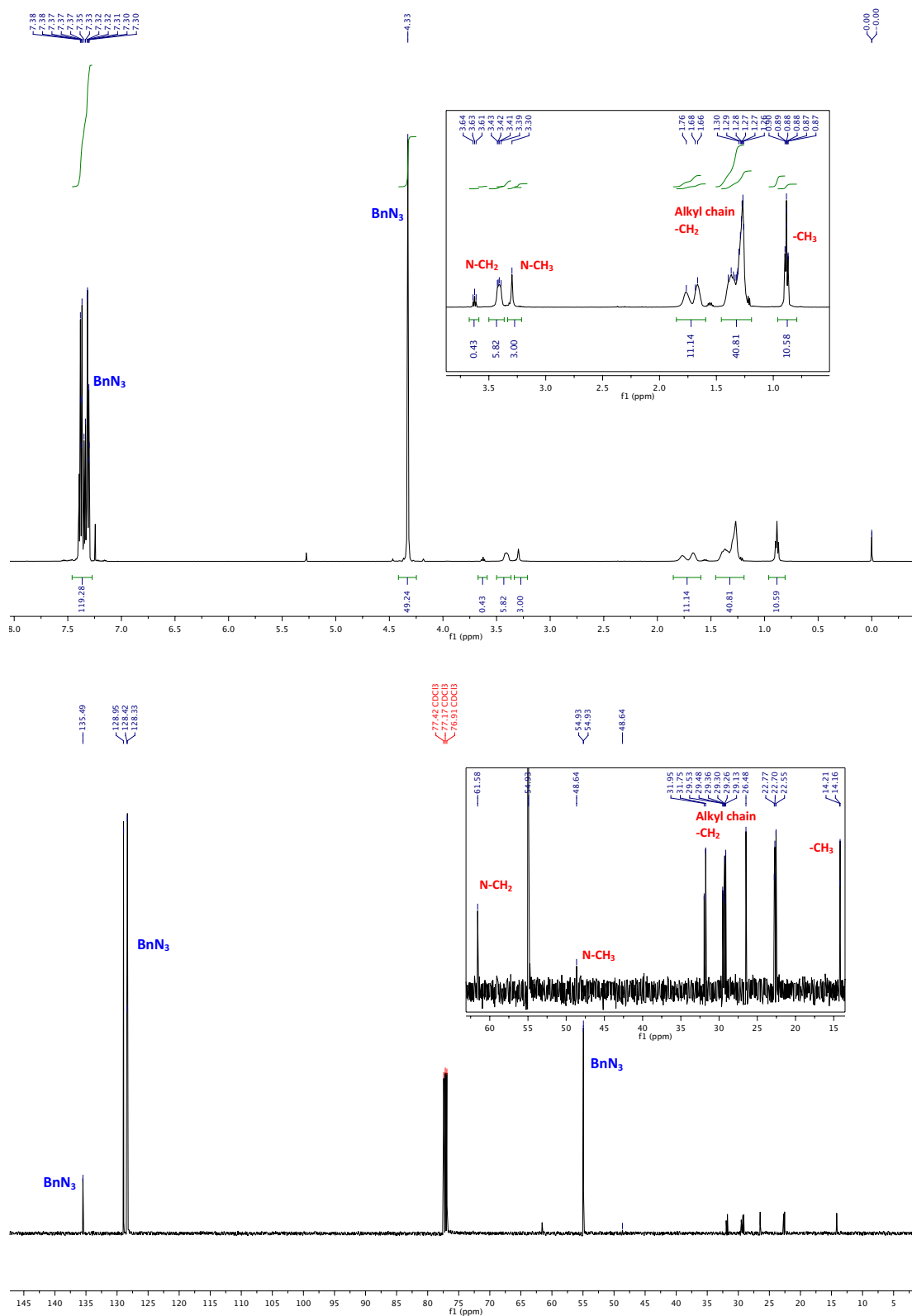


Figure 3.3 ¹H NMR (top, 500 MHz) and ¹³C NMR (bottom, 125 MHz) spectra (in CDCl₃) for benzyl azide from Alfa Aesar (Lot C25Z013).

With these clues in hand, we decided to understand the effect of this type of additives on the “click” reaction. We started by testing different types of amines and ammonium salts as additives in the model reaction, using our pure home-made benzyl azide (Figure 3.4). Ammonium salts were also tested due to the close agreement with the analysis by GC-MS-EI (the possible fragments obtained, Figure 3.2) and NMR.

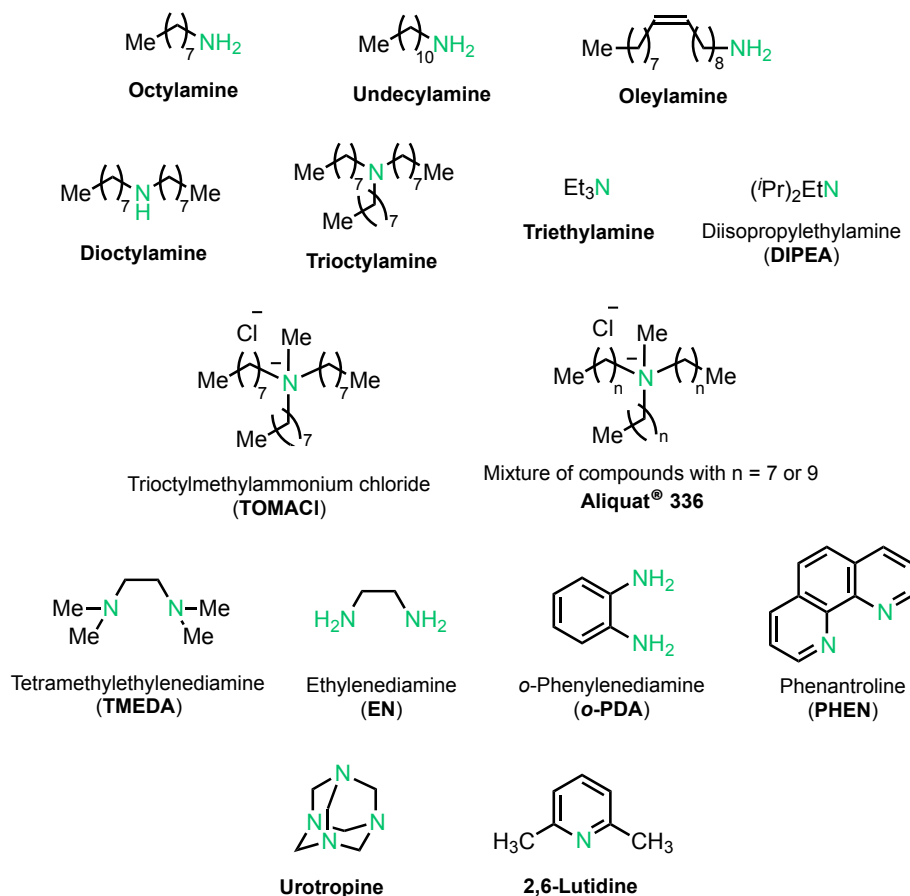


Figure 3.4 Amines and ammonium salts tested as additives in the benchmark CuAAC reaction, using pure home-made benzyl azide.

As shown in Table 3.2, primary, secondary and tertiary amines (Table 3.2, entries 1–5) bearing long aliphatic chains as additives (5 mol%) led to high yields of the corresponding 1,2,3-triazole **13a**. When the amount of the added amine was reduced to 1 mol%, the reaction also worked (Table 3.2, entries 1 and 3–5), especially for oleylamine, dioctylamine and trioctylamine. However, when the alkyl chain is shorter like in the case of NEt_3 or DIPEA (Table 3.2, entries 6–7), the reaction was less efficient. Ammonium salts, such as TOMACl and Aliquat® 336 (Table 3.2, entries 8–9) did not favour the cycloaddition neither. Diamines were also tested as additives; TMEDA led to a high conversion (Table 3.2, entry 10), whereas EN, *o*-PDA and PHEN did not promote the reaction. Finally, urotropine was not active in the reaction (Table 3.2, entry 14) and 2,6-lutidine (used as base in CuAAC reactions in water^[25]) gave a very low yield (Table 3.2, entry

15). It is important to note that the reaction was also carried out in the absence of CuI but in the presence of oleylamine, without observing any conversion.

Table 3.2 CuAAC between phenylacetylene and benzyl azide using CuI as catalytic precursor and in the presence of an amine.^[a]

$\text{Cul (1 mol\%)} \quad \text{Additive (5 mol\%)} \quad \text{1.5 h, rt, glycerol}$

Entry	Additive	Conversion (yield) (%) ^[b]
1	Octylamine	96 (93) 52 (44) ^[c]
2	Undecylamine	96 (93)
3	Oleylamine	100 (>99) 98 (94) ^[c]
4	Dioctylamine	100 (96) 95 (88) ^[c]
5	Trioctylamine	96 (88) 97 (73) ^[c]
6	NEt ₃	28 (16)
7	DIPEA	36 (6)
8	TOMACI	37 (19)
9	Aliquat® 336	20 (<5)
10	TMEDA	83 (70)
11	EN	30 (12)
12	<i>o</i> -PDA	30 (10)
13	PHEN	15 (6)
14	Urotropine	20 (<5)
15	2,6-Lutidine	34 (26)

^[a] Reaction conditions: CuI (1 mol%), additive (5 mol%), benzyl azide (0.5 mmol) and phenylacetylene (0.5 mmol) in glycerol (0.5 mL) at 25°C for 1.5 h. ^[b] Conversions (based on benzyl azide) and yields determined by ¹H NMR using 2-methoxynaphthalene as internal standard. ^[c] In italics, results using only 1 mol% of additive.

Using phenyl azide (**b**) instead of benzyl azide, the same trend could be observed (Table 3.3). In the absence of amine, the reaction did not work (Table 3.3, entry 1), while in the presence of amines with long aliphatic chains high yields were obtained (Table 3.3, entries 2–5). Once more, TMEDA favoured the reaction obtaining a good yield (Table 3.3, entry 7). In the

presence of NEt_3 , EN and urotropine, the system was nearly inactive (Table 3.3, entries 6 and 8–9).

Table 3.3 CuAAC between phenylacetylene and phenyl azide using CuI as catalytic precursor in the presence of an amine.^[a]

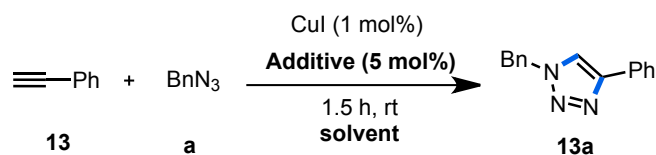
$\text{Ph-C}\equiv\text{C-H} + \text{PhN}_3 \xrightarrow[\text{glycerol, 1.5 h, rt}]{\text{CuI (1 mol\%), Additive (5 mol\%)}} \text{Ph-N}=\text{N}-\text{C}(\text{Ph})=\text{N}-\text{N}=\text{N}-\text{Ph}$

13 **b** **13b**

Entry	Additive	Conversion (yield) (%) ^[b]
1	–	<5
2	Octylamine	100 (94) <i>39 (9)</i> ^[c]
3	Oleylamine	100 (98) <i>100 (87)</i> ^[c]
4	Dioctylamine	83 (89) <i>88 (87)</i> ^[c]
5	Trioctylamine	88 (88) <i>100 (12)</i> ^[c]
6	NEt_3	10 (6)
7	TMEDA	70 (76)
8	EN	21 (19)
9	Urotropine	<5

^[a] Reaction conditions: CuI (1 mol%), additive (5 mol%), phenyl azide (0.5 mmol) and phenylacetylene (0.5 mmol) in glycerol (0.5 mL) at 25°C for 1.5 h. ^[b] Conversions (based on phenyl azide) and yields determined by ¹H NMR using 1,3,5-trimethoxybenzene as internal standard. ^[c] In italics, results using only 1 mol% of additive.

Our model reaction between phenylacetylene (**13**) and benzyl azide (**a**) using CuI as catalyst, was also tested in other polar solvents and in the presence of several amines (Table 3.4). In the absence of amine or in the presence of NEt_3 the reaction did not work (Table 3.4, entries 1–6). However, in the presence of dioctylamine or oleylamine the reactivity was much better (Table 3.4, entries 7–12); in water or 1,4-dioxane the reactivity was comparable to that observed in glycerol (Table 3.4, entries 7,9,10 and 12), whereas in ethanol the yields were lower (Table 3.4, entries 8 and 11).

Table 3.4 CuAAC between phenylacetylene and benzyl azide using CuI as catalytic precursor and an added amine in different solvents.^[a]

Entry	Additive	Solvent	Conversion (yield) (%) ^[b]
1	–	Water	22 (13)
2	–	Ethanol	12 (<5)
3	–	1,4-Dioxane	11 (<5)
4	NEt ₃	Water	15 (<5)
5	NEt ₃	Ethanol	17 (<5)
6	NEt ₃	1,4-Dioxane	24 (11)
7	Diocylamine	Water	100 (93)
8	Diocylamine	Ethanol	66 (48)
9	Diocylamine	1,4-Dioxane	100 (99)
10	Oleylamine	Water	99 (94)
11	Oleylamine	Ethanol	59 (48)
12	Oleylamine	1,4-Dioxane	94 (81)

^[a] Reaction conditions: CuI (1 mol%), additive (5 mol%), benzyl azide (0.5 mmol) and phenylacetylene (0.5 mmol) in the corresponding solvent (0.5 mL) at 25°C for 1.5 h. ^[b] Conversions (based on benzyl azide) and yields determined by ¹H NMR using 2-methoxynaphthalene as internal standard.

After this screening, a representative scope involving different alkynes (**13–22**) and organic azides (**a**, **b**) was carried out using oleylamine as additive. The corresponding 1,2,3-triazoles were obtained in high yields. Even using alkynes bearing alkyl substituents, triazoles were obtained from moderate to high yields (**15a**, **19a**, **19b**). No transesterification reactions with glycerol were observed when alkynes containing ester groups were used (**14a**, **16a**).

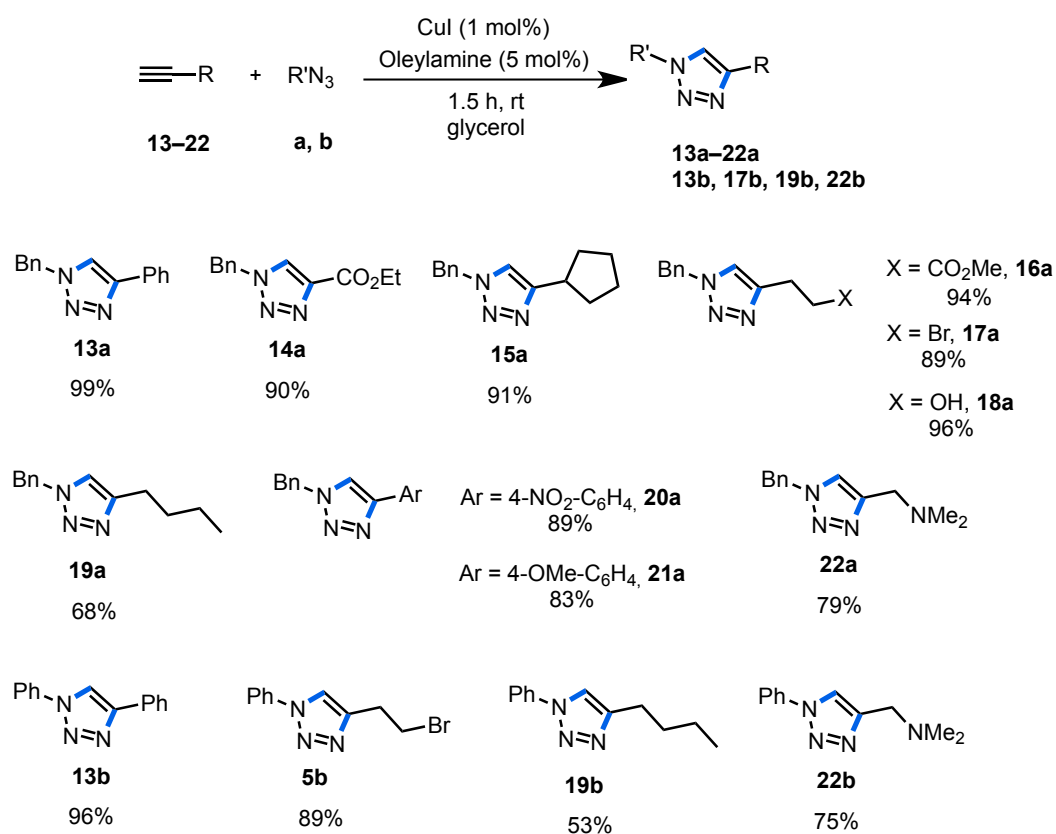
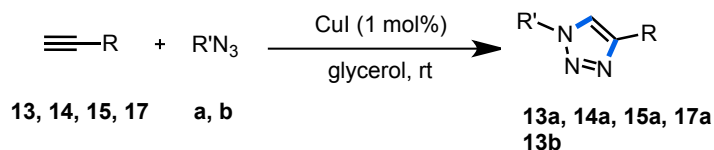
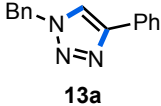
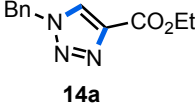
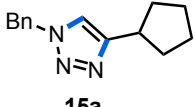
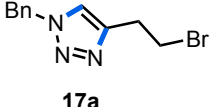
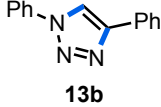


Figure 3.5 Scope of the azide-alkyne cycloaddition catalysed by CuI/Oleylamine system. Figures indicate the isolated yields.

In order to confirm the important effect of the added amine to promote the reaction, some selected triazoles were prepared under amine-free conditions, as control experiments (Table 3.5). In all cases, the yields obtained were very low even at longer reaction times (up to 7 h).

Table 3.5 Control experiments in the absence of amine.^[a]

Entry	Product	Time	Conversion (Yield) (%) ^[b]
1	 13a	1.5	16 (<5)
2	 14a	3	36 (25)
3	 15a	7	23 (<5)
4	 17a	7	6 (<5)
5	 13b	1.5	<5

^[a] Reaction conditions: CuI (1 mol%), azide (0.5 mmol) and phenylacetylene (0.5 mmol) in glycerol (0.5 mL) at 25°C. ^[b] Conversions (based on the azide) and yields determined by ¹H NMR using 2-methoxynaphthalene or 1,3,5-trimethoxybenzene as internal standard.

Unfortunately, our catalytic system was not active for the azide-alkyne cycloaddition using internal alkynes (**1**, **6**) and 1-iodoalkynes (**23**) (Figure 3.6). The corresponding fully substituted triazoles (**1a**, **6a**, **23a**) were not obtained under these mild conditions, even when the amount of CuI was increased and the reaction time was longer (tested in the case of **6a**). Internal alkynes usually require harder conditions to give the cycloaddition, as explained in chapter 2. In the specific case of iodoalkynes, they seem to be less reactive in glycerol, taking longer reaction times to afford good results (18 h, reported by García-Álvarez *et al.* using the

“active” benzyl azide).^[21] However, in aprotic organic solvents like THF,^[26] or even in water^[25a] (using other Cu(I) catalytic systems), the reactivity seems to be higher. A plausible explanation could be the trapping effect of glycerol due to its hydrogen bond network,^[27] preventing the iodoalkyne reactivity.

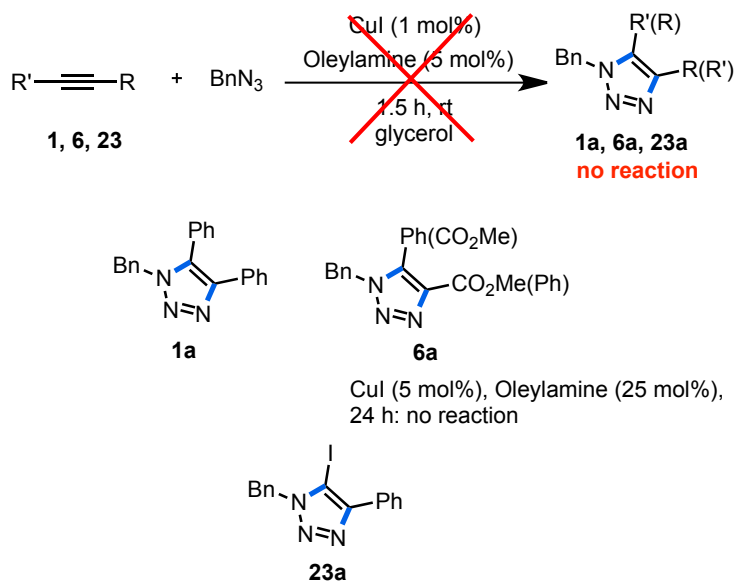


Figure 3.6 Azide-alkyne cycloaddition catalysed by CuI/Oleylamine system applied to internal alkynes.

It is important to note that the catalytic phase could be recycled up to four times without significant loss of activity (Figure 3.7). After each run, the obtained triazole (**13a**) was extracted from the glycerol phase with dichloromethane and the catalytic phase was maintained under vacuum for 30 min. The corresponding reagents were then added again under the same conditions of the preceding run. We demonstrate like this that glycerol is able to efficiently immobilise the catalyst. However, after the fourth run, the activity decreased dramatically, which is directly related to the leaching of copper (more than 1,000 ppm determined by ICP-MS).

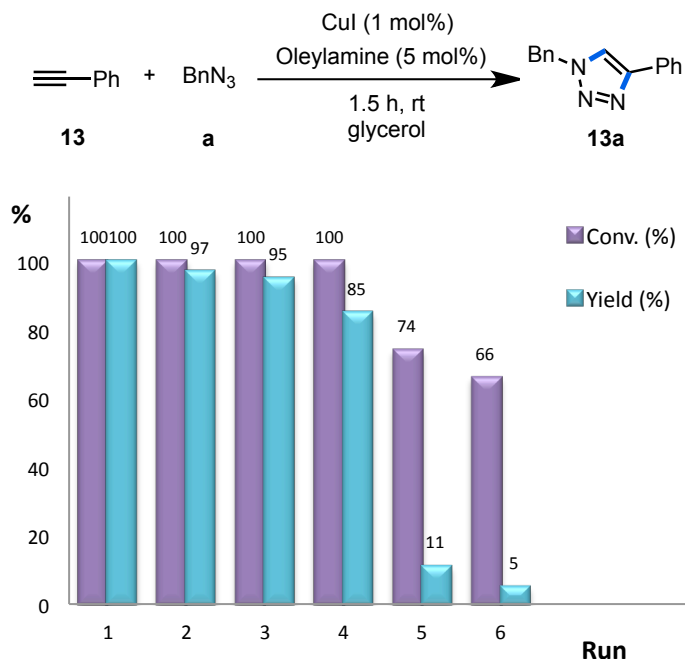


Figure 3.7 Recycling of the catalytic phase of the CuAAC reaction between phenylacetylene and benzyl azide to give **13a**. Conversions and yields determined by ^1H NMR using 2-methoxynaphthalene as internal standard.

With the aim of rationalising the results obtained, we analysed the structural behaviour of copper(I) salts in the presence of amines. Depending on the nature of the ligands and the reaction conditions, CuI motif leads to a large variety of structures, corresponding to discrete molecular complexes^[28] or polymeric networks.^[29] This variety is due to the versatile coordination numbers and geometries of both copper(I) and the halide anion. Copper(I) is a d^{10} ion favouring three different coordination numbers and in consequence leading to different structures around the metal centre: 2 (linear), 3 (trigonal-planar) and 4 (tetrahedral). On the other hand, the halide anion could act as terminal or μ^2 to μ^8 bridging ligand when it is bound to copper(I). These reasons explain such structural variety, which is especially remarkable when *N*-based ligands (mono- or bidentate) are present,^[30] particularly for diamines (EN, TMEDA, PHEN) or short-alkyl chain amines (NEt_3 , DIPEA).^[31] In addition to the good reactivity observed with long-alkyl chain amines, the system CuI/TMEDA gave also good yields. We could obtain a crystal structure of the complex “CuI-TMEDA” (Figure 3.8),^[32] confirming the ability of diamines to give complexes based on closed-cubane “ Cu_4I_4 ” tetramers in agreement with the reported structures.^[31e, 33]

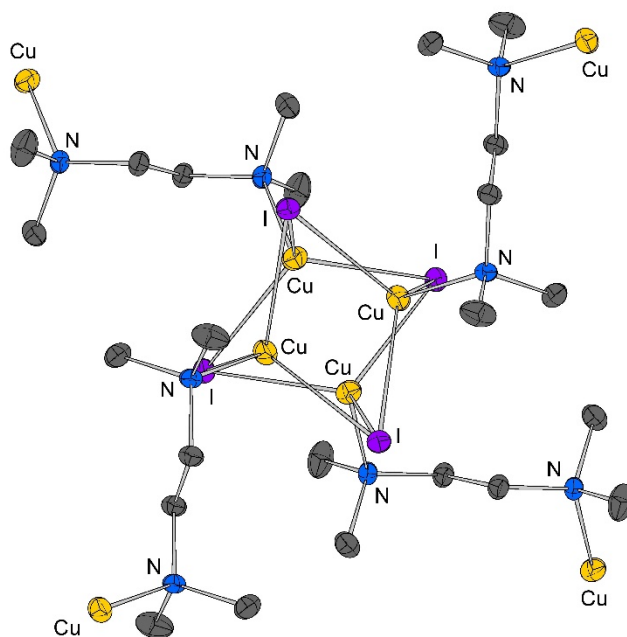


Figure 3.8. Plot of the XRD cubane-like structure of Cu_4I_4 -TMEDA (ellipsoids drawn at the 50% probability level); hydrogen atoms are omitted for clarity.

However, the reason why long-chain amines are promoting the CuAAC reaction should be different. It is well-known that these type of amines (considered weak ligands and in consequence they do not favour the formation of molecular complexes) favour the stabilisation of metal (and metal oxide) nanoparticles.^[34] Moreover, besides ionic liquids,^[35] polyols such as ethylene glycol, polyethylene glycol and, in the last decade, glycerol have been applied as solvents for the preparation of metal colloidal systems. They serve both as stabilisers and reducing agents. This synthetic approach is known as polyol methodology, which was first developed by Fièvet *et al.* in 1989.^[36] In this frame, the presence of both long-chain amines and glycerol, we wondered about the plausible presence of copper-based nanoparticles under our catalytic reaction conditions. Additionally, the broad research on copper nanoparticles^[15, 37] and also our experience in this subject working in glycerol medium,^[16, 38] reinforced this suspicion.

To verify this, we carried out TEM (Transmission Electron Microscopy) analyses of CuI in glycerol and in the presence of different amines (Annex 3.6.4). TEM analyses were carried out directly from the glycerol because of its negligible vapour pressure under high vacuum. In fact, well-dispersed and small nanoparticles (mean diameters in the range 1.8 - 2.8 nm) were observed for oleylamine, dioctylamine and TOMACI (Figure 3.9a, b and c). In contrast TEM analyses of the glycerol phases containing CuI/short-alkyl chains (such as EN, Figure 3.9e) showed the formation of agglomerates, as well as in the case of the system containing only CuI

in the absence of any added base (Figure 3.9d). Only few nanoparticles were observed in the case of CuI/TMEDA system (Figure 3.9f), together with agglomerates too. Correlating reactivity and structures, it seems that the formation of nanoparticles favours the catalytic process. (See Annex 3.6.4 for the rest of TEM images)

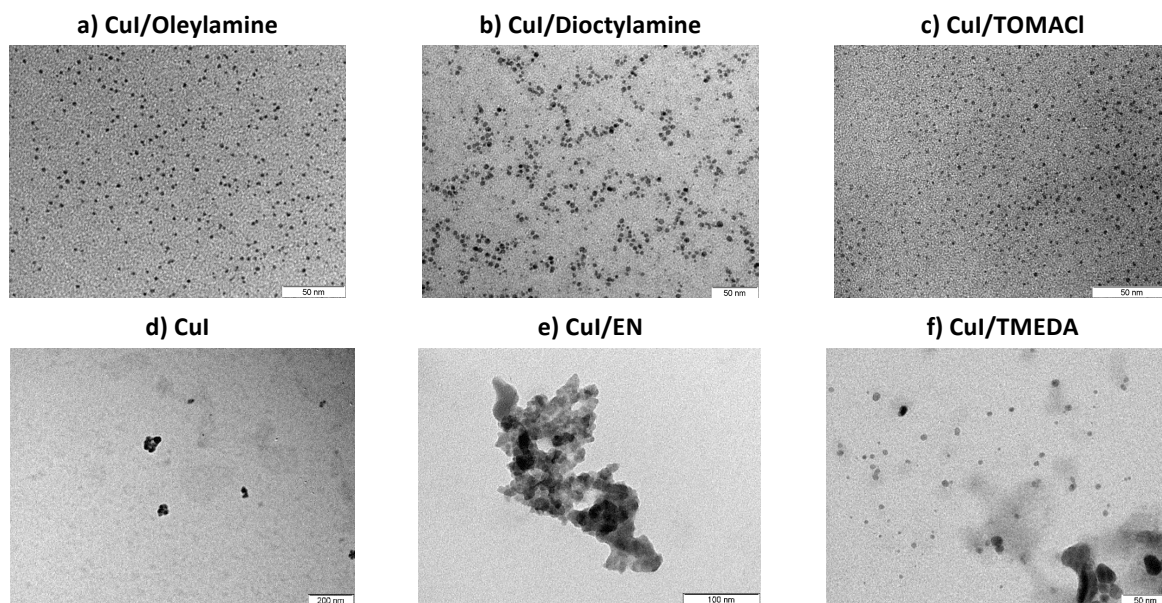


Figure 3.9 TEM images recorded in liquid phase for CuI-based systems containing oleylamine (a), dioctylamine (b) and TOMACI (c) in glycerol.

The adsorption of these long-chain amines, such as oleylamine or dioctylamine, at the surface of the particles provides a protective layer and prevent aggregation (Figure 3.10), by steric but also by coordination stabilisation.^[39] These labile amine ligands can be easily detached leading to free coordination sites in the surface of the copper-based nanoparticles, allowing the reaction to proceed.

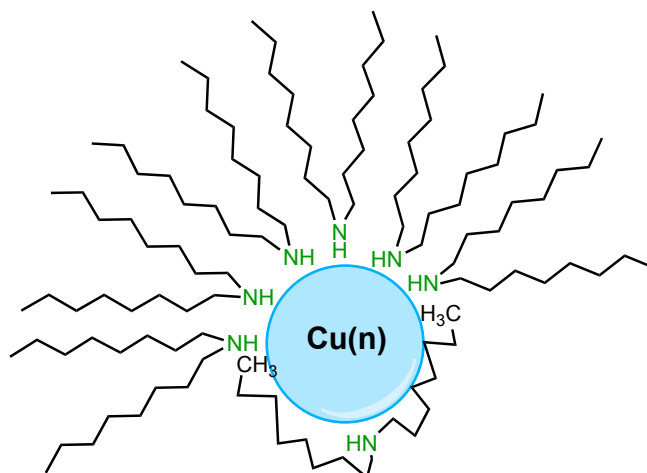


Figure 3.10 Scheme for the stabilisation of the metal core with long-chain amines (a secondary amine is considered to illustrate this stabilisation). Long-chain amines can be also coordinated at the surface by interaction of the alkyl chain.^[34a]

Curiously, although very well-dispersed nanoparticles were observed in the presence of ammonium derivatives (TOMACI and Aliquat[®] 336), the reaction was not working with these compounds as additives (Table 3.2, entries 8 and 9). In this case, the nanoparticles can be highly stabilised by strong electrostatic interactions between the ionic ligands and the nanoparticles, leading to very well-dispersed nanoparticles surrounded by anion/cation shells (Figure 3.11).^[39-40] However, this kind of stabilisation can probably be the reason of the poor reactivity shielding the nanoparticle surface and preventing the approach of the reactants to the catalytic copper centres.

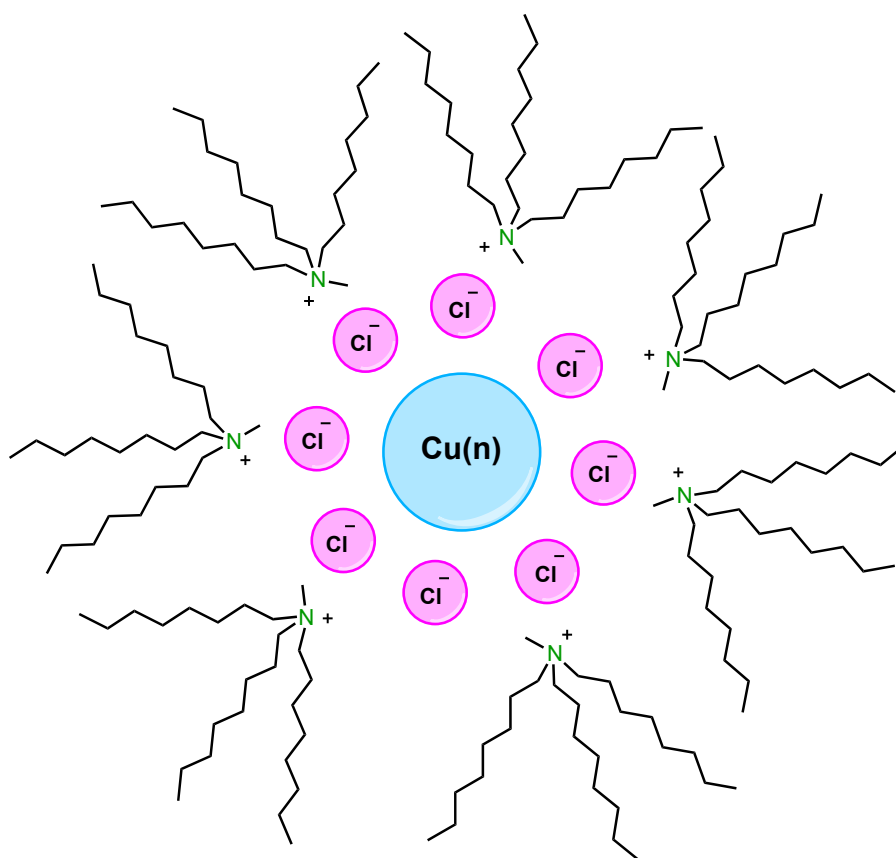


Figure 3.11 Scheme for the stabilisation of the metal core with ammonium derivatives (TOMACI is considered to illustrate this stabilisation).

On the contrary, when an equimolar mixture of the ammonium derivatives (TOMACI or Aliquat[®] 336) and a sodium salt (NaOAc or NaN₃) was added, the CuAAC reaction turned into active. TEM analyses of CuI in glycerol in the presence of the ammonium salt and the sodium salt, showed the formation of micelle-like arrangements (Figure 3.12). The arrangement of these structures can permit to have the copper centres more accessible to the reagents, where the more hydrophobic substituents (alkyl chains), are probably placed inside of these nano-

structures and the ionic/hydrophilic groups more in contact with glycerol. It is important to note that CuI/NaOAc and CuI/NaN₃ systems (1:5 ratio), in the absence of any N-based ligand, did not promote the reaction.

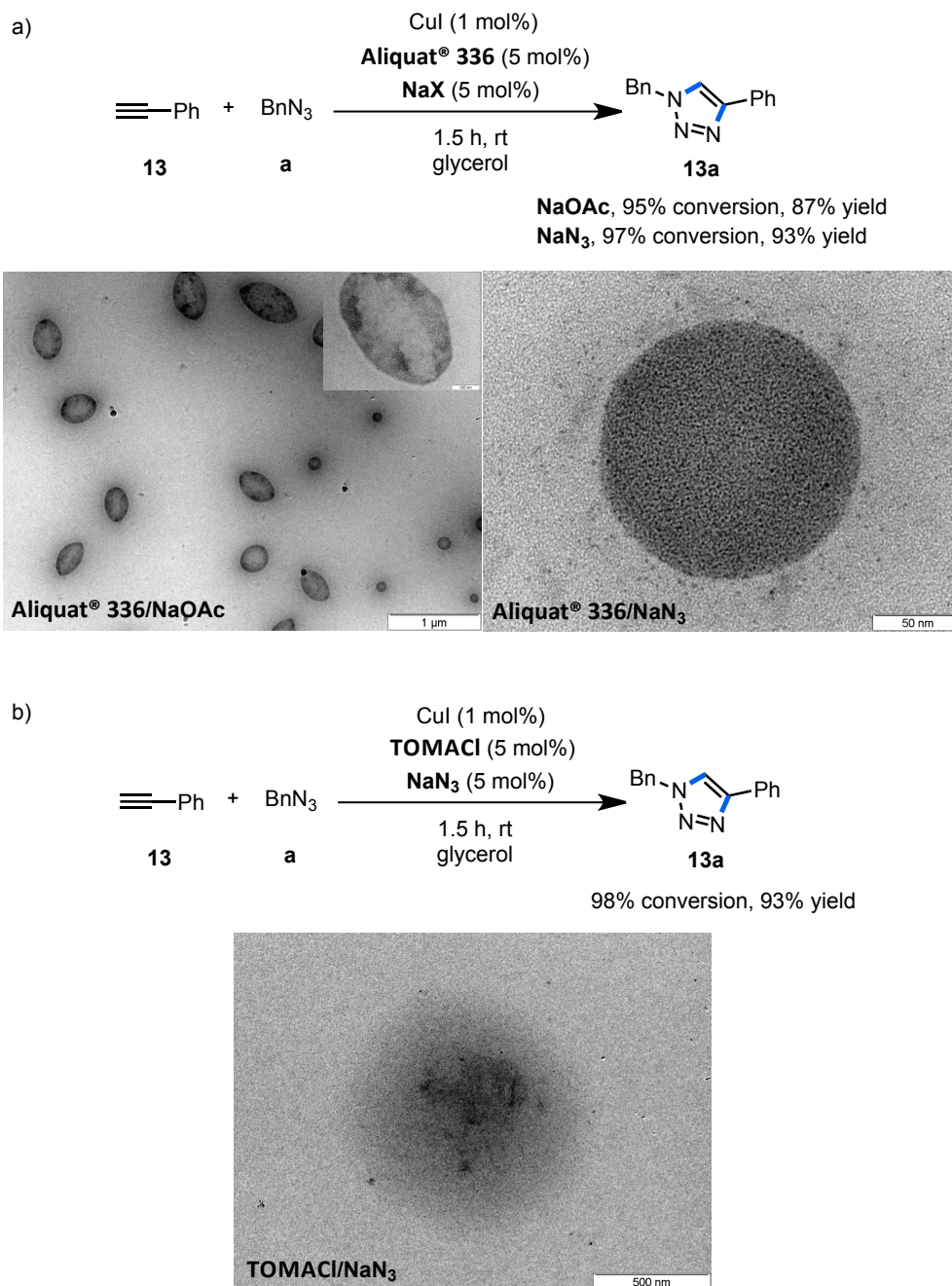
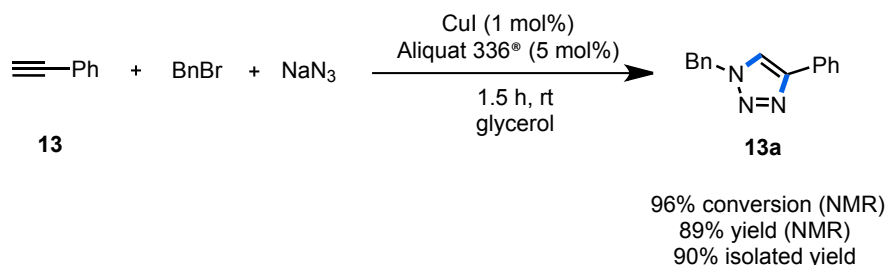


Figure 3.12 Effect of an added salt in CuAAC using ammonium derivatives as additives. a) Catalytic results using Aliquat[®] 336 and TEM images corresponding to the mixtures CuI, Aliquat[®] 336 and NaX (1:5:5 ratio) in glycerol: NaOAc (left), including an inserted image of one of the micelle-like object and NaN₃ (right). b) Catalytic results using TOMACI and TEM images corresponding to the mixtures CuI, TOMACI and NaN₃ (1:5:5 ratio) in glycerol.

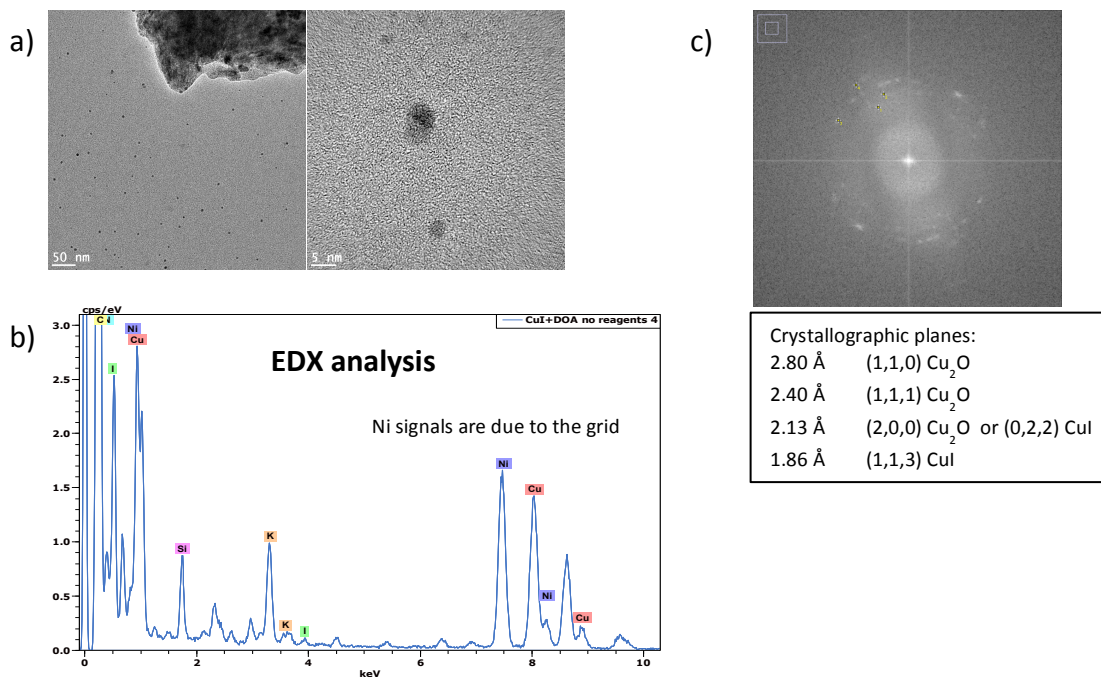
Taking into account this observed effect in the presence of sodium salts, the CuAAC one-pot three-component approach could also be feasible. Actually, using as reagents benzyl bromide, phenylacetylene and NaN_3 , **13a** was obtained in 90% isolated yield (Scheme 3.6).



Scheme 3.6 CuAAC one-pot three-component reaction.

In addition, we wanted to establish the oxidation state of copper of these Cu-based nanoparticles. HR-TEM (High Resolution Transmission Electron Microscopy) together with electron diffraction analysis of CuI/dioctylamine mixture confirmed the Cu(I) nature of the nanoparticles; EDX (Energy Dispersive X-Ray Analysis) analysis evidenced the presence of the amine and iodine on the nanoparticles surface, in addition to Cu_2O (Figure 3.13-I). For the same system but after catalysis, HR-TEM coupled to an electronic diffraction analysis showed that the nanoparticles were mainly constituted by Cu(0) (Figure 3.13-II). Moreover, we were not able to recycle this catalytic phase; the second run gave only a 22% yield in contrast with the 95% yield obtained in the first run, which indicates that Cu(I) species are the responsible of the catalytic activity.

I) Before catalysis



II) After catalysis

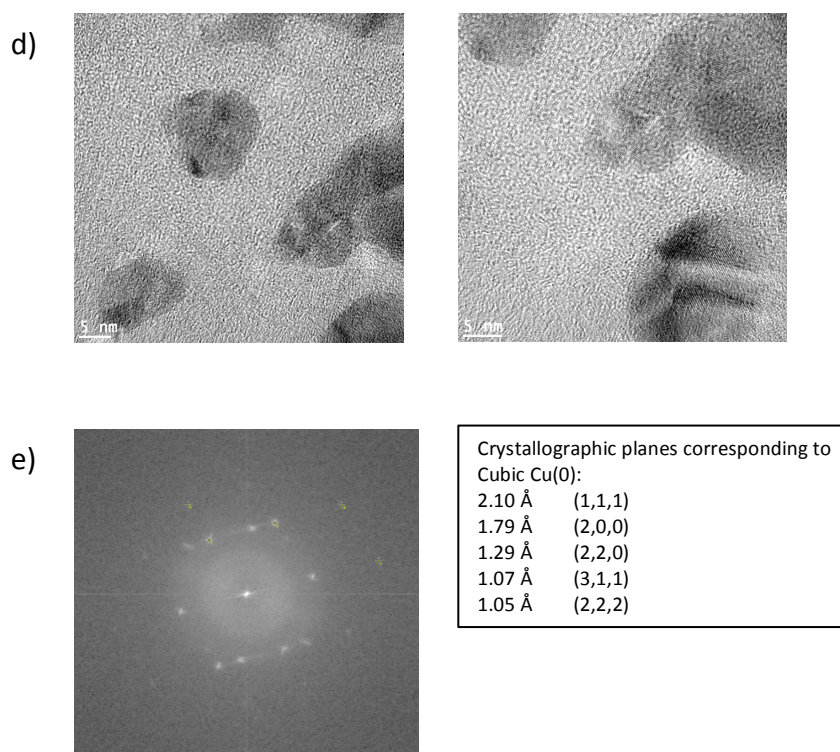


Figure 3.13. I) Before catalysis: HR-TEM images (a), EDX analysis (b) and electron diffraction together with crystallographic planes (c) corresponding to the mixture of CuI and dioctylamine in glycerol. A nickel grid was used for these analyses. **II) After Catalysis:** HR-TEM images (d) and electronic diffraction together with crystallographic planes (e) corresponding to the mixture of CuI and dioctylamine in glycerol after catalysis.

In contrast, the reutilization of CuI/oleylamine was possible as mentioned above (Figure 3.7). Indeed, HR-TEM/electronic diffraction analysis proved that nanoparticles were in this case mainly formed by Cu(I) after the first run. (Figure 3.14).

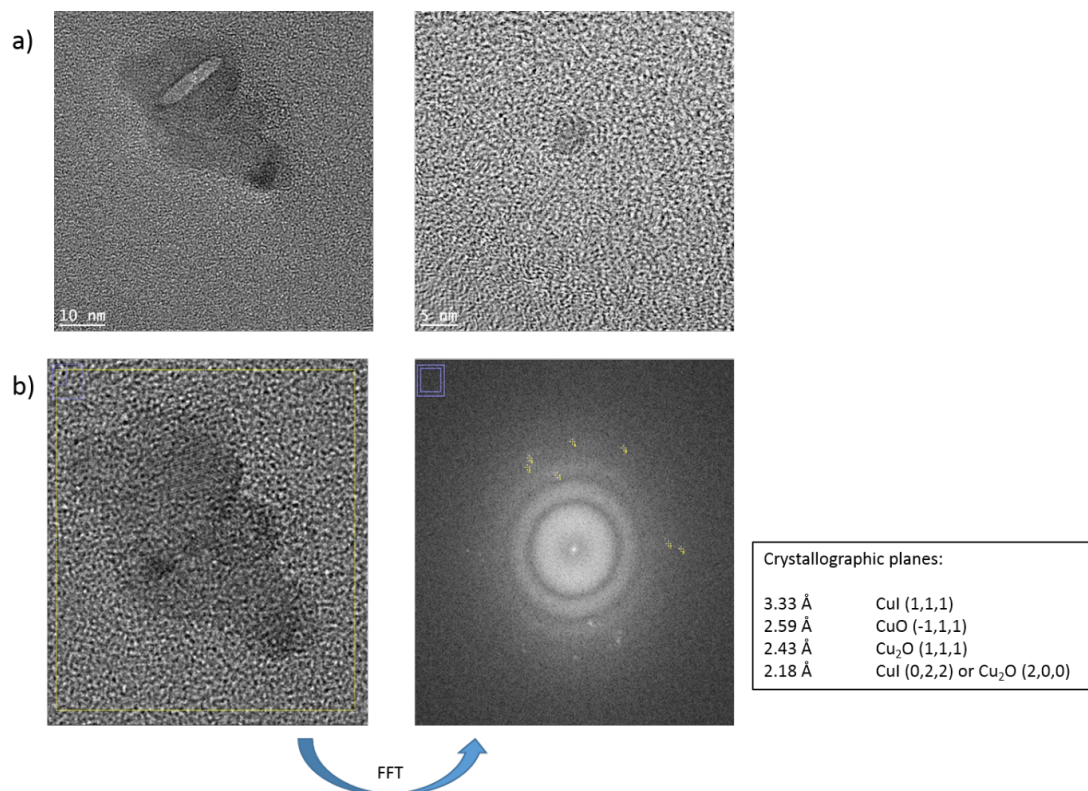


Figure 3.14. HR-TEM images (a) and electron diffraction together with (b) corresponding to the mixture of CuI and oleylamine in glycerol after catalysis (FFT = Fast Fourier Transform).

We also carried out XPS (X-Ray Photoelectron Spectroscopy) analyses with the aim of establishing the oxidation state of copper in the surface of nanoparticles (Figure 3.15). Cu(II) species can be usually clearly observed by the strong spin-orbit coupling, showing two satellites for each signal corresponding to Cu 2p_{1/2} and Cu 2p_{3/2} (Figure 3.15b). In our case, these satellites were not observed, which means the absence of Cu(II) species at the surface. In contrast, for Cu(I) and Cu(0) species these satellites show a weak intensity or are inexistent. Only with the XPS analyses we cannot conclude about the precise nature of Cu(I) and/or Cu(0) (Figure 3.15a, c and d).

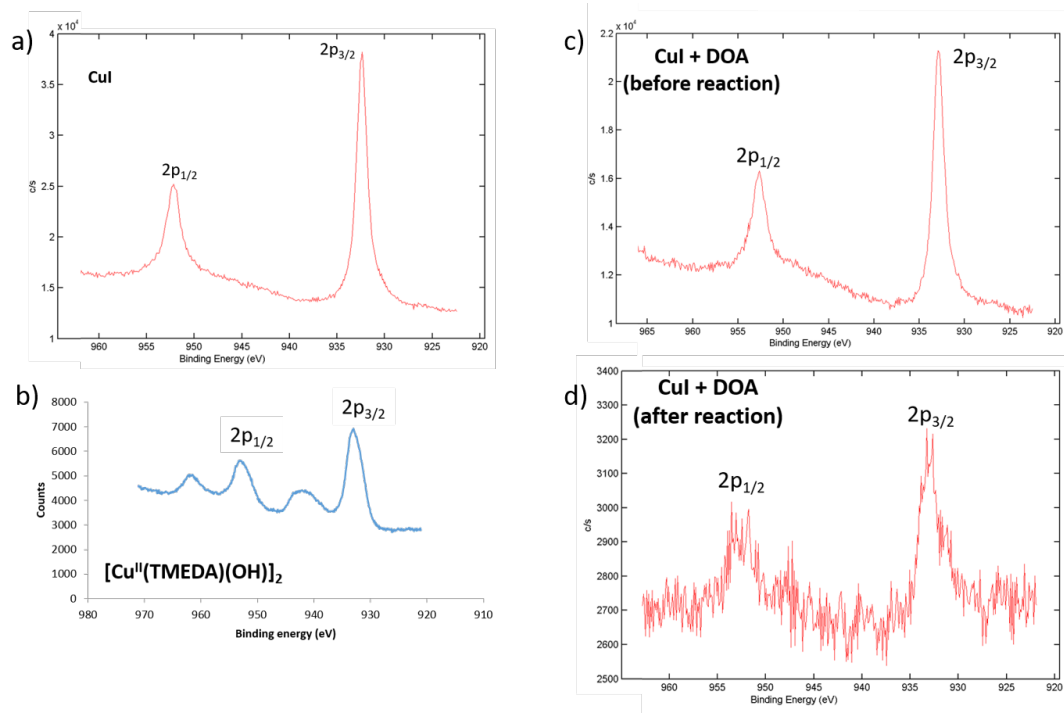


Figure 3.15. HR-XPS analyses of CuI (a), $[\text{Cu}^{\text{II}}(\text{TMEDA})(\text{OH})]_2$ (b), CuI + dioctylamine in glycerol (c) and CuI + dioctylamine in glycerol after ACC reaction (d).

3.3 Conclusions

The key role of “impurities” randomly present in commercial samples of benzyl azide is demonstrated in this chapter. The identified long-alkyl chain amines represent the crucial factor to accelerate the AAC using CuI as catalytic precursor in glycerol at room temperature. We established that the addition of small amounts (5 mol% or even 1 mol%) of primary, secondary or tertiary amines bearing long alkyl chains secures the success in the synthesis of 1,4-disubstituted-1,2,3-triazoles under mild reaction conditions. The use of glycerol, a non-volatile solvent, permitted us to analyse the catalytic phase before and after catalysis by (HR)TEM, which confirmed our suspicion: the *in-situ* formation of copper-based nanoparticles in the medium is the responsible of such good reactivity; furthermore, glycerol favours the immobilisation of the catalytic phase and permits the recycling. The presence of ammonium salts containing long alkyl chains (TOMACI or Aliquat® 336) did not promote the reaction, probably due to the efficient electrosteric stabilisation of the nanoparticles, which hinders the access of reagents to the Cu(I) centres. However, tuning the ionic species present in the reaction medium, the catalytic system turned into active through the formation of organised systems.

The lack of reproducibility found in a simple process, working under the “same” conditions, induced us the desire to understand and solve the problem, which also led us to

discover new issues for a well-known reaction. A warning should be made on the state-of-affairs of reagents, catalysts or solvents; the use of controlled-quality compounds reduces the casual effects, establishing reproducible protocols.

3.4 Experimental section

General

All manipulations were performed using standard Schlenk techniques under argon atmosphere unless otherwise noted.

Commercially available compounds (except glycerol) were used without previous purification. Glycerol (from Sigma- Aldrich, $\geq 99.5\%$ purity) was heated overnight at 80 °C under vacuum before use. After that, it was kept under inert atmosphere. Benzyl azide (**a**),^[24] pent-4-ynoic acid (**18**)^[41] and (iodoethynyl)benzene (**23**)^[42] were prepared according to the literature procedure.

NMR spectra were recorded in CDCl₃ (unless otherwise cited) using a Fourier 300 MHz Bruker, a Bruker Avance 400 Ultrashield or a Bruker Avance 500 Ultrashield apparatus at 298 K. ¹H NMR spectroscopy chemical shifts are quoted in ppm relative to tetramethylsilane (TMS). Chemical shifts are given in δ and coupling constants in Hz. ¹³C NMR spectra are decoupled from ¹H and the chemical shifts are quoted in ppm relative to CDCl₃ ($\delta = 77.16$).

GC analyses were performed with a Perkin–Elmer Clarus 500 chromatograph fitted with a FID and MS-detector, using dodecane as internal standard. The column employed was SGE BPX5 (30 m x 0.32 mm x 0.25 mm) phase composed by 5% of phenyl methylsiloxane.

TEM analyses of CuI/amine systems in glycerol were obtained by using a JEOL JEM 1011 microscope equipped with lanthanum hexaboride filament and running at 100 kV. A drop of solution was deposited on a holey carbon Cu grid, and the excess glycerol was removed to obtain a film as thin as possible. **HR-TEM** analyses were carried out from JEOL JEM 2100F instrument running at 200 kV and equipped with X PGT analyser (detection of light elements, resolution 135 eV).

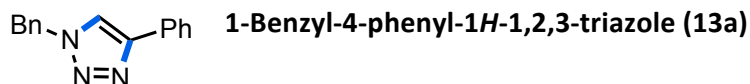
Flash chromatography was carried out using 60 mesh silica gel and dry-packed columns or with a Teledyne Isco CombiFlash system with UV detector. Thin layer chromatography was carried out using Merck TLC Silicagel 60 F254 aluminum sheets. Components were visualized by UV light ($\lambda = 254$ nm) and stained with KMnO₄ or phosphomolybdic dip.

Experimental procedures

General procedure for the azide-alkyne cycloaddition (GP3)

CuI (0.9 mg, 0.005 mmol) and the corresponding amine (0.005 – 0.25 mmol) were added to 0.5 mL of glycerol in a Schlenk tube equipped with a stirring bar under Ar atmosphere. The alkyne (0.5 mmol) and the azide (0.5 mmol: 67 mg for BnN₃ and 60 mg for PhN₃) were added consecutively to the reaction medium. The mixture was stirred at 25 °C for 1.5 h (or the stated time). The organic products were extracted from the catalytic mixture with dichloromethane (6 x 2 mL). The combined chlorinated organic layers were filtered through a Celite[®] pad and the resulting filtrate was concentrated under reduced pressure. The products were purified by chromatography (silica gel short column, eluent: cyclohexane/ethyl acetate) in order to determine the isolated yields of the corresponding triazoles.

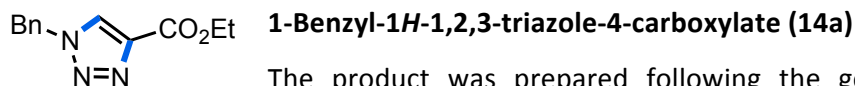
Characterisation of organic compounds



The product was prepared following the general procedure GP3 and purified by flash chromatography (cyclohexane/EtOAc 4:1). Isolated as a white solid in 99% yield (117 mg, 0.49 mmol). The following spectroscopic data matched with those reported in the literature.^[14]

¹H NMR (400 MHz, CDCl₃): δ 5.59 (s, 2H, CH₂), 7.30–7.46 (m, 8H, H_{Ar}), 7.69 (s, 1H, CH), 7.79–7.85 (m, 2H, H_{Ar}).

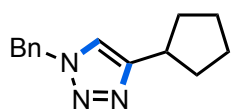
¹³C NMR (100 MHz, CDCl₃): δ 54.2 (CH₂), 119.5 (CH), 125.7 (CH_{Ar}), 128.0 (CH_{Ar}), 128.2 (CH_{Ar}), 128.8 (CH_{Ar}), 128.8 (CH_{Ar}), 129.1 (CH_{Ar}), 130.6 (C_{Ar}), 134.7 (C_{Ar}), 148.2 (C_{Ar}).



The product was prepared following the general procedure GP3 and purified by flash chromatography (cyclohexane/EtOAc 2:1). Isolated as a white solid in 90% yield (104 mg, 0.45 mmol). The following spectroscopic data matched with those reported in the literature.^[43]

¹H NMR (400 MHz, CDCl₃): δ 1.39 (t, ³J = 7.1 Hz, 3H, CH₃), 4.40 (q, ³J = 7.1 Hz, 2H, CH₂), 5.59 (s, 2H, CH₂), 7.24–7.35 (m, 2H, H_{Ar}), 7.36–7.45 (m, 3H, H_{Ar}), 7.99 (s, 1H, CH).

¹³C NMR (100 MHz, CDCl₃): δ 14.3 (CH₃), 54.5 (CH₂), 61.3 (CH₂), 127.3 (CH or CH_{Ar}), 128.2 (CH_{Ar}), 129.1 (CH or CH_{Ar}), 129.3 (CH_{Ar}), 133.7 (C), 140.6 (C), 160.7 (C=O).

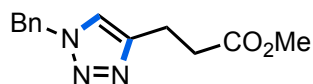


1-Benzyl-4-cyclopentyl-1H-1,2,3-triazole (15a)

The product was prepared following the general procedure GP3 and purified by flash chromatography (cyclohexane/EtOAc 4:1). Isolated as a white solid in 91% yield (103 mg, 0.45 mmol). The following spectroscopic data matched with those reported in the literature.^[44]

¹H NMR (400 MHz, CDCl₃): δ 1.58–1.81 (m, 6H, CH₂), 2.01–2.16 (m, 2H, CH₂), 3.10–3.23 (m, 1H, CH), 5.50 (s, 2H, CH₂), 7.18 (s, 1H, CH), 7.25–7.30 (m, 2H, H_{Ar}), 7.33–7.42 (m, 3H, H_{Ar}).

¹³C NMR (100 MHz, CDCl₃): δ 25.1 (CH₂), 33.2 (CH₂), 36.8 (CH), 54.0 (CH₂), 119.4 (CH), 128.0 (CH_{Ar}), 128.6 (CH_{Ar}), 129.0 (CH_{Ar}), 135.0 (C), 153.2 (C).

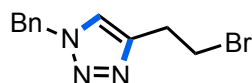


Methyl 3-(1-benzyl-1H-1,2,3-triazol-4-yl)propanoate (16a)

The product was prepared following the general procedure GP3 and purified by flash chromatography (cyclohexane/EtOAc 2:1). Isolated as a white solid in 94% yield (115 mg, 0.47 mmol). The following spectroscopic data matched with those reported in the literature.^[45]

¹H NMR (400 MHz, CDCl₃): δ 2.72 (t, ³J = 7.3 Hz, 2H, CH₂), 3.02 (t, ³J = 7.3 Hz, 2H, CH₂), 3.65 (s, 3H, CH₃), 5.49 (s, 2H, CH₂), 7.21–7.31 (m, 3H, H_{Ar} or + CH), 7.31–7.42 (m, 3H, H_{Ar} or + CH).

¹³C NMR (100 MHz, CDCl₃): δ 21.0 (CH₃), 33.4 (CH₂), 51.6 (CH₂), 54.0 (CH₂), 121.1 (CH), 128.0 (CH_{Ar}), 128.6 (CH_{Ar}), 129.0 (CH_{Ar}), 134.8 (C), 146.7 (C), 173.1 (C=O).

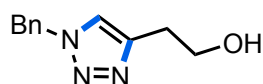


1-Benzyl-4-(2-bromoethyl)-1H-1,2,3-triazole (17a)

The product was prepared following the general procedure GP3 and purified by flash chromatography (cyclohexane/EtOAc 7:3). Isolated as a white solid in 89% yield (119 mg, 0.45 mmol). The following spectroscopic data matched with those reported in the literature.^[46]

¹H NMR (400 MHz, CDCl₃): δ 3.28 (t, ³J = 6.9 Hz, 2H, CH₂), 3.60 (t, ³J = 6.9 Hz, 2H, CH₂), 5.53 (s, 2H, CH₂), 7.24–7.31 (m, 2H, H_{Ar} or + CH), 7.34–7.43 (m, 4H, H_{Ar} or + CH).

¹³C NMR (125 MHz, CDCl₃): δ 29.5 (CH₂), 31.5 (CH₂), 54.1 (CH₂), 121.6 (CH), 128.0 (CH_{Ar}), 128.7 (CH_{Ar}), 129.1 (CH_{Ar}), 134.7 (C), 145.3 (C).



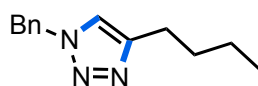
2-(1-Benzyl-1H-1,2,3-triazol-4-yl)ethanol (18a)

The product was prepared following the general procedure GP3 and

purified by flash chromatography (EtOAc). Isolated as an oil in 96% yield (98 mg, 0.48 mmol). The following spectroscopic data matched with those reported in the literature.^[47]

¹H NMR (500 MHz, CDCl₃): δ 2.92 (t, ³J = 6.0 Hz, 2H, CH₂), 3.05 (bs, 1H, OH) 3.91 (t, ³J = 6.0 Hz, 2H, CH₂), 5.49 (s, 2H, CH₂), 7.24–7.30 (m, 2H, H_{Ar} or + CH), 7.32–7.41 (m, 4H, H_{Ar} or + CH).

¹³C NMR (125 MHz, CDCl₃): δ 28.8 (CH₂), 54.1 (CH₂), 61.5 (CH₂), 121.5 (CH), 128.1 (CH_{Ar}), 128.7 (CH_{Ar}), 129.1 (CH_{Ar}), 134.7 (C), 146.0 (C).

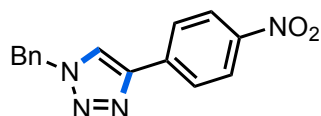


1-Benzyl-4-butyl-1H-1,2,3-triazole (19a)

The product was prepared following the general procedure GP3 and purified by flash chromatography (cyclohexane/EtOAc 4:1). Isolated as a white solid in 68% yield (73 mg, 0.34 mmol). The following spectroscopic data matched with those reported in the literature.^[48]

¹H NMR (400 MHz, CDCl₃): δ 0.92 (t, ³J = 7.3 Hz, 3H, CH₃), 1.32–1.43 (m, 2H, CH₂), 1.58–1.69 (m, 2H, CH₂), 2.70 (t, ³J = 7.8 Hz, 2H, CH₂), 5.50 (s, 2H, CH₂), 7.20 (s, 1H, CH), 7.23–7.29 (m, 2H, H_{Ar}), 7.32–7.41 (m, 3H, H_{Ar}).

¹³C NMR (100 MHz, CDCl₃): δ 13.8 (CH₃), 22.3 (CH₂), 25.4 (CH₂), 31.5 (CH₂), 53.9 (CH₂), 120.4 (CH), 127.9 (CH_{Ar}), 128.6 (CH_{Ar}), 129.0 (CH_{Ar}), 135.0 (C), 149.0 (C).

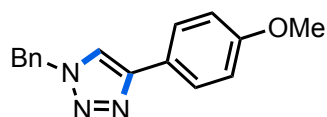


1-Benzyl-4-(4-nitrophenyl)-1H-1,2,3-triazole (20a)

The product was prepared following the general procedure GP3 and purified by flash chromatography (CombiFlash® system, 12 g, SiO₂ cartridge, 1st eluent: cyclohexane; 2nd eluent: 4:1 cyclohexane/ EtOAc). Isolated as a white solid in 89% yield (125 mg, 0.45 mmol). The following spectroscopic data matched with those reported in the literature.^[49]

¹H NMR (500 MHz, CDCl₃): δ 5.64 (s, 2H, CH₂), 7.34–7.39 (m, 2H, H_{Ar}(Ph)), 7.40–7.47 (m, 3H, H_{Ar}(Ph)), 7.82 (s, 1H, CH), 7.96–8.02 (m, 2H, H_{Ar}(4-NO₂Ph)), 8.26–8.31 (m, 2H, H_{Ar}(4-NO₂Ph)).

¹³C NMR (125 MHz, CDCl₃): δ 54.5 (CH₂), 121.0 (CH), 124.3 (CH_{Ar}), 126.1 (CH_{Ar}), 128.2 (CH_{Ar}), 129.1 (CH_{Ar}), 129.3 (CH_{Ar}), 134.2 (C), 136.8 (C), 146.0 (C), 147.3 (C).

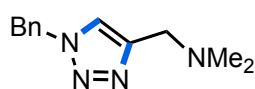


1-Benzyl-4-(4-methoxyphenyl)-1H-1,2,3-triazole (21a)

The product was prepared following the general procedure GP3 and purified by flash chromatography (cyclohexane/EtOAc 2:1). Isolated as a white solid in 83% yield (110 mg, 0.41 mmol). The following spectroscopic data matched with those reported in the literature.^[44]

$^1\text{H NMR}$ (500 MHz, CDCl_3): δ 3.84 (s, 3H, CH_3), 5.56 (s, 2H, CH_2), 6.92–6.98 (m, 2H, $H_{\text{Ar}}(4\text{-OMePh})$), 7.29–7.34 (m, 2H, $H_{\text{Ar}}(\text{Ph})$), 7.35–7.43 (m, 3H, $H_{\text{Ar}}(\text{Ph})$), 7.60 (s, 1H, CH), 7.71–7.77 (m, 2H, $H_{\text{Ar}}(4\text{-OMePh})$).

$^{13}\text{C NMR}$ (100 MHz, CDCl_3): δ 54.2 (CH_3 or CH_2), 55.3 (CH_3 or CH_2), 114.2 (CH_{Ar}), 118.7 (CH or C), 123.3 (CH or C), 127.0 (CH_{Ar}), 128.0 (CH_{Ar}), 128.7 (CH_{Ar}), 129.1 (CH_{Ar}), 134.8 (C), 148.0 (C), 159.6 (C).

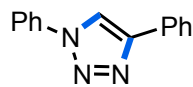


1-(1-Benzyl-1H-1,2,3-triazol-4-yl)-N,N-dimethylmethanamine (22a)

The product was prepared following the general procedure GP3 and purified by flash chromatography (EtOAc/EtOH 1:2). Isolated as an oil in 79% yield (86 mg, 0.40 mmol). The following spectroscopic data matched with those reported in the literature.^[20b]

$^1\text{H NMR}$ (500 MHz, CDCl_3): δ 2.25 (s, 6H, CH_3), 3.58 (s, 2H, CH_2), 5.51 (s, 2H, CH_2), 7.23–7.28 (m, 2H, H_{Ar}), 7.32–7.39 (m, 2H, H_{Ar}), 7.40 (s, 1H, CH).

$^{13}\text{C NMR}$ (125 MHz, CDCl_3): δ 45.1 (2x CH_3), 54.1 (CH_2), 54.4 (CH_2), 122.3 (CH), 128.1 (CH_{Ar}), 128.7 (CH_{Ar}), 129.1 (CH_{Ar}), 134.7 (C), 145.7 (C).

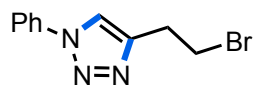


1,4-Diphenyl-1H-1,2,3-triazole (13b)

The product was prepared following the general procedure GP3 and purified by flash chromatography (CombiFlash® system, 12 g, SiO_2 cartridge, 1st eluent: cyclohexane; 2nd eluent: 95:5 cyclohexane/ EtOAc). Isolated as a white solid in 96% yield (95 mg, 0.43 mmol). The following spectroscopic data matched with those reported in the literature.^[44]

$^1\text{H NMR}$ (400 MHz, CDCl_3): δ 7.32–7.41 (m, 1H, H_{Ar}), 7.41–7.50 (m, 3H, H_{Ar}), 7.50–7.59 (m, 2H, H_{Ar}), 7.75–7.83 (m, 2H, H_{Ar}), 7.85–7.95 (m, 2H, H_{Ar}), 8.23 (s, 1H, CH).

$^{13}\text{C NMR}$ (125 MHz, CDCl_3): δ 117.8 (CH), 120.5 (CH_{Ar}), 125.8 (CH_{Ar}), 128.5 (CH_{Ar}), 128.9 (CH_{Ar}), 128.9 (CH_{Ar}), 129.8 (CH_{Ar}), 130.0 (C), 137.0 (C), 148.4 (C).

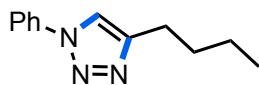


4-(2-Bromoethyl)-1-phenyl-1H-1,2,3-triazole (5b)

The product was prepared following the general procedure GP3 and purified by flash chromatography (cyclohexane/EtOAc 4:1). Isolated as a white solid in 89% yield (113 mg, 0.45 mmol). The following spectroscopic data matched with those reported in the literature.^[50]

$^1\text{H NMR}$ (400 MHz, CDCl_3): δ 3.41 (t, $^3J = 6.7$ Hz, 2H, CH_2), 3.74 (t, $^3J = 6.7$ Hz, 2H, CH_2), 7.42–7.49 (m, 1H, H_{Ar}), 7.50–7.59 (m, 2H, H_{Ar}), 7.72–7.79 (m, 2H, H_{Ar}), 7.93 (s, 1H, CH).

^{13}C NMR (100 MHz, CDCl_3): δ 29.5 (CH_2), 31.4 (CH_2), 119.9 (CH or CH_{Ar}), 120.5 (CH_{Ar}), 128.7 (CH or CH_{Ar}), 129.7 (CH_{Ar}), 137.1 (C), 145.5 (C).

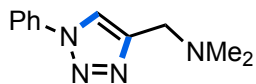


4-Butyl-1-phenyl-1H-1,2,3-triazole (19b)

The product was prepared following the general procedure GP3 and purified by flash chromatography (cyclohexane/EtOAc 12:1). Isolated as a yellow oil in 53% yield (54 mg, 0.27 mmol). The following spectroscopic data matched with those reported in the literature.^[51]

^1H NMR (400 MHz, CDCl_3): δ 0.97 (t, $^3J = 7.4$ Hz, 3H, CH_3), 1.39–1.50 (m, 2H, CH_2), 1.66–1.79 (m, 2H, CH_2), 2.81 (t, $^3J = 7.7$ Hz, 2H, CH_2), 7.38–7.45 (m, 1H, H_{Ar}), 7.47–7.55 (m, 2H, H_{Ar} or + CH), 7.69–7.78 (m, 3H, H_{Ar} or + CH).

^{13}C NMR (100 MHz, CDCl_3): δ 13.8 (CH_3), 22.3 (CH_2), 25.3 (CH_2), 31.5 (CH_2), 118.8 (CH), 120.4 (CH_{Ar}), 128.4 (CH_{Ar}), 129.6 (CH_{Ar}), 137.3 (C), 149.1 (C).



N,N-dimethyl-1-(1-phenyl-1H-1,2,3-triazol-4-yl)methanamine (22b)

The product was prepared following the general procedure GP3 and purified by flash chromatography (EtOAc/EtOH 1:2). Isolated as a yellow oil in 75% yield (75 mg, 0.37 mmol). The following spectroscopic data matched with those reported in the literature.^[20a]

^1H NMR (400 MHz, CDCl_3): δ 2.33 (s, 6H, CH_3), 3.70 (s, 2H, CH_2), 7.38–7.46 (m, 1H, H_{Ar}), 7.47–7.55 (m, 2H, H_{Ar}), 7.68–7.78 (m, 2H, H_{Ar}), 7.95 (s, 1H, CH).

^{13}C NMR (100 MHz, CDCl_3): δ 45.2 (2x CH_3), 54.4 (CH_2), 120.4 (CH_{Ar}), 120.5 (CH), 128.6 (CH_{Ar}), 129.7 (CH_{Ar}), 137.1 (C), 146.0 (C).

3.5 References

- [1] V. V. Rostovtsev, L. G. Green, V. V. Fokin, K. B. Sharpless, *Angew. Chem. Int. Ed.* **2002**, *41*, 2596–2599.
- [2] C. W. Tornøe, C. Christensen, M. Meldal, *J. Org. Chem.* **2002**, *67*, 3057–3064.
- [3] Data from SciFinder Scholar up to September 2016.
- [4] (a) J. E. Hein, V. V. Fokin, *Chem. Soc. Rev.* **2010**, *39*, 1302–1315; (b) L. Liang, D. Astruc, *Coord. Chem. Rev.* **2011**, *255*, 2933–2945; (c) S. Díez-González, *Catal. Sci. Technol.* **2011**, *1*, 166–178; (d) N. V. Sokolova, V. G. Nenajdenko, *RSC Adv.* **2013**, *3*, 16212–16242; (e) E. Haldón, M. C. Nicasio, P. J. Pérez, *Org. Biomol. Chem.* **2015**, *13*, 9528–9550; (f) S. Chassaing, V. Bénétteau, P. Pale, *Catal. Sci. Technol.* **2016**, *6*, 923–957; (g) A. Mandoli, *Molecules* **2016**, *21*, 1174.
- [5] H. C. Kolb, M. G. Finn, K. B. Sharpless, *Angew. Chem. Int. Ed.* **2001**, *40*, 2004–2021.
- [6] (a) M. Meldal, C. W. Tornøe, *Chem. Rev.* **2008**, *108*, 2952–3015; (b) R. Berg, B. F. Straub, *Beilstein J. Org. Chem.* **2013**, *9*, 2715–2750; (c) C. Wang, D. Ikhlef, S. Kahlal, J.-Y. Saillard, D. Astruc, *Coord. Chem. Rev.* **2016**, *316*, 1–20; (d) L. Zhu, C. J. Brassard, X. Zhang, P. M. Guha, R. J. Clark, *Chem. Rec.* **2016**, *16*, 1501–1517.
- [7] F. Himo, T. Lovell, R. Hilgraf, V. V. Rostovtsev, L. Noodleman, K. B. Sharpless, V. V. Fokin, *J. Am. Chem. Soc.* **2005**, *127*, 210–216.

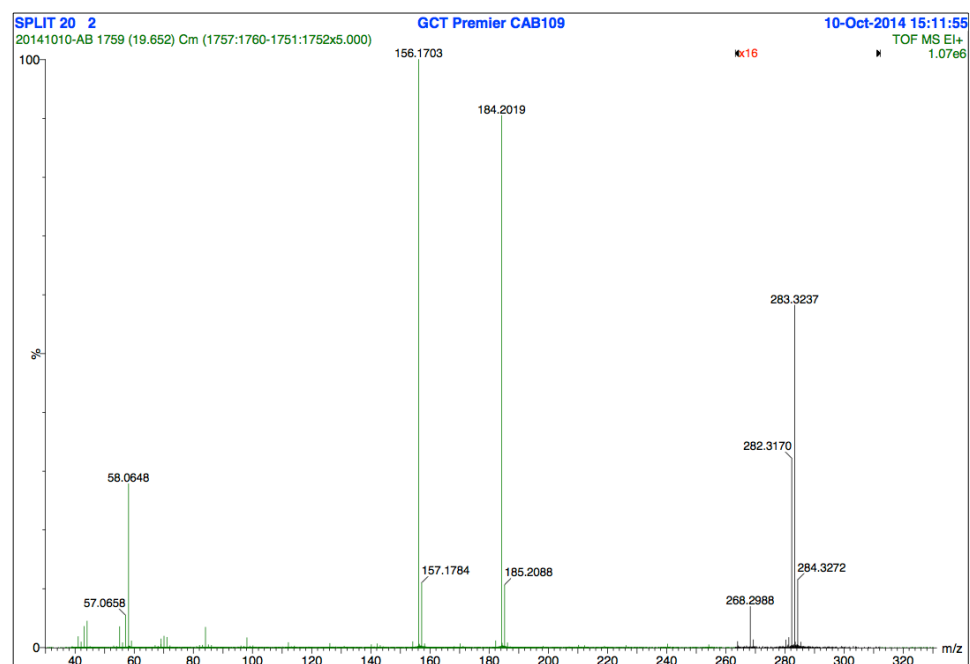
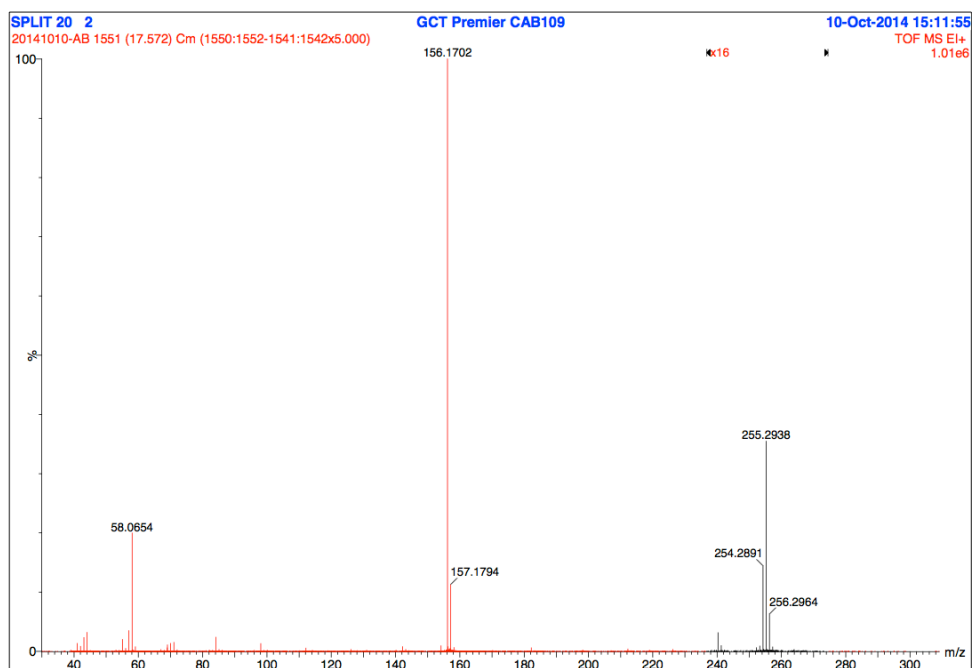
- [8] V. O. Rodionov, V. V. Fokin, M. G. Finn, *Angew. Chem. Int. Ed.* **2005**, *44*, 2210–2215.
- [9] (a) M. Ahlquist, V. V. Fokin, *Organometallics* **2007**, *26*, 4389–4391; (b) B. F. Straub, *Chem. Commun.* **2007**, 3868–3870.
- [10] (a) B. T. Worrell, J. A. Malik, V. V. Fokin, *Science* **2013**, *340*, 457–460; (b) C. Iacobucci, S. Reale, J.-F. Gal, F. De Angelis, *Angew. Chem. Int. Ed.* **2015**, *54*, 3065–3068; (c) L. Jin, D. R. Tolentino, M. Melaimi, G. Bertrand, *Sci. Adv.* **2015**, *1*, e1500304.
- [11] C. Nolte, P. Mayer, B. F. Straub, *Angew. Chem. Int. Ed.* **2007**, *46*, 2101–2103.
- [12] S. Díez-González, A. Correa, L. Cavallo, S. P. Nolan, *Chem. Eur. J.* **2006**, *12*, 7558–7564.
- [13] N. Candelon, D. Lastécouères, A. K. Diallo, J. Ruiz Aranzaes, D. Astruc, J.-M. Vincent, *Chem. Commun.* **2008**, 741–743.
- [14] P. Appukkuttan, W. Dehaen, V. V. Fokin, E. Van der Eycken, *Org. Lett.* **2004**, *6*, 4223–4225.
- [15] (a) F. Alonso, Y. Moglie, G. Radivoy, *Acc. Chem. Res.* **2015**, *48*, 2516–2528; (b) M. B. Gawande, A. Goswami, F.-X. Felpin, T. Asefa, X. Huang, R. Silva, X. Zou, R. Zboril, R. S. Varma, *Chem. Rev.* **2016**, *116*, 3722–3811.
- [16] F. Chahdoura, C. Pradel, M. Gómez, *ChemCatChem* **2014**, *6*, 2929–2936.
- [17] Solubility product constants for CuX: CuCl, 1.72×10^{-7} ; CuBr, 6.27×10^{-9} ; CuI, 1.27×10^{-12} ; data from CRC Handbook of Chemistry and Physics, Ed. D. R. Lide, 90th edition, 2009–2010, CRC Press, Boca Raton.
- [18] (a) T. R. Chan, R. Hilgraf, K. B. Sharpless, V. V. Fokin, *Org. Lett.* **2004**, *6*, 2853–2855; (b) W. G. Lewis, F. G. Magallon, V. V. Fokin, M. G. Finn, *J. Am. Chem. Soc.* **2004**, *126*, 9152–9153.
- [19] (a) V. O. Rodionov, S. I. Presolski, D. Díaz Díaz, V. V. Fokin, M. G. Finn, *J. Am. Chem. Soc.* **2007**, *129*, 12705–12712; (b) V. O. Rodionov, S. I. Presolski, S. Gardinier, Y.-H. Lim, M. G. Finn, *J. Am. Chem. Soc.* **2007**, *129*, 12696–12704; (c) S. I. Presolski, V. Hong, S.-H. Cho, M. G. Finn, *J. Am. Chem. Soc.* **2010**, *132*, 14570–14576.
- [20] (a) S. Özçubukçu, E. Ozkal, C. Jimeno, M. A. Pericàs, *Org. Lett.* **2009**, *11*, 4680–4683; (b) E. Ozkal, P. Llanes, F. Bravo, A. Ferrali, M. A. Pericàs, *Adv. Synth. Catal.* **2014**, *356*, 857–869; (c) P. Etayo, C. Ayats, M. A. Pericàs, *Chem. Commun.* **2016**, *52*, 1997–2010.
- [21] C. Vidal, J. García-Álvarez, *Green Chem.* **2014**, *16*, 3515–3521.
- [22] "It does, for example, no good to offer an elegant, difficult and expensive process to an industrial manufacturing chemist, whose ideal is something to be carried out in a disused bathtub by a one-armed man who cannot read, the product being collected continuously through the drain hole in 100% purity and yield" (J. Cornforth, *Chem. Brit.* 1975, 432).
- [23] B. C. Gibb, *Nature Chem.* **2014**, *6*, 653–654.
- [24] S. G. Alvarez, M. T. Alvarez, *Synthesis* **1997**, 413–414.
- [25] (a) J. García-Álvarez, J. Díez, J. Gimeno, *Green Chem.* **2010**, *12*, 2127–2130; (b) J. García-Álvarez, J. Díez, J. Gimeno, F. J. Suárez, C. Vincent, *Eur. J. Inorg. Chem.* **2012**, *2012*, 5854–5863.
- [26] J. E. Hein, J. C. Tripp, L. B. Krasnova, K. B. Sharpless, V. V. Fokin, *Angew. Chem. Int. Ed.* **2009**, *48*, 8018–8021.
- [27] T. Kusukawa, G. Niwa, T. Sasaki, R. Oosawa, W. Himeno, M. Kato, *Bull. Chem. Soc. Jpn.* **2013**, *86*, 351–353.
- [28] (a) M. Vitale, P. C. Ford, *Coord. Chem. Rev.* **2001**, *219–221*, 3–16; (b) F. De Angelis, S. Fantacci, A. Sgamellotti, E. Cariati, R. Ugo, P. C. Ford, *Inorg. Chem.* **2006**, *45*, 10576–10584.
- [29] (a) A. J. Blake, N. R. Brooks, N. R. Champness, L. R. Hanton, P. Hubberstey, M. Schröder, *Pure Appl. Chem.* **1998**, *70*, 2351–2357; (b) S. Kitagawa, R. Kitaura, S.-i. Noro, *Angew. Chem. Int. Ed.* **2004**, *43*, 2334–2375; (c) G. Férey, *Chem. Soc. Rev.* **2008**, *37*, 191–214.
- [30] (a) R. Peng, M. Li, D. Li, *Coord. Chem. Rev.* **2010**, *254*, 1–18; (b) S. Yuan, H. Wang, D.-X. Wang, H.-F. Lu, S.-Y. Feng, D. Sun, *CrystEngComm* **2013**, *15*, 7792–7802.
- [31] (a) P. C. Healy, C. Pakawatchai, C. L. Raston, B. W. Skelton, A. H. White, *J. Chem. Soc. Dalton Trans.* **1983**, 1905–1916; (b) M. F. Garbaskas, D. A. Haitko, J. S. Kasper, *J. Cryst. Spec. Res.* **1986**, *16*, 729–738; (c) J.-H. Yu, J.-Q. Xu, L. Han, T.-G. Wang, Z. Shi, W.-J. Jing, H. Ding, J.-N. Xu, H.-B. Jia, J. Hua, *Chin. J. Chem.* **2002**, *20*, 851–857; (d) Y. Yang, W. Chai, L. Song, K. Shu, *Acta Cryst.* **2010**, *E66*, m1486; (e) X. Chai, S. Zhang, Y. Chen, Y. Sun, H. Zhang, X. Xu, *Inorg. Chem. Commun.* **2010**, *13*, 240–243.
- [32] J.-J. Shen, J. Song, T.-L. Yu, Y.-L. Fu, *Chin. J. Struct. Chem.* **2014**, *33*, 1025–1030.
- [33] S. Zhang, Y. Cao, H. Zhang, X. Chai, Y. Chen, R. Sun, *J. Solid State Chem.* **2008**, *181*, 3327–3336.
- [34] (a) C. Pan, K. Pelzer, K. Philippot, B. Chaudret, F. Dassenoy, P. Lecante, M.-J. Casanove, *J. Am. Chem. Soc.* **2001**, *123*, 7584–7593; (b) E. Ramirez, L. Eradès, K. Philippot, P. Lecante, B. Chaudret, *Adv. Funct. Mater.* **2007**, *17*, 2219–2228; (c) G. Salas, C. C. Santini, K. Philippot, V. Collière, B. Chaudret, B. Fenet, P. F. Fazzini, *Dalton Trans.* **2011**, *40*, 4660–4668; (d) J. Cure, Y. Coppel, T. Dammak, P. F. Fazzini, A.

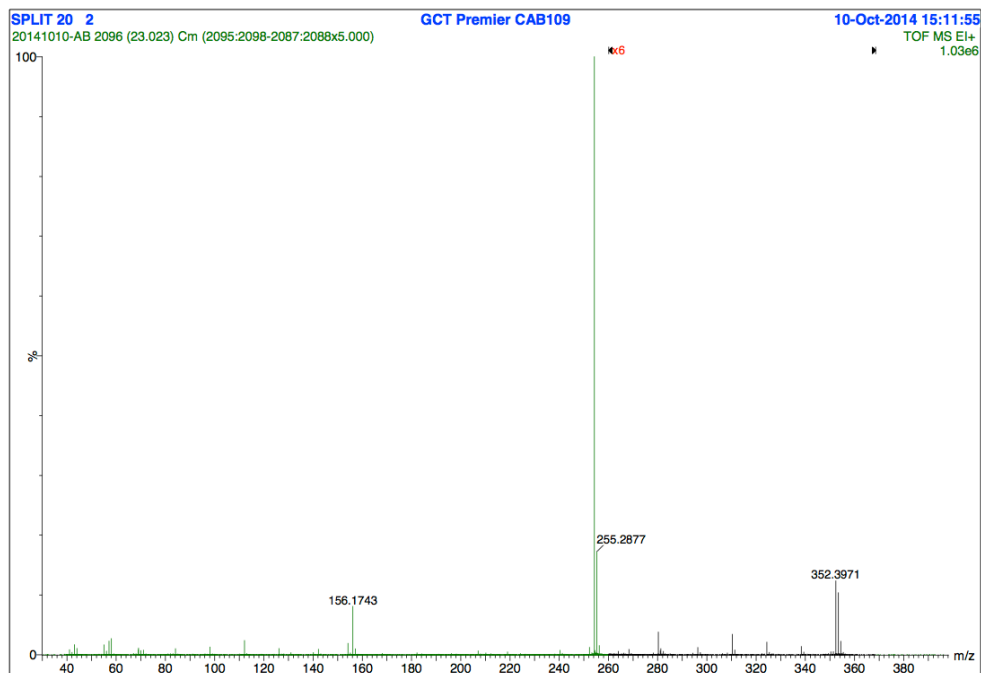
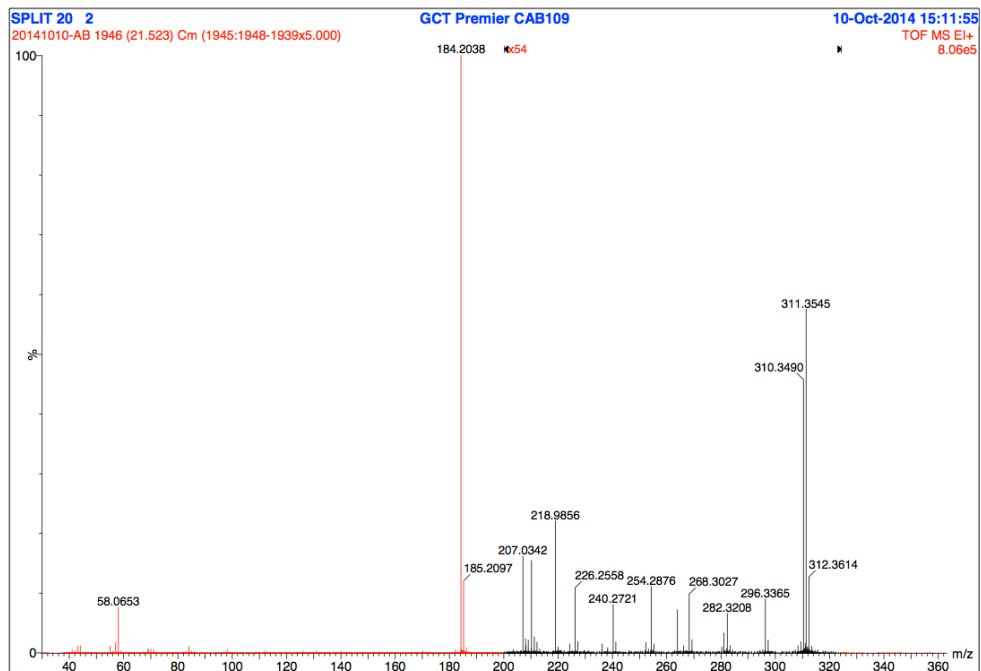
- Mlayah, B. Chaudret, P. Fau, *Langmuir* **2015**, *31*, 1362–1367; (e) H. You, X. Liu, H. Liu, J. Fang, *CrystEngComm* **2016**, *18*, 3934–3941.
- [35] (a) C. Vollmer, C. Janiak, *Coord. Chem. Rev.* **2011**, *255*, 2039–2057; (b) D. Freudenmann, S. Wolf, M. Wolff, C. Feldmann, *Angew. Chem. Int. Ed.* **2011**, *50*, 11050–11060; (c) J. D. Scholten, B. C. Leal, J. Dupont, *ACS Catalysis* **2012**, *2*, 184–200; (d) I. Favier, D. Madec, M. Gómez, in *Chapter 5 Metallic Nanoparticles in Ionic Liquids- Applications in Catalysis in Nanomaterials in Catalysis*, (Eds.: P. Serp, K. Philippot), Wiley-VCH, Weinheim, **2013**, pp. 203–249; (e) H.-P. Steinrück, P. Wasserscheid, *Catal. Lett.* **2015**, *145*, 380–397.
- [36] F. Fievet, J. P. Lagier, B. Blin, B. Beaudoin, M. Figlarz, *Solid State Ionics* **1989**, *32*, 198–205.
- [37] H. R. Ong, M. M. R. Khan, R. Ramli, Y. Du, S. Xi, R. M. Yunus, *RSC Adv.* **2015**, *5*, 24544–24549.
- [38] (a) F. Chahdoura, C. Pradel, M. Gómez, *Adv. Synth. Catal.* **2013**, *355*, 3648–3660; (b) F. Chahdoura, S. Mallet-Ladeira, M. Gómez, *Org. Chem. Front.* **2015**, *2*, 312–318; (c) F. Chahdoura, I. Favier, C. Pradel, S. Mallet-Ladeira, M. Gómez, *Catal. Commun.* **2015**, *63*, 47–51.
- [39] A. Roucoux, J. Schulz, H. Patin, *Chem. Rev.* **2002**, *102*, 3757–3778.
- [40] (a) H. Bönemann, W. Brijoux, R. Brinkmann, E. Dinjus, T. Joußen, B. Korall, *Angew. Chem. Int. Ed.* **1991**, *30*, 1312–1314; (b) S. Bucher, J. Hormes, H. Modrow, R. Brinkmann, N. Waldöfner, H. Bönemann, L. Beuermann, S. Krischok, W. Maus-Friedrichs, V. Kempter, *Surf. Sci.* **2002**, *497*, 321–332.
- [41] P. García-Domínguez, M. Weiss, I. Lepore, R. Álvarez, L. Altucci, H. Gronemeyer, Á. R. de Lera, *ChemMedChem* **2012**, *7*, 2101–2112.
- [42] D. Cheng, J. Li, J. Yan, *Synlett* **2007**, 2442–2444.
- [43] D. Gangaprasad, J. P. Raj, T. Kiranmye, S. S. Sadik, J. Elangovan, *RSC Adv.* **2015**, *5*, 63473–63477.
- [44] M. K. Barman, A. K. Sinha, S. Nembenna, *Green Chem.* **2016**, *18*, 2534–2541.
- [45] D. Reich, D. S. Müller, L. Schefzig, R. Zimmer, H.-U. Reissig, *Synlett* **2014**, *25*, 2265–2270.
- [46] V. Fiandanese, F. Iannone, G. Marchese, A. Punzi, *Tetrahedron* **2011**, *67*, 5254–5260.
- [47] V. H. Reddy, Y. V. R. Reddy, B. Sridhar, B. V. S. Reddy, *Adv. Synth. Catal.* **2016**, *358*, 1088–1092.
- [48] S. C. Sau, S. R. Roy, T. K. Sen, D. Mullangi, S. K. Mandal, *Adv. Synth. Catal.* **2013**, *355*, 2982–2991.
- [49] A. Pourjavadi, S. H. Hosseini, F. M. Moghaddam, S. E. Ayati, *RSC Adv.* **2015**, *5*, 29609–29617.
- [50] K. Wang, X. Bi, S. Xing, P. Liao, Z. Fang, X. Meng, Q. Zhang, Q. Liu, Y. Ji, *Green Chem.* **2011**, *13*, 562–565.
- [51] A. Ali, A. G. Corrêa, D. Alves, J. Zukerman-Schpector, B. Westermann, M. A. B. Ferreira, M. W. Paixão, *Chem. Commun.* **2014**, *50*, 11926–11929.

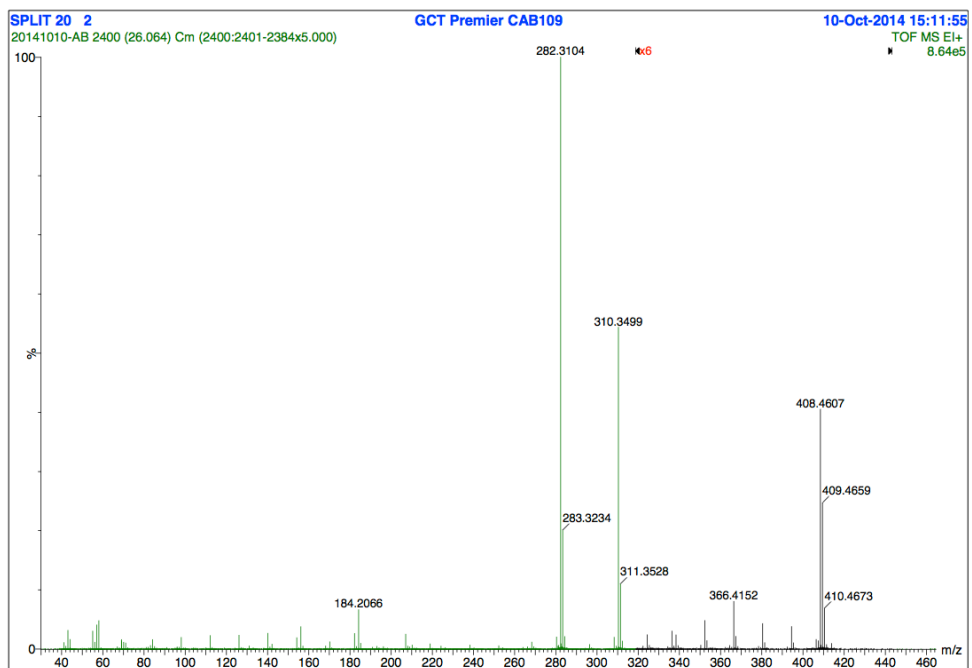
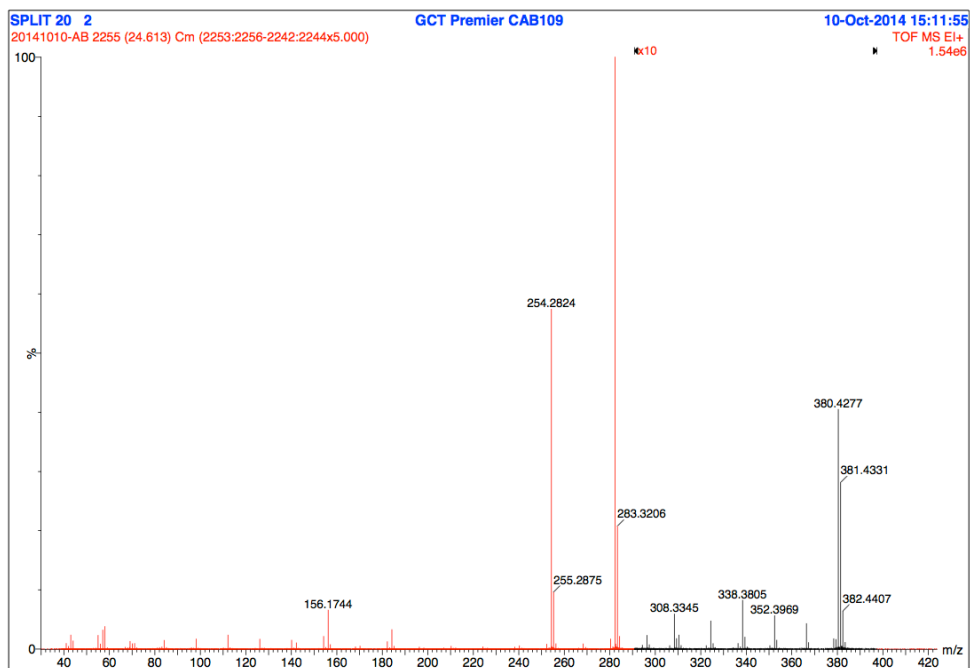
3.6 Annexes

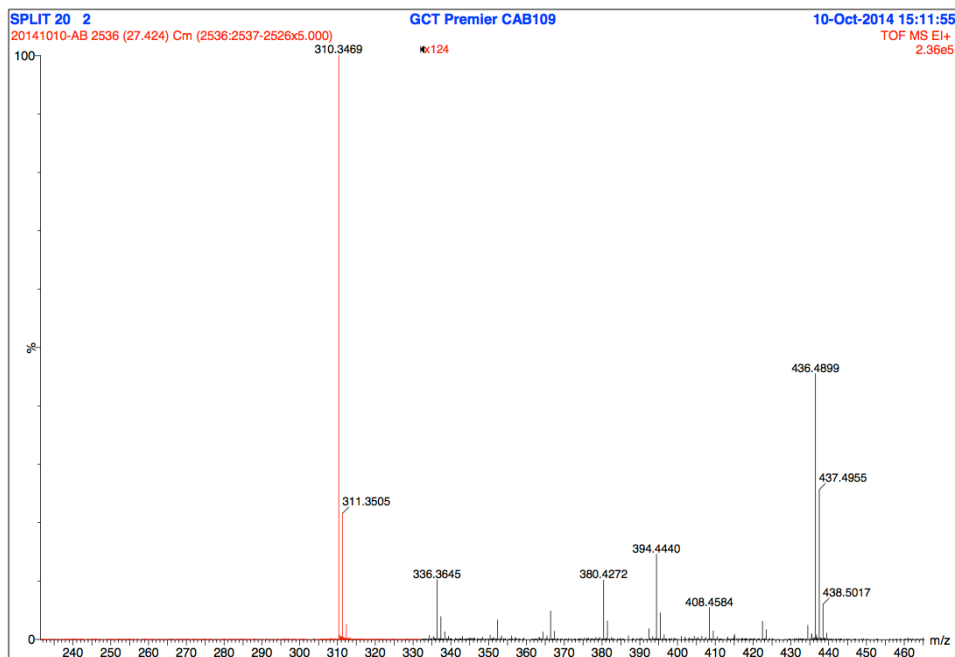
3.6.1 Mass spectra of the impurities of the contaminated benzyl azide

Mass spectra corresponding to the peaks appeared in the retention time between 17.5 and 27.5 minutes in the GC chromatogram shown in Figure 3.2.

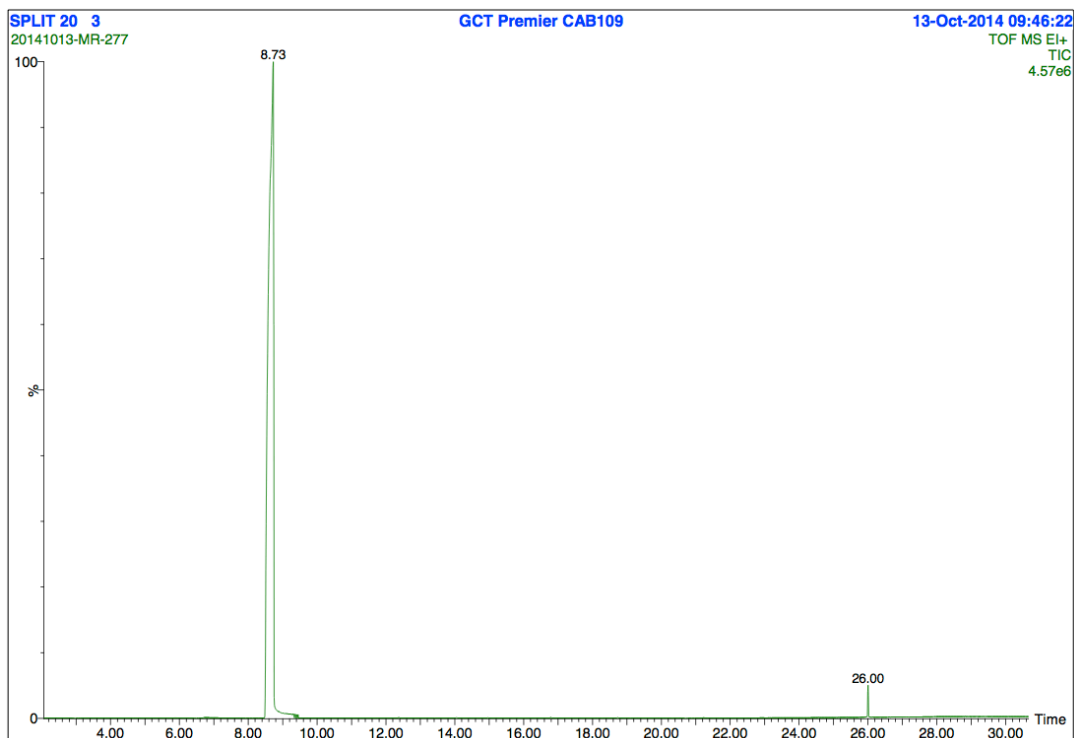






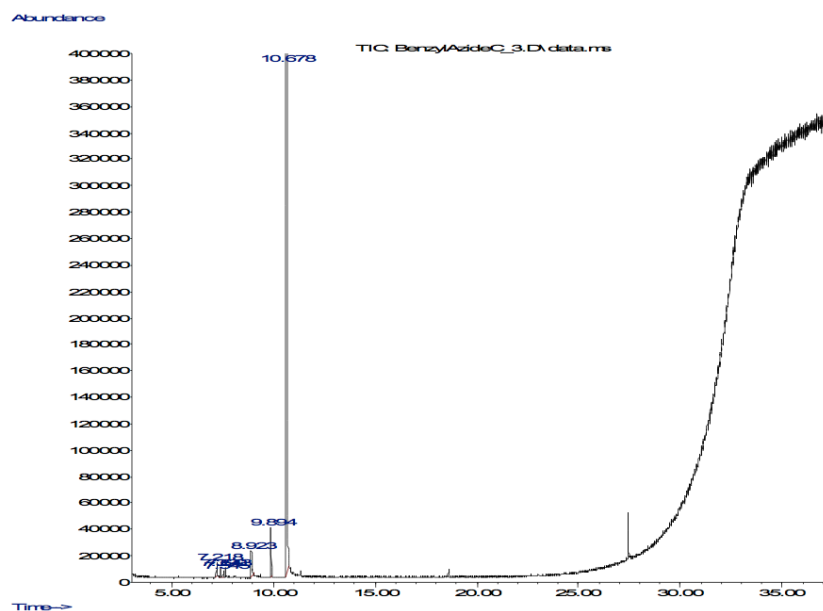


3.6.2 GC-MS-EI chromatograms of “inactive” benzyl azides



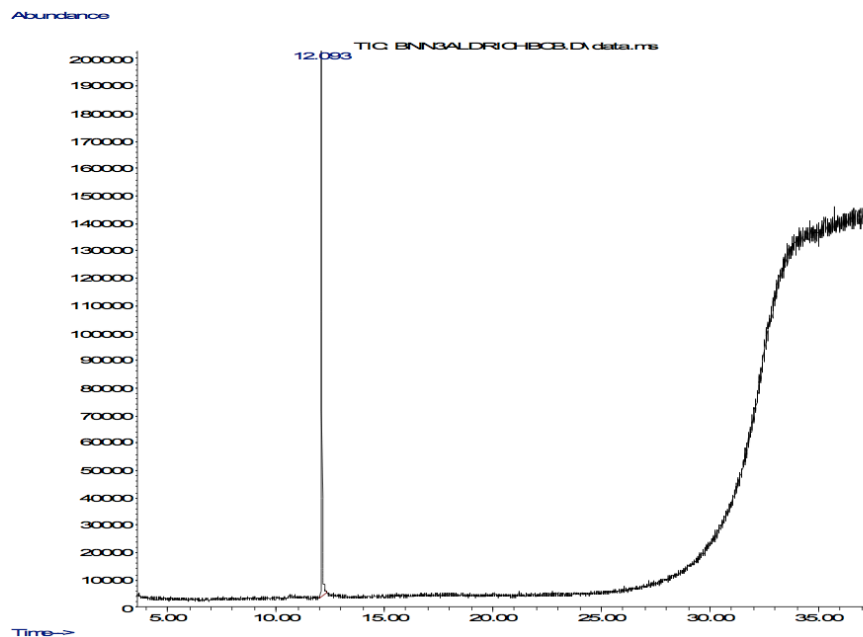
Home-made benzyl azide

HP5 30mx0.32mm, 0.25µm
Tinj/Aux 280°C
Flow 1.5mL/min
split 20:1 (1µL)
50°C(5')-325°C(5') /10°Cmin-1
Sample: in DCM



Benzyl azide from Alfa-Aesar (Lot AE040501)

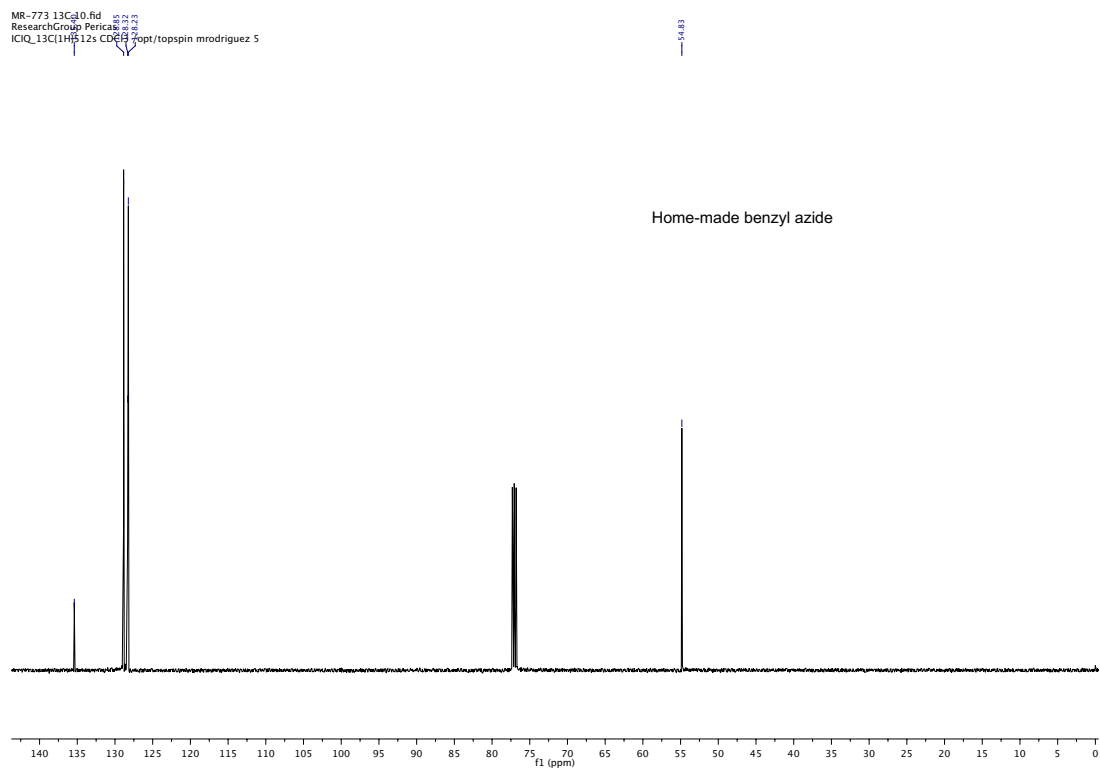
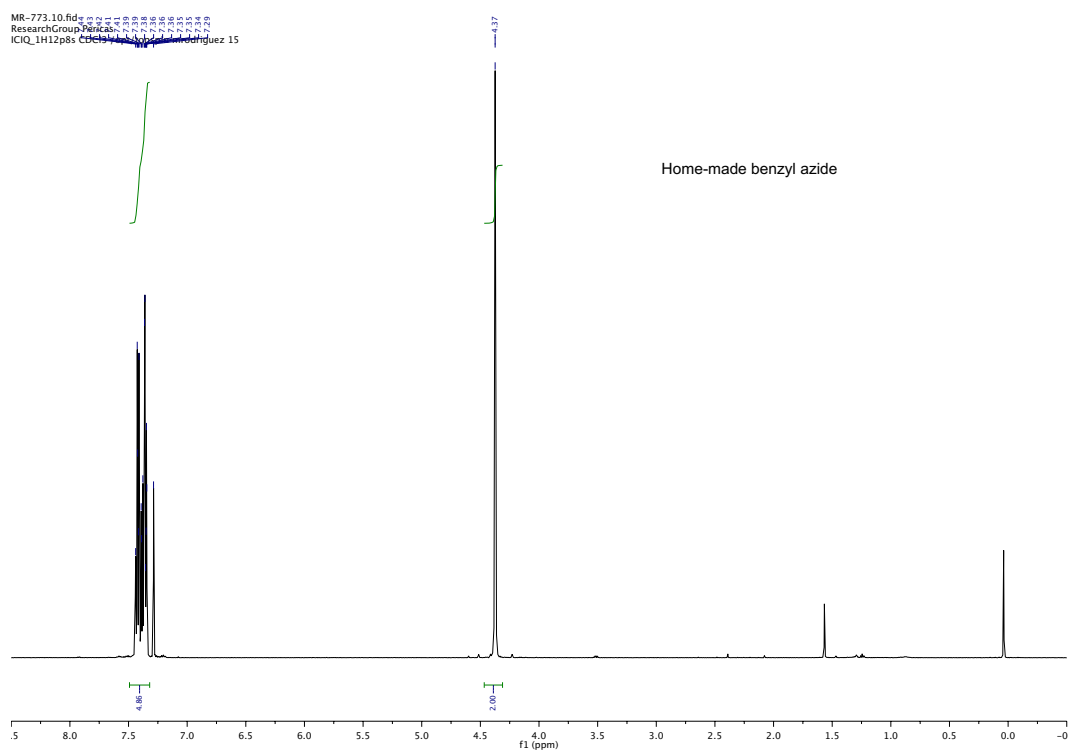
HP5 30mx0.32mm, 0.25µm
Tinj/Aux 280°C
Flow 1.5mL/min
split 20:1 (1µL)
50°C(5')-325°C(5') /10°Cmin-1
Sample: in DCM

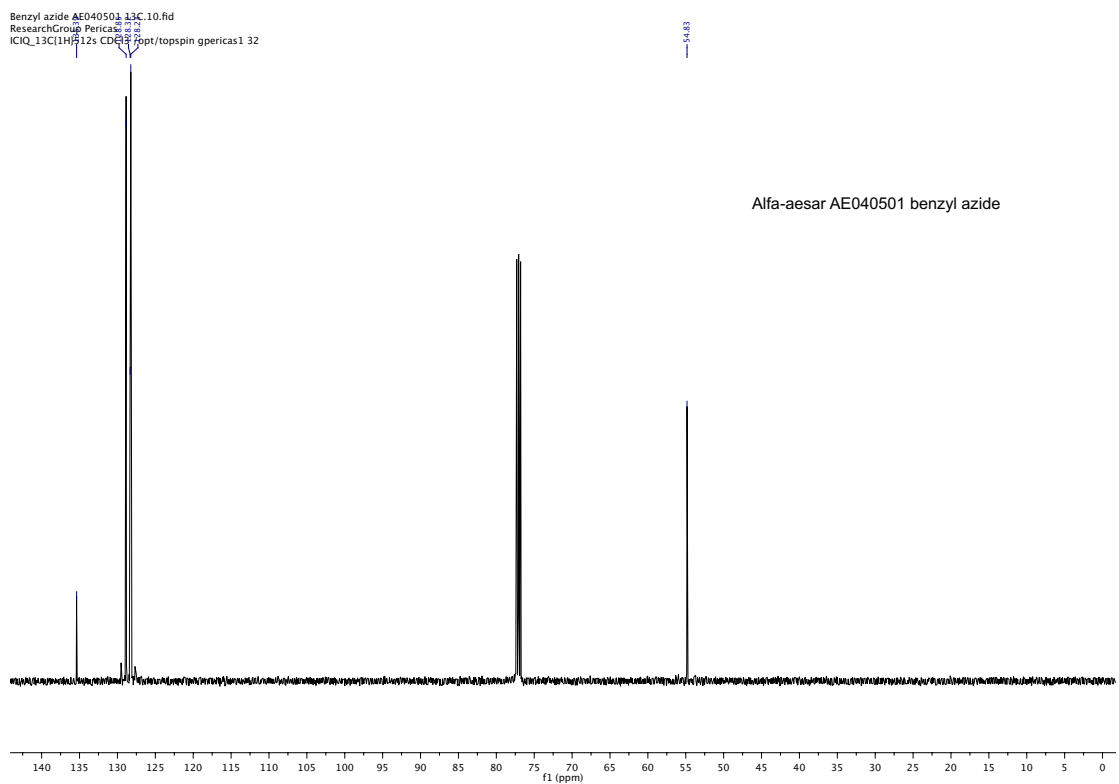
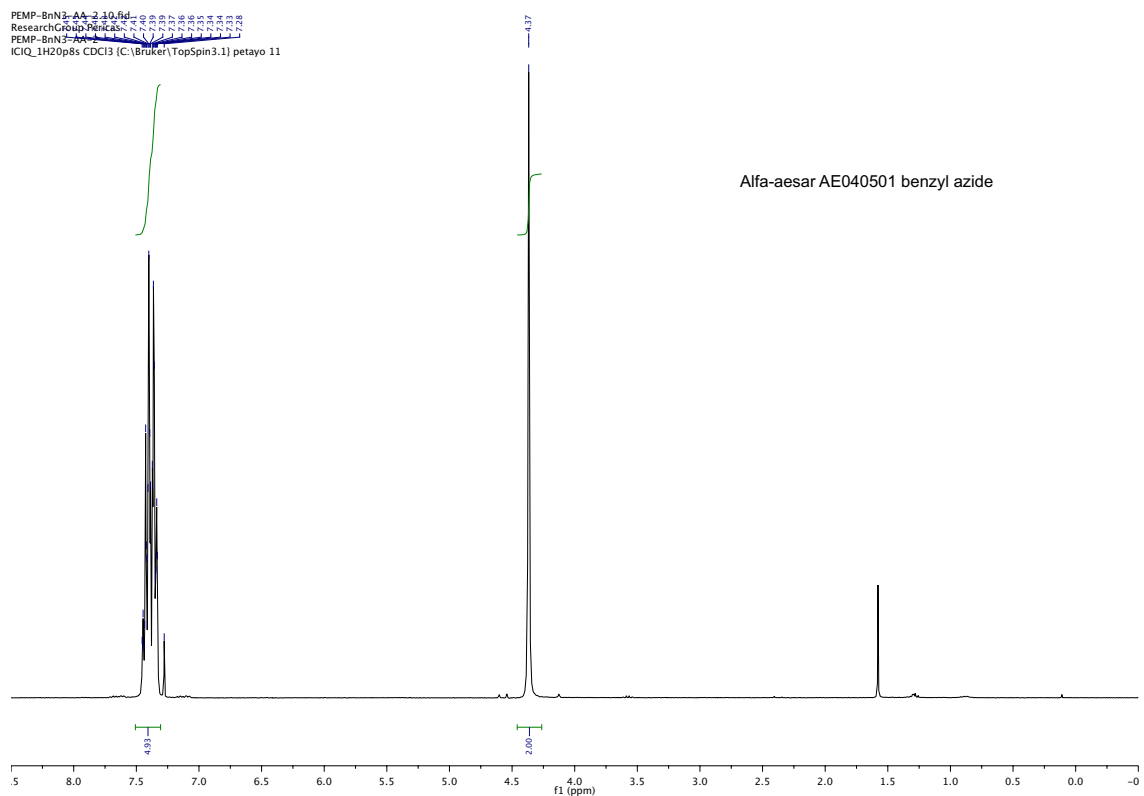


Benzyl azide from Aldrich (Lot BCBL4667V)

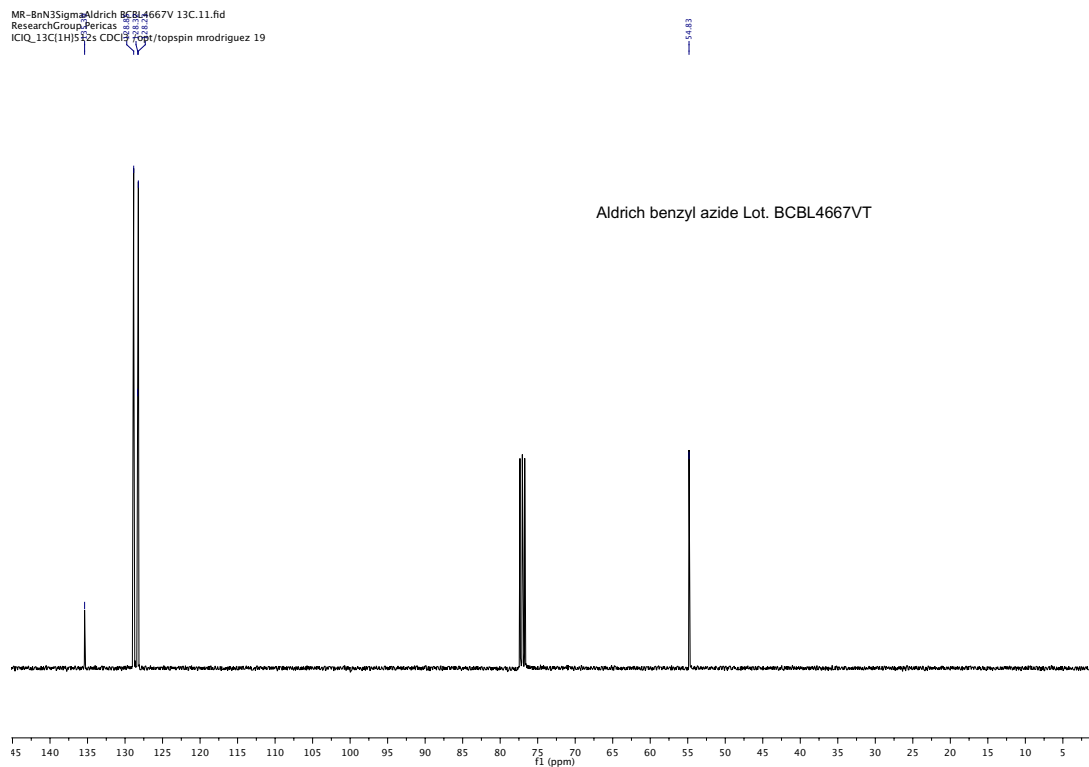
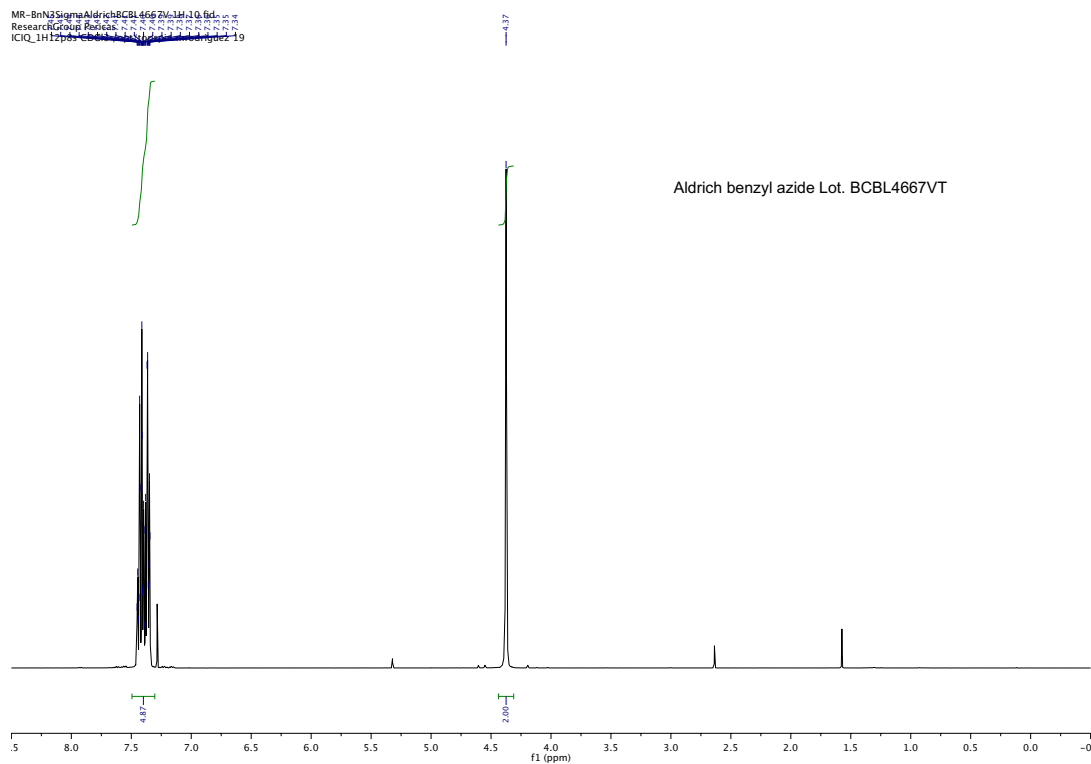
3.6.3 NMR spectra of “inactive” benzyl azides

^1H (top, 500 MHz) and ^{13}C (bottom, 125 MHz) NMR spectra (CDCl_3) for home-made BnN_3



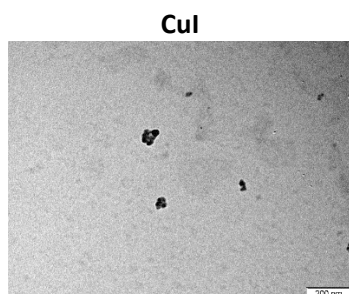
^1H (top, 300 MHz) and ^{13}C (bottom, 125 MHz) NMR spectra (CDCl_3) for BnN_3 from Alfa-Aesar (Lot AE040501)

^1H (top, 400 MHz) and ^{13}C (bottom, 100 MHz) NMR spectra (CDCl_3) for BnN_3 from Aldrich (Lot BCBL4667V)

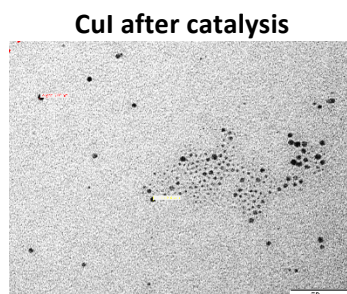


3.6.4 TEM images

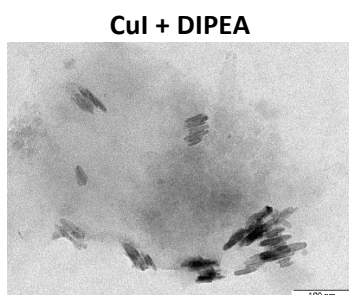
TEM images for CuI in the absence and in the presence of different amines in glycerol (left column) and the corresponding mixtures after the cycloaddition between phenylacetylene and benzyl azide (right column). Conversions and yields are indicated after catalysis.



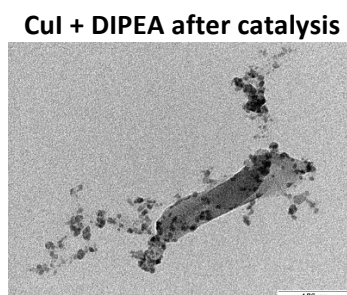
Only big agglomerates



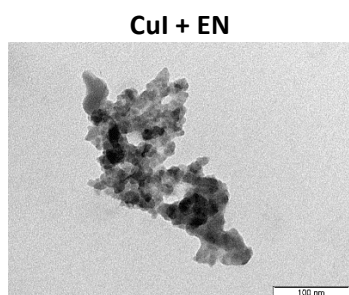
Few nanoparticles, not homogeneous in size
(conversion: <5%)



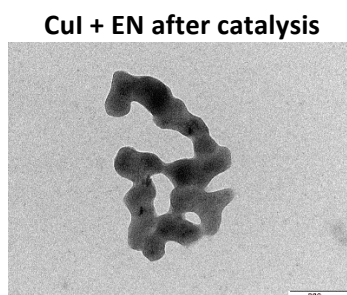
Agglomerates



Agglomerates
(conversion (yield): 36 (6%))

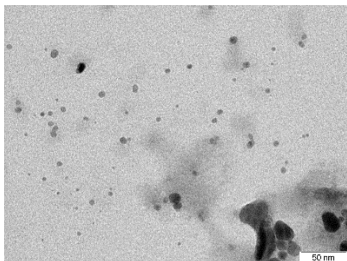


Agglomerates



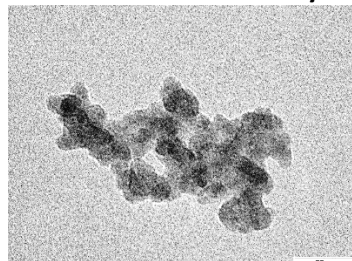
Agglomerates
(conversion (yield): 30 (12%))

CuI + TMEDA



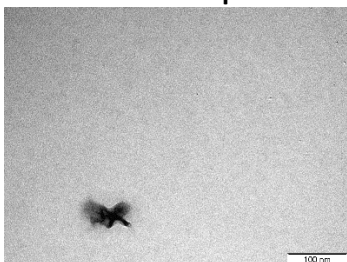
Few nanoparticles, mainly agglomerates

CuI + TMEDA after catalysis



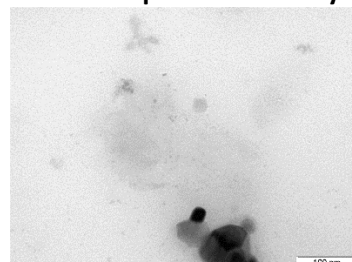
Only big agglomerates
(conversion (yield): 83 (70)%)

CuI + urotropine



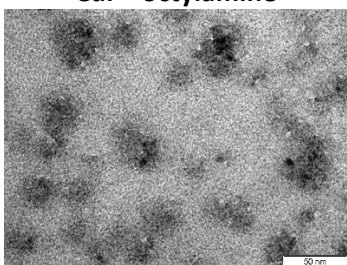
Only big agglomerates

CuI + urotropine after catalysis



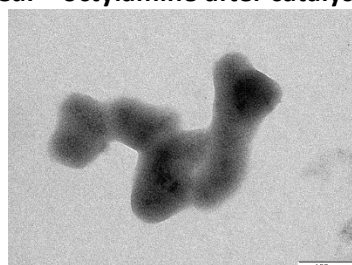
Only big agglomerates
(conversion (yield): 20 (<5)%)

CuI + octylamine



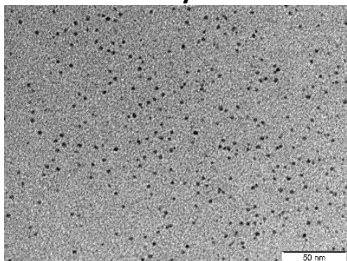
Trend to give assemblies

CuI + octylamine after catalysis



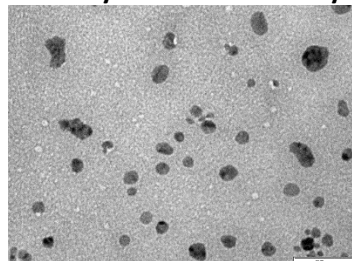
Mainly agglomerates
(conversion (yield): 96 (93)%)

CuI + oleylamine



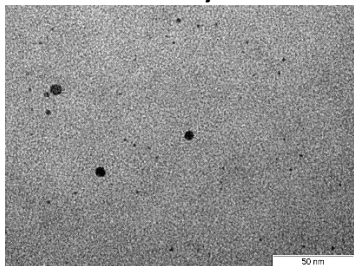
Well-dispersed nanoparticles,
 $d_{\text{mean}} = 2.7 \pm 0.8 \text{ nm}$ (for 934 NPs)

CuI + oleylamine after catalysis



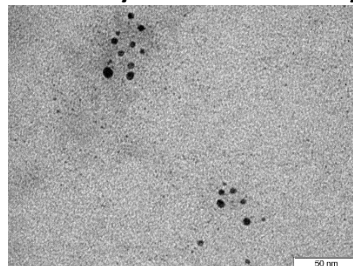
Mainly agglomerates
(conversion (yield): 100 (>99)%)

CuI + undecylamine



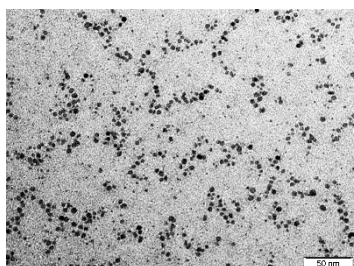
Few nanoparticles, not homogeneous in size

CuI + undecylamine after catalysis



Few nanoparticles, not homogeneous in size
(conversion (yield): 96 (93)%)

CuI + dioctylamine



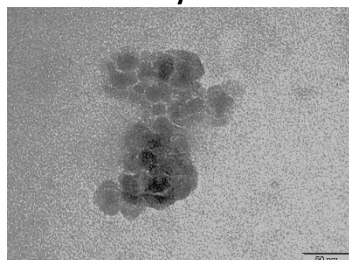
Well-dispersed nanoparticles,
 $d_{\text{mean}} = 2.1 \pm 0.8$ nm (for 605 NPs)

CuI + dioctylamine after catalysis



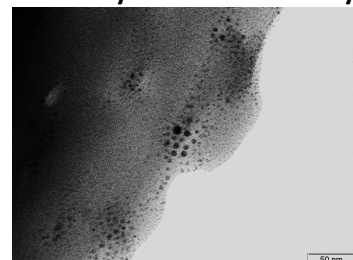
Well-dispersed nanoparticles,
 $d_{\text{mean}} = 1.4 \pm 0.6$ nm (for 1109 NPs)
(conversion (yield): 100 (96)%)

CuI + trioctylamine



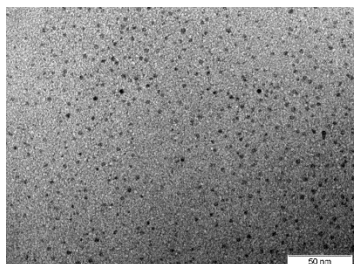
Agglomerates

CuI + trioctylamine after catalysis



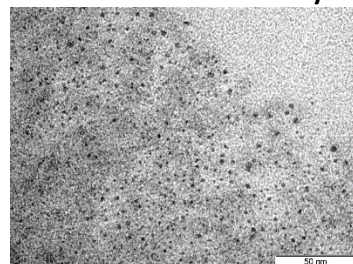
Big nanoparticles together with big objects
(conversion (yield): 96 (88)%)

CuI + TOMACI



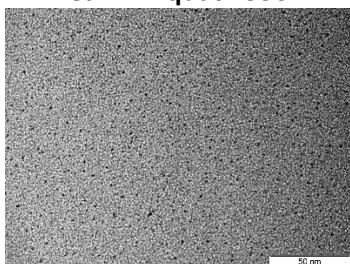
Well-dispersed nanoparticles,
 $d_{\text{mean}} = 1.8 \pm 0.6$ nm (for 684 NPs)

CuI + TOMACI after catalysis



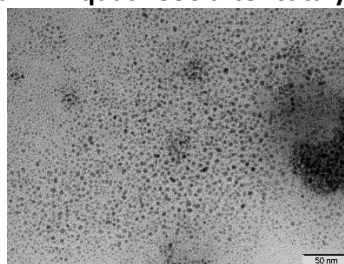
Well-dispersed nanoparticles,
 $d_{\text{mean}} = 1.6 \pm 0.5$ nm (for 314 NPs)
(conversion (yield): 37 (19)%)

CuI + Aliquat® 336



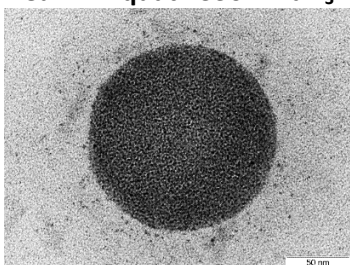
Well-dispersed nanoparticles,
 $d_{\text{mean}} = 1.7 \pm 0.7$ nm (for 1506 NPs)

CuI + Aliquat® 336 after catalysis



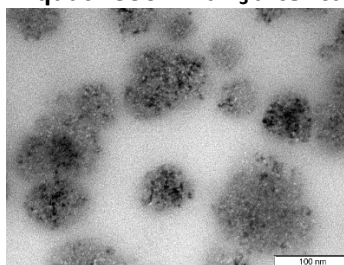
Well-dispersed nanoparticles,
 $d_{\text{mean}} = 2.7 \pm 1.0$ nm (for 1629 NPs)
(conversion (yield): 20 (<5)%)

CuI + Aliquat® 336 + NaN₃



Small nanoparticles, tending to give micelle-
like arrangements

CuI + Aliquat® 336 + NaN₃ after catalysis

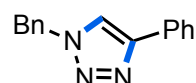
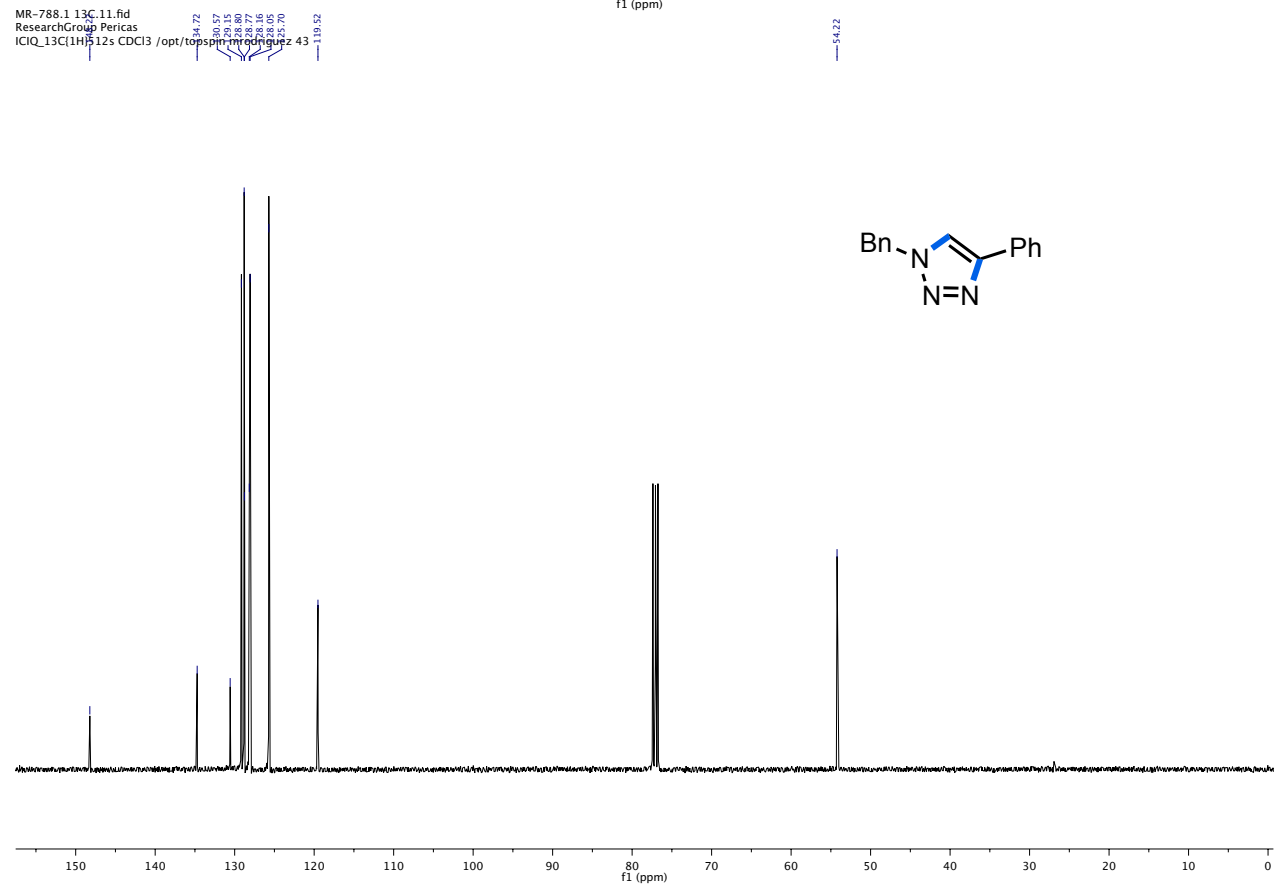
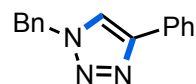
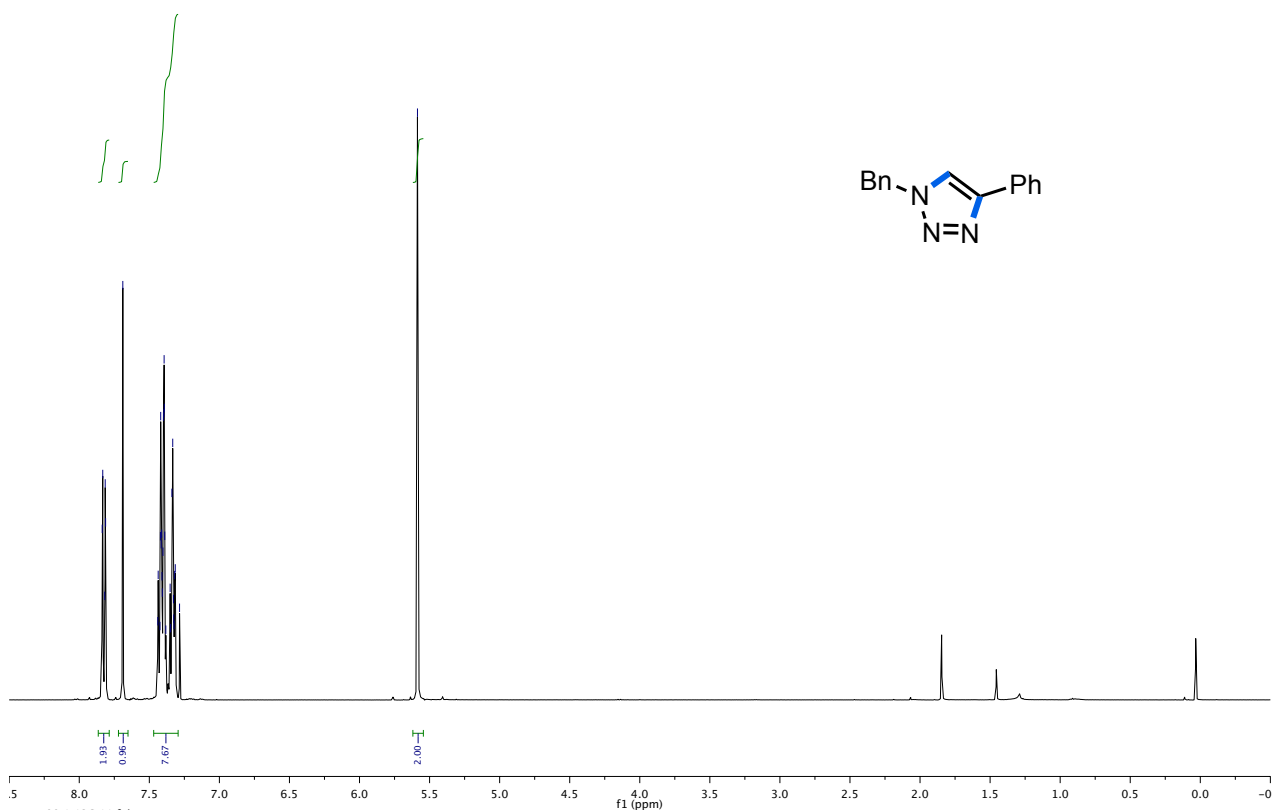


Particles tending to be associated
(conversion (yield): 97 (93)%)

3.6.5 NMR spectra of the isolated compounds

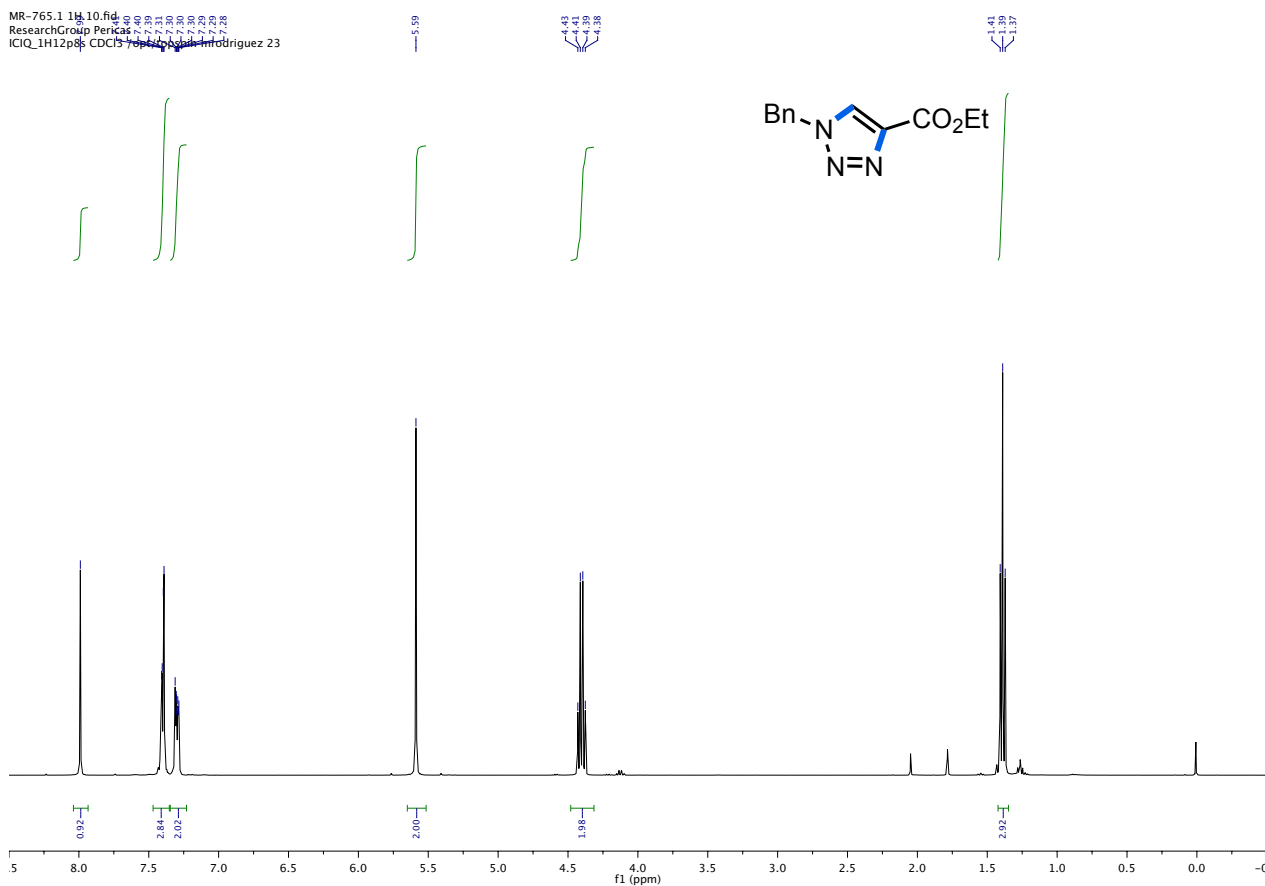
 ^1H NMR (400 MHz) (top) and ^{13}C NMR (100 MHz) (bottom) spectra in CDCl_3 for **13a**

MR-788.1 1H.10.fid
ResearchGroup Pericas
ICIQ_1H12p85-6123 /opt/topspin/mr09aug2

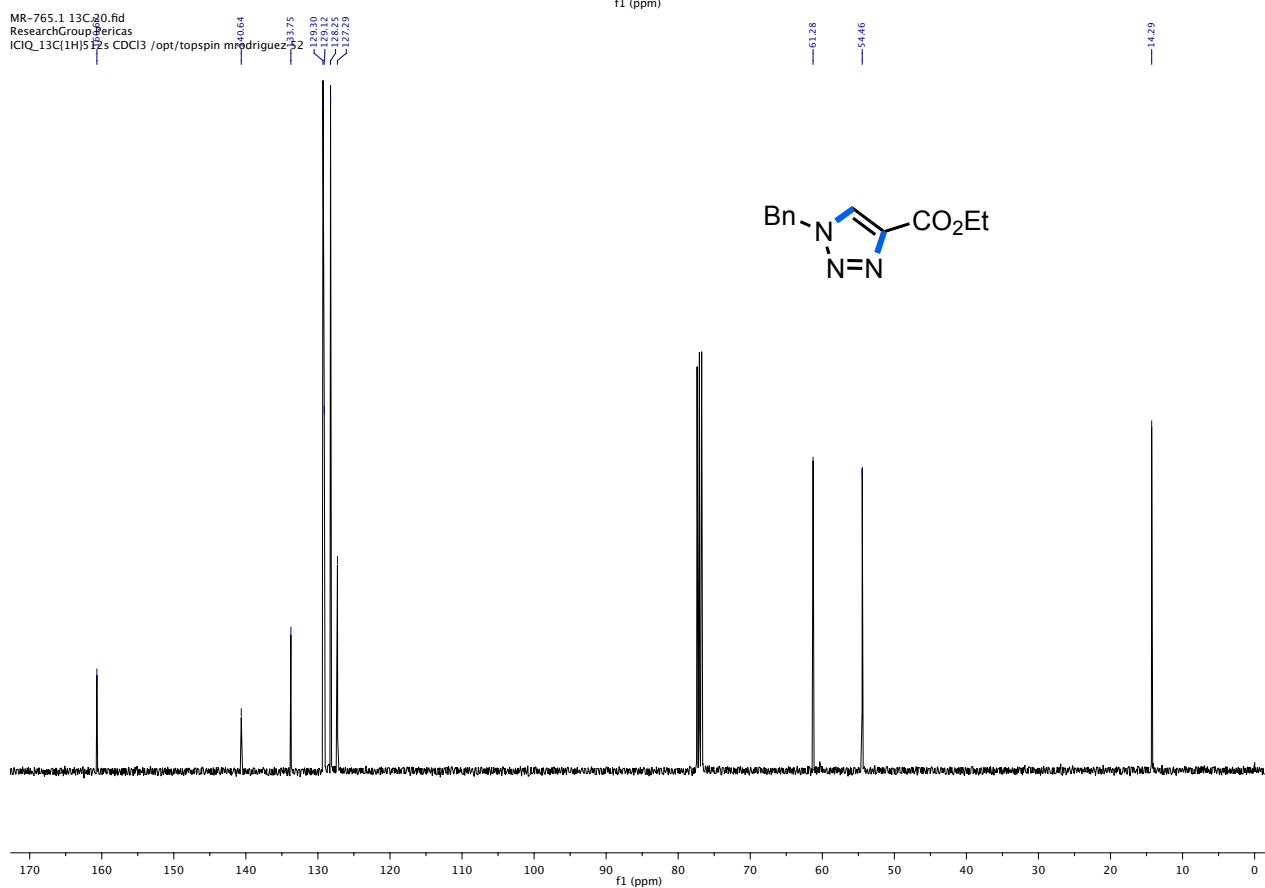


^1H NMR (400 MHz) (top) and ^{13}C NMR (100 MHz) (bottom) spectra in CDCl_3 for **14a**

MR-765.1 1H_10.fid
ResearchGroup.Pericas
ICIQ_1H12p8s CDCl3 /opt/topspin mrodriguez 23

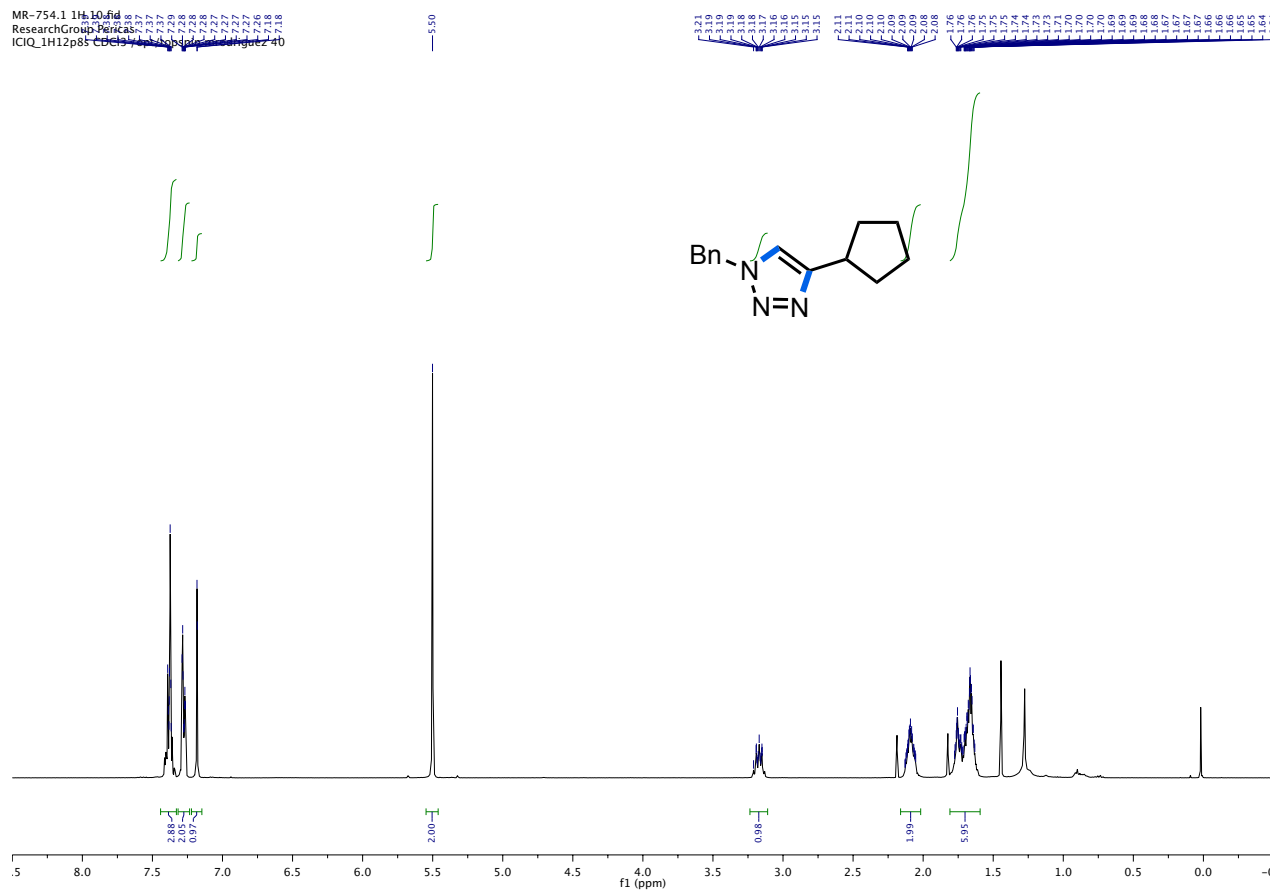


MR-765.1 13C_20.fid
ResearchGroup.Pericas
ICIQ_13C(1H)512s CDCl3 /opt/topspin mrodriguez 23

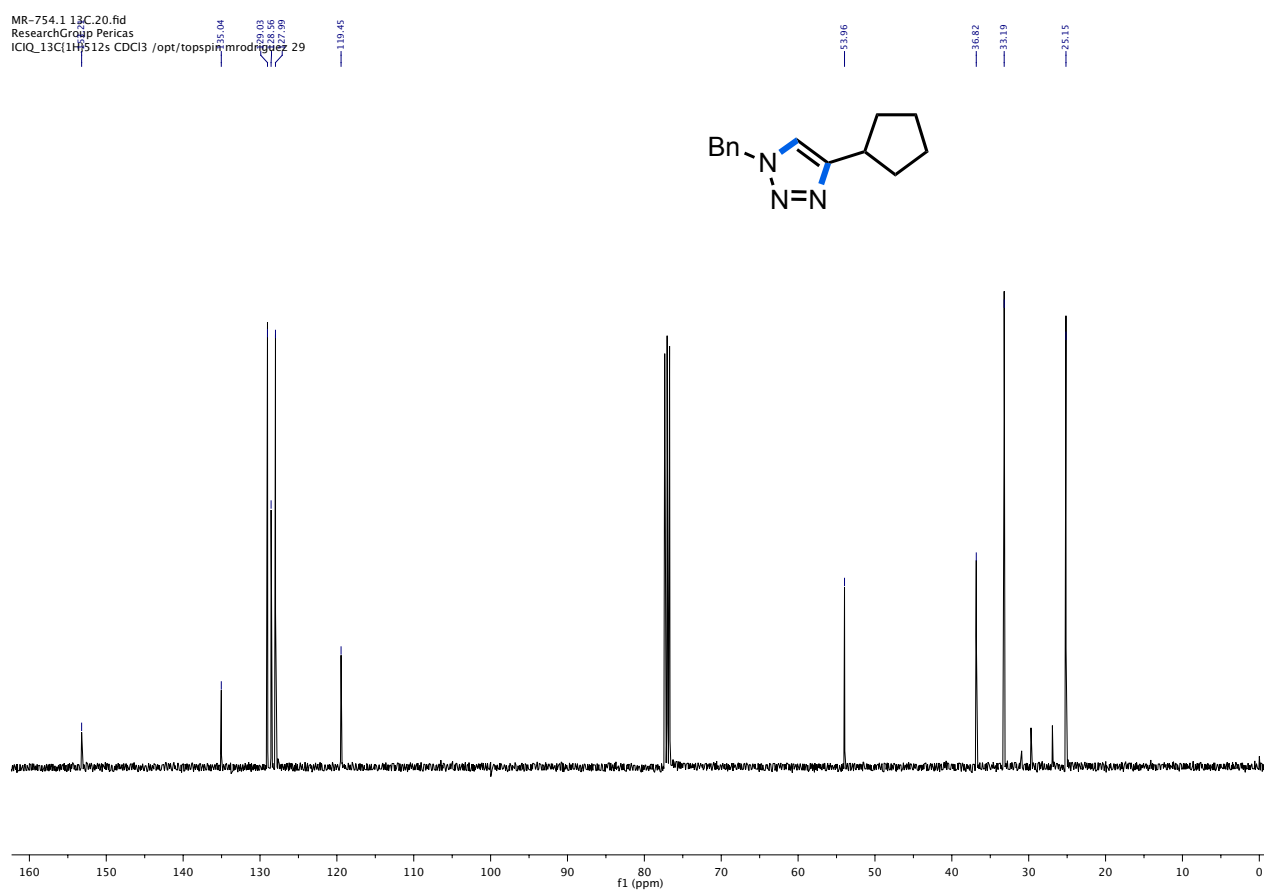


^1H NMR (400 MHz) (top) and ^{13}C NMR (100 MHz) (bottom) spectra in CDCl_3 for **15a**

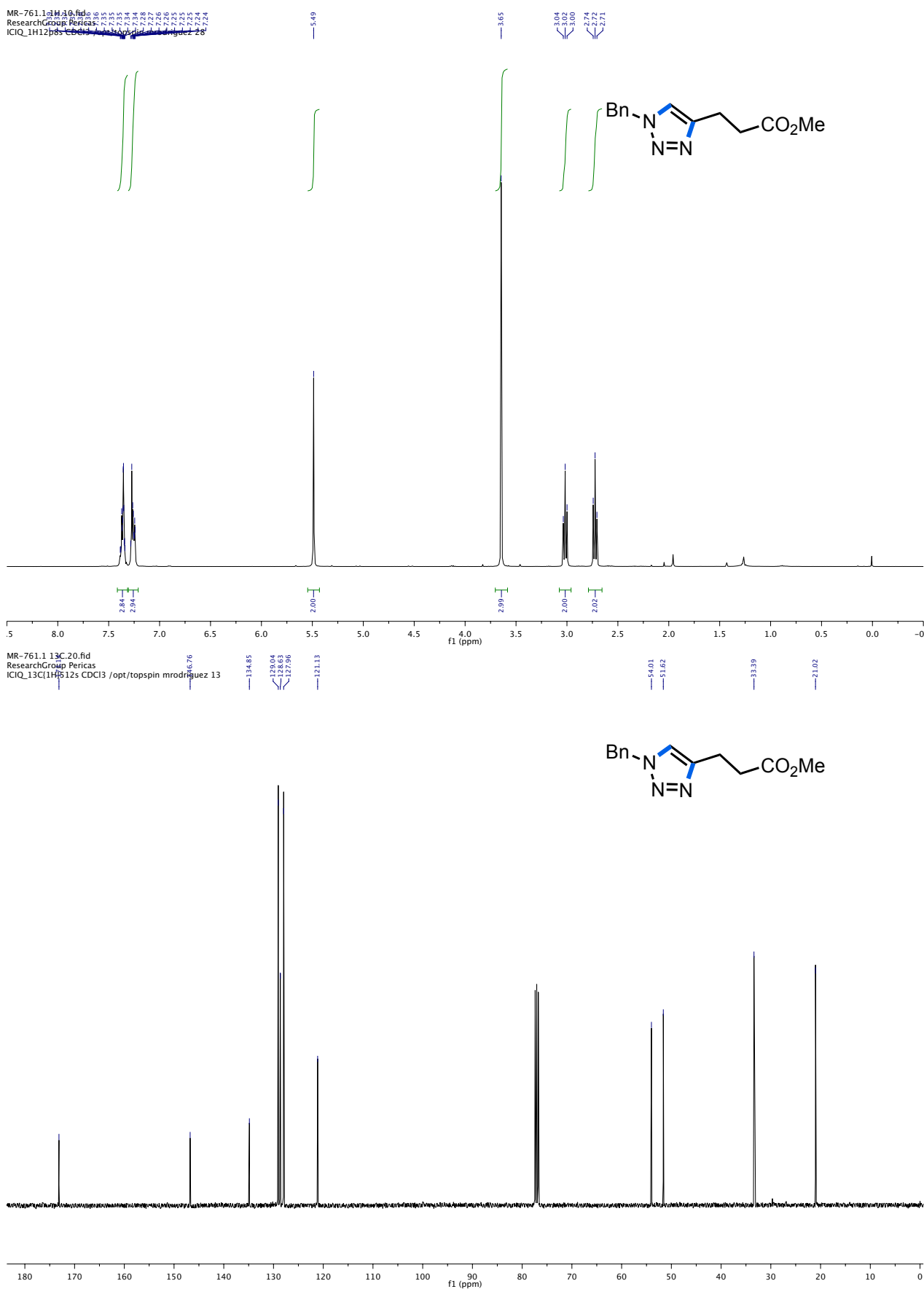
MR-754.1 1H.10.fid
 ResearchGroup Pericas
 ICIQ_1H12p85 CDCl3



MR-754.1 13C.20.fid
 ResearchGroup Pericas
 ICIQ_13C1H512s CDCl3 /opt/topspin/mrod/

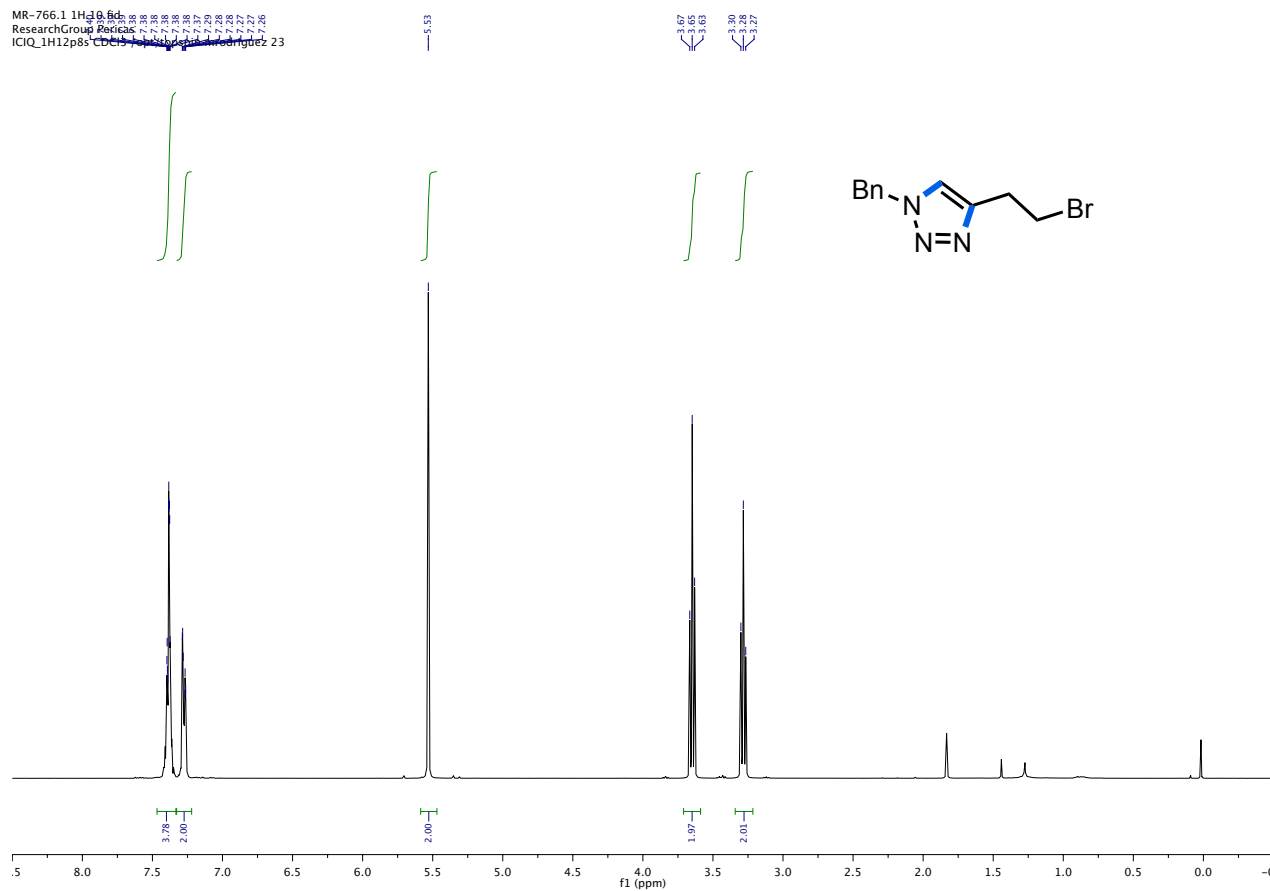


^1H NMR (400 MHz) (top) and ^{13}C NMR (100 MHz) (bottom) spectra in CDCl_3 for **16a**

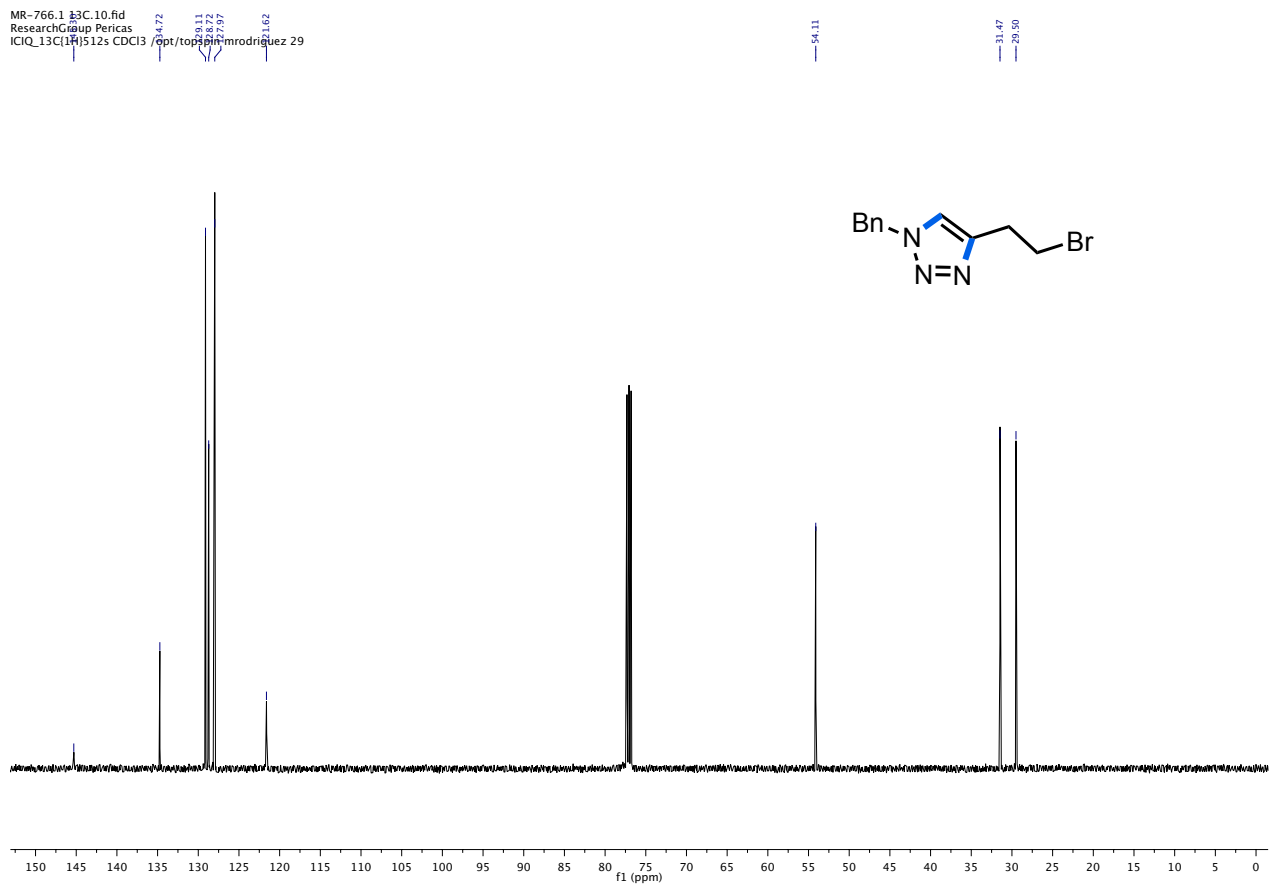


^1H NMR (400 MHz) (top) and ^{13}C NMR (125 MHz) (bottom) spectra in CDCl_3 for **17a**

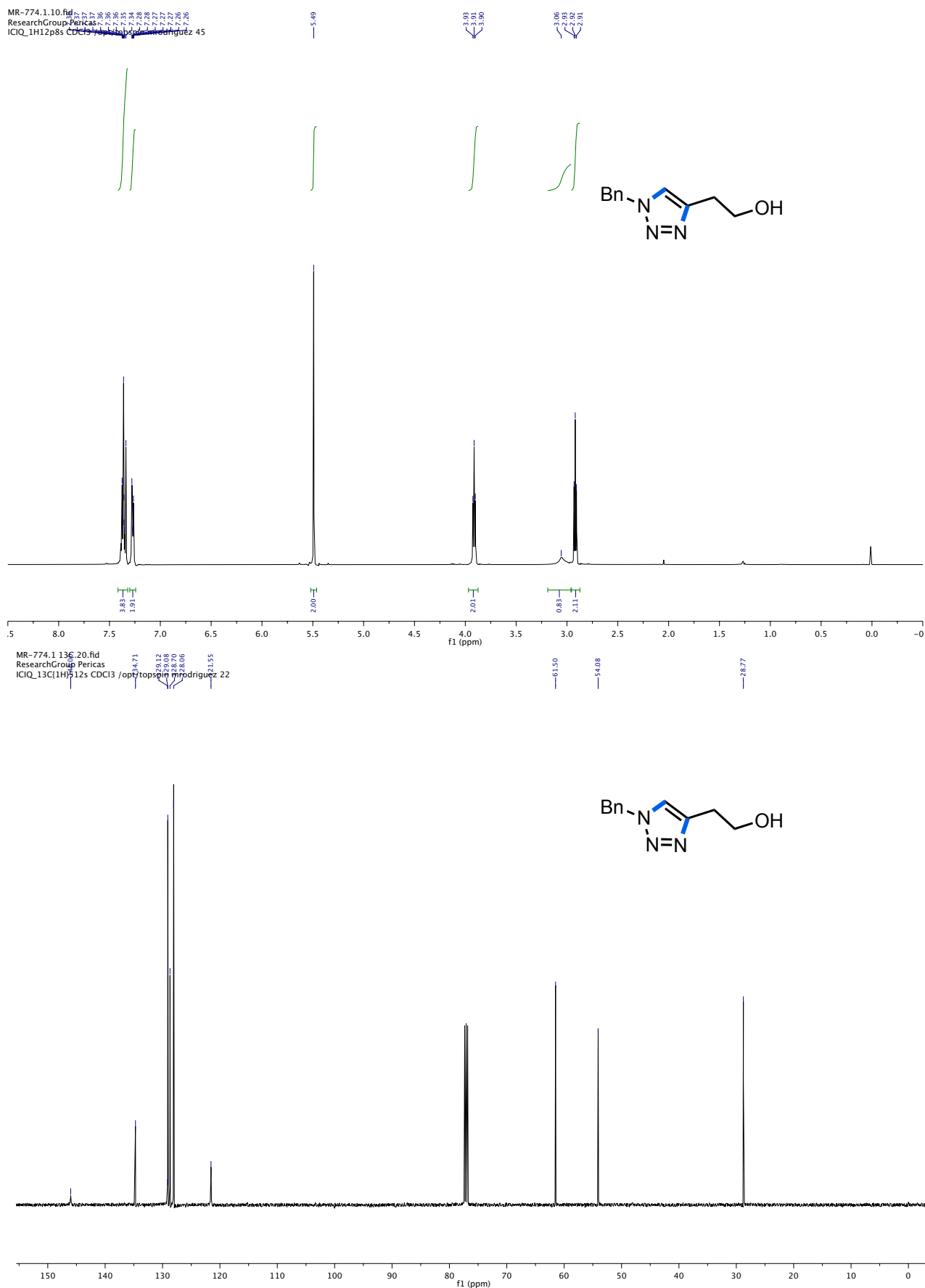
MR-766.1 1H10.fid
ResearchGroup Pericas
ICIQ_1H12p8s CDCl3 /opt/top/mrodriguez 23



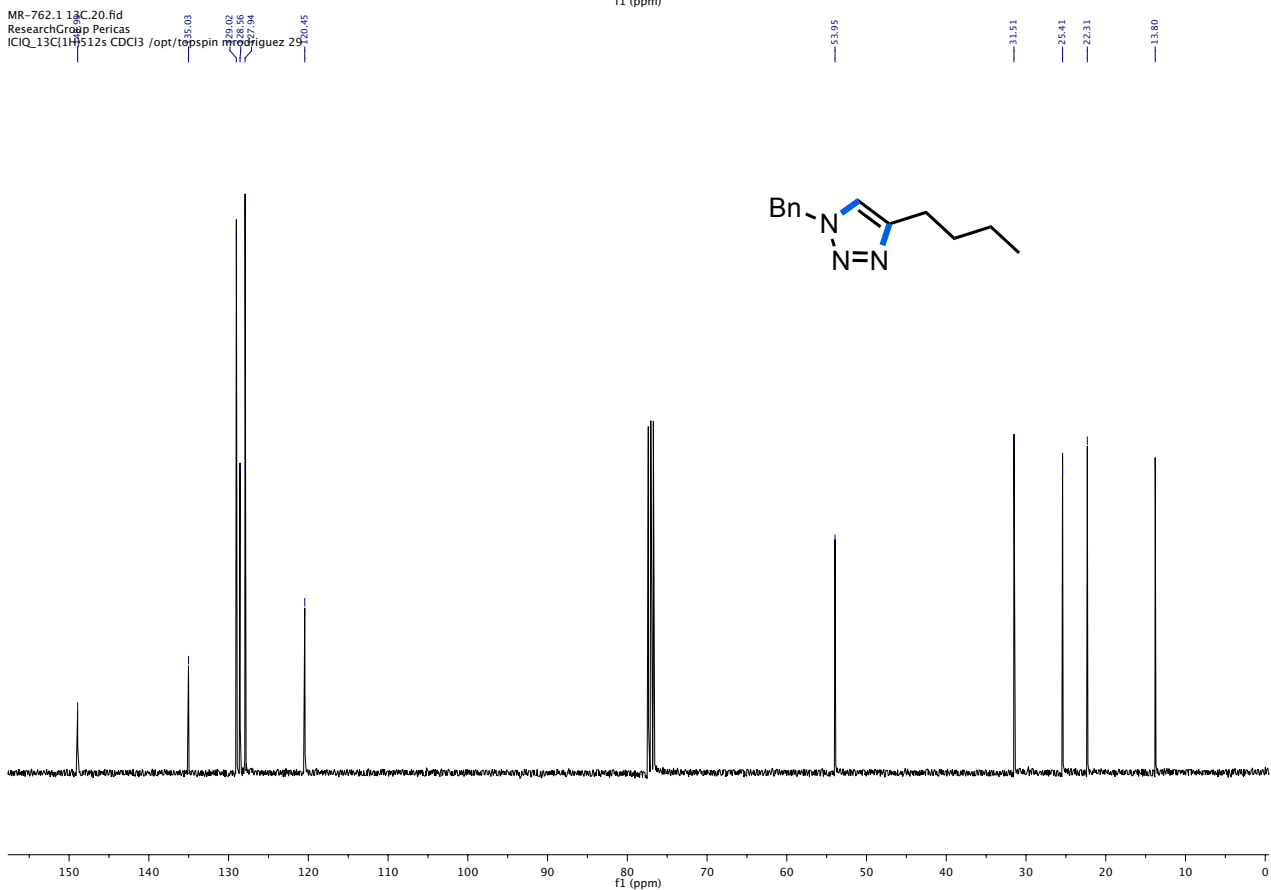
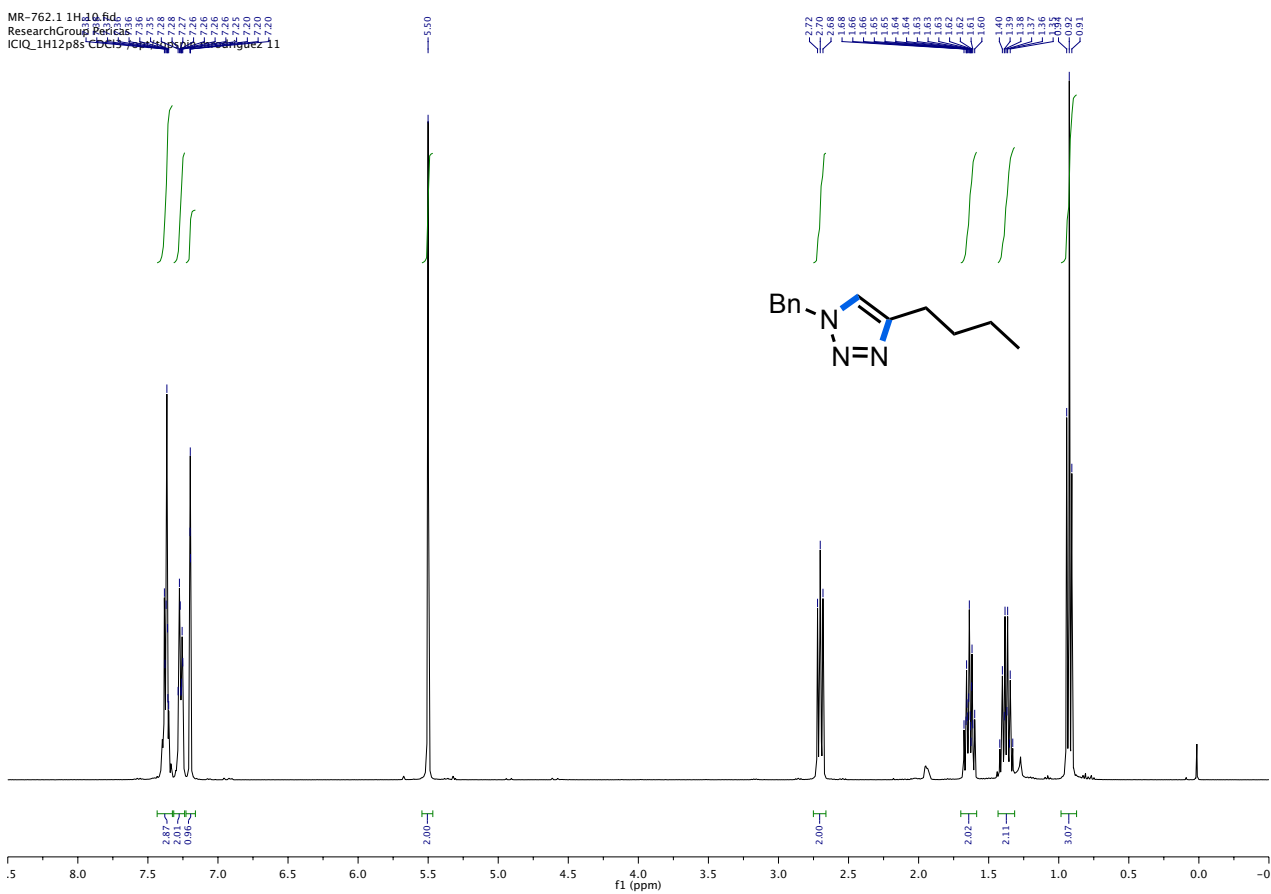
MR-766.1 13C.10.fid
ResearchGroup Pericas
ICIQ_13C14s12s CDCl3 /opt/top/mrodriguez 29



^1H NMR (500 MHz) (top) and ^{13}C NMR (125 MHz) (bottom) spectra in CDCl_3 for **18a**

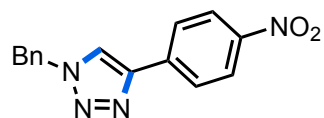
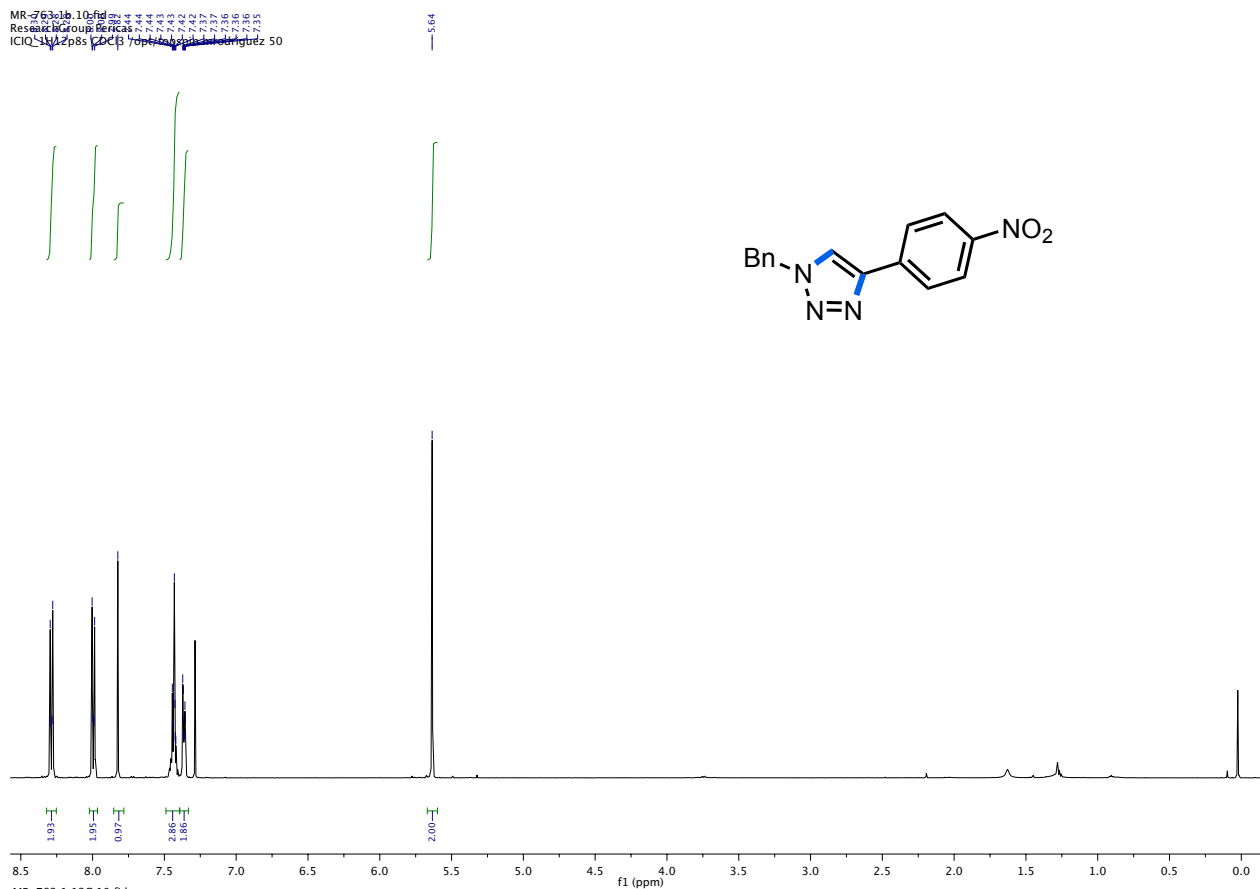


¹H NMR (400 MHz) (top) and ¹³C NMR (100 MHz) (bottom) spectra in CDCl₃ for **19a**

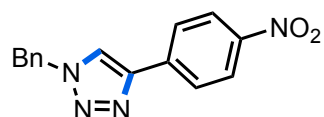
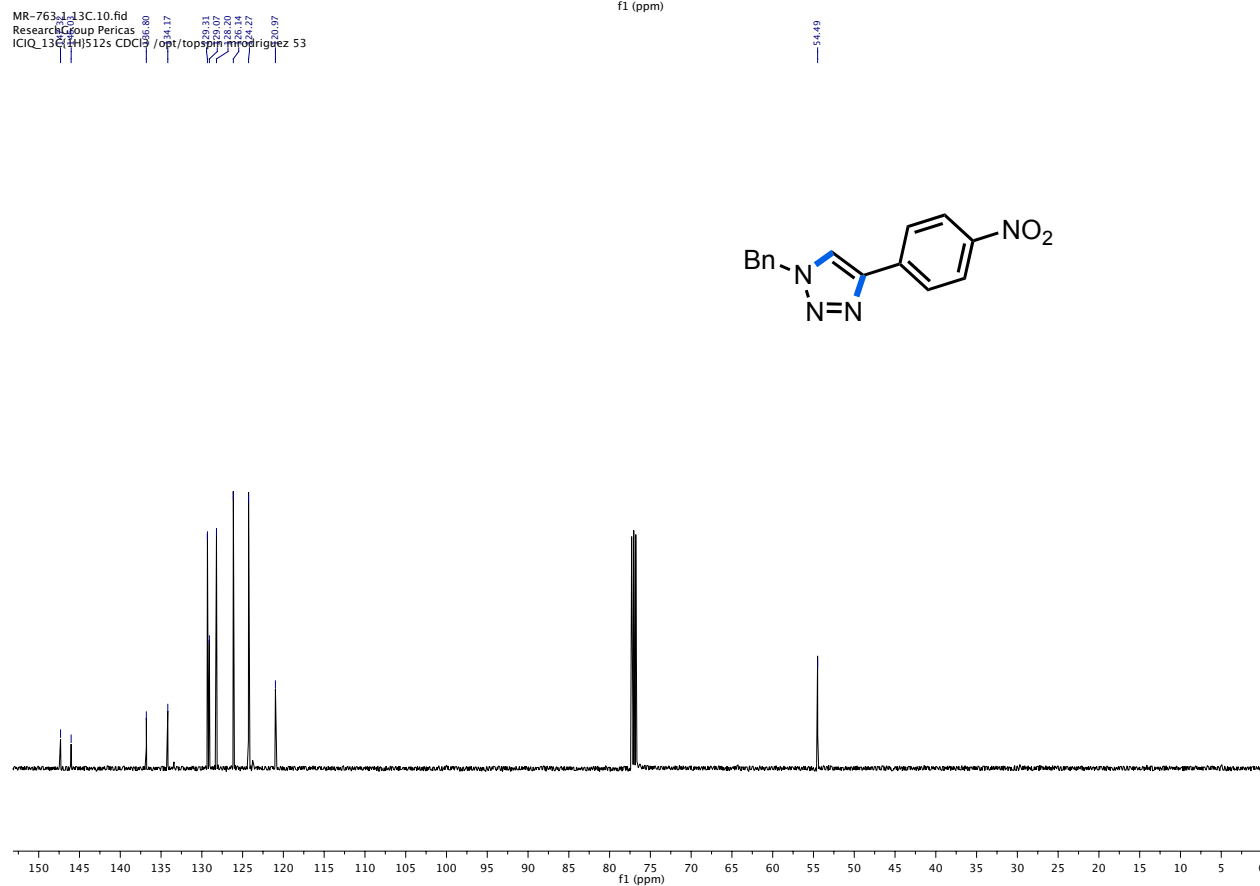


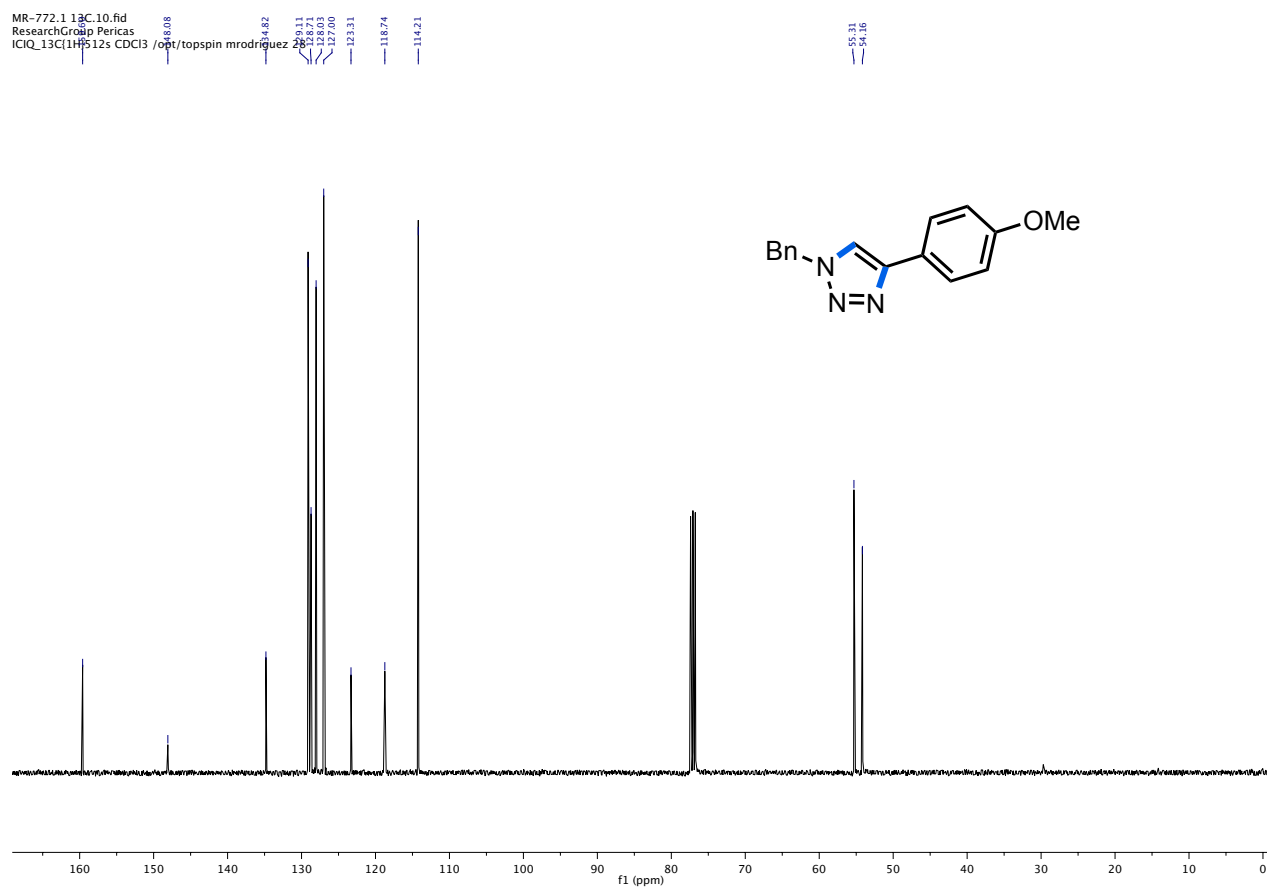
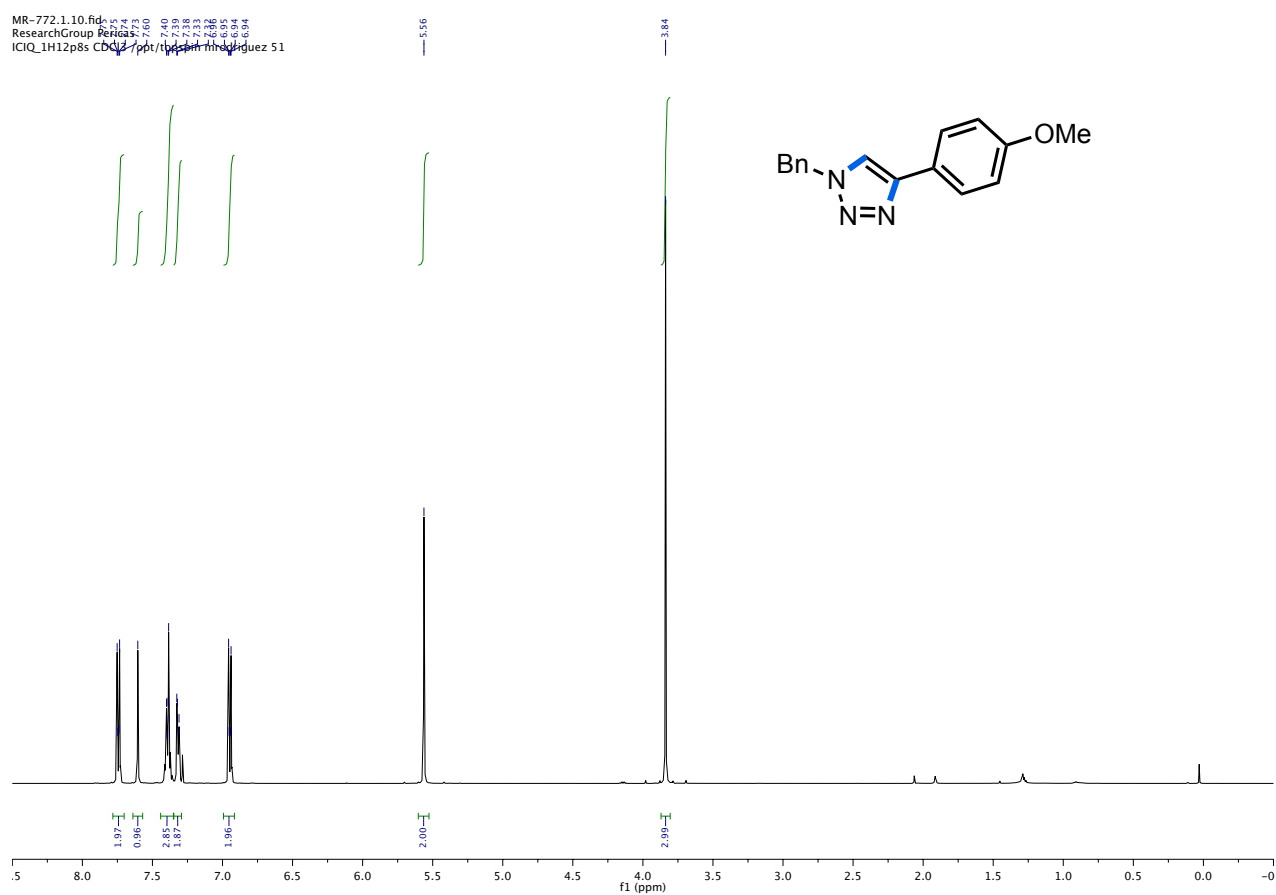
^1H NMR (500 MHz) (top) and ^{13}C NMR (125 MHz) (bottom) spectra in CDCl_3 for **20a**

MR-763-16_10.fid
Research Group Pericas
ICIQ_13C_112s CDCl₃ /opt/topspin/mrodriguez 50

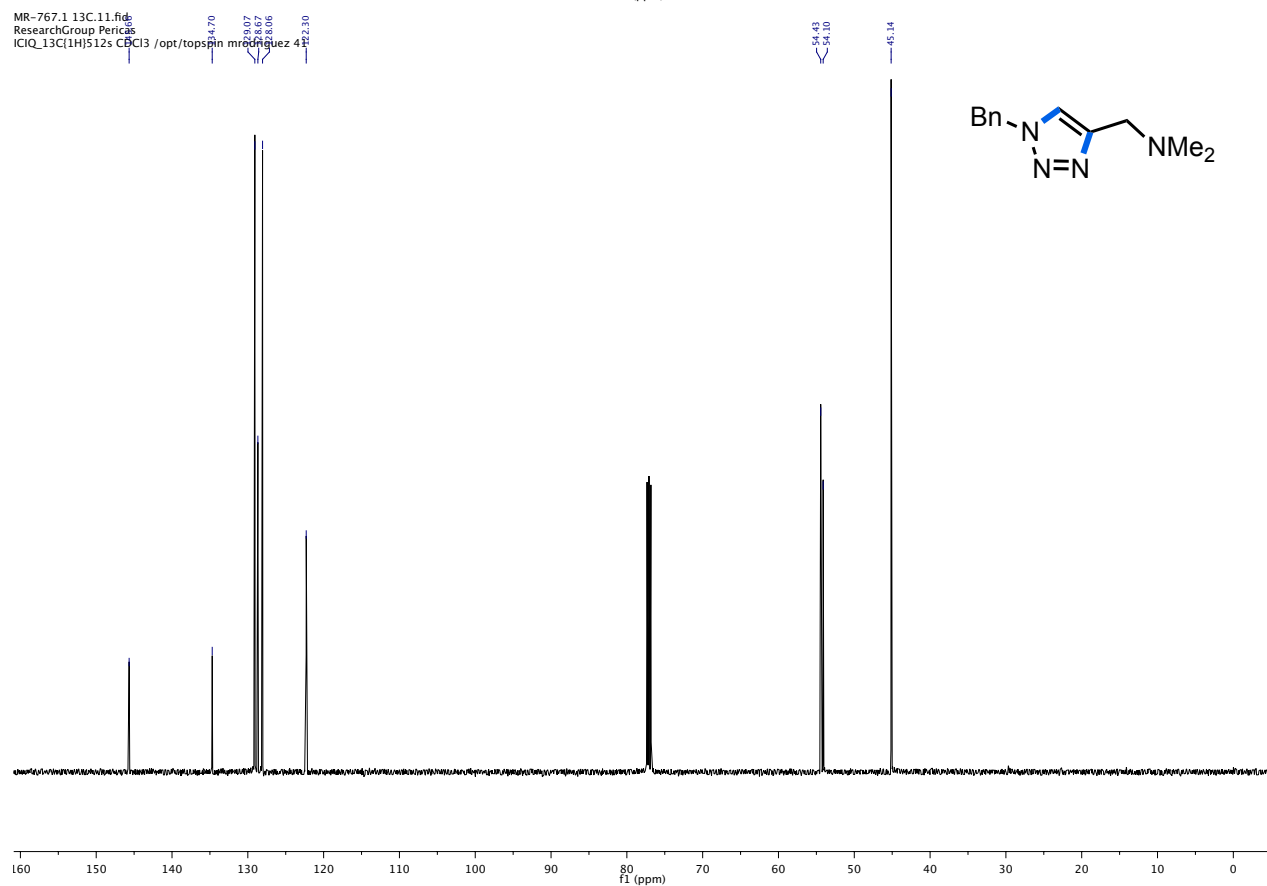
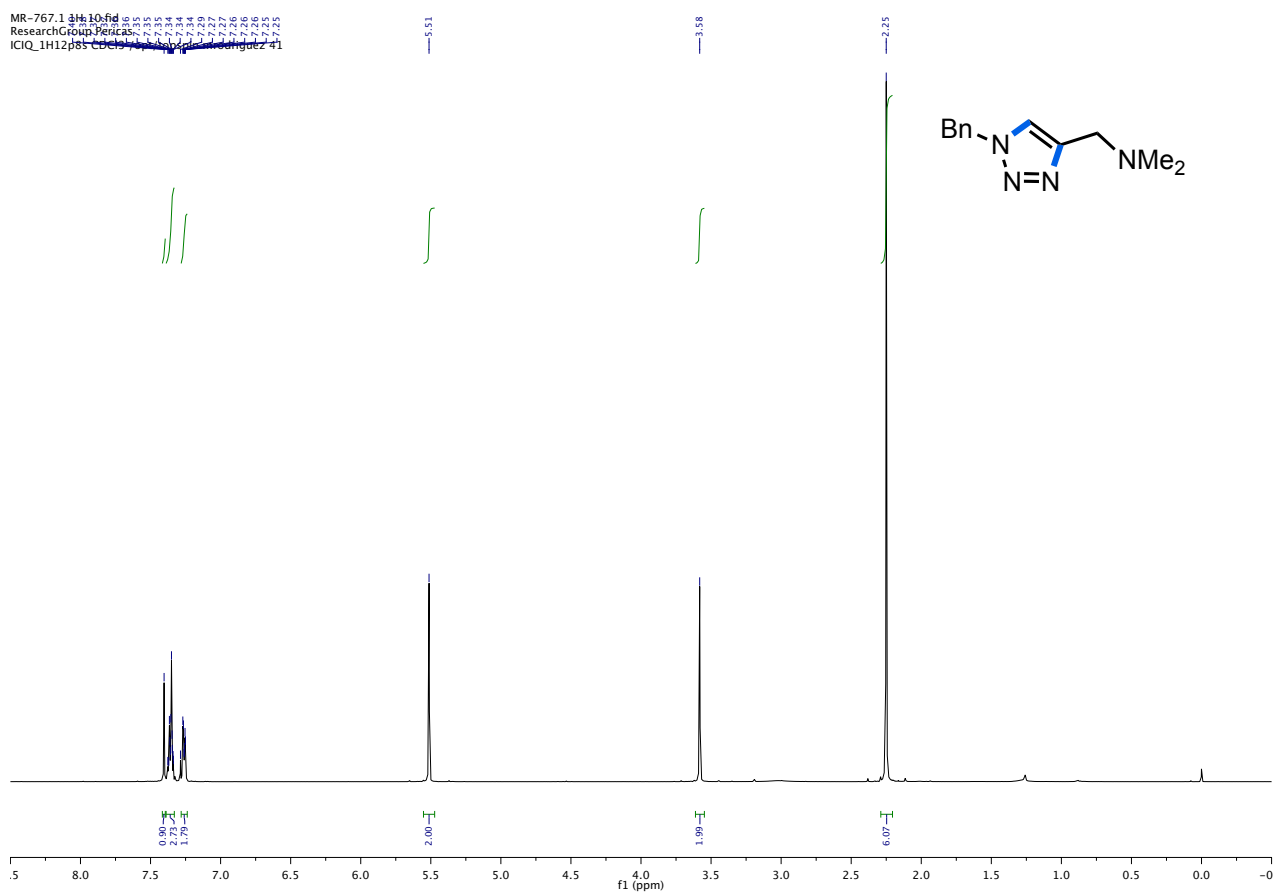


MR-763-16_13C.10.fid
Research Group Pericas
ICIQ_13C_112s CDCl₃ /opt/topspin/mrodriguez 53



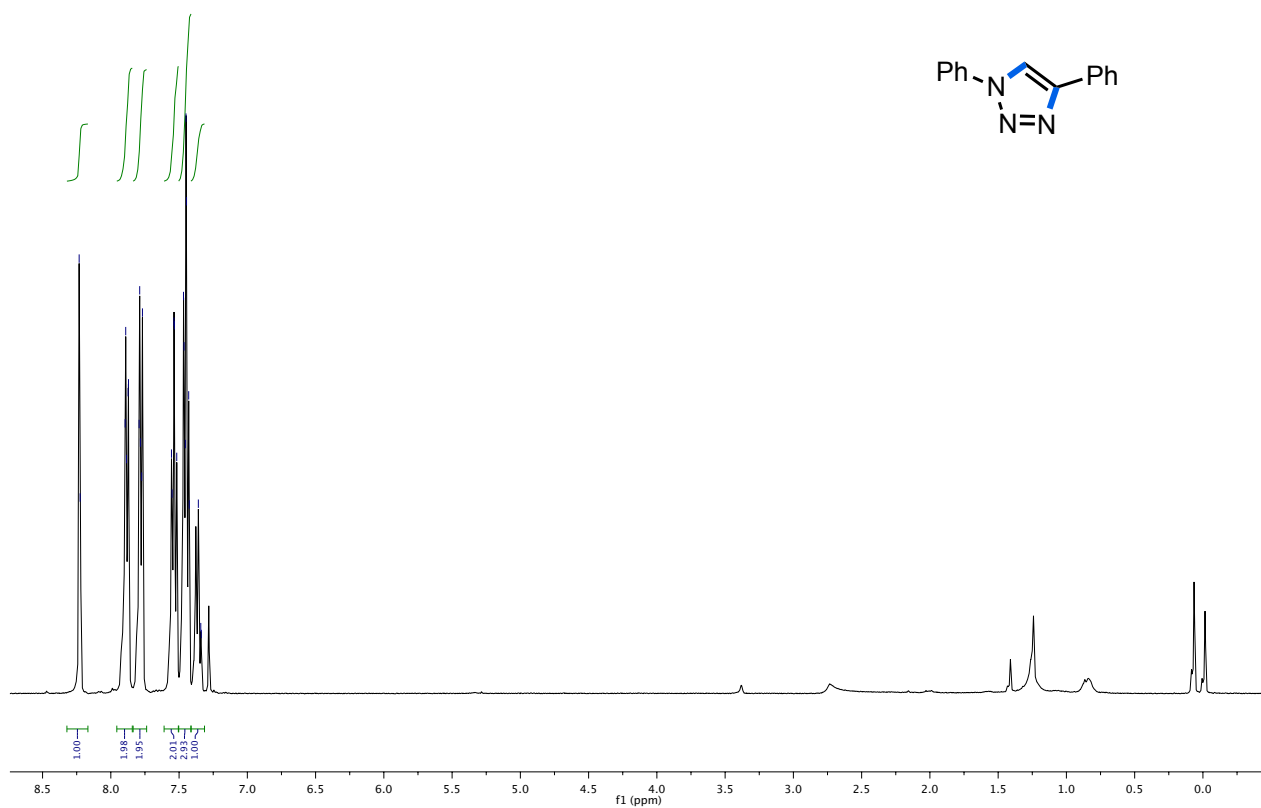
^1H NMR (500 MHz) (top) and ^{13}C NMR (100 MHz) (bottom) spectra in CDCl_3 for **21a**

^1H NMR (500 MHz) (top) and ^{13}C NMR (125 MHz) (bottom) spectra in CDCl_3 for **22a**

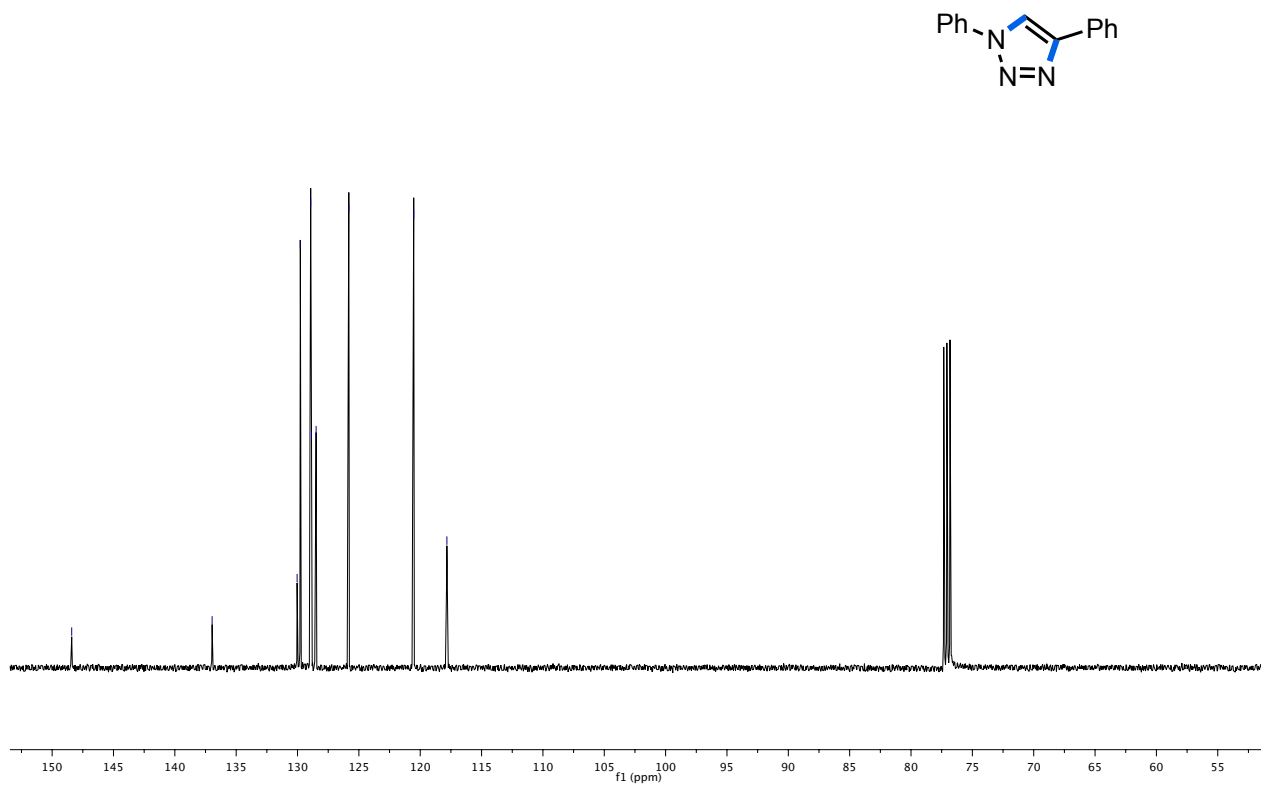


^1H NMR (400 MHz) (top) and ^{13}C NMR (125 MHz) (bottom) spectra in CDCl_3 for **13b**

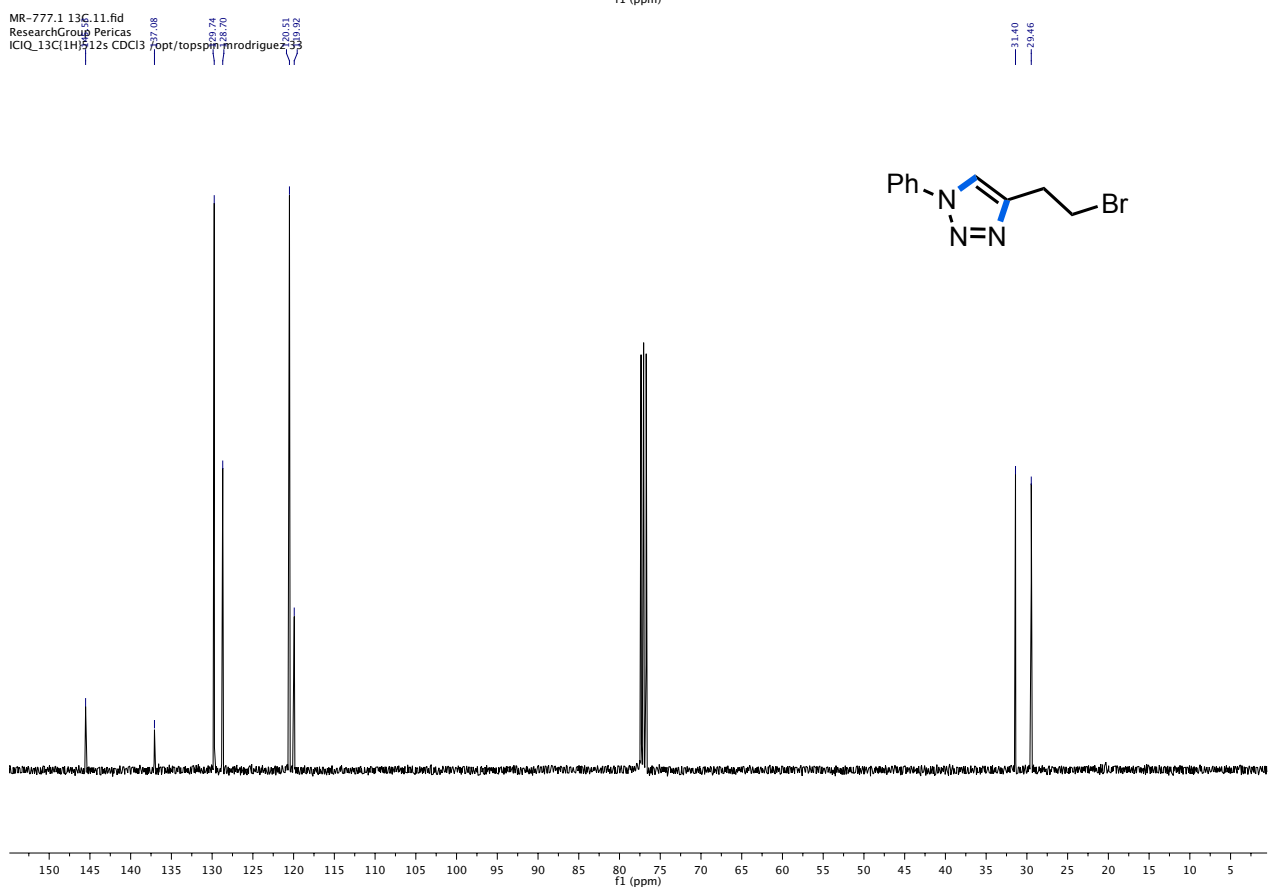
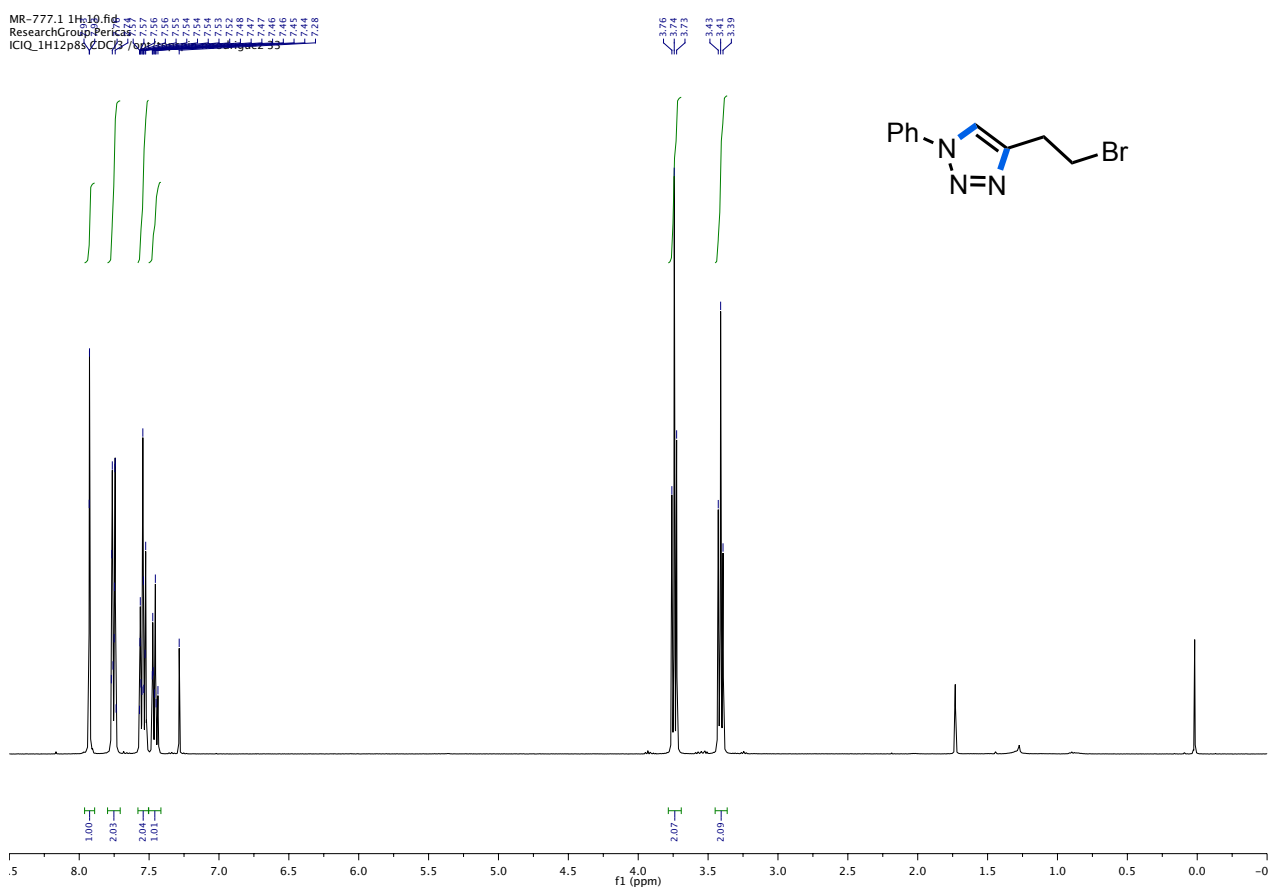
MR-776.1 1H.10.fid
ResearchGroup Pericas
ICIQ_1H12p5s CDCl3 /opt/topspin mrodrigue

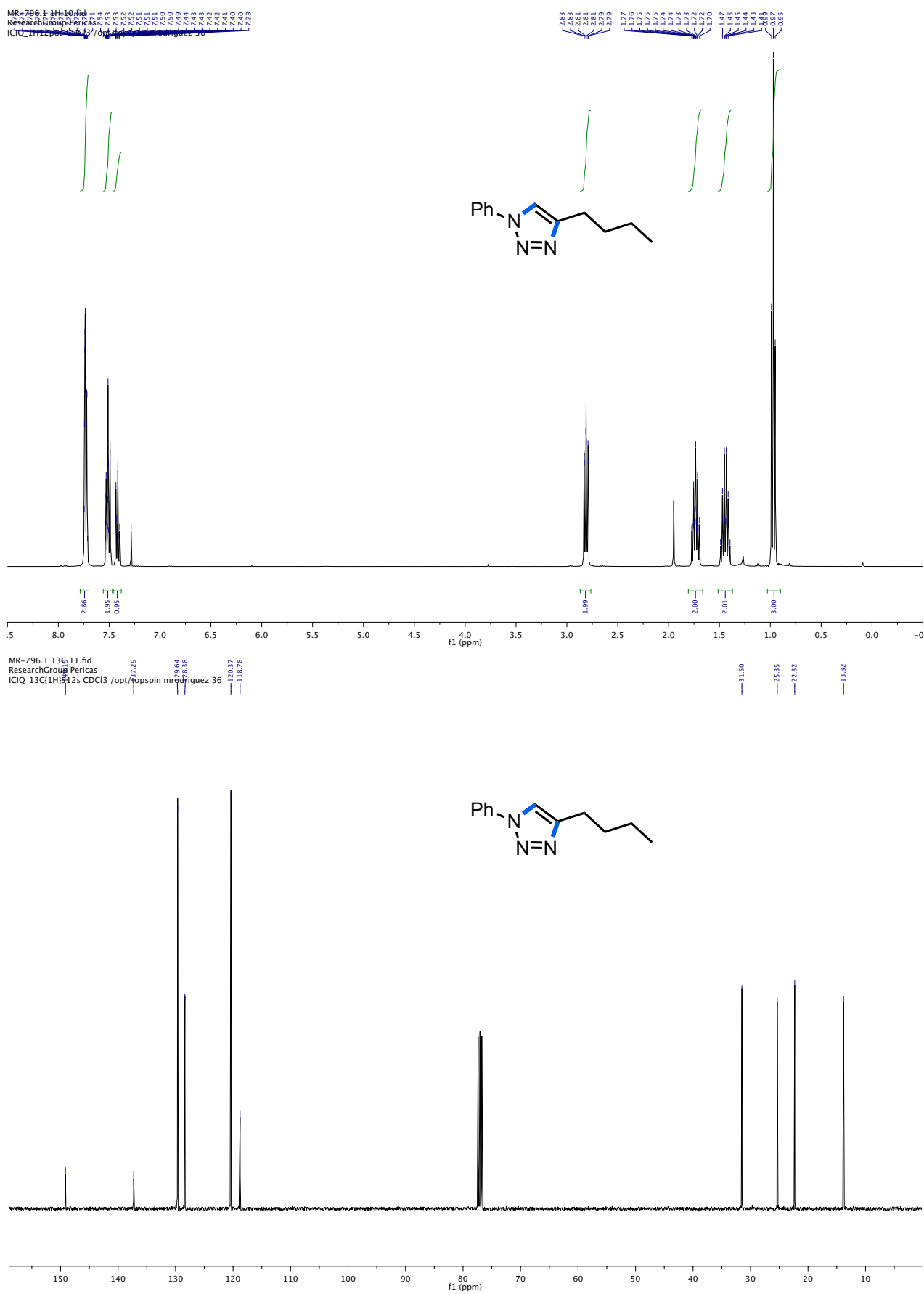


MR-776.1 13C.10.fid
ResearchGroup Pericas
ICIQ_13C13H512s CDCl3 /opt/topspin mrodrigue

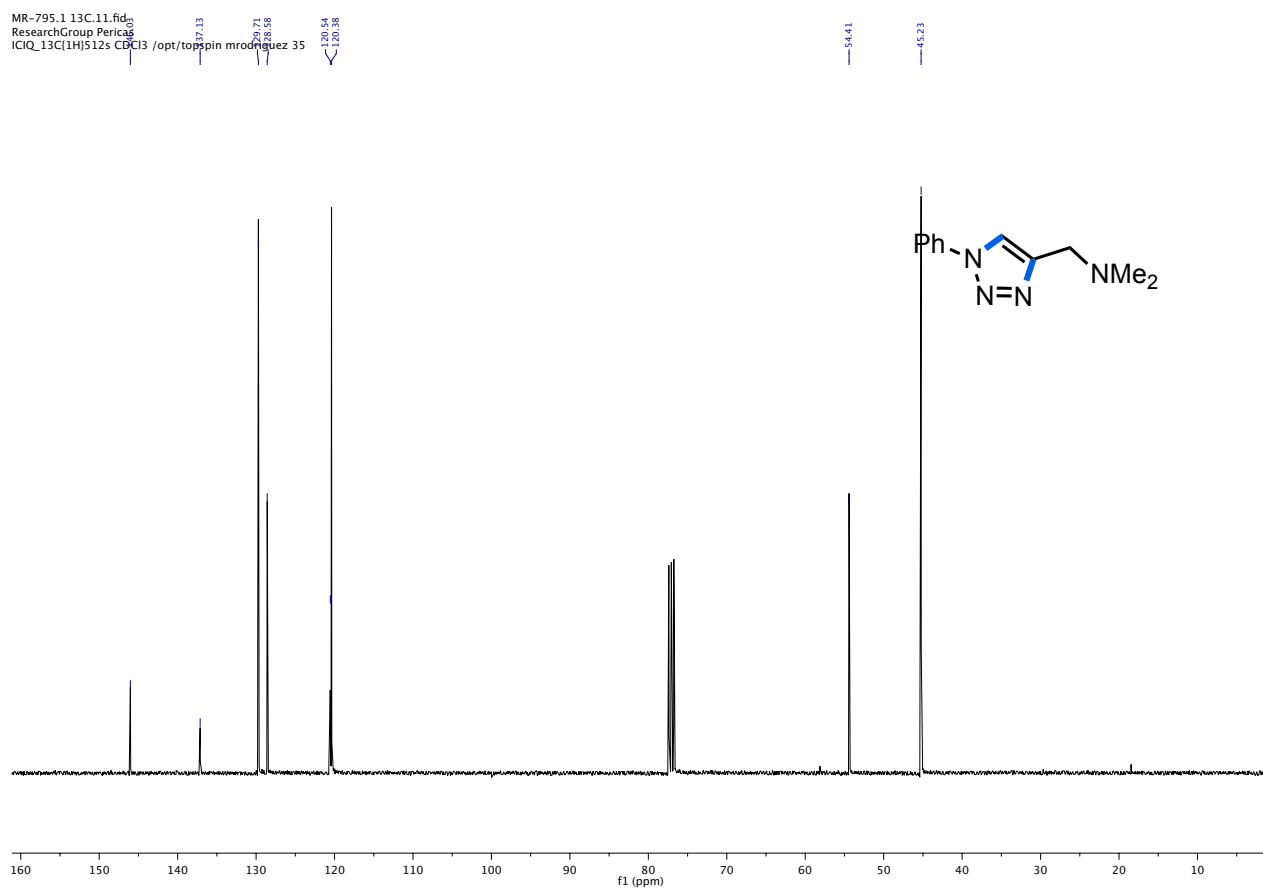
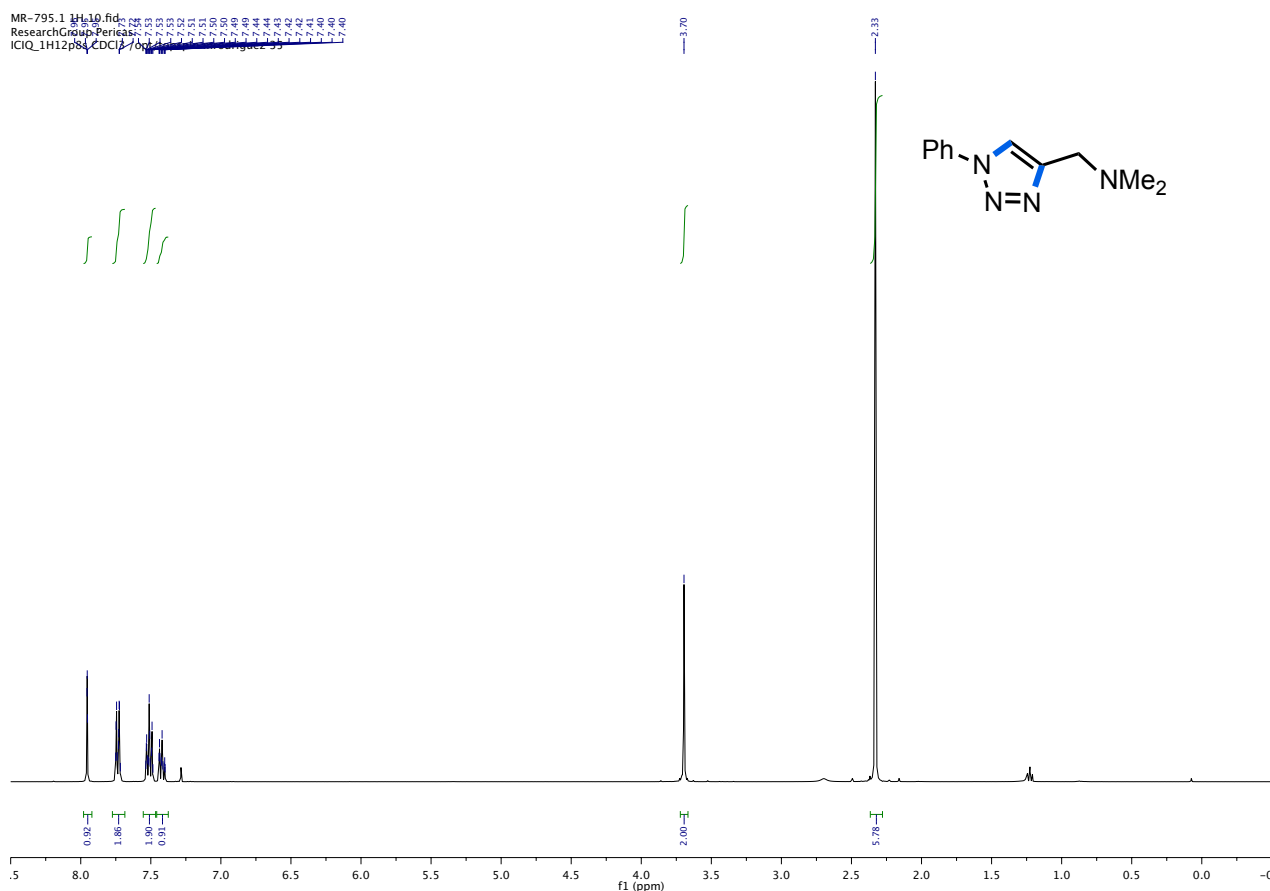


^1H NMR (400 MHz) (top) and ^{13}C NMR (100 MHz) (bottom) spectra in CDCl_3 for **5b**



^1H NMR (400 MHz) (top) and ^{13}C NMR (100 MHz) (bottom) spectra in CDCl_3 for **19b**

^1H NMR (400 MHz) (top) and ^{13}C NMR (100 MHz) (bottom) spectra in CDCl_3 for **22b**



3.6.6 Published paper



DOI: 10.1002/chem.201604048

CHEMISTRY
 A European Journal
 Full Paper

Copper Nanoparticles
Key Non-Metal Ingredients for Cu-catalyzed “Click” Reactions in Glycerol: Nanoparticles as Efficient Forwarders

 Marta Rodríguez-Rodríguez,^[a, b] Patricia Llanes,^[b] Christian Pradel,^[a] Miquel A. Pericàs,^{*,[b]} and Montserrat Gómez^{*,[a]}

Abstract: The effect of long-alkyl-chain amines in Cu^I-assisted azide–alkyne cycloadditions of terminal alkynes with organic azides in glycerol and other environmentally benign solvents (water, ethanol) has been examined. The presence of these additives favors the in situ formation of Cu^I-based nanoparticles and results in an increase of the catalytic reactivity. In glycerol, liquid-phase transmission electron micros-

copy (TEM) analyses, enabled by the negligible vapor pressure of this solvent, proved that Cu^I nanoparticles are responsible for the observed catalytic activity. The wide variety of alkynes and azides of which this effect has been investigated (14 combinations) confirms the role played by these additives in Cu-catalyzed Huisgen cycloadditions.

Introduction

Copper-catalyzed azide–alkyne cycloaddition (CuAAC) reactions represent a successful method for the synthesis of 1,2,3-triazoles,^[1] as indicated by the thousands of works published in this field,^[2a] including enantioselective CuAAC transformations.^[2b,c] This remarkable success is mainly due to the process versatility in terms of solvent compatibility, copper sources (salts, well-defined complexes, preformed nanoparticles, (un)-supported systems), functional group tolerance, and energy supplies (conventional heating, microwave activation) among others. However, this hands-on behavior leads to some concerns with regard to understanding (“who does what”), associated with the lack of conclusive studies in relation to CuAAC mechanism(s),^[3] in particular for in situ generated systems using Cu^I starting materials. The most frequently used precursors, copper halides, are quite insoluble in the common organic solvents, especially CuI.^[4] The presence of any additive (impurity) can improve the solubility of copper species in the medium, inducing then an increase of catalytic activity. In this context, organic bases play a decisive task, favoring both the coordination to metal (as Lewis bases) and the formation of active intermediates such as copper acetylides. Polydentate ni-

trogen-based ligands have been proved as particularly efficient copper partners, stabilizing Cu^I species^[5] and enhancing the rate of CuAAC processes.^[6] In this area, Cu^I complexes containing tris-(triazolyl)methane tripodal ligands, which are highly proficient in CuAAC reactions,^[11,7] represent an elegant approach to illustrate the role of Lewis bases (Figure 1). These ligands can efficiently stabilize catalytic precursors (I) and also intermediates acting as hemi-labile scaffolds (II), which generates vacant sites for the coordination of reagents.

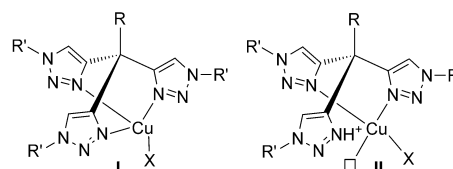


Figure 1. Tris(triazolyl)methane ligands for Cu^I-catalyzed AAC.^[11,7] Small square denotes vacant site on copper.

In agreement with these important, ancillary tasks, base-free catalytic CuAAC systems using Cu^I complexes as copper source are rare. To the best of our knowledge, only one recent publication by García-Alvarez and Vidal reports on a Cu^I system able to catalyze CuAAC reactions in glycerol in the absence of any added base.^[8]

Following our work on the use of glycerol as a solvent in metal-catalyzed processes^[9] and more recently in metal-free AAC for the synthesis of fully substituted 1,2,3-triazoles,^[10] in which the activation of both alkynes and benzylazide by glycerol was proved, we planned to evaluate the activity of Cu^I salts towards click reactions in this solvent, with the aim of un-

[a] M. Rodríguez-Rodríguez, C. Pradel, Prof. M. Gómez
 Laboratoire Hétérochimie Fondamentale et Appliquée (LHFA)
 UPS and CNRS UMR 5069
 Université de Toulouse
 118, route de Narbonne, 31062 Toulouse cedex 9 (France)
 E-mail: gomez@chimie.ups-tlse.fr

[b] M. Rodríguez-Rodríguez, Dr. P. Llanes, Prof. M. A. Pericàs
 Institute of Chemical Research of Catalonia (ICIQ)
 The Barcelona Institute of Science and Technology
 Avda. Països Catalans, 16, 43007 Tarragona (Spain)
 E-mail: mapericas@iciq.es

Supporting information for this article can be found under <http://dx.doi.org/10.1002/chem.201604048>.

Understanding the role of added exogenous base in glycerol medium.

Results and Discussion

We selected the cycloaddition between phenylacetylene and benzyl azide as the benchmark reaction, using CuI as catalyst source in neat glycerol at room temperature (Scheme of Table 1). The reaction did not work at all at short reaction times (1.5 h), 84% conversion being achieved after 24 h (entry 1, Table 1). In the course of our research, the high efficiency of this methodology under exactly the same "base-free" reaction conditions was reported, triazole **1a** being isolated by these authors in 94% yield in short reaction times.^[8] This serious discrepancy between independent runs of an easy-to-perform process, almost fulfilling the requirements in the Cornforth definition of an "ideal chemical process"^[11] led us to think that some uncontrolled factor was operating. Given the practical importance of azide-alkyne cycloadditions, we decided to deeply characterize the different components involved in the process in an attempt to rationalize this behavior.^[12] This analytical study showed that the success of the reaction depended on the quality (source) of BnN₃ (entries 2–4, Table 1) and that, rather surprisingly, high-purity samples of azide were unreactive. In fact only one commercially available lot of BnN₃ favored the cycloaddition (entry 2, Table 1).

Table 1. Azide-alkyne cycloaddition of phenylacetylene and benzyl azide in the presence of CuI.^[a]

Entry	Bn-N ₃ Source/Batch code ^[b]	Conv. (yield) [%] ^[c]
1 ^[d]	Home-made	< 5 84 (69) ^[e]
2	Alfa-Aesar/C252013 ^[f]	100 (80)
3	Alfa-Aesar/AE040501	< 5
4	Aldrich/BCBL4667V	< 5

[a] Reaction conditions: CuI (1 mol%), benzyl azide (0.5 mmol), and phenylacetylene (0.5 mmol) in glycerol (0.5 mL) at 25 °C for 1.5 h. Triazole **1a** was not obtained in the absence of copper (18% conversion, < 5% yield for **1a**); [b] for certificates of analyses, see the Supporting Information; [c] determined by ¹H NMR analysis using 2-methoxynaphthalene as internal standard; conversions based on BnN₃; [d] for BnN₃ synthesis, see ref. [24]; [e] in italics, data after 24 h reaction; [f] data coming from two different commercial flasks.

We analyzed the "active" BnN₃ by GC-MS and NMR (Figures S1–S3 in the Supporting Information). In contrast to the other BnN₃ samples (Figures S4–S9 in the Supporting Information), this one was contaminated by some compounds that, according to MS, appeared to correspond to amines containing long alkyl chains. To test the possible catalytic effect of these impurities, we carried out the cycloaddition in the presence of amines using high purity, home-made BnN₃ (Table 2). We ob-

Table 2. Azide-alkyne cycloaddition of phenylacetylene and the corresponding azide in the presence of CuI and amine.^[a,b]

Entry	Azide	Amine	Product, Conv. (yield) [%] ^[b]
1	a	NH ₂ (octyl)	1a , 96 (93) 52 (44) ^[c]
2	a	NH ₂ (undecyl)	1a , 96 (93)
3	a	Oleylamine	1a , 100 (> 99) 98 (94) ^[c] Run 4: 100 (85) ^[d]
4	a	NH(octyl) ₂	1a , 100 (96) 95 (88) ^[c]
5	a	N(octyl) ₃	1a , 96 (88) 97 (73) ^[c]
6	a	NEt ₃	1a , 28 (16)
7	a	NET(iPr) ₂	1a , 36 (6)
8	a	TOMACl	1a , 37 (19)
9 ^[e]	a	Aliquat [®] 336	1a , 20 (< 5)
10	a	TMEDA	1a , 83 (70)
11	a	EN	1a , 30 (12)
12	a	o-PDA	1a , 30 (10)
13	a	PHEN	1a , 15 (6)
14	a	Urotropine	1a , 20 (< 5)
15	a	2,6-lutidine	1a , 34(26)
16	b	–	1b , < 5
17	b	NH ₂ (octyl)	1b , 100 (94) 39 (9) ^[c]
18	b	Oleylamine	1b , 100 (98) 100 (87) ^[c]
19	b	NH(octyl) ₂	1b , 83 (89) 88 (87) ^[c]
20	b	N(octyl) ₃	1b , 88 (88) 100 (12) ^[c]
21	b	NEt ₃	1b , 10 (6)
22	b	TMEDA	1b , 70 (76)
23	b	EN	1b , 21 (19)
24	b	Urotropine	1b , < 5

[a] Reaction conditions: CuI (1 mol%), amine (5 mol%), benzyl or phenyl azide (0.5 mmol), and phenylacetylene (0.5 mmol) in glycerol (0.5 mL) at 25 °C for 1.5 h; [b] determined by ¹H NMR analysis using 2-methoxynaphthalene or 1,3,5-trimethoxybenzene as internal standard; conversions based on BnN₃; [c] in italics, conversion (yield) using 1 mol% of amine; [d] see Figure S10 in the Supporting Information for the recycling of the catalytic phase; [e] Aliquat[®] 336: Ammonium salts containing a mixture of C₈ and C₁₀ alkyl chains with C₈ predominating.

served that when 5 mol% of amine with respect to benzyl azide was used, primary (entries 1–3), secondary (entry 4), and tertiary (entry 5) long-alkyl-chain-based mono-amines led to high yields of the corresponding 1,2,3-triazole **1a**. For short-alkyl-chain derivatives, such as triethylamine or diisopropyl-

thylamine, low yields were achieved (<16%, entries 6 and 7, Table 2). When the amount of added amine decreased (1 mol%), the reaction also worked (entries 1 and 3–5), especially for oleylamine, dioctyl, and trioctyl amine (entries 3–5). Ammonium salts, such as trioctylmethylammonium chloride (TOMACl) and Aliquat[®]336 (ammonium salt containing a mixture of C8 and C10 alkyl chains, often used as a metal extraction reagent^[13]), did not favor the cycloaddition (entries 8 and 9).

Dinitrogenated (EN=ethylenediamine; *o*-PDA=ortho-phenylenediamine and PHEN=phenantroline, entries 11–13, Table 2) and tetranitrogenated (urotropine, entry 14) ligands did not trigger a positive outcome (yields <12%). TMEDA (tetramethylethylenediamine) was an exception to this behavior (70% yield, entry 10). The use of 2,6-lutidine, known by its performance in CuAAC in aqueous medium,^[14] gave a very low yield (entry 15).

The same trend could be found when phenyl azide was used instead of benzyl azide (entries 16–24, Table 2): the system was inactive in the absence of an added amine (entry 16). However, high yields could be isolated in the presence of amines containing a long alkyl chain (up to 94%, entries 17–20). For “light” amines (entries 21–24,), only the Cu/TMEDA system was active, as previously observed with BnN₃ (entries 10 and 22, Table 2).

Furthermore, this “super” amine effect was examined in other polar solvents, such as water, ethanol, or 1,4-dioxane. Under the same conditions as described above, the behavior was comparable to that observed in glycerol. Without any additive or in the presence of NEt₃, low yields were obtained (<13%, entries 1–6, Table 3). However, in the presence of dioctylamine (entries 7–9) or oleylamine (entries 10–12), the increase of catalytic activity was clearly apparent.

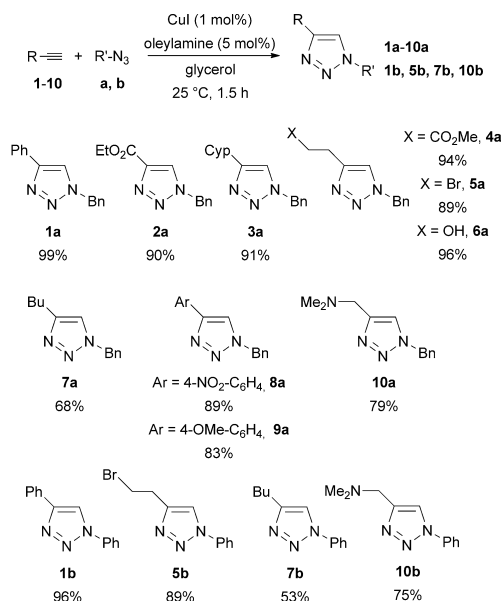
It is important to mention that the catalytic phase could be recycled up to four times without significant loss of efficiency (entry 3, Table 2; see Figure S10 in the Supporting Information), showing the ability of glycerol to immobilize the catalyst. The dramatic effect observed after the fourth run is undoubtedly related to the leaching of copper (more than 1000 ppm determined by ICP-MS).

With these results in hand, a representative set of Cu-catalyzed azide-alkyne cycloadditions involving the use of different alkynes (1–10) and organo-azides (a, b) (Scheme 1) was carried out in the presence of oleylamine. The corresponding triazoles were obtained in high to quantitative yield. Even those triazoles bearing alkyl substituents at C-4 (3a, 7a, 7b) were obtained in moderate to high yields (53–91%). No transesterification reactions with glycerol were detected for alkynes containing ester groups (2a, 4a). For selected triazoles, the reactions were also carried out in the absence of added amine, as control experiments. In all cases, low yields (<25%, see Table S1 in the Supporting Information) were recorded even at longer times (up to 7 h). Unfortunately, this catalytic system, working under favorable conditions, was not active using internal alkynes, such as diphenylacetylene, methyl phenylpropiolate, or 1-iodo-2-phenylacetylene (Figure S11 in the Supporting Information).

Table 3. Azide-alkyne cycloaddition of phenylacetylene and benzyl azide in the presence of CuI and amine.^[a]

Entry	Solvent	Amine	Conv. (yield) [%] ^[b]
1	H ₂ O	–	22 (13)
2	EtOH	–	12 (<5)
3	Dioxane	–	11 (<5)
4	H ₂ O	NEt ₃	15 (<5)
5	EtOH	NEt ₃	17 (<5)
6	Dioxane	NEt ₃	24 (11)
7	H ₂ O	NH(octyl) ₂	100 (93)
8	EtOH	NH(octyl) ₂	66 (48)
9	Dioxane	NH(octyl) ₂	100 (99)
10	H ₂ O	Oleylamine	99 (94)
11	EtOH	Oleylamine	59 (48)
12	Dioxane	Oleylamine	94 (81)

[a] Reaction conditions: CuI (1 mol%), amine (5 mol%), benzyl azide (0.5 mmol), and phenylacetylene (0.5 mmol) in the appropriate solvent (0.5 mL) at 25 °C for 1.5 h; [b] determined by ¹H NMR analysis using 2-methoxynaphthalene or 1,3,5-trimethoxybenzene as internal standard; conversions based on BnN₃.



Scheme 1. Scope of azide-alkyne cycloaddition catalyzed by CuI/amine system in glycerol. Figures indicate isolated yields.

With the aim of understanding the observed reactivity, we analyzed the structural behavior of copper salts. From a coordination point of view, the CuI motif leads to a large variety of structures corresponding to both discrete molecular com-

plexes^[15] and polymeric networks,^[16] depending on the nature of the ligands involved and also the reaction conditions. This structural variety is especially remarkable when N-based ligands are involved,^[17] in particular for diamines (EN, TMEDA, PHEN) and short-alkyl-chain tertiary amines (NEt₃, NEtPr₂) like those used in this work.^[18] Some of them give complex structures based on closed-cubane "Cu₄I₄" tetramers;^[18a,19] we could prove this trend by the X-ray diffraction analysis of the Cu₄I₄-TMEDA system (Figures S12 and S13 in the Supporting Information).^[20]

In contrast, long-alkyl-chain amines favor the stabilization of metal (and metal oxide) nanoparticles.^[21] Presuming the formation of copper-based nanoclusters under our reaction conditions,^[22] TEM analyses of CuI in glycerol and in the presence of different amines were carried out (Table S2 in the Supporting Information). Actually, the formation of well-dispersed nanoparticles was observed in the presence of long-alkyl-chain amines, including ammonium derivatives (Figure 2). HR-TEM and EDX analyses of a CuI/dioctylamine mixture in glycerol confirmed the Cu^I nature of the nanoparticles and the presence of the amine on the nanoparticle surface (Figure S14 in the Supporting Information). It is worth noting that ammonium salts such as TOMACI and Aliquat[®]336 did not lead to catalytically active systems, although the formation of well-dispersed nanoparticles was also observed. The lack of catalytic activity in these last cases is probably due to the very strong electrostatic interaction between the ionic ligands and the nanoparticles: As a result, Cu^I-based nanoparticles are tightly surrounded by anion/cation shells, and this leads to small and well-dispersed particles. However, this stabilizing interaction shields the surface of the nanoparticles and prevents the requisite approach of the reactants to the catalytic copper centers. In contrast, hemi-labile amine ligands, while still preventing particle agglomeration by steric shielding, can be easily detached, leading to free coordination sites on copper that are necessary for the reaction to proceed.^[23]

Interestingly, the presence of additional ionic compounds in the reaction medium was shown to influence the course of the reaction as well. Thus, when an equimolar mixture of Aliquat[®]336 and a sodium salt (NaOAc or NaN₃) was added to the non-productive reaction mixture, the system turned active (Figure 3). TEM analyses of CuI in glycerol in the presence of

both Aliquat[®]336 and sodium salt evidenced the formation of micelle-like arrangements, giving high local density of copper and therefore favoring the reactivity. This effect can especially be observed in the case of the mixture Aliquat[®]336/NaOAc, where cylindrical micelles were identified, containing the copper species at the surface (accessible to the reagents) and the more hydrophobic constituents (ammonium alkyl species) probably placed inside of these nano-objects. A similar trend could be observed using TOMACI/NaN₃ (Figure S15 in the Supporting Information). It is important to note that CuI/NaN₃ and CuI/NaOAc systems (in the absence of any nitrogen-based ligand) were not active. In addition, this reactivity behavior points to the feasibility of CuAAC by a one-pot three-component approach. Actually, with Bn-Br, NaN₃ and phenylacetylene as starting materials, **1a** was isolated in 90% yield (see Scheme S1 in the Supporting Information)

Correlating reactivity and structure, it seems that the formation of nanoparticles favors the catalytic process, which points to a beneficial (cooperative) effect between neighboring Cu^I centers for the activation of both azide and alkyne reactants during the cycloaddition, as already noted in our previous work involving the use of Cu₂O nanoparticles as catalytic precursors in glycerol medium.^[9a]

In fact, for short-chain alkyl amines such as DIPEA (DIPEA = *N,N*-diisopropylethylamine), ethylenediamine, or urotropine, agglomerates similar to those observed for CuI in the absence of any additive were formed (Table S2 in the Supporting Information), affording inactive catalytic systems (Table 2). Only CuI/TMEDA led to the simultaneous formation of nanoparticles and agglomerates. As we have already mentioned, this system depicted high catalytic activity in azide-alkyne cycloadditions (entries 10 and 22, Table 2).

We were also interested in establishing the oxidation state of copper involved in the active species. For that, we reused the catalytic phase corresponding to the active CuI/dioctylamine system (after reaction between phenylacetylene and benzyl azide). TEM analysis after catalysis showed smaller nanoparticles than before (ca. 1.4 nm (after) vs. 2.1 nm (before); Table S2 in the Supporting Information); the catalytic phase was then much less active (33% in the second run versus 100% in the first one). HR-TEM coupled to an electronic diffraction analysis showed that particles after the first catalytic

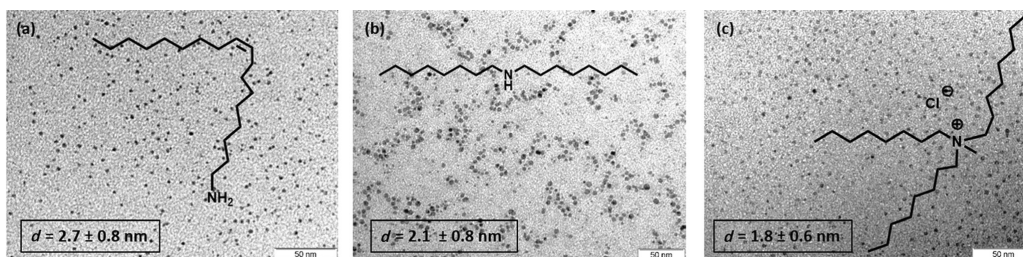


Figure 2. TEM images for CuI-based systems containing oleylamine (a), dioctylamine (b), and TOMACI (trioctylmethylammonium chloride) (c) in glycerol. Scale bars = 50 nm.

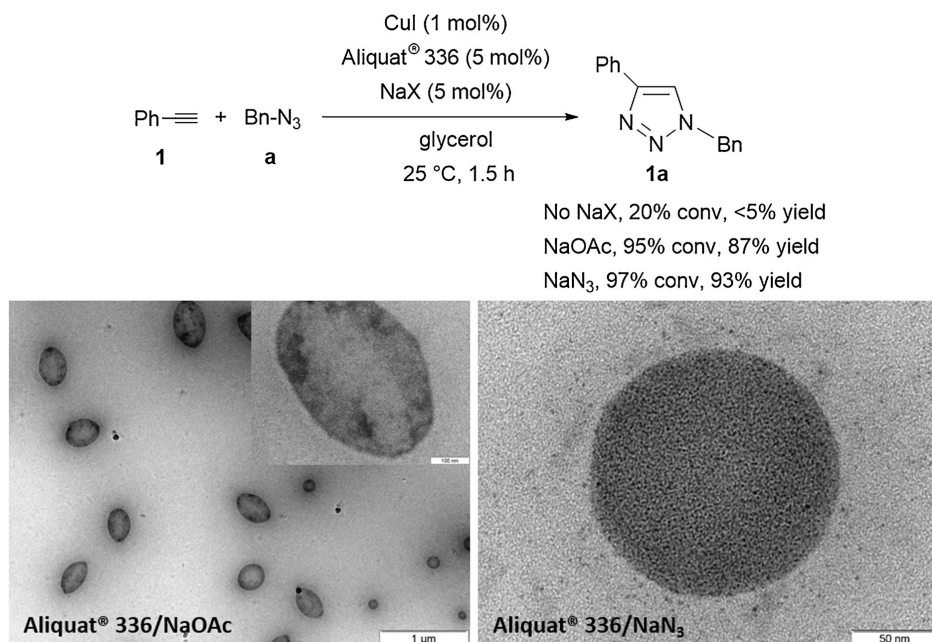


Figure 3. Effect of the salts in azide-alkyne cycloaddition. TEM images corresponding to the mixtures of CuI, Aliquat[®] 336, and NaX (1/5/5 ratio, respectively): NaOAc (left; scale bar = 1 μm, inset scale bar = 100 nm), including an inserted image of one of the cylindrical micelle-like objects; NaN₃ (right; scale bar = 50 nm).

run consisted of Cu⁰ (Figure S16 in the Supporting Information). This indicated to us that the initially formed Cu^I-rich nanoparticles suffer reductive deactivation as a concomitant off-cycle of the CuAAC reaction. In contrast, the reutilization of the CuI/oleylamine system gave the same activity as for the first run (for both cases, nearly full conversion). HR-TEM/electronic diffraction analysis proved that in this case, nanoparticles were mainly formed by Cu^I after catalysis (Figure S17 in the Supporting Information). In addition, XPS analysis evidenced the absence of Cu^{II} species after reaction (absence of the corresponding strong satellites, see Figure S18 in the Supporting Information). These data point to Cu^I-based nanoparticles as being responsible for the observed reactivity.

Conclusions

In this work, we could prove the key role of “impurities” randomly present in commercial samples of benzyl azide. Its accurate analyses led us to identify them (long-alkyl chain amines) and to examine their impact on CuI-based catalytic systems applied in azide-alkyne cycloadditions in different solvents. As a practical result of this study, we have been able to establish that the addition of small amounts (5 mol%) of primary, secondary, or tertiary amines containing C₈, C₁₁, or C₁₈ carbon chains (CuI/amine ratio = 1/1 or 1/5) secures the success in the syn-

thesis of 1,4-disubstituted 1,2,3-triazoles under mild reaction conditions (low metal loading of 1 mol%, short time of 1.5 h, and room temperature), in environmentally benign glycerol. As a consequence, a warning should be made on experimental procedures for the CuAAC reaction in polar solvents not involving the use of appropriate amines: Their success or failure strongly depends on the presence/absence of amine-type impurities in the employed azide. The use of glycerol as a non-volatile solvent enabled the (HR)TEM analysis of solutions constituted by CuI and amine, before and after catalysis. It could be learned from these studies that CuI, in the presence of long-alkyl-chain amines in glycerol at room temperature, gives rise to the formation of small and well-dispersed Cu^I nanoparticles, in contrast with the agglomerates formed from either bulk CuI or mixtures of CuI with low-weight amines. It is important to mention that the presence of ammonium salts mainly containing C₈ chains (TOMACI, Aliquat[®] 336) did not provide an efficient catalytic system in spite of the formation of well-dispersed nanoparticles. This was almost certainly caused by the stabilization of CuI nanoparticles by electrostatic effect, thus blocking the access of reagents to the Cu^I centers. However, tuning the ionic species present in the reaction medium, the catalytic system turned active through the formation of organized systems.

Altogether, this study led us to establish a correlation between the in situ formation of Cu^I nanoparticles in glycerol and other polar solvents and their catalytic activity. These nano-objects, generated due to the presence of long-alkyl-chain amines, favor the activation of both reagents, alkyne and azide partners, by cooperative effect between neighboring Cu^I centers.

The inconsistencies found working under the “same” conditions induce the desire to understand and discover new issues for known reactions. The use of controlled-quality compounds (reagents, catalysts, solvents) permits a dramatic reduction of these effects, establishing reproducible and sustainable protocols.

Experimental Section

General procedure for the azide-alkyne cycloaddition

CuI (0.9 mg, 0.005 mmol) and the corresponding amine (0.005–0.25 mmol) were added to glycerol (0.5 mL) in a Schlenk tube equipped with a stirring bar under Ar atmosphere. The alkyne (0.5 mmol) and the azide (0.5 mmol, 67 mg for BnN₃^[24] and 60 mg for PhN₃) were added consecutively to the reaction medium. The mixture was stirred at 25 °C for 1.5 h (or the stated time). The organic products were extracted from the catalytic mixture with dichloromethane (6 × 2 mL). The combined chlorinated organic layers were filtered through a Celite® pad and the resulting filtrate was concentrated under reduced pressure. The products were purified by chromatography (silica gel short column, eluent: cyclohexane/ethyl acetate) in order to determine the isolated yields of the corresponding triazoles.

Acknowledgements

Financial support from the Centre National de la Recherche Scientifique (CNRS), the Université de Toulouse 3—Paul Sabatier, MINECO (grants CTQ2012-38594-C02-01 and CTQ2015-69136-R), DEC (grant 2014SGR827) and ICIQ Foundation are gratefully acknowledged. S. Ladeira and R. Brousses are acknowledged for the resolution of the XRD structure. M.R. thanks the CNRS and MINECO (CTQ2012-38594-C02-01) for a PhD grant.

Keywords: azide-alkyne cycloaddition · copper · glycerol · long-chain amines · nanoparticles

- [1] For selected reviews, see: a) J. E. Hein, V. V. Fokin, *Chem. Soc. Rev.* **2010**, *39*, 1302–1315; b) S. Díez-González, *Catal. Sci. Technol.* **2011**, *1*, 166–178; c) F. Alonso, Y. Moglie, G. Radivoy, *Acc. Chem. Res.* **2015**, *48*, 2516–2528; d) E. Haldón, M. C. Nicasio, P. J. Pérez, *Org. Biomol. Chem.* **2015**, *13*, 9528–9550; e) S. Chassaing, V. Bénétreau, P. Pale, *Catal. Sci. Technol.* **2016**, *6*, 923–957; f) P. Etayo, C. Ayats, M. A. Pericàs, *Chem. Commun.* **2016**, *52*, 1997–2010.
- [2] a) More than 3400 references from SciFinder Scholar Database up to March 2016 (search containing “copper and azide alkyne cycloaddition” keywords); for selected recent asymmetric CuAAC contributions, see: b) T. Song, L. Li, W. Zhou, Z.-J. Zheng, Y. Deng, Z. Xu, L.-W. Xu, *Chem. Eur. J.* **2015**, *21*, 554–558; c) F. Zhou, C. Tan, J. Tang, Y.-Y. Zhang, W.-M. Gao, H.-H. Wu, Y.-H. Yu, J. Zhou, *J. Am. Chem. Soc.* **2013**, *135*, 10994–10997.
- [3] a) L. Jin, D. R. Tolentino, M. Melaimi, G. Bertrand, *Sci. Adv.* **2015**, *1*, e1500304; b) S. Calvo-Losada, M. S. Pino-González, J. J. Quirante, *J. Phys. Chem. B* **2015**, *119*, 1243–1258; c) R. Berg, B. F. Straub, *Beilstein J. Org. Chem.* **2013**, *9*, 2715–2750; d) D. Astruc, L. Liang, A. Rapakousiou, J. Ruiz, *Acc. Chem. Res.* **2012**, *45*, 630–640; e) M. Meldal, C. W. Tornøe, *Chem. Rev.* **2008**, *108*, 2952–3015; f) C. Wang, D. Ikhlef, S. Kahlal, J.-V. Saillard, D. Astruc, *Coord. Chem. Rev.* **2016**, *316*, 1–20.
- [4] Solubility product constants for CuX: CuCl, 1.72×10^{-7} ; CuBr, 6.27×10^{-9} ; CuI, 1.27×10^{-12} ; data from: *CRC Handbook of Chemistry and Physics*, 90th ed. (Ed.: D. R. Lide), **2009–2010**, CRC Press, Boca Raton.
- [5] a) T. R. Chan, R. Hilgraf, K. B. Sharpless, V. V. Fokin, *Org. Lett.* **2004**, *6*, 2853–2855; b) W. G. Lewis, F. G. Magallon, V. V. Fokin, M. G. Finn, *J. Am. Chem. Soc.* **2004**, *126*, 9152–9153.
- [6] a) V. O. Rodionov, S. I. Presolski, D. Díaz Díaz, V. V. Fokin, M. G. Finn, *J. Am. Chem. Soc.* **2007**, *129*, 12705–12712; b) V. O. Rodionov, S. I. Presolski, S. Gardinier, Y.-H. Lim, M. G. Finn, *J. Am. Chem. Soc.* **2007**, *129*, 12696–12704; c) S. I. Presolski, V. Hong, S.-H. Cho, M. G. Finn, *J. Am. Chem. Soc.* **2010**, *132*, 14570–14576.
- [7] For selected contributions, see: a) S. Özçubukçu, E. Ozkal, C. Jimeno, M. A. Pericàs, *Org. Lett.* **2009**, *11*, 4680–4683; b) E. Ozkal, P. Llanes, F. Bravo, A. Ferrali, M. A. Pericàs, *Adv. Synth. Catal.* **2014**, *356*, 857–869.
- [8] C. Vidal, J. García-Alvarez, *Green Chem.* **2014**, *16*, 3515–3521.
- [9] a) F. Chahdoura, C. Pradel, M. Gómez, *ChemCatChem* **2014**, *6*, 2929–2936; b) F. Chahdoura, S. Mallet-Ladeira, M. Gómez, *Org. Chem. Front.* **2015**, *2*, 312–318; c) F. Chahdoura, I. Favier, C. Pradel, S. Mallet-Ladeira, M. Gómez, *Catal. Commun.* **2015**, *63*, 47–51; d) F. Chahdoura, I. Favier, M. Gómez, *Chem. Eur. J.* **2014**, *20*, 10884–10893; e) F. Chahdoura, C. Pradel, M. Gómez, *Adv. Synth. Catal.* **2013**, *355*, 3648–3660.
- [10] M. Rodríguez-Rodríguez, E. Gras, M. A. Pericàs, M. Gómez, *Chem. Eur. J.* **2015**, *21*, 18706–18710.
- [11] “It does, for example, no good to offer an elegant, difficult and expensive process to an industrial manufacturing chemist, whose ideal is something to be carried out in a disused bathtub by a one-armed man who cannot read, the product being collected continuously through the drain hole in 100% purity and yield”: J. Cornforth, *Chem. Br.* **1975**, *11*, 432.
- [12] Different glycerol sources and different commercially available CuI salts were tested without observing any effect on the reactivity.
- [13] For representative recent contributions, see: a) S. Sharma, C.-M. Wu, N. Rajesh, *RSC Adv.* **2016**, *6*, 26668–26678; b) S. S. Swain, B. Nayak, N. Devi, S. Das, N. Swain, *Hydrometallurgy* **2016**, *162*, 63–70.
- [14] a) J. García-Alvarez, J. Díez, J. Gimeno, *Green Chem.* **2010**, *12*, 2127–2130; b) J. García-Alvarez, J. Díez, J. Gimeno, F. J. Suárez, C. Vincent, *Eur. J. Inorg. Chem.* **2012**, 5854–5863.
- [15] For selected contributions, see: a) M. Vitale, P. C. Ford, *Coord. Chem. Rev.* **2001**, *219–221*, 3–16; b) F. De Angelis, S. Fantacci, A. Sgamellotti, E. Cariati, R. Ugo, P. C. Ford, *Inorg. Chem.* **2006**, *45*, 10576–10584.
- [16] For selected contributions, see: a) S. Kitagawa, R. Kitaura, S.-i. Noro, *Angew. Chem. Int. Ed.* **2004**, *43*, 2334–2375; *Angew. Chem.* **2004**, *116*, 2388–2430; b) G. Férey, *Chem. Soc. Rev.* **2008**, *37*, 191–214; c) A. J. Blake, N. R. Brooks, N. R. Champness, L. R. Hanton, P. Hubberstey, M. Schröder, *Pure Appl. Chem.* **1998**, *70*, 2351–2357.
- [17] a) R. Peng, M. Li, D. Li, *Coord. Chem. Rev.* **2010**, *254*, 1–18; b) S. Yuan, H. Wang, D.-X. Wang, H.-F. Lu, S.-Y. Feng, S. Sun, *CrystEngComm* **2013**, *15*, 7792–7802.
- [18] For selected contributions, see: a) X. Chai, S. Zhang, Y. Chen, Y. Sun, H. Zhang, X. Xu, *Inorg. Chem. Commun.* **2010**, *13*, 240–243; b) Y. Yang, W. Chai, L. Song, K. Shu, *Acta Crystallogr. Sect. E* **2010**, *66*, m1486; c) J.-H. Yu, J.-Q. Xu, L. Han, T.-G. Wang, Z. Shi, W.-J. Jing, H. Dong, J.-N. Xu, H.-B. Jia, J. Hua, *Chin. J. Chem.* **2002**, *20*, 851–857; d) M. F. Garbaskas, D. A. Haitko, J. S. Kasper, *J. Cryst. Spec. Res.* **1986**, *16*, 729–738; e) P. C. Healy, C. Pakawatchai, C. L. Raston, B. W. Skelton, A. H. White, *J. Chem. Soc. Dalton Trans.* **1983**, 1905–1916.
- [19] S. Zhang, Y. Cao, H. Zhang, X. Chai, Y. Chen, R. Sun, *J. Solid State Chem.* **2008**, *181*, 3327.
- [20] X-ray diffraction structure recently published: J.-J. Shen, J. Song, T.-L. Yu, Y.-L. Fu, *Chin. J. Struct. Chem.* **2014**, *33*, 1025–1030.
- [21] For selected contributions, see: a) C. Pan, K. Pelzer, K. Philippot, B. Chaudret, F. Dassenoy, P. Lecante, M.-J. Casanove, *J. Am. Chem. Soc.* **2001**, *123*, 7584–7593; b) G. Salas, C. C. Santini, K. Philippot, V. Collière, B. Chaudret, B. Fenet, P. F. Fazzini, *Dalton Trans.* **2011**, *40*, 4660–4668; c) J.

- Cure, Y. Coppel, T. Dammak, P. F. Fazzini, A. Mlayah, B. Chaudret, P. Fau, *Langmuir* **2015**, *31*, 1362–1367.
- [22] For recent contributions concerning Cu-based nanoparticles, see: a) M. B. Gawande, A. Goswami, F.-X. Felpin, T. Asefa, X. Huang, R. Silva, X. Zou, R. Zboril, R. S. Varma, *Chem. Rev.* **2016**, *116*, 3722–3811; b) H. R. Ong, M. M. R. Khan, R. Ramli, Y. Du, S. Xi, R. M. Yunus, *RSC Adv.* **2015**, *5*, 24544–24549.
- [23] For a selected review concerning the stabilization of metal nanoparticles, see: A. Roucoux, J. Schulz, H. Patin, *Chem. Rev.* **2002**, *102*, 3757–3778.
- [24] S. G. Alvarez, M. T. Alvarez, *Synthesis* **1997**, 413–414.

Received: August 25, 2016
Published online on October 28, 2016

Chapter 4

Preparation of new enantiopure PTA-based derivatives. Some applications in enantioselective catalysis

Chapter 4. Preparation of new enantiopure PTA-based derivatives. Some applications in enantioselective catalysis

4.1 Introduction

1,3,5-Triaza-7-phosphaadamantane (Figure 4.1), usually abbreviated as PTA, was first reported by Daigle *et al.* in 1974.^[1] Although this “cage-like” phosphine^[2] has been scarcely used since its discovery, the increasing interest in the replacement of the common organic solvents employed in chemical companies by water or others environmental friendly solvents has caused the renaissance of PTA.^[3] The main reason is its solubility in water ($S_{25^{\circ}\text{C}} = 1.5 \text{ mol.L}^{-1}$, *ca.* 235 g.L⁻¹);^[4] water-soluble phosphines like PTA are suitable ligands for the development of new catalysts adapted to aqueous media. These water-soluble catalysts combine, in a certain way, the advantages of homogeneous and heterogeneous systems, being useful in aqueous/biphasic catalysis where the catalyst can be retained in the aqueous phase and the organic products can be extracted from the reaction mixture using other organic solvents.

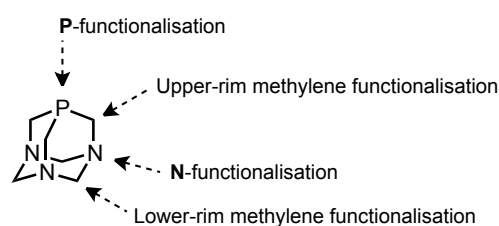


Figure 4.1 1,3,5-Triaza-7-phosphaadamantane (PTA), showing the sites to be functionalised

Apart from its solubility in water, another important property of PTA is its resistance to oxidation, which is more important than for other water-soluble phosphines like 3,3',3''-phosphanetriyltris(benzenesulfonic acid) trisodium salt (TPPTS). The reactivity of PTA is comparable to alkyl phosphines such as PMe_3 or PEt_3 , however it is stable when exposed to oxygen, whereas PMe_3 or PEt_3 are highly sensitive towards oxidation under air. Espenson *et al.*^[5] demonstrated that the rate constant of the oxidation of PTA by H_2O_2 using $[\text{ReO}_3(\text{CH}_3)]$ as catalyst is two orders of magnitude smaller than for PPh_3 . This behaviour might be attributed to the rigidity of the skeleton in the molecule (its cone angle is relatively small for an alkylphosphine, 103° (for comparison: 110° for PEt_3 ; 134° for PMe_3 ; 145° for PPh_3).^[3a] The rigidity of the PTA cage could make the lone electron pair of the phosphorus atom less accessible towards oxidation reagents.

PTA plays an important role in medicinal chemistry. Organometallic Ru(II)–arene complexes have shown promising results as anticancer agents, such as the $[(\text{RuCl}_2(\eta^6\text{-arene})(\text{PTA}))]$ family (abbreviated ruthenium(II)–arene–PTA or RAPTA, see Figure 4.2), developed by Dyson *et al.*^[6] The RAPTA compounds exhibit a piano-stool structure where three of the Ru coordination sites are occupied by a η^6 -coordinated arene ligand. Another coordination site is occupied by PTA ligand, which increases the solubility of the complexes in water, and the two remaining coordination sites usually occupied by labile chloro ligands that provide the opportunity for ligand exchange, generating vacant sites.

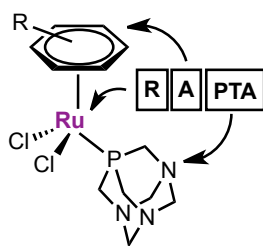


Figure 4.2 Generic structure of RAPTA anticancer agents.

In addition, the PTA structure can be modified, tuning its coordinative properties and in consequence offering other coordination modes. As indicated in Figure 4.1, this molecule can be functionalised at P and N atoms or at upper-rim or lower-rim methylene positions, maintaining the cage structure of PTA. In general, the “soft” P centre binds to low-valent transition metals, while protonation or alkylation occurs preferentially in the “hard” N atoms. The synthesis of *P*-alkylated PTA derivatives (Figure 4.3a) is done starting from phosphine sources such as PH_2R or $\text{P}(\text{CH}_2\text{OH})_3$.^[7] The basicity of PTA was determined by Darenbourg *et al.* ($\text{p}K_a$ of 5.70^[8]) and also by Fisher and Alyea *et al.* ($\text{p}K_a$ of 6.0.^[9]). In acidic aqueous solutions (pH lower than 6.5), PTA is *N*-protonated (Figure 4.3b), as expected considering the Lewis base character of the tertiary amino groups of PTA. Further *N*-protonation is thermodynamically less favourable due to the instability caused by the hybridization of nitrogen centres as well as by the destabilising electrostatic repulsion of two positive charges close within the same molecule, as proved by *ab initio* calculations.^[8a] PTA can be alkylated at N atoms (Figure 4.3c) by nucleophilic substitutions, using for instance MeI ^[10] or BnCl ^[9] as alkylating agents. Similar to the parent phosphine PTA, these quaternary ammonium derivatives are soluble in polar solvents. Nevertheless, they exhibit a lower solubility in organic solvents in relation to PTA, due to the presence of the ammonium functionality.^[11] Moving on to glycerol, the solvent of choice in this PhD Thesis, the *N*-alkylated PTA derivatives are glycerol-soluble, whereas PTA is insoluble in this solvent.^[12] In our group, several *N*-alkylated PTA compounds were synthesised and used for the stabilisation of palladium

nanoparticles (PdNPs) in glycerol.^[12b] The catalytic system was active in cross-coupling reactions, hydrogenations and one-pot tandem processes (see Scheme 1.11 in chapter 1).

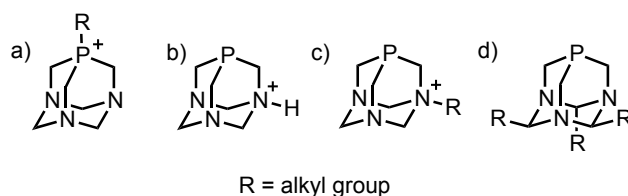
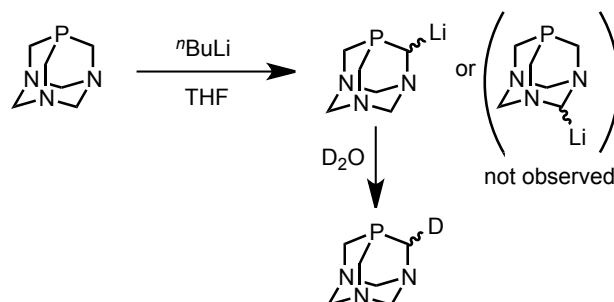


Figure 4.3 Functionalisation of PTA: a) P-Alkylation; b) N-Protonation; c) N-Alkylation; d) Lower-rim functionalisation.

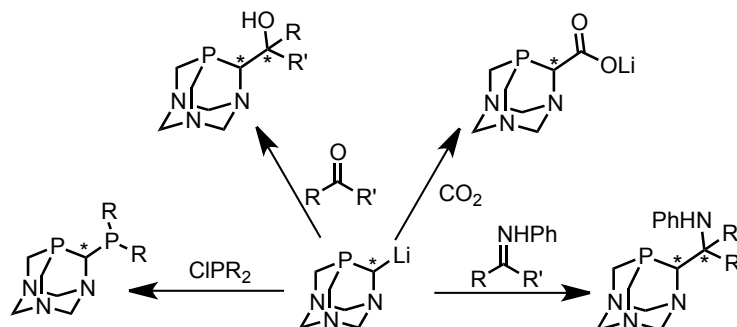
The lower-rim methylene positions (see Figure 4.1) have been also functionalised giving rise to PTA derivatives in which the 1,3,5-triazacyclohexane ring results 2,4,6-trisubstituted (Figure 4.3d).^[13] Nevertheless, the functionalisation at the upper-rim methylene position, adjacent to the P centre of PTA, is of paramount importance because these transformations lead to chiral PTA phosphines. A stereogenic centre is then generated in close proximity to the P atom, thus potentially enabling efficient ligand-to-metal transfer of the stereochemical information. In this way, a new class of chiral water-soluble PTA-based phosphines can be accessible. The first work reporting an upper-rim modification of PTA was published by Frost *et al.*^[14] They described for the first time the key step of lithiation of one upper-rim methylene position to obtain the corresponding PTA–Li derivative, which was isolated as a white highly pyrophoric powder in high yield (> 90%). Because of its pyrophoric nature, PTA–Li was indirectly characterised by reaction with D₂O. The deuteration selectively occurred at one of the α -P methylene positions. The selective lithiation at this site might be due to a better stabilisation of the formed carbanion.



Scheme 4.1 Lithiation of the upper-rim methylene position of PTA.

The thus resultant PTA–Li derivative opens the way to a great deal of possibilities in the development of new chiral PTA-based phosphine ligands. This highly reactive organolithium nucleophile can be added onto a variety of electrophiles (Scheme 4.2) such as

chlorophosphines,^[14-15] CO₂,^[16] aldehydes or ketones^[16-17] and imines.^[18] These synthetic strategies generate one or two stereogenic carbon centres.



Scheme 4.2 Reactivity of PTA–Li towards several electrophiles.

Some of these chiral PTA-based derivatives have been used as ligands in the synthesis of transition metal complexes (Figure 4.4), presenting high activity in different catalytic processes (nitrile hydrations^[15, 18] or transfer hydrogenations^[17b]). However, all the reported chiral PTA derivatives were not stereochemically pure, used as racemic mixture, and in consequence without inducing any stereoselectivity.

In 2011, Peruzzini and Gonsalvi *et al.*^[17b] reported on the use of Ir(I) complexes of PTA-based β -phosphino alcohols (Figure 4.4a), as suitable catalytic systems for the transfer hydrogenation of ketones as well as α,β -unsaturated carbonyl compounds. The same group also reported the first imidazolyl upper-rim PTA derivatives.^[17c] The Ru(II) complexes (Figure 4.4b) containing these hetero-donor ligands showed a moderate catalytic activity in the reduction of acetophenone. Following with the same metal, Frost *et al.* prepared PTA-based β -aminophosphines and coordinated them as bidentate ligands to Ru(II)–arene centres.^[18] These Ru(II) complexes (Figure 4.4c) were found to be active catalysts for the aqueous phase hydration of nitriles. More recently, the same group reported the synthesis of PTA-based P,P -donor ligands and their corresponding Ru(II)–arene complexes (Figure 4.4d), being also active in the nitrile hydration.^[15]

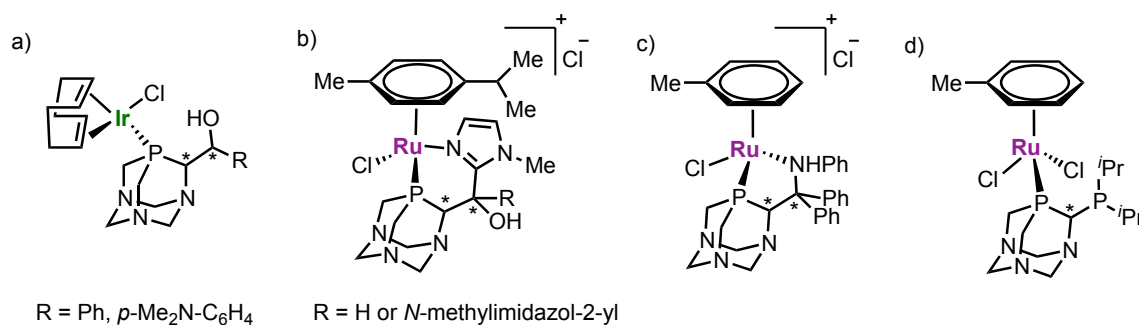


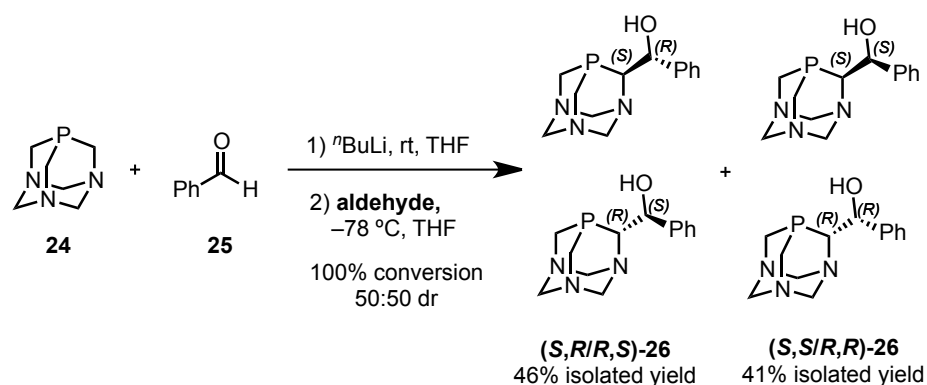
Figure 4.4 Transition metal complexes containing PTA-based ligands used in catalysis.

Nevertheless, to the best of our knowledge, enantiomerically pure PTA-based phosphines have not been previously reported in the literature. These compounds open the possibility of creating new glycerol (and water) soluble optically pure catalysts for asymmetric transformations of interest. This is actually the main goal of this chapter: to prepare new enantiopure PTA-based derivatives in order to use them as chiral ligands for transition metal-based complexes and also as chiral organocatalysts.

4.2 Results and discussion

4.2.1 Preparation of the enantiopure PTA phosphines

Following the strategy of Frost *et al.*^[14] for the upper-rim functionalisation of PTA (**24**) through the formation of the PTA–Li species, our first attempt was to prepare a β -phosphino alcohol using benzaldehyde (**25**) as electrophile (Scheme 4.3a).^[17a] The resulting mixture of stereoisomers, diastereomers **(S,R/R,S)-26** and **(S,S/R,R)-26**, was separated by column chromatography affording both diastereomers.



Scheme 4.3 Preparation of a racemic mixture of diastereomers of β -phosphino alcohol **26**.

With the aim of obtaining an enantiopure β -phosphino alcohol, the mixture of the four stereoisomers was separated by preparative chiral supercritical fluid chromatography (SFC), leading to a highly efficient separation (Figure 4.5a). Upon separation, suitable single crystals for X-ray diffraction analysis were obtained of one of the two enantiomers of each pair of diastereomers: **(R,R)-26** (Figure 4.5b) and **(S,R)-26** (Figure 4.5c), by slow evaporation of a dichloromethane solution. These structures, together with ^{31}P NMR spectra, allowed us determining the absolute configuration of each stereocentre.

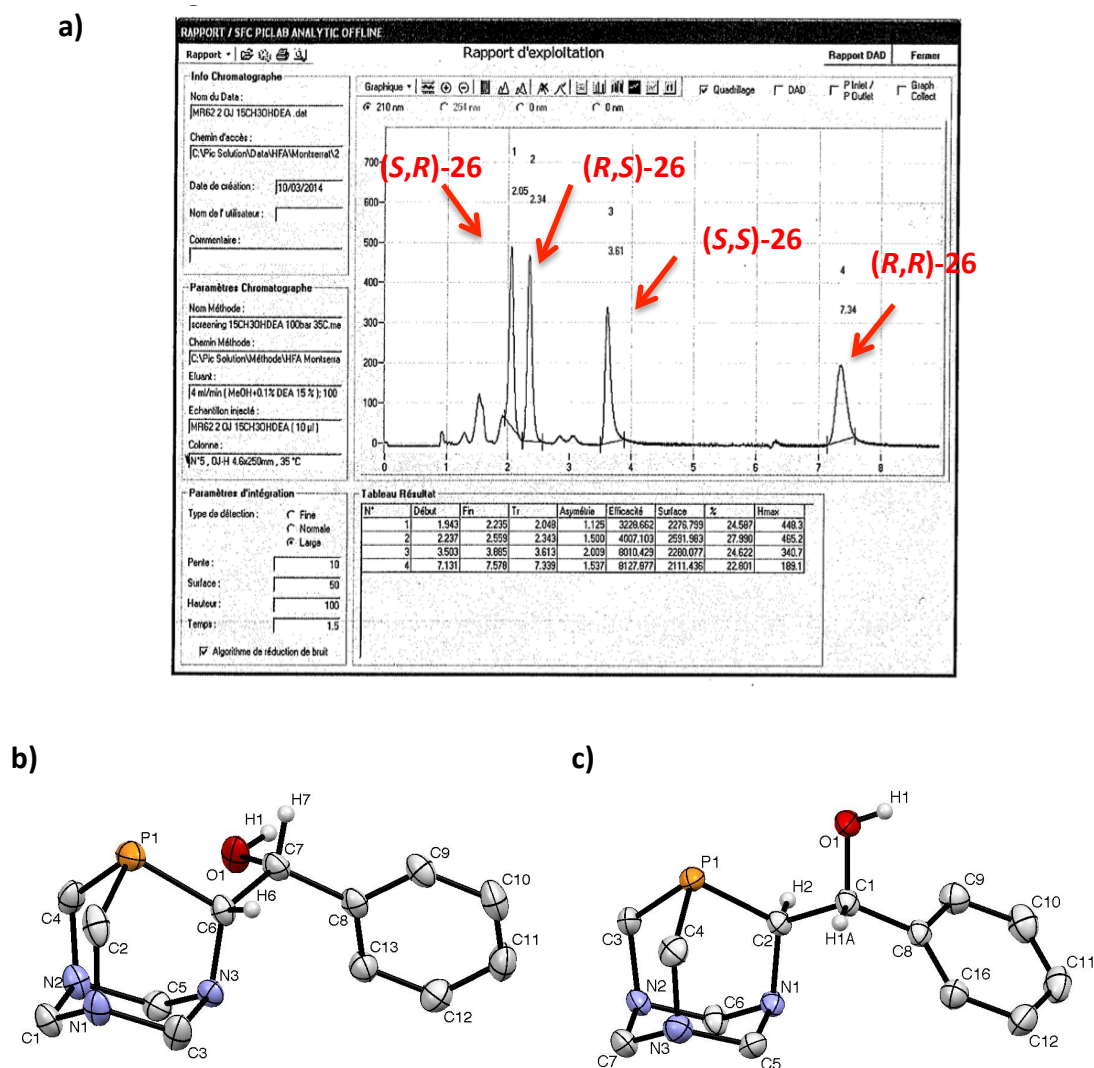
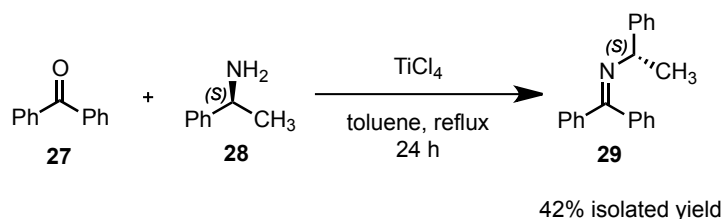


Figure 4.5 a) Chromatogram of the separation by SFC of a mixture of 4 stereoisomers for **26**: each peak has been assigned thanks to the X-ray diffraction structures and the ^{31}P NMR spectra; b) X-ray crystal structure of compound **(R,R)-26** (ellipsoids drawn at the 50% probability level); c) X-ray crystal structure of compound **(S,R)-26** (ellipsoids drawn at the 50% probability level). For clarity reasons, only hydrogens attached to oxygen and carbon atoms are shown.

In order to afford chiral bidentate PTA-based compounds, we decided to prepare enantiopure β -aminophosphines.^[18] In addition, this scaffold would be very useful, not only as chiral ligand for transition metal complexes, but also as bifunctional chiral organocatalyst.^[19]

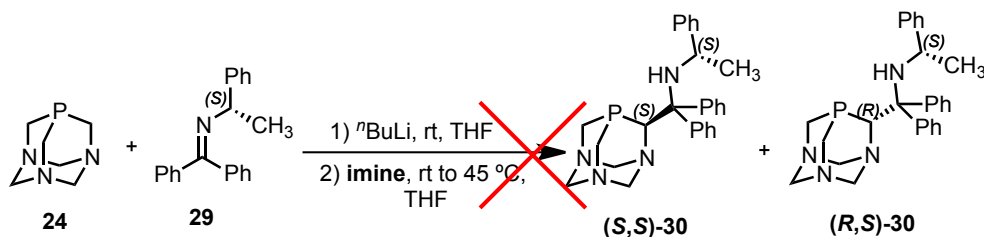
To prepare these optically pure β -aminophosphines, we envisioned the addition of PTA-Li to enantiopure imines, rendering in this way PTA derivatives featured by an amino group in β position to phosphorus. Our first attempt was to use an enantiopure ketimine as electrophile. The preparation of ketimine **29** involved the condensation of benzophenone (**27**) with the

enantiopure (*S*)-1-phenylethylamine (**28**) catalysed by TiCl_4 , affording 42% yield of the desired compound (Scheme 4.4).



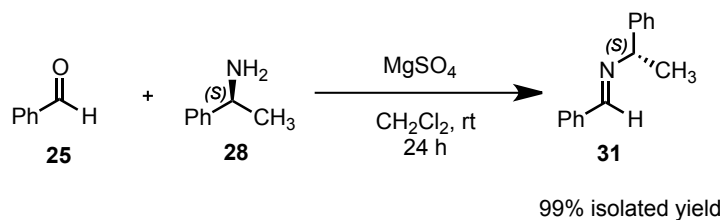
Scheme 4.4 Preparation of the chiral ketimine **29**.

The addition of PTA-Li to ketimine **29** did not work (Scheme 4.5), even increasing the temperature of the addition (in comparison with the preparation of the β -phosphino alcohols). It seems that the ketimine is not activated enough for the addition of PTA-Li. In order to enhance the reactivity, $\text{BF}_3 \cdot \text{OEt}_2$ was added as Lewis acid to the reaction mixture to activate the ketimine. However, what happened was the addition of $\text{BF}_3 \cdot \text{OEt}_2$ to PTA (probably forming a B-N bond)^[20], even when the boron reagent was previously mixed with the imine and added together to the solution containing the PTA-Li. The reaction was also carried out in the presence of TMEDA (tetramethylethylenediamine), in order to prevent the agglomeration of the organolithium. However, there was no conversion under such conditions.



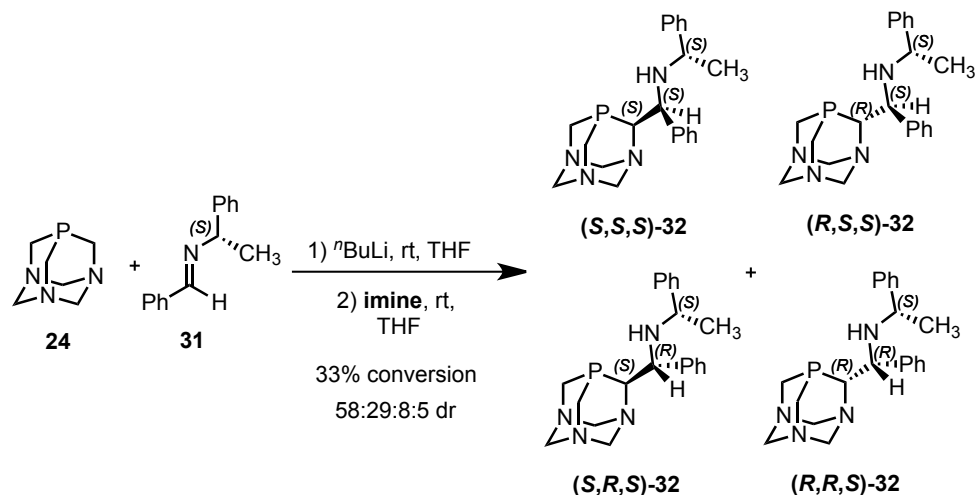
Scheme 4.5 Attempts to prepare a diastereomeric mixture of β -aminophosphine **30** by addition of PTA-Li to ketimine **29**.

In order to enhance the reactivity, we decided to use a less sterically demanding enantiopure aldimine instead of a ketimine, even though the number of diastereomers would increase due to the generation of one additional stereogenic carbon centre. Aldimine **31** was successfully prepared from benzaldehyde (**25**) and the enantiopure (*S*)-1-phenylethylamine (**28**), using MgSO_4 as dehydrating agent (Scheme 4.6).



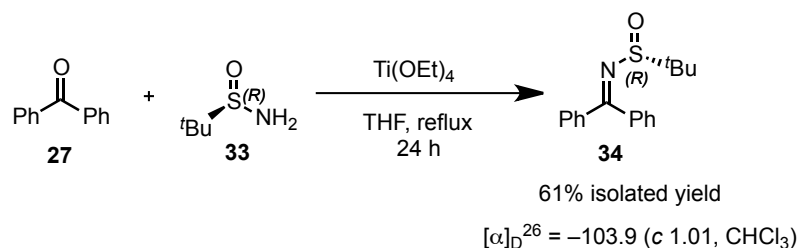
Scheme 4.6 Preparation of chiral aldimine **31**.

The addition of PTA–Li to chiral aldimine **31** led to low conversion (33%), obtaining a mixture of 3 diastereomers (ratio 58:29:8:5) (Scheme 4.7). The reaction was also conducted in the presence of $\text{BF}_3 \cdot \text{OEt}_2$ with the aim of enhancing the reactivity through Lewis acid-assisted activation of the electrophile. However, the desired products were not observed, appearing signals in ^{31}P NMR that presumably correspond to the addition of $\text{BF}_3 \cdot \text{OEt}_2$ to PTA.



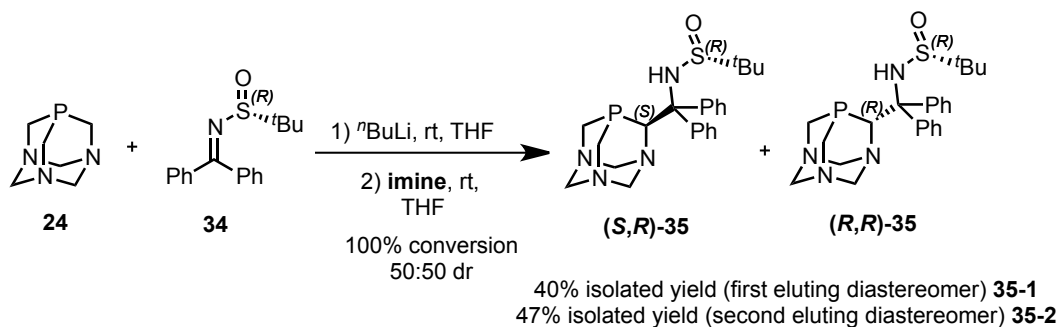
Scheme 4.7 Preparation of a diastereomeric mixture of β -aminophosphine **32** by addition of PTA–Li to aldimine **31**.

After these unsuccessful results using the enantiopure aldimine **31** and ketimine **29** as electrophiles in the addition of PTA–Li, we decided to move to optically pure *N*-*tert*-butylsulfinylketimines. The first synthesis of *N*-*tert*-butylsulfinylketimines was reported by Ellman *et al.* in 1999.^[21] The sulfinyl group has proven its efficiency as chiral auxiliary, because of both its ability to activate the imine with regard to nucleophilic addition and its ease to be removed (deprotection) under mild conditions by acid treatment.^[22] Although the synthesis of *N*-*tert*-butylsulfinylaldimines is less challenging than that of ketimines, we wanted to use an enantiopure ketimine derived from the condensation of benzophenone (**27**) and the enantiopure (*R*)-*tert*-butylsulfinamide (**33**; Scheme 4.8), with the aim of getting only two diastereomers by reaction with PTA–Li.



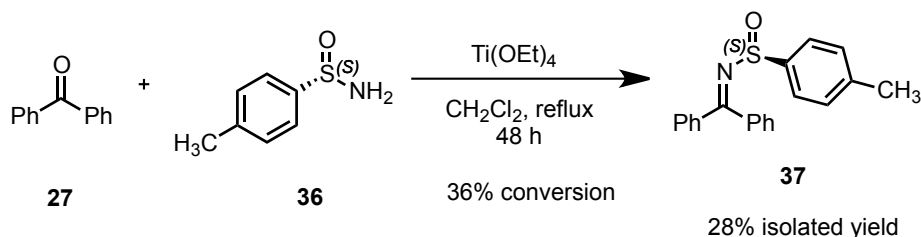
Scheme 4.8 Preparation of chiral ketimine **34**.

The addition of PTA–Li to the (*R*)-*N*-*tert*-butylsulfinylketimine **34** proceeded successfully (Scheme 4.9). The diastereomeric mixture was separated by column chromatography, obtaining 40% yield of the first eluting diastereomer and 47% yield of the second one. Unfortunately, we were not able to get suitable single crystals for X-ray diffraction analysis; therefore, the stereochemistry of both diastereomers is not assigned. For clarity reasons, the first eluting diastereomer is going to be called, from now on, **35-1** and the second one, **35-2**.



Scheme 4.9 Preparation of a diastereomeric mixture of β -phosphino sulfinamide **35** by addition of PTA–Li to sulfinylketimine **34**.

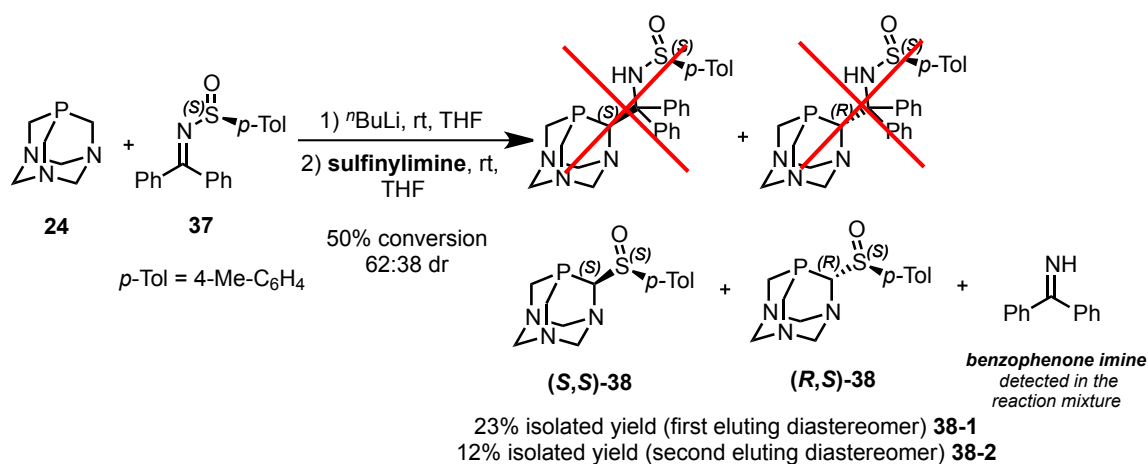
Following the same strategy, we also tackled the preparation of another β -phosphino sulfinamide derived from an enantiopure *N*-*p*-tolylsulfinylketimine. For this purpose, we prepared the sulfinylketimine **37** by condensation of benzophenone (**27**) and the enantiopure (*S*)-*p*-tolylsulfinamide (**36**) mediated by Ti(OEt)₄ (Scheme 4.10). Imine **37** was isolated in only 28% yield accounting the moderate conversion of the starting material (36%).



Scheme 4.10 Preparation of chiral ketimine **37**.

Nevertheless, the addition of PTA–Li to sulfinylketimine **37** did not lead to the expected β -phosphino sulfinamide. The nucleophilic addition of the organolithium did not occur on the imino group but onto the sulfinyl moiety (substitution reaction involving nucleophilic addition plus elimination of benzophenone imine), leading to an unexpected diastereomeric mixture (62:38 dr) of α -sulfinylphosphine **38** (Scheme 4.11). In this case, the diastereoselectivity was slightly favourable to one of the two diastereomers, which may be due to the asymmetric 1,2-induction controlled by the starting chiral imine.

The different behaviour observed using the *p*-tolylsulfinylimine in comparison with the *tert*-butylsulfinylimine has been already reported in the literature for related imines.^[23] In general, the addition of organometallic reagents to sulfinylimines could give two different nucleophilic attacks depending on the Grignard reagent, resulting on the formation of the substitution product or the addition product. While the *tert*-butyl group does not permit the substitution product at the stereogenic sulphur atom because of its steric hindrance, the *p*-tolyl group offers less steric impediment and nucleophiles are able to attack the sulphur atom leading to the substitution product, as we observed. Both diastereomers were separated by column chromatography isolating them in low yield (23% of the first eluting diastereomer and 12% of the second one). The conversion of this reaction was incomplete (around 50%) and we recovered unreacted imine plus benzophenone. The stereochemistry of both diastereomers was not assigned. Based on the literature precedents,^[24] we propose that the nucleophilic substitution reaction occurs with inversion of stereochemistry at the sulphur stereocentre. In this case the absolute configuration of the sulphur atom remains *S* due to a change in the priority of the substituents according to Cahn-Ingold-Prelog (CIP) rules. For clarity reasons, the first eluting diastereomer is going to be called, from now on, **38-1** and the second one, **38-2**.

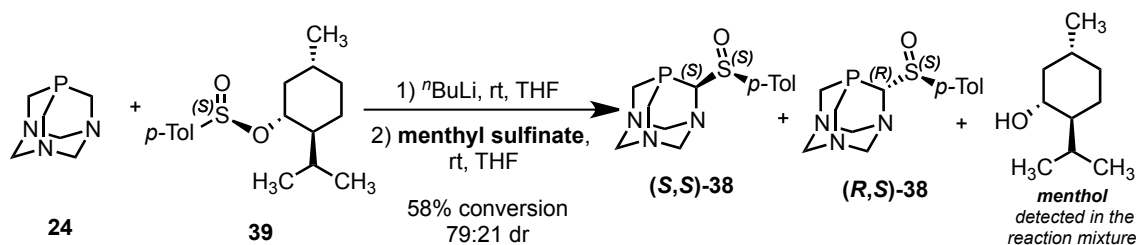


Scheme 4.11 Preparation of a diastereomeric mixture of α -sulfinylphosphine **38** by addition of PTA-Li to sulfinylketimine **37**.

Although compound **38** was unexpected, we should also pay attention to it because of it is a very interesting chiral PTA-derivative, which could be used as ligand for transition metal complexes. α -Sulfinylphosphines can act as bidentate ligands through the phosphorus and oxygen atoms. Moreover, the additional stereogenic carbon centre could help to increase the enantioselectivity regarding applications in asymmetric catalysis. In spite of the numerous literature reports on the use of phosphine-sulfoxides as ligands for many metal-mediated

transformations,^[25] scarce examples deal with α -sulfinylphosphine derivatives,^[26] some of them protected as phosphine-borane adducts.

With the aim of improving the synthesis of α -sulfinylphosphine **38**, we decided to use commercially available and enantiopure (1*R*,2*S*,5*R*)-menthyl (*S*)-*p*-toluenesulfinate (**39**) (also known as Andersen reagent)^[27] instead of the sulfinylketimine **37** as electrophile. The addition of PTA-Li would proceed necessarily onto the sulfinate group, thus generating menthol as concomitant product. However, we obtained the same reactivity than that using **37**, but with higher diastereoselectivity (79:21 dr), which may be due to the asymmetric 1,2-induction controlled by the starting chiral sulfinate. In this case the conversion (reaction monitored by ³¹P NMR), was also incomplete (58%) finding unreacted menthyl *p*-tolylsulfinate in the crude mixture.

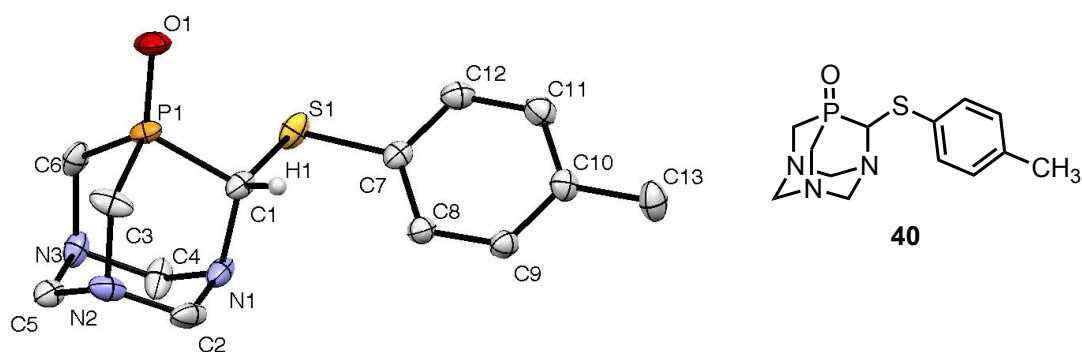


21% isolated yield (first eluting diastereomer) **38-1**
9% isolated yield (second eluting diastereomer) **38-2**

Scheme 4.12 Preparation of a diastereomeric mixture of α -sulfinylphosphine **38** by addition of PTA-Li to (1*R*,2*S*,5*R*)-menthyl (*S*)-*p*-toluenesulfinate (**39**).

In order to determine the absolute configuration of each diastereomer, we tried to get single crystals for X-ray diffraction analysis. Actually, we succeeded to obtain suitable crystals of the first eluting diastereomer. Surprisingly, the solved crystal structure revealed us another compound (Figure 4.6a). The oxygen was transferred from sulphur to phosphorus, yielding a thioether phosphine oxide (**40**). In addition, **40** crystallised in a centrosymmetric group as a racemic compound (Figure 4.6b). Inconsistently, the measurement of the optical rotation of the single crystals, immediately after the X-ray crystallography, gave a value distinct to zero ($[\alpha]_D^{26} = -29.3$ (*c* 1.00, CHCl₃)).

a)



b)

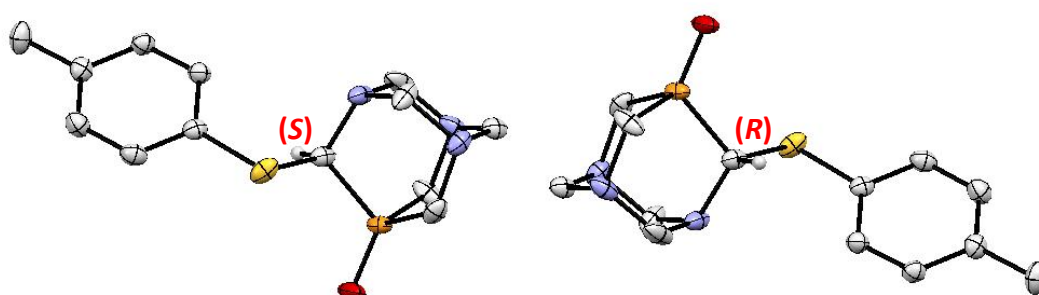
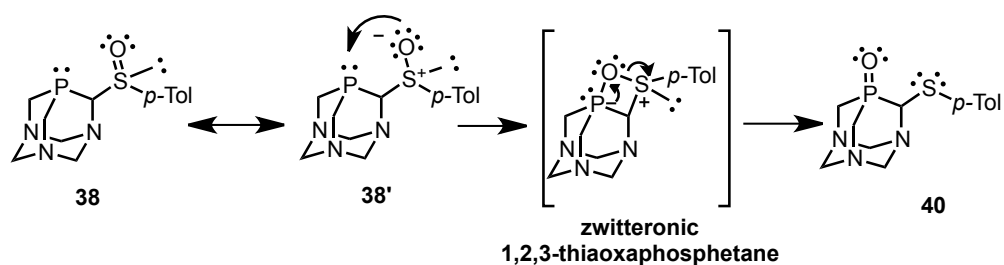


Figure 4.6 a) Crystal and chemical structure of compound **40** (ellipsoids drawn at the 50% probability level), hydrogen atoms are omitted for clarity; cocrystal with 1.5 molecules of water; b) Packing diagram showing only two molecules showing the configuration of the stereocentre.

In 1981, Vedejs *et al.* reported for the first time about the chemical instability of α -sulfinylphosphines. This class of compounds may easily suffer from a rapid internal redox process involving an intramolecular rearrangement, *via* migration of the oxygen atom of the sulfoxide group from sulphur to phosphorus.^[26a] The conversion of sulfinylphosphines into thioether phosphine oxide derivatives, *via* internal oxygen transfer, has also been suggested and even synthetically exploited by other authors.^[26b, 28] This plausible proposed mechanism could also take place in our case leading to the formation of thioether phosphine oxide **40** from α -sulfinylphosphine **38** (Scheme 4.13). Considering the zwitterionic resonance structure of **38** (**38'**), we propose an internal oxygen transfer from the sulfoxide moiety to the phosphino group. This oxygen migration could occur through the formation of a zwitterionic 1,2,3-thioxaphosphetane intermediate (structure depicted in Scheme 4.13). This kind of intermediate is reminiscent of 1,2-oxaphosphetanes, commonly proposed^[29] in the Wittig olefination reaction.^[29] Intramolecular rearrangement of zwitterionic 1,2,3-thioxaphosphetane would give rise to the isolated thioether phosphine oxide **40**.



Scheme 4.13 Plausible mechanism for the formation of compound **40**.

One of the advantages of using sulfinyl groups for the activation of imines is that they can be easily removed under mild acidic conditions. In the case of the two diastereomeric β -aminophosphines [**35-1** and **35-2**] prepared in this chapter, the cleavage of the sulfinyl group would lead to the corresponding enantiopure primary amines of opposite absolute configuration. From the point of view of organocatalysis, the primary aminophosphine that we would obtain is a promising bifunctional chiral organocatalyst. While the amino group can engage carbonyl compounds *via* the iminium ion/enamine activation mode,^[30] the trialkylphosphino fragment, can act as a nucleophile, activating an α,β -unsaturated carbonyl system through conjugate addition *via* phospho-Michael reaction.^[31]

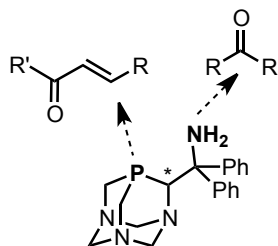
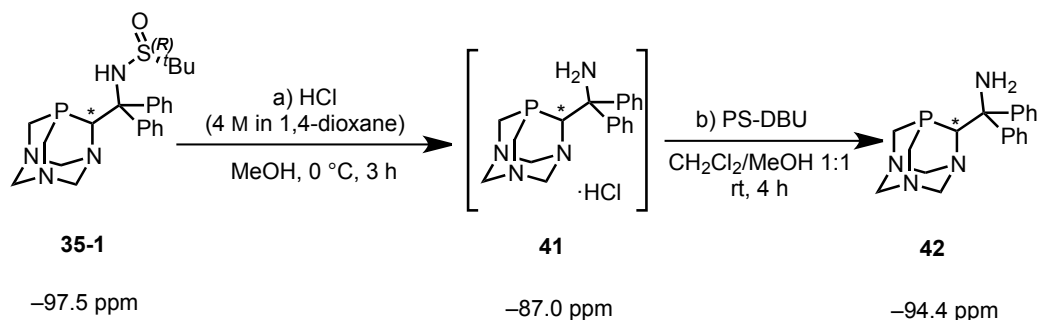


Figure 4.7 Envisioned dual behaviour of the PTA-based primary amine.

Following Ellman's procedure,^[22a] the cleavage of the *tert*-butylsulfinyl auxiliary group from **35-1** was carried out using a commercial solution of HCl, to yield the corresponding hydrochloride salt **41** (Scheme 4.14). The *tert*-butylsulfinyl chloride ($^t\text{BuSOCl}$) generated as a concomitant product was converted into methyl *tert*-butylsulfinatate ($^t\text{BuSO}_2\text{Me}$) in MeOH, which could be eliminated in the work-up of this first step. After testing different basic treatments (NaOH, NaOEt/EtOH, KO^tBu /MeOH), we found that the most convenient method is the use of the supported DBU (1,8-diazabicyclo[5.4.0]undec-7-ene) on polystyrene (PS-DBU) as base. Hence, a solution of the hydrochloride salt was treated with the immobilised base and, after that, the solution was separated from the polymer by simple filtration, getting full conversion into the desired primary aminophosphine **42**. The reaction was monitored by ^{31}P NMR (chemical shifts given in Scheme 4.14) to ensure full conversion of each step.



Scheme 4.14 Acid-promoted cleavage of the *tert*-butylsulfinyl auxiliary group (step a) and subsequent basic treatment using PS-DBU as base (step b). Below each compound, ^{31}P NMR (162 MHz, in CDCl_3) chemical shifts are indicated.

Nevertheless, although the conversion was complete, we could not get the primary aminophosphine **42** completely pure. Minor impurities were always formed in both steps. After purification by column chromatography, the hydrochloride salt **41**, as well as the primary aminophosphine **42**, were transformed into these impurities, and we were able to isolate one of them. This product was fully characterised as compound **43** (Figure 4.8), in which the PTA cage is opened (probably due to the acidic medium), and a fused 2-imidazoline ring is formed.

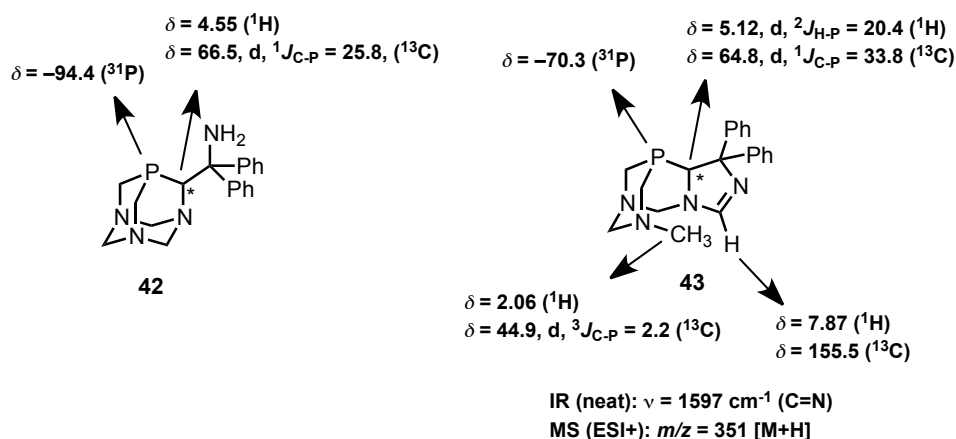
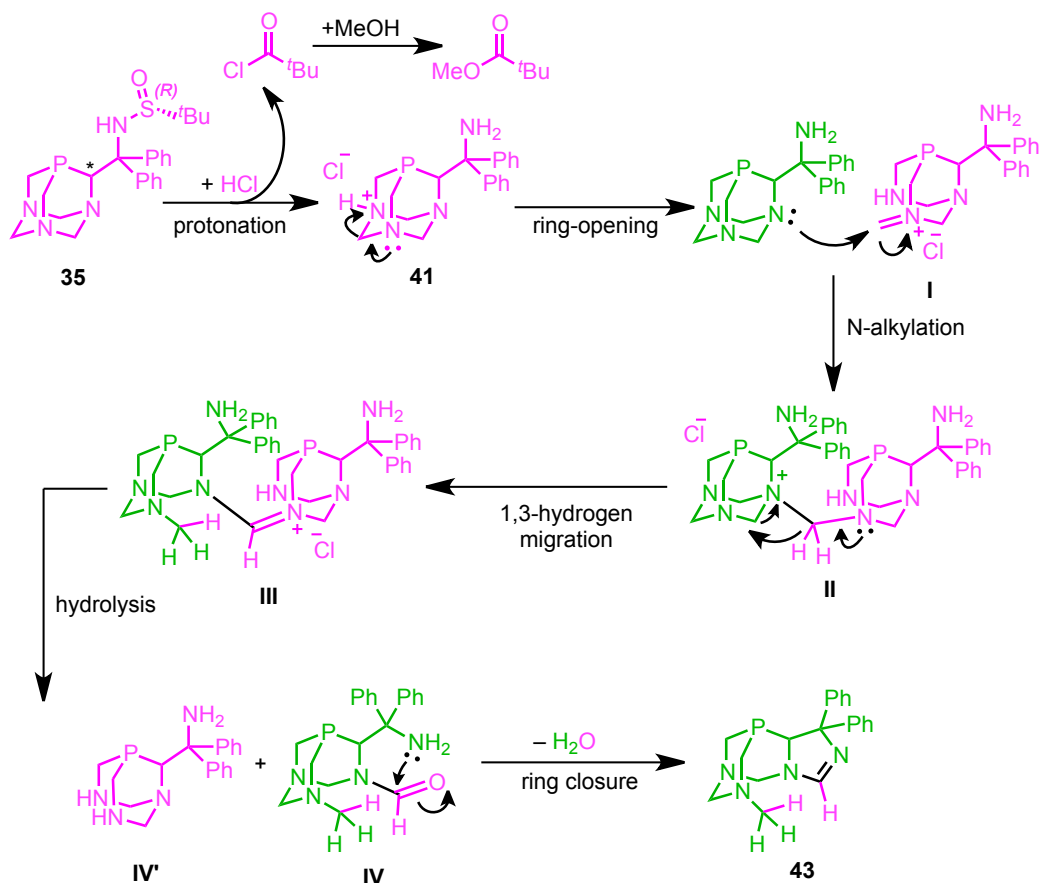


Figure 4.8 NMR signals of the amine **42** and the by-product formed in acid medium (**43**). NMR spectra were recorded in CDCl_3 . Chemical shifts given in ppm and coupling constants given in Hz.

We tried to rationalise how side product **43** could be formed, in order to improve the synthesis of the desired aminophosphine (**42**). The fused 2-imidazolidine ring formed in compound **43** contains an additional carbon atom, which might come from another aminophosphine molecule, as we propose in the following mechanism (Scheme 4.15). Acidic conditions are required to promote the cleavage of the *tert*-butylsulfinyl group in compound **35**, and under such conditions, the primary aminophosphine remains protonated (**41**). The analysis by RP-HPLC-MS of the protonated primary aminophosphine (**41**) seems to be in agreement with a mono-protonated species. If the protonation occurs in one of the three nitrogen atoms of the

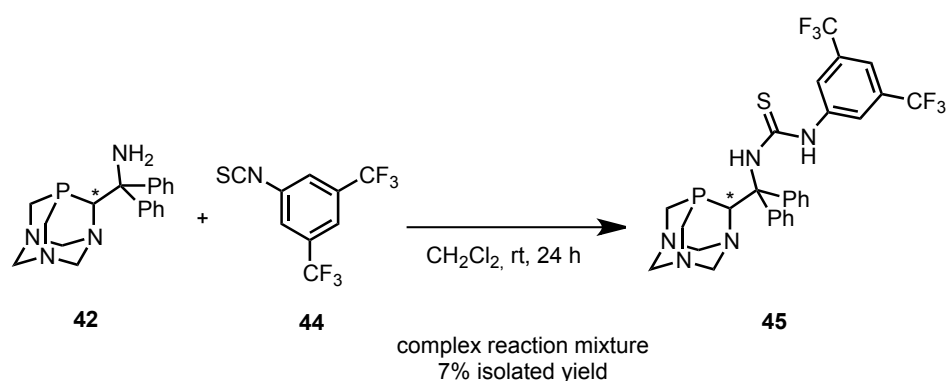
lower ring (tertiary amines), the PTA cage could be opened, thus leading to a PTA-derived formyliminium ion (**I**).^[32] At this point, the iminium ion could act as a Mannich acceptor being attacked by one of the tertiary amines of another molecule of aminophosphine, giving an aminated intermediate (**II**). This step is related to the Duff formylation reaction,^[33] which is a Friedel–Crafts acylation between an activated arene (usually phenols) and the iminium species resulting from protonation and ring-opening of hexamethylenetetramine (urotropine).^[34] A feasible 1,3-hydrogen migration could occur in the intermediate **II**, taking place with concomitant ring-opening, and thus leading to another iminium ion (**III**), which after hydrolysis would give rise to the corresponding formamide (**IV**), along with the PTA derivative **IV'**. This species could be assigned to an observed minor singlet at -62.2 ppm according to a ^{31}P NMR spectrum in which compound **43** is the major species (see Annexes 4.6.1, ^{31}P NMR spectra of compound **43**). An intramolecular condensation reaction with the primary amine would finally yield the isolated minor side product (**43**). Assuming the proposed mechanism is correct, it is clear that the acidic medium is the responsible for the formation of this side product. Consequently, a feasible solution to obtain the desired primary amine completely pure could be the avoiding of acidic conditions to cleavage the *tert*-butylsulfinyl group in **35**. A potential solution for avoiding the protonation of the tertiary amino groups of PTA (not already tested), something that triggers the proposed mechanism yielding the undesired compound **43**, could be the use of trimethylsilyl chloride^[35] in the presence of aprotic solvents, instead of HCl.



Scheme 4.15 Tentatively proposed mechanism to explain the formation of the side product **43**.

Although the primary aminophosphine was not obtained completely pure (around 86% chemical purity), we decided to carry on the synthesis of new PTA derivatives starting from the impure aminophosphine. The presence of the primary amino group provides the opportunity to obtain an enantiopure thiourea-phosphine^[36] by reaction with an isothiocyanate. In 1998, Jacobsen *et al.*^[37] reported that the use of urea and thiourea derivatives catalyse the asymmetric hydrocyanation of imines (the Strecker reaction). Later on, detailed mechanistic studies revealed that the responsible of the catalytic activity was the thiourea moiety, interacting with the substrate *via* a dual hydrogen-bond interaction.^[38] Since then, thioureas have been widely applied as Brønsted acid organocatalysts in a large number of organic transformations.^[39] Moreover, our envisioned chiral PTA-based thiourea-phosphine can also act as a bifunctional organocatalyst, due to the presence of the phosphino functionality. Chiral thiourea-phosphines have been also widely applied in enantioselective organic transformations such as allenolate–imine cycloadditions or (aza)-Morita-Baylis-Hillman reactions, demonstrating the essential role of both functional groups in catalysis.^[40]

With this end, we carried out the synthesis of the PTA-based thiourea **45** starting from the enantiopure primary aminophosphine **42** and using 3,5-bis(trifluoromethyl)phenyl isothiocyanate (**44**) as electrophile (Scheme 4.16). Unfortunately, we got a complex reaction mixture in which the isothiocyanate seems to be totally consumed according to the ^1H NMR spectrum. The signals of the desired thiourea (**45**) and also, again, the side product **43** were observed in the ^1H NMR spectrum of the crude mixture, more or less in equimolar ratio, although by ^{31}P NMR the thiourea seems to be the major product. With the aim of isolating the thiourea, the crude reaction mixture was purified by column chromatography, to get only 7% isolated yield of **45**, which was fully characterised.



Scheme 4.16 Synthesis of the PTA-based thiourea derivative **45**.

4.2.2 Applications of the enantiopure PTA derivatives

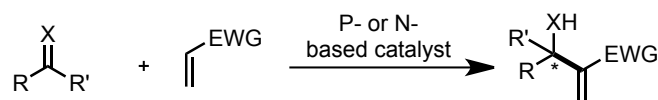
In the last part of my PhD Thesis, we explored the ability of these new enantiopure PTA-based compounds in some benchmark enantioselective reactions.

Morita-Baylis-Hillman reaction

The Morita-Baylis-Hillman (MBH) reaction,^[41] which couples aldehydes with activated olefins leading to functionalised allyl alcohols, is one of the most important methods for converting simple starting materials into highly functionalised products in an atom-economical way (Scheme 4.17a). In general, this reaction is catalysed by a nucleophilic organocatalyst, usually a tertiary amine such as 1,4-diazabicyclo[2.2.2]octane (DABCO) or a tertiary phosphine. The commonly accepted mechanism was already described in the earliest publications^[41] (Scheme 4.17b). The first step involves the conjugate addition of the catalyst, *via* aza- or phospho-Michael reaction, to the electron-deficient alkene to generate the corresponding zwitterionic species (**VI**). In the second step, **VI** attacks the carbonyl group *via* an aldol-type reaction leading to intermediate **VII**. The following intramolecular proton shift within **VII** to form

VIII in the third step, which generates the final MBH adduct recovering the catalyst in the elimination step. Nevertheless, the detailed mechanism, in particular for asymmetric MBH versions, remains still under discussion.^[42]

a) *Morita-Baylis-Hillman reaction*

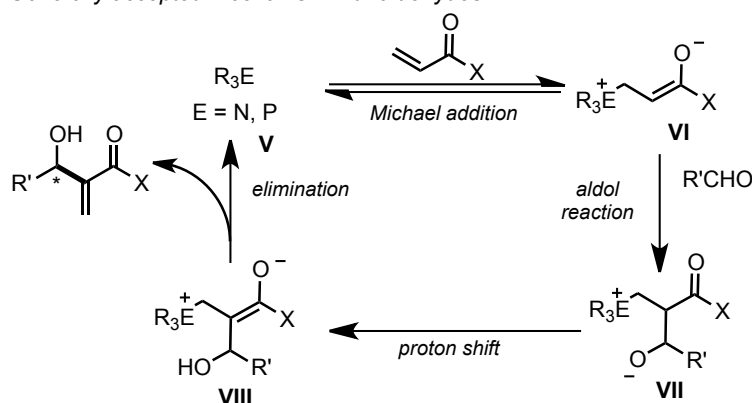


R = alkyl, aryl, heteroaryl, etc.; R' = H, CO₂R'', alkyl, aryl etc.

X = O, NCO₂R'', NSO₂Ar, NPOR₂'' etc.

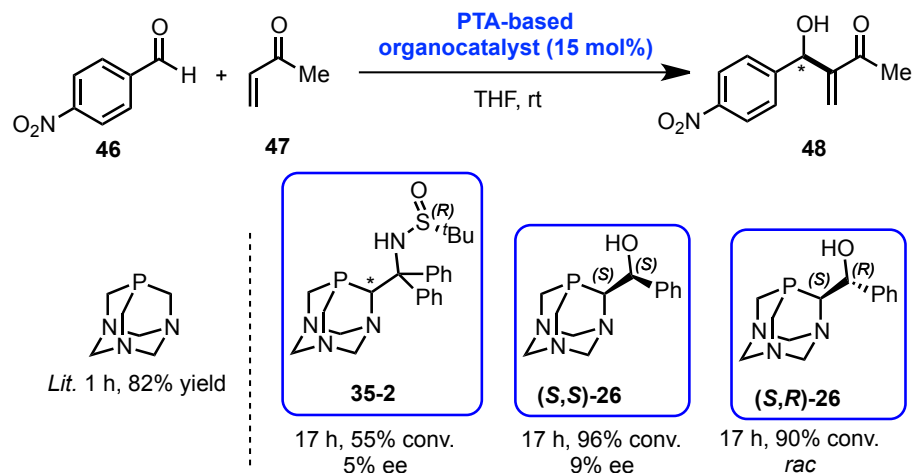
EWG = CO₂R'', CN, COR'', CHO, PO(OEt)₂, SO₂Ph, SO₃Ph, SPh, etc.

b) *Generally accepted mechanism with aldehydes*



Scheme 4.17 a) General scheme of MBH reaction; b) Generally accepted mechanism with aldehydes.

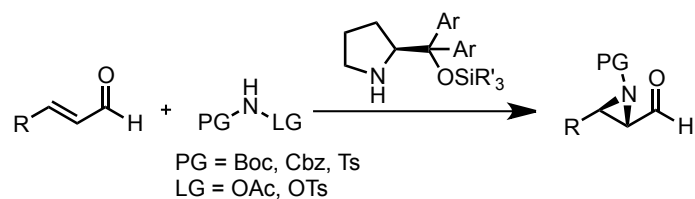
In 2006, He *et al.*^[31, 43] reported that the unfunctionalised PTA is an efficient organocatalyst for non-asymmetric MBH reactions. They isolated the zwitterionic adduct formed between PTA and ethyl acrylate confirming the occurrence of the phospho-Michael addition step in the catalytic cycle and proving that the phosphorus atom in PTA plays a critical role in the catalytic process. Taking into account these precedents, we planned to use our enantiopure PTA compounds as chiral organocatalysts in the asymmetric version of this reaction. Unfortunately, the PTA derivatives tested in the MBH reaction between 4-nitrobenzaldehyde (**46**) and methyl vinyl ketone (MVK, **47**) did not induce enantioselectivity in the product (**48**) (Scheme 4.18). One of the diastereomers of the *tert*-butylsulfinyl PTA **35-2** and both diastereomers of the phosphino alcohol PTA (**S,S**)-**26** and (**S,R**)-**26** were tested in order to study the matched/mismatched effect. The phosphino alcohol catalysts gave higher conversions than the *tert*-butylsulfinyl PTA derivative.



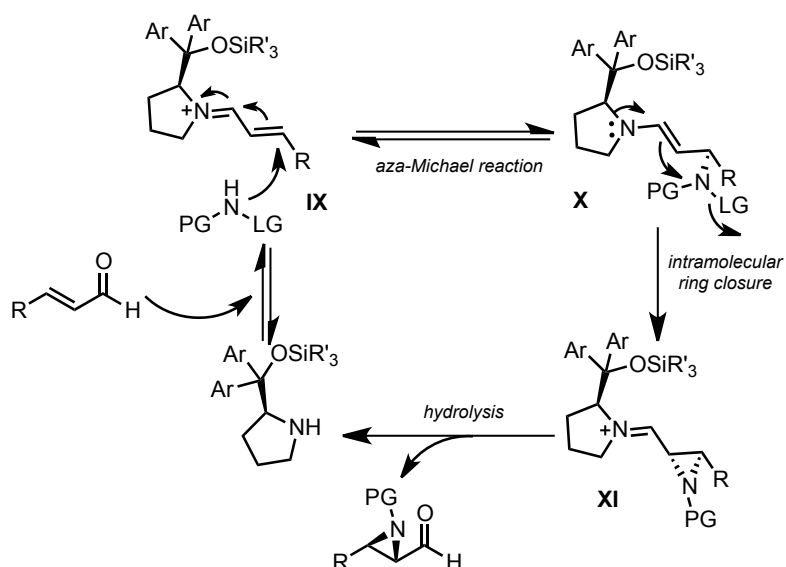
Scheme 4.18 MBH reaction catalyzed by enantiopure PTA-based derivatives.

Aziridination of α,β -unsaturated aldehydes

The catalytic asymmetric formation of aziridines represents a challenging and attractive target. The intrinsic ring-strain of these small heterocycles makes them versatile chiral building blocks in organic synthesis. The first protocols for the enantioselective synthesis of aziridines consisted in the use of chiral substrates or chiral auxiliaries.^[44] Asymmetric protocols using organometallic catalysts have been also widely used *via* nitrogen transfer to olefins and also *via* carbene insertion onto C=N double bonds.^[45] In the field of organocatalysis, Córdova *et al.*^[46] reported for the first time the use of chiral amines to provide simple asymmetric access to 2-formylaziridines from α,β -unsaturated aldehydes and O-acylated hydroxycarbamates (Scheme 4.19a). They proposed a reaction pathway (Scheme 4.19b) in which the first step is the formation of a chiral iminium intermediate (**IX**) between the aldehyde and the organocatalyst. Bulky groups in the catalyst control the stereoselectivity of the nucleophilic attack by the amino group, generating a chiral enamine intermediate (**X**). This intermediate can carry out a nucleophilic attack on the electrophilic nitrogen atom releasing the leaving group. The enantiopure aziridine is obtained by hydrolysis of intermediate **XI**.

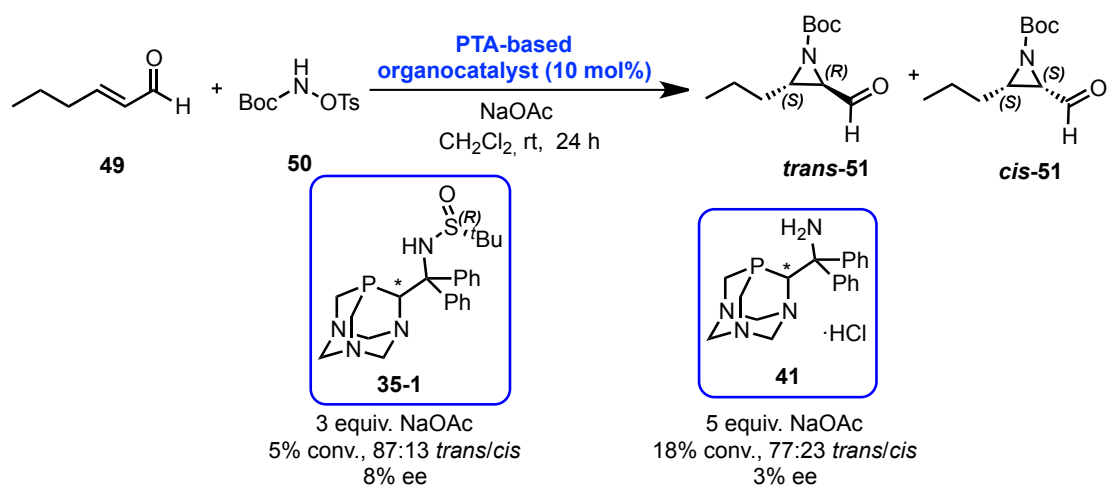
a) Organocatalysed aziridination reaction from α,β -unsaturated aldehydes

b) Proposed reaction pathway



Scheme 4.19 a) General scheme of organocatalysed aziridination reaction; b) Proposed reaction pathway.

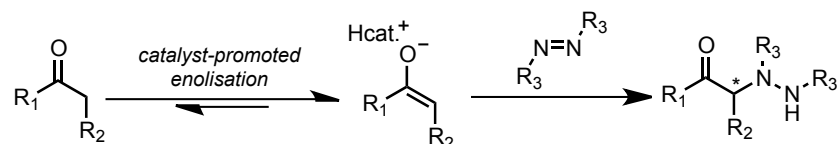
With these precedents in mind, we wanted to test our enantiopure PTA compounds as organocatalysts in the aziridination reaction between the *trans*-2-hexenal (**49**) and the *tert*-butyl *N*-(tosyloxy)carbamate (**50**) (Scheme 4.20). Conversions and enantioselectivities were very low using the *tert*-butylsulfinyl PTA derivative **35-1** or the hydrochloride salt **41** in the presence of an excess of base (*in situ* generation of the primary amine).



Scheme 4.20 Aziridination reaction catalyzed by enantiopure PTA-based derivatives.

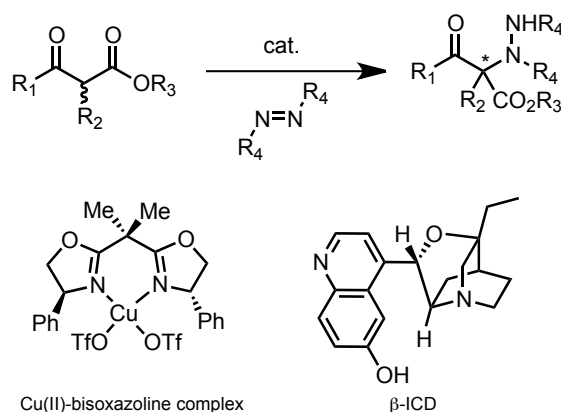
α -Amination reaction

The asymmetric α -amination of aldehydes,^[47] ketones^[48] and esters,^[49] is a powerful method to obtain α -amino acids, which represent fundamental building blocks for the construction of complex natural products and bioactive molecules. Basically, the reaction consists of an enolate (the enolisation process is promoted by a catalyst) reacting with an electrophilic nitrogen source, usually an azodicarboxylate reagent (Scheme 4.21).



Scheme 4.21 General reactivity pattern of α -amination reactions.

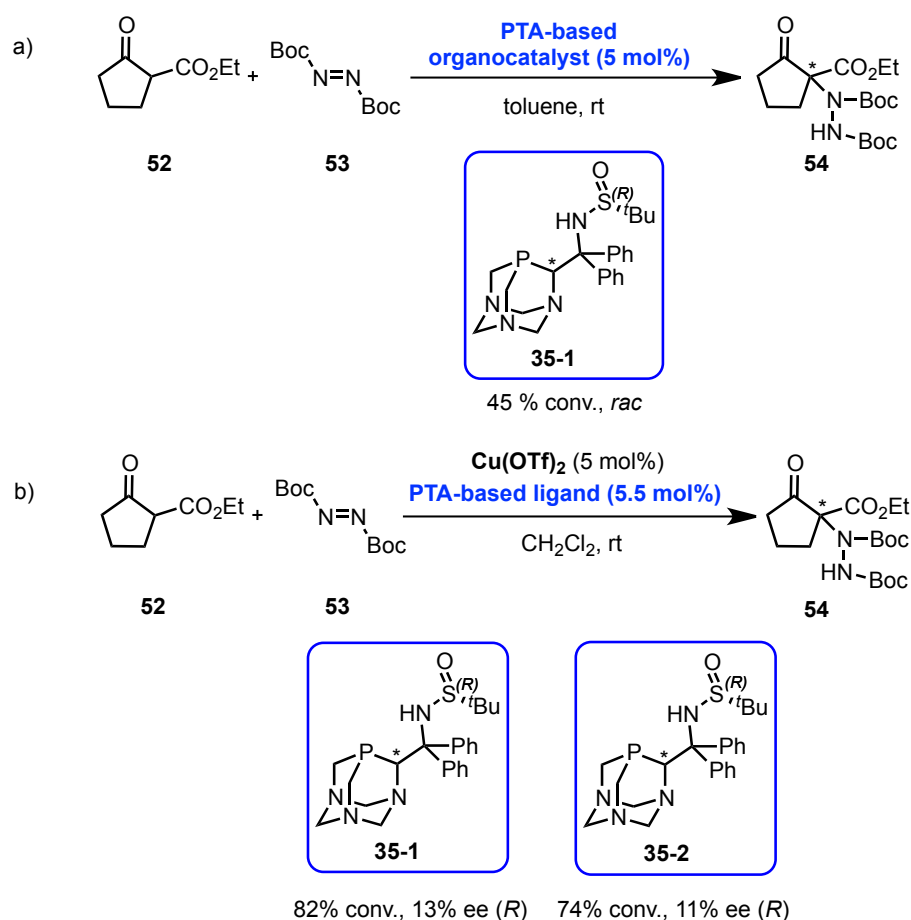
Focusing the attention on the α -amination of β -keto esters, this transformation has been widely explored, using both organocatalysts and metal-based catalysts.^[50] Jørgensen *et al.*^[51] reported for the first time the enantioselective α -amination of β -keto esters with azodicarboxylates catalysed by chiral copper(II)–bisoxazoline complexes (Scheme 4.22). The reaction most likely proceeds through a complex in which the distorted square planar Cu(II) centre is chelated to the β -keto ester enolate. The electrophilic attack of the azodicarboxylate occurs onto the less hindered face of the copper(II) enolate. From the other hand, the group of Jørgensen developed also the first organocatalysed α -amination of β -keto esters using a quinidine-derived alkaloid (β -isocupreidine, β -ICD) (Scheme 4.22).^[52] Although the authors did not provide mechanistic studies, they supposed that an enolate containing a chiral ammonium (β -ICD- H^+) counter ion is a likely intermediate.



Scheme 4.22 α -Amination of β -keto esters catalysed by a Cu-based complex or an organocatalyst (β -ICD).

After these two first reported examples using a metal- or an organo-based catalyst, other efficient catalytic systems have been described in the literature.^[53] We wanted to evaluate our

new PTA derivatives, both as chiral ligands using copper as transition metal and as chiral organocatalysts. Both catalytic systems were tested in the α -amination of ethyl 2-oxocyclopentanecarboxylate (**52**) and di-*tert*-butyl azodicarboxylate (**53**). The desired product (**54**) was obtained in low yield as a racemic mixture, using the *tert*-butylsulfinyl PTA derivative **35-1** as organocatalyst (Scheme 4.23a). Conversions were higher by adding copper(II) triflate as metal salt, using both diastereomers of the *tert*-butylsulfinyl PTA derivative **35-1** and **35-2**; however, the enantioselectivity was very low (up to 13% ee in favour of the *R* enantiomer) in both cases (Scheme 4.23b).

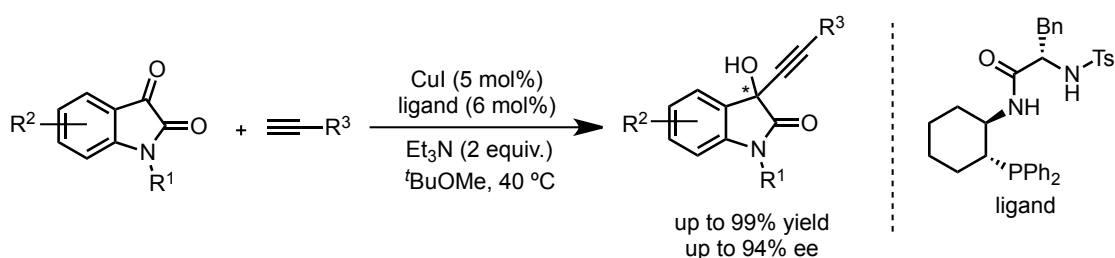


Scheme 4.23 a) Organocatalysed α -amination using **35-1** as organocatalyst; b) Cu-catalysed α -amination using **35-1** and **35-2** as ligands.

Addition of terminal alkynes to isatins

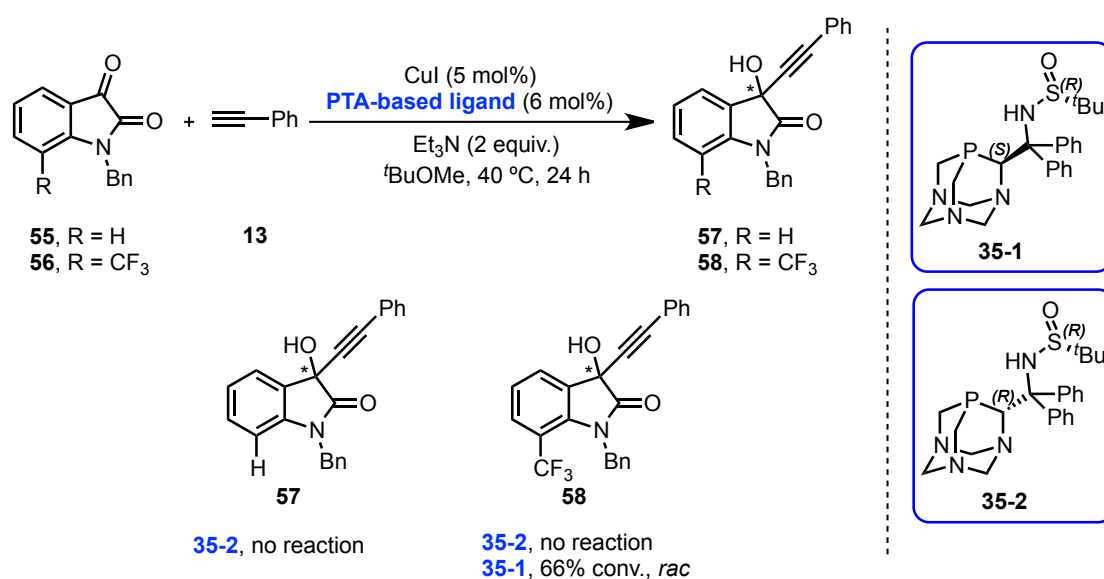
Nucleophilic additions to the C-3 carbonyl group of isatins to obtain 3-substituted 3-hydroxy-2-oxindole scaffolds are very useful reactions due to the presence of these motifs in natural products and drug candidates.^[54] One of these interesting transformations is the alkylation of isatins to afford 3-alkynyl-3-hydroxy-2-oxindoles. Non-symmetric versions have

been developed using diethyl zinc,^[55] using bis-*N*-heterocyclic carbene-derived silver complexes as catalysts^[56] or involving a CuI/DBU (1,8-diazabicyclo[5.4.0]undec-7-ene) system as catalyst.^[57] Very recently, the enantioselective version of this transformation was published independently by Liu *et al.*^[58] and Guo *et al.*^[59] The group of Liu reported that the system CuI/chiral guanidine provides an efficient route to these enantiomerically enriched propargylic alcohols. On the other hand, the group of Guo used a combination of CuI and a chiral phosphine ligand to afford the same class of compounds (Scheme 4.24).



Scheme 4.24 Alkynylation of isatins using CuI and a chiral phosphine reported by Guo *et al.*^[59]

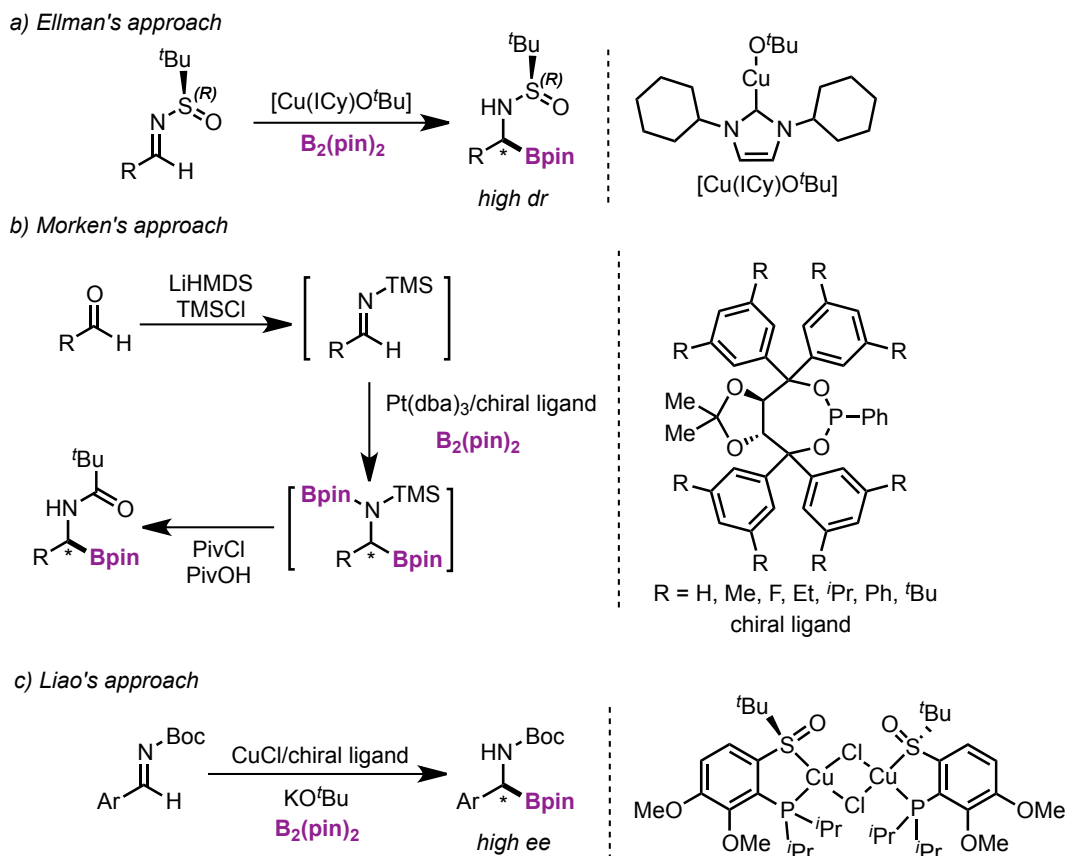
Following the work of Guo *et al.*, we decided to test the performance of our chiral phosphines as ligands in this asymmetric transformation (Scheme 4.25). In a first attempt, the reaction between *N*-benzylisatin (**55**) and phenylacetylene (**13**) using the *tert*-butylsulfinyl PTA **35-2** as ligand did not work. In order to increase the reactivity, *N*-benzylisatin was functionalised with a CF₃ group (compound **56**). In this case, using the same PTA derivative **35-2** as chiral ligand the reaction did not work neither. However, the **35-1** diastereomer led to a high conversion (66%), but unfortunately the product was racemic.



Scheme 4.25 Alkynylation of isatins using the diastereomers of **35** as chiral ligands.

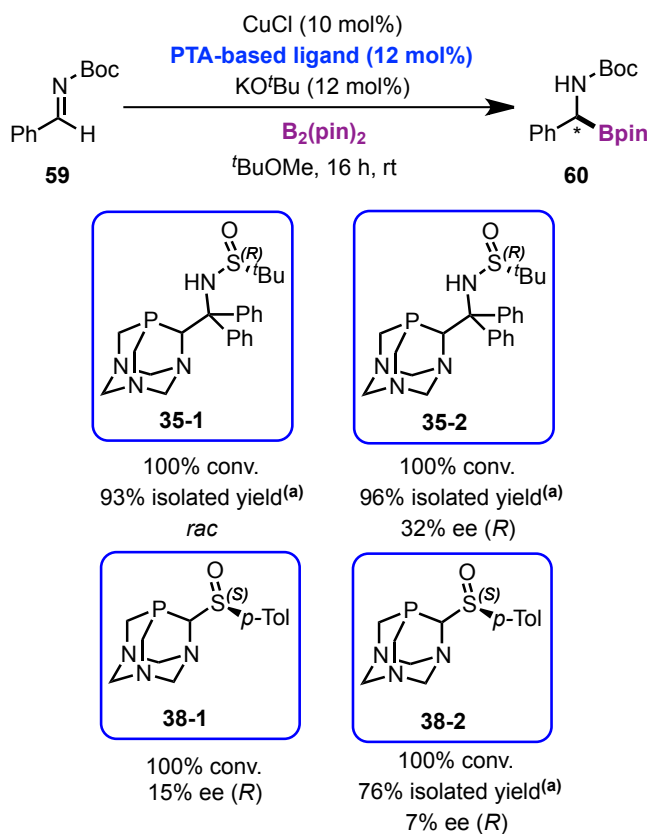
Hydroboration of *N*-Boc/Ts-protected imines

In the last years, boron-containing molecules have become very interesting in the pharmaceutical sector. Particularly, enantiopure α -amino boronic acids and esters have been used as potential enzyme inhibitors and therapeutic agents;^[60] these properties have stimulated a great deal of innovation on synthetic methods for their preparation.^[61] The addition of bis(pinacolato) diboron [B₂(pin)₂] reagent to imines catalysed by transition metal complexes is the most efficient approach to afford these products. Ellman *et al.*^[62] reported for the first time the borylation of enantiopure *N*-(*tert*-butylsulfinyl)aldimines in a highly diastereoselective way using catalytic amounts of (1,3-dicyclohexylimidazol-2-ylidene)copper(I) *tert*-butoxide [CuO^tBu(ICy)] (Scheme 4.26a). Morken *et al.*^[63] also contributed in this field reporting a strategy for the conversion of aldehydes to enantiomerically enriched α -amino boronates through the *in situ*-generated *N*-silylimine intermediate. The addition of B₂(pin)₂, catalysed by a Pt(0) phosphonite complex, occurs across the imine C=N double bond, leading to an intermediate that can directly be acylated to give a large variety of *N*-acyl- α -amino boronic esters (Scheme 4.26b). However, to simplify the process, Liao *et al.*^[25k] recently provided a directly borylation of *N*-Boc-protected imines, being in this case the *N*-Boc group easy to remove for synthetic purposes. They used as catalytic precursor a mixture of CuCl and the chiral phosphine–sulfoxide ligand proposing a bidentate coordination to copper through the sulphur and phosphorus atoms (Scheme 4.26c).



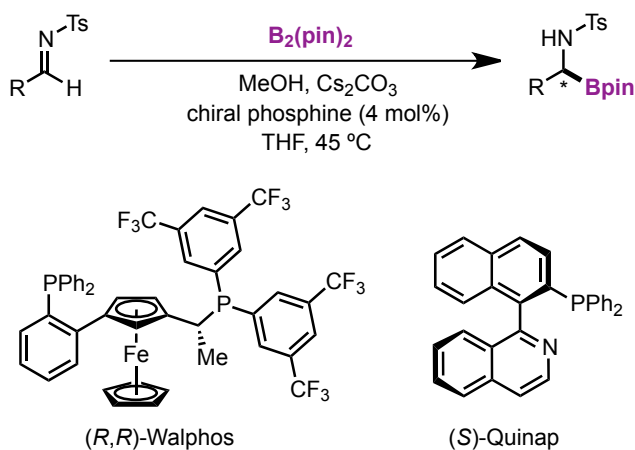
Scheme 4.26 Representative metal-catalysed approaches to obtain *N*-acyl α -amino boronic esters: a) Ellman *et al.*,^[62a] b) Morken *et al.*,^[63] c) Liao *et al.*^[25k]

Based on the work of Liao's group, we envisioned that our *tert*-butylsulfinyl PTA derivative **35** and also the α -sulfinylphosphine **38**, could act in a similar manner as the sulfoxide-phosphine ligand used by Liao *et al.* For this reason, we tested the addition of $B_2(\text{pin})_2$ to *N*-Boc aldimine **59** using our ligands (Scheme 4.27). Full conversions were achieved using both diastereomers of the *tert*-butylsulfinyl PTA derivative **35** as chiral ligands. The diastereomer **35-1** led to a racemic mixture of the α -amino boronic ester (**60**), whereas using the other diastereomer **35-2** the enantioselectivity was 32% ee (in favour of the *R* enantiomer). Using the two diastereomers of α -sulfinylphosphine **38**, conversions were also complete, however the asymmetric induction was very poor (less than 15% ee, in favour of the *R* enantiomer in both cases). It should be noted that, due to the rearrangement that **38** can suffer at room temperature to give **40** (see above), we cannot ensure that the ligand structure of **38** was preserved during the catalysis.



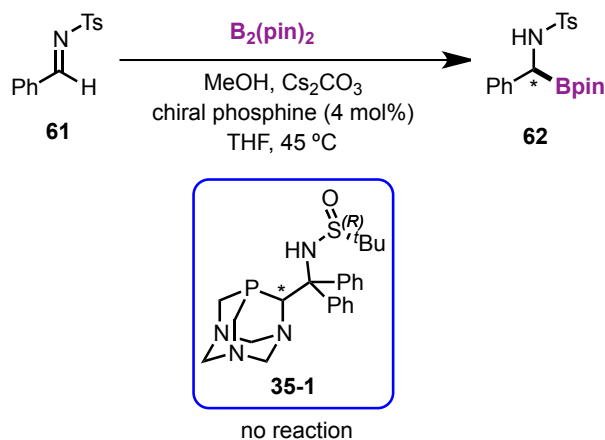
Scheme 4.27 Addition of $B_2(\text{pin})_2$ to N -Boc aldimine (**58**) using our PTA-based ligands. (a) The desired reaction product partially decomposes during chromatographic purification.

Fernández *et al.*^[64] provided an organocatalytic version to enantioselectively afford N -acyl- α -amino boronic esters. The nucleophilic boron addition to N -tosylaldimines was conducted in the presence of chiral phosphines as ligands (Scheme 4.28).



Scheme 4.28 Addition of $B_2(\text{pin})_2$ to N -tosylaldimines developed by Fernández *et al.*^[64]

With the conditions of this work, we tested also the performance of our PTA derivatives as organocatalysts (Scheme 4.29). Unfortunately, the process did not work.



Scheme 4.29 Organocatalysed addition of $\text{B}_2(\text{pin})_2$ to *N*-tosylaldimine **60**.

4.3 Summary and outlook

In this chapter, we have prepared the first enantiomerically pure PTA-based compounds. The PTA cage has been functionalised in the upper-rim methylene position, generating a stereogenic carbon centre in *alpha* position to the phosphorus atom. This ligand topology permit the mono- or bidentate coordination to a metal centre giving chiral metal-based catalytic precursors or the coordination to a substrate acting, in this case, as an organocatalyst.

The preparation of the enantiopure PTA-based β -phosphino alcohol (**26**) and β -phosphino sulfinamide (**35**) was successfully optimised obtaining both derivatives in good yields. The strategy to prepare both PTA-based derivatives consists on the selective lithiation of PTA to afford the nucleophilic PTA-Li that reacts with benzaldehyde or an enantiopure *tert*-butylsulfinylimine, respectively, to render the desired compounds.

The α -sulfinylphosphine PTA derivative (**38**) was also synthesised and fully characterised. In this case, the reaction outcome changed with respect to the previous imine. Whereas the addition of PTA-Li to an enantiopure *tert*-butylsulfinylimine proceeded on the C=N double bond, the addition to a *p*-tolylsulfinylimine went on the S=O moiety (nucleophilic addition plus elimination). We tried to optimise the preparation of this interesting PTA derivative using as electrophile enantiopure menthyl *p*-tolylsulfinate but the yields did not improve. Unfortunately, these compounds were found to be unstable, suffering from an unexpected rearrangement leading to a racemic thioether phosphine oxide (**40**), as we could prove by X-ray diffraction.

The cleavage of the *tert*-butylsulfinyl auxiliary group of β -phosphino sulfonamide (**35**) permitted the preparation of an enantiopure PTA-based primary aminophosphine (**42**) and from the last one, a PTA-based thiourea (**44**). These derivatives could be potential organocatalysts for asymmetric reactions. The preparation of both derivatives should be optimised in the future.

Although most of this part of the PhD project was devoted to the synthesis, we also tested the chiral PTA derivatives as ligands or organocatalysts in some model asymmetric transformations. The β -phosphino alcohols gave good conversions in the organocatalysed MBH reaction, however they did not induce enantioselectivity. *tert*-Butylsulfinyl PTA derivatives gave lower conversions in this reaction, probably due to the higher steric hindrance. The organocatalysed aziridination using our *tert*-butylsulfinyl PTA derivatives or the primary aminophosphine did not work. The α -amination reaction was tested using the *tert*-butylsulfinyl PTA derivatives as organocatalysts and also as ligands in the presence of a copper(II) salt. Good conversions were obtained in the last case, whereas the enantioselectivity was very low. It could be interesting in this case to carry out a screening of conditions and metal salts added as Lewis acids in order to improve the results. The alkylation of one 7-CF₃-substituted isatin worked only using one of the diastereomers of *tert*-butylsulfinyl PTA derivative leading to a racemic mixture. Finally, one of the most promising results was obtained in the Cu-catalysed hydroboration of *N*-Boc-protected imines using *tert*-butylsulfinyl PTA derivatives as ligands. This reaction should be studied deeply to try to improve the results.

Following our objective, that is to use these molecules in glycerol medium, solubility tests should be done in the future. If, like PTA, they are not soluble in this solvent, they could be *N*-alkylated as commented in the introduction in order to make them soluble by formation of the corresponding quaternary ammonium salts.

4.4 Experimental section

General

All manipulations were performed using standard Schlenk techniques under argon atmosphere unless otherwise noted.

Commercially available compounds (except benzaldehyde) were used without previous purification. Benzaldehyde was distilled prior to be used.

NMR spectra were recorded in CDCl₃ (unless otherwise cited) using a Fourier 300 MHz Bruker, a Bruker Avance 400 Ultrashield or a Bruker Avance 500 Ultrashield apparatus at 298 K. ¹H NMR (400 or 500 MHz) chemical shifts are quoted in ppm relative to tetramethylsilane (TMS). Chemical shifts are given in d and coupling constants in Hz. ¹³C NMR spectra (100 or 125 MHz) are decoupled from ¹H and the chemical shifts are quoted in ppm relative to CDCl₃ (d = 77.16). ³¹P NMR spectra (162 or 202 MHz) are decoupled from ¹H and the chemical shifts are quoted in ppm relative to 85% phosphoric acid in water.

Mass Spectrometry was measured on a Fisons V6-Quattro instrument, high resolution mass spectra by using electrospray ionisation (ESI) method were obtained on a Waters LCT Premier Instrument.

IR spectra were recorded on a Bruker Tensor 27 FT-IR spectrometer and are reported in wavenumbers (cm⁻¹). Neat samples were measured by using infrared spectroscopy under attenuated transmission reflectance (ATR) mode.

Flash chromatography was carried out using 60 (230–400 mesh) silica gel and dry-packed columns or with a Teledyne Isco CombiFlash[®] system equipped with UV detector. Thin layer chromatography was carried out using Merck TLC Silicagel 60 F254 aluminum sheets. Components were visualized by UV light (λ = 254 nm) and stained with KMnO₄, phosphomolybdic or cerium ammonium molybdate (CAM) dip.

High performance liquid chromatography (**HPLC**) was performed on Agilent Technologies chromatographs (Series 1100 and 1200), using columns with chiral stationary phases and guard columns. The next Daicel[®] chiral HPLC columns were used: IC, AD-H, AS-H.

GC analyses were carried out on an Agilent GC6890 with a flame ionization detector (FID) using Supelco[®] Beta-Dex 120 column.

Optical rotations were measured on a Jasco P-1030 polarimeter under ambient temperature by using sodium D line at 589 nm.

Melting points were measured in open capillaries on a Büchi B-540 instrument and are uncorrected.

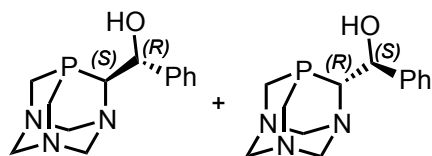
X-Ray Diffraction Analyses have been carried out on a Bruker-AXS APEX II Quazar diffractometer in the X-Ray service of Institut de Chimie de Toulouse and on a Bruker Kappa APEX II DUO diffractometer in the X-Ray Diffraction Unit of ICIQ.

Experimental procedures and characterization of organic compounds

Experimental procedure for the preparation of the β -phosphino alcohol PTA derivative

n-BuLi, 2.5 M solution in hexanes, (1.5 mL, 3.7 mmol) was syringed dropwise at room temperature over a suspension of dried PTA (589 mg, 3.7 mmol) in anhydrous THF (29 mL), over the course of 5 min under Ar atmosphere. The mixture was then left stirring for 5 h. After this period, a white solid corresponding to PTA–Li (highly pyrophoric) precipitated at the bottom of the Schlenk flask. A solution of freshly distilled benzaldehyde (0.25 mL, 2.5 mmol) in anhydrous THF (21 mL) was placed in a bath at -78 °C. The benzaldehyde solution was slowly syringed over the reaction mixture also cooled to -78 °C. The solution was stirred at this temperature for 15 min and after this time, the reaction was allowed to warm to room temperature and stirred overnight under Ar atmosphere. Afterwards, the reaction was warmed up at 0 °C and then, quenched with degassed water (1.3 mL) followed by stirring the solution for 1 h. The solvent was evaporated resulting in an orange and sticky solid. ^1H and ^{31}P NMR analyses of the crude mixture allowed determining the diastereomeric ratio to be 52:48. The crude product was purified by silica gel column chromatography (CombiFlash® system, 24 g SiO₂ cartridge, 1st eluent: 90:10 MeCN/EtOH, 2nd eluent: 80:20 MeCN/EtOH) affording 273 mg (41% isolated yield) of the first eluting diastereomer and 298 mg (45% isolated yield) of the second eluting diastereomer both as white and foamy solids.

The mixture was separated by preparative chiral supercritical fluid chromatography (SFC). Method: DAICEL Chiralcel OJ-H 5 μm (4.6 x 250) mm, *sc*CO₂/MeOH/HNEt₂ 90:10:0.1, 4 mL/min, 35 °C, 210 nm. The retention times were 2.0 min, 2.3 min, 3.6 min and 7.3 min. Starting from a racemic mixture of diastereomers of 560 mg, the separation afforded 59 mg of **(S,R)-26**, 29 mg of **(R,S)-26**, 44 mg of **(S,S)-26** and 77 mg of **(R,R)-26**.

**(S,R/R,S)-26****(R)--[(6S)-1,3,5-Triaza-7-phosphaadamantan-6-yl](phenyl)methanol****(S)--[(6R)-1,3,5-Triaza-7-phosphaadamantan-6-yl](phenyl)methanol**White solid; $R_f = 0.24$ (1:1 MeCN/EtOH); mp = 148.7–150.2 °C.

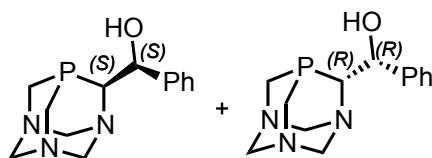
$^1\text{H NMR}$ (400 MHz, CDCl_3): δ 3.75–3.89 (m, 3H, PCH_N , $\text{PCH}_\text{aH}_\text{aN}$ and $\text{PCH}_\text{bH}_\text{bN}$), 4.09 (ddd, 1H, $^2J_{\text{HP}} = 14.3$, $^2J_{\text{HH}} = 11.8$ and $^4J_{\text{HH}} = 1.8$, $\text{PCH}_\text{aH}_\text{aN}$), 4.25 (dddd, 1H, $^2J_{\text{HP}} = 15.1$, $^2J_{\text{HH}} = 8.9$, $^4J_{\text{HH}} = 3.7$ and $^4J_{\text{HH}} = 1.6$, $\text{PCH}_\text{bH}_\text{bN}$), 4.37 (bd, 1H, $^2J_{\text{HH}} = 13.4$, $\text{NCH}_\text{aH}_\text{aN}$), 4.45 (ddd, 1H, $^2J_{\text{HH}} = 13.1$, $^4J_{\text{HH}} = 2.4$ and $^4J_{\text{HH}} = 2.4$, $\text{NCH}_\text{bH}_\text{bN}$), 4.42–4.46 (m, 2H, $\text{NCH}_\text{cH}_\text{cN}$ and $\text{NCH}_\text{cH}_\text{cN}$), 4.67 (dd, 1H, $^2J_{\text{HH}} = 13.1$ and $^4J_{\text{HH}} = 1.8$, $\text{NCH}_\text{bH}_\text{bN}$), 5.01 (ddd, 1H, $^2J_{\text{HH}} = 13.4$, $^4J_{\text{HH}} = 2.3$ and $^4J_{\text{HH}} = 2.3$, $\text{NCH}_\text{aH}_\text{aN}$), 5.23 (dd, 1H, $^3J_{\text{HH}} = 8.6$, $^3J_{\text{HP}} = 4.5$, CHOH), 7.30–7.51 (m, 5H, H_{Ar}).

$^{13}\text{C NMR}$ (125 MHz, CDCl_3): δ 48.4 (d, $^1J_{\text{CP}} = 24.0$, $\text{PCH}_\text{bH}_\text{bN}$), 51.5 (d, $^1J_{\text{CP}} = 19.9$, $\text{PCH}_\text{aH}_\text{aN}$), 65.7 (d, $^1J_{\text{CP}} = 23.6$, PCH_N), 67.8 (d, $^3J_{\text{CP}} = 3.5$, $\text{NCH}_\text{aH}_\text{aN}$), 74.0 (d, $^3J_{\text{CP}} = 2.6$, $\text{NCH}_\text{cH}_\text{cN}$), 76.7 ($\text{NCH}_\text{bH}_\text{bN}$), 77.9 (d, $^2J_{\text{CP}} = 6.7$, CHOH), 126.3 (d, $^4J_{\text{CP}} = 3.2$, $o\text{-CH}_{\text{Ar}}$), 128.0 (CH_{Ar}), 128.5 (CH_{Ar}), 143.1 (d, $^3J_{\text{CP}} = 1.8$, C_{Ar}).

$^{31}\text{P NMR}$ (162 MHz, CDCl_3): δ -100.3 (s).

IR absorption (neat): ν 3254 (O–H), 1600 ($\text{C}_{\text{Ar}}=\text{C}_{\text{Ar}}$).

HRMS (ESI $^+$): m/z $[\text{M}+\text{H}]^+$ calcd for $\text{C}_{13}\text{H}_{19}\text{N}_3\text{OP}$ 264.1260 found 264.1259.

**(S,S/R,R)-26****(S)--[(6S)-1,3,5-Triaza-7-phosphaadamantan-6-yl](phenyl)methanol****(R)--[(6R)-1,3,5-Triaza-7-phosphaadamantan-6-yl](phenyl)methanol**White solid; $R_f = 0.26$ (1:1 MeCN/EtOH)

$^1\text{H NMR}$ (400 MHz, CDCl_3): δ 3.63 (bdd, $^3J_{\text{HH}} = 11.0$ and $^2J_{\text{HP}} = 6.3$, 1H, PCH_N), 3.72 (dddd, 1H, $^2J_{\text{HP}} = 15.1$, $^2J_{\text{HH}} = 12.2$, $^4J_{\text{HH}} = 3.4$ and $^4J_{\text{HH}} = 2.1$, $\text{PCH}_\text{aH}_\text{aN}$), 3.90 (dddd, 1H, $^2J_{\text{HP}} = 15.3$, $^2J_{\text{HH}} = 10.7$, $^4J_{\text{HH}} = 2.2$ and $^4J_{\text{HH}} = 2.2$, $\text{PCH}_\text{bH}_\text{bN}$), 4.05 (ddd, 1H, $^2J_{\text{HP}} = 14.7$, $^2J_{\text{HH}} = 12.2$, and $^4J_{\text{HH}} = 1.9$, $\text{PCH}_\text{aH}_\text{aN}$), 4.04–4.17 (m, 1H, $\text{PCH}_\text{bH}_\text{bN}$), 4.45–4.59 (m, 3H, $\text{NCH}_\text{aH}_\text{aN}$, $\text{NCH}_\text{bH}_\text{bN}$ and $\text{NCH}_\text{cH}_\text{cN}$), 4.63 (bd, 1H, $^2J_{\text{HH}} = 13.4$, $\text{NCH}_\text{bH}_\text{bN}$), 4.79 (ddd, 1H, $^2J_{\text{HH}} = 13.7$, $^4J_{\text{HH}} = 2.4$ and $^4J_{\text{HH}} = 2.4$, $\text{NCH}_\text{aH}_\text{aN}$), 4.91 (bdd,

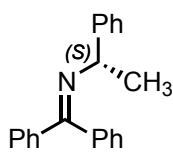
1H, $^2J_{\text{HH}} = 13.2$ and $^4J_{\text{HH}} = 1.5$, $\text{NCH}_c\text{H}_c\text{N}$), 5.18 (dd, 1H, $^3J_{\text{HH}} = 11.0$ and $^3J_{\text{HP}} = 3.5$, CHOH), 7.31–7.50 (m, 5H, H_{Ar})

^{13}C NMR (125 MHz, CDCl_3): δ 47.3 (d, $^1J_{\text{CP}} = 24.4$, $\text{PCH}_b\text{H}_b\text{N}$), 50.8 (d, $^1J_{\text{CP}} = 21.4$, $\text{PCH}_a\text{H}_a\text{N}$), 65.6 (d, $^1J_{\text{CP}} = 21.5$, PCHN), 66.4 (d, $^3J_{\text{CP}} = 2.7$, $\text{NCH}_a\text{H}_a\text{N}$), 71.5 (d, $^2J_{\text{CP}} = 15.1$, CHOH), 74.1 (d, $^3J_{\text{CP}} = 2.6$, $\text{NCH}_b\text{H}_b\text{N}$), 76.2 ($\text{NCH}_c\text{H}_c\text{N}$), 127.5 (d, $^4J_{\text{CP}} = 3.2$, $o\text{-CH}_{\text{Ar}}$), 128.3 (CH_{Ar}), 128.4 (CH_{Ar}), 140.4 (d, $^3J_{\text{CP}} = 1.7$, C_{Ar})

^{31}P NMR (162 MHz, CDCl_3): $\delta - 103.4$ (s).

IR absorption (neat): ν 3210 (O–H), 1601 and 1585 ($\text{C}_{\text{Ar}}=\text{C}_{\text{Ar}}$).

HRMS (ESI⁺): m/z $[\text{M}+\text{H}]^+$ calcd for $\text{C}_{13}\text{H}_{19}\text{N}_3\text{OP}$ 264.1260 found 264.1259.



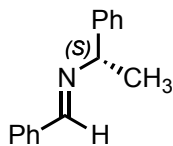
29

(S)-N-(Diphenylmethylene)-1-phenylethylamine

The product was prepared according to the literature procedure^[65] and isolated as an oil in 42% isolated yield (1.20 g, 4.20 mmol). The spectroscopic data matched with those reported in the literature.^[65]

^1H NMR (500 MHz, CDCl_3): δ 1.47 (d, $^3J_{\text{HH}} = 6.5$, 3H, CH_3), 4.54 (q, $^3J_{\text{HH}} = 6.5$, 1H, CH), 7.10–7.15 (m, 2H, H_{Ar}), 7.18–7.23 (m, 1H, H_{Ar}), 7.27–7.38 (m, 7H, H_{Ar}), 7.41–7.48 (m, 3H, H_{Ar}), 7.64–7.69 (m, 2H, H_{Ar}).

^{13}C NMR (125 MHz, CDCl_3): δ 25.0 (CH_3), 61.4 (CH), 126.5 (CH_{Ar}), 126.6 (CH_{Ar}), 127.7 (CH_{Ar}), 128.0 (CH_{Ar}), 128.3 (CH_{Ar}), 128.3 (CH_{Ar}), 128.4 (CH_{Ar}), 128.5 (CH_{Ar}), 129.8 (CH_{Ar}), 137.1 (C_{Ar}), 140.0 (C_{Ar}), 146.1 (C_{Ar}), 166.0 ($\text{C}=\text{N}$).



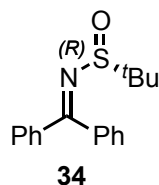
31

(S)-N-Benzylidene-1-phenylethylamine

The product was prepared according to the literature procedure^[66] and isolated as an oil in 99% yield (2.09 g, 9.98 mmol). The following spectroscopic data matched with those reported in the literature.^[66]

$^1\text{H NMR}$ (400 MHz, CDCl_3): δ 1.59 (d, $^3J_{\text{HH}} = 6.6$, 3H, CH_3), 4.54 (q, $^3J_{\text{HH}} = 6.6$, CH), 7.20–7.26 (m, 1H, H_{Ar}), 7.29–7.37 (m, 2H, H_{Ar}), 7.37–7.47 (m, 5H, H_{Ar}), 7.74–7.81 (m, 2H, H_{Ar}), 8.36 (s, 1H, $\text{CH}=\text{N}$).

$^{13}\text{C NMR}$ (100 MHz, CDCl_3): δ 25.0 (CH_3), 69.8 (CH), 126.8 (CH_{Ar}), 126.9 (CH_{Ar}), 128.4 (CH_{Ar}), 128.5 (CH_{Ar}), 128.6 (CH_{Ar}), 130.7 (CH_{Ar}), 136.6 (C_{Ar}), 145.3 (C_{Ar}), 159.6 ($\text{C}=\text{N}$).



(R)-N-(Diphenylmethylene)-tert-butylsulfonamide

The product was prepared according to the literature procedure^[22b] and isolated as a white-yellowish solid in 61% yield (2.89 g, 10.13 mmol).

$R_f = 0.24$ (1:4 EtOAc/cyclohexane); mp = 105.3–106.1 °C; $[\alpha]_{\text{D}}^{26} = -103.9$ (c 1.01, CHCl_3)

$^1\text{H NMR}$ (500 MHz, 328 K, CDCl_3): δ 1.33 (s, 9H, $t\text{Bu}$), 7.36–7.48 (m, 4H, H_{Ar}), 7.48–7.74 (m, 6H, H_{Ar}).

$^{13}\text{C NMR}$ (125 MHz, 328 K, CDCl_3): δ 22.3 [$\text{S}(=\text{O})\text{C}(\text{CH}_3)_3$], 56.8 [$\text{S}(=\text{O})\text{C}(\text{CH}_3)_3$], 128.1 (CH_{Ar}), 129.0 (CH_{Ar}), 130.8 (CH_{Ar}), 137.5 (C_{Ar}), 179.1 ($\text{C}=\text{N}$).

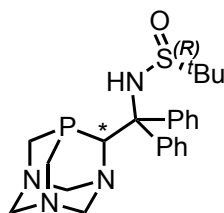
IR absorption (neat): ν 1584 ($\text{C}_{\text{Ar}}=\text{C}_{\text{Ar}}$), 1565 ($\text{C}=\text{N}$), 1087 and 1073 ($\text{S}=\text{O}$).

HRMS (ESI⁺): m/z [$\text{M}+\text{H}$]⁺ calcd for $\text{C}_{17}\text{H}_{20}\text{NOS}$ 286.1260, found 286.1258.

Experimental procedure for the preparation of the β -N-tert-butylsulfinyl PTA derivative

n-BuLi, 2.5 M solution in hexanes, (1.8 mL, 4.5 mmol) was syringed dropwise at room temperature over a suspension of dried PTA (707 mg, 4.5 mmol) in anhydrous THF (35 mL), over the course of 5 min under Ar atmosphere. The mixture was then left stirring for 5 h. After this period, a white solid corresponding to PTA–Li (highly pyrophoric) precipitated at the bottom of the Schlenk flask. To that suspension, a solution of dried chiral imine **34** (856 mg, 3 mmol) in anhydrous THF (26 mL) was slowly syringed at room temperature. The reaction mixture was stirred overnight at room temperature under Ar atmosphere. Afterwards, the reaction was cooled down at 0 °C and then, quenched with 1.5 mL of degassed water followed by stirring the solution for 1 h. The solvent was evaporated resulting in a yellowish and sticky solid. ^1H and ^{31}P NMR analyses of the crude mixture allowed determining the diastereomeric ratio to be 53:47. The crude product was purified by silica gel column chromatography (CombiFlash[®] system, 40 g SiO_2 cartridge, 1st eluent: MeCN, 2nd eluent: 90:10 MeCN/EtOH, 3rd eluent: 50:50 MeCN/EtOH)

affording 534 mg (40% isolated yield) of the 1st eluting diastereomer and 626 mg (47% isolated yield) of the 2nd eluting diastereomer both as white and foamy solids.



35-1

(R)-N-[(6S)-1,3,5-Triaza-7-phosphaadamantan-6-yl]diphenylmethyl-tert-butylsulfonamide

Foamy white solid; $R_f = 0.31$ (1:1 MeCN/EtOH); mp = 83.2–86.0 °C; $[\alpha]_D^{25} = -40.2$ (c 1.03, CHCl₃).

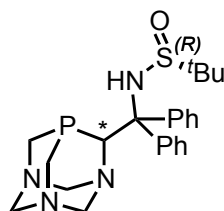
¹H NMR (400 MHz, CDCl₃): δ 1.08 (s, 9H, ^tBu), 3.18 (bdd, 1H, ²J_{HH} = 13.8 and ²J_{HP} = 13.8, PCH_aH_aN), 3.53 (bdd, 1H, ²J_{HH} = 13.8 and ²J_{HP} = 13.8, PCH_aH_aN), 3.66 (ddd, 1H, ²J_{HH} = 13.9, ⁴J_{HH} = 2.2 and ⁴J_{HH} = 2.2, NCH_aH_aN), 3.98-4.10 (m, 2H, NCH_aH_aN and PCH_bH_bN), 4.14 (ddd, 1H, ²J_{HH} = 14.1, ²J_{HP} = 14.1 and ⁴J_{HH} = 2.1, PCH_bH_bN), 4.36 (ddd, 1H, ²J_{HH} = 13.3, ⁴J_{HH} = 2.4 and ⁴J_{HH} = 2.4, NCH_bH_bN), 4.36 (bd, 1H, ²J_{HH} = 13.3, NCH_bH_bN), 4.71 (ddd, 1H, ²J_{HH} = 13.2, ⁴J_{HH} = 2.3 and ⁴J_{HH} = 2.3, NCH_cH_cN), 4.84 (bd, 1H, ²J_{HH} = 13.2, NCH_cH_cN), 4.88 (bs, 1H, PCHN), 5.88 (d, 1H, ⁴J_{HP} = 2.3, NH), 7.29-7.36 (m, 5H, H_{Ar}), 7.36-7.45 (m, 3H, H_{Ar}), 7.67-7.76 (m, 2H, H_{Ar}).

¹³C NMR (125 MHz, CDCl₃): δ 22.6 [S(=O)C(CH₃)₃], 47.1 (d, ¹J_{CP} = 25.7, PCH₂N), 52.9 (d, ¹J_{CP} = 21.5, PCH₂N), 56.3 [S(=O)C(CH₃)₃], 66.5 (d, ³J_{CP} = 3.0, NCH₂N), 67.0 (d, ¹J_{CP} = 26.0, PCHN), 69.6 (d, ²J_{CP} = 10.4, CPh₂), 74.4 (d, ³J_{CP} = 2.5, NCH₂N), 79.6 (s, NCH₂N), 127.9 (CH_{Ar}), 128.0 (CH_{Ar}), 128.1 (CH_{Ar}), 129.3 (CH_{Ar}), 130.21 (CH_{Ar}), 130.25 (CH_{Ar}), 142.2 (C_{Ar}), 142.7 (C_{Ar}).

³¹P NMR (162 MHz, CDCl₃): δ -97.5 (s).

IR absorption (neat): ν 3241 (N-H), 1599 (C_{Ar}=C_{Ar}), 1055 (S=O).

HRMS (ESI⁺): m/z [M+H]⁺ calcd for C₂₃H₃₂N₄OPS 443.2029, found 443.2034.



35-2

(R)-N-[(6R)-1,3,5-Triaza-7-phosphaadamantan-6-yl]diphenylmethyl-tert-butylsulfonamide

Foamy white solid; $R_f = 0.25$ (1:1 MeCN/EtOH); mp = 118.1–120.3 °C; $[\alpha]_D^{24} = -178.3$ (c 1.04, CHCl₃).

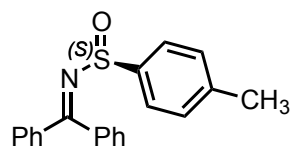
$^1\text{H NMR}$ (500 MHz, CDCl_3): δ 1.25 (s, 9H, ^tBu), 3.31 (bdd, 1H, $^2J_{\text{HH}} = 15.1$ and $^2J_{\text{HP}} = 9.9$, $\text{PCH}_\alpha\text{H}_\alpha\text{N}$), 3.51-3.62 (m, 2H, $\text{PCH}_\alpha\text{H}_\alpha\text{N}$ and $\text{NCH}_\alpha\text{H}_\alpha\text{N}$), 4.09-4.16 (m, 3H, $\text{PCH}_\beta\text{H}_\beta\text{N}$ and $\text{NCH}_\beta\text{H}_\beta\text{N}$), 4.38 (ddd, 1H, $^2J_{\text{HH}} = 13.2$, $^4J_{\text{HH}} = 2.1$ and $^4J_{\text{HH}} = 2.1$, $\text{NCH}_\beta\text{H}_\beta\text{N}$), 4.48 (bd, 1H, $^2J_{\text{HH}} = 13.2$, $\text{NCH}_\beta\text{H}_\beta\text{N}$), 4.74 (bd, 1H, $^2J_{\text{HH}} = 12.9$, $\text{NCH}_\gamma\text{H}_\gamma\text{N}$), 4.80 (ddd, 1H, $^2J_{\text{HH}} = 12.9$, $^4J_{\text{HH}} = 2.5$ and $^4J_{\text{HH}} = 2.5$, $\text{NCH}_\gamma\text{H}_\gamma\text{N}$), 5.06 (bs, 1H, PCHN), 6.33 (bs, NH), 7.29-7.41 (m, 8H, H_{Ar}), 7.43-7.54 (m, 2H, H_{Ar}).

$^{13}\text{C NMR}$ (100 MHz, CDCl_3): δ 23.0 [$\text{S(=O)C(CH}_3)_3$], 47.1 (d, $^1J_{\text{CP}} = 24.9$, PCH_2N), 52.7 (d, $^1J_{\text{CP}} = 19.9$, PCH_2N), 55.9 [$\text{S(=O)C(CH}_3)_3$], 65.2 (d, $^1J_{\text{CP}} = 30.0$, PCHN), 66.8 (d, $^3J_{\text{CP}} = 2.7$, NCH_2N), 67.7 (d, $^2J_{\text{CP}} = 6.6$, CPh_2), 74.5 (d, $^3J_{\text{CP}} = 2.2$, NCH_2N), 78.4 (s, NCH_2N), 127.6 (CH_{Ar}), 127.9 (CH_{Ar}), 128.1 (CH_{Ar}), 128.3 (CH_{Ar}), 130.3 (CH_{Ar}), 130.4 (x 2; CH_{Ar}), 140.9 (C_{Ar}), 145.9 (C_{Ar}).

$^{31}\text{P NMR}$ (202 MHz, CDCl_3): δ -90.1 (s).

IR absorption (neat): ν 3162 (N-H), 1597 ($\text{C}_{\text{Ar}}=\text{C}_{\text{Ar}}$), 1056 (S=O).

HRMS (ESI $^+$): m/z [$\text{M}+\text{H}$] $^+$ calcd for $\text{C}_{23}\text{H}_{32}\text{N}_4\text{OPS}$ 443.2029, found 443.2038.



37

(S)-N-(Diphenylmethylene)-p-tolylsulfonamide

The product was prepared according to the literature procedure^[67] and isolated as a white solid in 28% yield (579 mg, 1.81 mmol). The spectroscopic data matched with those reported in the literature.^[68]

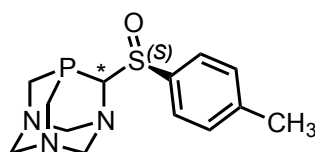
$^1\text{H NMR}$ (500 MHz, CDCl_3): δ 2.38 (s, 3H, CH_3), 7.14–7.30 (m, 3H, H_{Ar}), 7.31–7.58 (m, 7H, H_{Ar}), 7.58–7.62 (m, 2H, H_{Ar}), 7.63–7.89 (m, 2H, H_{Ar}).

$^{13}\text{C NMR}$ (100 MHz, CDCl_3): δ 21.6 (CH_3), 125.4 (CH_{Ar}), 128.3 (CH_{Ar}), 128.4 (CH_{Ar}), 129.8 (CH_{Ar}), 130.0 (CH_{Ar}), 142.3 (x2, C_{Ar}), 143.9 (C_{Ar}), 176.1 ($\text{C}=\text{N}$).

Experimental procedure for the preparation of the α -p-tolylsulfinyl PTA derivative

n-BuLi, 2.5 M solution in hexanes, (1.8 mL, 4.5 mmol) was syringed dropwise at room temperature over a suspension of dried PTA (707 mg, 4.5 mmol) in anhydrous THF (35 mL), over the course of 5 min under Ar atmosphere. The mixture was then left stirring for 5 h. After this period, a white solid corresponding to PTA–Li (highly pyrophoric) precipitated at the bottom of the Schlenk flask. To that suspension, a solution of dried (1*R*,2*S*,5*R*)-menthyl (*S*)-*p*-toluenesulfinate (883 mg, 3.0 mmol) in anhydrous THF (26 mL) was slowly syringed at room temperature. The reaction mixture was stirred overnight at room temperature under Ar

atmosphere. Afterwards, the reaction was cooled down at 0 °C and then, quenched with degassed water (1.5 mL) followed by stirring the solution for 1 h. The solvent was evaporated resulting in a yellowish and sticky solid. ^1H and ^{31}P NMR analyses of the crude mixture allowed determining the diastereomeric ratio to be 79:21. The crude product was purified by silica gel column chromatography (CombiFlash® system, 40 g SiO_2 cartridge, 1st eluent: MeCN, 2nd eluent: 90:10 MeCN/EtOH, 3rd eluent: 85:15 MeCN/EtOH) affording 188 mg (21% isolated yield) of the first eluting diastereomer and 77 mg (9% isolated yield) of the second eluting diastereomer both as white and foamy solids.



38-1

(S)-6-[(S)-p-Tolylsulfinyl]-1,3,5-triaza-7-phosphaadamantane

White solid; $R_f = 0.27$ (1:1 MeCN/EtOH); mp = 64.7–66.8 °C (decomp.); $[\alpha]_D^{25} = -81.8$ (c 0.87, CHCl_3).

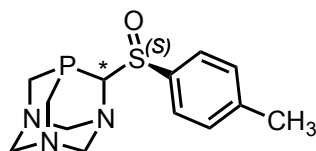
^1H NMR (500 MHz, CDCl_3): δ 2.43 (s, 3H, CH_3), 3.74–3.83 (m, 1H, $\text{PCH}_a\text{H}_a\text{N}$), 3.84–3.93 (m, 1H, $\text{PCH}_b\text{H}_b\text{N}$), 4.16 (ddd, 1H, $^2J_{\text{HP}} = 16.6$, $^2J_{\text{HH}} = 14.5$ and $^4J_{\text{HH}} = 2.2$, $\text{PCH}_a\text{H}_a\text{N}$), 4.42 (ddd, 1H, $^2J_{\text{HH}} = 13.3$, $^4J_{\text{HH}} = 2.4$ and $^4J_{\text{HH}} = 2.4$, $\text{NCH}_a\text{H}_a\text{N}$), 4.50 (ddd, 1H, $^2J_{\text{HH}} = 13.3$, $^4J_{\text{HH}} = 2.2$ and $^4J_{\text{HH}} = 2.2$, $\text{NCH}_b\text{H}_b\text{N}$), 4.52–4.63 (m, 3H, $\text{NCH}_b\text{H}_b\text{N}$, $\text{NCH}_c\text{H}_c\text{N}$ and $\text{PCH}_b\text{H}_b\text{N}$), 4.75 (bd, 1H, $^2J_{\text{HP}} = 7.4$, PCHN), 4.79 (bdd, 1H, $^2J_{\text{HH}} = 13.3$ and $^4J_{\text{HH}} = 2.0$, $\text{NCH}_a\text{H}_a\text{N}$), 5.33 (ddd, 1H, $^2J_{\text{HH}} = 13.7$, $^4J_{\text{HH}} = 2.5$ and $^4J_{\text{HH}} = 2.5$, $\text{NCH}_c\text{H}_c\text{N}$), 7.31–7.39 (m, 2H, $m\text{-H}_{\text{Ar}}$), 7.58–7.64 (m, 2H, $o\text{-H}_{\text{Ar}}$).

^{13}C NMR (125 MHz, CDCl_3): δ 21.5 (CH_3), 48.8 (d, $^1J_{\text{CP}} = 24.7$, $\text{PCH}_b\text{H}_b\text{N}$), 51.9 (d, $^1J_{\text{CP}} = 23.2$, $\text{PCH}_a\text{H}_a\text{N}$), 68.8 (d, $^3J_{\text{CP}} = 2.8$, $\text{NCH}_c\text{H}_c\text{N}$), 73.6 (d, $^3J_{\text{CP}} = 2.6$, $\text{NCH}_b\text{H}_b\text{N}$), 76.8 ($\text{NCH}_a\text{H}_a\text{N}$), 86.9 (d, $^1J_{\text{CP}} = 39.5$, PCHN), 124.5 (d, $^4J_{\text{CP}} = 2.3$, $o\text{-CH}_{\text{Ar}}$), 129.8 ($m\text{-CH}_{\text{Ar}}$), 139.1 (d, $^3J_{\text{CP}} = 1.9$, $\text{C}_{\text{Ar}}\text{-S}$), 141.8 ($\text{C}_{\text{Ar}}\text{-CH}_3$).

^{31}P NMR (202 MHz, CDCl_3): δ -106.1 (s).

IR absorption (neat): ν 1595 ($\text{C}_{\text{Ar}}=\text{C}_{\text{Ar}}$), 1032 and 1011 (S=O).

HRMS (ESI $^+$): m/z $[\text{M}+\text{Na}]^+$ calcd for $\text{C}_{13}\text{H}_{18}\text{N}_3\text{NaOPS}$ 318.0800, found 318.0815.



38-2

(R)-6-[(S)-p-Tolylsulfinyl]-1,3,5-triaza-7-phosphaadamantane

White solid; $R_f = 0.22$ (1:1 MeCN/EtOH); mp = 87.6–89.7 °C (decomp.); $[\alpha]_D^{25} = +146.5$ (c 0.97, CHCl₃).

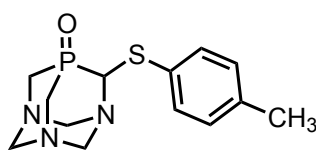
¹H NMR (500 MHz, CDCl₃): δ 2.44 (s, 3H, CH₃), 3.79–3.87 (m, 1H, PCH_aH_aN), 3.93 (dddd, 1H, ²J_{HP} = 15.0, ²J_{HH} = 12.6, ⁴J_{HH} = 2.2 and ⁴J_{HH} = 2.2, PCH_bH_bN), 4.15 (ddd, 1H, ²J_{HP} = 16.5, ²J_{HH} = 14.1 and ⁴J_{HH} = 2.2, PCH_aH_aN), 4.28–4.36 (m, 1H, PCH_bH_bN), 4.44 (ddd, ²J_{HH} = 13.5, ⁴J_{HH} = 2.3 and ⁴J_{HH} = 2.3, NCH_aH_aN), 4.50–4.57 (m, 2H, NCH_bH_bN and NCH_cH_cN), 4.60 (bd, 1H, ²J_{HH} = 13.5, NCH_bH_bN), 4.73 (bd, 1H, ²J_{HP} = 6.7, PCHN), 4.85 (dd, 1H, ²J_{HH} = 13.5 and ⁴J_{HH} = 1.8, NCH_aH_aN), 5.19 (ddd, 1H, ²J_{HH} = 13.9, ⁴J_{HH} = 2.4 and ⁴J_{HH} = 2.4, NCH_cH_cN), 7.32–7.40 (m, 2H, *m*-H_{Ar}), 7.61–7.68 (m, 2H, *o*-H_{Ar}).

¹³C NMR (125 MHz, CDCl₃): δ 21.6 (CH₃), 47.8 (d, ¹J_{CP} = 23.5, PCH_bH_bN), 51.5 (d, ¹J_{CP} = 24.3, PCH_aH_aN), 68.3 (d, ³J_{CP} = 2.8, NCH_cH_cN), 73.6 (d, ³J_{CP} = 2.8, NCH_bH_bN), 76.5 (NCH_aH_aN), 83.9 (d, ¹J_{CP} = 34.9, PCHN), 125.8 (d, ⁴J_{CP} = 3.7, *o*-CH_{Ar}), 129.8 (*m*-CH_{Ar}), 137.5 (d, ³J_{CP} = 3.5, C_{Ar}-S), 142.4 (C_{Ar}-CH₃).

³¹P NMR (202 MHz, CDCl₃): δ -102.6 (s).

IR absorption (neat): ν 1595 (C_{Ar}=C_{Ar}), 1032 and 1012 (S=O).

HRMS (ESI⁺): m/z [M+Na]⁺ calcd for C₁₃H₁₈N₃NaOPS 318.0800, found 318.0793.



40

6-(p-Tolylthio)-1,3,5-triaza-7-phosphaadamantane 7-oxide

Obtained during the crystallisation process (slow evaporation of a dichloromethane solution) as a white-yellowish solid.

$[\alpha]_D^{26} = -29.3$ (c 1.00, CHCl₃).

¹H NMR (400 MHz, CDCl₃): δ 2.33 (s, 3H, CH₃), 3.70–3.84 (m, 2H, PCH_aH_aN and PCH_bH_bN), 3.94 (ddd, 1H, ²J_{HP} = 15.3, ²J_{HH} = 8.5 and ⁴J_{HH} = 2.1, PCH_aH_aN), 4.03–4.20 (m, 4H, PCH_bH_bN, NCH_aH_aN, NCH_bH_bN and NCH_cH_cN), 4.38 (bd, 1H, ²J_{HH} = 13.8, NCH_aH_aN), 4.51 (dd, 1H, ²J_{HH} = 13.8 and ⁴J_{HH} =

1.8, $\text{NCH}_b\text{H}_b\text{N}$), 4.94 (ddd, 1H, $^2J_{\text{HH}} = 14.0$, $^4J_{\text{HH}} = 2.5$ and $^4J_{\text{HH}} = 2.5$, $\text{NCH}_c\text{H}_c\text{N}$), 5.14 (dd, 1H, $^2J_{\text{HP}} = 10.6$ and $^4J_{\text{HH}} = 3.0$, PCHN), 7.10–7.16 (m, 2H, H_{Ar}), 7.43–7.48 (m, 2H, H_{Ar}).

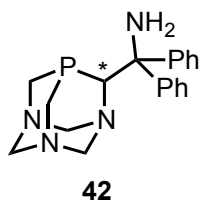
^{13}C NMR (125 MHz, CDCl_3): δ 21.2 (CH_3), 53.1 (d, $^1J_{\text{CP}} = 53.2$, $\text{PCH}_a\text{H}_a\text{N}$), 56.7 (d, $^1J_{\text{CP}} = 48.9$, $\text{PCH}_b\text{H}_b\text{N}$), 65.2 (d, $^3J_{\text{CP}} = 10.6$, $\text{NCH}_c\text{H}_c\text{N}$), 72.9 (d, $^3J_{\text{CP}} = 9.1$, $\text{NCH}_a\text{H}_a\text{N}$), 73.1 (d, $^1J_{\text{CP}} = 46.6$, PCHN), 73.9 (d, $^3J_{\text{CP}} = 6.7$, $\text{NCH}_b\text{H}_b\text{N}$), 130.0 (CH_{Ar}), 132.7 (CH_{Ar}), 138.5 (x2, C_{Ar}).

^{31}P NMR (162 MHz, CDCl_3): δ -7.00 (s).

Experimental procedure for the preparation of primary β -aminophosphine PTA derivative

HCl, 4 M solution in 1,4-dioxane, (0.1 mL, 0.36 mmol) was syringed dropwise under Ar atmosphere over a solution of **35-2** in anhydrous MeOH (1.2 mL) previously cooled down to 0 °C. The mixture was then left stirring for 3 h allowing the solution to reach room temperature. The solvent was evaporated resulting in a white solid. This solid was diluted in water (4 mL) and the solution was washed with Et_2O (3 x 5 mL) in order to eliminate the methyl *tert*-butylsulfinate generated as reaction byproduct. The water was eliminated under reduced pressure affording the corresponding hydrochloride **41** as a white solid. ^1H and ^{31}P NMR analyses in $\text{MeOH}-d_4$ allowed determining the formation of this species.

The hydrochloride **41** was dissolved in anhydrous MeOH (2 mL) under Ar atmosphere. PS-DBU, polymer-bound 1.8 mmol/g, (0.55 mmol, 303 mg) was placed in another Schlenk flask equipped with a stirring bar and anhydrous CH_2Cl_2 (2 mL) was added over it. The corresponding suspension was stirred 5 min at room temperature. The hydrochloride solution was syringed dropwise over the PS-DBU suspension and the mixture was stirred for 4 h at room temperature. The solution was filtered with a cannula washing the PS-DBU with anhydrous CH_2Cl_2 (3 x 2 mL). The solvent was evaporated and the corresponding primary amine **42** was obtained as a foamy white solid.



[(6S)-1,3,5-Triaza-7-phosphaadamantan-6-yl]diphenylmethanamine

Isolated in around 86% chemical purity.

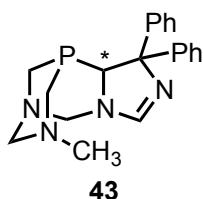
^1H NMR (400 MHz, CDCl_3): δ 2.35 (bd, 2H, NH_2), 3.42–3.53 (m, 1H, $\text{PCH}_a\text{H}_a\text{N}$), 3.56–3.66 (m, 1H, $\text{PCH}_a\text{H}_a\text{N}$), 4.01 (dddd, 1H, $^2J_{\text{HP}} = 14.8$, $^2J_{\text{HH}} = 9.6$, $^4J_{\text{HH}} = 1.7$ and $^4J_{\text{HH}} = 1.7$, $\text{PCH}_b\text{H}_b\text{N}$), 4.08–4.18 (m, 2H, $\text{PCH}_b\text{H}_b\text{N}$ and $\text{NCH}_a\text{H}_a\text{N}$), 4.31–4.42 (m, 2H, $\text{NCH}_a\text{H}_a\text{N}$ and $\text{NCH}_b\text{H}_b\text{N}$), 4.47 (bd, 1H, $^2J_{\text{HH}} =$

13.1, $\text{NCH}_b\text{H}_b\text{N}$), 4.51–4.55 (m, 1H, PCHN), 4.61 (ddd, 1H, $^2J_{\text{HH}} = 13.1$, $^4J_{\text{HH}} = 2.4$ and $^4J_{\text{HH}} = 2.4$, $\text{NCH}_c\text{H}_c\text{N}$), 4.77 (d, 1H, $^2J_{\text{HH}} = 13.1$, $\text{NCH}_c\text{H}_c\text{N}$), 7.18–7.40 (m, 8H, H_{Ar}), 7.45–7.52 (m, 2H, H_{Ar}).

^{13}C NMR (100 MHz, CDCl_3): δ 47.9 (d, $^1J_{\text{CP}} = 25.1$, $\text{PCH}_a\text{H}_a\text{N}$), 52.9 (d, $^1J_{\text{CP}} = 20.1$, $\text{PCH}_b\text{H}_b\text{N}$), 64.9 (d, $^2J_{\text{CP}} = 8.2$, CPh_2), 66.6 (d, $^1J_{\text{CP}} = 25.9$, PCHN), 67.0 ($\text{NCH}_a\text{H}_a\text{N}$), 74.6 ($\text{NCH}_b\text{H}_b\text{N}$), 79.4 ($\text{NCH}_c\text{H}_c\text{N}$), 126.9 (CH_{Ar}), 127.1 (CH_{Ar}), 127.6 (CH_{Ar}), 127.9 (CH_{Ar}), 128.1 (CH_{Ar}), 128.5 (CH_{Ar}), 147.4 (C_{Ar}) 147.9 (C_{Ar}).

^{31}P NMR (162 MHz, CDCl_3): δ -94.5 (s).

IR absorption (neat): ν 3346 and 3281 (N–H), 1597 and 1579 ($\text{C}_{\text{Ar}}=\text{C}_{\text{Ar}}$).



(S)-3-Methyl-10,10-diphenyl-2,3,4,6,10,10a-hexahydro-1,5-methanoimidazo[1,5-e][1,3,5,7]triazaphosphocine

Isolated in around 95% chemical purity.

^1H NMR (400 MHz, CDCl_3): δ 1.95 (s, 3H, NCH_3), 2.24 (ddd, 1H, $^2J_{\text{HP}} = 15.9$, $^2J_{\text{HH}} = 14.8$ and $^4J_{\text{HH}} = 1.6$, $\text{PCH}_a\text{H}_a\text{N}$), 2.50–2.60 (m, 1H, $\text{PCH}_a\text{H}_a\text{N}$), 3.30–3.36 (m, 1H, $\text{NCH}_a\text{H}_a\text{N}$), 3.43–3.51 (m, 1H, $\text{PCH}_b\text{H}_b\text{N}$), 3.59 (ddd, 1H, $^2J_{\text{HP}} = 15.4$, $^2J_{\text{HH}} = 9.8$ and $^4J_{\text{HH}} = 2.5$, $\text{PCH}_b\text{H}_b\text{N}$), 3.91 (d, 1H, $^2J_{\text{HH}} = 11.7$, $\text{NCH}_a\text{H}_a\text{N}$), 4.75 (d, 1H, $^2J_{\text{HH}} = 13.8$, $\text{NCH}_b\text{H}_b\text{N}$), 4.99 (d, 1H, $^2J_{\text{HH}} = 13.8$, $\text{NCH}_b\text{H}_b\text{N}$), 5.10 (bd, 1H, $^2J_{\text{HP}} = 20.5$, PCHN), 7.19–7.38 (m, 6H, H_{Ar}), 7.46–7.53 (m, 2H, H_{Ar}), 7.54–7.60 (m, 2H, H_{Ar}), 7.84 (s, 1H, NCHN).

^{13}C NMR (100 MHz, CDCl_3): δ 45.1 (d, $^3J_{\text{CP}} = 2.2$, NCH_3), 47.2 (d, $^1J_{\text{CP}} = 17.0$, $\text{PCH}_b\text{H}_b\text{N}$), 50.1 (d, $^1J_{\text{CP}} = 22.9$, $\text{PCH}_a\text{H}_a\text{N}$), 64.9 (d, $^1J_{\text{CP}} = 33.9$, PCHN), 67.0 ($\text{NCH}_b\text{H}_b\text{N}$), 76.9 ($\text{NCH}_a\text{H}_a\text{N}$), 80.1 (CPh_2), 126.0 (x 2, CH_{Ar}), 127.7 (d, $^5J_{\text{CP}} = 4.2$, $o\text{-CH}_{\text{Ar}}$), 128.2 (CH_{Ar}), 128.5 (d, $^5J_{\text{CP}} = 3.2$, $o\text{-CH}_{\text{Ar}}$), 128.7 (CH_{Ar}), 141.4 (C_{Ar}), 145.9 (C_{Ar}), 155.6 (NCHN).

^{31}P NMR (162 MHz, CDCl_3): δ -70.3 (s).

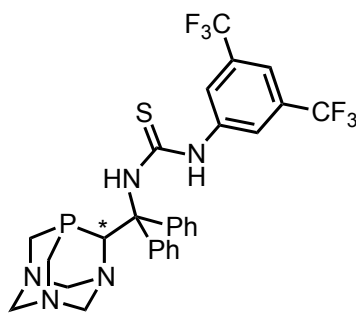
IR absorption (neat): ν 1597 (C=N), 1576 ($\text{C}_{\text{Ar}}=\text{C}_{\text{Ar}}$).

HRMS (ESI⁺): m/z $[\text{M}+\text{H}]^+$ calcd for $\text{C}_{20}\text{H}_{24}\text{N}_4\text{P}$ 351.1733, found 351.1729.

Experimental procedure for the preparation of the thiourea PTA derivative

The primary amine was dissolved in anhydrous CH_2Cl_2 (1 mL) under Ar atmosphere. 3,5-Bis(trifluoromethyl)phenyl isothiocyanate was added dropwise at room temperature. The

reaction mixture was stirred overnight. After this period, the solvent was evaporated. The crude product was purified by silica gel column chromatography (CombiFlash® system, 4 g SiO₂ cartridge, 1st eluent: MeCN, 2nd eluent: 90:10 MeCN/EtOH, 3rd eluent: 50:50 MeCN/EtOH) affording 8 mg (7% isolated yield) of the desired product as white and foamy solid.



45

1-[(6S)-1,3,5-Triaza-7-phosphaadamantan-6-yl]diphenylmethyl-3-[3,5-bis(trifluoromethyl)phenyl]thiourea

White solid; R_f = 0.46 (1:1 MeCN/EtOH); mp = 107.6–109.5 °C; $[\alpha]_D^{25}$ = –36.5 (c 0.40, CHCl₃).

¹H NMR (400 MHz, CDCl₃): δ 3.33–3.44 (m, 1H, PCH_aH_aN), 3.48–3.63 (m, 2H, PCH_aH_aN and NCH_aH_aN), 3.77–3.87 (m, 1H, PCH_bH_bN), 4.07 (ddd, 1H, ²J_{HP} = 14.6, ²J_{HH} = 14.6 and ⁴J_{HH} = 1.5, PCH_bH_bN), 4.15 (bd, 1H, ²J_{HH} = 13.8, NCH_aH_aN), 4.35 (bd, 1H, ²J_{HH} = 13.2, NCH_bH_bN), 4.48 (bd, 1H, ²J_{HH} = 13.2, NCH_bH_bN), 4.56–4.61 (m, 1H, PCHN), 4.73 (ddd, 1H, ²J_{HH} = 13.3, ⁴J_{HH} = 2.2 and ⁴J_{HH} = 2.2, NCH_cH_cN), 4.92 (bd, 1H, ²J_{HH} = 13.3, NCH_cH_cN), 6.75 (s, 1H, NH), 7.27–7.32 (m, 2H, CH_{Ar}), 7.48–7.70 (m, 7H, CH_{Ar}), 7.82–7.96 (m, 4H, CH_{Ar}), 8.90 (s, 1H, NH).

¹³C NMR (100 MHz, CDCl₃): δ 47.5 (d, ¹J_{CP} = 25.1, PCH_aH_aN), 53.1 (d, ¹J_{CP} = 20.1, PCH_bH_bN), 66.0 (d, ³J_{CP} = 3.0, NCH_aH_aN), 69.8 [(d, ²J_{CP} = 12, C(Ph)₂], 71.2 (d, ¹J_{CP} = 28.5, PCHN), 74.4 (d, ³J_{CP} = 2.0, NCH_bH_bN), 79.4 (NCH_cH_cN), 118.9 (sept, ³J_{CF} = 3.8, CH_{Ar}), 122.8 (q, ¹J_{CF} = 272.7, CF₃), 123.9–124.1 (m, CH_{Ar}), 128.5 (CH_{Ar}), 129.2 (CH_{Ar}), 129.3 (d, ⁴J_{CP} = 7.7, CH_{Ar}), 129.4 (CH_{Ar}), 129.7 (CH_{Ar}), 130.1 (CH_{Ar}), 131.4 (q, ²J_{CF} = 33.6, C-CF₃), 135.1 (C_{Ar}), 139.7 (C_{Ar}), 140.2 (d, ³J_{CP} = 2.1, C_{Ar}), 179.8 (C=S).

³¹P NMR (162 MHz, CDCl₃): δ –96.4 (s).

¹⁹F NMR (376 MHz, CDCl₃): δ –63.2 (s).

IR absorption (neat): ν 3344 and 3245 (N–H), 1274 (C=S), 1171 and 1126 (C–F).

HRMS (ESI⁺): m/z [M+H]⁺ calcd for C₂₈H₂₇F₆N₅PS 610.1623, found 610.1625.

Experimental procedure for the Morita-Baylis-Hillman reaction^[31a]

A solution of the corresponding PTA-based organocatalyst (15 mol%) and 4-nitrobenzaldehyde (**46**; 37.8 mg, 0.250 mmol) in THF (0.50 mL) under inert atmosphere was prepared inside a Schlenck tube containing a stirring bar. Methyl vinyl ketone (**47**; 61 μ L, 0.750 mmol) was syringed over the previous solution under stirring at rt. The reaction mixture was stirred at rt. After 17 h, the reaction mixture was concentrated under reduced pressure.

Chiral HPLC analysis [Daicel Chiralpak IC, 95:5 *n*-hexane/2-propanol, 1.0 mL/min, 220 and 254 nm, t_R (1st enantiomer) = 28.8 min, t_R (2nd enantiomer) = 31.0 min] allowed determining the enantioselectivity for desired MBH adduct.

Experimental procedure for the aziridination reaction^[46b]

A suspension of PTA-based organocatalyst (10 mol%), sodium acetate (3 equiv. or 5 equiv.) and *tert*-butyl *N*-(tosyloxy)carbamate (**50**; 52 mg, 0.181 mmol) in CH₂Cl₂ (0.6 mL) under inert atmosphere was prepared inside a Schlenck tube containing a stirring bar. *trans*-2-Hexenal (**49**; 42.0 μ L, 0.362 mmol) was added over the previous suspension under smooth stirring at rt. The reaction mixture was stirred smoothly at rt. After 7 h at rt the reaction mixture was diluted with CH₂Cl₂ (20 mL) and was washed with water (20 mL). After separation of phases the aqueous phase was further extracted with CH₂Cl₂ (1 x 20 mL). The combined organic layers were dried over anhydrous Na₂SO₄, filtered and concentrated under reduced pressure. ¹H NMR analysis of the crude mixture allowed determining the diastereomeric *trans/cis* ratio of the aziridination product.

Chiral GC analysis [Supelco Beta-Dex 120, isothermal 100 °C, *trans* diastereomer: t_R (1st enantiomer) = 74.6 min, t_R (2nd enantiomer) = 77.5 min] allowed determining the enantioselectivity for the major *trans*-aziridine.

Experimental procedure for the organocatalysed α -amination reaction^[53d]

A solution of the corresponding PTA-based organocatalyst (5 mol%) in toluene (0.60 mL) under inert atmosphere was prepared inside a Schlenck tube containing a stirring bar. Ethyl 2-oxocyclopentane-1-carboxylate (**52**; 24 μ L, 0.160 mmol) was added over the previous solution under stirring at rt followed by addition of di-*tert*-butyl azodicarboxylate (**53**; 55.3 mg, 0.240 mmol) in one portion as a solid. The reaction mixture was stirred at rt. After 21 h at rt the reaction mixture was concentrated under reduced pressure.

Chiral HPLC analysis [Daicel Chiralpak AD-H, 95:5 *n*-hexane/2-propanol, 1.0 mL/min, 210 nm, t_R (1st enantiomer) = 10.6 min, t_R (2nd enantiomer) = 18.7 min] allowed determining the enantioselectivity for desired α -amination product.

Experimental procedure for Cu-catalysed α -amination reaction^[53a]

A solution of $\text{Cu}(\text{OTf})_2$ (2.89 mg, 0.008 mmol) and PTA-based ligand (5.5 mol%) in CH_2Cl_2 (1.0 mL) under inert atmosphere was prepared inside a Schlenck tube containing a stirring bar and stirred for 30 min at rt. Ethyl 2-oxocyclopentane-1-carboxylate (**52**; 24 μL , 0.160 mmol) was added over the previous light blue solution under stirring at rt. A dark yellow solution of di-*tert*-butyl azodicarboxylate (**53**; 44.2 mg, 0.192 mmol) in CH_2Cl_2 (0.5 mL) was then added into the reaction mixture and the solution was stirred at rt. After 26 h the reaction mixture was concentrated under reduced pressure.

Chiral HPLC analysis [Daicel Chiralpak AD-H, 95:5 *n*-hexane/2-propanol, 1.0 mL/min, 210 nm, t_R (1st enantiomer) = 10.6 min, t_R (2nd enantiomer) = 18.7 min] allowed determining the enantioselectivity for desired α -amination product.

Experimental procedure for the addition of terminal alkynes to isatins^[59]

A mixture of CuI (1.9 mg, 0.01 mmol) and PTA-based ligand (6 mol%) in *tert*-butyl methyl ether ($t\text{BuOMe}$) (0.5 mL) was prepared under Ar atmosphere and the mixture was stirred at rt for 30 min. Then, the corresponding isatin (**55** or **56**; 0.2 mmol), phenylacetylene (**13**; 23 μL , 0.21 mmol) and triethylamine (56 μl , 0.4 mmol) were added to the mixture, followed by 0.5 mL more of $t\text{BuOMe}$. The mixture was stirred at 40 °C. After 24 h, the mixture was cooled to rt and passed through a short column of Celite® with EtOAc as eluent. The solvent was evaporated under reduced pressure.

Chiral HPLC analysis [Daicel Chiralpak AD-H, 90:10 *n*-hexane/2-propanol, 0.9 mL/min, 254 nm, t_R (1st enantiomer) = 15.6 min, t_R (2nd enantiomer) = 25.0 min] allowed determining the enantioselectivity for desired product.

Experimental procedure for the Cu-catalysed hydroboration of *N*-Boc-protected imines^[25k]

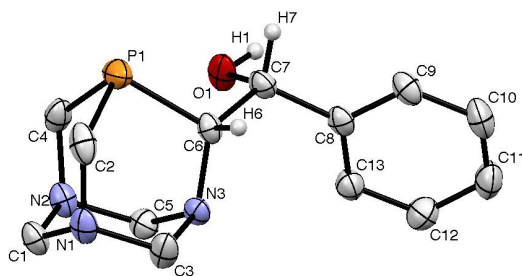
A Schlenk tube containing a stirring bar was charged with CuCl (1.9 mg, 0.02 mmol), PTA-based ligand (12 mol%), KO^tBu (2.69 mg, 0.024 mmol) and $t\text{BuOMe}$ (0.6 mL). The mixture was stirred for 30 min at rt under Ar atmosphere. Then, a solution of B_2pin_2 in $t\text{BuOMe}$ (0.4 mL) and a

solution of *N*-Boc aldimine **59** in *t*BuOMe (0.4 mL) were added successively. The reaction mixture was stirred at rt. After 16 h, the reaction mixture was passed through a short column of Celite® with EtOAc as eluent. The solvent was evaporated under reduced pressure. The product was isolated by rapid silica gel chromatography on deactivated silica gel (35 wt% H₂O, prepared by mixing vigorously silica gel and deionized water in a 65:35 ratio by weight) using a mixture 95:5 cyclohexane/EtOAc. The TLCs were revealed with CAM. *The product suffers partial decomposition during the purification.*

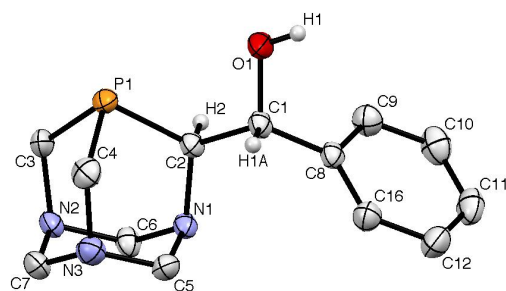
Chiral HPLC analysis [Daicel Chiralpak AS-H, 98:2 *n*-hexane/2-propanol, 0.5 mL/min, 254 nm, 220 nm, 210 nm, *t*_R(1st enantiomer) = 10.6 min, *t*_R(2nd enantiomer) = 14.4 min] allowed determining the enantioselectivity for desired product.

Experimental procedure for the organocatalysed hydroboration of *N*-Ts-protected imines^[64]

A Schlenk tube containing a stirring bar was charged with Cs₂CO₃ (12.1 mg, 0.037 mmol), PTA-based ligand (5 mol%), B₂pin₂ (76.2 mg, 0.30 mmol) and THF (0.75 mL). To this mixture, a solution of *N*-Ts aldimine **61** in THF (0.25 mL) was added, followed by methanol (0.1 mL, 2.5 mmol). The reaction mixture was stirred at 40 °C. After 24 h, the solvent was eliminated under reduced pressure.

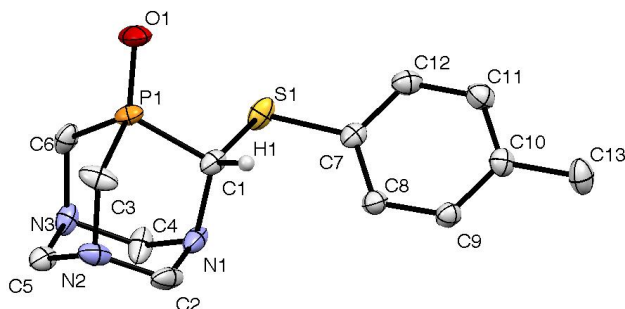
Compound (*R,R*)-26

Empirical formula	$C_{13}H_{18}N_3OP$
Formula weight	263.27
Temperature	193(2) K
Wavelength	0.71073 Å
Crystal system	Monoclinic
Space group	P 21
Unit cell dimensions	$a = 6.0511(4)$ Å $\alpha = 90^\circ$ $b = 7.6950(5)$ Å $\beta = 94.401(4)^\circ$ $c = 13.8031(10)$ Å $\gamma = 90^\circ$
Volume	$640.82(8)$ Å ³
Z	2
Density (calculated)	1.364 mg/m ³
Absorption coefficient	0.207 mm ⁻¹
F(000)	280
Crystal size	$0.24 \times 0.06 \times 0.04$ mm ³
Theta range for data collection	5.17 to 26.37°
Index ranges	$-7 \leq h \leq 7$, $-9 \leq k \leq 9$, $-17 \leq l \leq 17$
Reflections collected	11585
Independent reflections	2616 [R(int) = 0.0307]
Completeness to theta = 26.37°	98.9 %
Max. and min. transmission	0.9918 and 0.9521
Refinement method	Full-matrix least-squares on F ²
Data / restraints / parameters	2616 / 2 / 166
Goodness-of-fit on F ²	1.064
Final R indices [I > 2σ(I)]	R1 = 0.0325, wR2 = 0.0850
R indices (all data)	R1 = 0.0348, wR2 = 0.0867
Absolute structure parameter	-0.03(8)
Largest diff. peak and hole	0.391 and -0.161 e. Å ⁻³

Compound (*S,R*)-26

Empirical formula	$C_{13}H_{18}N_3OP$
Formula weight	263.27
Temperature	193(2) K
Wavelength	0.71073 Å
Crystal system	Monoclinic
Space group	P2(1)
Unit cell dimensions	$a = 7.1217(7)$ Å $\alpha = 90^\circ$ $b = 7.8503(8)$ Å $\beta = 99.365(5)^\circ$ $c = 11.7164(12)$ Å $\gamma = 90^\circ$
Volume	$646.30(11)$ Å ³
Z	2
Density (calculated)	1.353 Mg/m ³
Absorption coefficient	0.205 mm ⁻¹
F(000)	280
Crystal size	0.29 x 0.21 x 0.13 mm ³
Theta range for data collection	4.07 to 33.28°
Index ranges	-10 ≤ h ≤ 10, -12 ≤ k ≤ 12, -18 ≤ l ≤ 18
Reflections collected	17882
Independent reflections	4905 [R(int) = 0.0330]
Completeness to theta = 33.28 °	98.9 %
Absorption correction	Semi-empirical from equivalents
Max. and min. transmission	0.9741 and 0.9432
Refinement method	Full-matrix least-squares on F ²
Data / restraints / parameters	4905 / 1 / 167
Goodness-of-fit on F ²	1.037
Final R indices [I > 2σ(I)]	R1 = 0.0376, wR2 = 0.0877
R indices (all data)	R1 = 0.0466, wR2 = 0.0927
Absolute structure parameter	-0.02(6)
Largest diff. peak and hole	0.281 and -0.226 e. Å ⁻³

Compound 40



Empirical formula	$C_{13}H_{21}N_3O_{2.5}PS$ ($C_{13}H_{18}N_3OPS \cdot 1.5H_2O$)
Formula weight	322.36
Temperature	100(2) K
Wavelength	0.71073 Å
Crystal system	Monoclinic
Space group	C2/c
Unit cell dimensions	$a = 35.064(3)$ Å $\alpha = 90^\circ$ $b = 6.9930(5)$ Å $\beta = 96.737(2)^\circ$ $c = 12.4040(10)$ Å $\gamma = 90^\circ$
Volume	$3020.5(4)$ Å ³
Z	8
Density (calculated)	1.418 Mg/m ³
Absorption coefficient	0.330 mm ⁻¹
F(000)	1368
Crystal size	0.40 x 0.20 x 0.05 mm ³
Theta range for data collection	2.340 to 33.928°
Index ranges	-54 ≤ h ≤ 52, -7 ≤ k ≤ 10, -19 ≤ l ≤ 19
Reflections collected	14510
Independent reflections	5790 [R(int) = 0.0243]
Completeness to theta = 33.928 °	94.6%
Absorption correction	Multi-scan
Max. and min. transmission	0.984 and 0.856
Refinement method	Full-matrix least-squares on F ²
Data / restraints / parameters	5790 / 9 / 220
Goodness-of-fit on F ²	1.033
Final R indices [I > 2σ(I)]	R1 = 0.0428, wR2 = 0.1140
R indices (all data)	R1 = 0.0550, wR2 = 0.1230
Largest diff. peak and hole	0.515 and -0.577 e. Å ⁻³

4.5 References

- [1] D. J. Daigle, A. B. Pepperman, S. L. Vail, *J. Heterocycl. Chem.* **1974**, *11*, 407–408.
- [2] M. Zablocka, A. Hameau, A.-M. Caminade, J.-P. Majoral, *Adv. Synth. Catal.* **2010**, *352*, 2341–2358.
- [3] (a) A. D. Phillips, L. Gonsalvi, A. Romerosa, F. Vizza, M. Peruzzini, *Coord. Chem. Rev.* **2004**, *248*, 955–993; (b) J. Bravo, S. Bolaño, L. Gonsalvi, M. Peruzzini, *Coord. Chem. Rev.* **2010**, *254*, 555–607; (c) L. Gonsalvi, M. Peruzzini, in *Phosphorus Compounds: Advanced Tools in Catalysis and Material Sciences* (Eds.: M. Peruzzini, L. Gonsalvi), Springer Netherlands, Dordrecht, **2011**, pp. 183–212; (d) L. Gonsalvi, A. Guerriero, F. Hapiot, D. A. Krogstad, E. Monflier, G. Reginato, M. Peruzzini, *Pure Appl. Chem.* **2013**, *85*, 385–396.
- [4] L. Gonsalvi, M. Peruzzini, in *Encyclopedia of Reagents for Organic Synthesis*, John Wiley & Sons, Ltd, **2001**.
- [5] M. M. Abu-Omar, J. H. Espenson, *J. Am. Chem. Soc.* **1995**, *117*, 272–280.
- [6] (a) C. S. Allardyce, P. J. Dyson, D. J. Ellis, S. L. Heath, *Chem. Commun.* **2001**, 1396–1397; (b) C. Scolaro, A. Bergamo, L. Brescacin, R. Delfino, M. Cocchietto, G. Laurenczy, T. J. Geldbach, G. Sava, P. J. Dyson, *J. Med. Chem.* **2005**, *48*, 4161–4171; (c) B. S. Murray, M. V. Babak, C. G. Hartinger, P. J. Dyson, *Coord. Chem. Rev.* **2016**, *306*, 86–114.
- [7] (a) E. Fluck, H. J. Weissgraeber, *Chem. Ztg* **1977**, *101*, 304; (b) B. Assmann, K. Angermaier, M. Paul, J. Riede, H. Schmidbaur, *Chem. Ber.* **1995**, *128*, 891–900.
- [8] (a) D. J. Darensbourg, T. J. Decuir, J. H. Reibenspies, in *Aqueous Organometallic Chemistry and Catalysis* (Eds.: I. T. Horváth, F. Joó), Kluwer Academic Publishers, Dordrecht, **1995**, pp. 61–80; (b) D. J. Darensbourg, J. B. Robertson, D. L. Larkins, J. H. Reibenspies, *Inorg. Chem.* **1999**, *38*, 2473–2481.
- [9] K. J. Fisher, E. C. Alyea, N. Shahnazarian, *Phosphorus, Sulfur Silicon Relat. Elem.* **1990**, *48*, 37–40.
- [10] D. J. Daigle, A. B. Pepperman, *J. Heterocycl. Chem.* **1975**, *12*, 579–580.
- [11] D. J. Daigle, T. J. Decuir, J. B. Robertson, D. J. Darensbourg, in *Inorg. Synth.*, John Wiley & Sons, Inc., **2007**, pp. 40–45.
- [12] (a) A. E. Díaz-Álvarez, P. Crochet, V. Cadierno, *Catal. Commun.* **2011**, *13*, 91–96; (b) F. Chahdoura, I. Favier, C. Pradel, S. Mallet-Ladeira, M. Gómez, *Catal. Commun.* **2015**, *63*, 47–51.
- [13] R. Huang, B. J. Frost, *Inorg. Chem.* **2007**, *46*, 10962–10964.
- [14] G. W. Wong, J. L. Harkreader, C. A. Mebi, B. J. Frost, *Inorg. Chem.* **2006**, *45*, 6748–6755.
- [15] J. M. Sears, W.-C. Lee, B. J. Frost, *Inorg. Chim. Acta* **2015**, *431*, 248–257.
- [16] G. W. Wong, W.-C. Lee, B. J. Frost, *Inorg. Chem.* **2008**, *47*, 612–620.
- [17] (a) M. Erlandsson, L. Gonsalvi, A. Ienco, M. Peruzzini, *Inorg. Chem.* **2008**, *47*, 8–10; (b) A. Guerriero, M. Erlandsson, A. Ienco, D. A. Krogstad, M. Peruzzini, G. Reginato, L. Gonsalvi, *Organometallics* **2011**, *30*, 1874–1884; (c) D. A. Krogstad, A. Guerriero, A. Ienco, G. Manca, M. Peruzzini, G. Reginato, L. Gonsalvi, *Organometallics* **2011**, *30*, 6292–6302.
- [18] W.-C. Lee, J. M. Sears, R. A. Enow, K. Eads, D. A. Krogstad, B. J. Frost, *Inorg. Chem.* **2013**, *52*, 1737–1746.
- [19] W. Li, J. Zhang, *Chem. Soc. Rev.* **2016**, *45*, 1657–1677.
- [20] B. J. Frost, C. A. Mebi, P. W. Gingrich, *Eur. J. Inorg. Chem.* **2006**, 1182–1189.
- [21] (a) G. Liu, D. A. Cogan, T. D. Owens, T. P. Tang, J. A. Ellman, *J. Org. Chem.* **1999**, *64*, 1278–1284; (b) D. A. Cogan, J. A. Ellman, *J. Am. Chem. Soc.* **1999**, *121*, 268–269.
- [22] (a) G. Liu, D. A. Cogan, J. A. Ellman, *J. Am. Chem. Soc.* **1997**, *119*, 9913–9914; (b) D. Morton, D. Pearson, R. A. Field, R. A. Stockman, *Chem. Commun.* **2006**, 1833–1835; (c) V. K. Aggarwal, N. Barbero, E. M. McGarrigle, G. Mickle, R. Navas, J. R. Suárez, M. G. Unthank, M. Yar, *Tetrahedron Lett.* **2009**, *50*, 3482–3484; (d) F. Ferreira, C. Botuha, F. Chemla, A. Pérez-Luna, *Chem. Soc. Rev.* **2009**, *38*, 1162–1186; (e) M. T. Robak, M. A. Herbage, J. A. Ellman, *Chem. Rev.* **2010**, *110*, 3600–3740.
- [23] (a) P. Moreau, M. Essiz, J.-Y. Mérour, D. Bouzard, *Tetrahedron: Asymmetry* **1997**, *8*, 591–598; (b) W. H. Chan, A. W. M. Lee, P. F. Xia, W. Y. Wong, *Tetrahedron Lett.* **2000**, *41*, 5725–5728; (c) J. A. Ellman, T. D. Owens, T. P. Tang, *Acc. Chem. Res.* **2002**, *35*, 984–995; (d) P. Zhou, B.-C. Chen, F. A. Davis, *Tetrahedron* **2004**, *60*, 8003–8030.
- [24] R. Zurawinski, B. Donnadiou, M. Mikolajczyk, R. Chauvin, *J. Organomet. Chem.* **2004**, *689*, 380–386.
- [25] (a) K. Hiroi, Y. Suzuki, I. Abe, R. Kawagishi, *Tetrahedron* **2000**, *56*, 4701–4710; (b) S. Nakamura, T. Fukuzumi, T. Toru, *Chirality* **2004**, *16*, 10–12; (c) J. Chen, D. Li, H. Ma, L. Cun, J. Zhu, J. Deng, J. Liao, *Tetrahedron Lett.* **2008**, *49*, 6921–6923; (d) F. Lang, G. Chen, L. Li, J. Xing, F. Han, L. Cun, J. Liao, *Chem. Eur. J.* **2011**, *17*, 5242–5245; (e) J. Gui, G. Chen, P. Cao, J. Liao, *Tetrahedron: Asymmetry* **2012**, *23*, 554–

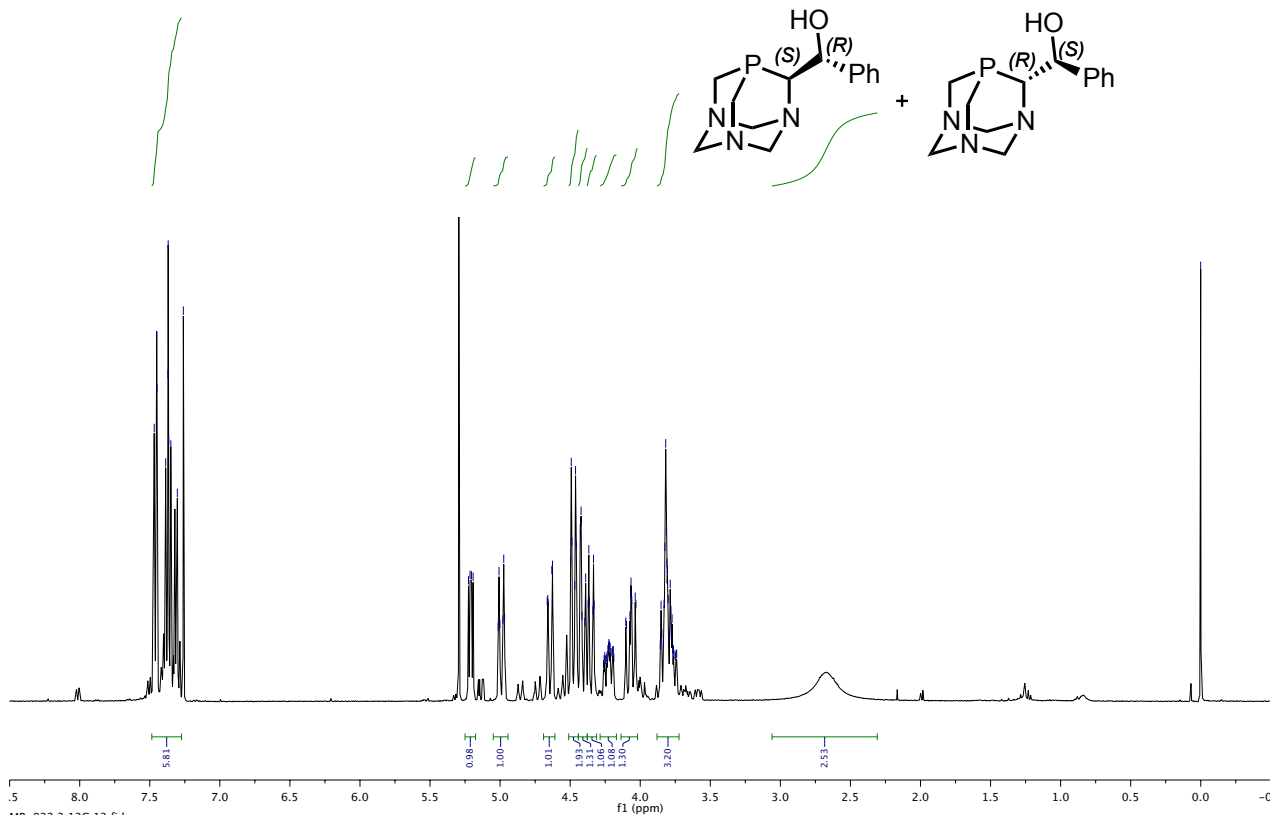
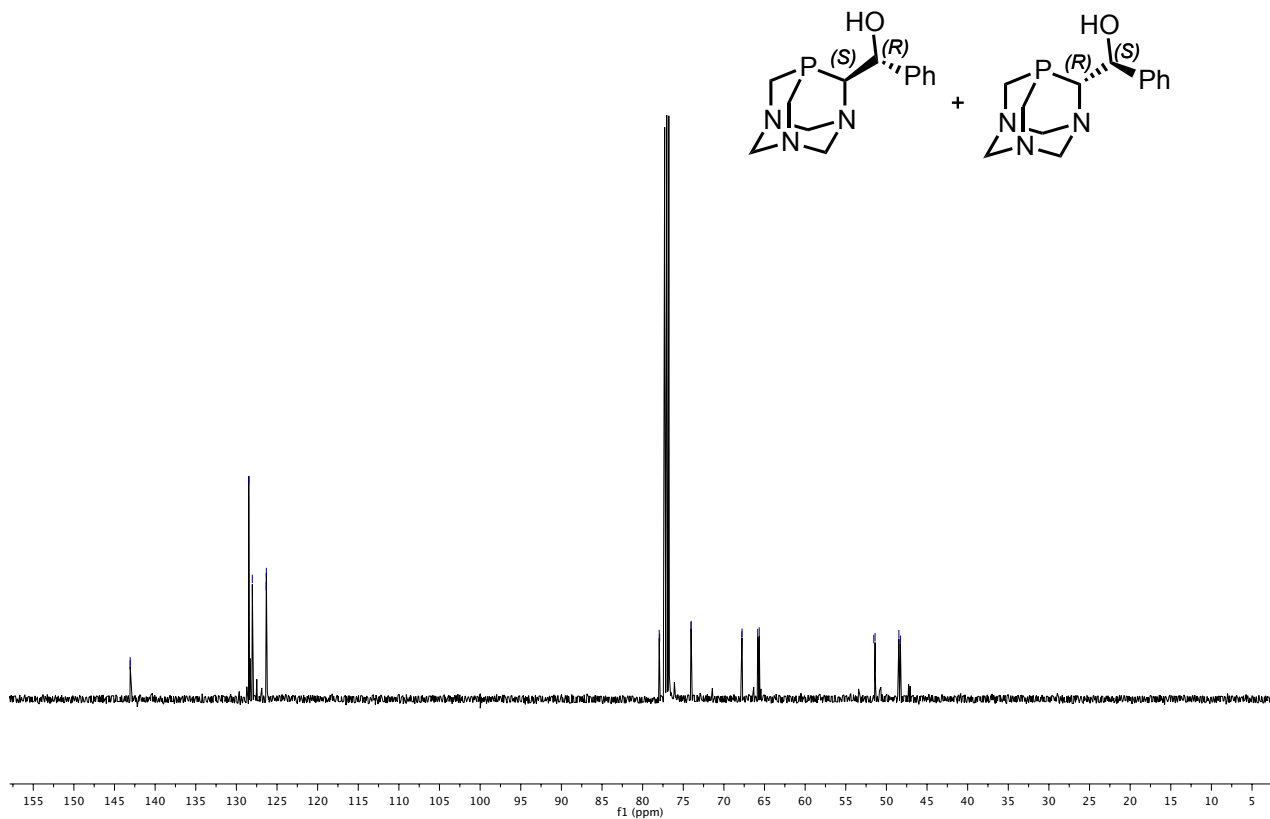
- 563; (f) R. Malacea, J.-C. Daran, R. Poli, E. Manoury, *Tetrahedron: Asymmetry* **2013**, *24*, 612–620; (g) H.-G. Cheng, B. Feng, L.-Y. Chen, W. Guo, X.-Y. Yu, L.-Q. Lu, J.-R. Chen, W.-J. Xiao, *Chem. Commun.* **2014**, *50*, 2873–2875; (h) A. Berthelot-Bréhier, A. Panossian, F. Colobert, F. R. Leroux, *Org. Chem. Front.* **2015**, *2*, 634–644; (i) L.-Y. Chen, X.-Y. Yu, J.-R. Chen, B. Feng, H. Zhang, Y.-H. Qi, W.-J. Xiao, *Org. Lett.* **2015**, *17*, 1381–1384; (j) Y. Lou, P. Cao, T. Jia, Y. Zhang, M. Wang, J. Liao, *Angew. Chem. Int. Ed.* **2015**, *54*, 12134–12138; (k) D. Wang, P. Cao, B. Wang, T. Jia, Y. Lou, M. Wang, J. Liao, *Org. Lett.* **2015**, *17*, 2420–2423; (l) T. Yang, Y. Zhang, P. Cao, M. Wang, L. Li, D. Li, J. Liao, *Tetrahedron* **2016**, *72*, 2707–2711.
- [26] (a) E. Vedejs, H. Mastalerz, G. P. Meier, D. W. Powell, *J. Org. Chem.* **1981**, *46*, 5253–5254; (b) C. Ferrer, A. Riera, X. Verdaguier, *Organometallics* **2009**, *28*, 4571–4576; (c) M. Abdalillah, R. Zurawinski, Y. Canac, B. Laleu, J. Lacour, C. Lepetit, G. Magro, G. Bernardinelli, B. Donnadieu, C. Duhayon, M. Mikolajczyk, R. Chauvin, *Dalton Trans.* **2009**, 8493–8508; (d) R. Zurawinski, C. Lepetit, Y. Canac, L. Vendier, M. Mikolajczyk, R. Chauvin, *Tetrahedron: Asymmetry* **2010**, *21*, 1777–1787; (e) I. Alvarado-Beltran, M. Lozano González, Y. Escudié, E. Maerten, N. Saffon-Merceron, I. Fabing, C. Alvarez Toledano, A. Baceiredo, *Tetrahedron* **2016**, *72*, 1662–1667.
- [27] K. K. Andersen, *Tetrahedron Lett.* **1962**, 93–95.
- [28] (a) N. W. Alcock, J. M. Brown, P. L. Evans, *J. Organomet. Chem.* **1988**, *356*, 233–247; (b) E. Vedejs, R. A. Buchanan, Y. Watanabe, *J. Am. Chem. Soc.* **1989**, *111*, 8430–8438; (c) S. Y. M. Chooi, S. Y. Siah, P. H. Leung, K. F. Mok, *Inorg. Chem.* **1993**, *32*, 4812–4818; (d) K. Hiroi, Y. Suzuki, R. Kawagishi, *Tetrahedron Lett.* **1999**, *40*, 715–718; (e) M. Revés, T. Achard, J. Solà, A. Riera, X. Verdaguier, *J. Org. Chem.* **2008**, *73*, 7080–7087.
- [29] P. A. Byrne, D. G. Gilheany, *Chem. Soc. Rev.* **2013**, *42*, 6670–6696.
- [30] P. Melchiorre, *Angew. Chem. Int. Ed.* **2012**, *51*, 9748–9770.
- [31] (a) Z. He, X. Tang, Y. Chen, Z. He, *Adv. Synth. Catal.* **2006**, *348*, 413–417; (b) X. Tang, B. Zhang, Z. He, R. Gao, Z. He, *Adv. Synth. Catal.* **2007**, *349*, 2007–2017.
- [32] A. García-Fernández, J. Díez, M. P. Gamasa, E. Lastra, *Inorg. Chem.* **2009**, *48*, 2471–2481.
- [33] (a) J. C. Duff, E. J. Bills, *J. Chem. Soc.* **1932**, 1987–1988; (b) J. C. Duff, E. J. Bills, *J. Chem. Soc.* **1934**, 1305–1308.
- [34] N. Grimblat, A. M. Sarotti, T. S. Kaufman, S. O. Simonetti, *Org. Biomol. Chem.* **2016**, *14*, 10497–10501.
- [35] R. K. Chambers, N. Chaipukdee, T. Thaima, K. Kanokmedhakul, S. G. Pyne, *Eur. J. Org. Chem.* **2016**, 3765–3772.
- [36] Y.-L. Sun, Y. Wei, M. Shi, *ChemCatChem* **2016**, DOI: 10.1002/cctc.201601144.
- [37] M. S. Sigman, E. N. Jacobsen, *J. Am. Chem. Soc.* **1998**, *120*, 4901–4902.
- [38] P. Vachal, E. N. Jacobsen, *J. Am. Chem. Soc.* **2002**, *124*, 10012–10014.
- [39] (a) M. S. Taylor, E. N. Jacobsen, *Angew. Chem. Int. Ed.* **2006**, *45*, 1520–1543; (b) S. J. Connon, *Chem. Eur. J.* **2006**, *12*, 5418–5427.
- [40] (a) Y.-L. Shi, M. Shi, *Adv. Synth. Catal.* **2007**, *349*, 2129–2135; (b) Y.-Q. Fang, E. N. Jacobsen, *J. Am. Chem. Soc.* **2008**, *130*, 5660–5661.
- [41] (a) M. Ken-ichi, S. Zennosuke, H. Hiromitsu, *Bull. Chem. Soc. Jpn.* **1968**, *41*, 2815–2815; (b) A. B. Baylis, M. E. D. Hillman, German Patent 2155113, **1972**.
- [42] (a) D. Basavaiah, K. Venkateswara Rao, R. Jannapu Reddy, *Chem. Soc. Rev.* **2007**, *36*, 1581–1588; (b) Y. Wei, M. Shi, *Chem. Rev.* **2013**, *113*, 6659–6690.
- [43] X. Xu, C. Wang, Z. Zhou, X. Tang, Z. He, C. Tang, *Eur. J. Org. Chem.* **2007**, 4487–4491.
- [44] (a) H. M. I. Osborn, J. Sweeney, *Tetrahedron: Asymmetry* **1997**, *8*, 1693–1715; (b) G. Righi, S. Pietrantonio, C. Bonini, *Tetrahedron* **2001**, *57*, 10039–10046.
- [45] P. Müller, C. Fruit, *Chem. Rev.* **2003**, *103*, 2905–2920.
- [46] (a) J. Vesely, I. Ibrahim, G.-L. Zhao, R. Rios, A. Córdova, *Angew. Chem. Int. Ed.* **2007**, *46*, 778–781; (b) L. Deiana, P. Dziedzic, G.-L. Zhao, J. Vesely, I. Ibrahim, R. Rios, J. Sun, A. Córdova, *Chem. Eur. J.* **2011**, *17*, 7904–7917.
- [47] (a) B. List, *J. Am. Chem. Soc.* **2002**, *124*, 5656–5657; (b) A. Bøgevig, K. Juhl, N. Kumaragurubaran, W. Zhuang, K. A. Jørgensen, *Angew. Chem. Int. Ed.* **2002**, *41*, 1790–1793.
- [48] N. Kumaragurubaran, K. Juhl, W. Zhuang, A. Bøgevig, K. A. Jørgensen, *J. Am. Chem. Soc.* **2002**, *124*, 6254–6255.
- [49] K. Juhl, K. A. Jørgensen, *J. Am. Chem. Soc.* **2002**, *124*, 2420–2421.
- [50] (a) J. M. Janey, *Angew. Chem. Int. Ed.* **2005**, *44*, 4292–4300; (b) T. Vilaivan, W. Bhanthumnavin, *Molecules* **2010**, *15*, 917–958.
- [51] M. Marigo, K. Juhl, K. A. Jørgensen, *Angew. Chem. Int. Ed.* **2003**, *42*, 1367–1369.

- [52] S. Saaby, M. Bella, K. A. Jørgensen, *J. Am. Chem. Soc.* **2004**, *126*, 8120–8121.
- [53] (a) C. Foltz, B. Stecker, G. Marconi, S. Bellemin-Laponnaz, H. Wadepohl, L. H. Gade, *Chem. Commun.* **2005**, 5115–5117; (b) M. Terada, M. Nakano, H. Ube, *J. Am. Chem. Soc.* **2006**, *128*, 16044–16045; (c) R. He, X. Wang, T. Hashimoto, K. Maruoka, *Angew. Chem. Int. Ed.* **2008**, *47*, 9466–9468; (d) K. Murai, S. Fukushima, A. Nakamura, M. Shimura, H. Fujioka, *Tetrahedron* **2011**, *67*, 4862–4868; (e) P. Kasaplar, E. Ozkal, C. Rodríguez-Esrich, M. A. Pericàs, *Green Chem.* **2015**, *17*, 3122–3129.
- [54] (a) S. Peddibhotla, *Curr. Bioact. Compd.* **2009**, *5*, 20–38; (b) A. Kumar, S. S. Chimni, *RSC Adv.* **2012**, *2*, 9748–9762; (c) S. Mohammadi, R. Heiran, R. P. Herrera, E. Marqués-López, *ChemCatChem* **2013**, *5*, 2131–2148; (d) B. Yu, H. Xing, D.-Q. Yu, H.-M. Liu, *Beilstein J. Org. Chem.* **2016**, *12*, 1000–1039.
- [55] G. Chen, Y. Wang, S. Gao, H.-P. He, S.-L. Li, J.-X. Zhang, J. Ding, X.-J. Hao, *J. Heterocycl. Chem.* **2009**, *46*, 217–220.
- [56] F. Lazreg, M. Lesieur, A. J. Samson, C. S. J. Cazin, *ChemCatChem* **2016**, *8*, 209–213.
- [57] M. Chouhan, K. Ram Senwar, K. Kumar, R. Sharma, V. A. Nair, *Synthesis* **2014**, *46*, 195–202.
- [58] Q. Chen, Y. Tang, T. Huang, X. Liu, L. Lin, X. Feng, *Angew. Chem. Int. Ed.* **2016**, *55*, 5286–5289.
- [59] N. Xu, D.-W. Gu, J. Zi, X.-Y. Wu, X.-X. Guo, *Org. Lett.* **2016**, *18*, 2439–2442.
- [60] (a) W. Yang, X. Gao, B. Wang, *Med. Res. Rev.* **2003**, *23*, 346–368; (b) S. J. Baker, C. Z. Ding, T. Akama, Y.-K. Zhang, V. Hernandez, Y. Xia, *Future Med. Chem.* **2009**, *1*, 1275–1288; (c) S. J. Baker, J. W. Tomsho, S. J. Benkovic, *Chem. Soc. Rev.* **2011**, *40*, 4279–4285.
- [61] P. Andrés, G. Ballano, M. I. Calaza, C. Cativiela, *Chem. Soc. Rev.* **2016**, *45*, 2291–2307.
- [62] (a) M. A. Beenen, C. An, J. A. Ellman, *J. Am. Chem. Soc.* **2008**, *130*, 6910–6911; (b) A. W. Buesking, V. Bacauanu, I. Cai, J. A. Ellman, *J. Org. Chem.* **2014**, *79*, 3671–3677.
- [63] K. Hong, J. P. Morken, *J. Am. Chem. Soc.* **2013**, *135*, 9252–9254.
- [64] C. Solé, H. Gulyás, E. Fernández, *Chem. Commun.* **2012**, *48*, 3769–3771.
- [65] J. Albert, J. Granell, R. Qadir, J. Quirante, C. Calvis, R. Messeguer, J. Badía, L. Baldomà, M. Font-Bardia, T. Calvet, *Organometallics* **2014**, *33*, 7284–7292.
- [66] L. Huang, Y. Zhang, R. J. Staples, R. H. Huang, W. D. Wulff, *Chem. Eur. J.* **2012**, *18*, 5302–5313.
- [67] J. L. García Ruano, J. Alemán, M. Belén Cid, A. Parra, *Org. Lett.* **2005**, *7*, 179–182.
- [68] Q. Wang, Y. Li, Z. Qi, F. Xie, Y. Lan, X. Li, *ACS Catal.* **2016**, *6*, 1971–1980.

4.6 Annex: NMR spectra of the isolated compounds

 ^1H NMR (400 MHz), ^{13}C NMR (125 MHz) and ^{31}P (162 MHz) spectra in CDCl_3 for (*S,R/R,S*)-26MR-822.3 1H.10.fid
ResearchGroup Perica
ICIQ_1H12p8s CDCl3-7-265.23
5.21
5.20
5.19
5.18
5.01
4.97
4.63
4.63
4.49
4.49
4.46
4.43
4.42
3.85
3.85
3.83
3.82
3.81
3.81
3.80
3.80
3.79
3.78
3.77
3.76
3.75
3.74

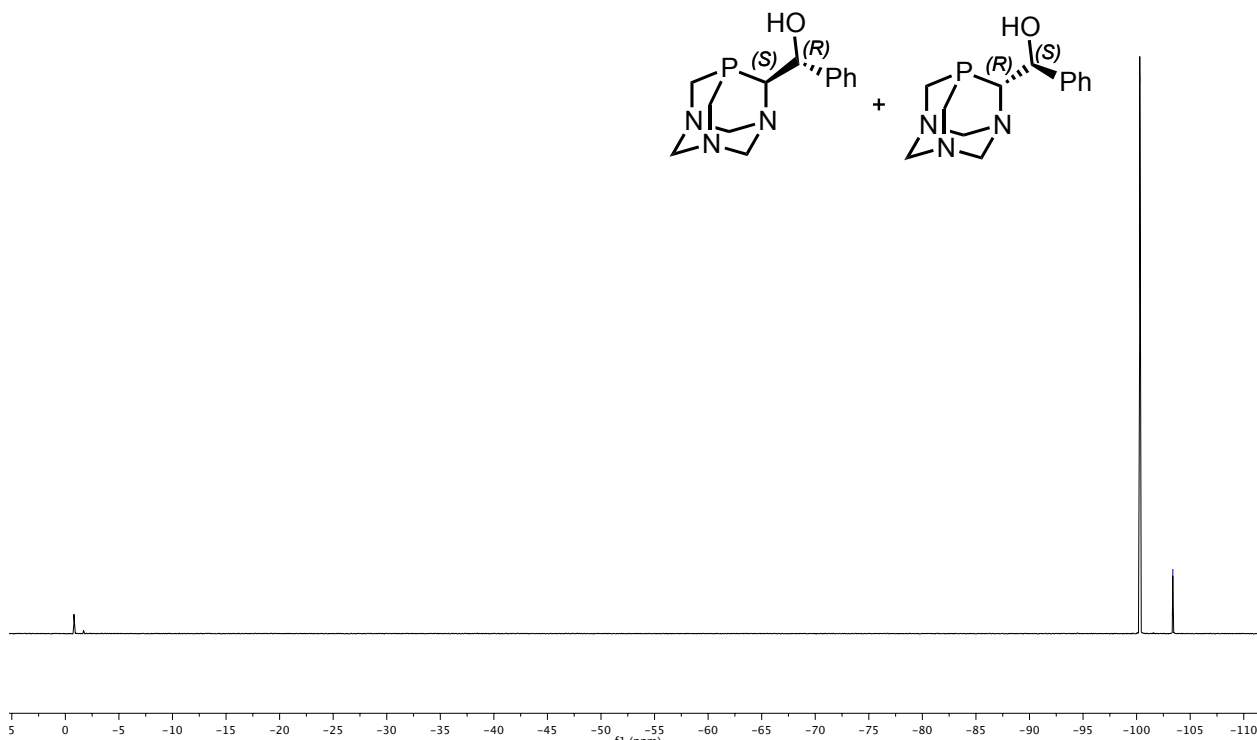
0.00

MR-822.3 13C.13.fid
ResearchGroup Perica
ICIQ_13C(1H)512s CDCl3-7-2677.96
77.91
74.05
74.03
67.79
67.76
65.84
65.85
51.55
51.39
48.77
48.27

Preparation of new enantiopure PTA-based derivatives. Some applications in enantioselective catalysis.

ResearchGroup Pericas
ICIQ_31P{1H} CDCl3 /opt/topspin mrodriguez 4

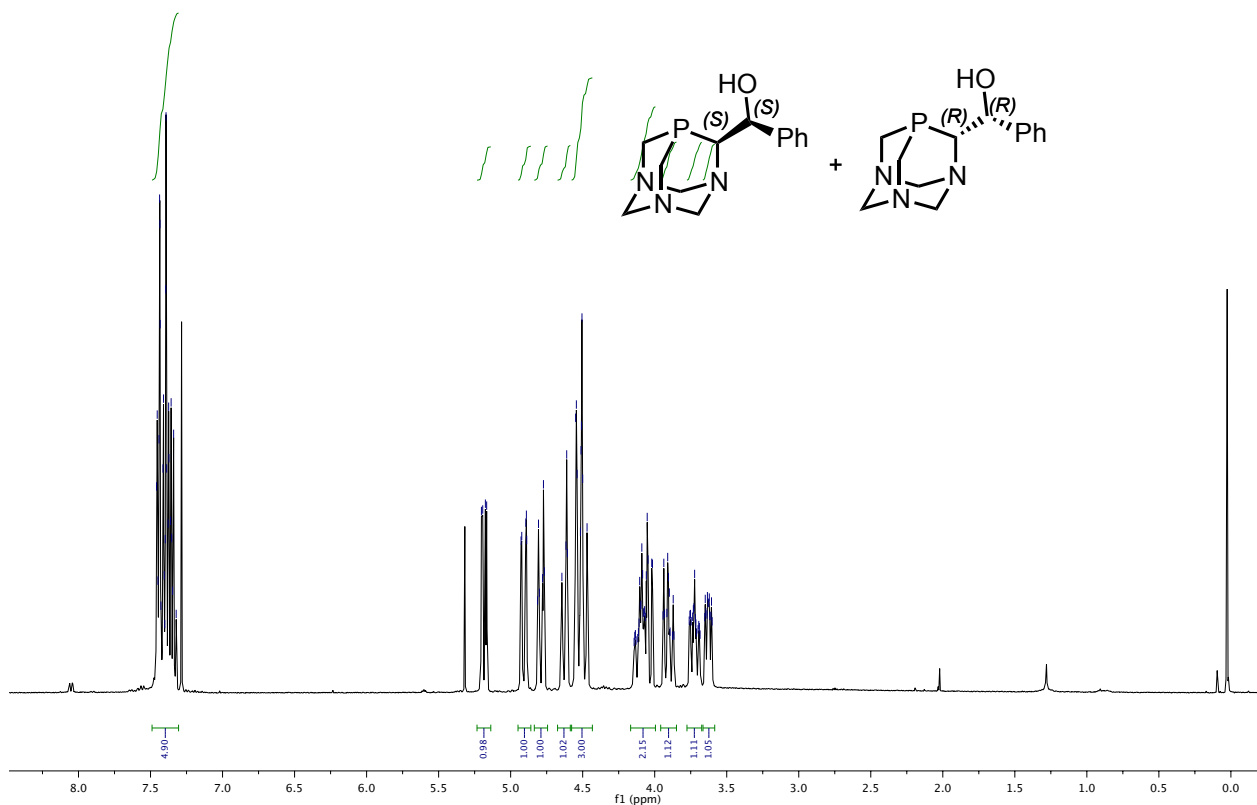
100.2
103.2



^1H NMR (400 MHz), ^{13}C NMR (125 MHz) and ^{31}P (162 MHz) spectra in CDCl_3 for **(S,S/R,R)-26**

MR-822.1 1H.10.fid
ResearchGroup Pericas
ICIQ_1H1205 CDCl3 /opt/topspin mrodriguez 2

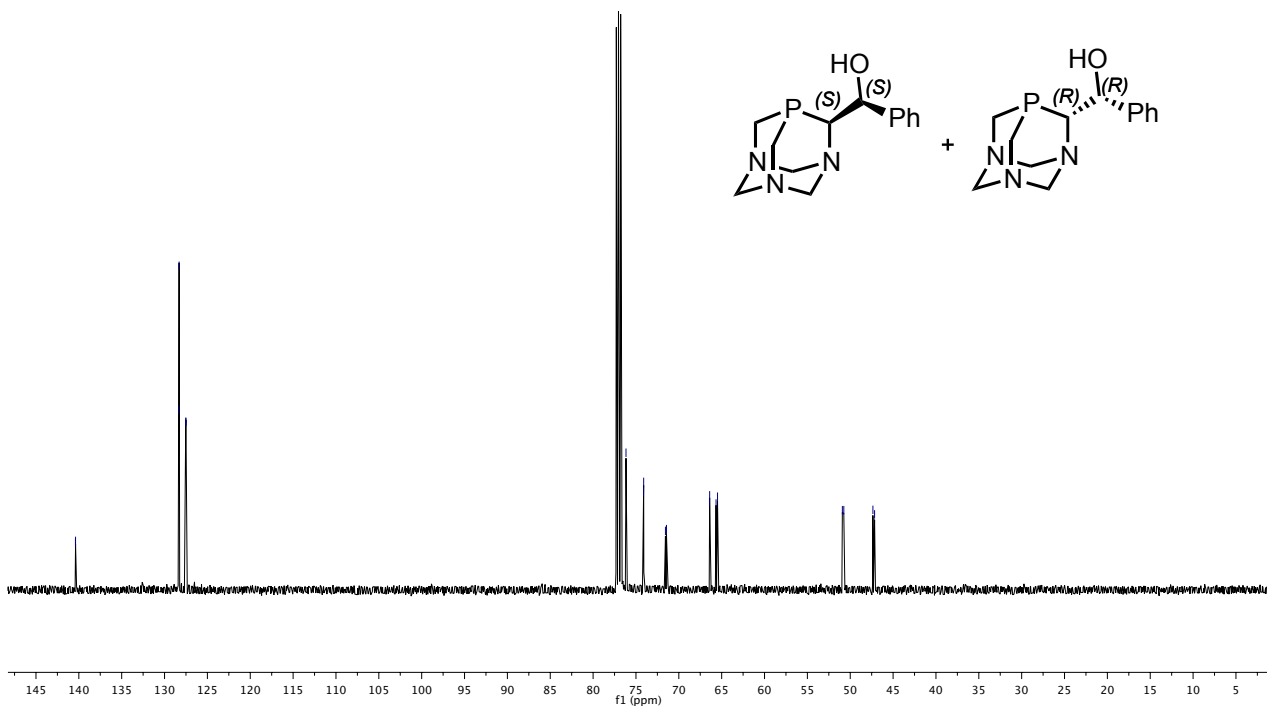
5.30
5.19
5.18
5.17
4.77
4.61
4.54
4.54
4.51
4.51
4.50
4.39
4.14
4.13
4.12
4.12
4.11
4.10
4.10
4.09
4.08
4.08
4.07
4.07
4.06
4.06
4.05
3.94
3.94
3.92
3.90
3.89
3.89
3.87
3.87
3.76
3.75
3.72
3.72
3.71
3.71
3.70
3.69
3.68
3.65
3.65
3.64
3.63
3.62
3.61
3.60



MR-822.1 13C.13.fid
 ResearchGroup Pericas
 ICIQ_13C[1H]S12s CDCI3 /opt/topspin mrodriguez 35

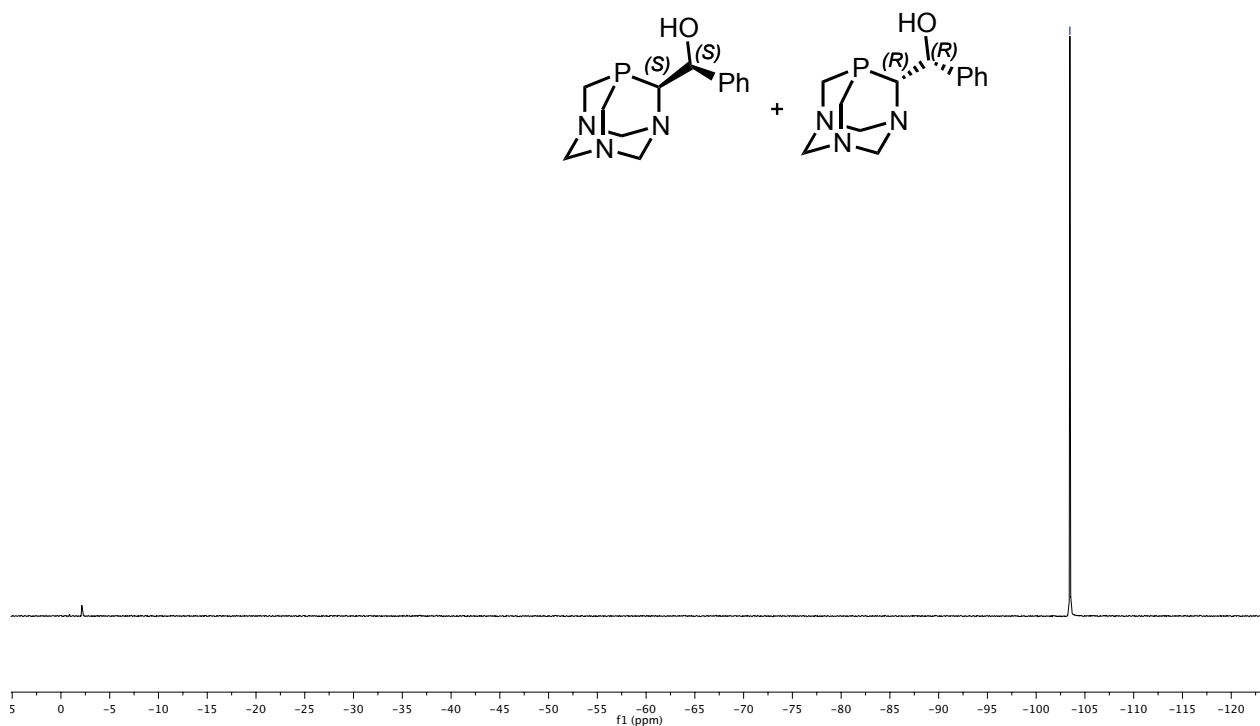
76.16
 74.12
 74.10
 71.86
 71.64
 66.42
 66.40
 65.88

50.92
 50.75
 47.35
 47.16

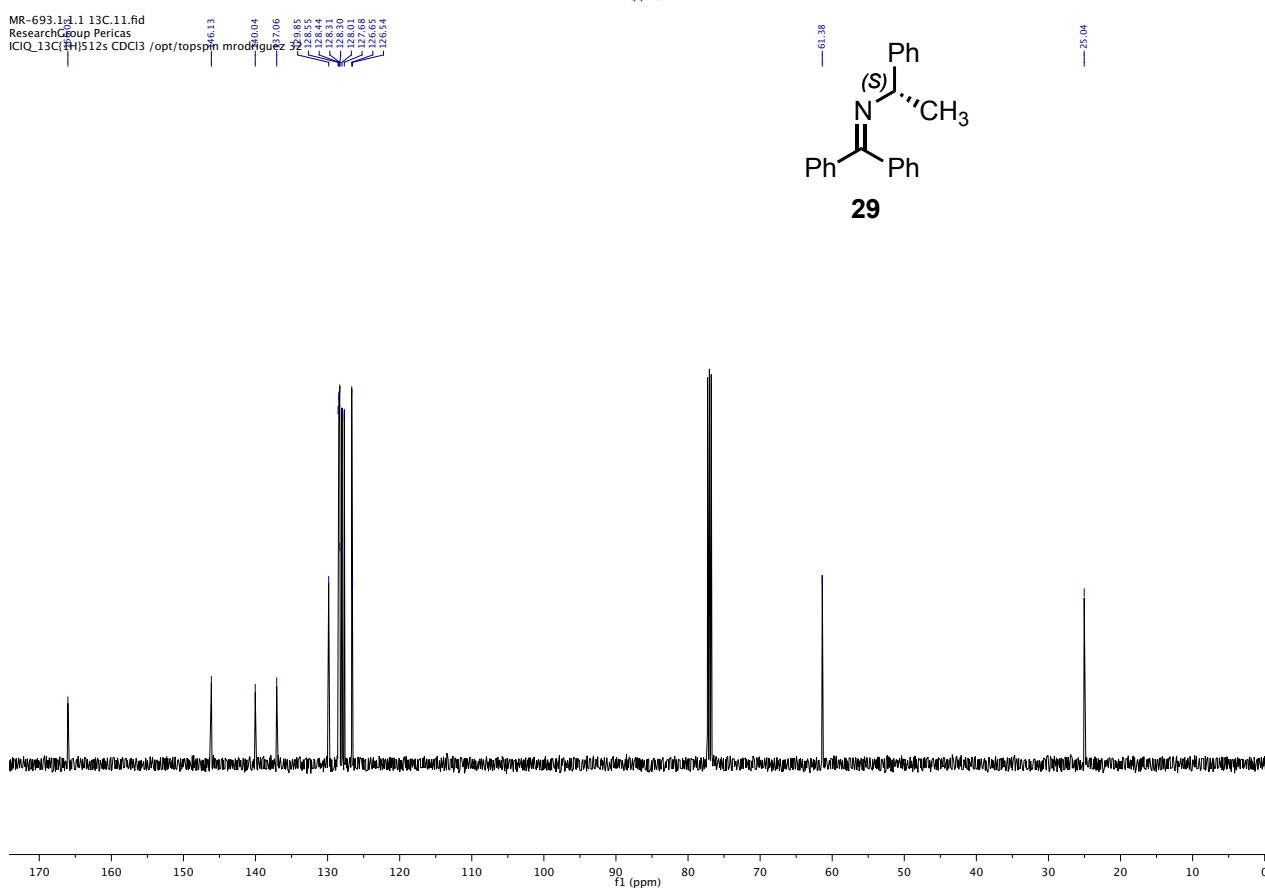
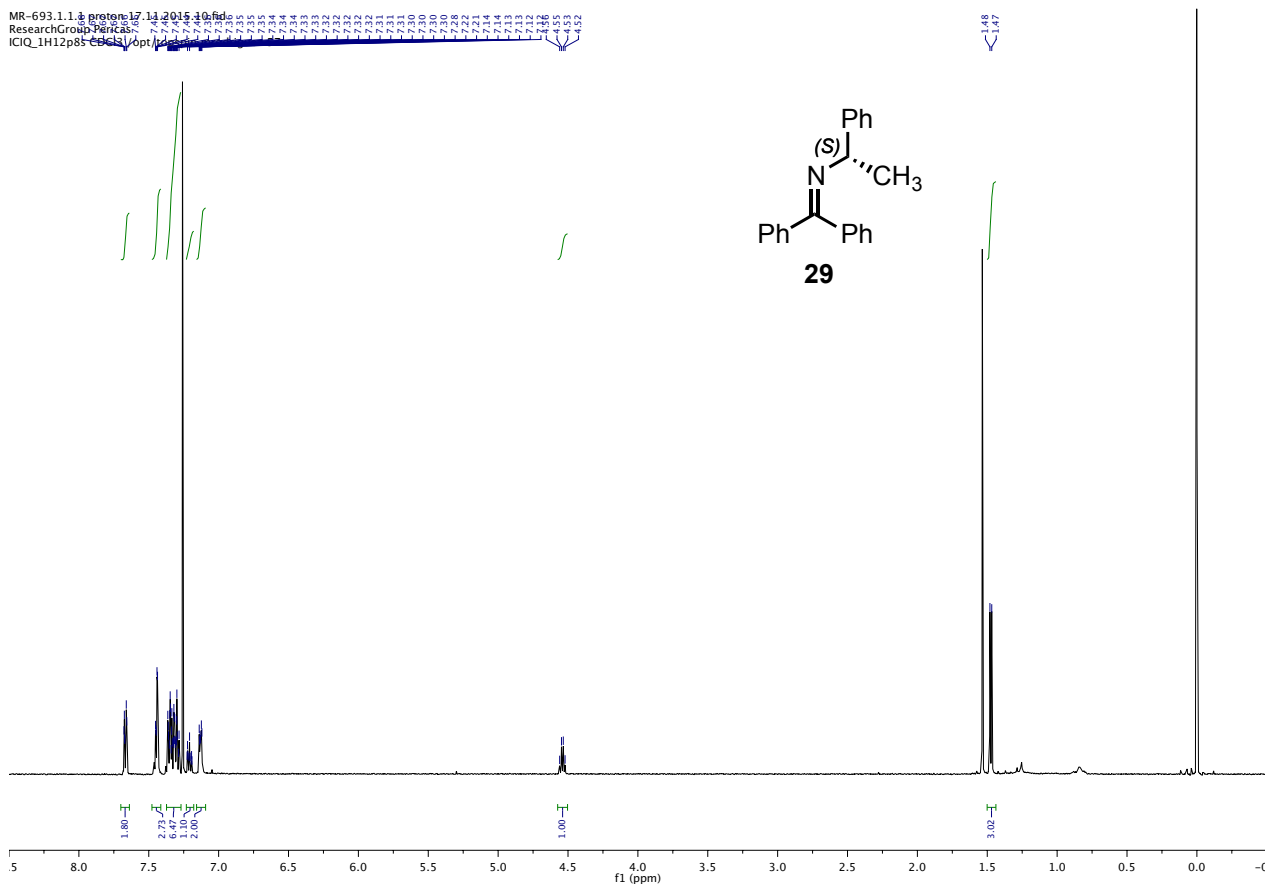


MR-822.1 31P[1H].11.fid
 ResearchGroup Pericas
 ICIQ_31P[1H] CDCI3 /opt/topspin mrodriguez 2

103.46

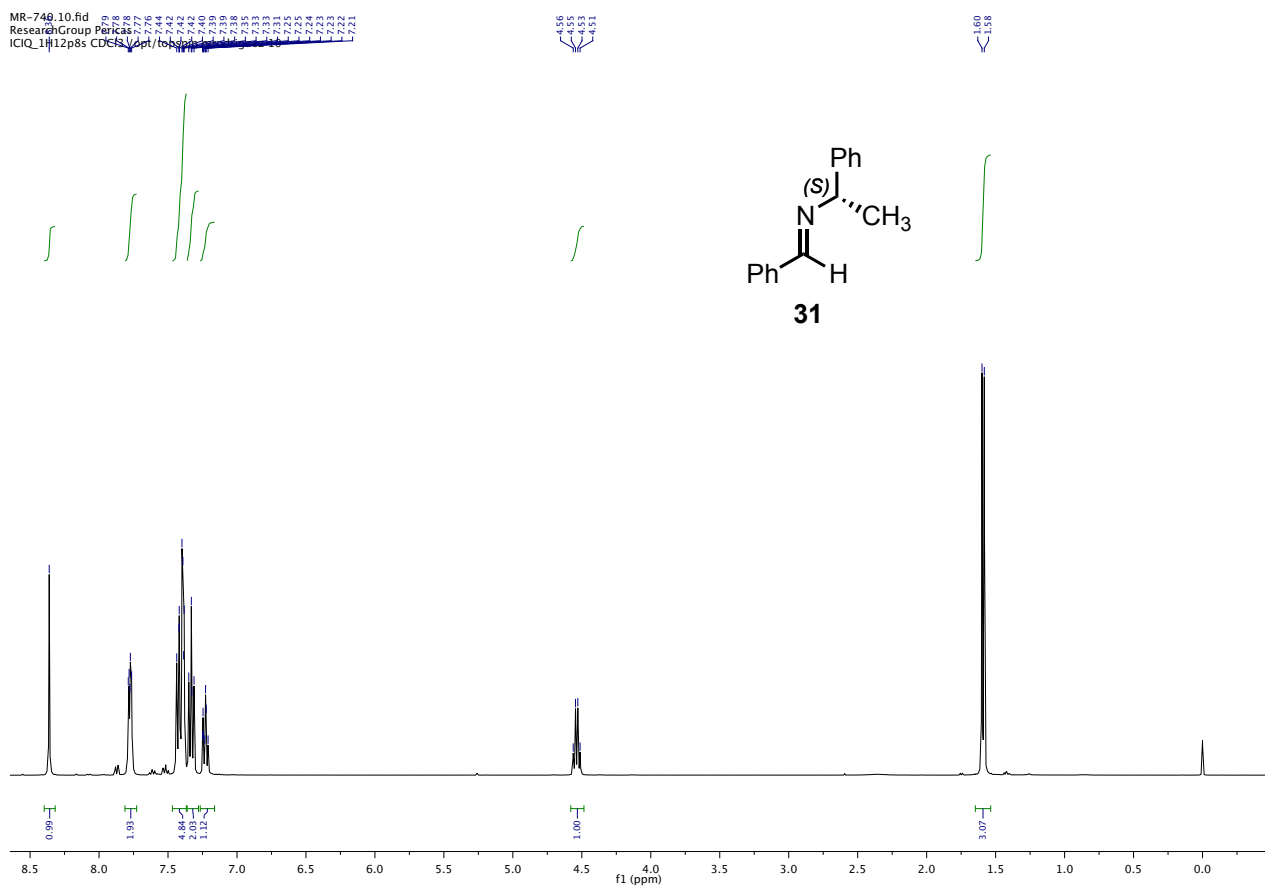


^1H NMR (500 MHz), ^{13}C NMR (125 MHz) spectra in CDCl_3 for **29**

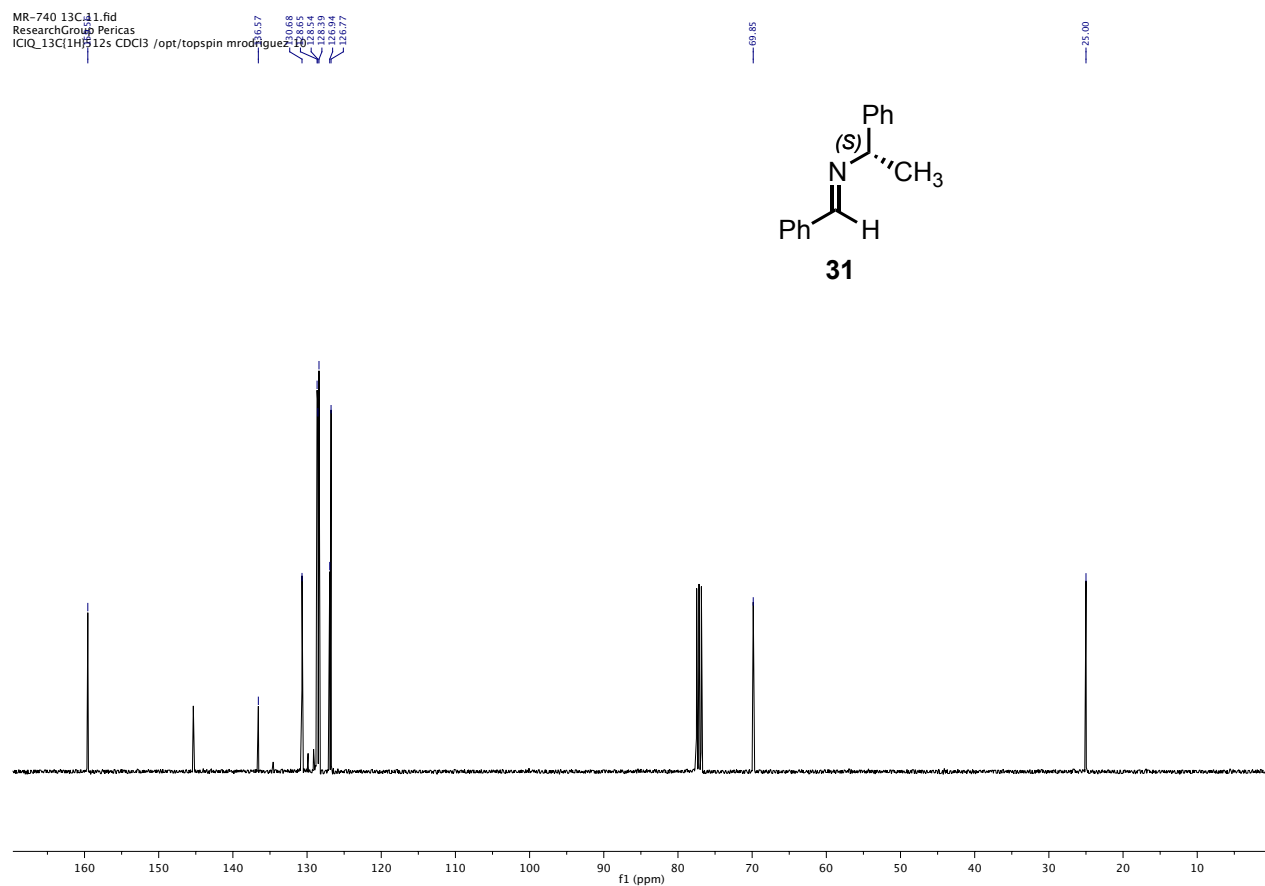


^1H NMR (400 MHz), ^{13}C NMR (100 MHz) spectra in CDCl_3 for **31**

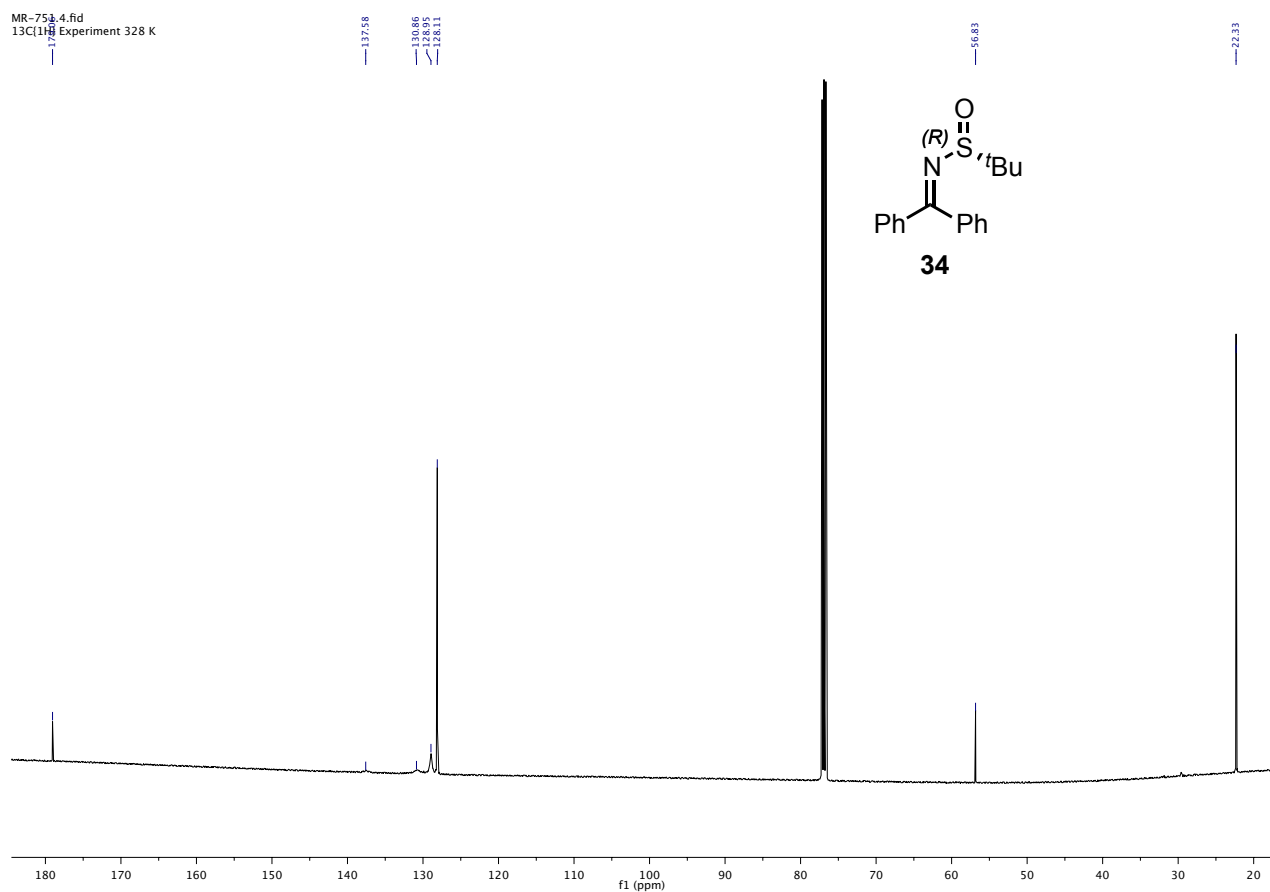
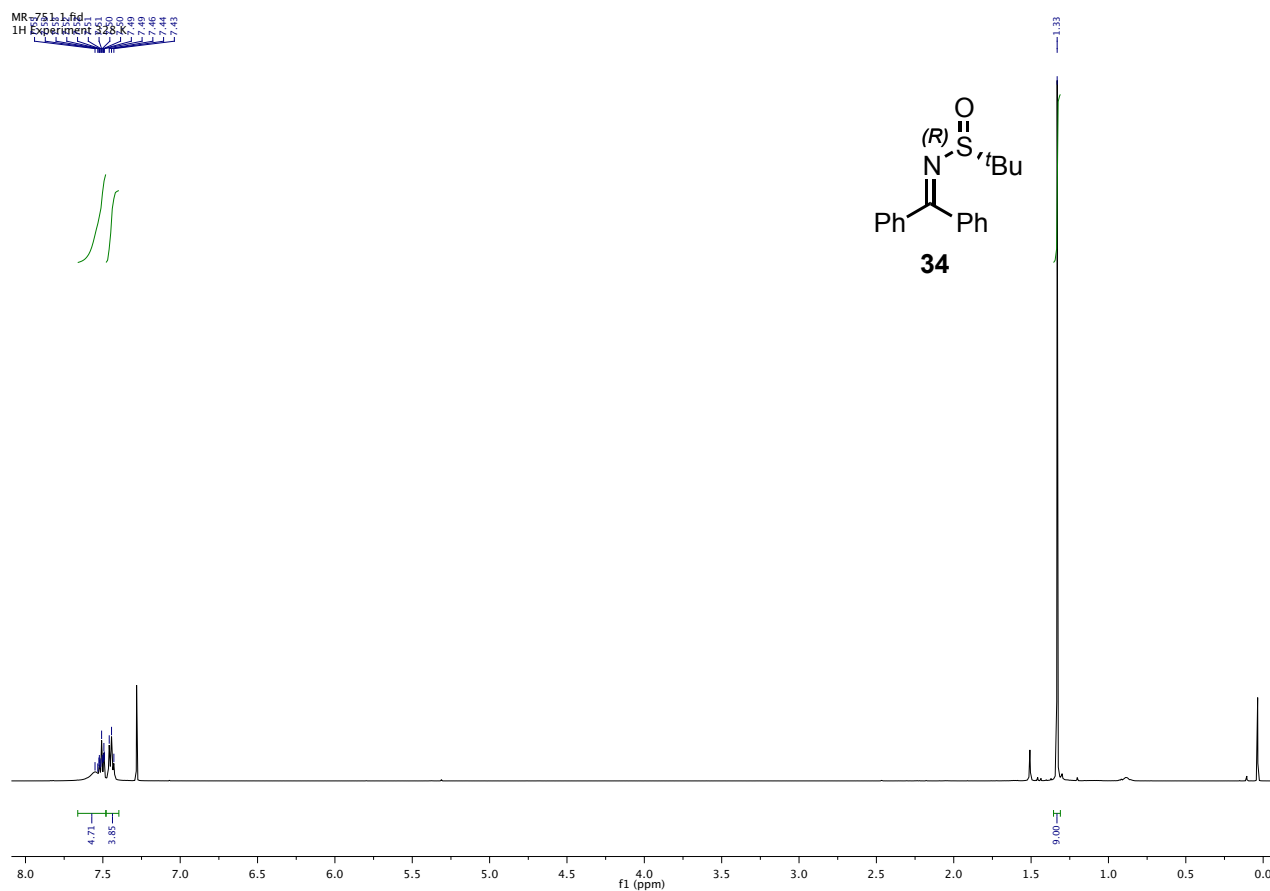
MR-740_10.fid
ResearchGroup Pericas
ICIQ_1H12p8s CDCl3 /opt/topspin



MR-740_13C_11.fid
ResearchGroup Pericas
ICIQ_13C11H512s CDCl3 /opt/topspin

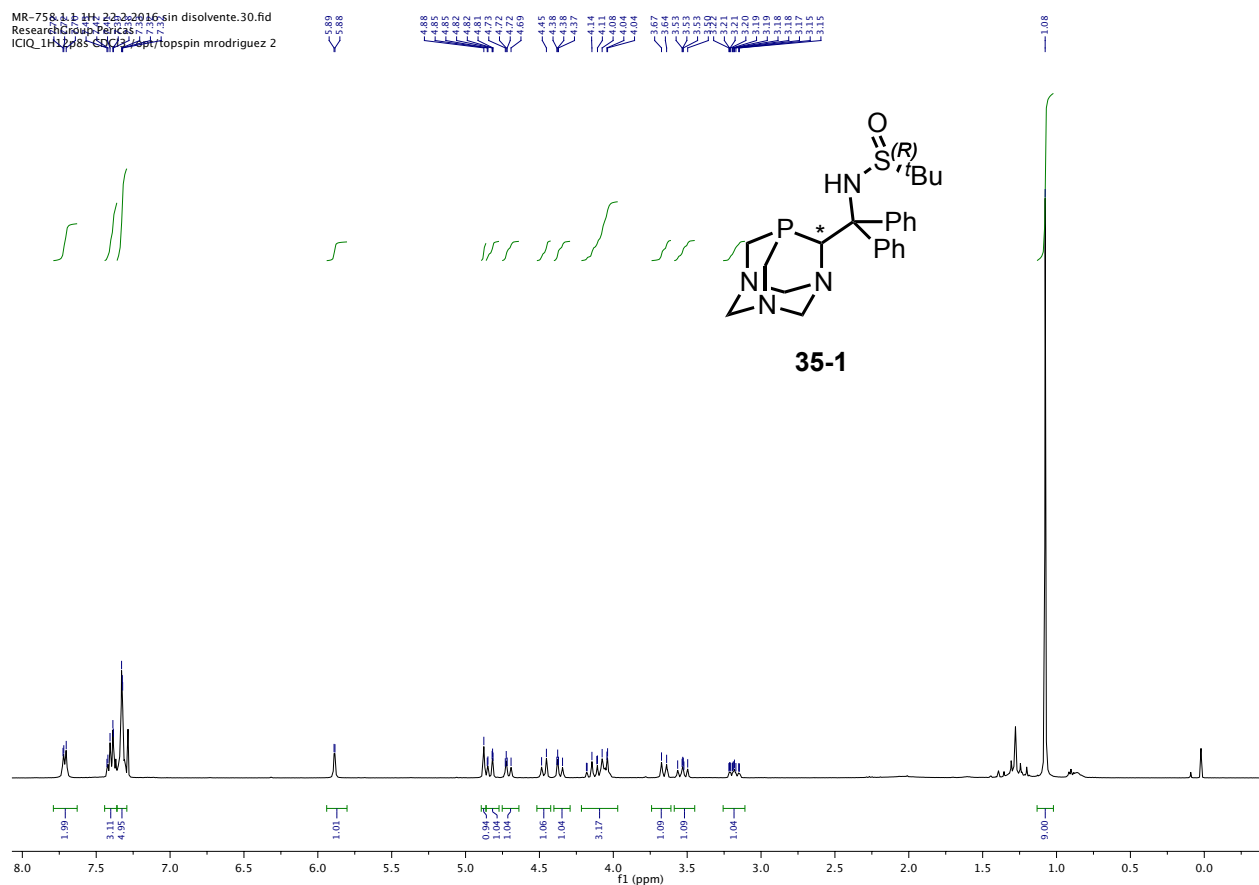


^1H NMR (500 MHz), ^{13}C NMR (125 MHz) spectra in CDCl_3 for **34**

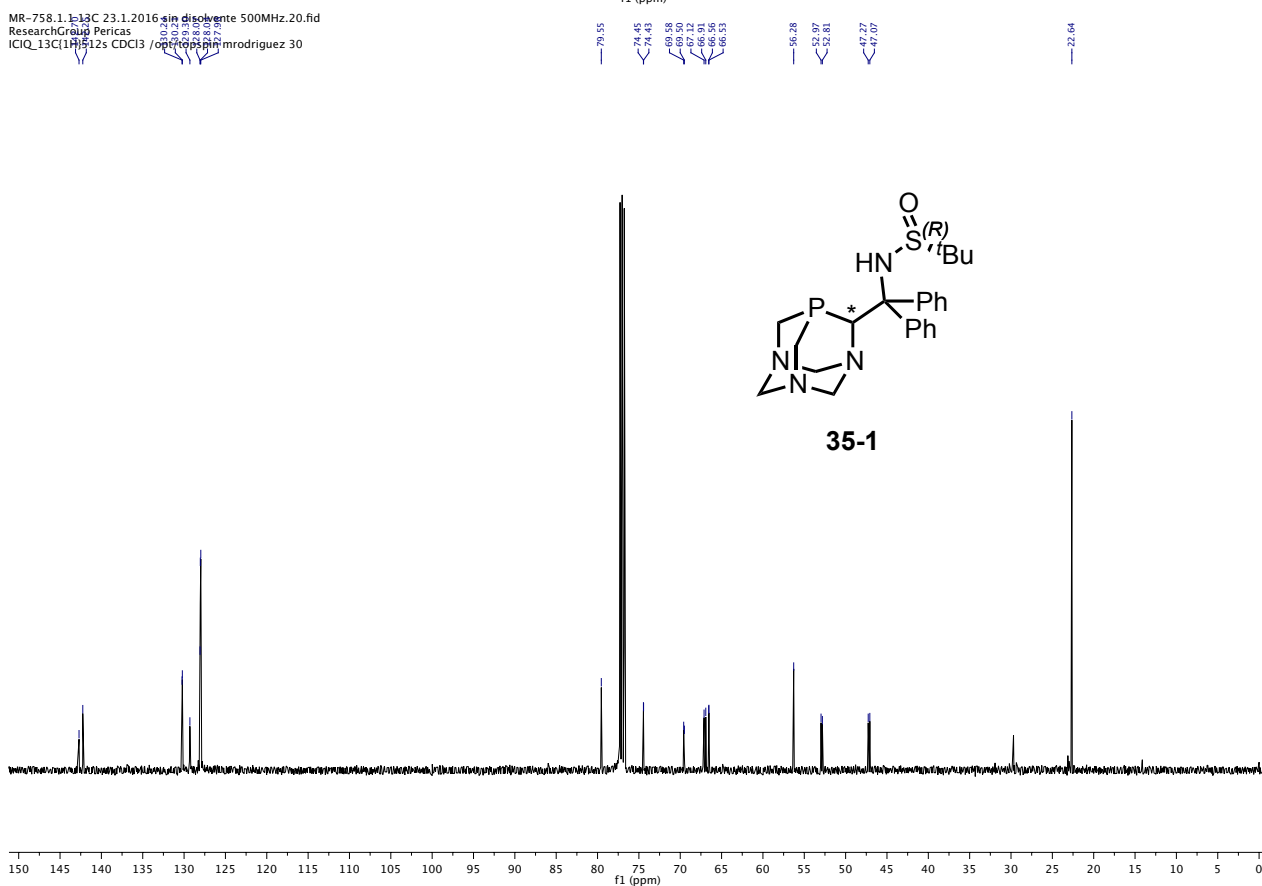


^1H NMR (400 MHz), ^{13}C NMR (125 MHz) and ^{31}P (162 MHz) spectra in CDCl_3 for **35-1**

MR-758.1.1-1H-22.2.2016 sin disolvente.30.fid
ResearchGroup Pericas
ICIQ_1H185-500MHz/opsin mrodriguez 2

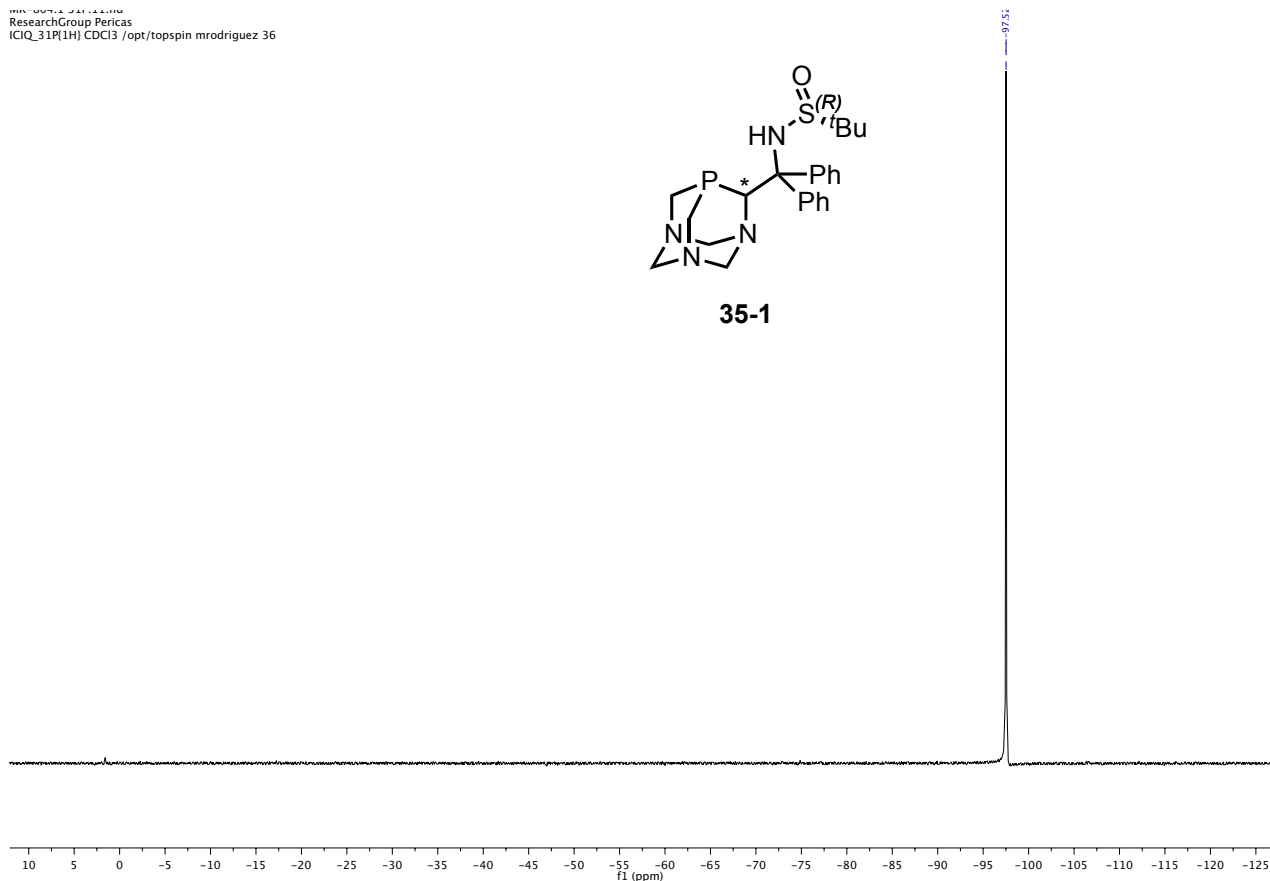
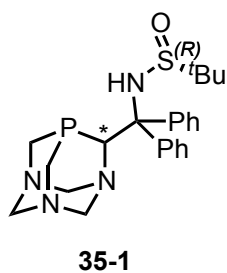


MR-758.1.1-13C-23.1.2016 sin disolvente 500MHz.20.fid
ResearchGroup Pericas
ICIQ_13C185-125MHz/opsin mrodriguez 30



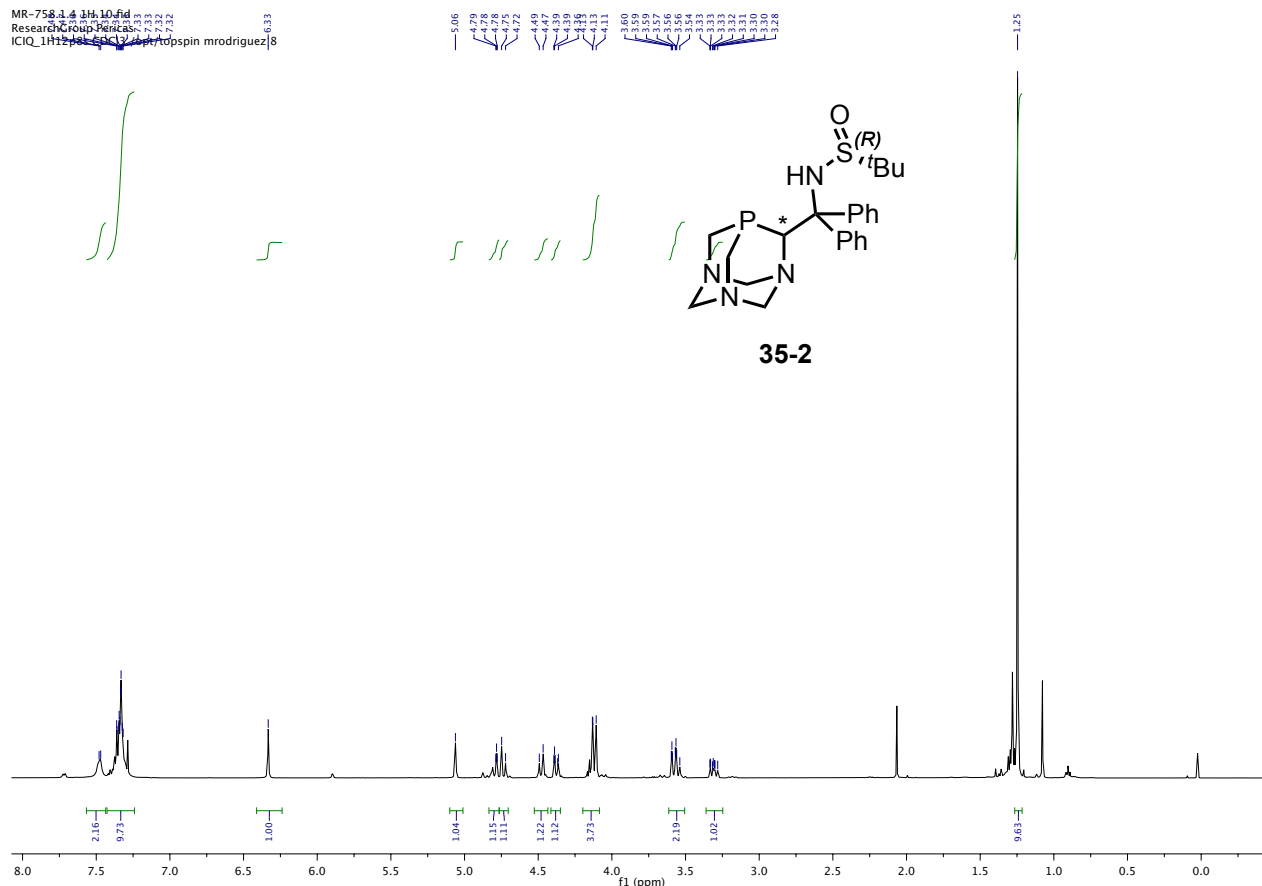
Preparation of new enantiopure PTA-based derivatives. Some applications in enantioselective catalysis.

MR-00714 24112410M
 ResearchGroup Pericas
 ICIQ_31P[1H] CDCl3 /opt/topspin mrodriguez 36

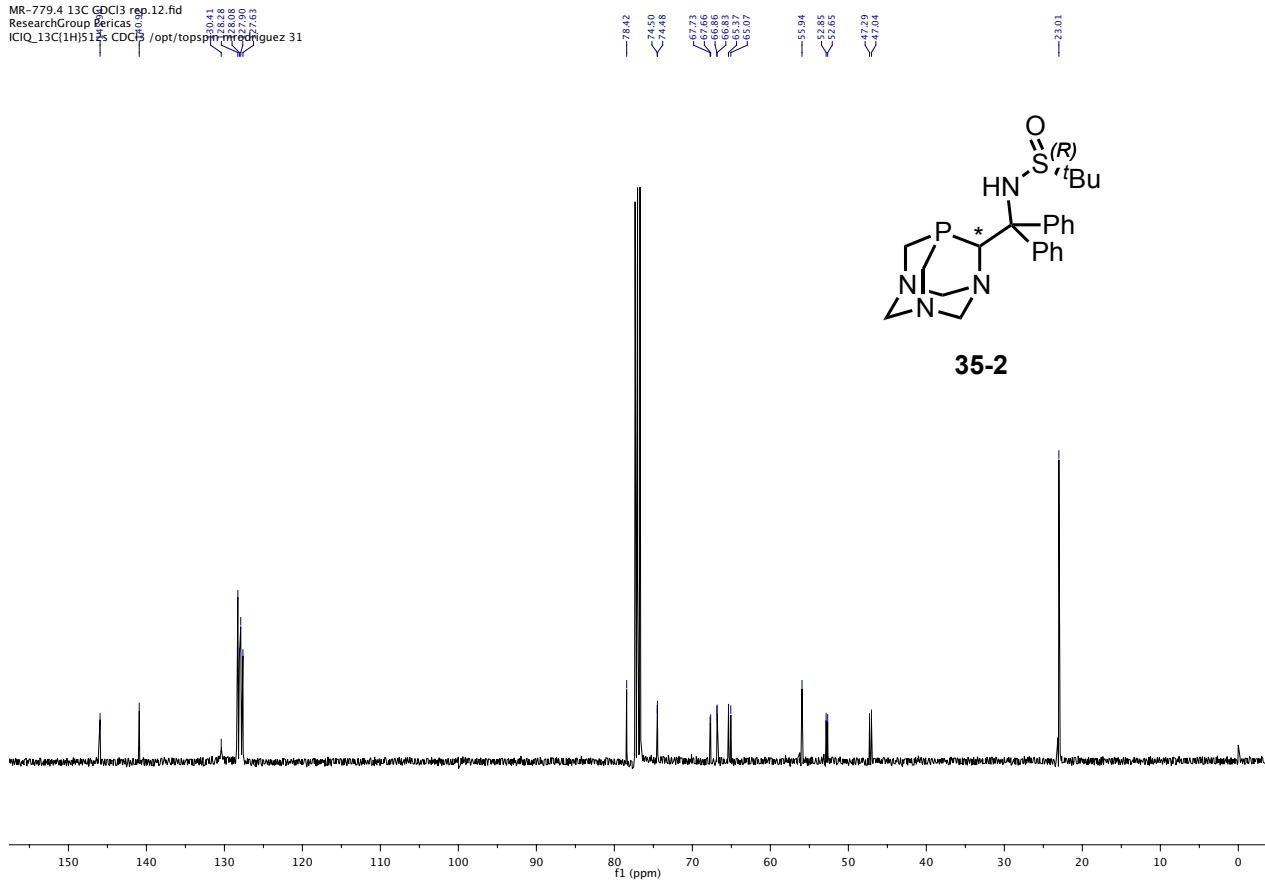


^1H NMR (500 MHz), ^{13}C NMR (100 MHz) and ^{31}P (202 MHz) spectra in CDCl_3 for **35-2**

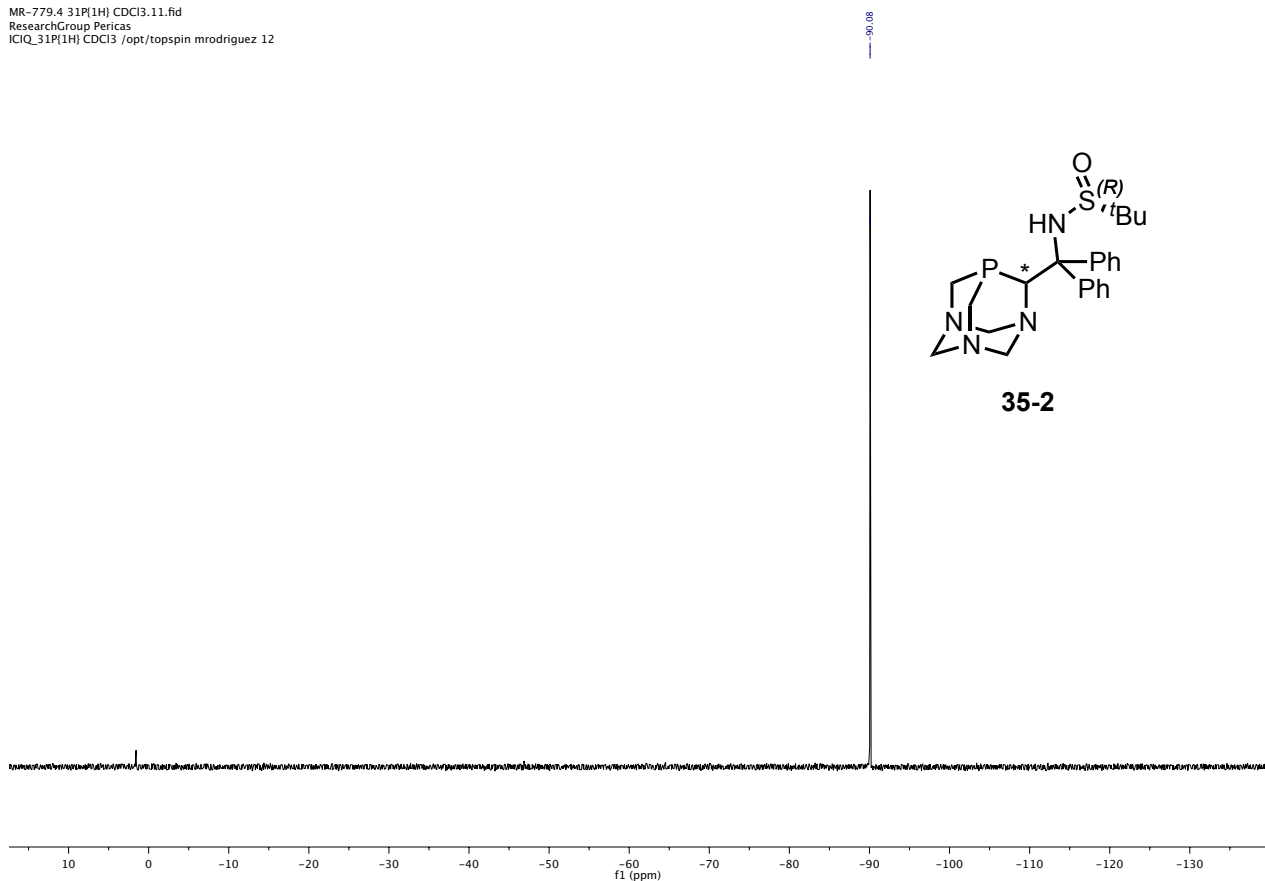
MR-75814 1H10.fid
 ResearchGroup Pericas
 ICIQ_1H12[1H] CDCl3 /opt/topspin mrodriguez 8



MR-779.4 13C GPC13 rep.12.fid
 ResearchGroup Pericas
 ICIQ_13C(1H)512s CDCl3 /opt/topspin-mrodriguez 31

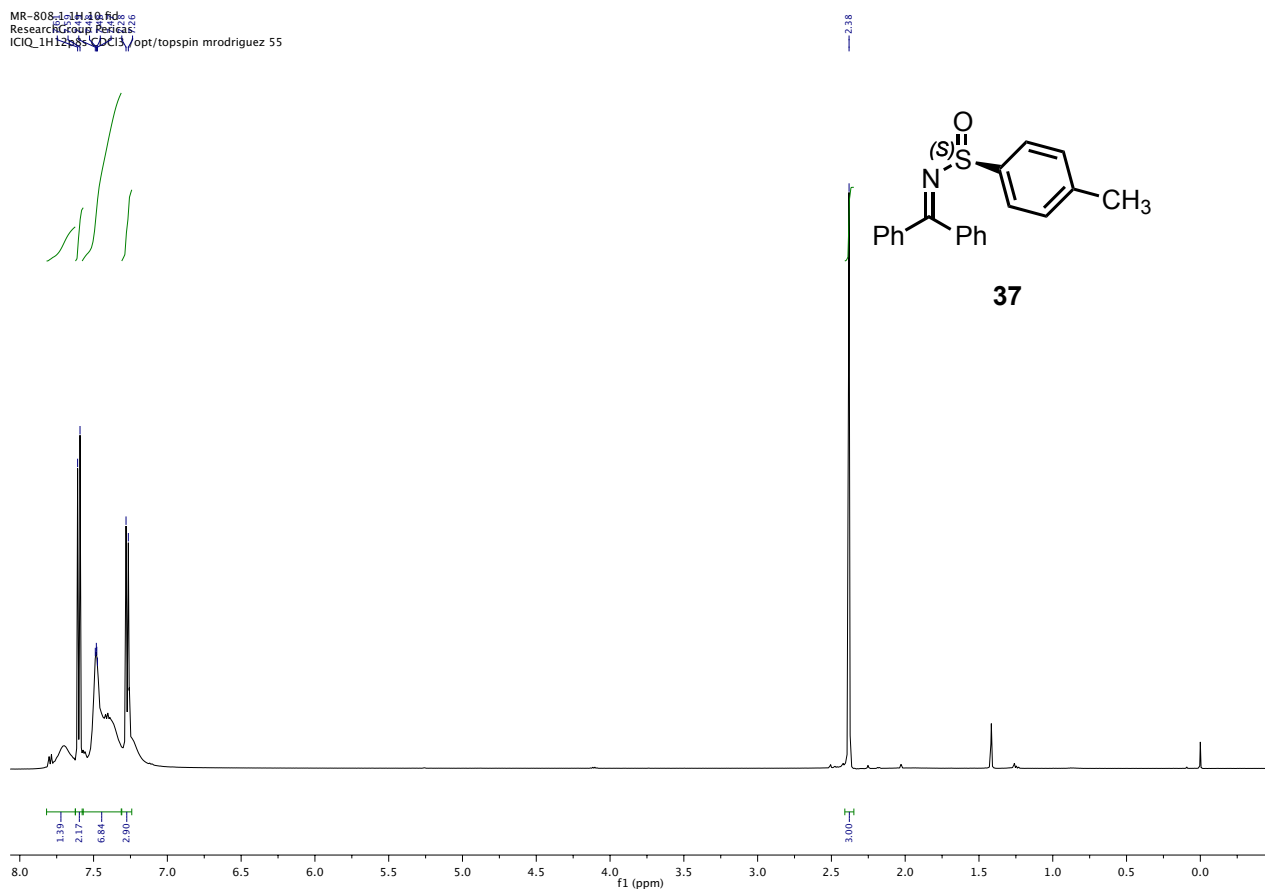


MR-779.4 31P(1H) CDCl3.11.fid
 ResearchGroup Pericas
 ICIQ_31P(1H) CDCl3 /opt/topspin mrodriguez 12

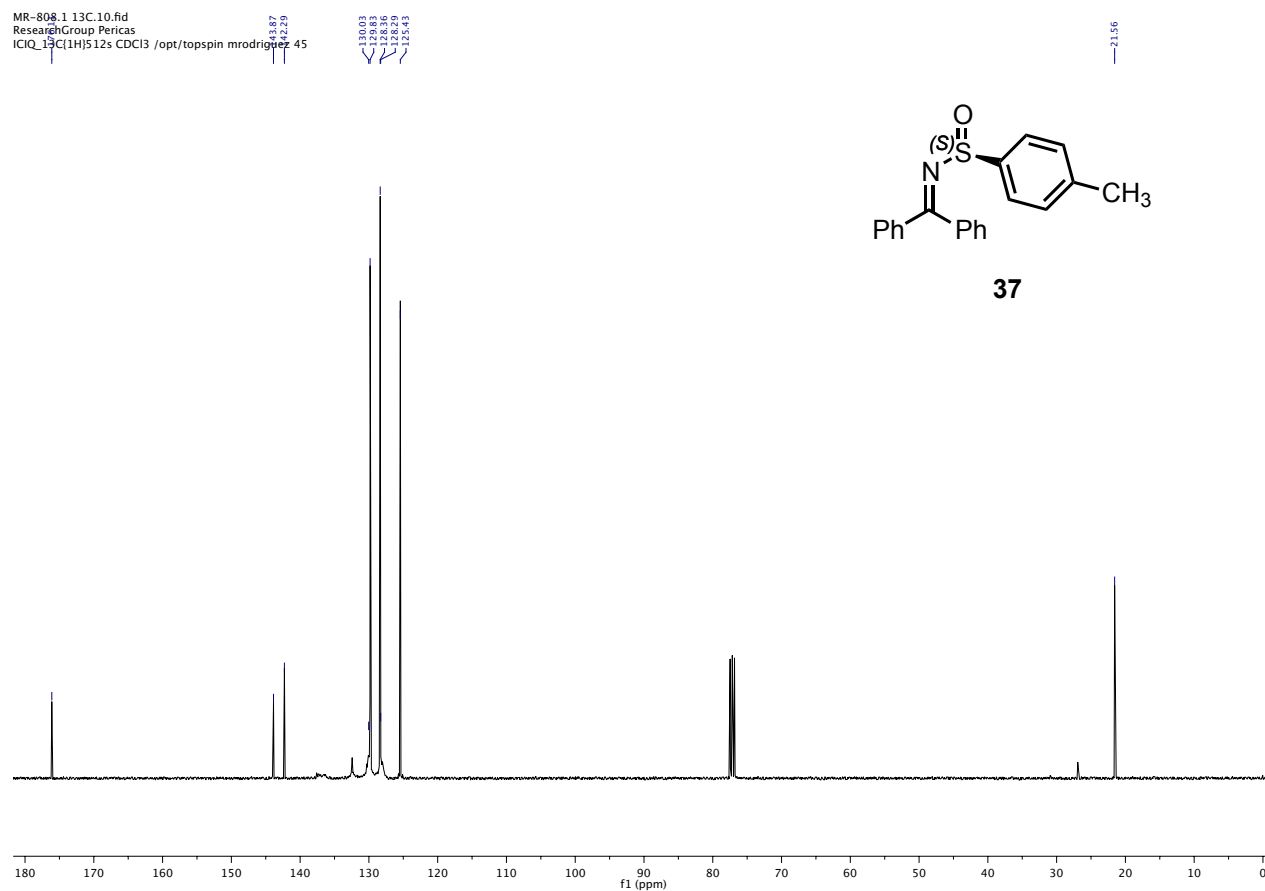


^1H NMR (500 MHz), ^{13}C NMR (100 MHz) spectra in CDCl_3 for **37**

MR-808_1 1H 500.fid
Research Group Pericas
ICIQ_1H12s CDCl3 /opt/topspin mrodriguez 55



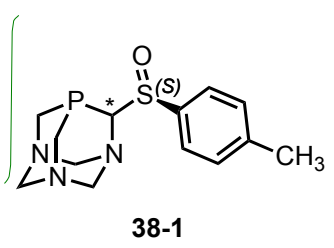
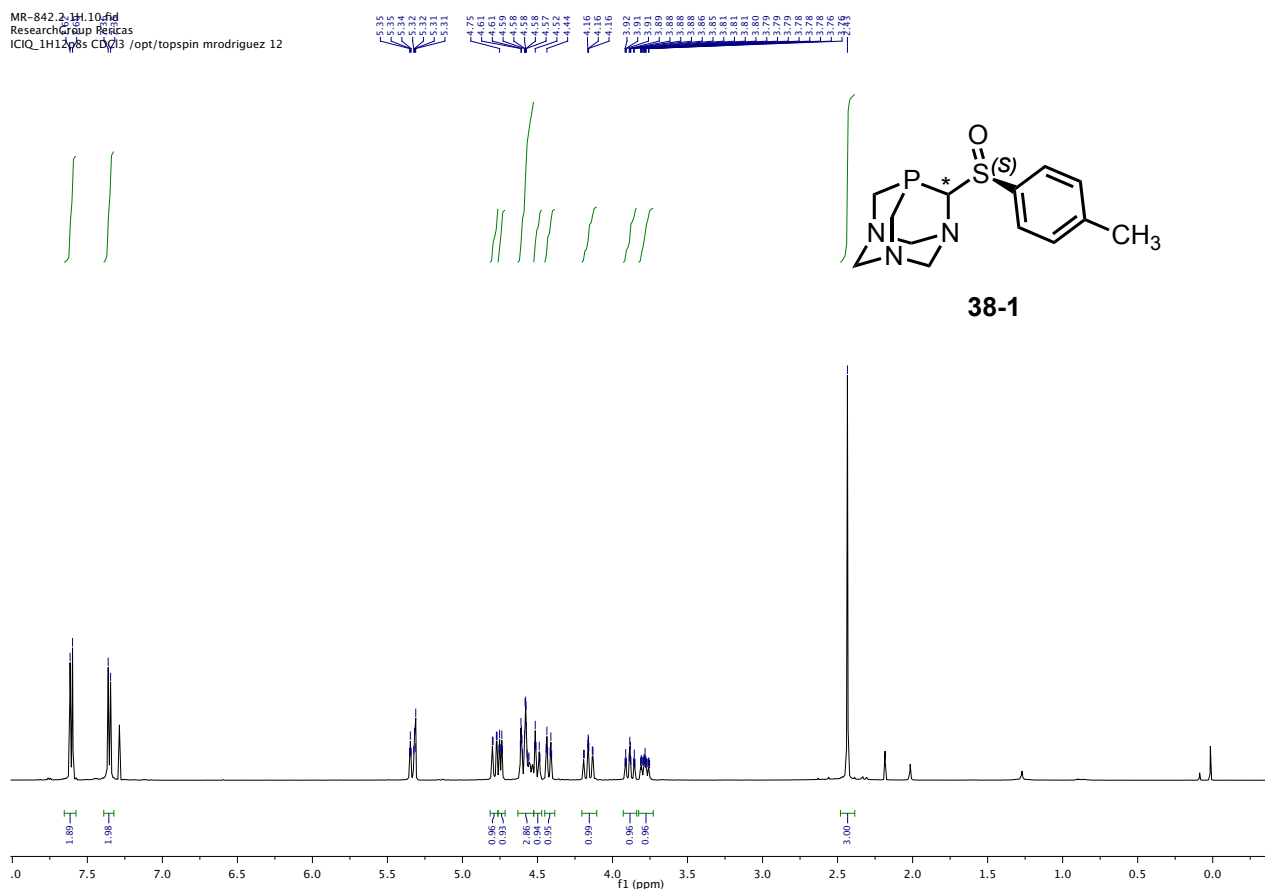
MR-808_1 13C 10.fid
Research Group Pericas
ICIQ_13C(1H)512s CDCl3 /opt/topspin mrodriguez 45



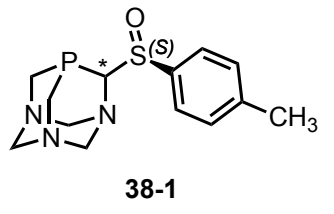
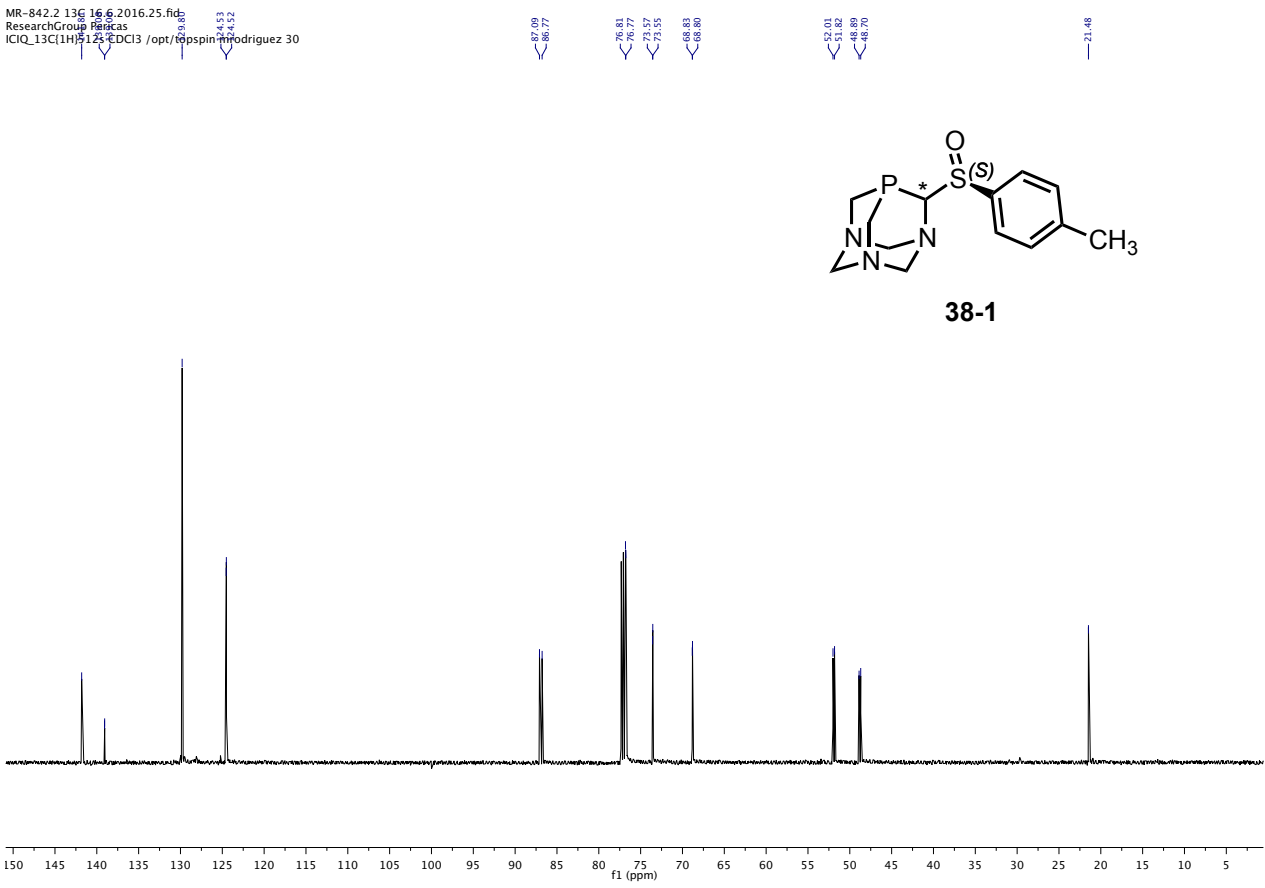
Chapter IV

^1H NMR (500 MHz), ^{13}C NMR (125 MHz) and ^{31}P (202 MHz) spectra in CDCl_3 for **38-1**

MR-842.2.1H.10.fid
Research Group Pericas
ICIQ_1H125.pbs CDCl3 /opt/topspin mrodriguez 12



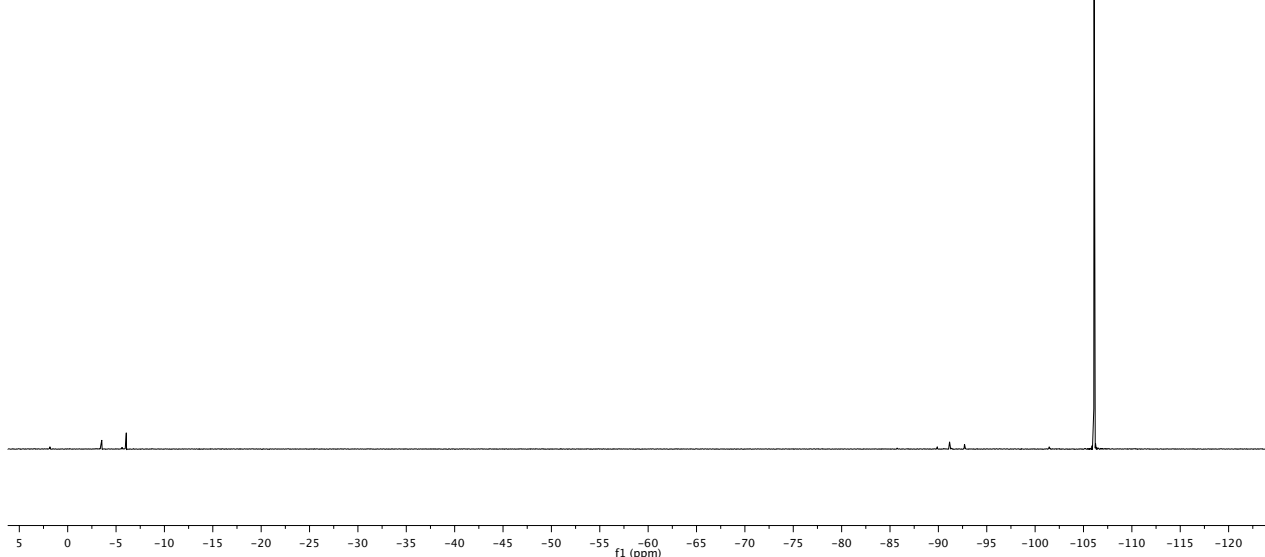
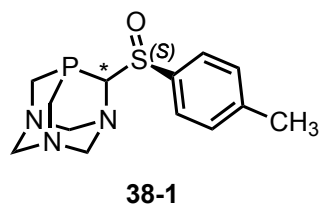
MR-842.2.13C.16.6.2016.25.fid
Research Group Pericas
ICIQ_13C1125.pbs CDCl3 /opt/topspin mrodriguez 30



Preparation of new enantiopure PTA-based derivatives. Some applications in enantioselective catalysis.

MR-842.2 31P[1H] 16.6.2016.21.fid
 ResearchGroup Pericas
 ICIQ_31P[1H] CDCl3 /opt/topspin mrodriguez 30

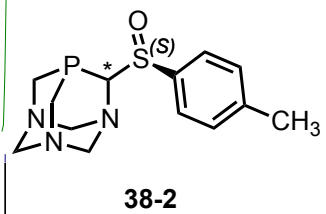
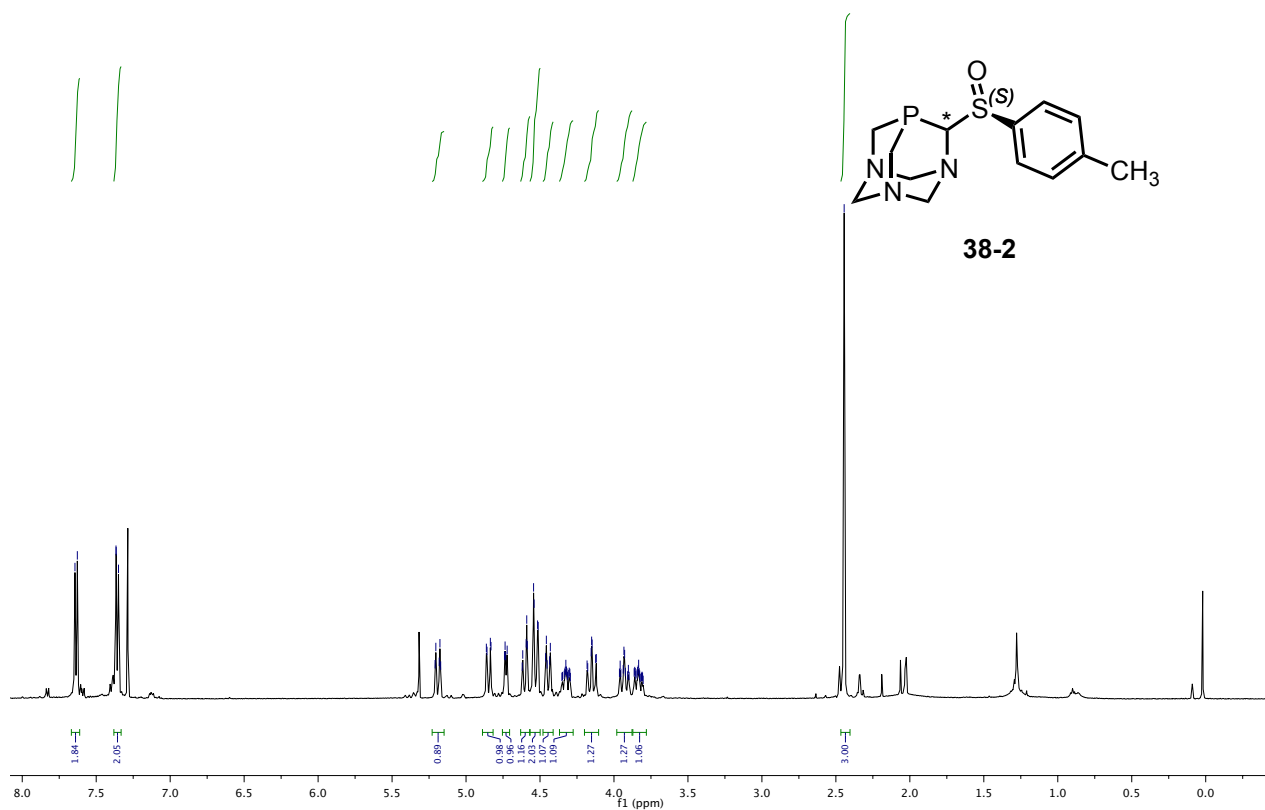
106.09



¹H NMR (500 MHz), ¹³C NMR (125 MHz) and ³¹P (202 MHz) spectra in CDCl₃ for **38-2**

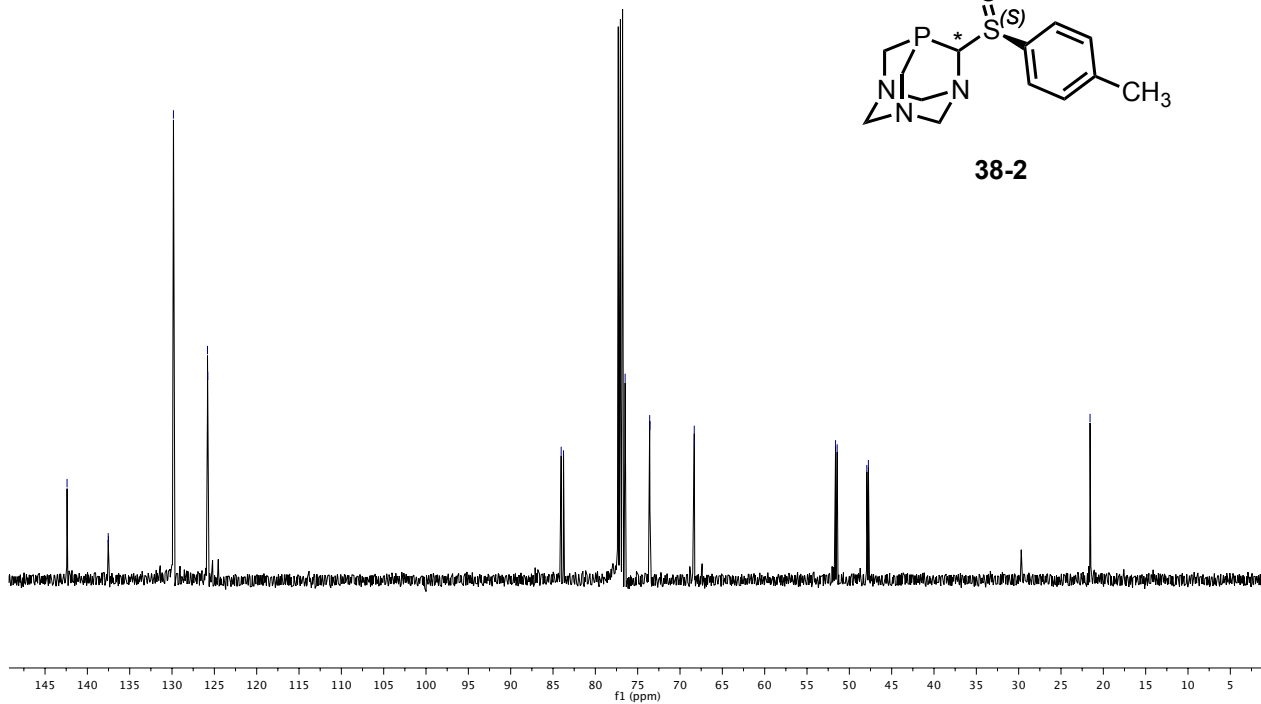
MR-842.4 1H 16.6.2016.20.fid
 ResearchGroup Pericas
 ICIQ_1H125 16.6.2016.20.fid /opt/topspin mrodriguez 31

5.20
5.18
5.17
4.85
4.74
4.59
4.59
4.54
4.52
4.51
4.15
3.96
3.95
3.94
3.93
3.90
3.86
3.86
3.84
3.83
3.83
2.34



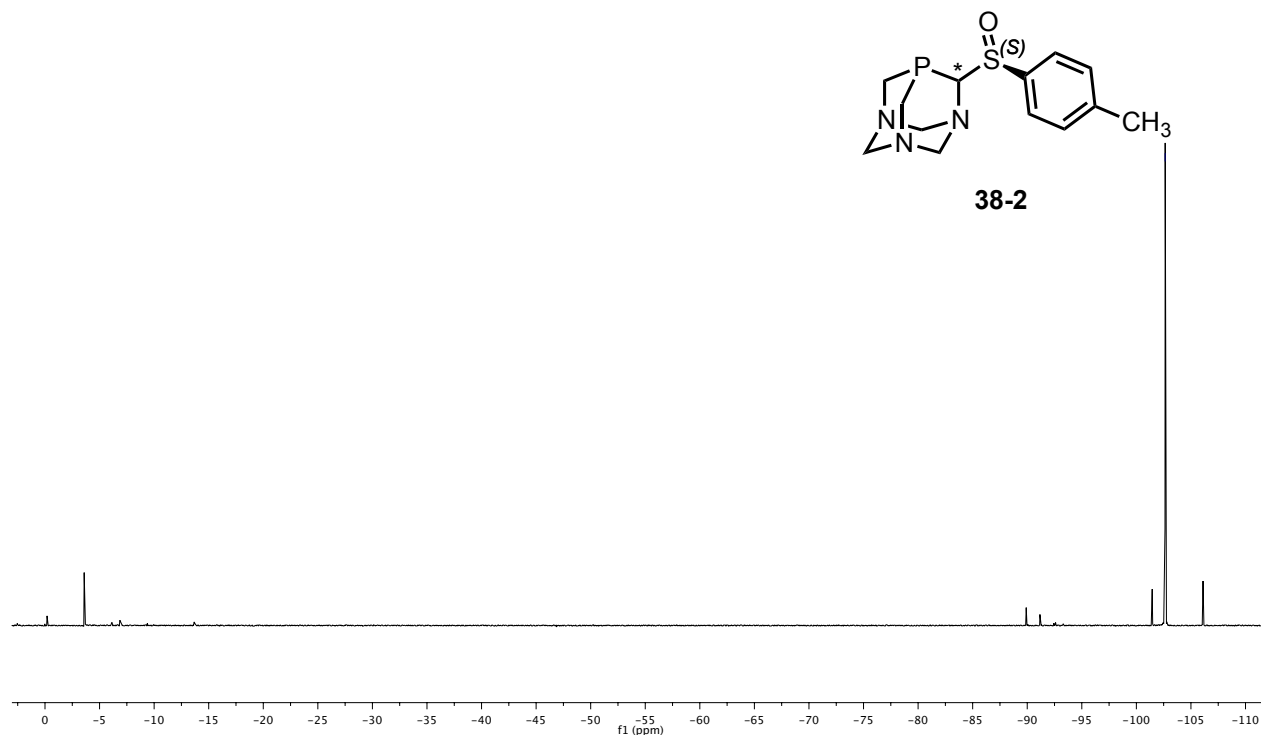
MR-842.4_13C 16.6.2016.25.fid
 ResearchGroup Pericas
 ICIQ_13C[1H]5125 CDCl3 /opt/topspin mrodriguez 31

85.06
 83.09
 76.48
 73.58
 73.56
 68.32
 68.30
 51.63
 51.43
 47.94
 47.75
 21.57



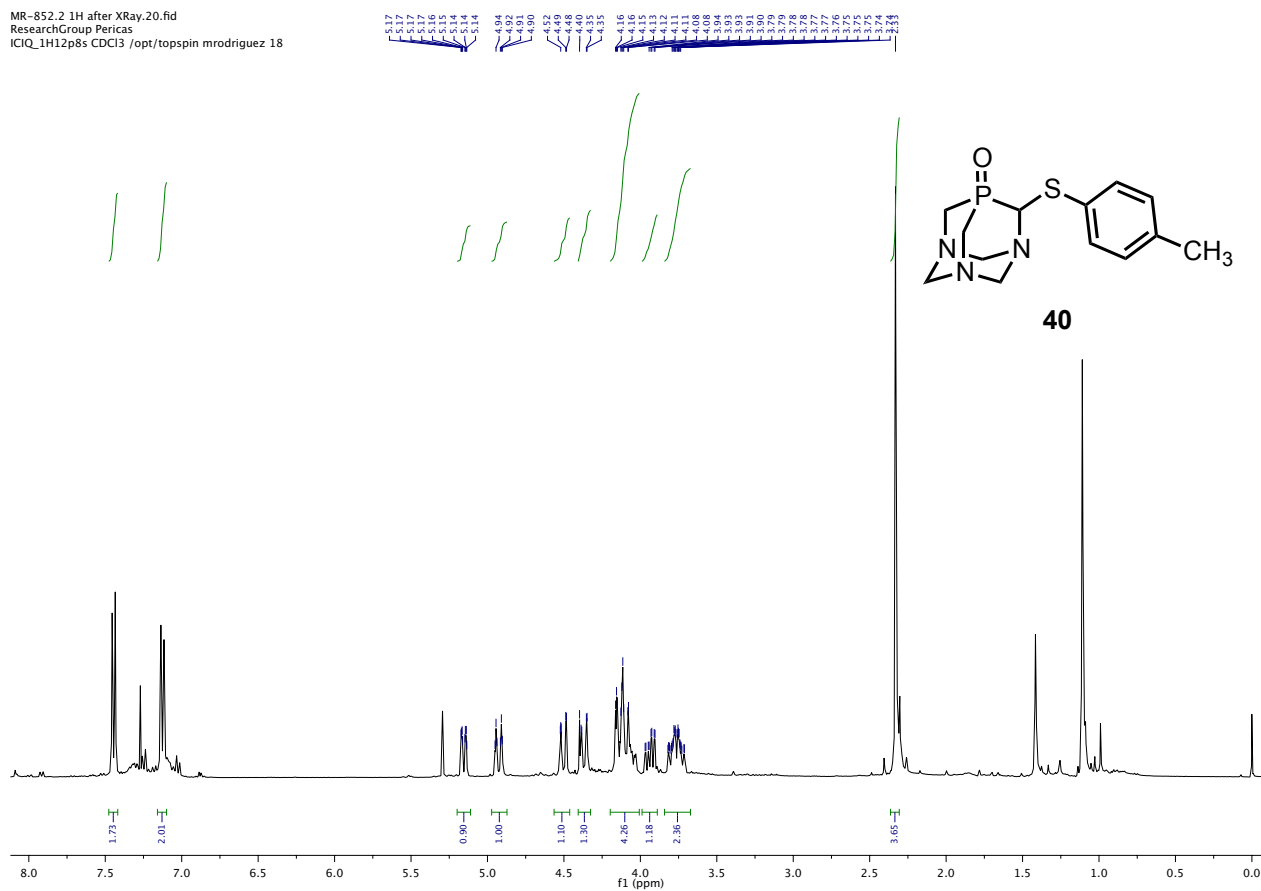
MR-842.4_31P[1H] 16.6.2016.21.fid
 ResearchGroup Pericas
 ICIQ_31P[1H] CDCl3 /opt/topspin mrodriguez 31

102.64

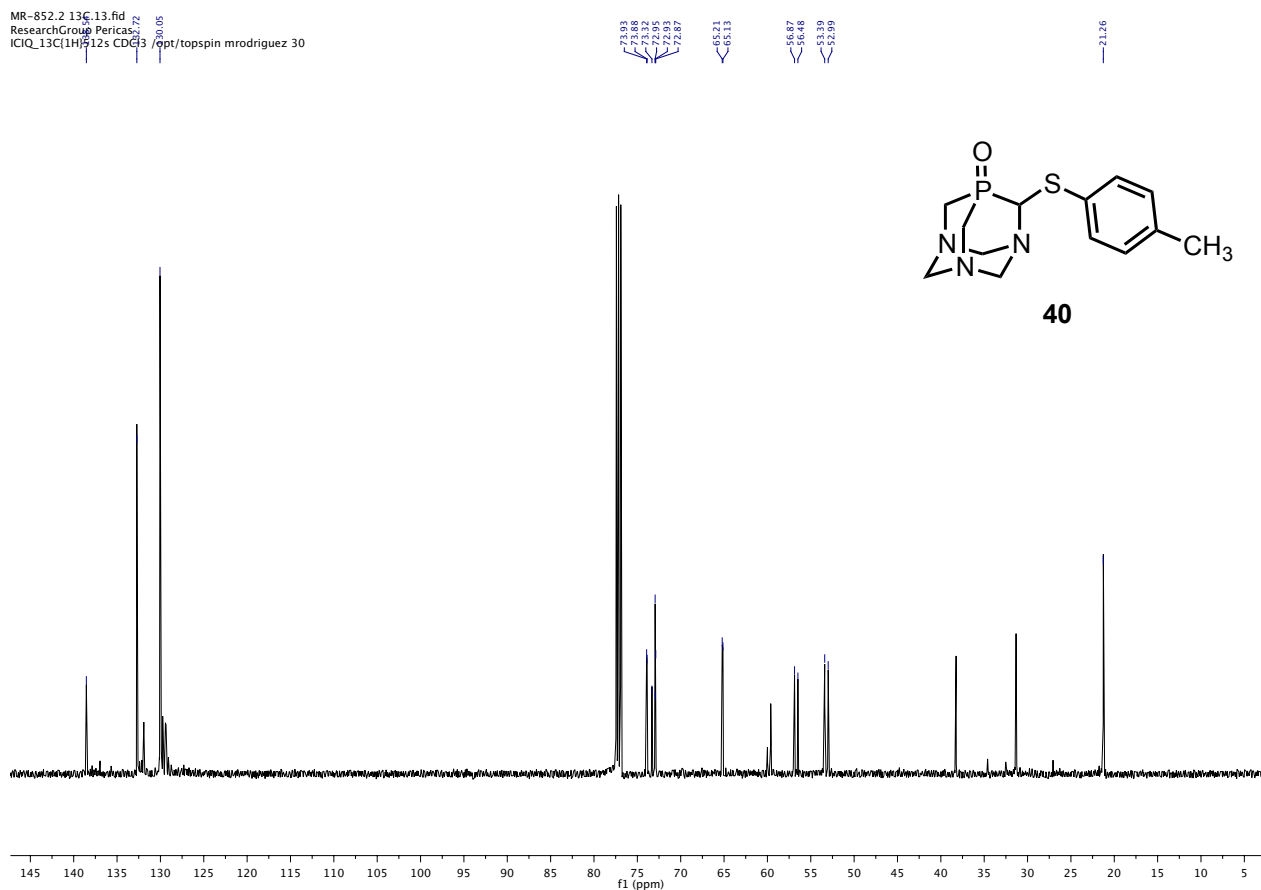


^1H NMR (400 MHz), ^{13}C NMR (125 MHz) and ^{31}P (162 MHz) spectra in CDCl_3 for **40**

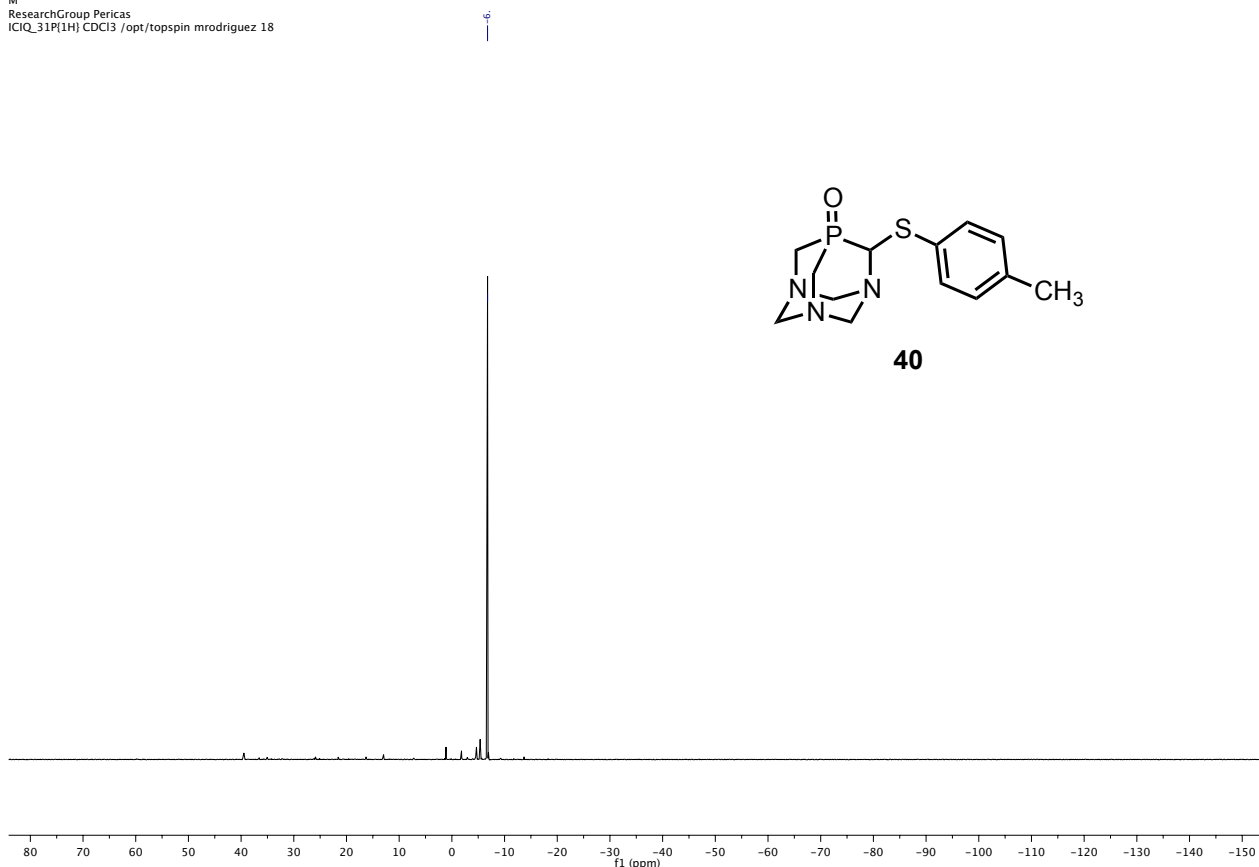
MR-852.2 1H after XRay.20.fid
ResearchGroup Pericas
ICIQ_1H12p8s CDCl3 /opt/topspin mrodriguez 18



MR-852.2 13C.13.fid
ResearchGroup Pericas
ICIQ_13C(1H)12s CDCl3 /opt/topspin mrodriguez 30

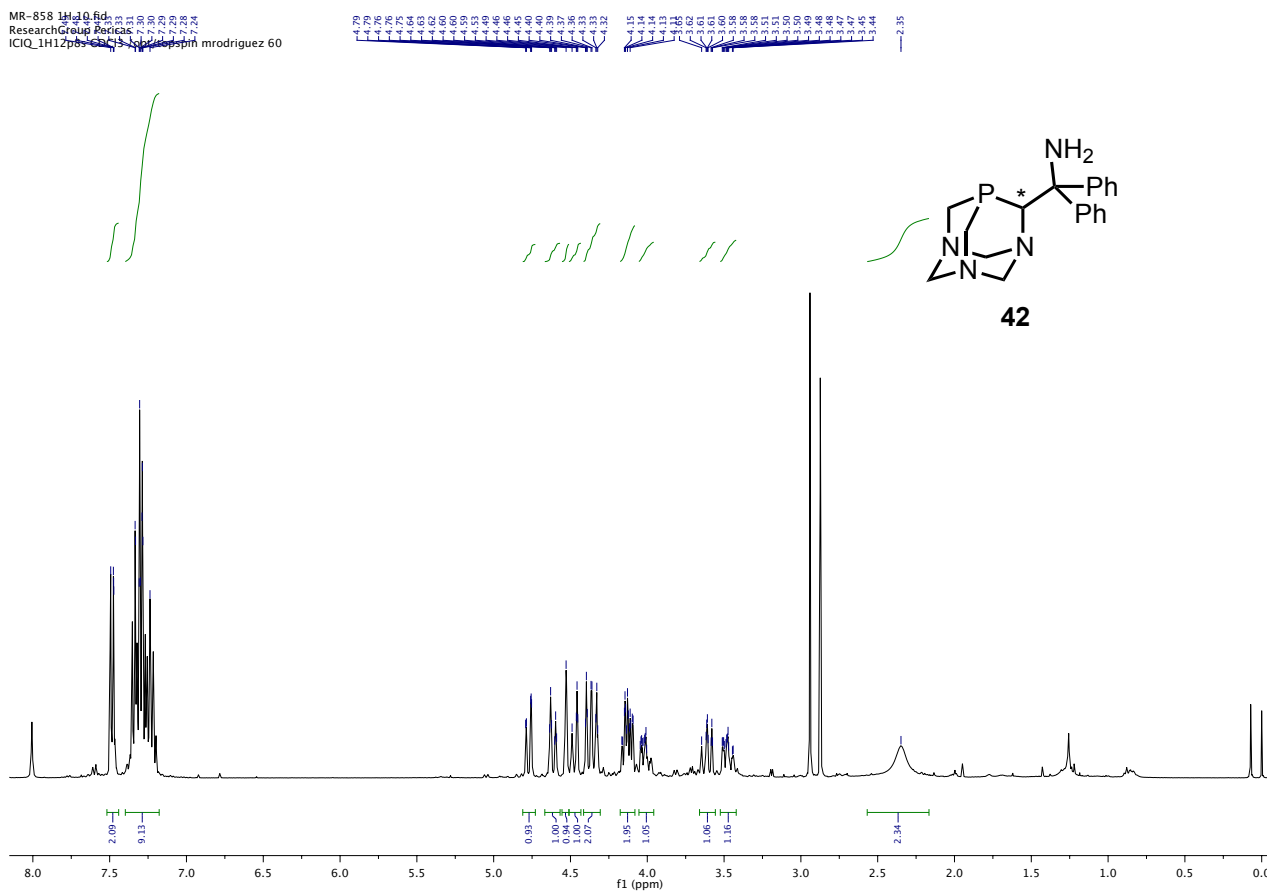


M
 ResearchGroup Pericas
 ICIQ_31P(1H) CDCl3 /opt/topspin mrodriguez 18



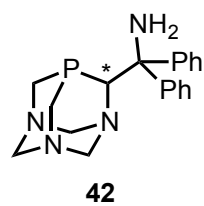
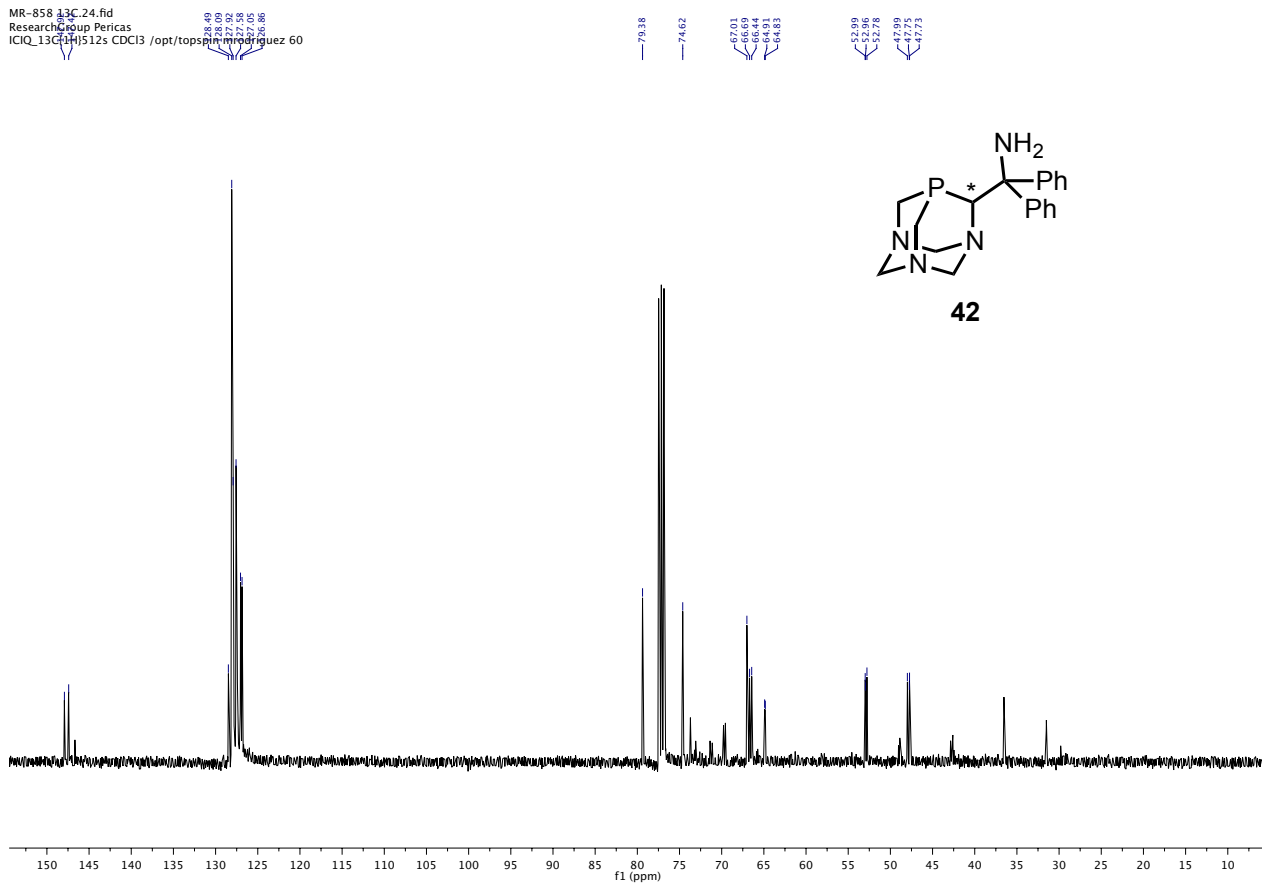
¹H NMR (400 MHz), ¹³C NMR (100 MHz) and ³¹P (162 MHz) spectra in CDCl₃ for **42**

MR-858 1H(0).f1
 ResearchGroup Pericas
 ICIQ_1H(1H) CDCl3 /opt/topspin mrodriguez 60

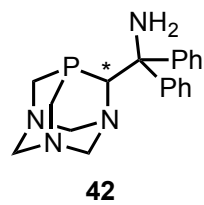
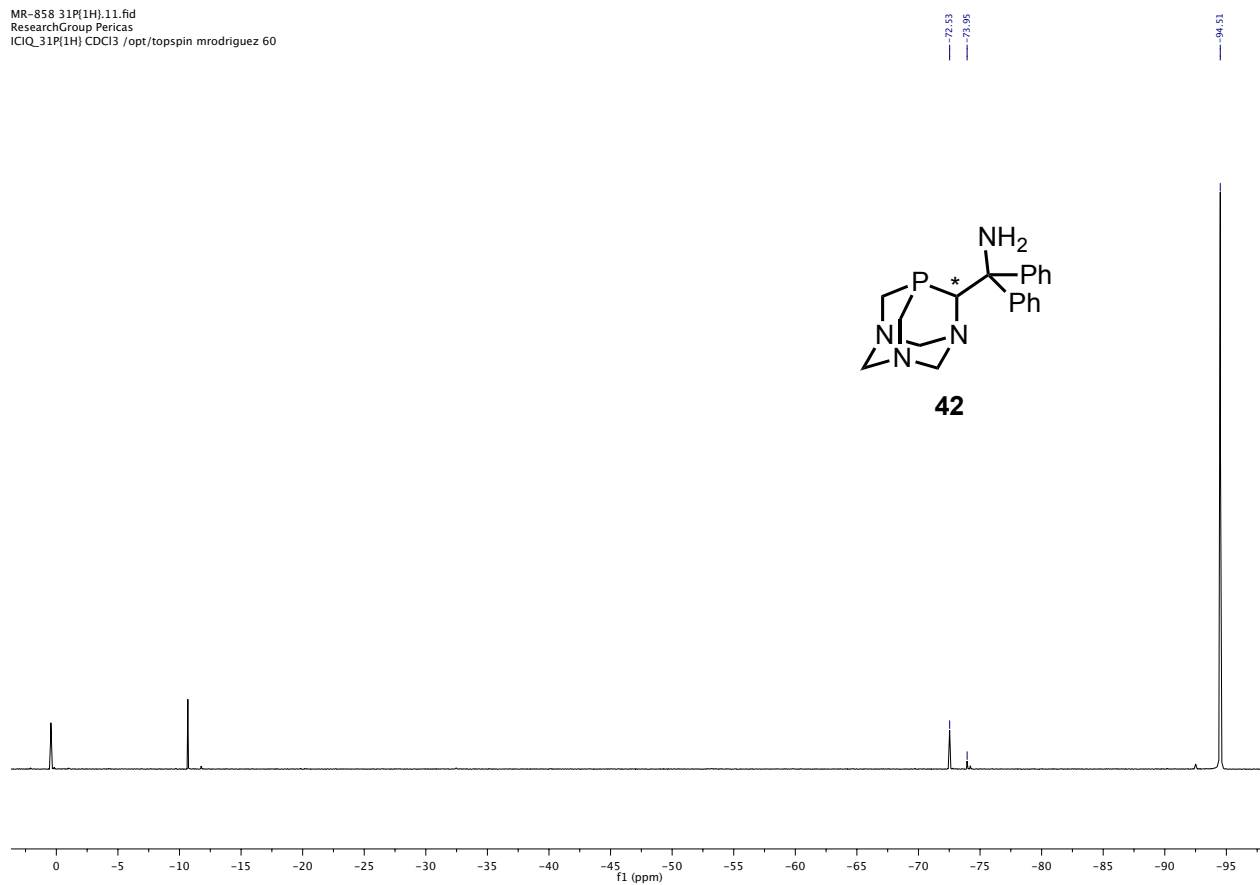


Preparation of new enantiopure PTA-based derivatives. Some applications in enantioselective catalysis.

MR-858 13C.24.fid
ResearchGroup Pericas
ICIQ_13C[1H]512s CDCl3 /opt/topspin mrodriguez 60

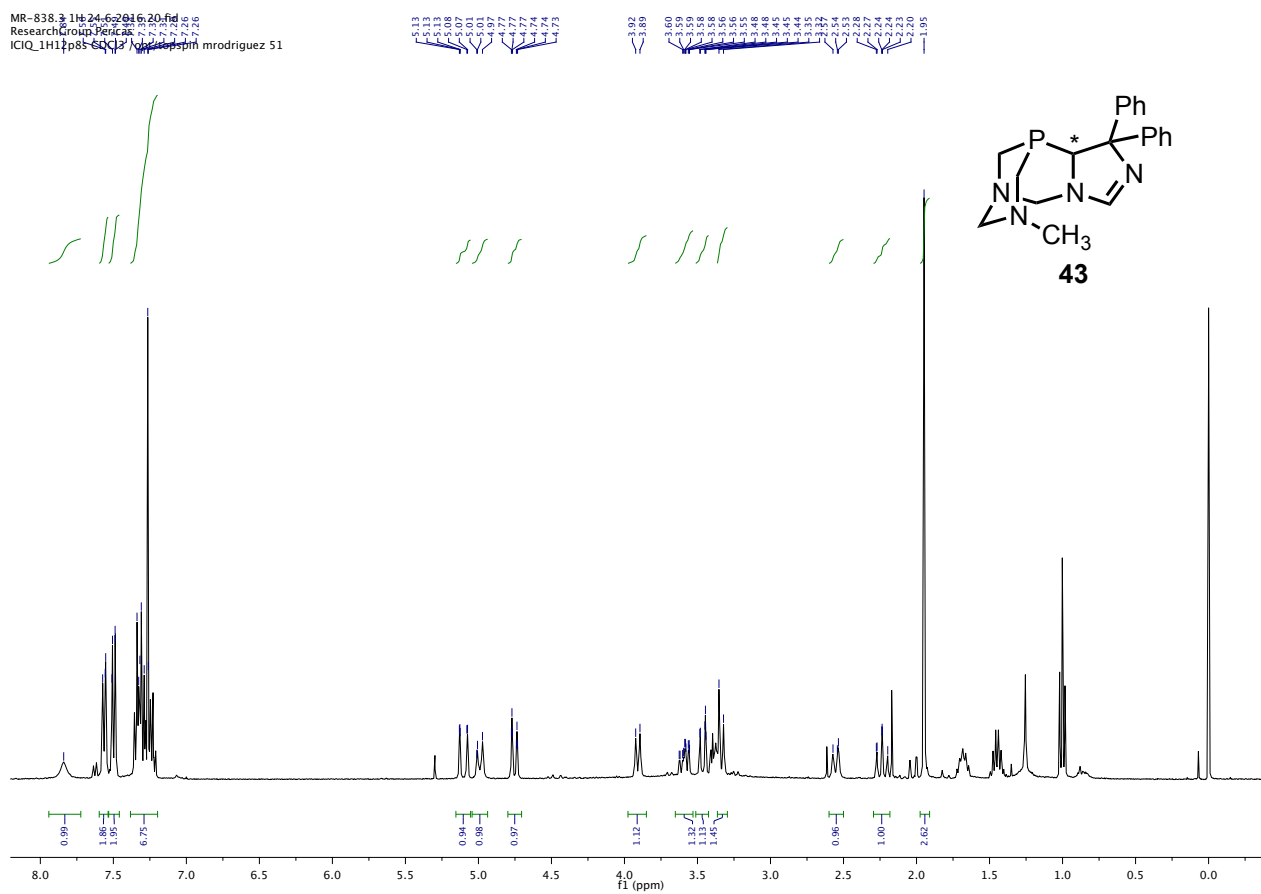


MR-858 31P[1H].11.fid
ResearchGroup Pericas
ICIQ_31P[1H] CDCl3 /opt/topspin mrodriguez 60

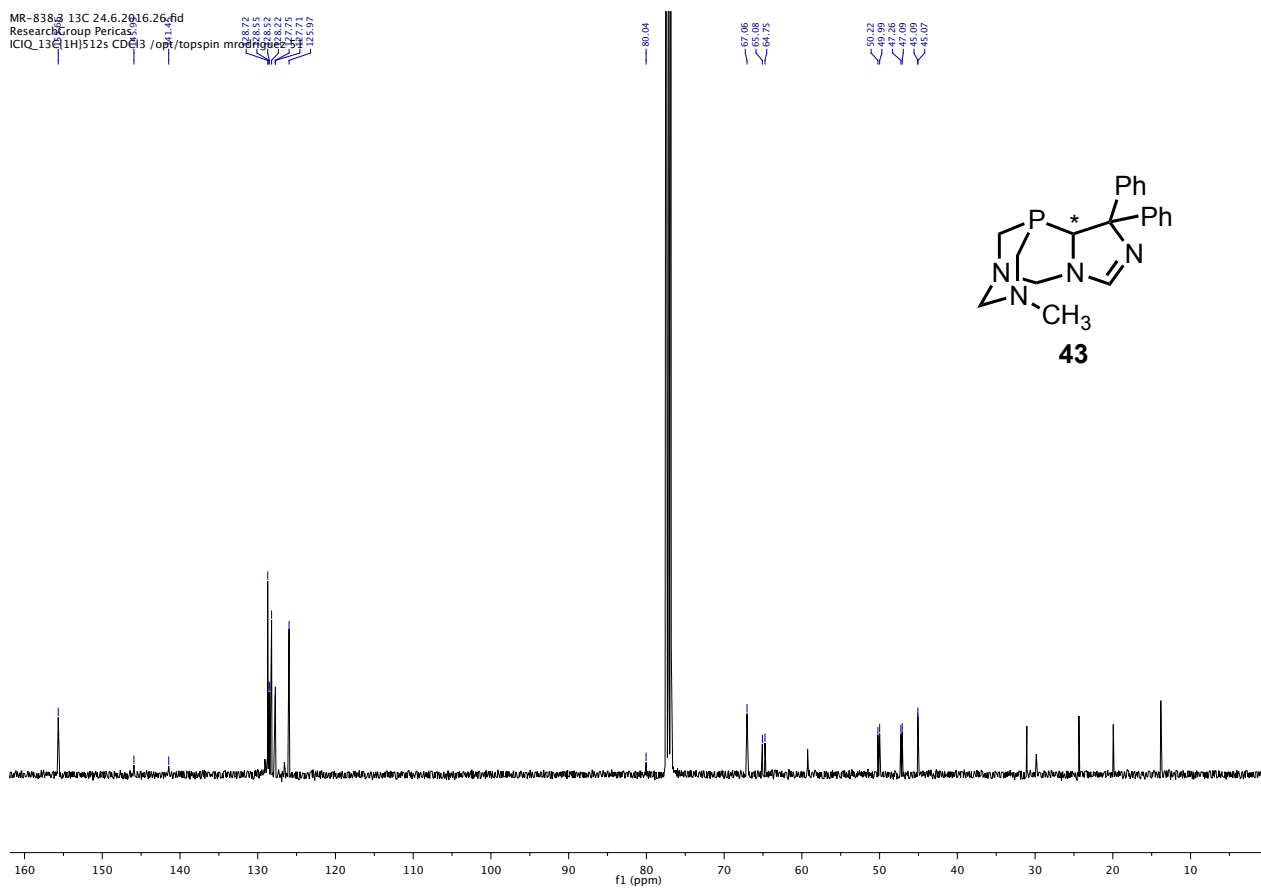


^1H NMR (400 MHz), ^{13}C NMR (100 MHz) and ^{31}P (162 MHz) spectra in CDCl_3 for **43**

MR-838_3 1H 24.6.2016.fid
 ResearchGroup Perica
 ICIQ_1H11p85-84 (3) /opt/topspin mrodriguez 51

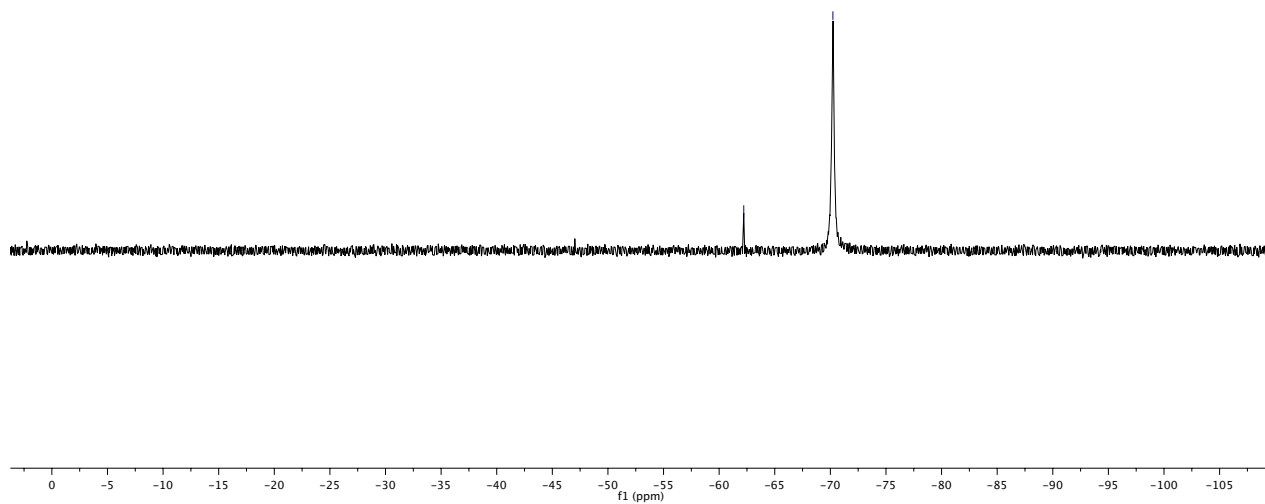
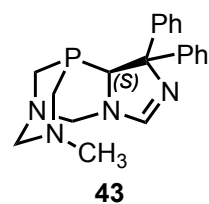


MR-838_2 13C 24.6.2016.fid
 ResearchGroup Perica
 ICIQ_13C11H1512s CDCl3 /opt/topspin mrodriguez 51



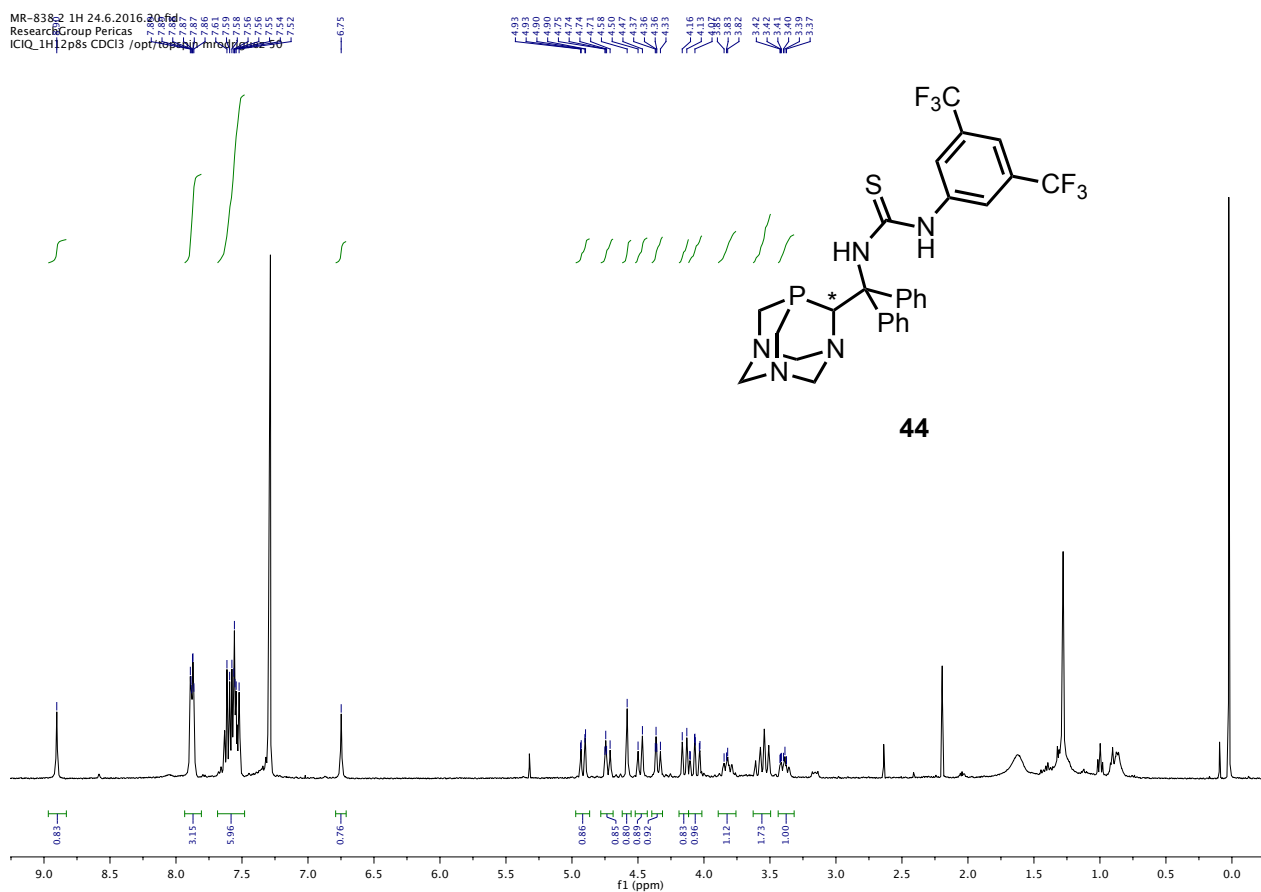
Preparation of new enantiopure PTA-based derivatives. Some applications in enantioselective catalysis.

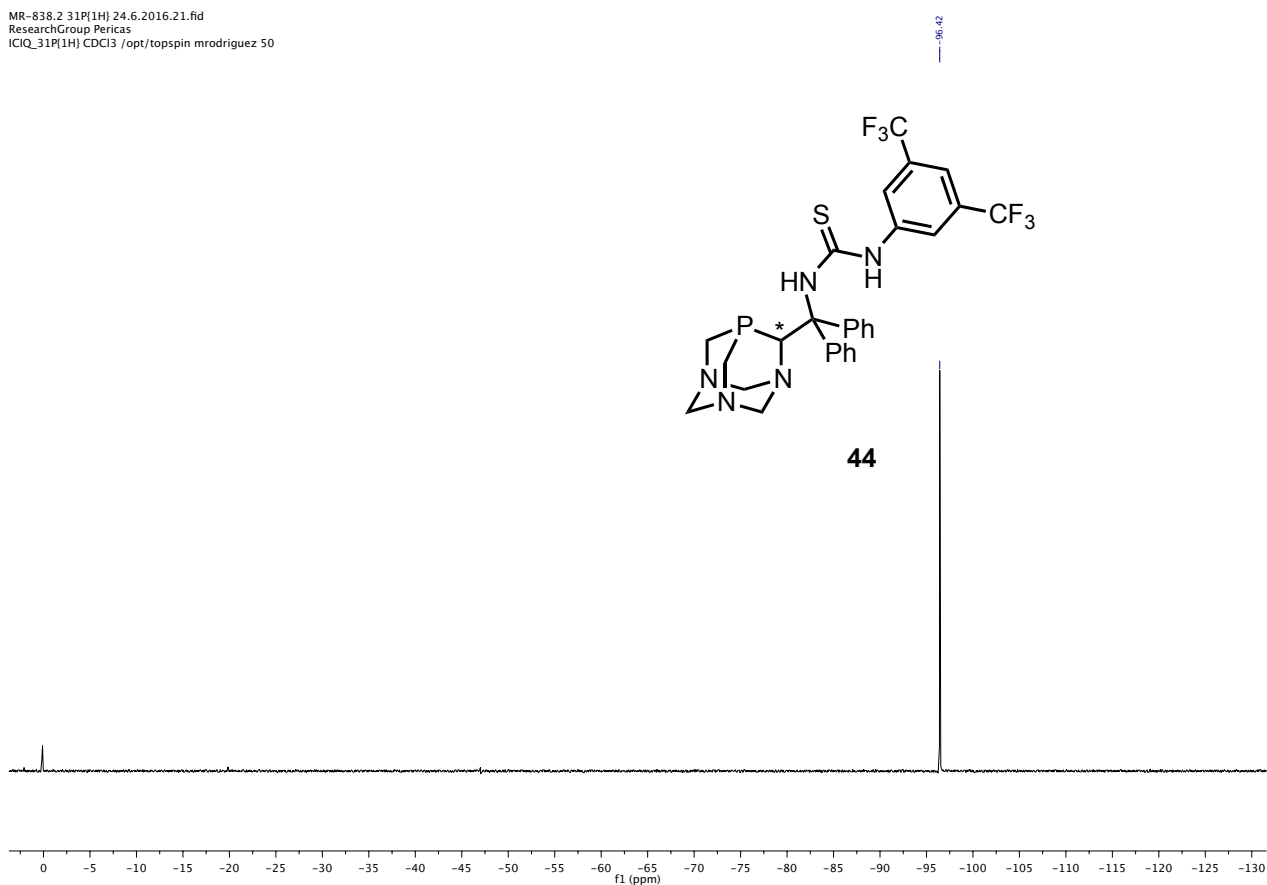
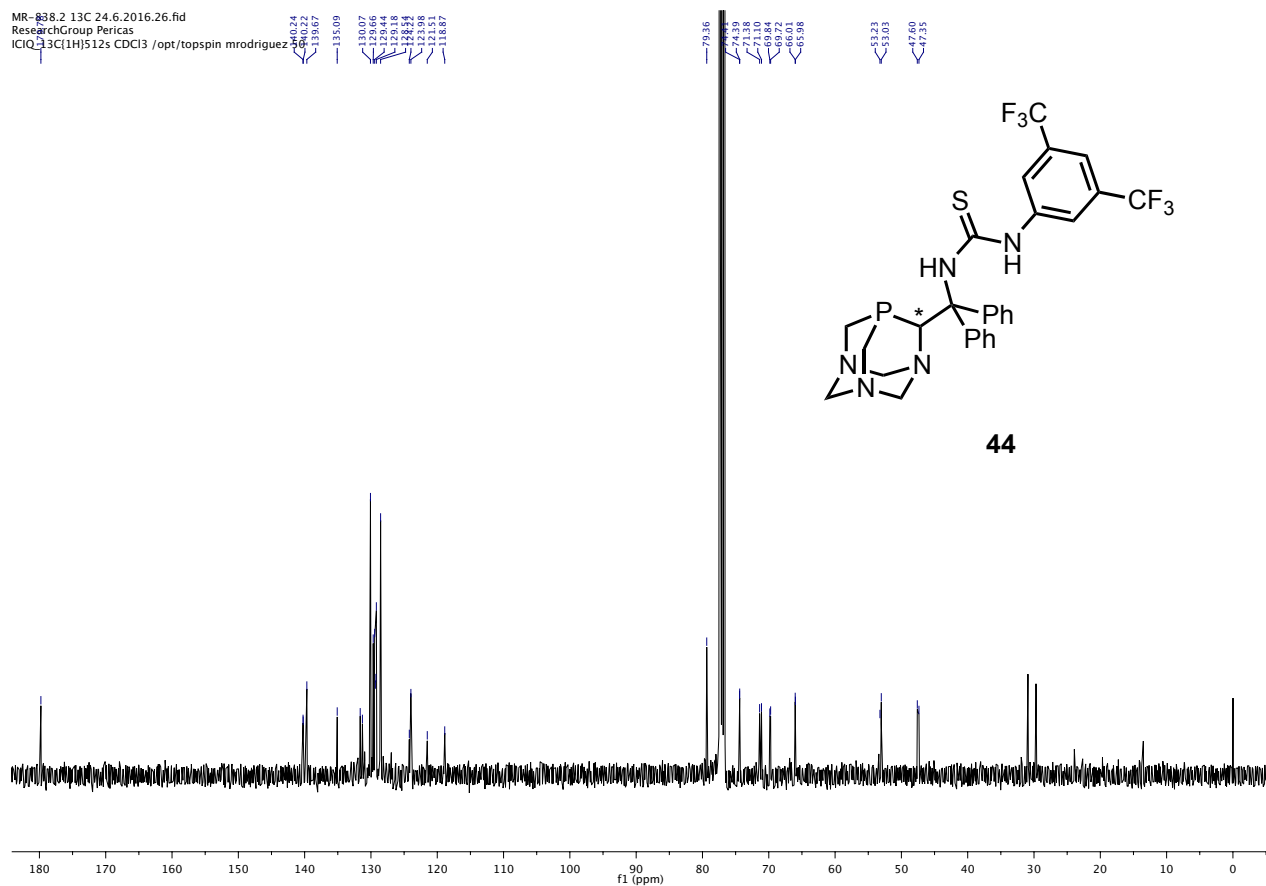
ICIQ_31P[1H] CDCl3 /opt/topspin mrodriguez 51



^1H NMR (400 MHz), ^{13}C NMR (100 MHz), ^{31}P (162 MHz), ^{19}F NMR (376 MHz) spectra in CDCl_3 for **44**

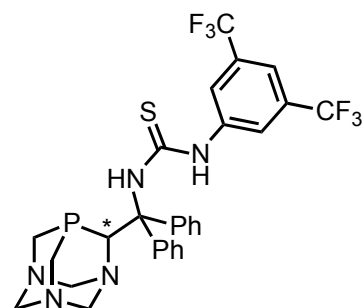
MR-838-2 1H 24.6.2016 20.fid
Research Group Pericas
ICIQ_1H12p8s CDCl3 /opt/topspin mrodriguez 50



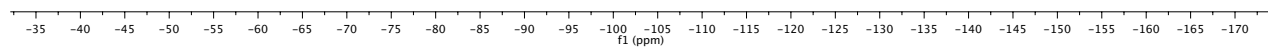


Preparation of new enantiopure PTA-based derivatives. Some applications in enantioselective catalysis.

MR-838.2 19F[1H] 24.6.2016.22.fid
ResearchGroup Pericas
ICIQ_19F[1H] CDCl3 /opt/topspin mrodriguez 50



44



Conclusions and perspectives

Conclusions and perspectives

Solvents are used daily in a wide variety of applications and, in most of the cases, its utilisation represent an environmental and safety problem for the planet and our society due to their toxicity. With the aim of doing our bit to help to the sustainable development of the world, the work presented in this Doctoral Thesis has been focused on the use of glycerol as solvent for chemical transformations. Glycerol is a biodegradable compound produced in huge amounts as an undesired by-product in biodiesel industries. The search of new uses of this compound is a matter of importance to allow the development of renewable resources such as biodiesel.

With this idea in mind, the usefulness of using glycerol as solvent in microwave assisted azide-alkyne cycloadditions between non-activated internal alkynes and organic azides under metal-free conditions has been demonstrated (Chapter 2). Under classical heating, this process takes long times and requires high temperatures to afford the desired fully substituted triazoles. However, the interesting physicochemical properties of glycerol permit the acceleration of the process under microwave dielectric heating much more than using other protic solvents. The ability of glycerol to form multiple hydrogen bonds might be the responsible for this significant enhancement of reactivity; this hydrogen-bonding network leads to a longer relaxation time in comparison with other protic solvents, which seems to be crucial for the reaction acceleration. Moreover, theoretical calculations demonstrated that the reaction is favoured due to the lower energy of $\text{BnN}_3/\text{glycerol}$ LUMO frontier orbital, in comparison with the one of neat benzyl azide or other adducts (like $\text{BnN}_3/\text{ethylene glycol}$ or $\text{BnN}_3/\text{propane-1,2-diol}$); this fact permits a better overlapping with the HOMO of the internal alkyne enhancing the reactivity. The presence of copper did not change the results in any case, except for silyl-based alkynes. Using this type of alkynes, the addition of a catalytic amount of copper led to desilylated 1,2,3-triazoles that were not observed in the absence of metal.

We have been also interested in the effect of glycerol in the same kind of reactivity, but under regioselectivity control (Chapter 3). Therefore, the Cu-catalysed azide-alkyne cycloaddition between terminal alkynes and organic azides have been studied. Surprisingly, we have found that the presence of impurities in commercial samples of benzyl azide disturbs this catalytic reaction. These impurities have been identified as long aliphatic chain amines and we have demonstrated that they are convenient stabilisers for the formation of highly reactive

copper nanoparticles in this medium under very mild conditions (room temperature, 1 mol% CuI). The catalytic glycerol phase could be analysed by (HR)TEM thanks to the negligible vapour pressure of the solvent, which allowed us to evidence the presence of nanoparticles. In addition, the nanoparticles are efficiently immobilised in this solvent, enabling the recycling of the catalytic phase after extracting the organic products with an immiscible solvent. Another major conclusion of this work is the importance of checking the quality of the commercial products that we use, in order to avoid these reproducibility issues.

The work carried out in the last part of this Thesis has consisted on the preparation of new enantiopure PTA derivatives that are potential glycerol-soluble molecules (Chapter 4). This is the first time that PTA-based derivatives are prepared in an enantiopure form and they open the door for the generation of new catalytic systems in glycerol (or water) medium for asymmetric reactions. The synthesis of β -phosphino alcohol (**26**) and β -phosphino sulfinamide (**35**) PTA-based derivatives has been established, whereas the synthesis of α -sulfinylphosphine PTA derivative (**38**), PTA-based primary aminophosphine (**42**) and PTA-based thiourea (**44**) requires further optimisation. Several preliminary tests have been carried out to check their activity as ligands for transition metal catalysed reactions or as organocatalysts in transformations as the organocatalysed MBH reaction, the aziridination reaction, the α -amination reaction, the Cu-catalysed addition of terminal alkynes to isatins and the Cu-catalysed hydroboration of isatins. This last transformation is the most promising result in terms of reactivity (around 96% yield) and enantioselectivity (32%), using one of the diastereomers of β -phosphino sulfinamide (**35**). A future optimisation of the process could lead to a better enantioselectivity of the final product. The search for applications of these PTA-based ligands is still ongoing. In addition to their potential role as ligands for transition metal complexes with application in catalysis, they might also act as stabilisers for metal nanoparticles or as organocatalysts by themselves.

With this work, we have revealed how useful glycerol can be as solvent in chemical transformations, having in some cases a non-innocent role in the process, which leads to the success of the reaction. Our efforts in this topic pretend to open the door to more synthetic alternatives in this environmentally friendly medium in Fine Chemistry sector. The study of asymmetric catalytic processes, supported catalytic systems and flow processes are interesting fields to be explored in glycerol medium.

